

# UC Riverside

## UC Riverside Electronic Theses and Dissertations

### Title

Synthetic Studies Toward the Total Syntheses of Norcrassin A and Berbamine & Development of Dual Brønsted/Lewis Acid Catalysis for Site-Selective Friedel–Crafts Alkylation of Phenols

### Permalink

<https://escholarship.org/uc/item/81j610hv>

### Author

Nguyen, Vivienne

### Publication Date

2023

Peer reviewed|Thesis/dissertation

UNIVERSITY OF CALIFORNIA  
RIVERSIDE

Synthetic Studies Toward the Total Syntheses of Norcrassin A and Berbamine &  
Development of Dual Brønsted/Lewis Acid Catalysis for Site-Selective Friedel–Crafts  
Alkylation of Phenols

A Dissertation submitted in partial satisfaction  
of the requirements for the degree of

Doctor of Philosophy

in

Chemistry

by

Viviene Kim Nguyen

December 2023

Dissertation Committee:

Dr. Kevin Kou, Chairperson

Dr. Catharine Larsen

Dr. Christopher Switzer

Copyright by  
Viviene Kim Nguyen  
2023

The Dissertation of Vivienne Kim Nguyen is approved:

---

---

---

Committee Chairperson

University of California, Riverside

## ABSTRACT OF THE DISSERTATION

Synthetic Studies Toward the Total Syntheses of Norcrassin A and Berbamine & Development of Dual Brønsted/Lewis Acid Catalysis for Site-Selective Friedel–Crafts Alkylation of Phenols

by

Viviene Kim Nguyen

Doctor of Philosophy, Graduate Program in Chemistry  
University of California, Riverside, December 2023  
Dr. Kevin Kou, Chairperson

Norcrassin A is a C<sub>16</sub> tetranorditerpenoid characterized by a unique 5/5/5/6 tetracyclic framework – a structural feature not previously reported in natural products. Further evaluation of norcrassin A also showed its exciting promise as an anti-Alzheimer’s disease (AD) compound. Given its novel molecular structure and reported biological profile, a concise and convergent synthesis to this structurally and functionally important molecule was envisioned from cost-effective starting materials through straightforward chemical transformations. The salient features of the developed route include a multi-gram, eight-step synthesis of an advanced bicyclic lactone intermediate and a one-pot aldol/aldol/lactonization sequence to gain rapid entry to the tetracyclic skeleton.

Berbamine is a cyclic bisbenzylisoquinoline alkaloid (bisBIA) with a well-documented history of usage in clinical practice for treating inflammation, cancer, and autoimmune diseases. Despite its exciting biology, only limited hit-to-lead optimizations are possible due to the lack of functional group handles for derivatizations and the absence of a total synthesis for modifications in the core scaffold. While current access relies on isolation from natural sources, commercial samples acquired by us and our collaborator Dr. Wendong Huang at City of Hope National Medical Center between 2018–2021 revealed compromised authenticities by NMR analysis. Hence, a practical synthesis would provide indisputable access to berbamine and its diverse analogs. An array of scalable, multi-step synthetic strategies were designed and progressed en route to berbamine. The intention is to explore opportunities for derivatization, substrate- versus catalyst-controlled hydrogenation, as well as atropisomerism of the hindered diaryl ether linkage.

The Friedel–Crafts alkylation provides an intuitive bond disconnection for C(sp<sup>2</sup>)–C(sp<sup>3</sup>) bond retrosynthesis. Prior investigations in the Kou laboratory reported conditions for setting quaternary carbon centers in site-selective Friedel–Crafts reactions using unactivated tertiary alcohols and catalytic combinations of FeX<sub>3</sub>/HX. Encouraged by this previous work, a new combination of catalytic ZnCl<sub>2</sub> and catalytic camphorsulfonic acid (CSA) led to the first site-selective Friedel–Crafts alkylation of phenols with unactivated secondary alcohols, affording the desired products in up to 85% yield. This dual catalytic system favored *ortho*-selectivity in the absence of steric

influence while starting from minimally prefunctionalized reaction precursors, serving as a departure from conventional transition-metal-catalyzed cross-coupling methods.

## Acknowledgements

Thank you to my advisor, Professor Kevin Kou, for the opportunity to explore the field of synthetic chemistry and its breadth of applications. There was never a dull moment, especially given the challenges that came with pursuing total synthesis. His steadfast support and patience knew no bounds and I am incredibly grateful for the guidance he provided throughout my tenure at the University of California, Riverside. The technical knowledge and skills he so graciously bestowed upon me has shaped the researcher that I am today, allowing me to persevere in the face of adversity. It fills me with sorrow to be parting ways with the group. Yet, there is a feeling of pride knowing that I will leave a better chemist than I ever thought I could be. It is that for which I am deeply thankful for.

I would also like to acknowledge the other members of my dissertation committee, Professors Christopher Switzer and Catharine Larsen, for serving in this capacity and who were critical for the completion of this work. I must acknowledge the tireless UCR ACIF staff spectroscopists for their assistance in operating the analytical instrumentation. To Barbara Outzen-Hill and Christina Youhas for coordinating all exam dates and ensuring that administrative paperwork is completed by the requisite deadlines. I am also appreciative of Professor Michael Pirrung for his welcoming presence during my brief period in his group.

The past and current members of the Kou lab have provided such a supportive and enriching environment over the course of my graduate career. It was an absolute pleasure being in the company of these wonderful individuals who were a consistent source of

advice and inspiration. I owe a deep gratitude to Aaron Pan not only for his key involvement in the work presented herein, but also as a trusted confidante who so selflessly supported me over the years. A genuine comrade in arms. To Andy Trinh for being a familiar source of comfort in the midst of all of the uncertainty. Of all places, it was unbelievable that we had crossed paths again here. A warm thank you to Roni Manasi for offering a memorable and surprisingly profound friendship. To Dr. Taylor Alexander who had kept my seat warm and gave me much needed assurance. I would like to acknowledge Manuel Larach and Berkley Lujan for their dedication and contributions toward the respective total syntheses. To the undergraduates I mentored. It was a privilege. Lastly, to my family for their unconditional love and being the champions of my success. The ambitions I have would not have been possible without their encouragement.

## Table of Contents

ABSTRACT OF THE DISSERTATION .....	iv
Acknowledgements.....	vii
List of Tables .....	xiv
List of Figures .....	xv
List of Schemes.....	xvi
<b>1 Chapter One: Synthetic Efforts Toward Norcrassin A.....</b>	<b>1</b>
1.1 Introduction.....	1
1.1.1 Classification of Terpenes and Diterpenes .....	1
1.1.2 Biosynthetic Roots of Diterpenes .....	5
1.1.3 Biological Activity of Diterpenes .....	8
1.1.4 Synthetic Strategies Toward Diterpenes.....	13
1.1.4.1 ent-Halimic Acid Precursor .....	13
1.1.4.2 Polyene Cyclizations.....	16
1.1.4.2.1 Lewis Acid-Mediated Cyclizations.....	17
1.1.4.2.2 Halogen Electrophile Triggered Polyene Cyclizations.....	19
1.1.4.2.3 Transition-Metal Induced Polyene Cyclizations.....	22

1.1.4.2.4	Radical Polyene Cyclizations .....	25
1.2	Norcrassin A .....	27
1.2.1	Isolation and Structure .....	27
1.2.2	Biological Activity .....	29
1.2.3	Biosynthetic Pathway of Norcrassin A .....	29
1.3	Results and Discussion .....	30
1.3.1	Retrosynthetic Analysis of Norcrassin A.....	31
1.3.2	Synthesis of Keto Diester <b>124</b> .....	32
1.3.3	Construction of Epoxycyclohexanone <b>128</b> .....	33
1.3.4	First Generation Attempts to Lactone <b>127</b> .....	38
1.3.5	Second Generation Strategies to Lactone <b>127</b> .....	41
1.3.6	Third Generation Attempts at Lactone <b>127</b> .....	45
1.3.7	Aldol/Aldol/Lactonization Studies .....	48
1.3.8	Additional Optimization Studies.....	53
1.3.8.1	Conversion of Enol Side Product to Lactone.....	53
1.3.8.2	1,3-Transpositions of Allyl Alcohols.....	54
1.3.8.3	Enantioselective Strategy .....	55
1.4	Conclusion .....	56

1.5	Experimental Section .....	59
1.5.1	General Experimental .....	59
1.5.2	Experimental Procedures .....	61
1.6	References.....	81
1.7	Selected NMR Spectra .....	94
<b>2</b>	<b>Chapter Two: Synthetic Efforts Toward Berbamine .....</b>	<b>114</b>
2.1	Introduction.....	114
2.1.1	Classification of Bisbenzylisoquinoline Alkaloids (BisBIAs) .....	114
2.1.2	Biosynthesis .....	115
2.1.3	Biological Activity .....	117
2.1.3.1	Tetrandrine .....	119
2.1.3.2	Berbamine .....	121
2.1.3.3	Neferine and Dauricine .....	122
2.1.4	Total Syntheses of bisBIAs.....	124
2.1.4.1	Synthesis of Coclaurine and its Derivatives .....	124
2.1.4.2	Synthesis of Acyclic bisBIAs .....	126
2.1.4.3	Synthesis of Cyclic bisBIAs .....	134
2.2	Berbamine .....	138

2.3	Retrosynthetic Analysis of Berbamine .....	140
2.4	Results and Discussion .....	141
2.4.1	Synthesis of Amine Fragment.....	141
2.4.2	Synthesis of Phenylacetic Acid <b>268</b> .....	145
2.4.3	Clockwise Approach.....	149
2.4.4	Counterclockwise Approach.....	151
2.4.5	Diaryl Ether Studies.....	153
2.5	Conclusions.....	155
2.6	Experimental Section .....	158
2.6.1	General Experimental .....	158
2.6.2	Experimental Procedures .....	160
2.7	References.....	180
2.8	Selected NMR Spectra.....	192
<b>3</b>	<b>Chapter Three: Dual Brønsted/Lewis Acid Catalysis for Site-Selective</b>	
	<b>Friedel–Crafts Alkylation of Phenols .....</b>	<b>212</b>
3.1	Introduction.....	212
3.1.1	Friedel–Crafts Alkylation.....	212
3.2	Results and Discussion .....	214

3.2.1	Optimization Studies.....	215
3.2.2	Reaction Scope.....	217
3.2.3	Probing the Site-Selectivity .....	221
3.2.4	Mechanism of the Reaction .....	223
3.3	Conclusion .....	226
3.4	Experimental Section .....	227
3.4.1	General Experimental .....	227
3.4.2	Experimental Procedures .....	229
3.5	References.....	250
3.6	Selected NMR Spectra .....	253

## List of Tables

<b>Table 1.</b> Diastereoselective reduction of enone <b>138</b> .....	36
<b>Table 2.</b> Ketene silyl acetal-mediated cis-epoxide ring-opening methods.....	39
<b>Table 3.</b> Optimization of Ullmann coupling between 5-bromovanillin ( <b>245</b> ) and methyl vanillate ( <b>246</b> ) .....	154
<b>Table 4.</b> Survey of conditions for direct Friedel–Crafts alkylation of phenolic <b>309</b> with alcohol <b>310</b> .....	216

## List of Figures

<b>Figure 1.</b> Structures of common terpenes as well as isoprene ( <b>5</b> ).....	1
<b>Figure 2.</b> Structures of phytol ( <b>6</b> ) and tagetones A ( <b>7</b> ) and B ( <b>8</b> ) .....	3
<b>Figure 3.</b> Example diterpene skeletal types .....	4
<b>Figure 4.</b> Representative diterpenoids with promising bioactivity .....	10
<b>Figure 5.</b> Structure of ent-halimic acid ( <b>42</b> ) and structurally related natural products ....	13
<b>Figure 6.</b> Norcrassin A ( <b>112</b> ) and other related diterpenoids.....	28
<b>Figure 7.</b> Selected bioactive bisBIAs.....	118
<b>Figure 8.</b> Exploring scope of Friedel–Crafts alkylations with unactivated secondary alcohols. Conditions: phenolic <b>306</b> (0.2 mmol), alcohol <b>307</b> (0.6 mmol), ZnCl <sub>2</sub> (0.01 mmol), (R)-CSA (0.15 mmol), PhCl (0.2 mL, 1 M), 140 °C, 18 h. <sup>a</sup> With 5 equiv alcohol <b>307</b> . <sup>b</sup> With phenolic <b>306</b> (1 mmol), alcohol <b>307</b> (1.1 mmol), ZnCl <sub>2</sub> (0.05 mmol), (R)-CSA (0.75 mmol), PhCl 1 mL, 1 M), 140 °C, 18 h. <sup>c</sup> With 2 equiv alcohol <b>307</b> . <sup>d</sup> With 1.1 equiv alcohol <b>307</b> . <sup>e</sup> With 1 mol% ZnCl <sub>2</sub> . .....	218
<b>Figure 9.</b> Examples of para- and dialkyl-substituted phenols. Conditions: phenolic <b>306</b> (0.2 mmol), alcohol <b>307</b> (0.6 mmol), ZnCl <sub>2</sub> (0.01 mmol), (R)-CSA (0.15 mmol), PhCl (0.2 mL, 1 M), 140 °C, 18 h. <sup>a</sup> With 2 equiv alcohol <b>307</b> . <sup>b</sup> With 1.1 equiv alcohol <b>307</b> . <sup>c</sup> With 1 mol% ZnCl <sub>2</sub> . .....	219
<b>Figure 10.</b> Plots of initial rates .....	224

## List of Schemes

<b>Scheme 1.</b> Biosynthesis of GGPP ( <b>9</b> ) from DMAPP ( <b>12</b> ) and IPP ( <b>13</b> ) .....	5
<b>Scheme 2.</b> Mevalonate pathway via MVA ( <b>17</b> ) .....	6
<b>Scheme 3.</b> Mevalonate-independent pathway via MEP/DOXP .....	7
<b>Scheme 4.</b> Mechanisms of action for type I and type II diterpene synthases.....	8
<b>Scheme 5.</b> Synthesis of chettaphanins I ( <b>43</b> ) and II ( <b>44</b> ).....	15
<b>Scheme 6.</b> Enantioselective Lewis acid/Brønsted acid cyclization of polyprenoids.....	17
<b>Scheme 7.</b> Enantioselective polyene cyclization of homo(polyprenyl)arenes).....	18
<b>Scheme 8.</b> New artificial cyclase for enantioselective total synthesis of <b>67</b> and <b>69</b> .....	18
<b>Scheme 9.</b> Synthesis of chiral tetracycle using SbCl <sub>5</sub> and BINOL-derived complex .....	19
<b>Scheme 10.</b> Enantioselective halocyclization with nucleophilic phosphoramidites .....	20
<b>Scheme 11.</b> Catalytic asymmetric bromocyclization of geranylbenzenes and geranylphenols .....	21
<b>Scheme 12.</b> Haliranium-mediated cyclizations using morpholine and HFIP.....	22
<b>Scheme 13.</b> Enantioselective oxidative [Pt <sup>2+</sup> ]-catalyzed polycyclization .....	22
<b>Scheme 14.</b> Platinum-catalyzed formation of polycycles .....	23
<b>Scheme 15.</b> Cationic gold(I) polyene cyclizations .....	23
<b>Scheme 16.</b> Total synthesis of <b>99</b> via iridium-catalyzed polyene cyclization.....	24
<b>Scheme 17.</b> Iridium-induced polycyclization in the synthesis of <b>102</b> and <b>103</b> .....	25
<b>Scheme 18.</b> Radical asymmetric polyene cyclization via organo-SOMO catalysis.....	26
<b>Scheme 19.</b> Construction of <b>111</b> via HAT-based cyclization .....	27
<b>Scheme 20.</b> Possible biosynthetic route to norcrassin A ( <b>112</b> ) .....	30

<b>Scheme 21.</b> Retrosynthesis of norcrassin A ( <b>112</b> ).....	32
<b>Scheme 22.</b> Synthesis of orthoester <b>131</b> and allylic alcohol <b>134</b> .....	33
<b>Scheme 23.</b> Completed synthesis of 2-oxoglutarate <b>136</b> .....	33
<b>Scheme 24.</b> Proposed epoxide ring opening approach.....	34
<b>Scheme 25.</b> Synthesis of epoxycyclohexanones <b>128</b> .....	35
<b>Scheme 26.</b> Other methods of diastereoselective epoxidation of enone <b>138</b> .....	37
<b>Scheme 27.</b> Formation of enol, or 2-hydroxy-3,4-dimethyl-2-cyclohexenone <b>149</b> .....	40
<b>Scheme 28.</b> Mukaiyama–Michael addition and Rubottom oxidation strategy to lactone	42
<b>Scheme 29.</b> Use of softer nucleophiles en route to lactone <b>127</b> .....	43
<b>Scheme 30.</b> One-pot ZnCl <sub>2</sub> -mediated Reformatsky reaction toward lactone <b>127</b> .....	44
<b>Scheme 31.</b> Stepwise Reformatsky reaction toward lactone.....	44
<b>Scheme 32.</b> Revised retrosynthesis of lactone ( <b>127</b> ).....	46
<b>Scheme 33.</b> Synthesis of lactone <b>127</b> via Eschenmoser–Claisen rearrangement and Kornblum oxidation .....	47
<b>Scheme 34.</b> Completion of lactone <b>127</b> .....	48
<b>Scheme 35.</b> Deuterium incorporation into lactone .....	48
<b>Scheme 36.</b> Anticipated strategy of base-mediated aldol/aldol/lactonization.....	49
<b>Scheme 37.</b> Possible retro-aldol reaction pathways .....	50
<b>Scheme 38.</b> Formation of O-methylated lactone .....	51
<b>Scheme 39.</b> Proposed silyl acetal variation of aldol/aldol/lactonization .....	51
<b>Scheme 40.</b> Synthesis of silyl acetal derivative of keto-diester .....	53
<b>Scheme 41.</b> Attempts to convert enol <b>149</b> to lactone <b>127</b> .....	54

<b>Scheme 42.</b> Rhenium-catalyzed 1,3-transposition .....	54
<b>Scheme 43.</b> Vanadium- and enzyme-mediated 1,3-transposition .....	55
<b>Scheme 44.</b> Kinetic resolution of 2-methylcyclohexanone ( <b>176</b> ) .....	56
<b>Scheme 45.</b> Developed production of lactone <b>127</b> .....	57
<b>Scheme 46.</b> Formation of norcrassin A ( <b>112</b> ) .....	58
<b>Scheme 47.</b> Coclaurine ( <b>179</b> and <b>180</b> ) and/or reticuline ( <b>181</b> ) are the biosynthetic building blocks of the majority of bisBIAs.....	114
<b>Scheme 48.</b> Current understanding of the bisBIA biosynthetic pathway.....	116
<b>Scheme 49.</b> Total synthesis of ( $\pm$ )-coclaurine ( <b>179</b> ) .....	124
<b>Scheme 50.</b> Hiemstra's strategy to access ten benzyltetrahydroisoquinolines ( <b>201</b> ).....	125
<b>Scheme 51.</b> Total synthesis of ( $\pm$ )-dauricine ( <b>191</b> , no yields reported) .....	127
<b>Scheme 52.</b> Total synthesis of (+)-O-methylthalibrine ( <b>213</b> ). .....	129
<b>Scheme 53.</b> Electrochemical methods to synthesize a) ( $\pm$ )-dauricine ( <b>191</b> ) and b) (+)-O-methylthalibrine ( <b>213</b> ) .....	131
<b>Scheme 54.</b> Huang and Lumb's synthesis of (S,S)-tetramethylmagnolamine ( <b>229</b> ). .....	133
<b>Scheme 55.</b> Opatz's synthesis of ( $\pm$ )-curine ( <b>188</b> ) and ( $\pm$ )-tubocurine ( <b>238</b> ) and formal total synthesis of ( $\pm$ )-tubocurarine ( <b>239</b> ) .....	135
<b>Scheme 56.</b> Bracher's modular total synthesis of ( $\pm$ )-tetrandrine ( <b>186</b> ) and isotetrandrine ( <b>241</b> ). Conditions for Ullmann couplings: CuBr•SMe <sub>2</sub> , Cs <sub>2</sub> CO <sub>3</sub> , pyridine, 110 °C; Pictet–Spengler reactions: TFA, CH <sub>2</sub> Cl <sub>2</sub> .....	137
<b>Scheme 57.</b> Retrosynthesis of berbamine ( <b>187</b> ).....	140
<b>Scheme 58.</b> Synthesis of aryethylamine <b>252</b> .....	142

<b>Scheme 59.</b> Synthetic route employing N-Boc-protected amine (254).....	143
<b>Scheme 60.</b> Synthetic route employing N-tosyl-protected amine (256) .....	144
<b>Scheme 61.</b> Synthesis of N-nosyl-protected bis(arylethyl)amine (263).....	145
<b>Scheme 62.</b> Attempted synthesis of phenylacetic acid (268).....	146
<b>Scheme 63.</b> Proposed completion of berbamine (187) via macrolactam (243) and double Bischler–Napieralski reaction strategy .....	148
<b>Scheme 64.</b> Retrosynthesis of 187 incorporating clockwise synthetic strategy .....	149
<b>Scheme 65.</b> Synthesis of O-protected phenylacetic acid analogs.....	150
<b>Scheme 66.</b> Synthesis of berbamine (187) through anticipated clockwise approach.....	151
<b>Scheme 67.</b> Counterclockwise strategy starting from free arylethylamine 252 .....	152
<b>Scheme 68.</b> Synthesis of iodophenylacetic acid 287.....	153
<b>Scheme 69.</b> Synthesis of 5-iodovanillin (290) .....	155
<b>Scheme 70.</b> Current synthesis toward diethylamine fragment 259 .....	156
<b>Scheme 71.</b> Potential remaining synthetic steps to berbamine (187).....	157
<b>Scheme 72.</b> Iovel's Fe-catalyzed arylation of benzyl alcohols and benzyl carboxylates	212
<b>Scheme 73.</b> Friedel–Crafts reactions via direct substitution of unactivated alcohols ....	213
<b>Scheme 74.</b> Developed Brønsted/Lewis acid-catalyzed Friedel–Crafts alkylations.....	214
<b>Scheme 75.</b> Application to late-stage derivatizations.....	221
<b>Scheme 76.</b> Mechanistic studies.....	222
<b>Scheme 77.</b> Proposed mechanism .....	226

# 1 Chapter One: Synthetic Efforts Toward Norcrassin A

## 1.1 Introduction

### 1.1.1 Classification of Terpenes and Diterpenes

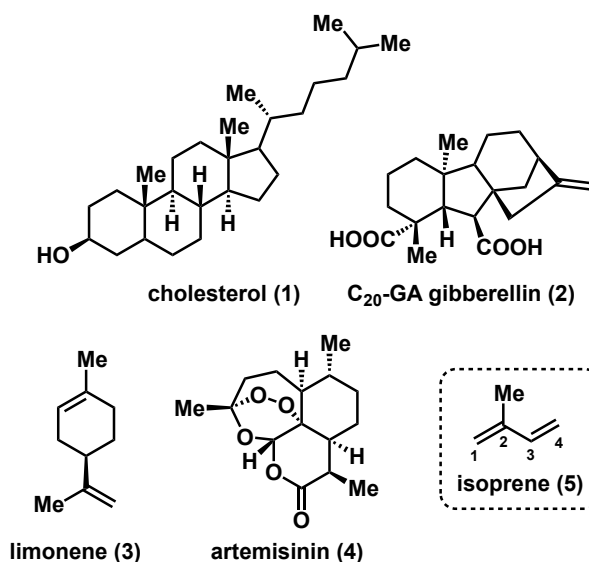


**Figure 1.** Structures of common terpenes as well as isoprene (5)

Terpenes comprise the largest and most structurally diverse class of natural products.<sup>1</sup> Currently numbering in the tens of thousands, this vast chemical library accounts for nearly one-third of all compounds currently characterized in the Dictionary of Natural Products.<sup>2</sup> Isolated from marine and terrestrial organisms, including fungi, plants, marine sponges, and bacteria, these substances are some of the most well documented natural products and display an assortment of structural and functional roles.<sup>3-5</sup> For example, steroids such as cholesterol (1) are fundamental for lipid membrane structure and cell signaling, gibberellins (2) are crucial in plant developmental processes, limonene (3) is a monoterpene that plays a role in the fragrance of citrus rinds, while

artemisinin (**4**) and its semisynthetic derivatives are used to treat parasitic worm and malarial infections (Figure 1).<sup>6,7</sup>

The high variety of the described effects is a reflection of the significant and intriguing molecular diversity of these natural products. Yet, belying the structural complexity of the terpenome are rather modest biosynthetic origins: head-to-tail or tail-to-head coupling reactions of a five-carbon unit called isoprene, or 2-methyl-butadiene ( $C_5H_8$ , **5**, Figure 1).<sup>8,9</sup> All terpenes are constructed from at least isoprene precursors, and the number of carbon atoms in their backbone determines its classification as hemi-, mono-, sesqui-, di-, sester-, tri-, sesquar-, and tetraterpenes.<sup>8</sup> Monoterpenes, such as pinene and myrcene, are hydrocarbons with the chemical formula  $C_{10}H_{16}$ . Hemiterpenes ( $C_5H_8$ ) contain half the number of carbons of a monoterpene, or only a single isoprene unit. Sesquiterpenes ( $C_{15}H_{24}$ ) possess three isoprene units while diterpenes ( $C_{20}H_{32}$ ) consist of four. Sester-, tri-, sesquar-, and tetraterpenes encompass twenty-five, thirty, thirty-five, and forty-carbon atoms, respectively. Based on these arrangements, a sizable number of underlying acyclic (linear) and cyclic sub-classes exist. Discrete structural types, including cembrane and amphilectane skeletons, as well as unusual isothiocyanate, nicotinoyl, halogenated, and methylbutanoyl functionalities broadly occur in these secondary metabolites.<sup>10</sup> Such functional modifications of the original hydrocarbon framework via substitution, oxidation, or skeletal rearrangements are coined terpenoids or isoprenoids, which are used interchangeably with the term terpenes in the scientific literature.

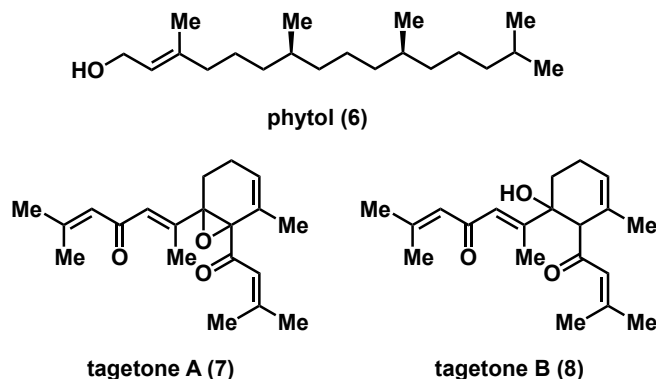


**Figure 2.** Structures of phytol (6) and tagetones A (7) and B (8)

Within the terpenome, diterpenes and diterpenoids, represent a group of over twenty-thousand natural compounds. Diterpenes are categorized in accordance with their biogenesis, resulting in approximately one-hundred thirty unique carbon scaffolds that are further discriminated by the number of rings and cyclization patterns present in their chemical structures.<sup>11</sup> Among the least distributed in nature are linear and monocyclic skeletal types. Representative examples include the acyclic diterpene phytol (6), a constituent of chlorophyll A and vitamin K<sub>1</sub>, and monocyclic diterpenoids tagetones A (7) and B (8) from the flowers of *Tagetes minuta* (Figure 2). The most abundant are polycyclic diterpenes, classified as bicyclic (halimane, labdane, and clerodane), tricyclic (rosane, pimarane, cassane, chinane, vouacapane, abietane, and podocarpane), tetracyclic (gibberellane, scopadulane, kaurene, trachylobane, stemarane, atisane, stemodane, aphidicolane, and beyerene), and macrocyclic (jatrophane, daphnane, tigliane, cembrane, taxane, and ingenane) (Figure 3).<sup>12</sup>

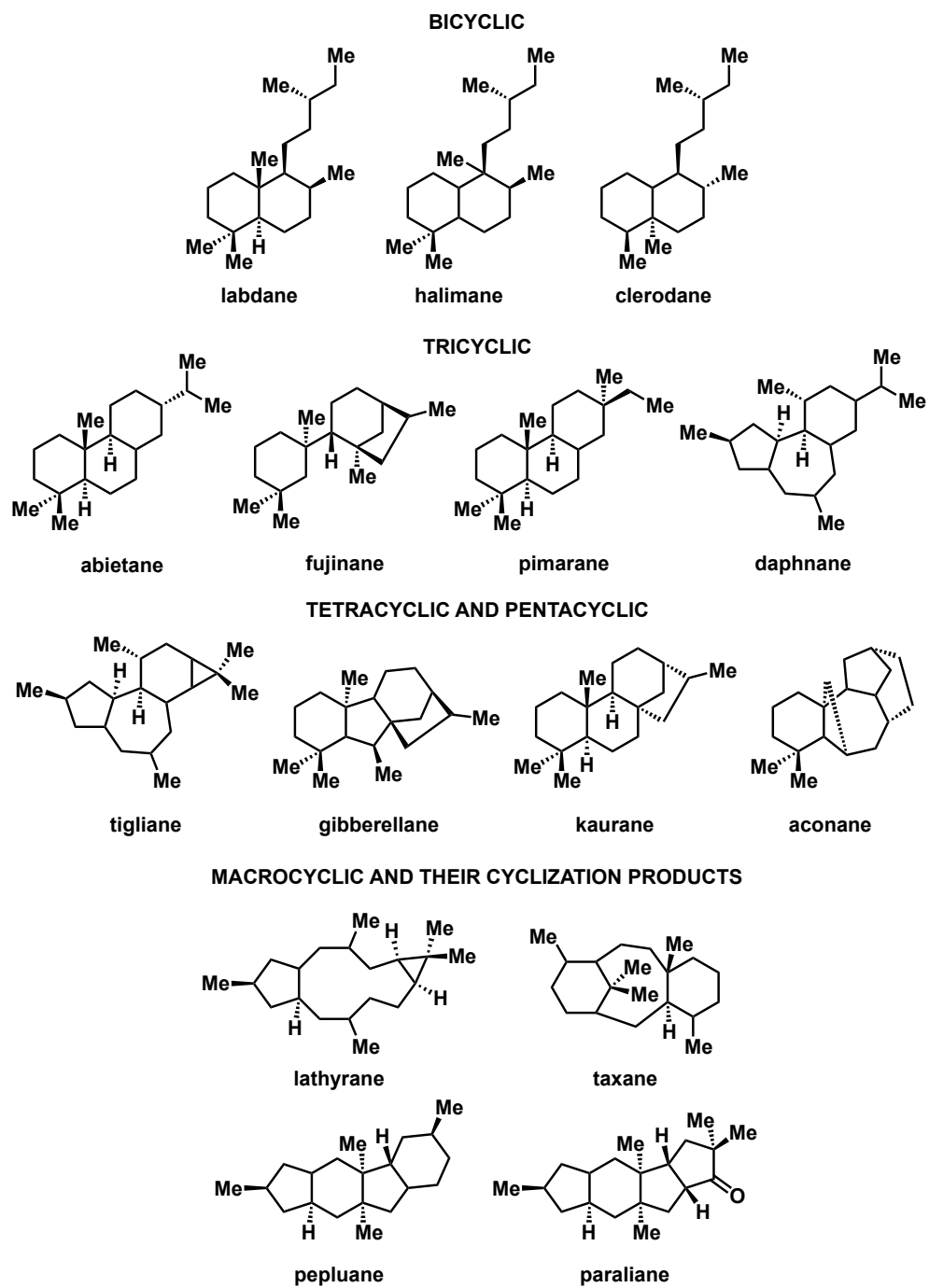
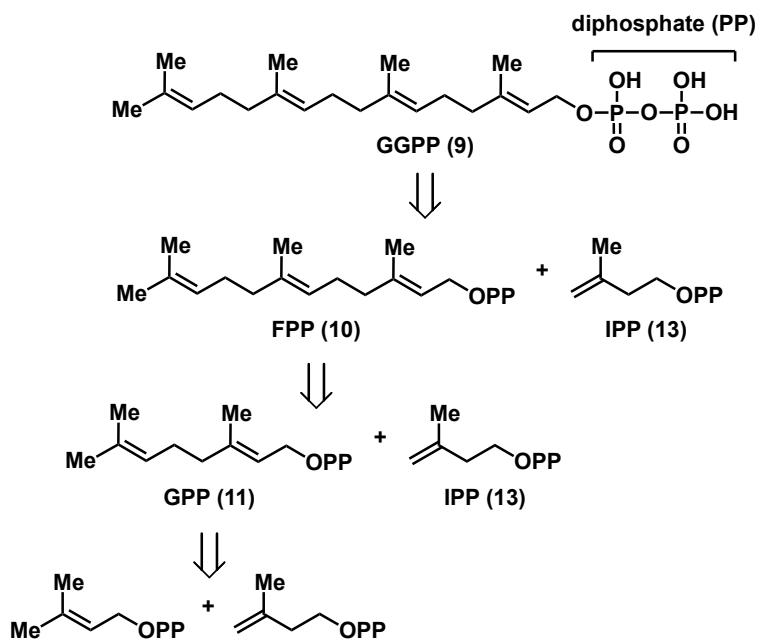


**Figure 3.** Example diterpene skeletal types

### 1.1.2 Biosynthetic Roots of Diterpenes

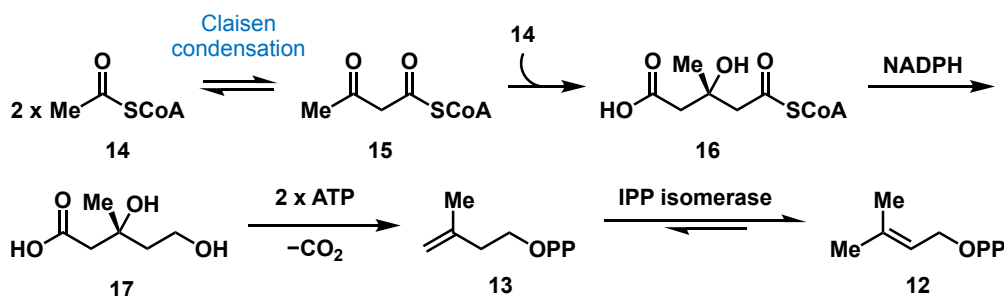
Originating from a single precursor molecule called geranylgeranyl diphosphate (GGPP, **9**), diterpenes are composed of four isoprene units: one dimethylallyl diphosphate (DMAPP, **12**) starter and three isopentenyl diphosphate (IPP, **13**) elongation units (Scheme 1).<sup>13</sup>



**Scheme 1.** Biosynthesis of GGPP (**9**) from DMAPP (**12**) and IPP (**13**)

These biochemically active pyrophosphate ester building blocks are the products of two distinct biosynthetic routes: the mevalonate, or mevalonic acid (MVA), pathway and the mevalonate-independent pathway via methylerythritol phosphate/deoxyxylulose phosphate (MEP/DOXP).<sup>14,15</sup> The former, the first discovered, has been established in fungi, bacteria, mammals, and in the cytosol of plants, proceeding with acetyl-coenzyme A (**14**, acetyl-CoA) as the sole carbon feedstock derived from carbohydrate and fatty acid catabolism (Scheme 2).<sup>16</sup> The initial thiolase-catalyzed step of the mevalonate pathway

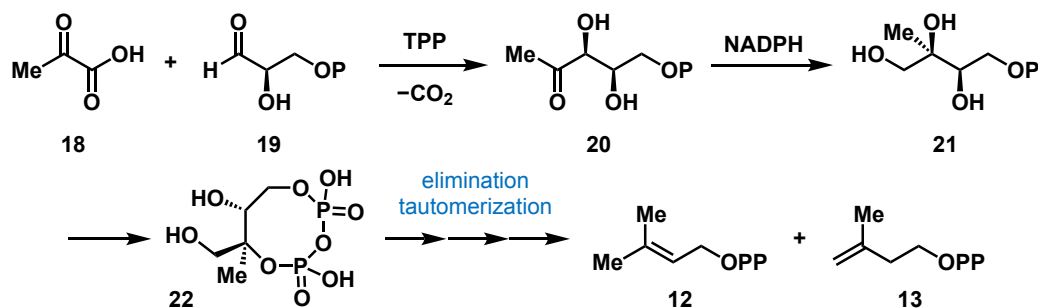
combines two acetyl-CoA molecules via a Claisen condensation to yield acetoacetyl-CoA (**15**). Following an aldol-type reaction with a third molecule of acetyl-CoA to form  $\beta$ -hydroxy- $\beta$ -methylglutaryl-coenzyme A (HMG-CoA, **16**), an irreversible reduction affords (R)-mevalonic acid (**17**).<sup>17</sup> Successive phosphorylation and decarboxylation of MVA provides a pool of IPP (**13**), which can be isomerized to DMAPP (**12**) by IPP isomerase.<sup>18</sup>



**Scheme 2.** Mevalonate pathway via MVA (**17**)

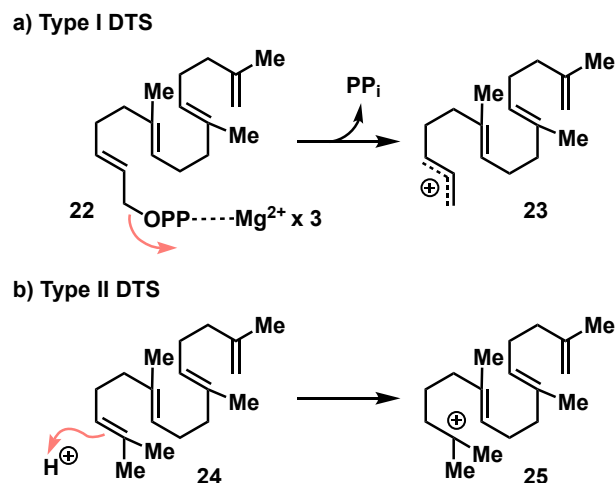
The mevalonate-independent pathway is initiated by the condensation of pyruvate (**18**) and glyceraldehyde-3-phosphate (**19**) to generate DOXP (**20**, Scheme 3).<sup>18,19</sup> Rearrangement and reduction of DOXP (**20**) to MEP (**21**) via a reductoisomerase prompts a series of substitution and phosphorylation events to produce cyclic intermediate 2-C-methyl-D-erythritol-2,4-cyclodiphosphate (MEcPP, **22**).<sup>18,19</sup> DMAPP (**12**) and IPP (**13**) are then synthesized in the final steps of the non-mevalonate route through independent elimination and tautomerization pathways catalyzed by 4-hydroxy-3-methylbut-2-enyl diphosphate (HMB-PP) reductase.<sup>18,19</sup> Ensuing head (isopropylidene) to tail (alcohol) or vice versa linkage of DMAPP and IPP yields C<sub>10</sub> geranyl pyrophosphate (GPP, **10**), which can undergo condensation with additional IPP molecules to afford C<sub>15</sub> farnesyl

diphosphate (FPP, **11**) and eventually, the linear and achiral C<sub>20</sub> geranylgeranyl diphosphate (**9**) with methyl branches along its unsaturated chain (Scheme 1).<sup>17</sup> These isoprenoid diphosphates can cyclize via intricate carbocation-initiated rearrangement, elimination, and cyclization cascades to provide a myriad of products containing multiple stereocenters and mono- and polycyclic carbon skeletons.<sup>20,21</sup>



**Scheme 3.** Mevalonate-independent pathway via MEP/DOXP

The enzymes that facilitate such hallmark reactions through a combination of controlled carbocation quenching, substrate preference and folding, and transient carbocation stabilization are termed diterpene synthases (DTSs), or diterpene cyclases (DTCs).<sup>22</sup> Depending on how they generate the initial catalysis-triggering carbocation, DTSs are further divided into two main classes.<sup>23</sup> In type I DTSs, a trinuclear Mg<sup>2+</sup> cluster favors ionization of a diphosphate moiety, leaving behind an allylic carbocation (**23**, Scheme 4a).<sup>24</sup> Type II DTSs form a tertiary carbocation (**25**) by protonation of an epoxide or alkene functional group, often exercising a central aspartic acid as the catalytic Brønsted acid (Scheme 4b).<sup>22,23,25</sup>



**Scheme 4.** Mechanisms of action for type I and type II diterpene synthases

After the carbocation is generated, both type I and type II DTSs facilitate similar chemical transformations, such as hydride shifts, cation- $\pi$  cyclizations, and a variety of alkyl shifts, ring expansions, and ring contractions to induce extraordinary changes in stereochemistry, bonding, and hybridization of the substrate carbon atoms.<sup>22,23</sup>

Alternatively, irregular cyclopropanation, branching, or cyclobutane reactions can afford non-canonical carbon frameworks, contributing to the stereochemical and structural diversity of diterpenes and diterpenoids.<sup>26</sup>

### 1.1.3 Biological Activity of Diterpenes

Isolated from diverse sponge, insect, plant, fungal, and marine species, formulations containing diterpenes and diterpenoids have been traditionally used in different parts of the world as treatments for various diseases and infections. *Croton tonkinensis*, a medicinal herb with the ent-kaurane diterpenoid ent-18-acetoxy-7 $\beta$ -hydroxy kaur-15-oxo-16-ene (CrT1, **41**) as the major constituent, is widely utilized in traditional Vietnamese medicine to treat gastric and duodenal ulcers, malaria, abscess,

and impetigo (Figure 4).<sup>27</sup> The extract and oils sourced from *Plectranthus madagascariensis* contain abietane diterpenes that have been used in South African communities to treat respiratory and dermatological ailments, such as coughs, bronchitis, asthma, and cutaneous wounds.<sup>28</sup> Shrubs from the *Vitex* genus contain an abundance of natural labdane-type diterpenoids and have a long history of use throughout Japan, Southeast Asia, and the Pacific Islands as treatments for reproductive disorders, inflammatory diseases, and gastrointestinal conditions.<sup>27,29</sup> Many daphnane, tigliane, and lathyrane diterpenoids from the genus *Daphne* have also been exploited for their cholesterol-lowering effects as well as anti-inflammatory and analgesic characteristics.<sup>30</sup>

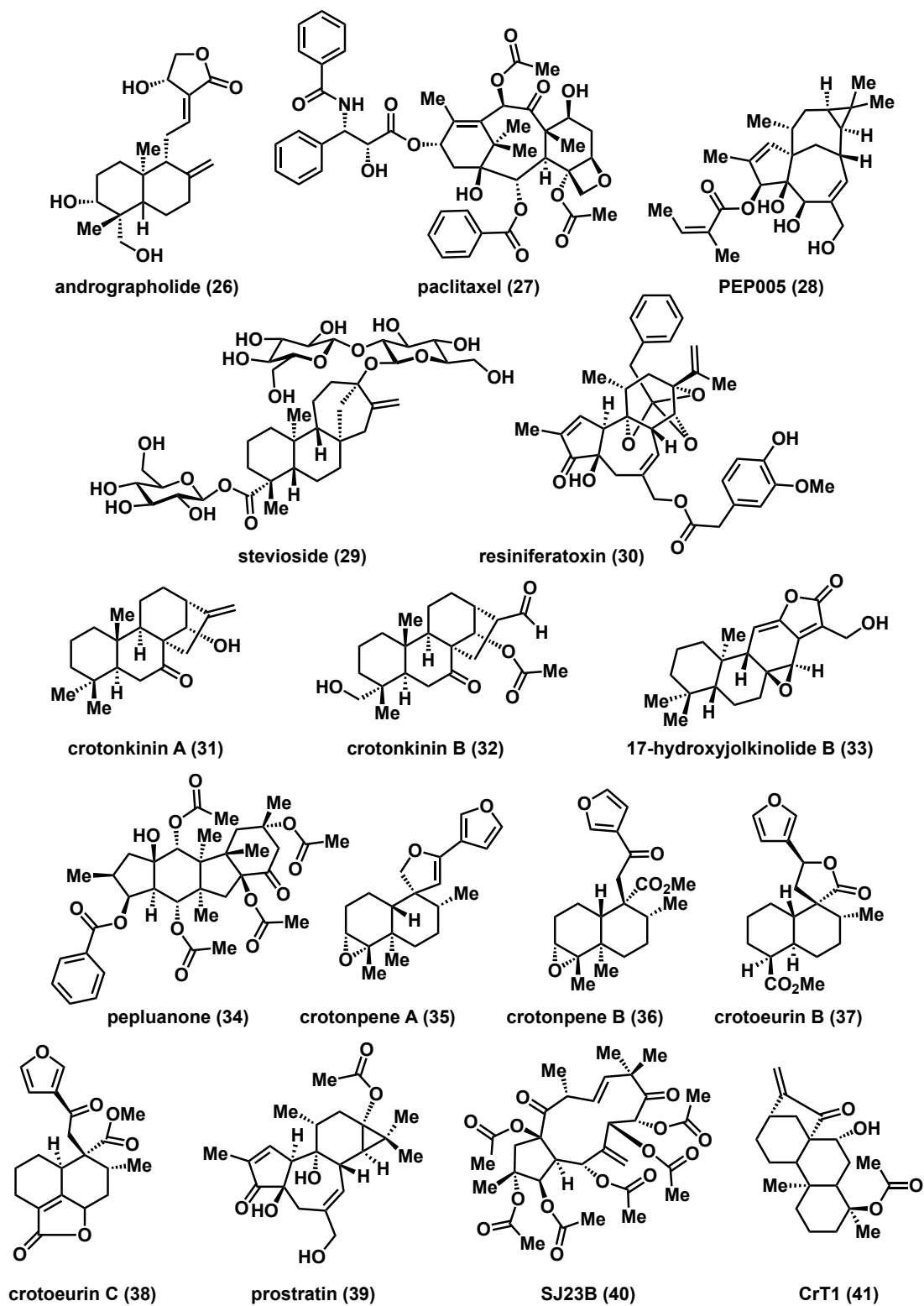


**Figure 4.** Representative diterpenoids with promising bioactivity

As such, these compounds have become the focus of natural product drug discovery and are continuously being investigated for their therapeutic potential. A number of existing herbal medicines and conventional drugs, such as andrographolide (**26**) and paclitaxel (**27**), are diterpenoids with potent pharmacological activities and unique structural skeletons (Figure 4).<sup>12</sup> Within the past decade, the hydrophobic diterpene ester ingenol 3-angelate (PEP005, **28**) attracted considerable interest as a treatment for actinic keratosis, a precancerous lesion that can progress to invasive squamous cell carcinoma.<sup>31</sup> Approved by the Food and Drug Administration (FDA) in 2012, PEP005 is an agonist of classical and novel protein kinase C (PKC) isoenzymes, which can slow cell proliferation, trigger cell cycle arrest, and promote apoptosis in several malignant cell lines.<sup>32</sup> Other promising diterpenes under clinical investigation include ginkgo diterpene lactone meglumine (GDLM), a formulation of mainly ginkgolides and bilobalide, as a neuroprotective treatment of ischemic stroke.<sup>33</sup> The kaurene glycoside stevioside (**29**) is used as non-toxic zero calorie sweetener and has been shown to modulate diabetes-induced complications while retaining a minute effect on blood glucose levels.<sup>34</sup> Resiniferatoxin (RTX, **30**), a capsaicin analogue of the daphnane subtype, is an ultrapotent transient receptor potential vanilloid 1 (TRPV1) calcium channel agonist currently under clinical evaluation as an analgesic for advanced forms of cancer and osteoarthritis.<sup>35–37</sup>

The immunomodulatory, neurite outgrowth-promoting, and antiviral properties of diterpene- and diterpenoid-rich species have also been examined.<sup>38,39</sup> Kuo *et al.* identified two novel kaurane diterpenoids, crotonkinins A (**31**) and B (**32**), evaluating their anti-

inflammatory potentials on nitric oxide (NO) and NADPH-oxidase (NOX)-dependent reactive oxygen species (ROS) production in microglial cells (Figure 4).<sup>40</sup> 17-Hydroxyjolkinolide B (**33**) was found to be a strong inhibitor of the lipopolysaccharide-induced production of pro-inflammatory mediators and cytokines, such as interleukin 6 (IL-6) and tumor necrosis factor alpha (TNF- $\alpha$ ).<sup>41</sup> Comparably, the diterpene component of *Euphorbia peplus*, pepluanone (**34**), possessed a noteworthy in vivo anti-inflammatory effect in carrageenin-induced rat paw edema.<sup>42</sup>

Sun *et al.* reported that nerve growth factor (NGF)-mediated neurite outgrowth was enhanced by clerodane diterpenoids crotonpenes A (**35**) and B (**36**) in PC12 cells at 15  $\mu$ M (Figure 4).<sup>43</sup> At a concentration of 10  $\mu$ M, crotoeurins B (**37**) and C (**38**) presented similar neurite outgrowth-stimulating activity on NGF-mediated PC12 cells.<sup>44</sup> Prostratin (**39**), a phorbol ester first isolated from Strathmore weed *Pimelea prostrate*, was shown to activate latent viral reservoirs of HIV-1 (human immunodeficiency virus 1) via activation of PKC-dependent nuclear factor- $\kappa$ B (NF- $\kappa$ B), protecting healthy CD4<sup>+</sup> cells from further HIV-1 infection.<sup>45</sup> The anti-viral influence of a series of formerly isolated jatrophone diterpenes were moreover probed by Bedoya *et al.*<sup>46,47</sup> One of the molecules, SJ23B (**40**), wielded a potent antagonistic effect on HIV-1 latency and infection. Through the downregulation of HIV receptors such as CCR5, CXCR4, and CD4, this non-tumorigenic diterpene prevented viral infection in human primary T cells with an IC<sub>50</sub> value of 2 nM. Moreover, SJ23B induced viral reactivation, behaving as an in vivo agent to purge dormant HIV-1 proviruses with a much higher efficacy than that of prostratin (**39**).

## 1.1.4 Synthetic Strategies Toward Diterpenes

### 1.1.4.1 *ent*-Halimic Acid Precursor

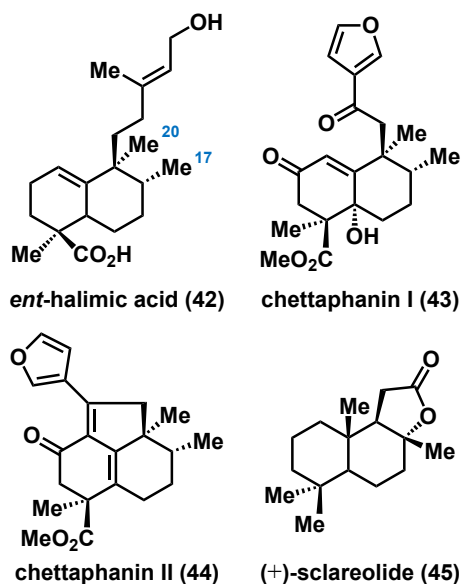
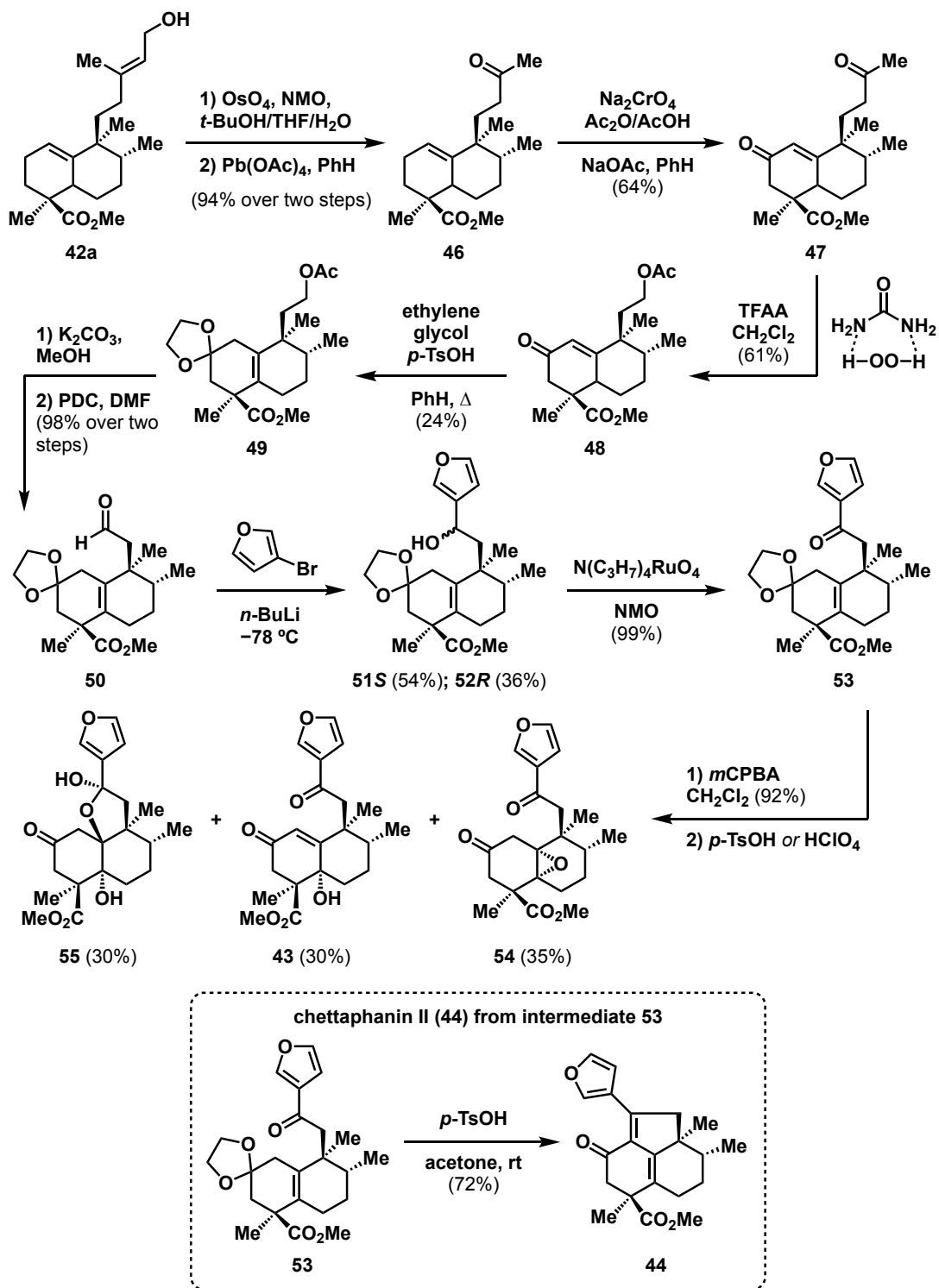


**Figure 5.** Structure of *ent*-halimic acid (42) and structurally related natural products

*ent*-Halimic acid (42) is the primary component of *Halimium viscosum* and can be easily isolated (Figure 5).<sup>11</sup> This compound is a bicyclic diterpene with an *ent*-halimane skeleton, the structure of which makes it a versatile molecule and appropriate starting material for the synthesis of several bioactive and other interesting compounds.<sup>11</sup>

The *ent* classification of compound 42 is largely determined by the arrangement of methyls Me-17 and Me-20 (Figure 5).<sup>11</sup> Halimane derivatives in which Me-17 and Me-20 exhibit a *cis* relationship are designated as normal or *ent*-halimanes. Conversely, halimanes with an 8-*epi*- or 8-*epi-ent* configuration feature a *trans* orientation between Me-17 and Me-20. *ent*-Halimic acid (42) was used in the synthesis of furanoditerpenoids chettaphanin I (43) and II (44), and in that of *ent*-halimanolides and anti-tumoral

sesterterpenolide analogues of dysidiolide (Scheme 5).<sup>48</sup> The synthesis of **43** and **44** commenced with oxidation of the methyl ester of *ent*-halimic acid with OsO<sub>4</sub> and lead(IV) acetate to give ketone **46**. An ensuing Na<sub>2</sub>CrO<sub>4</sub> oxidation provided  $\alpha,\beta$ -unsaturated ketone **47**, which was subjected to Bayer–Villiger reaction using urea hydrogen peroxide and trifluoroacetic acid anhydride (TFAA) to generate **48** in 61% yield, eliminating the remaining two carbons of the side chain. Following protection of the carbonyl as a dioxolane (**49**), saponification with K<sub>2</sub>CO<sub>3</sub> in MeOH and oxidation of the resultant alcohol gave aldehyde **50**. Introduction of the furan ring fragment was accomplished by means of a furyl-lithium species generated from 3-bromofuran and *n*-BuLi, furnishing hydroxyderivatives **51** and **52**. Treatment of **51** and **52** with tetrapropylammonium perruthenate (TPAP) and *N*-methylmorpholine *N*-oxide (NMO) gave ketone **53**, which was reacted with *m*CPBA and *p*-TsOH to yield chettaphanin I (**43**) as mixture with **54** and **55**. Chettaphanin II (**44**) was assembled in 71% yield via reaction of intermediate **53** with *p*-TsOH (Scheme 5). *ent*-Halimic acid (**42**) was also applied by Marcos and co-workers in the construction of propellanes and a series of tetranor diterpenes from (+)-sclareolide (**45**).<sup>49–51</sup>



**Scheme 5.** Synthesis of chettaphanins I (**43**) and II (**44**)

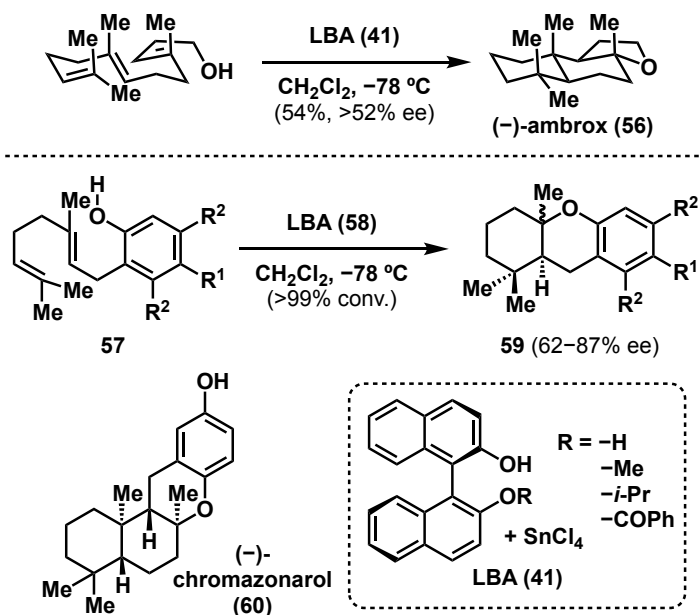
Though the chemical functionality of *ent*-halimic acid (**42**) has proven useful in the synthesis of tetranor compounds, such approaches are heavily reliant on the need for *ent*-halimic acid which is routinely extracted from considerable amounts of *Halimium viscosum* (0.34% with respect to the dry plant weight).<sup>11,52</sup> In this manner, syntheses that commence from this starting material may result in a broad reduction of the plant species. It should also be noted that of the known synthetic routes using *ent*-halimic acid or other known natural products, several were fairly inefficient and displayed only a modest level of scalability.<sup>53,54</sup>

#### 1.1.4.2 Polyene Cyclizations

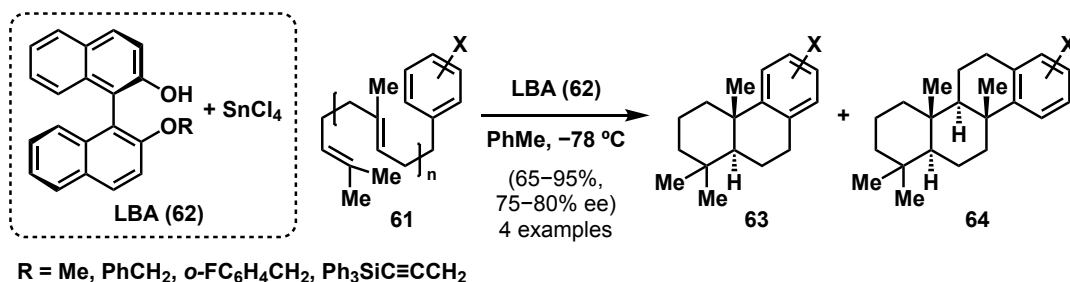
The carbon skeleton common to diterpenes and their derivatives is assembled biosynthetically from GGPP through a polyolefin cyclization pathway enabled by class II DTCs.<sup>23</sup> Followed by a series of downstream biosynthetic modifications that lead to the introduction of additional functionality, it is estimated that a substantial number of polycyclic diterpenoids arise from this preliminary cyclization. Pioneered by van Tamelen, Johnson, and Goldsmith, a number of asymmetric biomimetic polyene cyclizations have been identified in the literature,<sup>55-58</sup> many of which induced the cation-olefin polycyclization through organocatalysis or treatment with a variety of Lewis and protic acids. However, successful applications of these nonenzymatic processes in natural product synthesis are scarce, with only a handful of reports spanning the past two decades. Classic and/or recent successful examples are described below.

#### 1.1.4.2.1 Lewis Acid-Mediated Cyclizations

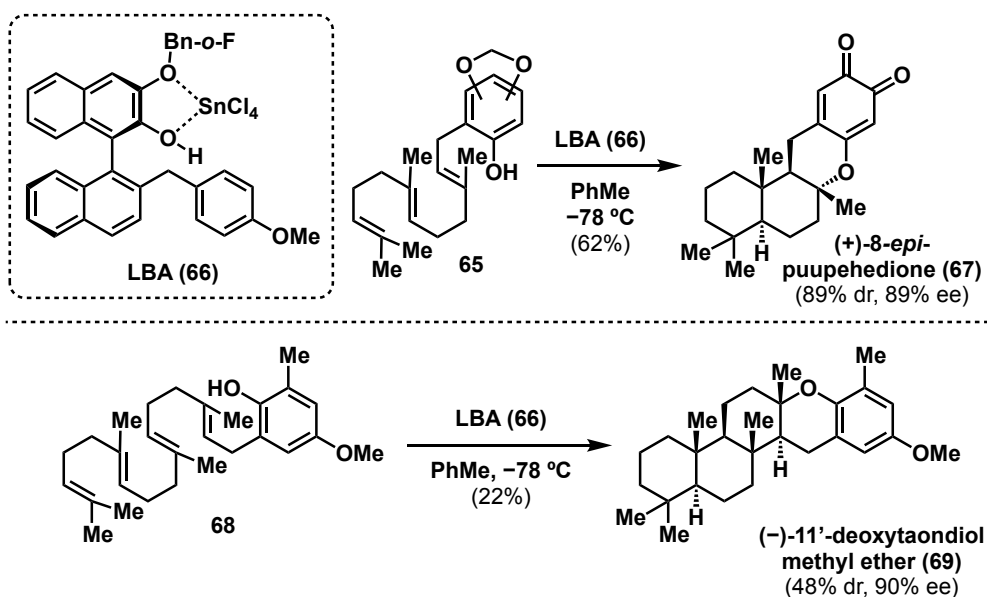
Ishihara *et al.* described a combined Lewis acid and chiral Brønsted acid (LBA) system that enabled the first enantioselective biomimetic cyclization of 2-polyprenylphenols (Scheme 6).<sup>59</sup> Prepared from SnCl<sub>4</sub> and the monobenzoylester of (*R*)-(+)-1,1'-binaphthalene-2,2'-diol (BINOL), these artificial farnesyl and geranyl cyclases (**58**) were implicated in the asymmetric preparation of (–)-ambrox (**56**), a commercial substitute for ambergris, via cyclization of homofarnesol. Several tricyclic compounds (**59**) and (–)-chromazonarol (**60**), a constituent of the Pacific seaweed *Dictyopteris undulata*, were also constructed from the corresponding geranyl and farnesyl substrates to evaluate the generality of the LBA-promoted strategy, although with modest yields and stereoselectivity.



**Scheme 6.** Enantioselective Lewis acid/Brønsted acid cyclization of polyprenoids



**Scheme 7.** Enantioselective polyene cyclization of homo(polyprenyl)arenes)

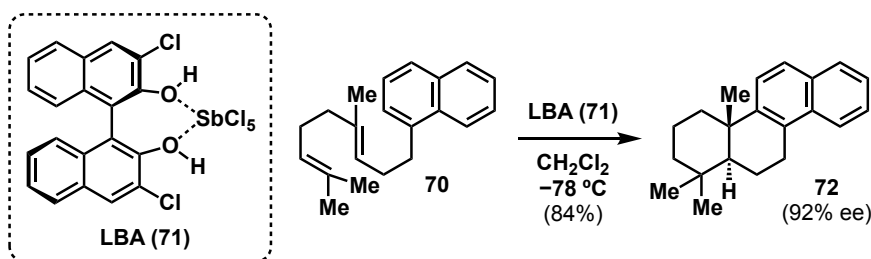


**Scheme 8.** New artificial cyclase for enantioselective total synthesis of **67** and **69**

Two years later, Ishihara *et al.* outlined an application of this approach in the biomimetic cyclization of homo(polyprenyl)arenes (**61**) possessing a less-nucleophilic aryl terminator, supplying access to representative (+)-podcarpa-8,11,13-triene diterpenoids (**63**) and (–)-tetracyclic polyprenoids (**64**, Scheme 7).<sup>60</sup> Not long after, a new artificial cyclase (**66**) that incorporated a chiral catechol-derived Brønsted acid into the established SnCl<sub>4</sub> system was introduced by the same group to yield several polycyclic

terpenoids bearing a chroman scaffold, such as (+)-8-epi-puupehedione (**67**) and (-)-11'-deoxytaondiol methyl ether (**69**, Scheme 8).<sup>61</sup>

An analogous report by Surendra and Corey delivered a range of chiral polycyclic molecules from achiral polyene precursors (Scheme 9).<sup>62</sup> The polycyclization was initiated by a one-to-one complex of SbCl<sub>5</sub> and o,o'-dichloro-BINOL (**71**), delivering excellent enantioselectivity of up to 92% enantiomeric excess (ee) and ~90% yield per ring formed. Serving as an extension of their prior indium(III) bromide or iodide-mediated approach, the *Lewis* acid functioned as a proton equivalent, initiating the cation–olefin cyclization via selective activation of the terminal C–C double bond of the polyene to control the absolute configuration of the product.<sup>63</sup>

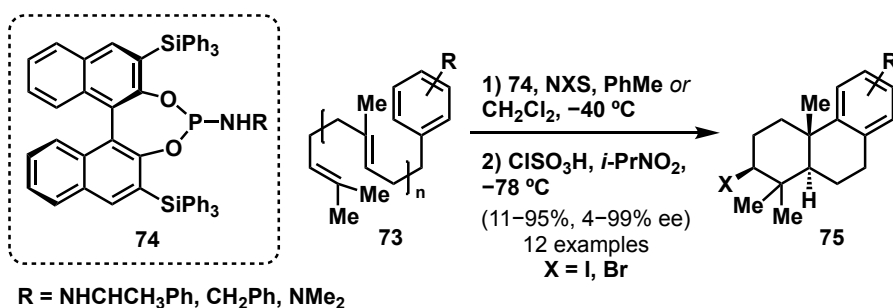


**Scheme 9.** Synthesis of chiral tetracycle using SbCl<sub>5</sub> and BINOL-derived complex

#### 1.1.4.2.2 Halogen Electrophile Triggered Polyene Cyclizations

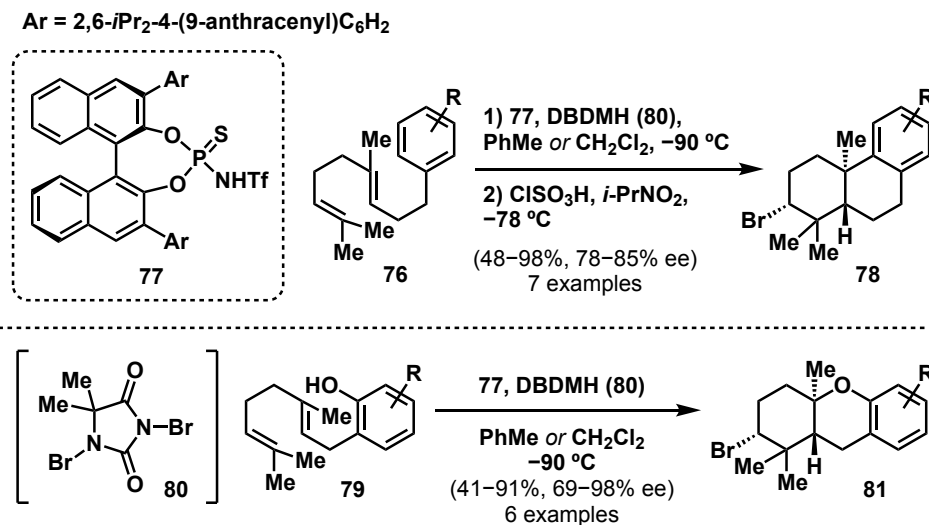
Sakakura and co-workers employed stoichiometric amounts of chiral phosphoramidites with *N*-halosuccinimide (NXS) to achieve the enantioselective halocyclization of simple polycyclic terpenoids (Scheme 10).<sup>64</sup> The nucleophilic phosphoramidite (**74**), designed with two triphenylsilyl groups at the 3 and 3' positions, provided access to polycyclic 3-haloterpenoids (**75**) more easily than conventional multistep syntheses. By placing the activated halogen atom of the *N*-halosuccinimide

closer to the chiral environment of the nucleophilic promoter, this reaction yielded the requisite products in up to 99% diastereomeric and enantiomeric excesses, serving as a direct contrast to the *Lewis* acid approach.



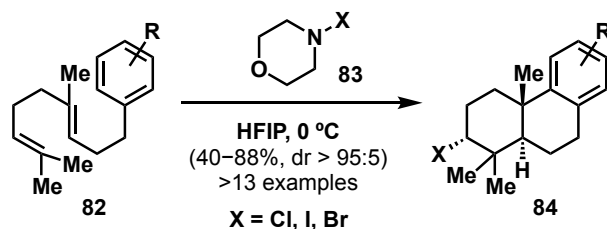
**Scheme 10.** Enantioselective halocyclization with nucleophilic phosphoramidites

The first catalytic enantioselective bromonium-induced polyene cyclization was reported by Samanta and Yamamoto (Scheme 11).<sup>65</sup> This process was catalyzed by a chiral BINOL-derived thiophosphoramidate (**77**) and used 1,3-dibromo-5,5-dimethylhydantoin (DBDMH, **80**) as the electrophilic bromine source. Bromocyclization of homogeranylbenzenes (**76**) afforded a mixture of completely cyclized and partially cyclized products. Treatment of the crude reaction mixture with chlorosulfonic acid promoted the full cyclization of the partially cyclized material to furnish bromides **78**. Under the same conditions, geranylphenols (**79**) delivered the fully bromocyclized products (**81**) as single diastereomers with high yields and enantioselectivities.



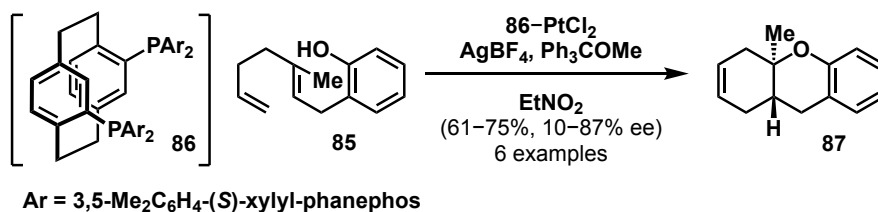
**Scheme 11.** Catalytic asymmetric bromocyclization of geranylbenzenes and geranylphenols

In 2018, Arnold *et al.* discovered that an electrophilic halogen source in the presence of morpholine and hexafluoroisopropanol (HFIP) mediated the halocyclization of polyenes (Scheme 12).<sup>66</sup> Reaction of the morpholine Lewis base and either 1,3-dichloro-5,5-dimethylhydantoin (DCDMH) or a *N*-halosuccinimide generated the halogenating agent *N*-halomorpholine **83**, which successfully converted homogeranyl benzene **82** into fully cyclized halides **84**. HFIP was essential for its strongly hydrogen-bond donating, highly polar, and Lewis acidic, yet weakly nucleophilic qualities. It not only activated the *N*-halomorpholine (**83**) for halogenation to occur, but also facilitated the cyclization by prearranging the aryl diene via hydrophobic interactions.



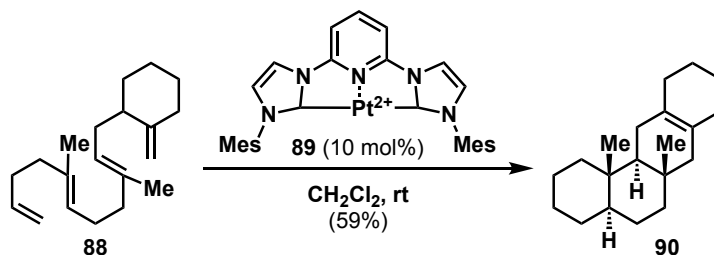
**Scheme 12.** Haliranium-mediated cyclizations using morpholine and HFIP

#### 1.1.4.2.3 Transition-Metal Induced Polyene Cyclizations



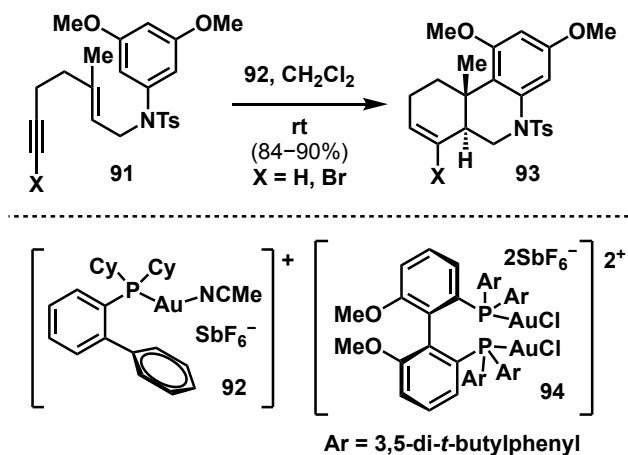
**Scheme 13.** Enantioselective oxidative  $[\text{Pt}^{2+}]_2$ -catalyzed polycyclization

An oxidative method catalyzed by  $[(\text{xylyl-phanephos})\text{PtCl}_2]$  (**86**) and  $\text{AgBF}_4$  was shown to regioselectively, diastereoselectively, and enantioselectively enable the polycyclization of polyene-ols (**87**, Scheme 13).<sup>67</sup> In 2014, a new platinum(II) complex (**89**) containing a tridentate N-heterocyclic carbene (NHC) pincer ligand was developed for the synthesis of sterol-like polycyclic compounds (**90**, Scheme 14).<sup>68</sup> Initiated by selective coordination of electrophilic platinum(II) to the least substituted olefin and subsequent protodemetalation to regenerate the metal catalyst, a variety of polyene substrates (**88**) were diastereoselectively converted to their corresponding di-, tri-, and tetracyclic counterparts.

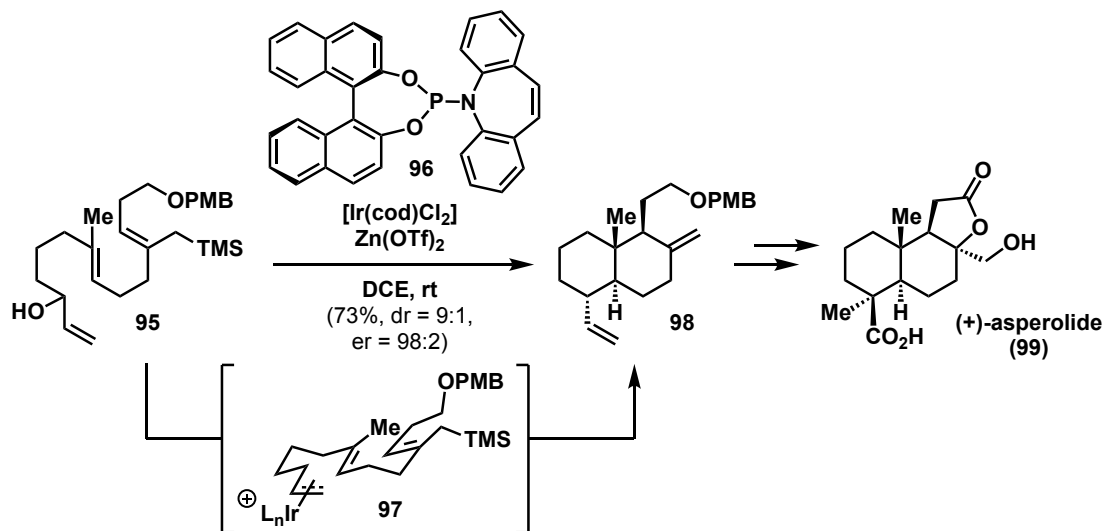


**Scheme 14.** Platinum-catalyzed formation of polycycles

Rong and Echavarren explored the extension of a cationic gold(I) complex (**92**) to polyene cyclizations, leading to the synthesis of steroid-like molecules under mild conditions with minimal catalyst loadings (1–3 mol%) (Scheme 15).<sup>69</sup> The reaction illustrated broad substrate compatibility and high stereoselectivity, encompassing terminal alkynes, 1-bromo-1,5-enynes, and diverse nucleophiles to efficiently construct carbo- and heterocyclic compounds. An enantioselective variant was also surveyed using a dinuclear gold(I) complex of MeO-DTB-BIPHEP (**94**) in the presence of  $\text{AgNTf}_2$ . Despite the excellent yields, only moderate enantioselectivities were observed.

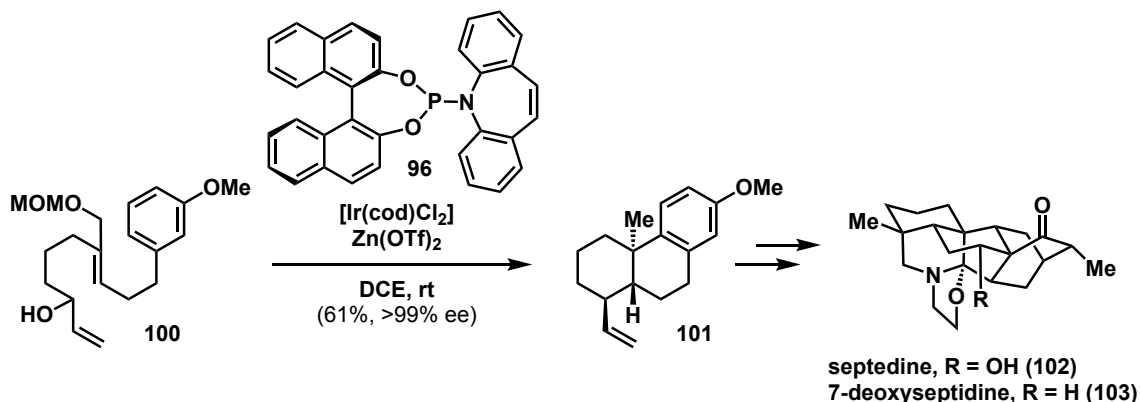


**Scheme 15.** Cationic gold(I) polyene cyclizations



**Scheme 16.** Total synthesis of **99** via iridium-catalyzed polyene cyclization

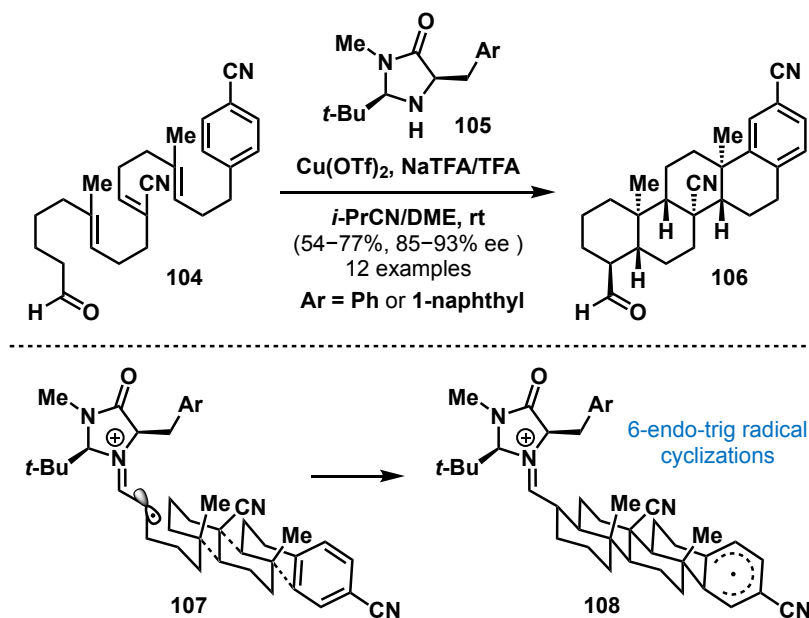
Jeker *et al.* developed a synthetic entry into the labdane-type diterpenoids based on an pivotal iridium-catalyzed polyene cyclization cascade involving an allyl silane as the terminating group (Scheme 16).<sup>70</sup> Showcased in the total synthesis of (+)-asperolide C (**99**), a tetranorlabdane diterpenoid, a  $\pi$ -allyl iridium complex (**97**) generated from a linear allylic alcohol (**95**) underwent a series of stereoselective cyclizations to form the carbobicyclic core (**98**). The synthesis continued with a series of stepwise oxidations and chemo- and diastereoselective alkylations to afford the final product. In the total synthesis of septedine (**102**) and 7-deoxyseptedine (**103**), an analogous polyene cyclization tactic was used to prepare the key abietatriene intermediate (**101**) from allylic alcohol **100** (Scheme 17).<sup>71</sup> Employing  $[\text{Ir}(\text{cod})\text{Cl}]_2$ , a chiral phosphoramidite ligand (**83**), and  $\text{Zn}(\text{OTf})_2$ , the desired transformation was accomplished on decagram scale in 61% yield with an ee exceeding 99%.



**Scheme 17.** Iridium-induced polycyclization in the synthesis of **102** and **103**

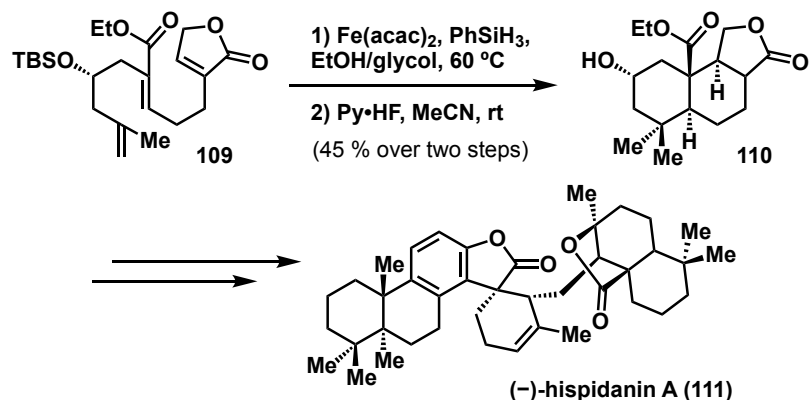
#### 1.1.4.2.4 Radical Polyene Cyclizations

Radical-based polyene cyclizations have received noticeably less consideration. Despite reports of auxiliary- and substrate-based radical cyclizations, asymmetric variants have remained largely elusive. In 2010, Rendler and MacMillan employed a formerly developed singly occupied molecular orbital (SOMO) activation strategy to accomplish the first enantioselective radical polycyclization of polyenals (**104**) under ambient-temperature (Scheme 18).<sup>72</sup> The presented method relied on a selective copper(II)-induced oxidation of chiral enamines formed by condensation with an imidazolidinone catalyst (**105**). To deliver cyclohexadienyl radical **108**, the resultant  $\alpha$ -amino radical intermediate **107** engaged in a series of single-electron 6-endo-trig cyclizations, which was then terminated by a suitable arene. Oxidation to the cyclohexadienyl cation followed by rearomatization and release of the catalyst furnished several bi-, tri-, tetra-, penta-, and hexacyclic aldehydes (**106**) in up to 77% yield and 93% ee.



**Scheme 18.** Radical asymmetric polyene cyclization via organo-SOMO catalysis

The synthetic utility of transition metal-initiated radical cyclizations was demonstrated in the asymmetric total synthesis of (–)-hispidanin A (**111**), a dimeric diterpenoid with promising anti-cancer properties (Scheme 19).<sup>73</sup> Accordingly, from terminal alkene **109**, the use of iron(III) acetylacetonate and triphenylsilane as the hydrogen source delivered the primary tricyclic core (**110**) of (–)-hispidanin A (**111**) via hydrogen atom transfer (HAT) in 45% yield over two steps.



**Scheme 19.** Construction of **111** via HAT-based cyclization

## 1.2 Norcrassin A

### 1.2.1 Isolation and Structure

The genus *Croton*, one of the largest genera in the family Euphorbiaceae, is a complex and diverse taxonomic group of plants. Many species of *Croton* are well documented in different parts of the world as treatments for a wide variety of ailments. Popular uses include treatment of digestive disorders, external wounds, and inflammation, as well as hypertension, dysentery, and malaria.<sup>27,74,75</sup> For example, *Croton tiglium* has been used as a purgative to relieve intestinal inflammation, peptic ulcers, visceral pain, and dyspepsia.<sup>76,77</sup> The mature trees of *Croton lechleri* in South America produce a thick red latex, commonly referred to as sangre de grado (blood of the tree), that contains significant hemostatic properties relevant to wound healing.<sup>78</sup> Ethnomedical uses of the latex include topical treatment of lacerations and abrasions and protection against severe gastrointestinal distress when taken orally in a dilute form.<sup>79</sup> In traditional Thai medicine, *Croton oblongifolius* is applied externally to the hepatic region to ease chronic inflammation and enlargement of the liver.<sup>80</sup> Additionally, a decoction of the

leaves of *Croton zambesicus* is used broadly by indigenous cultures of West Africa as an anti-microbial and anti-hypertensive.<sup>81</sup>

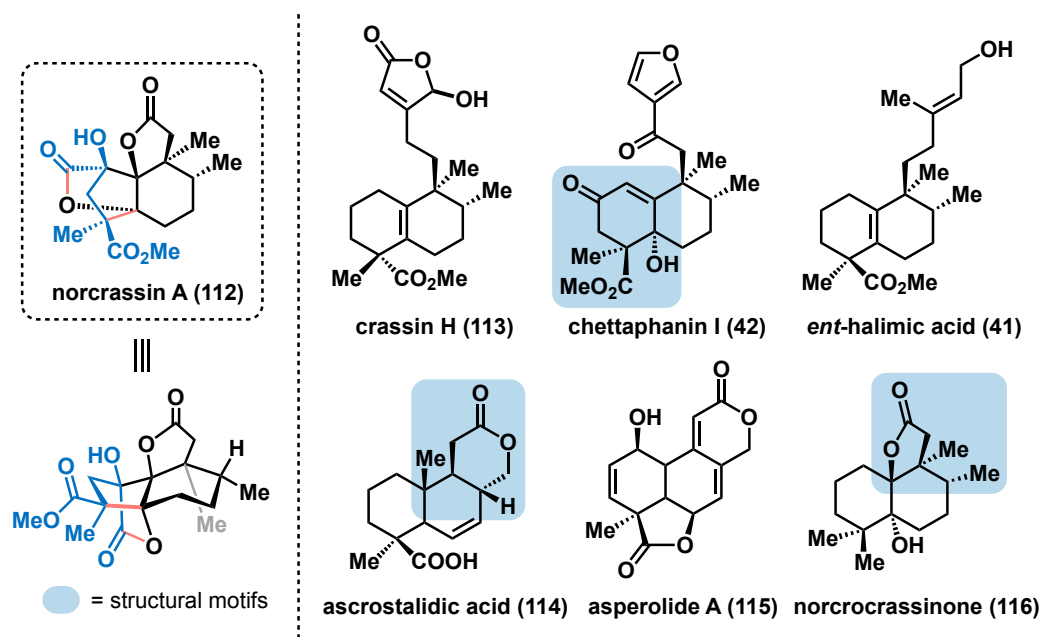


**Figure 6.** Norcrassin A (112) and other related diterpenoids

Phytochemical investigations of *Croton* species have proven their richness in bioactive secondary metabolites, making them especially valuable for pharmacological research studies. With the predominant isolates identified as sesquiterpenes and clerodane- and labdane-type diterpenes, these substances have been reported to show potent biological effects, such as anti-tumor consequences, anti-inflammation, and cytotoxicity.<sup>82–86</sup> Recently, a C<sup>16</sup> tetranorditerpenoid with an unprecedented molecular architecture was isolated from *C. crassifolius* by Zhang and co-workers.<sup>87</sup> Designated as norcrassin A (112), the compound is characterized by an uncommon 5/5/5/6 tetracyclic ring system and six contiguous stereocenters, three of which are quaternary carbon atoms.

The fused cyclic core is particularly noteworthy as it is a structural feature not previously reported in natural products (Figure 6).

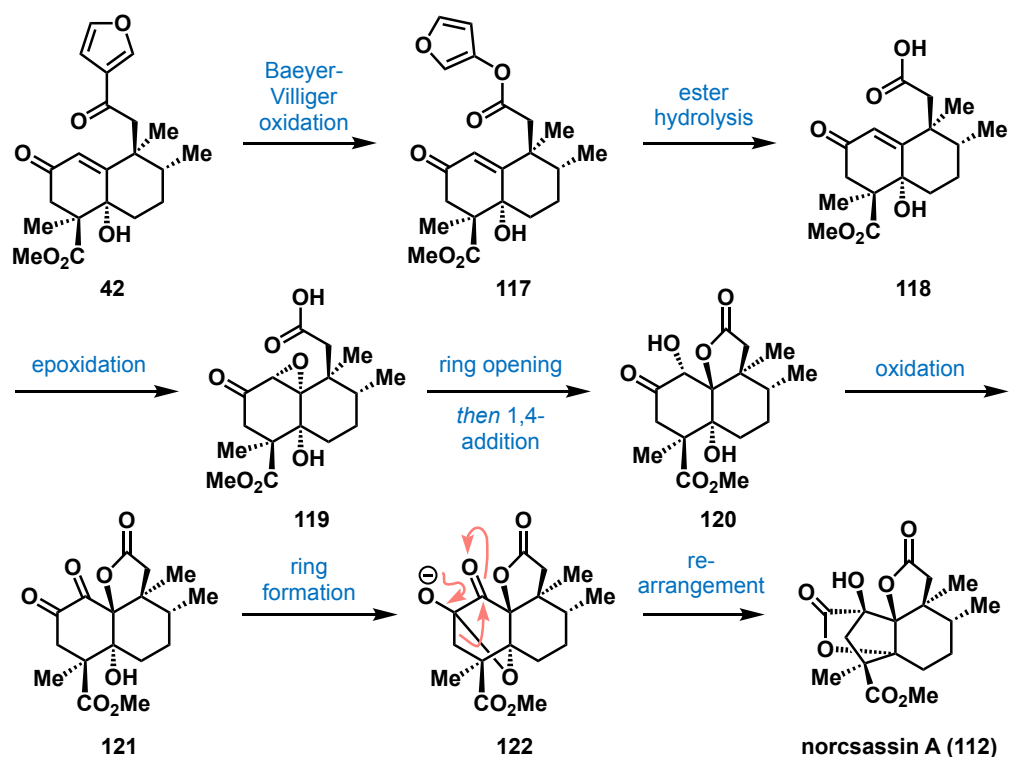
### 1.2.2 Biological Activity

Upon further evaluation using a *Caenorhabditis elegans* Alzheimer's disease (AD) pathological model, norcrassin A (**112**) also showed promise to act as an anti-AD compound candidate (Figure 6).<sup>87</sup> In the isolation study, *C. elegans* was embedded with the human gene of amyloid beta (A $\beta$ ) downstream of the muscle promoter to exhibit AD-like symptoms of paralysis. Norcrassin A was found to significantly delay worm paralysis at a 50  $\mu$ M concentration compared to the negative control with 0.1% DMSO only. However, when compared to memantine, a known N-methyl-D-aspartate (NMDA) receptor antagonist, norcrassin A exerted relatively lower anti-AD activity, only delaying worm paralysis up to forty hours. While not as potent as the established positive control, memantine, norcrassin A revealed its potential as a candidate for further assessment toward combating neurodegenerative disorders.

### 1.2.3 Biosynthetic Pathway of Norcrassin A

While the specific details are not fully understood, the biogenetic pathway for norcrassin A (**112**) may originate from chettaphanin I (**42**) as presented in Scheme 20.<sup>87</sup> Following Baeyer–Villiger oxidation and selective ester hydrolysis to produce carboxylic acid **118**, epoxidation of the  $\Delta^1$  alkene would lead to the formation of epoxy ketone **119**. The ensuing lactone (**120**) would be generated via an epoxide ring opening and intramolecular 1,4-addition reaction. Finally, an oxidative event would provide the

corresponding diketone (**121**), which would undergo a subsequent intramolecular anion assisted rearrangement to yield norcrassin A (**112**).



**Scheme 20.** Possible biosynthetic route to norcrassin A (**112**)

### 1.3 Results and Discussion

Proposed by Zhang *et al.*, norcrassin A (**112**) may be generated from its biosynthetic precursor chettaphanin I (**42**, Figure 6). Yet, the synthesis of ent-halimane **42** would require either a pre-functionalized ent-halimic acid precursor (Section 1.1.4.1) or a rather tenuous acid-induced polycyclization cascade (Section 1.1.4.2). A method capable of resolving the above limitations and constructing **112** using well-established reaction pathways is necessary for a scalable and concise synthesis. This would allow for extended testing, where **122** could be re-subjected to biological screenings for additional

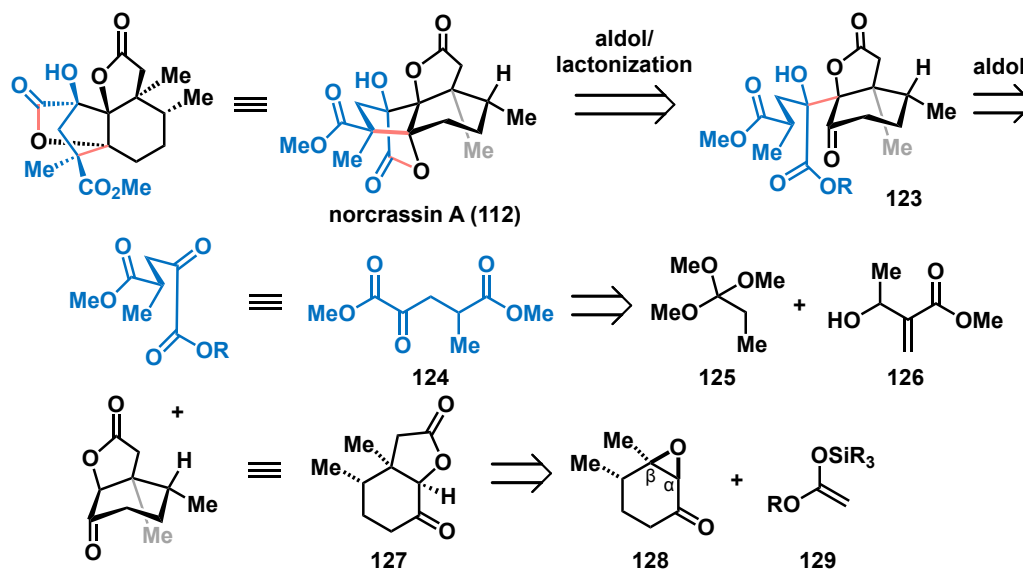
insight into its potential mechanism of amyloid- $\beta$  inhibition. Investigations toward the synthesis of **112** would also form part of an ongoing interest in the synthesis and medicinal chemistry of tetranor, clerodane, and ent-halimane derivatives such as crassin H (**113**) and norcrocrassinone (**116**, Figure 6).<sup>88</sup> In particular, the 2-oxoglutarate (**124**) and fused bicyclic lactone (**127**) thus obtained from the proposed route below would be valuable intermediates in the synthesis of various tetranor diterpenoid derivatives with tetracyclic dilactone scaffolds (Scheme 21).

The presence of six contiguous stereocenters and a rare fused tetracyclic framework render this natural product a veritable challenge in synthetic chemistry. The salient features of this route include a one-pot aldol/aldol/lactonization sequence to gain rapid entry to the tetracyclic framework. This strategy should allow for a short, convergent synthesis to this structurally and functionally important natural product and its analogues from cost-effective starting materials through straightforward chemical transformations. Herein, we describe a prospective total synthesis of this novel compound and summarize the research progress to date.

### 1.3.1 Retrosynthetic Analysis of Norcrassin A

Retrosynthetically, a two-bond disconnection at the bridged [2.2.1] bicyclic lactone moiety of norcrassin A effectively simplifies the tetracyclic natural product to bicyclic intermediate **123** (Scheme 21). In the forward sense, a tandem aldol/lactonization sequence would provide norcrassin A (**112**). Further simplification of **123** can be achieved by disconnecting the hindered C–C bond, which could be forged through an

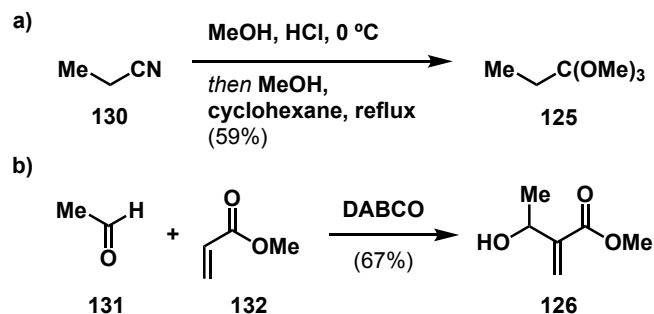
aldol reaction between two relatively simple fragments: literature reported keto diester **124** and fused bicyclic lactone **127**.



**Scheme 21.** Retrosynthesis of norcrassin A (**112**)

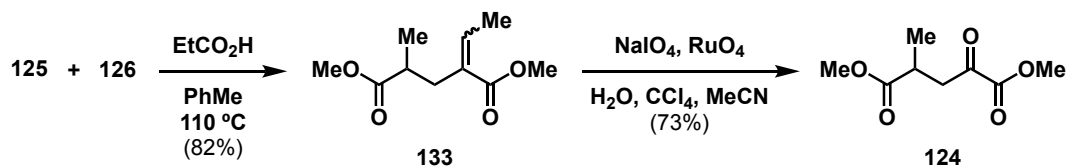
### 1.3.2 Synthesis of Keto Diester **124**

The western fragment, 2-oxoglutarate **124**, to which lactone **127** reacts with, was carried out in our lab by Manuel Larach. Orthoester **125** was readily prepared from the appropriate nitrile precursor (**130**) using the Pinner method (Scheme 22a).<sup>89</sup> A base-catalyzed Baylis–Hillman reaction, the addition of methyl acrylate (**132**) to acetaldehyde (**131**), gave 3-hydroxy-2-methylenealkanoate (**126**, Scheme 22b).<sup>90</sup>



**Scheme 22.** Synthesis of orthoester **131** and allylic alcohol **134**

Johnson–Claisen rearrangement between the corresponding orthoester (**125**) and allylic alcohol (**126**) delivered dimethyl 2-ethylidene-4-alkylglutarate (**133**) in 82% yield (Scheme 23). Oxidative cleavage of the C–C double bond with sodium periodate (NaIO<sub>4</sub>) in the presence of catalytic ruthenium tetroxide (RuO<sub>4</sub>) yielded the desired keto diester (**124**) in 73% yield.

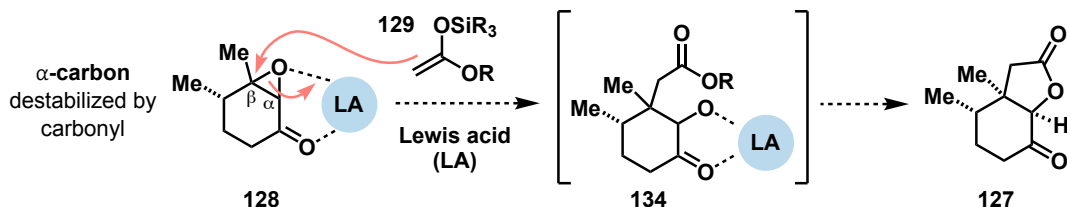


**Scheme 23.** Completed synthesis of 2-oxoglutarate **136**

### 1.3.3 Construction of Epoxycyclohexanone **128**

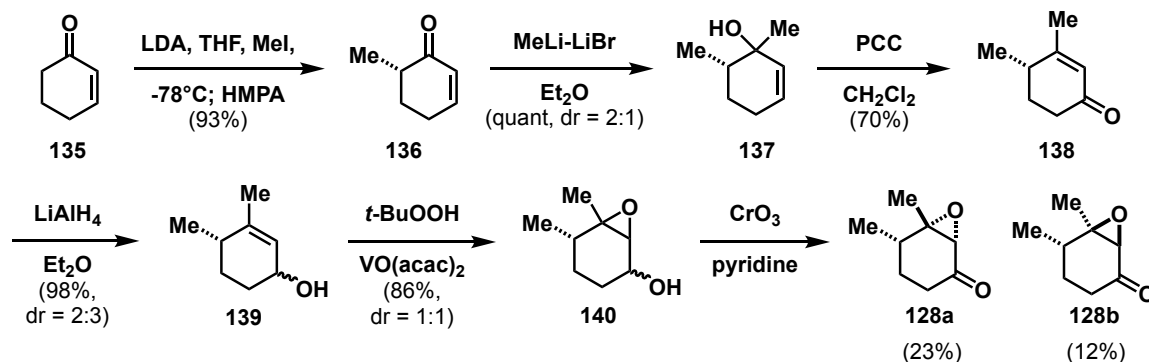
Preparation of norcrassin A (**112**) was categorically dependent upon the availability of the  $\gamma$ -butyrolactone (**127**). We thus planned an initial epoxide ring-expansion approach to access the lactone that was based on the premise that a ketene silyl acetal (KSA, **129**) would add to the  $\beta$ -position of epoxyketone **128** (Scheme 24). Although direct nucleophilic attack into the more-hindered  $\beta$ -position may not be favorable, addition of a Lewis acid (LA) can coordinate to both the ketone and epoxide,

prompting the ring to open, forming a discrete carbocation. Compared to the  $\alpha$ -carbon, the carbocation formed at the  $\beta$ -carbon would be tertiary. It would also not experience the destabilizing effects of being adjacent to an electron-withdrawing carbonyl. Taking advantage of the inherent electronics of the epoxide substrate (**128**), the KSA should attack the coordinated epoxyketone (**128**) and subsequently lactonize.



**Scheme 24.** Proposed epoxide ring opening approach

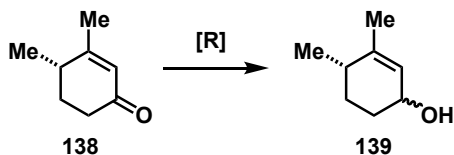
Hence, the construction of 2,3-epoxy-cis-3,4-dimethylcyclohexanone (**128**) commenced from cyclohexenone **135** (Scheme 25). Methylation of **135** afforded the modestly volatile 6-methyl-2-cyclohexen-1-one (**136**, 93% yield).<sup>91</sup> Subsequent MeLi•LiBr-mediated methylation afforded 1,6-dimethyl-2-cyclohexen-1-ol (**137**) in quantitative yield as an inconsequential mixture of diastereomers (dr = 2:1),<sup>92</sup> which is slightly higher than the 1:1 dr as reported by Jiang and co-workers when using MeLi instead of MeLi-LiBr.<sup>93</sup> Treating tertiary allylic alcohol (**137**) with pyridinium chlorochromate (PCC) followed by aqueous workup provided 3,4-dimethyl-2-cyclohexen-1-one (**138**) in 70% yield.<sup>92</sup>



**Scheme 25.** Synthesis of epoxycyclohexanones **128**

Further transformation of 3,4-dimethyl-2-cyclohexen-1-one (**138**) was carried out via a three-step sequence, as shown in Scheme 25.<sup>94</sup> LiAlH<sub>4</sub>-mediated reduction of **138** afforded 3,4-dimethyl-2-cyclohexen-1-ol (**139**, 98% yield) as a 2:3 mixture of 1,4-cis and 1,4-trans isomers, which was used directly in the next step without purification. It should also be noted that additional means for diastereoselective reduction of enone **138** were assessed. Treatment of **138** with bis(2-methoxyethoxy)aluminum hydride (Red-Al, dr = 3:2), L-Selectride (dr = 2:1) as well as a cerium (III) chloride assisted protocol (dr = 4:5) yielded allylic alcohol **139** in varying diastereomeric ratios (Table 1). A reversal of selectivity was also observed when using Red-Al and L-Selectride. Sodium triacetoxyborohydride (STAB) exhibited little reductive activity.

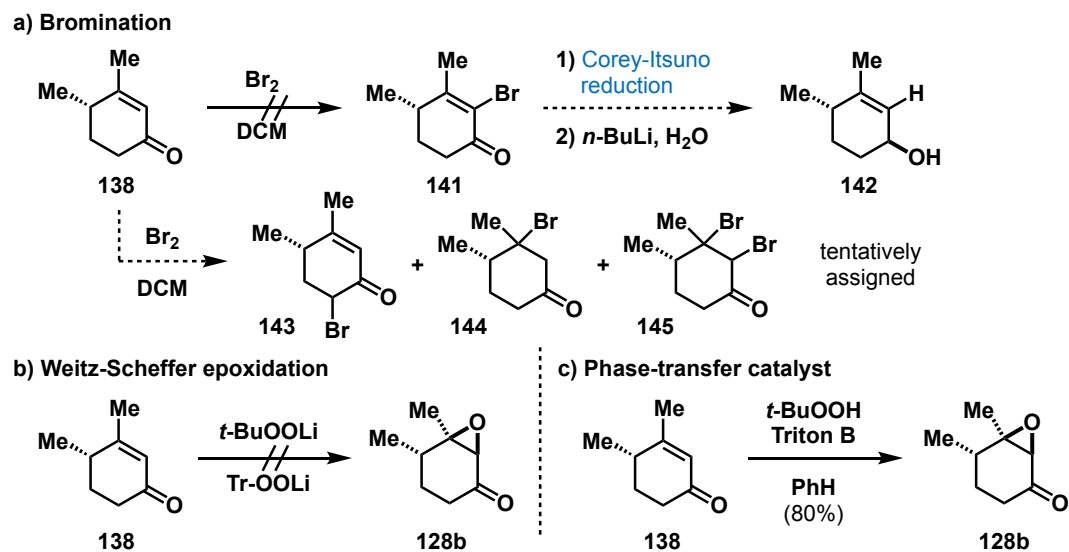
**Table 1.** Diastereoselective reduction of enone **138**



Reducing Agent	Diastereomeric Ratio (dr) <sup>a</sup>
Red-Al	3:2
L-Selectride	2:1
NaBH <sub>4</sub> , CeCl <sub>3</sub> •7H <sub>2</sub> O	4:5
STAB	N.R.
<sup>a</sup> N.R. = no reactivity.	

Vanadium-catalyzed alkene epoxidation of allylic alcohol **139** yielded a yellowish oil (**140**, 86% crude yield), containing a 1:1 isomeric mixture of epoxy alcohols.

Oxidation of the crude epoxy alcohol (**140**) with a CrO<sub>3</sub>–pyridine complex furnished a mixture of 2,3-epoxy-3,4-dimethylcyclohexanones (**128**). Isolation of the stereoisomers by gradient flash chromatography afforded the trans- (**128a**) and cis- (**128b**) dimethyl isomers in 23% and 12% yields, respectively, over two steps.<sup>91,92,94</sup>



**Scheme 26.** Other methods of diastereoselective epoxidation of enone **138**

With multi-gram quantities of 3,4-dimethyl-2-cyclohexen-1-one (**138**), we surveyed three other methods for diastereoselective epoxidation. Bromination of the endocyclic alkene of **138** could afford a substrate for a planned Corey–Itsuno reduction (Scheme 26a).<sup>95</sup> <sup>1</sup>H NMR analysis of the crude mixture suggested the presence of three plausible compounds:  $\alpha$ -bromination at the aliphatic position and mono/dibromination of the alkene. Unfortunately, no brominated product corresponding to **141** was observed, presumably due to rapid decomposition of the crude product to the corresponding phenol. Further investigation into the aforementioned approaches were halted.

Dimethyl enone **138** was also subjected to Weitz–Scheffer epoxidation using *t*-BuOOLi and Tr-OOLi (Scheme 26b).<sup>96</sup> <sup>1</sup>H NMR analysis of the crude reaction mixtures suggested marginal formation of the desired epoxide, albeit with substantial quantities of starting material. However, to our delight, Triton B-catalyzed Weitz–Scheffer epoxidation of enone **138** exclusively afforded the moderately volatile 2,3-epoxy-3,4-*cis*-

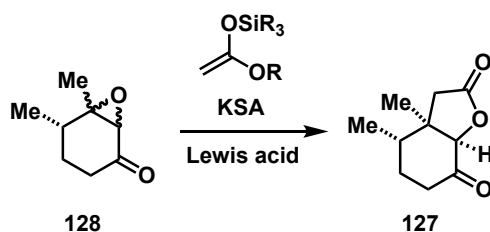
dimethylcyclohexanone (**128b**) in 73% yield (Scheme 26c).<sup>97</sup> Repeating the above reaction using triple the phase-transfer catalyst loading and an additional equivalent of oxidant increased the yield to 80%, though accompanied with t-BuOH as a minor byproduct that is difficult to remove by purification.

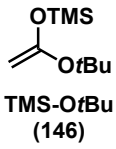
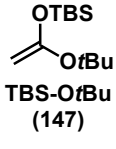
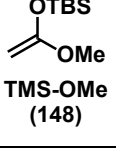
#### 1.3.4 First Generation Attempts to Lactone **127**

With ample access to epoxy ketones **128**, we began to analyze epoxide ring-opening methods for generating lactone **127** (Scheme 24). Enolate-mediated conditions were probed, albeit with no significant outcome.<sup>98</sup> To this extent, cis-dimethyl epoxy ketone **128b** was exposed to Lewis-acidic Et<sub>2</sub>AlCl and the lithium enolate of tert-butyl acetate.<sup>11</sup> <sup>1</sup>H NMR analysis of the crude mixture suggested formation of a new species. Yet, the endo-cyclic methylene protons could not be explicitly accounted for. To achieve regioselective ring-opening of the epoxide, **128b** was subsequently treated with the LHMDS-generated enolate of tert-butyl acetate. Instead of Et<sub>2</sub>AlCl, ZnCl<sub>2</sub> was used for chelation of the enolate and BF<sub>3</sub>-OEt<sub>2</sub> for the activation of the epoxide. <sup>1</sup>H NMR analysis of the crude material did not indicate formation of the anticipated product.

To expand our current synthetic approach, we assessed reactions of ketene silyl acetals with epoxides in the presence of various Lewis acids (Table 2).<sup>99</sup> Upon treatment of epoxy ketone **128b** with trimethylsilyl (TMS)-protected KSA (**146**) in the presence of BF<sub>3</sub>-OEt<sub>2</sub> in CH<sub>2</sub>Cl<sub>2</sub> at -78°C, TLC analysis of the reaction mixtures implied the formation of two products (Table 2, Entry 7). Unfortunately, the hydroxy ester could not be clearly deduced from the <sup>1</sup>H NMR spectrum of the crude reaction mixture due to decomposition.

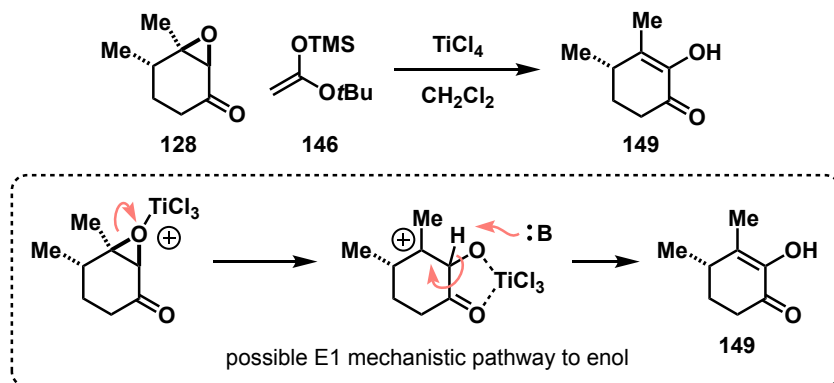
**Table 2.** Ketene silyl acetal-mediated *cis*-epoxide ring-opening methods



Entry	KSA	Lewis Acid <sup>a</sup>	Solvent	Result <sup>b</sup>
1	 <b>TMS-OTBu (146)</b>	FeCl <sub>3</sub>	DCE	Decomposition
2		FeCl <sub>2</sub>	DCE	Decomposition
3		FeCl <sub>2</sub> + FeCl <sub>3</sub>	DCE	Decomposition
4		AlCl <sub>3</sub>	DCE	Decomposition + S.M.
5		TiCl <sub>4</sub> <sup>c</sup>	CH <sub>2</sub> Cl <sub>2</sub>	Enol + S.M.
6		LiClO <sub>4</sub> <sup>c</sup>	CH <sub>2</sub> Cl <sub>2</sub> Et <sub>2</sub> O	S.M. S.M.
7		BF <sub>3</sub> •OEt <sub>2</sub>	CH <sub>2</sub> Cl <sub>2</sub>	Decomposition
8	 <b>TBS-OTBu (147)</b>	ZnCl <sub>2</sub>	CH <sub>2</sub> Cl <sub>2</sub>	S.M.
9		Et <sub>2</sub> AlCl	CH <sub>2</sub> Cl <sub>2</sub>	Enol + S.M.
10		Y(OTf) <sub>3</sub>	CH <sub>2</sub> Cl <sub>2</sub>	S.M.
11		Yb(OTf) <sub>3</sub>	CH <sub>2</sub> Cl <sub>2</sub>	S.M.
12		LiClO <sub>4</sub> <sup>c</sup>	CH <sub>2</sub> Cl <sub>2</sub> Et <sub>2</sub> O	S.M. S.M.
13		TiCl <sub>4</sub> <sup>c</sup>	CH <sub>2</sub> Cl <sub>2</sub>	Enol
14		Ti(OiPr) <sub>4</sub>	CH <sub>2</sub> Cl <sub>2</sub>	Enol + S.M.
15	Mg(ClO <sub>4</sub> ) <sub>2</sub>	CH <sub>2</sub> Cl <sub>2</sub>	S.M.	
16	 <b>TMS-OMe (148)</b>	Cu(OTf) <sub>2</sub> <sup>c</sup>	Et <sub>2</sub> O	S.M.
17		Phenylboronic acid	THF	S.M.

<sup>a</sup>1.0 equiv except for LiClO<sub>4</sub>, TiCl<sub>4</sub>, Yb(OTf)<sub>3</sub>, Cu(OTf)<sub>2</sub>, and phenylboronic acid. <sup>b</sup> S.M. = starting material. <sup>c</sup>Performed on *trans*- and *cis*-diastereomers.

LiClO<sub>4</sub> (in excess or catalytic amounts) has been used by Fontaine *et al.* as an effective Lewis acid to induce chelation-controlled group transfer Mukaiyama aldol reaction of epoxyaldehydes with ketene silyl acetals.<sup>100</sup> Treatment of epoxy ketones **128** with catalytic (5%), moderate (1.5 equiv) and excess (10 equiv) amounts of LiClO<sub>4</sub> in varying concentrations using Et<sub>2</sub>O as well as CH<sub>2</sub>Cl<sub>2</sub> as the solvents yielded moderate to significant quantities of unreacted starting material (Table 2, Entry 6 & 12). *cis*-Dimethyl epoxy ketone **128b** was also subjected to an iron-catalyzed protocol developed by our group (Table 2, Entry 1–3) as well as AlCl<sub>3</sub> (Table 2, Entry 4). Analysis of the <sup>1</sup>H NMR spectra heavily alluded to substrate decomposition.



**Scheme 27.** Formation of enol, or 2-hydroxy-3,4-dimethyl-2-cyclohexenone **149**

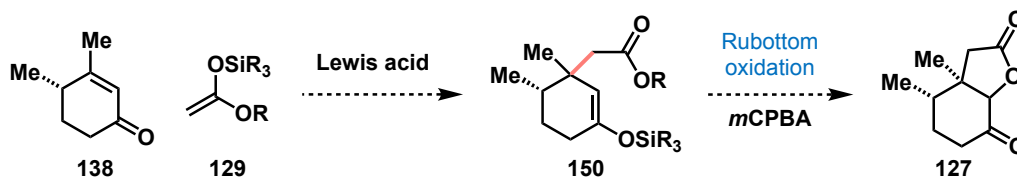
Lastly, a solution of TMS-protected KSA and epoxy ketones **128** were submitted to reaction with TiCl<sub>4</sub> (Table 1, Entry 5 & 13). Results indicated that 2-hydroxy-3,4-dimethyl-2-cyclohexenone (**149**) was formed using 0.5 equivalents of TiCl<sub>4</sub> (22% yield) via a possible E1 mechanistic pathway (Scheme 27). Presumably, TiCl<sub>4</sub> prompted ring-opening of the epoxide, resulting in the formation of a tertiary carbocation at the β-

position. However, deactivation of the nucleophile by the Lewis acid promoted a competing elimination reaction to ultimately furnish enol **149**. This observation was supported by additional control experiments, in which TMS-protected KSA and epoxy ketones **128** were individually treated with  $\text{TiCl}_4$ .  $^1\text{H}$  NMR analyses of the crude reaction mixtures indicated deprotection of the KSA to the corresponding tert-butyl acetate, rendering the nucleophile ineffective. Meanwhile, subjecting both epoxy ketones to  $\text{TiCl}_4$  strictly afforded the enol product. Similarly, treatment of cis- and trans-epoxy ketones **128** with  $\text{Ti}(\text{OiPr})_4$ ,  $\text{BF}_3\text{-OEt}_2$ ,  $\text{ZnCl}_2$ ,  $\text{Mg}(\text{ClO}_4)_2$ ,  $\text{Et}_2\text{AlCl}$ ,  $\text{Y}(\text{OTf})_3$ ,  $\text{Yb}(\text{OTf})_3$ ,  $\text{Cu}(\text{OTf})_2$ , and phenylboronic acid afforded starting material, decomposition, or the enol side product (**149**).

### 1.3.5 Second Generation Strategies to Lactone **127**

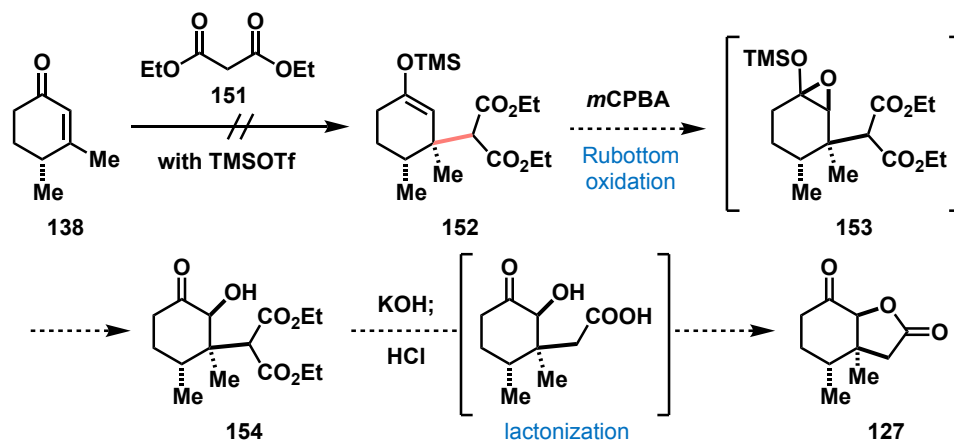
Other means of generating lactone **127** using fewer synthetic steps were also examined due to the inefficacy of the above Lewis acid-promoted epoxide ring opening reactions with KSAs. To this end, Rubottom oxidation following Mukaiyama conjugate addition to enone **138** was assessed using an assortment of KSA (**129**) and Lewis acid partners (Scheme 28).<sup>101</sup> Treatment of enone **138** with  $\text{LiClO}_4$ ,  $\text{SnCl}_4$ ,  $\text{ZnCl}_2$ ,  $\text{Et}_2\text{AlCl}$ ,  $\text{Y}(\text{OTf})_3$ , and  $\text{Yb}(\text{OTf})_3$  at 0.05 M, 0.1 M, 0.25 M, 0.4 M, 0.5 M, and 1.0 M concentrations resulted in predominantly unreacted starting materials. Moreover, attempts to activate the KSA nucleophile in situ using potassium fluoride (KF) and tetrabutylammonium fluoride (TBAF) furnished similar results, though the quality of the corresponding fluoride sources may have been questionable. At this point, it was hypothesized that the presence of the distal methyl group in enone **138** may have

impeded the reaction because the analogous reaction of 3-methylcyclohexenone (**138**) has been reported to undergo a similar Mukaiyama reaction.<sup>102</sup>



**Scheme 28.** Mukaiyama–Michael addition and Rubottom oxidation strategy to lactone

Softer nucleophilic and basic conditions were hence examined to induce the appropriate reactivity.<sup>103</sup> The course of nucleophilic conjugate additions is dominated by orbital, rather than electrostatic, considerations.<sup>104</sup> In an  $\alpha,\beta$ -unsaturated carbonyl system, such as the one in enone **138**, the electrophilic  $\beta$ -carbon has a predominantly large coefficient.<sup>105</sup> Nucleophiles with similar, if not greater, frontier orbital attributes would more readily react. Therefore, when compared to previously used KSAs, malonate esters or suitable alternatives would be considered softer reagents that would allow for supposedly facile carbon-carbon bond formation, especially in the construction of relatively difficult quaternary carbon centers.

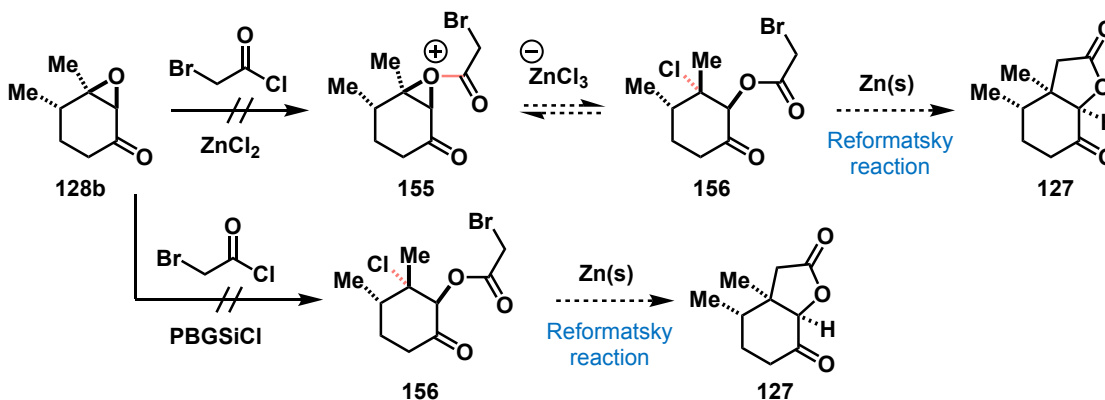


**Scheme 29.** Use of softer nucleophiles en route to lactone **127**

Applied directly to enone **138**, following 1,4-addition of diethyl malonate (**151**), the ensuing product would be trapped as a silyl enol ether (**152**, Scheme 29). Epoxidation of the enol ether olefin would generate a siloxy oxirane (**153**), which would rearrange to the alpha-hydroxy ketone (**154**). Subsequent hydrolysis and decarboxylation would allow for the final lactonization to occur. However, as opposed to the desired diester product (**152**),  $^1\text{H}$  NMR analysis of the crude material displayed a significant amount of starting enone **138**. Consistent with our prior rationale, the sterically demanding environment adjacent to the olefin presumably hampered nucleophilic attack by the diethyl malonate.

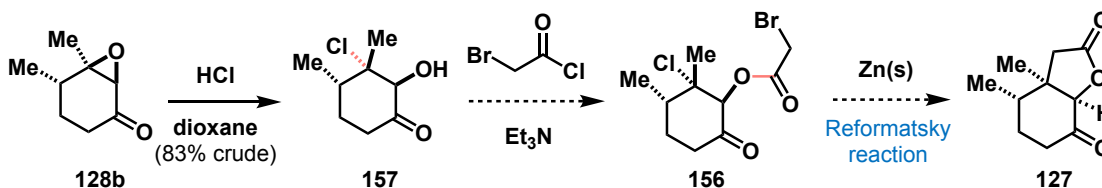
We also probed a Reformatsky-type reaction facilitated by addition of epoxy ketone **128b** to an acid chloride (Scheme 30). In this one-step process,  $\text{ZnCl}_2$  would promote addition of the epoxide (**128b**) to the acid chloride, prompting formation of  $\alpha$ -bromo ester **156**. Introduction of metallic  $\text{Zn}_{(s)}$  would form the zinc enolate, which would attack the intramolecular carbon-chloride bond to generate the target lactone (**127**). The reaction was also anticipated to proceed through a  $\text{S}_{\text{N}}1$ -type pathway in which the  $\text{ZnCl}_2$

may abstract the halide to form the tertiary carbocation center. However, attempts to enable this one-pot process led to primarily decomposition of the starting material.



**Scheme 30.** One-pot  $\text{ZnCl}_2$ -mediated Reformatsky reaction toward lactone **127**

Instead, as preceded by Gros *et al.*, silica-supported guanidinium chloride (PBGSiCl) was successfully prepared to promote the chemo- and regioselective ring opening of the epoxide.<sup>106</sup> Epoxyketone **128b** was then subjected to the functionalized silica catalyst and bromoacetyl chloride (Scheme 30). Unfortunately, the  $\beta$ -chloro- $\alpha$ -oxyester product (**156**) was not observed, seemingly due to significant product instability. Additional runs involved varying the temperature and treating the crude reaction mixture immediately with  $\text{Zn}_{(s)}$ . Yet, the desired transformation could not be achieved and only rapid decomposition of the substrate was observed.

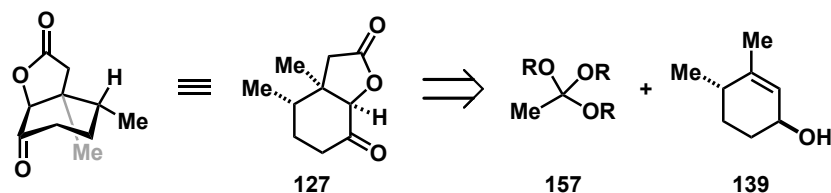


**Scheme 31.** Stepwise Reformatsky reaction toward lactone

Additionally, the Reformatsky-type reaction was attempted in a stepwise manner (Scheme 31). However, initial attempts into the acid-induced ring opening of the epoxide with HCl (i.e. aqueous, EtOH, MeOH), could not be effected.  $^1\text{H}$  NMR analysis of the crude reaction mixtures did not indicate formation of the anticipated vicinal chlorohydrin (**157**). Rather, formation of 2-hydroxy-3,4-dimethyl-2-cyclohexenone (**149**) was often seen. Yet, HCl solution in dioxane effectively produced the chlorohydrin (**157**), which was supported via  $^1\text{H}$  NMR analysis of the crude reaction mixture.<sup>107</sup> A similar chlorohydrin product was also produced utilizing a DBU-TiCl<sub>4</sub> mediated protocol.<sup>108</sup> Acylation of the crude material with 2-bromoacetyl chloride and NEt<sub>3</sub> did not display any reactivity. Instead, reversion to epoxide **128** was frequently detected, which was indicative of a base-triggered re-epoxidation pathway. While substitution of NEt<sub>3</sub> with pyridine suggested otherwise, peaks corresponding to the anticipated bromoacetate (**156**) could not be discerned via  $^1\text{H}$  NMR analysis of the isolated fractions upon purification. This may have been due to instability of the material on silica gel. The crude mixture (**157**) was also immediately subjected to Zn<sub>(s)</sub>. However,  $^1\text{H}$  NMR analysis of the crude material indicated decomposition of the starting material.

#### 1.3.6 Third Generation Attempts at Lactone **127**

Given the above discussed approaches did not pan out as expected, a different route was conceived in which a sigmatropic rearrangement would grant access to the desired bicyclic lactone (**127**) starting from a previously synthesized allylic alcohol intermediate (**139**, Scheme 32).

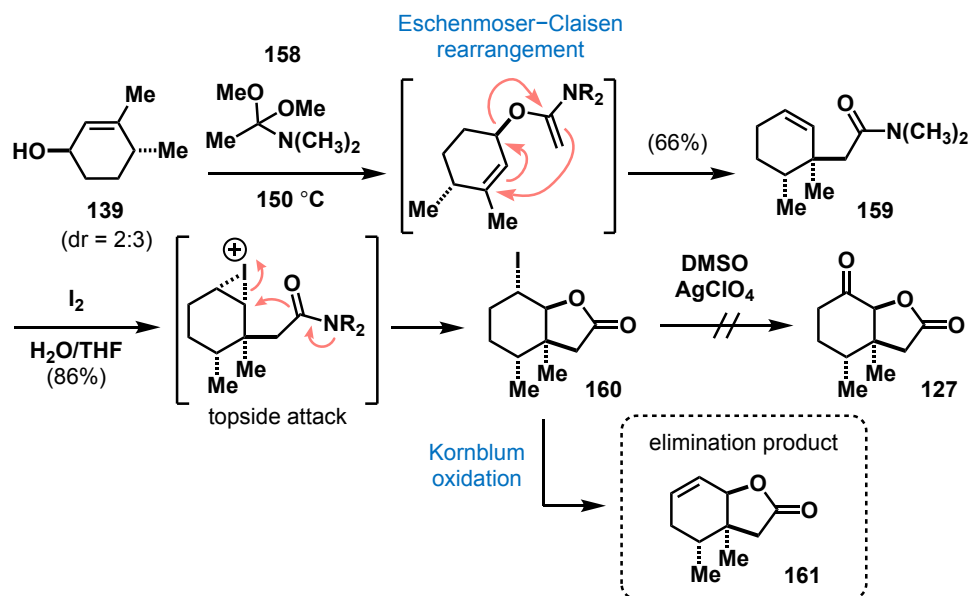


**Scheme 32.** Revised retrosynthesis of lactone (**127**)

Halolactonization is an intramolecular variant of the halohydrin synthesis reaction that effectively generates a lactone via addition of an oxygen and iodine across a carbon-carbon double bond.<sup>109</sup> It is a reaction that encompasses a number of nuances that affect ideal product formation, including regioselectivity and ring size preference. Hence, iodolactonization represents a straightforward opportunity to access lactone **127** (Scheme 33). Centered on work done by Bisai and Sarpong, treatment of allylic alcohol **139** with commercially available dimethyl acetal of *N,N*-dimethylacetamide (DMA-DMA, **158**) successfully produced the  $\gamma,\delta$ -unsaturated dimethyl amide (**159**, 66% yield).<sup>110</sup> Subsequent iodolactonization of amide **159** yielded fused iodolactone **160** in 86% yield.

Lastly, transformation of the secondary halide to the desired carbonyl (**127**) was surveyed via a silver assisted dimethyl sulfoxide oxidation.<sup>111</sup> This slight variation to the traditional Kornblum oxidation, in which reaction of a primary halide with DMSO forms an aldehyde, could resolve the difficulty of DMSO in displacing an unactivated secondary halide to form the appropriate alkoxy-sulphonium intermediate and ultimately, the bicyclic lactone (**127**). However, treatment of iodolactone **160** with  $\text{AgBF}_4$ ,  $\text{AgNO}_3$  and  $\text{AgClO}_4$  afforded primarily the elimination side product (**161**) as well as moderate amounts of unreacted starting material. Alternatively, a Wacker–Tsuji oxidation will be

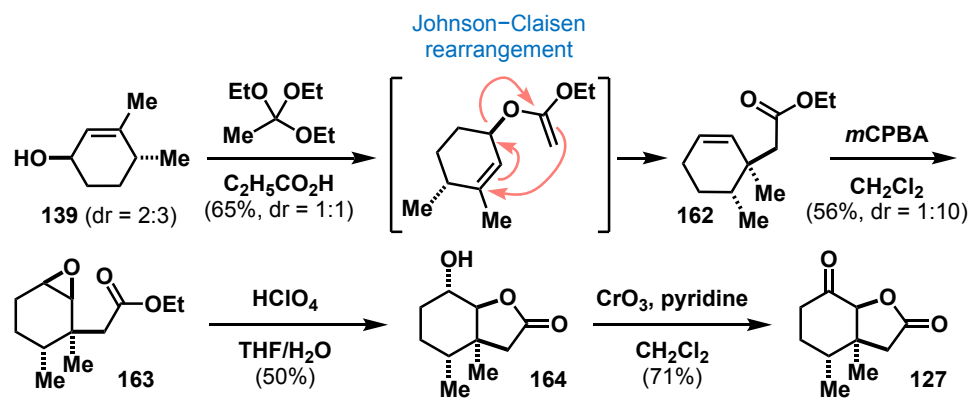
considered on any remaining elimination product to obtain desired lactone **127** in future studies.



**Scheme 33.** Synthesis of lactone **127** via Eschenmoser–Claisen rearrangement and Kornblum oxidation

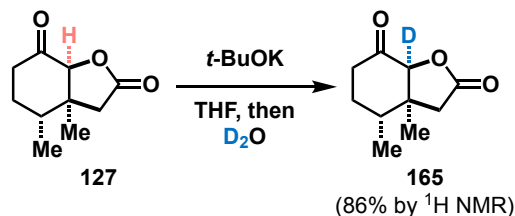
Another strategy was adapted from Olejniczak *et al.* that decisively yielded the desired lactone (**127**) in four synthetic steps (Scheme 34).<sup>112</sup> Allyl alcohol **139**, obtained in the reduction of enone **138**, was subjected to Johnson–Claisen rearrangement leading to  $\gamma,\delta$ -unsaturated ethyl ester **162** in 65% yield (dr = 1:1). Preferential epoxidation of cis-**162** via mCPBA gave epoxide **163** in 56% yield as a mixture of cis- and trans-diastereomers. The resultant epoxy ester underwent an acid-induced cyclization to hydroxy lactone **164**, which was further oxidized with a CrO<sub>3</sub>–pyridine complex to the anticipated lactone (**127**) in 71% yield, rendering its construction complete. The lactone

was isolated as a single diastereomer with stereochemistry of the methyl groups assigned as syn via NOE.



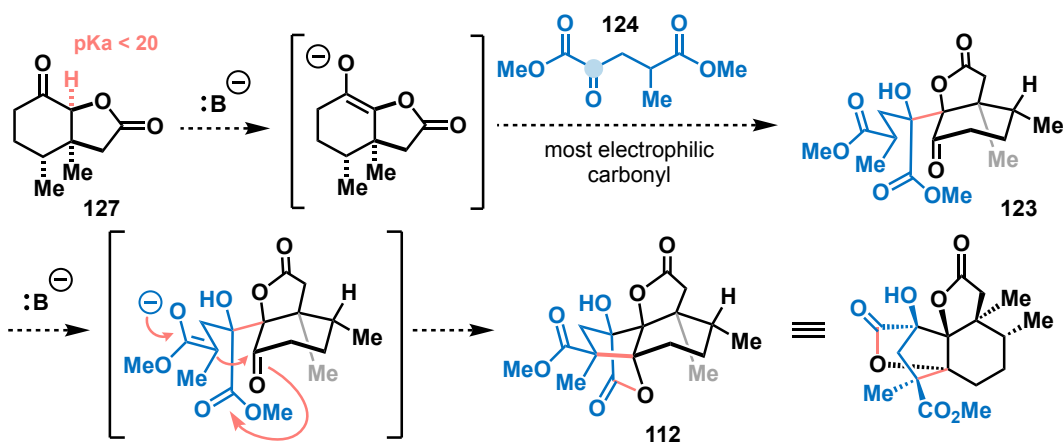
### 1.3.7 Aldol/Aldol/Lactonization Studies

With effective access to both fragments (**124** and **127**), the novel aldol/aldol/lactonization sequence was probed. Deuterium oxide ( $D_2O$ ) studies indicated that deuterium was being incorporated at the desired alpha position of lactone **127**, suggesting that deprotonation and enolate formation was occurring at the required site for the initial aldol reaction (Scheme 35).



That information in hand, enolate formation would thus commence from lactone (**127**), in which the highlighted hydrogen atom would be preferentially deprotonated due

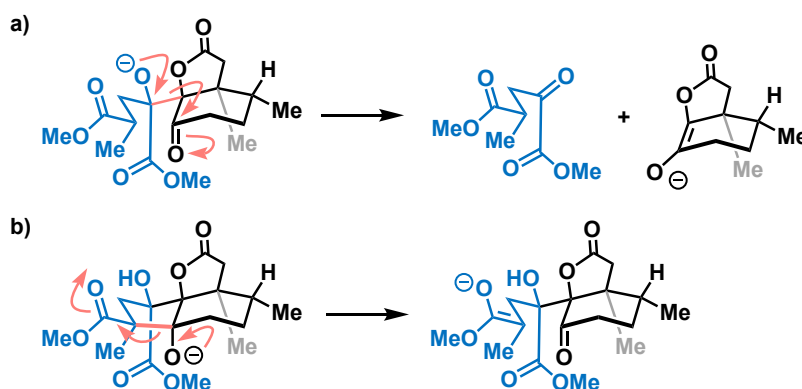
to its relative acidity (Scheme 36). Introduction of oxoglutarate **124** would prompt an intermolecular attack by the enolate upon the ketone (marked in blue), which would be deemed as the more reactive carbonyl. The basic conditions of the initial addition should prompt an ensuing intramolecular aldol reaction via the ester enolate, which upon lactonization would provide norcrassin A (**112**), potentially in one cascading step.



**Scheme 36.** Anticipated strategy of base-mediated aldol/aldol/lactonization

In this regard, the base surveyed at the outset was KOt-Bu (1 and 2 equiv) in *t*-BuOH under ambient temperature (rt, 20–25 °C) and reflux. Upon purification by preparatory TLC,  $^1\text{H}$  NMR analysis of the isolated materials did not bear anything significant other than minimal amounts of unreacted keto diester **124**. Resubjecting **124** and **127** to KOt-Bu in THF at 0 °C, rt, or under reflux showed signs of reactivity via  $^1\text{H}$  NMR analysis of the crude material. Yet, purification of the reaction mixtures did not reveal any diagnostic signals telling of initial aldol addition product **123** nor norcrassin A (**112**). Instead, it was likely that the generated bicyclic intermediate (**123**) may have been hydrolyzed in situ, thwarting the second aldol reaction. Additional treatment of lactone

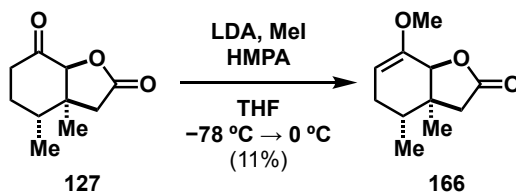
**127** and keto diester **124** with varying equivalents (1.0, 1.5, and 2.0 equiv) of KOt-Bu, KHMDS, LiHMDS, and NaH using t-BuOH and THF as the solvents at  $-78\text{ }^{\circ}\text{C}$ ,  $0\text{ }^{\circ}\text{C}$ , rt, or under reflux did not yield the anticipated product. Neither did exposure to LDA (2 equiv) in the presence of DMPU (5 equiv).<sup>113</sup> In most cases, the keto diester component (**124**) seemed to have condensed onto itself once added into the reaction mixture. Degradation of the two starting materials was also detected. At this stage, it was surmised that a retro-aldol reaction may have occurred, fragmenting the  $\beta$ -hydroxy ketones back to their respective enolates (Scheme 37). This could have induced undesirable results, such as side reactivity or product decomposition, especially given the accessibility of other electrophilic centers on **124** and **127**.



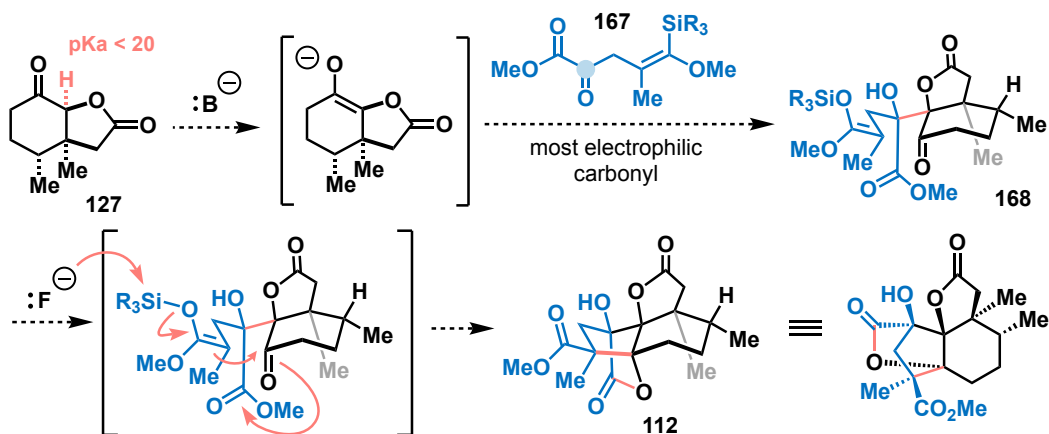
**Scheme 37.** Possible retro-aldol reaction pathways

Therefore, lactone **127** was treated with a simpler electrophile to confirm the appropriate reactivity. Enolization of **127** with LDA followed by addition of MeI as well as HMPA provided O-methylated product **166** (Scheme 38). The observed O-alkylation was anticipated as addition of HMPA decreases the prevalence of ion clustering, favoring a dissociated and often more reactive oxygen-centered enolate anion.<sup>114</sup> However,

compared to the outcome depicted in Scheme 35, the olefin seen in enol ether **166** implied opposite selectivity for deprotonation, which readily transpired at the more sterically accessible  $\alpha$ -carbon despite the use of less than one equivalent of base. Future work will entail resubjecting **127** with KO $t$ -Bu in THF, conditions featured in the preceding D<sub>2</sub>O experiment, to achieve the preferred deprotonation.



**Scheme 38.** Formation of O-methylated lactone

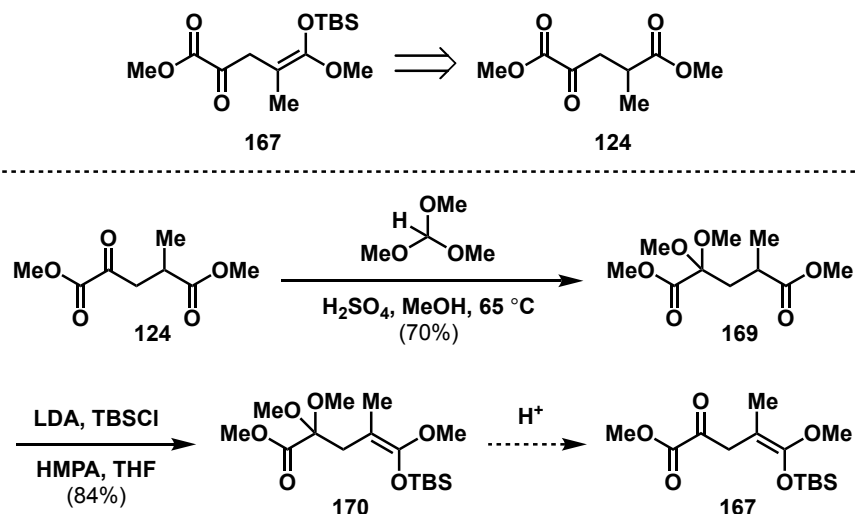


**Scheme 39.** Proposed silyl acetal variation of aldol/aldol/lactonization

Likewise, an alternative coupling partner (**167**) to which lactone **127** reacts with was assessed. Compared to the original 2-oxoglutarate (**124**), the KSA variant (**167**) would follow the initial aldol sequence outlined in Scheme 39. However, rather than relying on a second in-situ deprotonation to activate the methyl ester, the silyl acetal would serve as a pre-activated enolate equivalent. Addition of a fluoride source would

cleave the silyl group, facilitating the second aldol reaction, which could then lactonize to afford the natural product (**112**).

En route to silyl acetal **167**, a H<sub>2</sub>SO<sub>4</sub>-mediated ketalization of diester **124** provided dimethyl ketal **169** in 70% yield (Scheme 40). Subsequent formation of the TBS-protected KSA (**170**) proceeded in 84% yield as a mixture of *cis*- and *trans*-isomers through a similar method reported by Danishefsky *et al.*<sup>115</sup> The concluding deprotection of **170** was then surveyed. In this regard, treatment of **170** with silica gel in MeCN as well as H<sub>2</sub>O and acetone at 80 °C and 60 °C afforded either starting material or dimethyl ketal **169**.<sup>116</sup> Alternatively, diester **124** was subjected to two successive deprotonations with NaH and *n*-BuLi in an attempt to selectively form the TMS-ether and TBS-KSA, albeit to no avail. Alternative means of ketal removal were also examined, including a purportedly chemoselective Er(OTf)<sub>3</sub>-catalyzed method in wet nitromethane (MeNO<sub>2</sub>) and standard hydrolyzing conditions using *p*-TsOH in either acetone or H<sub>2</sub>O.<sup>117,118</sup> All of which selectively cleaved the TBS-protected KSA, rendering the dimethyl ketal untouched.

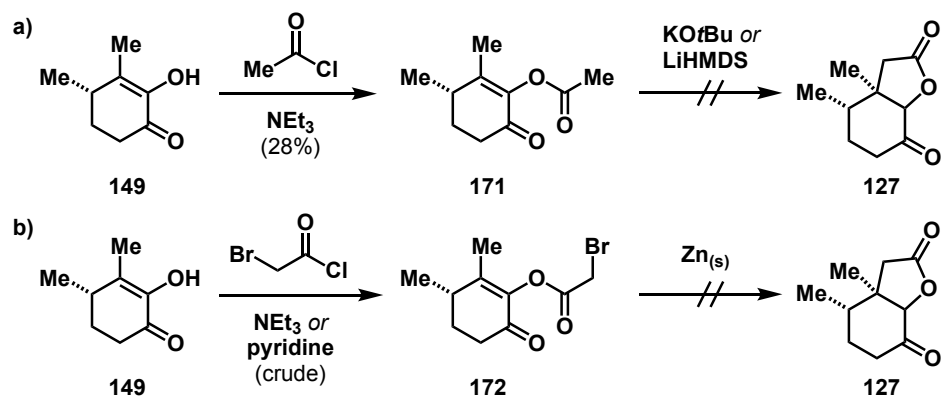


**Scheme 40.** Synthesis of silyl acetal derivative of keto-diester

### 1.3.8 Additional Optimization Studies

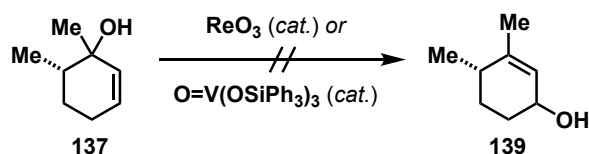
#### 1.3.8.1 Conversion of Enol Side Product to Lactone

We also attempted to exploit the 2-hydroxy-3,4-dimethyl-2-cyclohexenone (**149**) side-product. To this end, acylation of **149** with acetyl chloride and  $\text{NEt}_3$  yielded the acetate (**171**) in 28% yield (Scheme 41a).<sup>119</sup> Note that a similar product was also produced that employed a pyridine-mediated protocol.<sup>120</sup> However, initial efforts into the base-induced intramolecular Michael addition could not be achieved using  $\text{KOTBu}$  and  $\text{LiHMDS}$ .  $^1\text{H}$  NMR analysis of the crude reaction mixtures afforded predominantly starting material. An intramolecular Reformatsky-type reaction was also surveyed, in which enol **149** was subjected to bromoacetyl chloride and pyridine or  $\text{NEt}_3$  (Scheme 41b). Upon treatment of the crude mixture with  $\text{Zn}_{(\text{s})}$ , peaks corresponding to lactone **127** could not be discerned via  $^1\text{H}$  NMR analysis. Instead, decomposition of  $\alpha$ -bromoester **172** was observed.



**Scheme 41.** Attempts to convert enol **149** to lactone **127**

### 1.3.8.2 1,3-Transpositions of Allyl Alcohols

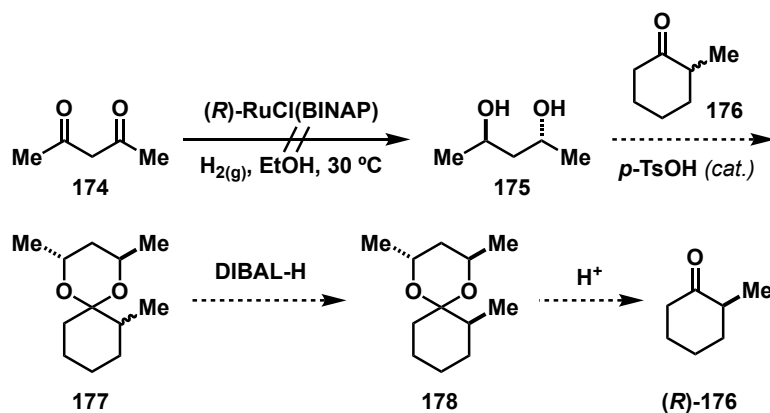


**Scheme 42.** Rhenium-catalyzed 1,3-transposition

The 1,3-transposition of allyl alcohols has been studied over several decades mainly using metal-oxo catalysts. Methyltrioxorhenium (MTO,  $\text{ReO}_3$ ) has been used by Jacob *et al.* as an effective Lewis acid to induce such allyl bond transpositions.<sup>121</sup> Hence, 1,3-transpositions represent a straightforward opportunity to abridge the current approach to allyl alcohol **139** by one step (Scheme 25). Unfortunately, treatment of tertiary alcohol **137** with catalytic (5%) amounts of MTO and  $\text{OV}(\text{OSiPh}_3)_3$  yielded mostly unreacted starting material (Scheme 42).



acetal (**177**) with triisobutylaluminum (TIBA) or diisobutylaluminum hydride (DIBAL-H) at low temperature followed by mild acid hydrolysis would elicit a kinetic resolution, transforming **177** to the optically pure ketone (**176**). However, attempts to construct (–)-(2R,4R)-2,4-pentanediol (**175**) from acetylacetone (**174**) could not be accomplished due to pressure irregularities with the hydrogenation vessel, resulting in reisolation of unreacted diketone.<sup>124</sup>

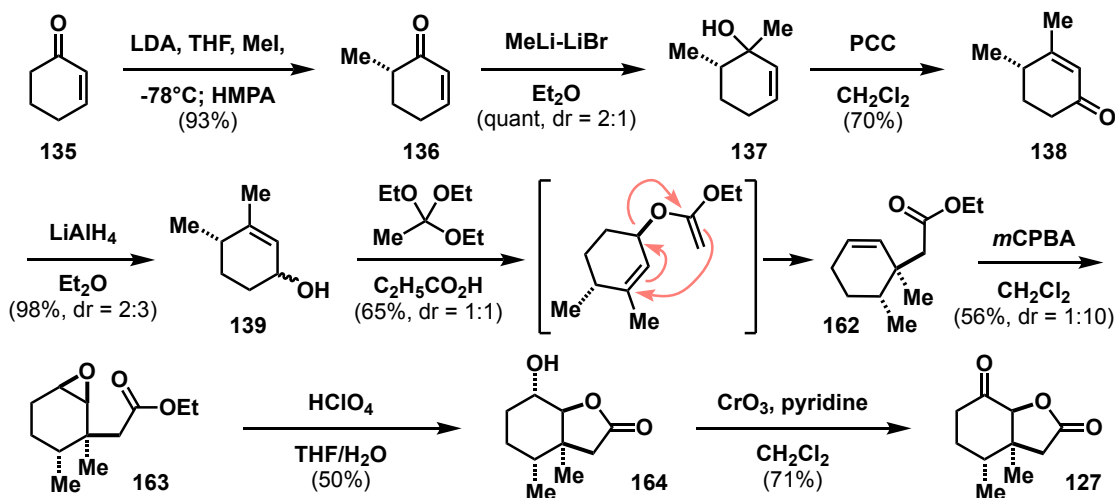


**Scheme 44.** Kinetic resolution of 2-methylcyclohexanone (**176**)

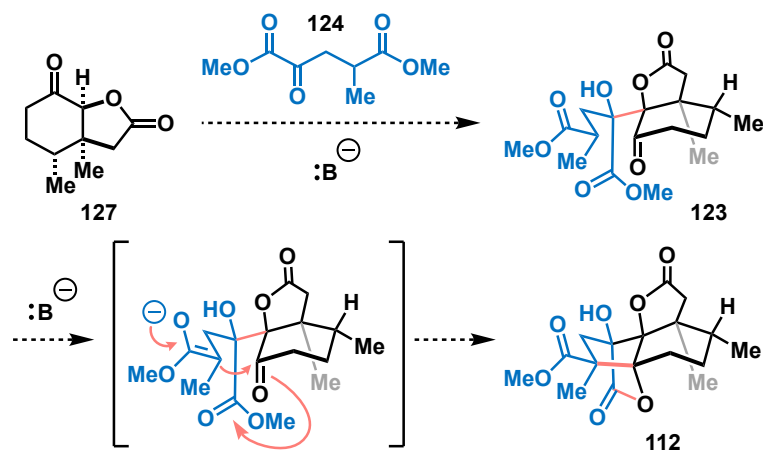
#### 1.4 Conclusion

Although much work has been completed en-route to norcrassin A (**112**), the target itself has not been completed. However, a number of vital advancements were made toward its synthesis. A scalable, eight-step route was developed to complete the synthesis of lactone **127** with the preferred stereochemical configuration (Scheme 45). Transformations include the dialkylation and subsequent Babler–Dauben oxidation of commercially available cyclohexenone **135**, generating enone **138** in high yield. Further elaboration of enone **138** via a  $\text{LiAlH}_4$  reduction provided allyl alcohol **139**, which was subjected to Johnson–Claisen rearrangement leading to the  $\gamma,\delta$ -unsaturated methyl ester

**162.** Followed by an oxidation with *m*CPBA, the resultant epoxy ester underwent an acid-induced cyclization via an intermediary diol ester to generate hydroxy lactone **164**, which was further oxidized to the lactone **127**. This sequence provided access to substantial quantities of each respective intermediate with modest diastereoselectivities. Accordingly, cyclohexenone **135** will be advanced through these steps to produce lactone **127** on scale, quantities of which will be required for successful completion of norcrassin A (**112**).



**Scheme 45.** Developed production of lactone **127**



**Scheme 46.** Formation of norcrassin A (**112**)

Conditions will then need to be worked out to perform the novel aldol/aldol/lactonization sequence upon reaction of fused bicyclic lactone **127** with pre-synthesized 2-oxoglutarate (**124**, Scheme 46). A plethora of reaction conditions, such as other bases, solvents, temperatures, and workups, will need to be explored to affect the desired selectivity and reactivity. Once the racemic synthesis of **112** is completed, an enantioselective approach from a chiral intermediate will be targeted via a potential resolution of methyl cyclohexenone **136** as depicted in Scheme 44. Ultimately, these advancements represent significant progress toward norcrassin A (**112**) and provide useful foundation for further work toward the natural product family. Members of which demonstrate potent bioactivities and offer continuing inspiration for the development of new chemical methods.

## 1.5 Experimental Section

### 1.5.1 General Experimental

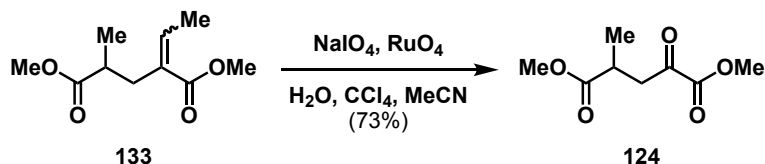
Commercial reagents were purchased from MilliporeSigma, Acros Organics, Chem-Impex, TCI, Oakwood, and Alfa Aesar, and used without additional purification. Solvents were purchased from Fisher Scientific, Acros Organics, Alfa Aesar, and Sigma Aldrich. Tetrahydrofuran (THF), diethyl ether (Et<sub>2</sub>O), acetonitrile (MeCN), dichloromethane (CH<sub>2</sub>Cl<sub>2</sub>), toluene (PhMe), 1,4-dioxane, and triethylamine (Et<sub>3</sub>N) were sparged with argon and dried by passing through alumina columns using argon in a Glass Contour (Pure Process Technology) solvent purification system. Benzene (PhH) was distilled over calcium hydride (CaH<sub>2</sub>) under a nitrogen (N<sub>2</sub>) atmosphere, degassed via freeze-pump-thaw (three cycles), and stored over 4 Å molecular sieves in a Schlenk flask under N<sub>2</sub>. Dimethylformamide (DMF), dimethyl sulfoxide (DMSO), dichloroethane (DCE), and solutions of MeLi, n-BuLi, and LDA were purchased in Sure/Seal or AcroSeal bottling and dispensed under N<sub>2</sub>. Deuterated solvents were obtained from Cambridge Isotope Laboratories, Inc. or MilliporeSigma.

Unless otherwise noted in the experimental procedures, reactions were carried out in flame or oven-dried glassware under a positive pressure of N<sub>2</sub> in anhydrous solvents using standard Schlenk techniques. Reaction progresses were monitored using thin-layer chromatography (TLC) on EMD Silica Gel 60 F254 or Macherey–Nagel SIL HD (60 Å mean pore size, 0.75 mL/g specific pore volume, 5–17 μm particle size, with fluorescent indicator) silica gel plates. Visualization of the developed plates was performed under UV light (254 nm). Purification and isolation of products were performed via silica gel

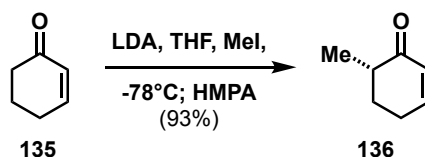
chromatography (both column and preparative thin-layer chromatography). Organic solutions were concentrated under reduced pressure on IKA® temperature-controlled rotary evaporator equipped with an ethylene glycol/water condenser.

Melting points were measured with the MEL-TEMP melting point apparatus. Proton nuclear magnetic resonance ( $^1\text{H}$  NMR) spectra, carbon nuclear magnetic resonance ( $^{13}\text{C}$  NMR) spectra and fluorine nuclear magnetic resonance ( $^{19}\text{F}$  NMR) spectra were recorded on Bruker Avance NEO 400 (not  $^1\text{H}$  decoupled) or Bruker Avance 600 MHz spectrometers ( $^1\text{H}$  decoupled). Chemical shifts ( $\delta$ ) are reported in ppm relative to the residual solvent signal ( $\delta$  7.26 for  $^1\text{H}$  NMR,  $\delta$  77.16 for  $^{13}\text{C}$  NMR in  $\text{CDCl}_3$ ).<sup>1</sup> Data for  $^1\text{H}$  NMR spectroscopy are reported as follows: chemical shift ( $\delta$  ppm), multiplicity (s = singlet, d = doublet, t = triplet, q = quartet, m = multiplet, br = broad, dd = doublet of doublets, dt = doublet of triplets), coupling constant (Hz), integration. Data for  $^{13}\text{C}$  and  $^{19}\text{F}$  NMR spectroscopy are reported in terms of chemical shift ( $\delta$  ppm). IR spectroscopic data were recorded on a NICOLET 6700 FT-IR spectrophotometer using a diamond attenuated total reflectance (ATR) accessory. Samples are loaded onto the diamond surface either neat or as a solution in organic solvent and the data acquired after the solvent had evaporated. High resolution accurate mass (ESI) spectral data were obtained from the Analytical Chemistry Instrumentation Facility at the University of California, Riverside, on an Agilent 6545 Q-TOF LC/MS instrument (supported by NSF grant CHE-1828782).

## 1.5.2 Experimental Procedures

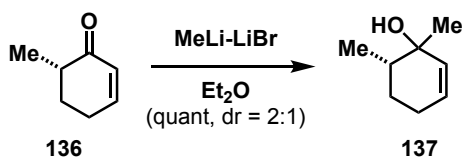


**Dimethyl 2-methyl-3-oxosuccinate (136).** To a solution of **133** (1.48 g, 7.39 mmol, 1 equiv) in a mixture of  $\text{CCl}_4$  (17 mL, 172 mmol, 23 equiv) and MeCN (17 mL, 319 mmol, 43 equiv) was added a solution of  $\text{NaIO}_4$  (6.33 g, 29.6 mmol, 4 equiv) in  $\text{H}_2\text{O}$  (22 mL) and  $\text{RuO}_2$  (98 mg, 0.74 mmol, 0.1 equiv). The mixture was stirred at rt for 24 h, then filtered over a pad of Celite. The biphasic mixture was extracted with  $\text{CH}_2\text{Cl}_2$  (2 x 10 mL). The combined organic extract was washed with brine (10 mL), dried over  $\text{MgSO}_4$ , filtered, and concentrated in vacuo to afford a pale-yellow oil. The crude product was purified by flash chromatography eluting with EtOAc/hexanes (1:5 v/v) to give compound **124** as colorless oil (930 mg, 73%).  $R_f$ : 0.34 (1:5 EtOAc/hexane, UV,  $\text{KMnO}_4$  stain).  $^1\text{H}$  NMR (400 MHz,  $\text{CDCl}_3$ )  $\delta$  3.88 (s, 3H), 3.68 (s, 3H), 3.32 (dd,  $J = 18.6, 8.4$  Hz, 1H), 3.02 (dq,  $J = 8.3, 7.2, 5.2$  Hz, 1H), 2.88 (dd,  $J = 18.5, 5.3$  Hz, 1H), 1.25 (d,  $J = 7.2$  Hz, 3H). All spectroscopic data are consistent with those previously reported.<sup>89</sup>



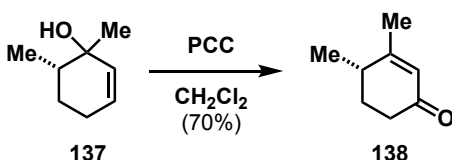
**6-Methyl-2-cyclohexen-1-one (136).** To a 500 mL round-bottomed flask was added 2-cyclohexenone (**135**, 4.00 g, 40 mmol, 1 equiv) and anhydrous THF (70 mL). The solution was cooled to  $-78^\circ\text{C}$  and a solution of LDA (2 M solution, 28 mL, 57 mmol, 1.4 equiv) was added dropwise. The solution was stirred for 30 min followed by dropwise

addition of MeI (5.2 mL, 83 mmol, 2 equiv). After stirring for 30 min at  $-78\text{ }^{\circ}\text{C}$ , HMPA (24 mL, 138 mmol) was added and the yellow mixture was stirred at  $-78\text{ }^{\circ}\text{C}$  for 2 h. Et<sub>2</sub>O (80 mL) was added to the mixture at  $0\text{ }^{\circ}\text{C}$  and the organic extract was washed with sat. NH<sub>4</sub>Cl<sub>(aq)</sub> (5 x 20 mL) and brine (3 x 20 mL), dried over Na<sub>2</sub>SO<sub>4</sub>, and concentrated in vacuo. The crude product was purified by flash chromatography eluting with hexanes/Et<sub>2</sub>O (1:1 v/v) to give compound **136** as a volatile yellow liquid (3.70 g, 83%). R<sub>f</sub>: 0.26 (1:10 EtOAc/hexane, UV). <sup>1</sup>H NMR (400 MHz, CDCl<sub>3</sub>) δ 6.92 (m, 1H), 5.97 (dt, 1H), 2.39 (m, 3H), 2.06 (m, 1H), 1.73 (m, 1H), 1.13 (d, 3H). All spectroscopic data are consistent with those previously reported.<sup>91</sup>

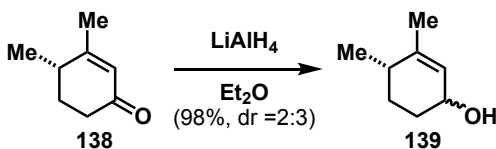


**1,6-Dimethyl-2-cyclohexen-1-ol (137)**. Enone **136** (3.20 g, 28.6 mmol, 1 equiv) was taken in anhydrous Et<sub>2</sub>O (53 mL) and cooled to  $-78\text{ }^{\circ}\text{C}$ . A solution of MeLi-LiBr complex in Et<sub>2</sub>O (1.5 M, 20.6 mL, 30.9 mmol, 1.08 equiv) was added via syringe over 20 min. The cooling bath was removed, and the mixture was stirred at rt for 3 h. After 3 h, the mixture was cooled to  $0\text{ }^{\circ}\text{C}$  and H<sub>2</sub>O (25 mL) was slowly added to the yellow solution. The biphasic mixture was extracted with Et<sub>2</sub>O (2 x 30 mL). The combined organic extract was washed with H<sub>2</sub>O (30 mL), dried over MgSO<sub>4</sub>, filtered, and concentrated in vacuo to afford cyclohexenol **137** (3.20 g, 89%, dr = 2:1) as a bright yellow oil which was used in the following step without further purification. R<sub>f</sub>: 0.24 (1:4 EtOAc/hexane, UV, vanillin stain). <sup>1</sup>H NMR (400 MHz, CDCl<sub>3</sub>, both diastereomers) δ

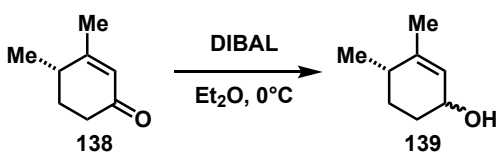
5.71 (m, 2H), 2.05 (m, 2H), 1.74 (m, 1H), 1.56 (m, 1H), 1.42 (m, 1H), 1.16 (s, 3H), 1.03 (d, 3H), 0.96 (d, 3H). All spectroscopic data are consistent with those previously reported.<sup>92</sup>



**3,4-Dimethyl-2-cyclohexen-1-one (138).** To a 250 mL round-bottomed flask under N<sub>2</sub> was added PCC (10.95 g, 50.8 mmol, 2 equiv) and CH<sub>2</sub>Cl<sub>2</sub> (50 mL). A solution of crude cyclohexenol **137** (3.20 g, 25.4 mmol, 1 equiv) in CH<sub>2</sub>Cl<sub>2</sub> (16 mL) was transferred to the reaction mixture via cannula over 5 min, and the solution was stirred at rt for 3 h. The reaction mixture was diluted with Et<sub>2</sub>O (80 mL), decanted, and the remaining black resin was washed with Et<sub>2</sub>O (3 x 33 mL). The combined brown Et<sub>2</sub>O extract was washed with 1.25 M NaOH<sub>(aq)</sub> (2 x 60 mL), 1.37 M HCl<sub>(aq)</sub> (60 mL) and sat. NaHCO<sub>3(aq)</sub> (2 x 33 mL), dried over MgSO<sub>4</sub>, filtered, and concentrated in vacuo to give the crude product (2.84 g) as a yellow oil. Purification by column chromatography (eluting with 1:6 Et<sub>2</sub>O/pentane, then 1:1 Et<sub>2</sub>O/pentane) yielded dimethyl enone **138** as a yellow oil (1.90 g, 63%). R<sub>f</sub>: 0.45 (1:2 EtOAc/hexane, UV, p-anisaldehyde stain); <sup>1</sup>H NMR (400 MHz, CDCl<sub>3</sub>) δ 5.79 (s, 1H), 2.42 (m, 2H), 2.29 (m, 1H), 2.09 (m, 1H), 1.93 (s, 3H), 1.73 (m, 1H), 1.17 (d, 3H); <sup>13</sup>C NMR (400 MHz, CDCl<sub>3</sub>) δ 199.6, 166.6, 126.3, 34.6, 34.4, 30.3, 22.7, 17.7. All spectroscopic data are consistent with those previously reported.<sup>92</sup>

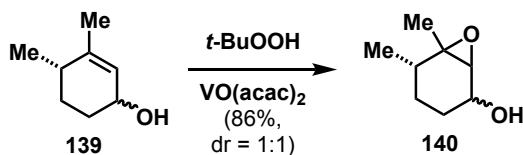


**3,4-Dimethyl-2-cyclohexen-1-ol (138).** To a solution of  $\text{LiAlH}_4$  (153 mg, 4.03 mmol, 1 equiv) in  $\text{Et}_2\text{O}$  (6 mL) under  $\text{N}_2$  was slowly added a solution of enone **139** (500 mg, 4.03 mmol, 1 equiv) in  $\text{Et}_2\text{O}$  (40 mL) at  $0^\circ\text{C}$ . The reaction mixture was stirred at  $0^\circ\text{C}$  for 3 h, quenched with  $\text{H}_2\text{O}$  (5 mL) and sat.  $\text{NH}_4\text{Cl}_{(\text{aq})}$  (10 mL) and extracted with  $\text{Et}_2\text{O}$  ( $3 \times 8$  mL). The combined organic extract was dried over  $\text{MgSO}_4$ , filtered, and concentrated in vacuo to afford allylic alcohol **139** (490 mg, 96%, dr = 2:3) as a pale-yellow oil, which was used in the following step without further purification.  $R_f$ : 0.57 (1:2 EtOAc/hexanes, UV, vanillin stain);  $^1\text{H}$  NMR (400 MHz,  $\text{CDCl}_3$ , both diastereomers)  $\delta$  5.46 (m, 1H + 1H), 4.14 (m, 1H + 1H), 2.04 (m, 2H), 1.87 (m, 2H), 1.73–1.61 (m, 3H), 1.69 (s, 3H + 3H), 1.49 (m, 2H), 1.26 (m, 1H), 1.05 (d, 3H), 0.97 (d, 3H). All spectroscopic data are consistent with those previously reported.<sup>94</sup>

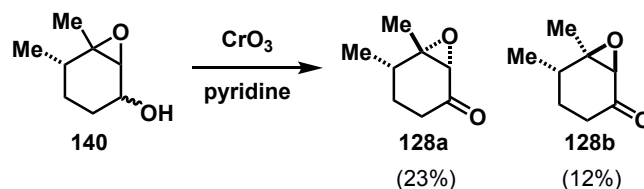


**3,4-Dimethyl-2-cyclohexen-1-ol (139).** Enone **138** (450 mg, 3.6 mmol, 1 equiv) was taken in  $\text{Et}_2\text{O}$  (36 mL) under  $\text{N}_2$  and cooled to  $0^\circ\text{C}$ . A solution of DIBAL-H (1.2 M solution, 3.6 mL, 4.3 mmol, 1 equiv) was added and the mixture was stirred at  $0^\circ\text{C}$  for 2 h. The reaction mixture was diluted with  $\text{Et}_2\text{O}$  and slowly quenched with  $\text{H}_2\text{O}$  (1 mL). Following addition of 15%  $\text{NaOH}_{(\text{aq})}$  (1 mL) and  $\text{H}_2\text{O}$  (1 mL) at  $0^\circ\text{C}$ , the mixture was stirred for 15 min at rt. Upon addition of  $\text{MgSO}_4$ , the solution was stirred for an

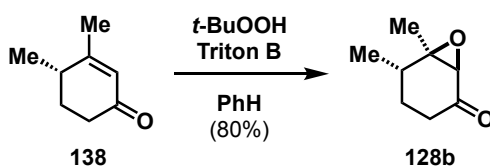
additional 15 min, filtered, and concentrated in vacuo to yield allylic alcohol **139** (438 mg, 96% yield, dr = 1:1) as a yellow oil which was used in the following step without further purification. R<sub>f</sub>: 0.37 (1:4 EtOAc/hexanes, UV, KMnO<sub>4</sub> stain). <sup>1</sup>H NMR (400 MHz, CDCl<sub>3</sub>, both diastereomers) δ 5.46 (m, 1H + 1H), 4.14 (m, 1H + 1H), 2.04 (m, 2H), 1.87 (m, 2H), 1.73–1.61 (m, 3H), 1.69 (s, 3H + 3H), 1.49 (m, 2H), 1.26 (m, 1H), 1.05 (d, 3H), 0.97 (d, 3H). All spectroscopic data are consistent with those previously reported.<sup>94</sup>



**2,3-Epoxy-3,4-dimethylcyclohexan-1-ol (140).** Allylic alcohol **139** (490 mg, 3.8 mmol, 1 equiv) was taken in anhydrous benzene (11 mL), along with VO(acac)<sub>2</sub> (5.0 mg, 0.019 mmol, 0.005 equiv). A solution of 70% t-BuOOH (0.75 mL, 4.2 mmol, 1.07 equiv) in anhydrous benzene (2 mL) was added and the mixture was stirred for 30 h at rt. The reaction mixture was quenched with sat. Na<sub>2</sub>SO<sub>3(aq)</sub> (8 mL), extracted with Et<sub>2</sub>O (3 x 8 mL), and dried over MgSO<sub>4</sub>. Evaporation in vacuo afforded compound **140** (420 mg, 86% crude yield, dr = 1:1) as a crude yellow oil. This material was clean by <sup>1</sup>H NMR analysis and was therefore used in the following step without further purification. R<sub>f</sub>: 0.31 (1:2 EtOAc/hexanes, UV, p-anisaldehyde stain). <sup>1</sup>H NMR (400 MHz, CDCl<sub>3</sub>, crude, both diastereomers) δ 4.02 (m, 1H), 3.16 (d, 1H, J = 3.7 Hz), 3.10 (d, 1H, J = 3.1 Hz), 2.10–1.41 (m, 5H), 1.32 (s, 3H), 1.30 (s, 3H) 1.05 (d, 3H), 1.01 (d, 3H). All spectroscopic data are consistent with those previously reported.<sup>94</sup>

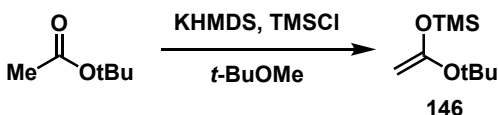


**2,3-Epoxy-3,4-*trans*-dimethylcyclohexanone (128a/b).** To a 0 °C solution of anhydrous pyridine (2 mL, 25 mmol, 10 equiv) in CH<sub>2</sub>Cl<sub>2</sub> (21 mL) was added CrO<sub>3</sub> (1.23 g, 12.3 mmol, 5.0 equiv). After stirring for 15 min at 0 °C, a solution of crude epoxy alcohol **140** (350 mg, 2.46 mmol, 1.0 equiv) in CH<sub>2</sub>Cl<sub>2</sub> (1.5 mL) was slowly added to the oxidizing mixture and stirred additionally for 1 h at 0 °C. The liquid portion was decanted from the gummy residue and rinsed exhaustively with CH<sub>2</sub>Cl<sub>2</sub>. The combined organic extract was washed with sat. NaHCO<sub>3(aq)</sub> and brine, dried over MgSO<sub>4</sub>, and concentrated in vacuo. The crude product was purified by flash chromatography eluting with Et<sub>2</sub>O/hexanes (1:3 v/v) to yield *trans*-(**128a**, 25.3 mg, 23%) and *cis*-(**128b**, 12.8 mg, 12%) isomers as volatile colorless liquids (25.3 mg, 23%). R<sub>f</sub>: 0.27 (1:3 ether/hexane, UV, KMnO<sub>4</sub> stain). <sup>1</sup>H NMR for **128a** (500 MHz, CDCl<sub>3</sub>) δ 3.01 (s, 1H), 2.52–2.44 (ddd, 1H), 2.1–1.99 (m, 2H), 1.75–1.56 (m, 2H), 1.39 (s, 3H), 1.16 (d, 3H). All spectroscopic data are consistent with those previously reported.<sup>94</sup>

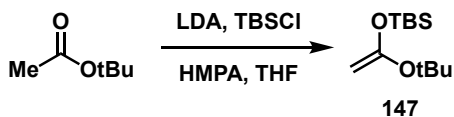


**2,3-Epoxy-3,4-*cis*-dimethylcyclohexanone (128b).** To a solution of cyclohexenone **138** (200 mg, 1.6 mmol, 1 equiv) in anhydrous benzene (2 mL) was added 70% t-BuOOH (270 μL, 2.09 mmol, 1.3 equiv) followed by 40% Triton B in methanol (58 μL, 0.14

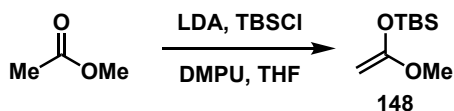
mmol, 0.086 equiv). The reaction mixture was stirred at rt for 48 h, quenched with H<sub>2</sub>O (2 mL) and extracted with Et<sub>2</sub>O (3 x 3 mL). The combined organic extract was washed with sat. Na<sub>2</sub>SO<sub>3(aq)</sub> (3 x 3 mL) and brine (3 x 3 mL), dried over MgSO<sub>4</sub>, and concentrated in vacuo. The crude product was purified by flash chromatography eluting with EtOAc/hexanes (1:3 v/v) to yield compound **128b** as a volatile colorless liquid (163 mg, 73%). R<sub>f</sub>: 0.62 (1:4 EtOAc/hexanes, UV, KMnO<sub>4</sub> stain). <sup>1</sup>H NMR (500 MHz, CDCl<sub>3</sub>) δ 3.10 (s, 1H), 2.40–2.17 (m, 5H), 1.44 (s, 3H), 1.07 (d, 3H, J = 7.1 Hz). All spectroscopic data are consistent with those previously reported.<sup>94</sup>



**1-tert-Butoxy-1-(trimethylsilyloxy) ethylene (146).** To a 0–5 °C solution of anhydrous KHMDS (0.7 M solution, 22 mL, 15.5 mmol, 1.2 equiv) in t-BuOMe (10 mL) was added a solution of tert-butyl acetate (1.5 g, 13 mmol, 1.0 equiv) in t-BuOMe (3 mL) over 7 min. After stirring for 30 min at 0–5 °C, TMSCl (2 mL, 16.8 mmol, 1.3 equiv) was added over 3 min and the solution was stirred at 0–5 °C for 30 min. The reaction mixture was warmed to rt and stirred for 2 h. The solution was poured into ice water (6 mL) and hexanes (6 mL). The biphasic mixture was extracted with hexanes (3 x 6 mL), washed with brine (6 mL), dried over Na<sub>2</sub>SO<sub>4</sub>, and concentrated in vacuo. The crude yellow oil was purified by vacuum distillation to give the desired ketene acetal as a colorless oil (1.78 g, 73%). bp 61–65°C/20 mTorr; <sup>1</sup>H NMR (500 MHz, CDCl<sub>3</sub>): δ 0.23 (9H, s), 1.34 (9H, s), 3.41 (1H, d, J = 1.4 Hz), 3.44 (1H, d, J = 1.4 Hz). All spectroscopic data are consistent with those previously reported.<sup>125</sup>

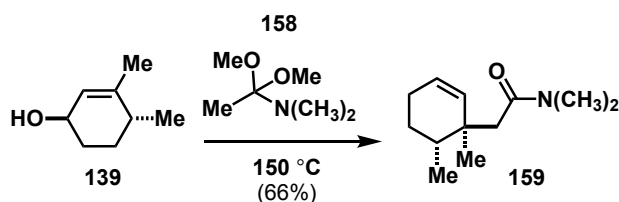


**1-(*tert*-Butyldimethylsilyloxy)-1-*tert*-butoxyethylene (147).** To a  $-78\text{ }^{\circ}\text{C}$  solution of anhydrous LDA (2 M solution, 11.5 mL, 14.2 mmol, 1.1 equiv) was added *tert*-butyl acetate (1.5 g, 13 mmol, 1 equiv) over 10 min. The mixture was stirred for an additional 15 min and then HMPA (2 mL) was added, followed by a solution of TBSCl (2.04 g, 13.5 mmol, 1.05 equiv) in THF (4.5 mL). The solution was warmed to rt and the solvent was removed in vacuo. The residue was taken up in hexanes (70 mL), washed with  $\text{H}_2\text{O}$  (3 x 30 mL) and brine (15 mL), dried over  $\text{Na}_2\text{SO}_4$ , and concentrated in vacuo to afford crude ketene acetal as a transparent, yellow liquid suitable for use without further purification (2.10 g, 71%).  $^1\text{H NMR}$  (400 MHz,  $\text{CDCl}_3$ )  $\delta$  3.50 (d,  $J = 1.3$  Hz, 1H), 3.48 (d,  $J = 1.2$  Hz, 1H), 1.37 (s, 9H), 0.96 (s, 9H), 0.21 (s, 6H). All spectroscopic data are consistent with those previously reported.<sup>115</sup>



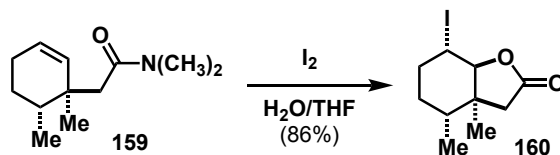
**1-(*tert*-Butyldimethylsilyloxy)-1-methoxyethylene (148).** To a  $-78\text{ }^{\circ}\text{C}$  solution of anhydrous LDA (2.0 M solution, 8.3 mL, 16.5 mmol, 1.1 equiv) in THF (38 mL) was added methyl acetate (1.2 mL, 15 mmol, 1 equiv) over 10 min. After stirring for 30 min at  $-78\text{ }^{\circ}\text{C}$ , DMPU (3 mL, 25 mmol, 1.7 equiv) was added dropwise, followed by a solution of TBSCl (2.71 g, 18.0 mmol, 1.2 equiv) in THF (5 mL). The mixture was

stirred at  $-78\text{ }^{\circ}\text{C}$  for 30 min, then warmed to rt over 1 h. The solvent was removed in vacuo and the residue was taken up in pentane (100 mL), washed with  $\text{H}_2\text{O}$  (50 mL),  $\text{CuSO}_4$  (50 mL),  $\text{NaHCO}_3$  (50 mL), and brine (15 mL), dried over  $\text{Na}_2\text{SO}_4$ , and concentrated in vacuo to afford crude ketene acetal as a clear, yellow liquid. The crude material was further purified via vacuum distillation to yield the desired product as a colorless oil (1.79 g, 64%). bp  $72\text{--}74\text{ }^{\circ}\text{C}/20\text{ mTorr}$ ;  $^1\text{H NMR}$  (400 MHz,  $\text{CDCl}_3$ )  $\delta$  3.54 (s, 3H), 3.23 (d, 1H,  $J = 2.6\text{ Hz}$ ), 3.10 (d, 1H,  $J = 2.6\text{ Hz}$ ), 0.93 (s, 9H), 0.17 (s, 6H). All spectroscopic data are consistent with those previously reported.<sup>115</sup>

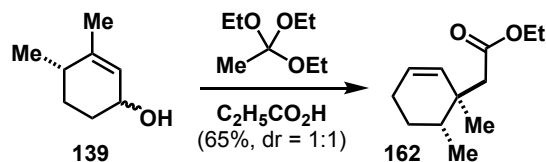


**2-(1,6-dimethylcyclohex-2-en-1-yl)-*N,N*-dimethylacetamide (159).** To a solution of alcohol **139** (300 mg, 2.37 mmol, 1 equiv) in anhydrous *p*-xylene (10 mL) was added *N,N*-dimethylacetamide dimethyl acetal (**158**, 3.46 mL, 23.7 mmol, 10 equiv). The solution was sparged with  $\text{N}_2$ , sealed and heated for 14 h at  $150\text{ }^{\circ}\text{C}$ . The reaction mixture was allowed to cool to rt and concentrated in vacuo. The crude product was purified by column chromatography (50% EtOAc/hexanes) to afford amide **159** as pale-yellow oil (300 mg, 66%, d.r. = 1:1).  $^1\text{H NMR}$  (600 MHz,  $\text{CDCl}_3$ ) 5.60 (d,  $J = 1.8\text{ Hz}$ , 1H), 5.57 – 5.44 (m, 1H), 2.94 (s, 6H), 2.47 (d,  $J = 13.2\text{ Hz}$ , 1H), 2.09 (dd,  $J = 13.3, 1.4\text{ Hz}$ , 1H), 2.03 – 1.95 (m, 2H), 1.84 – 1.76 (m, 1H), 1.48 – 1.37 (m, 2H), 1.22 (s, 3H), 0.93 (d, 2.48H), 0.91 (d, 2.30H).  $^{13}\text{C NMR}$  (600 MHz,  $\text{CDCl}_3$ )  $\delta$  171.8, 135.0, 126.6, 41.4, 39.9, 37.6, 32.9, 26.3, 25.1, 23.6, 19.2, 14.3. IR (ATR): 3022, 2919, 1635, 1495, 1452, 1389, 1200,

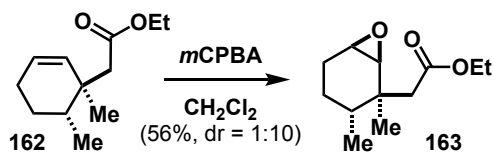
1034  $\text{cm}^{-1}$ . HRMS (ESI+)  $m/z$  calculated for  $\text{C}_{12}\text{H}_{22}\text{NO}$   $[\text{M}+\text{H}]^+$ : 196.1696, found: 196.1693;  $m/z$  calculated for  $\text{NaC}_{12}\text{H}_{21}\text{NO}$   $[\text{M}+\text{Na}]^+$ : 218.1515, found: 218.1507.



**7-iodo-3a,4-dimethylhexahydrobenzofuran-2(3H)-one (160)**. To a solution of amide **159** (100 mg, 0.51 mmol, 1 equiv) in 50:50 THF/ $\text{H}_2\text{O}$  was added iodine (194 mg, 1.53 mmol, 3 equiv). The reaction mixture was heated for 4 h at 60  $^\circ\text{C}$  and cooled to rt. The solution was quenched with  $\text{NaHSO}_4(\text{aq})$  and extracted with  $\text{Et}_2\text{O}$  (3 x 5 mL). The combined organic extracts were washed with brine (5 mL), dried over  $\text{MgSO}_4$ , and concentrated in vacuo. The crude product was purified by column chromatography (50%  $\text{EtOAc}$ /hexanes) to afford iodolactone **160** as yellow gummy solid (130 mg, 86%).  $^1\text{H}$  NMR (600 MHz,  $\text{CDCl}_3$ , mixture of diastereomers)  $\delta$  4.33 (d,  $J = 9.8$  Hz, 1H), 3.79 (ddd,  $J = 13.8, 9.8, 4.4$  Hz, 1H), 2.52 (dd,  $J = 17.0, 7.6$  Hz, 2H), 2.30 (d, 1H), 2.05–1.97 (m, 3H), 1.93 (d, 1H), 1.71–1.60 (m, 2H), 1.55–1.43 (m, 3H), 1.36 (s, 3H), 1.24 (s, 3H), 0.93 (ddd,  $J = 8.2, 6.7, 1.2$  Hz, 6H).  $^{13}\text{C}$  NMR (600 MHz,  $\text{CDCl}_3$ , mixture of diastereomers)  $\delta$  175.1, 174.4, 92.1, 87.9, 45.6, 44.0, 42.5, 37.7, 36.3, 34.5, 34.5, 32.5, 31.4, 28.4, 26.5, 25.8, 23.2, 20.3, 17.0, 16.1. IR (ATR): 2927, 2859, 1778, 1674, 1596, 1573, 1418, 1299, 1262, 1206, 1192, 1081, 1003, 931  $\text{cm}^{-1}$ . HRMS (ESI+)  $m/z$  calculated for  $\text{C}_{10}\text{H}_{16}\text{IO}_2$   $[\text{M}+\text{H}]^+$ : 295.0189, found: 295.0177.

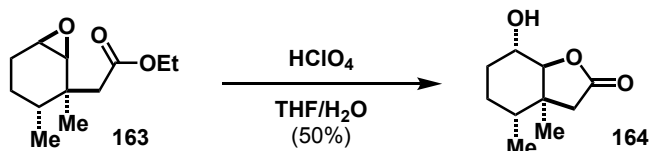


**Ethyl(1,6-dimethylcyclohex-2-en-1-yl)acetate (162).** A mixture of cyclohexenol **139** (500 mg, 3.96 mmol, 1 equiv), triethyl orthoacetate (TEOA, 5.5 mL, 30 mmol, 7.6 equiv) and propionic acid (2.2  $\mu\text{L}$ , 0.03 mmol, 0.007 equiv) was heated to 140  $^\circ\text{C}$  for 23 h in a flask equipped with a distillation head. The excess triethyl orthoacetate was removed via simple distillation, and the yellow liquid was purified by column chromatography eluting with acetone/hexanes (1:19 v/v) to afford a diastereomeric mixture of ester **162** as a colorless oil (320 mg, 41%, dr = 1:1).  $R_f$ : 0.36 (5:95 EtOAc/hexanes, UV,  $\text{KMnO}_4$  stain).  $^1\text{H}$  NMR (400 MHz,  $\text{CDCl}_3$ )  $\delta$  5.61 (m, 1H), 5.51 (dt,  $J = 10.1, 2.1$  Hz, 1H), 4.11 (q, 2H,  $J = 7.1$  Hz), 2.31 (s, 1H), 2.22 (d, 1H), 2.00 (m, 1H), 1.69 (m, 1H), 1.56 (m, 1H), 1.40 (m, 1H), 1.25 (t, 3H,  $J = 7.1$  Hz), 1.16 (s, 3H), 0.92 (d, 1.24H), 0.90 (d, 1.16H).  $^{13}\text{C}$  NMR (400 MHz,  $\text{CDCl}_3$ )  $\delta$  172.7, 60.1, 59.5, 54.9, 39.4, 36.3, 25.6, 24.2, 23.5, 21.2, 16.0, 14.3. IR (ATR): 3122, 2941, 2932, 1770, 1682, 1555, 1320, 1288, 1133, 1112, 1031, 1010  $\text{cm}^{-1}$ . HRMS (ESI+)  $m/z$  calculated for  $\text{C}_{12}\text{H}_{21}\text{O}_2$   $[\text{M}+\text{H}]^+$ : 197.1545, found: 197.1552



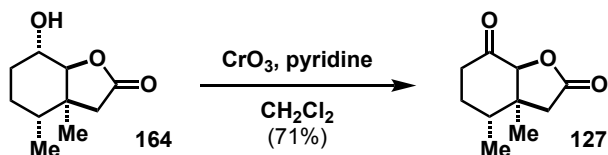
**Ethyl(2,3-dimethyl-7-oxabicyclo [4.1.0]heptan-2-yl)acetate (163).** To a solution of ester **162** (950 mg, 4.84 mmol, 1 equiv) in  $\text{CH}_2\text{Cl}_2$  (11 mL) was added *m*-chloroperbenzoic acid (2.00 g, 9.69 mmol, 2 equiv, 83.1% pure) portion-wise. After stirring for 8 h to 12 h at rt, the solution was quenched with  $\text{H}_2\text{O}$  and  $\text{Na}_2\text{SO}_3(\text{s})$  and

diluted with EtOAc (20 mL). The organic extract was washed with NaHCO<sub>3(aq)</sub> (3 x 10 mL), dried over Na<sub>2</sub>SO<sub>4</sub>, concentrated in vacuo, and purified by column chromatography eluting with EtOAc/hexanes (1:4 v/v) to afford epoxy ester **163** as a volatile colorless oil (706 mg, 69%). <sup>1</sup>H NMR (400 MHz, CDCl<sub>3</sub>) δ 4.15 (q, 2H), 3.26–3.06 (m, 2H), 2.48 (m, 2H), 2.09 (m, 2H), 1.88 (m, 1H), 1.72 (m, 1H), 1.59 (m, 1H), 1.27 (t, 3H), 1.25 (s, 3H), 1.23 (m, 1H), 0.80 (d, 3H). <sup>13</sup>C NMR (400 MHz, CDCl<sub>3</sub>) δ 172.7, 60.1, 59.5, 54.9, 39.4, 36.3, 25.6, 24.2, 23.5, 21.2, 16.0, 14.3. IR (ATR): 2962, 2857, 1764, 1579, 1342, 1289, 1263, 1151 cm<sup>-1</sup>. HRMS (ESI+) m/z calculated for C<sub>20</sub>H<sub>21</sub>O<sub>3</sub> [M+H]<sup>+</sup>: 213.1485, found: 213.1489.

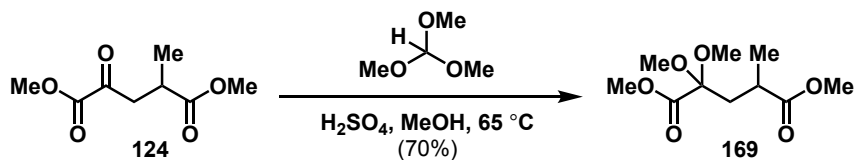


**1,6-Dimethyl-9-hydroxy-2-oxabicyclo[4.3.0]nonan-3-one (164)**. Epoxy ester **163** (506 mg, 2.38 mmol, 1 equiv) was taken in a mixture of THF/H<sub>2</sub>O/HClO<sub>4</sub> (10:5:0.5 v/v). After stirring for 20 h at rt, the solution was neutralized with 20% NaHCO<sub>3(aq)</sub> (1 mL) and extracted with Et<sub>2</sub>O (4 x 2 mL). The combined organic extract was dried over Na<sub>2</sub>SO<sub>4</sub>, concentrated in vacuo, and purified by column chromatography (40–45% EtOAc/hexanes) to afford hydroxy lactone **164** as colorless oil (220 mg, 50%). <sup>1</sup>H NMR (600 MHz, CDCl<sub>3</sub>) δ 3.88 (d, J = 8.2 Hz, 1H), 3.52 (ddd, J = 12.6, 8.2, 4.7 Hz, 1H), 2.40 (d, J = 17.0 Hz, 1H), 1.97 (d, J = 17.0 Hz, 1H), 1.92 (ddt, J = 13.0, 4.5, 3.1 Hz, 1H), 1.70 – 1.64 (m, 1H), 1.54 (dtd, J = 13.7, 6.8, 4.3 Hz, 1H), 1.39 – 1.30 (m, 2H), 1.22 (s, 3H), 0.93 (d, J = 6.8 Hz, 3H). <sup>13</sup>C NMR (600 MHz, CDCl<sub>3</sub>) δ 176.3, 91.8, 73.1, 44.5, 38.0,

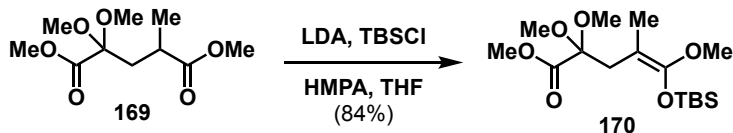
35.8, 29.9, 28.6, 26.5, 16.8. IR (ATR): 3431, 2936, 2874, 1772, 1487, 1262, 1101, 846  $\text{cm}^{-1}$ . HRMS (ESI<sup>-</sup>)  $m/z$  calculated for  $\text{C}_{10}\text{H}_{15}\text{O}_3$   $[\text{M}-\text{H}]^-$ : 183.1027, found: 183.1030.



**1,6-Dimethyl-2,9-oxabicyclo[4.3.0]nonan-3-one (127)**. To a  $0\text{ }^\circ\text{C}$  solution of anhydrous pyridine (25  $\mu\text{L}$ , 0.31 mmol, 6 equiv) in  $\text{CH}_2\text{Cl}_2$  (260  $\mu\text{L}$ ) was added  $\text{CrO}_3$  (15.6 mg, 0.16 mmol, 3 equiv). After stirring for 15 min at  $0\text{ }^\circ\text{C}$ , a solution of hydroxy lactone **164** (10 mg, 0.05 mmol, 1 equiv) in  $\text{CH}_2\text{Cl}_2$  (28  $\mu\text{L}$ ) was slowly added to the oxidizing mixture and stirred additionally for 20 h at  $0\text{ }^\circ\text{C}$ . The solution was decanted from the gummy residue and rinsed exhaustively with  $\text{CH}_2\text{Cl}_2$ . The combined organic extract was washed with sat.  $\text{NaHCO}_3(\text{aq})$  and brine, dried over  $\text{MgSO}_4$ , and concentrated in vacuo to yield lactone **127** as a brown oil (6.3 mg, 71%).  $^1\text{H}$  NMR (600 MHz,  $\text{CDCl}_3$ )  $\delta$  4.45 (s, 1H), 2.60 – 2.39 (m, 2H), 2.25 (d,  $J = 16.9$  Hz, 1H), 2.08 – 2.02 (m, 1H), 2.00 (dd,  $J = 16.8, 0.9$  Hz, 1H), 1.59 – 1.49 (m, 1H), 1.38 (d,  $J = 0.9$  Hz, 3H), 1.00 (d,  $J = 6.6$  Hz, 3H).  $^{13}\text{C}$  NMR (600 MHz,  $\text{CDCl}_3$ )  $\delta$  204.0, 173.3, 86.1, 48.7, 38.2, 36.7, 33.1, 28.6, 25.3, 15.3. IR (ATR): 2959, 2937, 2874, 1777, 1573, 1455, 1419, 1299, 1207, 1179, 1133, 1102, 1081, 1003, 958  $\text{cm}^{-1}$ . HRMS (ESI<sup>+</sup>)  $m/z$  calculated for  $\text{C}_{10}\text{H}_{15}\text{O}_3$   $[\text{M}+\text{H}]^+$ : 183.1016, found: 183.1018.

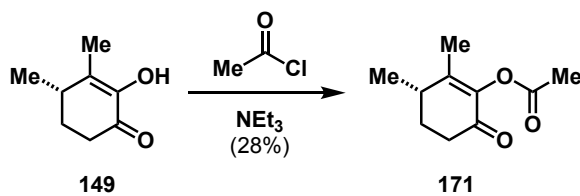


**Dimethyl-2,2-dimethoxy-4-methylpentanedioate (169).** To a solution of keto-diester **124** (139 mg, 0.73 mmol, 1 equiv) in anhydrous MeOH (0.3 mL) was added trimethyl orthoformate (0.20 mL, 1.80 mmol, 2.4 equiv) and H<sub>2</sub>SO<sub>4</sub> (1 drops). The reaction mixture was heated for 24 h at 65 °C and cooled to rt. The solution was quenched with NaHCO<sub>3(aq)</sub> and extracted with EtOAc (3 x 3 mL). The combined organic extract was dried over MgSO<sub>4</sub> and concentrated in vacuo to afford crude acetal **169** as a transparent, yellow liquid suitable for use without further purification (120 mg, 70%). <sup>1</sup>H NMR (500 MHz, CDCl<sub>3</sub>) δ 3.79 (d, J = 1.1 Hz, 3H), 3.66 (d, J = 1.1 Hz, 3H), 3.25 (s, 6H), 2.53 (dq, J = 13.1, 7.1 Hz, 1H), 2.44 (dd, J = 14.5, 8.4 Hz, 1H), 1.88 (dd, J = 14.6, 4.5 Hz, 1H), 1.17 (d, J = 7.0 Hz, 3H). <sup>13</sup>C NMR (500 MHz, CDCl<sub>3</sub>) δ 160.3, 159.6, 108.4, 63.6, 52.5, 50.0, 49.9, 37.1, 34.6, 18.5. IR (ATR): 2927, 2859, 1742, 1585, 1473, 1418, 1279, 1207, 1182, 1052, 1010 cm<sup>-1</sup>. HRMS (ESI+) m/z calculated for C<sub>10</sub>H<sub>19</sub>O<sub>6</sub> [M+H]<sup>+</sup>: 235.1176, found: 235.1176.



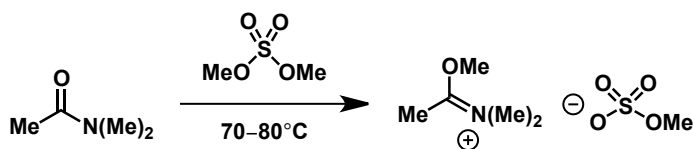
**Methyl-5-((*tert*-butyldimethylsilyl)oxy)-2,2,5-trimethoxy-4-methylpent-4-enoate (170).** To a -78 °C solution of anhydrous LDA (2 M solution, 0.2 mL, 0.47 mmol, 1.1 equiv) was added a solution of dimethyl acetal **169** (100 mg, 0.43 mmol, 1 equiv) in THF (1 mL) over 10 min. The mixture was stirred for an additional 15 min and then HMPA

(0.1 mL) was added, followed by a solution of TBSCl (68 mg, 0.45 mmol, 1.05 equiv) in THF (4.5 mL). The solution was warmed to rt and the solvent was removed in vacuo. The residue was taken up in hexanes (5 mL), washed with H<sub>2</sub>O (3 x 3 mL) and brine (3 mL), dried over Na<sub>2</sub>SO<sub>4</sub>, and concentrated in vacuo to afford crude ketene acetal **170** as a transparent, yellow liquid suitable for use without further purification (125 mg, 84%, 2:1 mixture of E/Z isomers). <sup>1</sup>H NMR for (*E*)-**170** (500 MHz, CDCl<sub>3</sub>) δ 3.76 (s, 3H), 3.49 (s, 3H), 3.28 (s, 6H), 2.59 (s, 2H), 1.56 (s, 3H), 0.95 (s, 9H), 0.14 (s, 6H). <sup>1</sup>H NMR for (*Z*)-**170** (500 MHz, CDCl<sub>3</sub>) δ 3.78 (s, 3H), 3.45 (s, 3H), 3.28 (s, 6H), 2.63 (s, 2H), 1.55 (s, 3H), 0.98 (s, 9H), 0.14 (s, 6H). <sup>13</sup>C NMR for (*E*)-**170** (500 MHz, CDCl<sub>3</sub>) δ 169.4, 152.7, 128.1, 101.3, 57.7, 52.1, 49.8, 35.1, 31.0, 25.5, 17.9, 14.8, -4.8. <sup>13</sup>C NMR for (*Z*)-**170** (500 MHz, CDCl<sub>3</sub>) δ 169.3, 151.9, 128.3, 102.7, 57.7, 52.5, 49.9, 37.1, 34.6, 25.6, 18.5, 13.6, -4.7. IR (ATR): 3087, 2897, 2844, 1749, 1483, 1317, 1289, 1229, 1177, 1051, 982 cm<sup>-1</sup>. HRMS (ESI+) m/z calculated for C<sub>16</sub>H<sub>33</sub>O<sub>6</sub>Si [M+H]<sup>+</sup>: 349.2041, found: 349.2054.

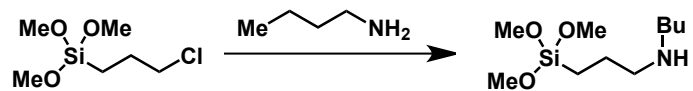


**2,3-Dimethyl-6-oxocyclohexenyl acetate (171).** To a 0 °C solution of enol **149** (10 mg, 0.07 mmol, 1 equiv) in CH<sub>2</sub>Cl<sub>2</sub> (160 μL) was added acetyl chloride (8 μL, 0.11 mmol, 1.50 equiv) dropwise. After stirring for 2 h at 0 °C, the mixture was quenched with H<sub>2</sub>O (1 mL), extracted with CH<sub>2</sub>Cl<sub>2</sub> (3 x 1 mL), dried over Na<sub>2</sub>SO<sub>4</sub>, and concentrated in vacuo. Purification by column chromatography (eluting with 30:70 EtOAc/hexanes) yielded acetate **171** as a pale-yellow oil (3.4 mg, 28%). R<sub>f</sub>: 0.34 (1:3 EtOAc/hexanes, UV, KMO<sub>4</sub>

stain);  $^1\text{H NMR}$  (400 MHz,  $\text{CDCl}_3$ )  $\delta$  2.62 (ddd,  $J = 17.1, 9.9, 5.7$  Hz, 2H), 2.45 (ddd,  $J = 17.1, 7.7, 4.9$  Hz, 1H), 2.25 (s, 3H), 2.23 – 2.16 (m, 2H), 1.85 (s, 3H), 1.78 (ddt,  $J = 10.5, 7.6, 5.3$  Hz, 1H), 1.24 (s, 3H). All spectroscopic data are consistent with those previously reported.<sup>126</sup>

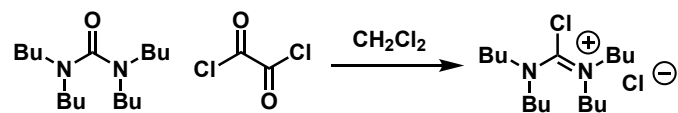


***N,N*-dimethylacetamide dimethyl sulfate complex.** To a 100 mL three-necked round bottom flask with thermometer and dry nitrogen inlet was added dimethyl sulfate (10.0 mL, 105 mmol, 1 equiv) and dimethylacetamide (10.0 mL, 108 mmol, 1 equiv). The mixture was heated to 70–80 °C for 3 h. After cooling in an ice-water bath, the solution was washed with dry PhH (7 mL) and dry  $\text{Et}_2\text{O}$  (2 x 6 mL). The washings were removed with a large syringe and the last traces of solvent were removed in vacuo to yield a colorless, viscous oil (21.32 g, 87%).  $^1\text{H NMR}$  (600 MHz,  $\text{CDCl}_3$ )  $\delta$  4.30 (s, 3H), 3.71 (s, 3H), 3.49 (s, 3H), 3.32 (s, 3H), 2.66 (s, 3H). All spectroscopic data are consistent with those previously reported.<sup>127</sup>

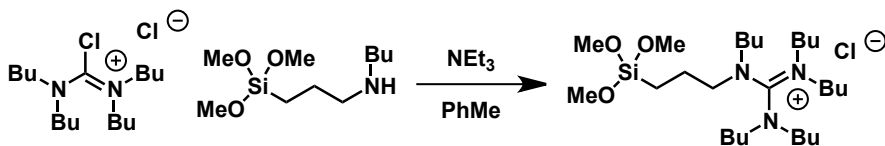


**[(*N*-butylamino) propyl] trimethoxysilane.** *n*-Butylamine (16 mL, 164 mmol, 3 equiv) was heated to 80 °C and (3-chloropropyl)trimethoxysilane (10 mL, 54 mmol, 1 equiv) was added dropwise. The temperature was maintained for 8 h. Warm petroleum ether (40 °C, 20 mL) was added at rt and the white precipitate was filtered at 0 °C. Evaporation of the solvent produced a tacky yellow slush that was passed through silica to afford the

appropriate product as a clear yellow liquid (11.9 g, 94%).  $^1\text{H}$  NMR (400 MHz,  $\text{CDCl}_3$ )  $\delta$  3.60 (s, 9H), 2.7 (q, 4H), 1.7–1.2 (m, 8H), 0.9–0.6 (m, 7H). All spectroscopic data are consistent with those previously reported.<sup>106</sup>

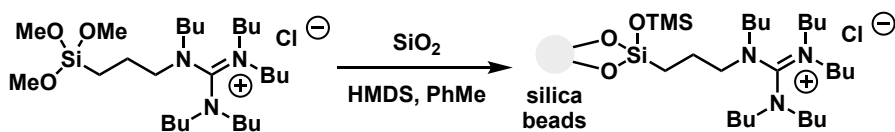


**Tetrabutylchloroformamidinium chloride salt (TBCA).** To a 0 °C solution of 1,1,3,3-tetrabutylurea (1 mL, 3.5 mmol, 1.0 equiv) in anhydrous PhMe (35 mL) was added oxalyl chloride (360  $\mu\text{L}$ , 4.2 mmol, 1.2 equiv). The solution was stirred at rt for 2 h, then warmed to 60 °C for 20 h. The dark yellow mixture was cooled, filtered under reduced pressure, and concentrated *in vacuo* to yield a dark brown oil suitable for use without further purification (1.12 g, 94%).  $^1\text{H}$  NMR (500 MHz,  $\text{CDCl}_3$ )  $\delta$  3.88 (t, 4H), 3.33 (t, 4H), 1.76–1.59 (m, 8H), 1.51–1.34 (m, 8H), 0.89 (t, 6H), 0.83 (t, 6H). All spectroscopic data are consistent with those previously reported.<sup>128</sup>

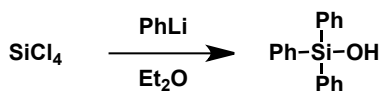


**Pentabutylpropyltrimethoxysilane guanidinium chloride.** [(N-butylamino) propyl] silane (820  $\mu\text{L}$ , 3.27 mmol, 1.0 equiv) and  $\text{NEt}_3$  (660  $\mu\text{L}$ , 4.71 mmol, 1.44 equiv) was taken in anhydrous PhMe (5 mL). A solution of tetrabutylchloroformamidinium chloride (TBCA) (1.12 g, 3.30 mmol, 1.01 equiv) in anhydrous PhMe (2 mL) was added. The temperature was raised to 70 °C and maintained for 4 h. Triethylammonium chloride was filtered by vacuum filtration and following removal of PhMe *in vacuo*, the guanidinium silane was obtained as a brown oil (1.78 g, quantitative).  $^1\text{H}$  NMR (500 MHz,  $\text{CDCl}_3$ )  $\delta$

3.6 (s, 9H), 3.2–2.9 (m, 12H), 1.91–1.1 (m, 22H), 0.9–0.6 (m, 17H). All spectroscopic data are consistent with those previously reported.<sup>128</sup>

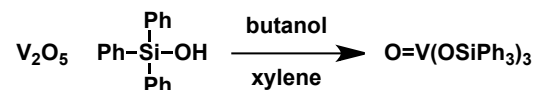


**Silica-supported pentabutyl propyl guanidinium chloride (PBGSiCl).** Silica (8.4 g) dried at 70 °C/20 mTorr was suspended in anhydrous PhMe (22 mL). A solution of guanidinium silane (1.78 g, 3.31 mmol, 1.0 equiv) in PhMe (4.5 mL) was added and the mixture was heated at reflux for 8 h. After filtration, washing with PhMe, and drying (18 h at 80 °C/20 mTorr), HMDS (860  $\mu$ L, 4.10 mmol, 1.24 equiv) was added to the functionalized silica in PhMe (50 mL) and the suspension was refluxed for 4 h. The beads were filtered, washed with PhMe, and dried for 18 h at 80 °C/20 mTorr to yield the catalyst as tan silica beads (8.5 g). All data are consistent with those previously reported.<sup>128</sup>

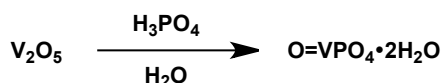


**Triphenylsilanol.** To a solution of silicon tetrachloride (2.5 mL, 21.8 mmol, 1 equiv) and Et<sub>2</sub>O (170 mL) at 0 °C was added a solution of phenyl lithium (1.9M solution, 34 mL, 65.3 mmol, 3 equiv) in Et<sub>2</sub>O over 3 h. The mixture was stirred overnight at rt, hydrolyzed with H<sub>2</sub>O and sat. NH<sub>4</sub>Cl<sub>(aq)</sub> at 0 °C and extracted with Et<sub>2</sub>O (2 x 15 mL). The combined organic layers were dried over Na<sub>2</sub>SO<sub>4</sub>, decolorized by stirring with charcoal (3 g) for 5 min, and concentrated in vacuo. The resulting residue was dissolved in boiling petroleum ether. Slow cooling to rt and refrigeration gave a white powder (3.23 g, 54%), which was

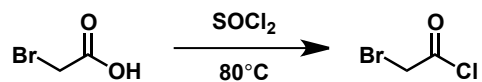
filtered off, washed with several portions of petroleum ether, and dried at 60 °C under vacuum. <sup>1</sup>H NMR (500 MHz, CDCl<sub>3</sub>) δ 7.84 – 7.32 (m, 18H), 2.48 (s, 1H). All spectroscopic data are consistent with those previously reported.<sup>129</sup>



**Tris(triphenylsilyl)vanadate(V).** Vanadium pentoxide (433 mg, 2.4 mmol, 1 equiv), triphenylsilanol (3.23g, 11.7 mmol, 4.9 equiv), butanol (1.0 mL, 11.7 mmol, 4.9 equiv), and xylene (14 mL) were refluxed, and the water formed was continuously removed using a Dean-Stark apparatus during 7 h. The black material was removed by filtration, washed with boiling xylenes (5 x 3 mL) and dried *in vacuo*. The combined filtrate was allowed to cool, and the pale gray solid (3.90 g) was isolated by filtration, washed with xylenes and hexanes, and dried over vacuum filtration. m.p. 222–225 °C. <sup>1</sup>H NMR (600 MHz, CDCl<sub>3</sub>) δ 7.54 – 7.46 (m, 18H), 7.45 – 7.36 (m, 9H), 7.22 (t, 18H). All data are consistent with those previously reported.<sup>129</sup>



**Vanadium phosphate.** Vanadium pentoxide (1.0 g, 5.5 mmol, 1 equiv) was refluxed in a solution of H<sub>2</sub>O (24 mL, 1337 mmol, 243 equiv) and concentrated H<sub>3</sub>PO<sub>4</sub> (13 mL, 109 mmol, 19.8 equiv) for 16 h under air. A green, crystalline solid (1.33 g) was isolated by vacuum filtration. The product was washed with small volumes of H<sub>2</sub>O and then ethanol and dried by suction in air. IR: 3540 (br), 1050 (s), 910 (s) cm<sup>-1</sup>. All data are consistent with those previously reported.<sup>130</sup>



**2-Bromoacetyl chloride.** A stirred solution of bromoacetic acid (2.5 g, 18.0 mmol, 1 equiv) in thionyl chloride (12.5 mL, 172 mmol, 9.6 equiv) was refluxed for 6 h. The reaction mixture was concentrated in vacuo to yield bromoacetyl chloride as a yellow liquid (2.52 g, 90%). <sup>1</sup>H NMR (500 MHz, CDCl<sub>3</sub>) δ 4.35 (s, 2H). All spectroscopic data are consistent with those previously reported.<sup>131</sup>

## 1.6 References

- (1) Christianson, D. W. Roots of Biosynthetic Diversity. *Science* **2007**, *316* (5821), 60–61. <https://doi.org/10.1126/science.1141630>.
- (2) Christianson, D. W. Structural and Chemical Biology of Terpenoid Cyclases. *Chem. Rev.* **2017**, *117* (17), 11570–11648. <https://doi.org/10.1021/acs.chemrev.7b00287>.
- (3) Blunt, J. W.; Copp, B. R.; Keyzers, R. A.; Munro, M. H. G.; Prinsep, M. R. Marine Natural Products. *Nat. Prod. Rep.* **2014**, *31* (2), 160–258. <https://doi.org/10.1039/C3NP70117D>.
- (4) Hanson, J. R. Diterpenoids of Terrestrial Origin. *Nat. Prod. Rep.* **2016**, *33* (10), 1227–1238. <https://doi.org/10.1039/C6NP00059B>.
- (5) Hanson, J. R. Diterpenoids of Terrestrial Origin. *Nat. Prod. Rep.* **2017**, *34* (10), 1233–1243. <https://doi.org/10.1039/C7NP00040E>.
- (6) Zhao, H.; Sun, L.; Kong, C.; Mei, W.; Dai, H.; Xu, F.; Huang, S. Phytochemical and Pharmacological Review of Diterpenoids from the Genus *Euphorbia* Linn (2012–2021). *J. Ethnopharmacol.* **2022**, *298*, 115574. <https://doi.org/10.1016/j.jep.2022.115574>.
- (7) Oldfield, E.; Lin, F.-Y. Terpene Biosynthesis: Modularity Rules. *Angew. Chem. Int. Ed.* **2012**, *51* (5), 1124–1137. <https://doi.org/10.1002/anie.201103110>.
- (8) Weston-Green, K.; Clunas, H.; Jimenez Naranjo, C. A Review of the Potential Use of Pinene and Linalool as Terpene-Based Medicines for Brain Health: Discovering Novel Therapeutics in the Flavours and Fragrances of Cannabis. *Front. Psychiatry* **2021**, *12*.
- (9) Hillier, S. G.; Lathe, R. Terpenes, Hormones and Life: Isoprene Rule Revisited. *J. Endocrinol.* **2019**, *242* (2), R9–R22. <https://doi.org/10.1530/JOE-19-0084>.
- (10) Wang, K. Terpenoids From the Sea: Chemical Diversity and Bioactivity. *Curr. Org. Chem.* *18* (7), 840–866.
- (11) Roncero, A. M.; Tobal, I. E.; Moro, R. F.; Díez, D.; Marcos, I. S. Halimane Diterpenoids: Sources, Structures, Nomenclature and Biological Activities. *Nat. Prod. Rep.* **2018**, *35* (9), 955–991. <https://doi.org/10.1039/C8NP00016F>.
- (12) Saha, P.; Rahman, F. I.; Hussain, F.; Rahman, S. M. A.; Rahman, M. M. Antimicrobial Diterpenes: Recent Development From Natural Sources. *Front. Pharmacol.* **2022**, *12*.

- (13) Dickschat, J. S. 1.16 - Biosynthesis of Diterpenoid Natural Products. In *Comprehensive Natural Products III*; Liu, H.-W. (Ben), Begley, T. P., Eds.; Elsevier: Oxford, 2020; pp 506–552. <https://doi.org/10.1016/B978-0-12-409547-2.14624-4>.
- (14) González-Burgos, E.; Gómez-Serranillos, M. P. Terpene Compounds in Nature: A Review of Their Potential Antioxidant Activity. *Curr. Med. Chem.* **2012**, *19* (31), 5319–5341. <https://doi.org/10.2174/092986712803833335>.
- (15) Devappa, R. K.; Makkar, H. P. S.; Becker, K. Jatropha Diterpenes: A Review. *J. Am. Oil Chem. Soc.* **2011**, *88* (3), 301–322. <https://doi.org/10.1007/s11746-010-1720-9>.
- (16) Miziorako, H. M. Enzymes of the Mevalonate Pathway of Isoprenoid Biosynthesis. *Arch. Biochem. Biophys.* **2011**, *505* (2), 131–143. <https://doi.org/10.1016/j.abb.2010.09.028>.
- (17) Lanzotti, V. Diterpenes for Therapeutic Use. In *Natural Products: Phytochemistry, Botany and Metabolism of Alkaloids, Phenolics and Terpenes*; Ramawat, K. G., Mérillon, J.-M., Eds.; Springer: Berlin, Heidelberg, 2013; pp 3173–3191. [https://doi.org/10.1007/978-3-642-22144-6\\_192](https://doi.org/10.1007/978-3-642-22144-6_192).
- (18) Jordão, F. M.; Kimura, E. A.; Katzin, A. M. Isoprenoid Biosynthesis in the Erythrocytic Stages of Plasmodium Falciparum. *Mem. Inst. Oswaldo Cruz* **2011**, *106*, 134–141. <https://doi.org/10.1590/S0074-02762011000900018>.
- (19) Eisenreich, W.; Bacher, A.; Arigoni, D.; Rohdich, F. Biosynthesis of Isoprenoids via the Non-Mevalonate Pathway. *Cell. Mol. Life Sci. CMLS* **2004**, *61* (12), 1401–1426. <https://doi.org/10.1007/s00018-004-3381-z>.
- (20) Karunanithi, P. S.; Zerbe, P. Terpene Synthases as Metabolic Gatekeepers in the Evolution of Plant Terpenoid Chemical Diversity. *Front. Plant Sci.* **2019**, *10*.
- (21) Yamada, Y.; Cane, D. E.; Ikeda, H. Chapter Seven - Diversity and Analysis of Bacterial Terpene Synthases. In *Methods in Enzymology*; Hopwood, D. A., Ed.; Natural Product Biosynthesis by Microorganisms and Plants, Part A; Academic Press, 2012; Vol. 515, pp 123–162. <https://doi.org/10.1016/B978-0-12-394290-6.00007-0>.
- (22) Rudolf, J. D.; Chang, C.-Y. Terpene Synthases in Disguise: Enzymology, Structure, and Opportunities of Non-Canonical Terpene Synthases. *Nat. Prod. Rep.* **2020**, *37* (3), 425–463. <https://doi.org/10.1039/c9np00051h>.
- (23) Dickschat, J. S. Bacterial Diterpene Biosynthesis. *Angew. Chem. Int. Ed.* **2019**, *58* (45), 15964–15976. <https://doi.org/10.1002/anie.201905312>.

- (24) Aaron, J. A.; Christianson, David. W. Trinuclear Metal Clusters in Catalysis by Terpenoid Synthases. *Pure Appl. Chem. Chim. Pure Appl.* **2010**, *82* (8), 1585–1597. <https://doi.org/10.1351/PAC-CON-09-09-37>.
- (25) Zi, J.; Mafu, S.; Peters, R. J. To Gibberellins and Beyond! Surveying the Evolution of (Di)Terpenoid Metabolism. *Annu. Rev. Plant Biol.* **2014**, *65* (1), 259–286. <https://doi.org/10.1146/annurev-arplant-050213-035705>.
- (26) Sacchettini, J. C.; Poulter, C. D. Creating Isoprenoid Diversity. *Science* **1997**, *277* (5333), 1788–1789. <https://doi.org/10.1126/science.277.5333.1788>.
- (27) Sul, Y. H.; Lee, M. S.; Cha, E. Y.; Thuong, P. T.; Khoi, N. M.; Song, I. S. An *Ent*-Kaurane Diterpenoid from *Croton Tonkinensis* Induces Apoptosis by Regulating AMP-Activated Protein Kinase in SK-HEP1 Human Hepatocellular Carcinoma Cells. *Biol. Pharm. Bull.* **2013**, *36* (1), 158–164. <https://doi.org/10.1248/bpb.b12-00873>.
- (28) Lambrechts, I. A.; Lall, N. Traditional Usage and Biological Activity of *Plectranthus Madagascariensis* and Its Varieties: A Review. *J. Ethnopharmacol.* **2021**, *269*, 113663. <https://doi.org/10.1016/j.jep.2020.113663>.
- (29) Kamal, N.; Mio Asni, N. S.; Rozlan, I. N. A.; Mohd Azmi, M. A. H.; Mazlan, N. W.; Mediani, A.; Baharum, S. N.; Latip, J.; Assaw, S.; Edrada-Ebel, R. A. Traditional Medicinal Uses, Phytochemistry, Biological Properties, and Health Applications of *Vitex Sp.* *Plants* **2022**, *11* (15), 1944. <https://doi.org/10.3390/plants11151944>.
- (30) Nie, Y.-W.; Li, Y.; Luo, L.; Zhang, C.-Y.; Fan, W.; Gu, W.-Y.; Shi, K.-R.; Zhai, X.-X.; Zhu, J.-Y. Phytochemistry and Pharmacological Activities of the Diterpenoids from the Genus *Daphne*. *Molecules* **2021**, *26* (21), 6598. <https://doi.org/10.3390/molecules26216598>.
- (31) Sumarni, U.; Reidel, U.; Eberle, J. Targeting Cutaneous T-Cell Lymphoma Cells by Ingenol Mebutate (PEP005) Correlates with PKC $\delta$  Activation, ROS Induction as Well as Downregulation of XIAP and c-FLIP. *Cells* **2021**, *10* (5), 987. <https://doi.org/10.3390/cells10050987>.
- (32) Ersvaer, E.; Kittang, A. O.; Hampson, P.; Sand, K.; Gjertsen, B. T.; Lord, J. M.; Bruserud, Ø. The Protein Kinase C Agonist PEP005 (Ingenol 3-Angelate) in the Treatment of Human Cancer: A Balance between Efficacy and Toxicity. *Toxins* **2010**, *2* (1), 174–194. <https://doi.org/10.3390/toxins2010174>.
- (33) Zhang, Q.; Wang, A.; Xu, Q.; Xia, X.; Tian, X.; Zhang, Y.; Li, X.; Yang, X.; Wang, X.; Peng, J.; Li, Y.; Liu, L.; Jin, S.; Meng, X.; Zhao, X.; GDLM group. Efficacy and Safety of Ginkgo Diterpene Lactone Meglumine in Acute Ischemic Stroke: A Randomized Clinical Trial. *JAMA Netw. Open* **2023**, *6* (8), e2328828. <https://doi.org/10.1001/jamanetworkopen.2023.28828>.

- (34) Mohammed, A.; Tajuddeen, N.; Ibrahim, M. A.; Isah, M. B.; Aliyu, A. B.; Islam, Md. S. Potential of Diterpenes as Antidiabetic Agents: Evidence from Clinical and Pre-Clinical Studies. *Pharmacol. Res.* **2022**, *179*, 106158. <https://doi.org/10.1016/j.phrs.2022.106158>.
- (35) Leiman, D.; Minkowitz, H.; Levitt, R. C.; Solanki, D.; Horn, D.; Janfaza, D.; Sarno, D.; Albores-Ibarra, N.; Bai, X.; Takeshita, K.; Zhao, T.; Lu, C.-W.; Bharathi, P.; Ahern, J.; Klineciewicz, S.; Nedeljkovic, S. S. Preliminary Results from a Phase 1b Double-Blind Study to Assess the Safety, Tolerability and Efficacy of Intra-Articular Administration of Resiniferatoxin or Placebo for the Treatment of Moderate to Severe Pain Due to Osteoarthritis of the Knee. *Osteoarthritis Cartilage* **2020**, *28*, S138. <https://doi.org/10.1016/j.joca.2020.02.228>.
- (36) Szallasi, A.; Blumberg, P. M. Resiniferatoxin and Its Analogs Provide Novel Insights into the Pharmacology of the Vanilloid (Capsaicin) Receptor. *Life Sci.* **1990**, *47* (16), 1399–1408. [https://doi.org/10.1016/0024-3205\(90\)90518-V](https://doi.org/10.1016/0024-3205(90)90518-V).
- (37) Kissin, I.; Szallasi, A. Therapeutic Targeting of TRPV1 by Resiniferatoxin, from Preclinical Studies to Clinical Trials. *Curr. Top. Med. Chem.* **11** (17), 2159–2170.
- (38) Xu, W.-H.; Liu, W.-Y.; Liang, Q. Chemical Constituents from Croton Species and Their Biological Activities. *Mol. J. Synth. Chem. Nat. Prod. Chem.* **2018**, *23* (9), 2333. <https://doi.org/10.3390/molecules23092333>.
- (39) Vasas, A.; Hohmann, J. Euphorbia Diterpenes: Isolation, Structure, Biological Activity, and Synthesis (2008–2012). *Chem. Rev.* **2014**, *114* (17), 8579–8612. <https://doi.org/10.1021/cr400541j>.
- (40) Kuo, P.-C.; Shen, Y.-C.; Yang, M.-L.; Wang, S.-H.; Thang, T. D.; Dung, N. X.; Chiang, P.-C.; Lee, K.-H.; Lee, E.-J.; Wu, T.-S. Crotonkinins A and B and Related Diterpenoids from Croton Tonkinensis as Anti-Inflammatory and Antitumor Agents. *J. Nat. Prod.* **2007**, *70* (12), 1906–1909. <https://doi.org/10.1021/np070383f>.
- (41) Uto, T.; Qin, G.-W.; Morinaga, O.; Shoyama, Y. 17-Hydroxy-Jolkinolide B, a Diterpenoid from Euphorbia Fischeriana, Inhibits Inflammatory Mediators but Activates Heme Oxygenase-1 Expression in Lipopolysaccharide-Stimulated Murine Macrophages. *Int. Immunopharmacol.* **2012**, *12* (1), 101–109. <https://doi.org/10.1016/j.intimp.2011.10.020>.
- (42) Corea, G.; Fattorusso, E.; Lanzotti, V.; Di Meglio, P.; Maffia, P.; Grassia, G.; Ialenti, A.; Ianaro, A. Discovery and Biological Evaluation of the Novel Naturally Occurring Diterpene Pepluanone as Antiinflammatory Agent. *J. Med. Chem.* **2005**, *48* (22), 7055–7062. <https://doi.org/10.1021/jm050321r>.

- (43) Sun, Y.; Wang, M.; Ren, Q.; Li, S.; Xu, J.; Ohizumi, Y.; Xie, C.; Jin, D.-Q.; Guo, Y. Two Novel Clerodane Diterpenenes with NGF-Potentiating Activities from the Twigs of *Croton Yanhuii*. *Fitoterapia* **2014**, *95*, 229–233. <https://doi.org/10.1016/j.fitote.2014.03.012>.
- (44) Pan, Z.; Ning, D.; Wu, X.; Huang, S.; Li, D.; Lv, S. New Clerodane Diterpenoids from the Twigs and Leaves of *Croton Euryphyllus*. *Bioorg. Med. Chem. Lett.* **2015**, *25* (6), 1329–1332. <https://doi.org/10.1016/j.bmcl.2015.01.033>.
- (45) Miana, G. A.; Riaz, M.; Shahzad-ul-Hussan, S.; Paracha, R. Z.; Paracha, U. Z. Prostratin: An Overview. *Mini-Rev. Med. Chem.* **15** (13), 1122–1130.
- (46) Bedoya, L. M.; Márquez, N.; Martínez, N.; Gutiérrez-Eisman, S.; Álvarez, A.; Calzado, M. A.; Rojas, J. M.; Appendino, G.; Muñoz, E.; Alcamí, J. SJ23B, a Jatrophone Diterpene Activates Classical PKCs and Displays Strong Activity against HIV in Vitro. *Biochem. Pharmacol.* **2009**, *77* (6), 965–978. <https://doi.org/10.1016/j.bcp.2008.11.025>.
- (47) Wardana, A. P.; Aminah, N. S.; Rosyda, M.; Abdjan, M. I.; Kristanti, A. N.; Tun, K. N. W.; Choudhary, M. I.; Takaya, Y. Potential of Diterpene Compounds as Antivirals, a Review. *Heliyon* **2021**, *7* (8), e07777. <https://doi.org/10.1016/j.heliyon.2021.e07777>.
- (48) Marcos, I. S.; Hernández, F. A.; Sexmero, M. J.; Díez, D.; Basabe, P.; Pedrero, A. B.; García, N.; Urones, J. G. Synthesis and Absolute Configuration of (–)-Chettaphanin I and (–)-Chettaphanin II. *Tetrahedron* **2003**, *59* (5), 685–694. [https://doi.org/10.1016/S0040-0\(02\)01564-8](https://doi.org/10.1016/S0040-0(02)01564-8).
- (49) Marcos, I.; Martínez, B.; Sexmero, M.; Díez, D.; Basabe, P.; Urones, J. Chemistry of Ent-Halimic Acid: Synthesis of [4.3.3]Propellanes. *Synthesis* **2006**, *2006* (22), 3865–3873. <https://doi.org/10.1055/s-2006-950300>.
- (50) Fráter, G.; Helmlinger, D.; Kraft, P. Synthesis of [4.3.3]Propellanes by Carbenium-Ion Rearrangement and Their Olfactory Characterization. *Helv. Chim. Acta* **2003**, *86* (3), 678–696. <https://doi.org/10.1002/hlca.200390067>.
- (51) Kraft, P.; Bajgrowicz, J. A.; Denis, C.; Fráter, G. Odds and Trends: Recent Developments in the Chemistry of Odorants. *Angew. Chem. Int. Ed.* **2000**, *39* (17), 2980–3010. [https://doi.org/10.1002/1521-3773\(20000901\)39:17<2980::AID-ANIE2980>3.0.CO;2-#](https://doi.org/10.1002/1521-3773(20000901)39:17<2980::AID-ANIE2980>3.0.CO;2-#).
- (52) Roncero, A. M.; Tobal, I. E.; Moro, R. F.; Díez, D.; Marcos, I. S. Halimanes and Cancer: Ent-Halimic Acid as a Starting Material for the Synthesis of Antitumor Drugs. *Front. Chem.* **2023**, *11*.

- (53) Silva, L.; Gomes, A. C.; Rodilla, J. M. L. Diterpene Lactones with Labdane, Halimane and Clerodane Frameworks. *Nat. Prod. Commun.* **2011**, *6* (4), 1934578X1100600410. <https://doi.org/10.1177/1934578X1100600410>.
- (54) Zhang, Y.; Li, X.; Xu, T. Total Synthesis of Bioactive Tetracyclic Norditerpene Dilactones. *Org. Biomol. Chem.* **2021**, *19* (42), 9138–9147. <https://doi.org/10.1039/D1OB01535D>.
- (55) Van Tamelen, E. E. Bioorganic Chemistry: Sterols and Acrylic Terpene Terminal Epoxides. *Acc. Chem. Res.* **1968**, *1* (4), 111–120. <https://doi.org/10.1021/ar50004a003>.
- (56) Johnson, W. S.; Kinnel, R. B. Stereospecific Tricyclization of a Polyolefinic Acetal. *J. Am. Chem. Soc.* **1966**, *88* (16), 3861–3862. <https://doi.org/10.1021/ja00968a035>.
- (57) Goldsmith, D. J.; Phillips, C. F. Structural and Stereochemical Course of in Vitro Epoxy Olefin Cyclization. Diterpenoid Intermediates. *J. Am. Chem. Soc.* **1969**, *91* (21), 5862–5870. <https://doi.org/10.1021/ja01049a028>.
- (58) Barrett, A.; Ma, T.-K.; Mies, T. Recent Developments in Polyene Cyclizations and Their Applications in Natural Product Synthesis. *Synthesis* **2019**, *51* (01), 67–82. <https://doi.org/10.1055/s-0037-1610382>.
- (59) Ishihara, K.; Nakamura, S.; Yamamoto, H. The First Enantioselective Biomimetic Cyclization of Polyprenoids. *J. Am. Chem. Soc.* **1999**, *121* (20), 4906–4907. <https://doi.org/10.1021/ja984064+>.
- (60) Ishihara, K.; Ishibashi, H.; Yamamoto, H. Enantioselective Biomimetic Cyclization of Homo(Polyprenyl)Arenes. A New Entry to (+)-Podcarpa-8,11,13-Triene Diterpenoids and (–)-Tetracyclic Polyprenoid of Sedimentary Origin. *J. Am. Chem. Soc.* **2001**, *123* (7), 1505–1506. <https://doi.org/10.1021/ja003541x>.
- (61) Ishibashi, H.; Ishihara, K.; Yamamoto, H. A New Artificial Cyclase for Polyprenoids: Enantioselective Total Synthesis of (–)-Chromazonarol, (+)-8-Epi-Puupehedione, and (–)-11'-Deoxytaondiol Methyl Ether. *J. Am. Chem. Soc.* **2004**, *126* (36), 11122–11123. <https://doi.org/10.1021/ja0472026>.
- (62) Surendra, K.; Corey, E. J. Highly Enantioselective Proton-Initiated Polycyclization of Polyenes. *J. Am. Chem. Soc.* **2012**, *134* (29), 11992–11994. <https://doi.org/10.1021/ja305851h>.
- (63) Surendra, K.; Qiu, W.; Corey, E. J. A Powerful New Construction of Complex Chiral Polycycles by an Indium(III)-Catalyzed Cationic Cascade. *J. Am. Chem. Soc.* **2011**, *133* (25), 9724–9726. <https://doi.org/10.1021/ja204142n>.

- (64) Sakakura, A.; Ukai, A.; Ishihara, K. Enantioselective Halocyclization of Polyprenoids Induced by Nucleophilic Phosphoramidites. *Nature* **2007**, *445* (7130), 900–903. <https://doi.org/10.1038/nature05553>.
- (65) Samanta, R. C.; Yamamoto, H. Catalytic Asymmetric Bromocyclization of Polyenes. *J. Am. Chem. Soc.* **2017**, *139* (4), 1460–1463. <https://doi.org/10.1021/jacs.6b13193>.
- (66) Arnold, A. M.; Pöthig, A.; Drees, M.; Gulder, T. NXS, Morpholine, and HFIP: The Ideal Combination for Biomimetic Haliranium-Induced Polyene Cyclizations. *J. Am. Chem. Soc.* **2018**, *140* (12), 4344–4353. <https://doi.org/10.1021/jacs.8b00113>.
- (67) Mullen, C. A.; Campbell, A. N.; Gagné, M. R. Asymmetric Oxidative Cation/Olefin Cyclization of Polyenes: Evidence for Reversible Cascade Cyclization. *Angew. Chem. Int. Ed.* **2008**, *47* (32), 6011–6014. <https://doi.org/10.1002/anie.200801423>.
- (68) Geier, M. J.; Gagné, M. R. Diastereoselective Pt Catalyzed Cycloisomerization of Polyenes to Polycycles. *J. Am. Chem. Soc.* **2014**, *136* (8), 3032–3035. <https://doi.org/10.1021/ja500656k>.
- (69) Rong, Z.; Echavarren, A. M. Broad Scope Gold(I)-Catalysed Polyenyne Cyclisations for the Formation of up to Four Carbon–Carbon Bonds. *Org. Biomol. Chem.* **2017**, *15* (10), 2163–2167. <https://doi.org/10.1039/C7OB00235A>.
- (70) Jeker, O. F.; Kravina, A. G.; Carreira, E. M. Total Synthesis of (+)-Asperolide C by Iridium-Catalyzed Enantioselective Polyene Cyclization. *Angew. Chem. Int. Ed.* **2013**, *52* (46), 12166–12169. <https://doi.org/10.1002/anie.201307187>.
- (71) Zhou, S.; Guo, R.; Yang, P.; Li, A. Total Synthesis of Septedine and 7-Deoxyseptedine. *J. Am. Chem. Soc.* **2018**, *140* (29), 9025–9029. <https://doi.org/10.1021/jacs.8b03712>.
- (72) Rendler, S.; MacMillan, D. W. C. Enantioselective Polyene Cyclization via Organo-SOMO Catalysis. *J. Am. Chem. Soc.* **2010**, *132* (14), 5027–5029. <https://doi.org/10.1021/ja100185p>.
- (73) Deng, H.; Cao, W.; Liu, R.; Zhang, Y.; Liu, B. Asymmetric Total Synthesis of Hispidanin A. *Angew. Chem. Int. Ed.* **2017**, *56* (21), 5849–5852. <https://doi.org/10.1002/anie.201700958>.
- (74) Aderogba, M. A.; Ndhlala, A. R.; Van Staden, J. Acetylcholinesterase Inhibitory Activity and Mutagenic Effects of Croton Penduliflorus Leaf Extract Constituents. *South Afr. J. Bot.* **2013**, *87*, 48–51. <https://doi.org/10.1016/j.sajb.2013.03.013>.

- (75) Lee, S. E.; Hwang, H. J.; Ha, J.-S.; Jeong, H.-S.; Kim, J. H. Screening of Medicinal Plant Extracts for Antioxidant Activity. *Life Sci.* **2003**, *73* (2), 167–179. [https://doi.org/10.1016/S0024-3205\(03\)00259-5](https://doi.org/10.1016/S0024-3205(03)00259-5).
- (76) Pal, P. K.; Nandi, M. K.; Singh, N. K. Detoxification of Croton Tiglium L. Seeds by Ayurvedic Process of Śodhana. *Anc. Sci. Life* **2014**, *33* (3), 157–161. <https://doi.org/10.4103/0257-7941.144619>.
- (77) Liu, Z.; Gao, W.; Zhang, J.; Hu, J. Antinociceptive and Smooth Muscle Relaxant Activity of Croton Tiglium L Seed: An In-Vitro and In-Vivo Study. *Iran. J. Pharm. Res. IJPR* **2012**, *11* (2), 611–620.
- (78) Jones, K. Review of Sangre de Drago (Croton Lechleri) - A South American Tree Sap in the Treatment of Diarrhea, Inflammation, Insect Bites, Viral Infections, and Wounds: Traditional Uses to Clinical Research. *J. Altern. Complement. Med.* **2003**, *9* (6), 877–896. <https://doi.org/10.1089/107555303771952235>.
- (79) Miller, M. J. S.; Vergnolle, N.; McKnight, W.; Musah, R. A.; Davison, C. A.; Trentacosti, A. M.; Thompson, J. H.; Sandoval, M.; Wallace, J. L. Inhibition of Neurogenic Inflammation by the Amazonian Herbal Medicine Sangre de Grado. *J. Invest. Dermatol.* **2001**, *117* (3), 725–730. <https://doi.org/10.1046/j.0022-202x.2001.01446.x>.
- (80) Ahmed, B.; Alam, T.; Varshney, M.; Khan, S. A. Hepatoprotective Activity of Two Plants Belonging to the Apiaceae and the Euphorbiaceae Family. *J. Ethnopharmacol.* **2002**, *79* (3), 313–316. [https://doi.org/10.1016/S0378-8741\(01\)00392-0](https://doi.org/10.1016/S0378-8741(01)00392-0).
- (81) Ngadjui, B. T.; Abegaz, B. M.; Keumedjio, F.; Folefoc, G. N.; Kapche, G. W. F. Diterpenoids from the Stem Bark of Croton Zambesicus. *Phytochemistry* **2002**, *60* (4), 345–349. [https://doi.org/10.1016/S0031-9422\(02\)00034-1](https://doi.org/10.1016/S0031-9422(02)00034-1).
- (82) Hanson, J. R. Diterpenoids. *Nat. Prod. Rep.* **2004**, *21* (6), 785–793. <https://doi.org/10.1039/B414026P>.
- (83) Sun, Y.; Wang, M.; Ren, Q.; Li, S.; Xu, J.; Ohizumi, Y.; Xie, C.; Jin, D.-Q.; Guo, Y. Two Novel Clerodane Diterpenes with NGF-Potentiating Activities from the Twigs of Croton Yanhuii. *Fitoterapia* **2014**, *95*, 229–233. <https://doi.org/10.1016/j.fitote.2014.03.012>.
- (84) Wang, G.-C.; Li, J.-G.; Li, G.-Q.; Xu, J.-J.; Wu, X.; Ye, W.-C.; Li, Y.-L. Clerodane Diterpenoids from Croton Crassifolius. *J. Nat. Prod.* **2012**, *75* (12), 2188–2192. <https://doi.org/10.1021/np300636k>.

- (85) Boonyarathanakornkit, L.; Che, C.; Fong, H. H. S.; Farnsworth, N. R. Constituents of Croton Crassifolius Roots. *Planta Med.* **1988**, *54* (01), 61–63. <https://doi.org/10.1055/s-2006-962339>.
- (86) Li, C.; Sun, X.; Yin, W.; Zhan, Z.; Tang, Q.; Wang, W.; Zhuo, X.; Wu, Z.; Zhang, H.; Li, Y.; Zhang, Y.; Wang, G. Crassifolins Q–W: Clerodane Diterpenoids From Croton Crassifolius With Anti-Inflammatory and Anti-Angiogenesis Activities. *Front. Chem.* **2021**, *9*, 733350. <https://doi.org/10.3389/fchem.2021.733350>.
- (87) Zhang, Z.-X.; Wu, P.-Q.; Li, H.-H.; Qi, F.-M.; Fei, D.-Q.; Hu, Q.-L.; Liu, Y.-H.; Huang, X.-L. Norcrassin A, a Novel C16 Tetranorditerpenoid, and Bicrotonol A, an Unusual Dimeric Labdane-Type Diterpenoid, from the Roots of Croton Crassifolius. *Org. Biomol. Chem.* **2018**, *16* (10), 1745–1750. <https://doi.org/10.1039/C7OB02991H>.
- (88) Zhang, Z.-X.; Li, H.-H.; Zhi, D.-J.; Wu, P.-Q.; Hu, Q.-L.; Yu, Y.-F.; Zhao, Y.; Yu, C.-X.; Fei, D.-Q. Norcrocrassinone: A Novel Tetranorditerpenoid Possessing a 6/6/5 Fused Ring System from Croton Crassifolius. *Tetrahedron Lett.* **2018**, *59* (45), 4028–4030. <https://doi.org/10.1016/j.tetlet.2018.09.060>.
- (89) Alaux, S.; Kusk, M.; Sagot, E.; Bolte, J.; Jensen, A. A.; Bräuner-Osborne, H.; Gefflaut, T.; Bunch, L. Chemoenzymatic Synthesis of a Series of 4-Substituted Glutamate Analogues and Pharmacological Characterization at Human Glutamate Transporters Subtypes 1–3. *J. Med. Chem.* **2005**, *48* (25), 7980–7992. <https://doi.org/10.1021/jm050597z>.
- (90) Wang, S.-Z.; Yamamoto, K.; Yamada, H.; Takahashi, T. Stereochemical Study on the Palladium(O)-Catalyzed Carbonylation of 3-(Methoxycarbonyloxy)-2-Methylenealkanoates and Analogues. *Tetrahedron* **1992**, *48* (12), 2333–2348. [https://doi.org/10.1016/S0040-4020\(01\)88755-X](https://doi.org/10.1016/S0040-4020(01)88755-X).
- (91) Marques, F. A.; Lenz, C. A.; Simonelli, F.; Maia, B. H. L. N. S.; Vellasco, A. P.; Eberlin, M. N. Structure Confirmation of a Bioactive Lactone Isolated from Otoba Parvifolia through the Synthesis of a Model Compound. *J. Nat. Prod.* **2004**, *67* (11), 1939–1941. <https://doi.org/10.1021/np049771x>.
- (92) White, J. D.; Grether, U. M.; Lee, C.-S. (R)-(+)-3,4-DIMETHYLCYCLOHEX-2-EN-1-ONE. *Org. Synth.* **2005**, *82*, 108. <https://doi.org/10.15227/orgsyn.082.0108>.
- (93) Jiang, C.-H.; Bhattacharyya, A.; Sha, C.-K. Enantiospecific Total Synthesis of (–)-Bakkenolide III and Formal Total Synthesis of (–)-Bakkenolides B, C, H, L, V, and X. *Org. Lett.* **2007**, *9* (17), 3241–3243. <https://doi.org/10.1021/ol071124k>.
- (94) Marino, J. P.; Jaen, J. C. Stereospecific Umpolung .Alpha.' Substitution of Ketones via Reactions of Organocuprates with Enol Ethers of .Alpha.,.Beta.-

- Epoxycyclohexanones. *J. Am. Chem. Soc.* **1982**, *104* (11), 3165–3172.  
<https://doi.org/10.1021/ja00375a039>.
- (95) Nicolaou, K. C.; Ding, H.; Richard, J.-A.; Chen, D. Y.-K. Total Synthesis of Echinopines A and B. *J. Am. Chem. Soc.* **2010**, *132* (11), 3815–3818.  
<https://doi.org/10.1021/ja9093988>.
- (96) Kou, K. G. M.; Li, B. X.; Lee, J. C.; Gallego, G. M.; Lebold, T. P.; DiPasquale, A. G.; Sarpong, R. Syntheses of Denudatine Diterpenoid Alkaloids: Cochlearenine, N-Ethyl-1 $\alpha$ -Hydroxy-17-Veratroyldictyzine, and Paniculamine. *J. Am. Chem. Soc.* **2016**, *138* (34), 10830–10833. <https://doi.org/10.1021/jacs.6b07268>.
- (97) Yang, N. C.; Finnegan, R. A. A New Method for the Epoxidation of  $\alpha,\beta$ -Unsaturated Ketones. *J. Am. Chem. Soc.* **1958**, *80* (21), 5845–5848.  
<https://doi.org/10.1021/ja01554a066>.
- (98) Taylor, S. K.; Fried, J. A.; Grassl, Y. N.; Marolewski, A. E.; Pelton, E. A.; Poel, T. J.; Rezanka, D. S.; Whittaker, M. R. Stereoselective Reactions of Ester Enolates with Epoxides. *J. Org. Chem.* **1993**, *58* (25), 7304–7307.  
<https://doi.org/10.1021/jo00077a069>.
- (99) Maslak, V.; Matović, R.; Saičić, R. N. Titanium Tetrachloride Promoted Reaction of Silyl Ketene Acetals with Epoxides: A New Method for the Synthesis of  $\gamma$ -Butanolides. *Tetrahedron Lett.* **2002**, *43* (31), 5411–5413.  
[https://doi.org/10.1016/S0040-4039\(02\)01070-5](https://doi.org/10.1016/S0040-4039(02)01070-5).
- (100) Fontaine, E.; Baltas, M.; Escudier, J.-M.; Gorrichon, L. Diastereoselectivity in the Lewis Acid Mediated Aldol Reaction of Chiral  $\alpha,\beta$ -Epoxyaldehydes with a Ketene Silyl Acetal. *Monatshefte Für Chem. Chem. Mon.* **1996**, *127* (5), 519–528.  
<https://doi.org/10.1007/BF00807077>.
- (101) Reetz, M. T.; Fox, D. N. A. Carbon-Carbon Bond Formation Catalyzed by Lithium Perchlorate in Dichloromethane. *Tetrahedron Lett.* **1993**, *34* (7), 1119–1122.  
[https://doi.org/10.1016/S0040-4039\(00\)77505-8](https://doi.org/10.1016/S0040-4039(00)77505-8).
- (102) Gnaneshwar, R.; Wadgaonkar, P. P.; Sivaram, S. The Mukaiyama–Michael Addition of a  $\beta,\beta$ -Dimethyl Substituted Silyl Ketene Acetal to  $\alpha,\beta$ -Unsaturated Ketones Using Tetra-n-Butylammonium Bibenzoate as a Nucleophilic Catalyst. *Tetrahedron Lett.* **2003**, *44* (32), 6047–6049. [https://doi.org/10.1016/S0040-4039\(03\)01511-9](https://doi.org/10.1016/S0040-4039(03)01511-9).
- (103) Poupart, M.-A.; Lassalle, G.; Paquette, L. A. INTRAMOLECULAR OXIDATIVE COUPLING OF A BIENOLATE: 4-METHYLTRICYCLO[2.2.2.0<sup>3,5</sup>]OCTANE-2,6-DIONE. *Org. Synth.* **1990**, *69*, 173.  
<https://doi.org/10.15227/orgsyn.069.0173>.

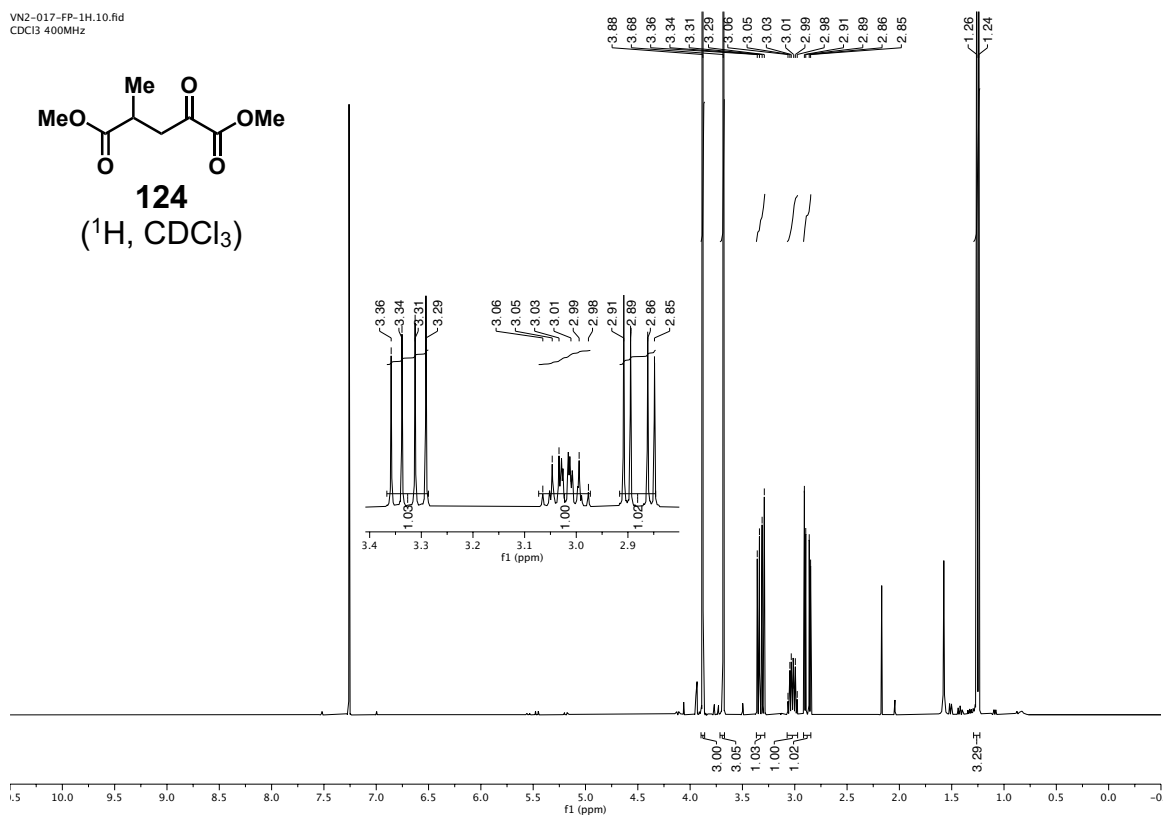
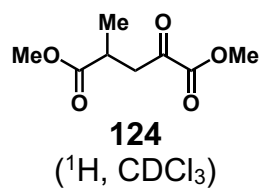
- (104) Bergmann, E. D.; Ginsburg, D.; Pappo, R. The Michael Reaction \* This Cooperative Study Was Begun When the Three Authors Were Working at the Weizmann Institute of Science, Rehovoth. In *Organic Reactions*; John Wiley & Sons, Ltd, 2011; pp 179–556. <https://doi.org/10.1002/0471264180.or010.03>.
- (105) Ho, T.-L. Hard Soft Acids Bases (HSAB) Principle and Organic Chemistry. *Chem. Rev.* **1975**, *75* (1), 1–20. <https://doi.org/10.1021/cr60293a001>.
- (106) Gros, P.; Le Perchec, P.; Senet, J. P. Reaction of Epoxides with Chlorocarbonylated Compounds Catalyzed by Hexaalkylguanidinium Chloride. *J. Org. Chem.* **1994**, *59* (17), 4925–4930. <https://doi.org/10.1021/jo00096a040>.
- (107) Chini, M.; Crotti, P.; Gardelli, C.; Macchia, F. Regio- and Stereoselective Synthesis of  $\beta$ -Halohydrins from 1,2-Epoxides with Ammonium Halides in the Presence of Metal Salts. *Tetrahedron* **1992**, *48* (18), 3805–3812. [https://doi.org/10.1016/S0040-4020\(01\)92271-9](https://doi.org/10.1016/S0040-4020(01)92271-9).
- (108) Spawn, C.-L.; Drtina, G. J.; Wiemer, D. F. Facile Conversion of Epoxides to Chlorohydrins with Titanium(IV) Chloride/ 1,8-Diazabicyclo[5.4.0]Undec-7-Ene. *Synthesis* **1986**, *1986* (04), 315–317. <https://doi.org/10.1055/s-1986-31596>.
- (109) Dowle, M. D.; Davies, D. I. Synthesis and Synthetic Utility of Halolactones. *Chem. Soc. Rev.* **1979**, *8* (2), 171–197. <https://doi.org/10.1039/CS9790800171>.
- (110) Bisai, V.; Sarpong, R. Methoxypyridines in the Synthesis of Lycopodium Alkaloids: Total Synthesis of ( $\pm$ )-Lycoposerramine R. *Org. Lett.* **2010**, *12* (11), 2551–2553. <https://doi.org/10.1021/ol100823t>.
- (111) Epstein, W. W.; Ollinger, J. Silver Ion Assisted Dimethyl Sulphoxide Oxidations of Organic Halides. *J. Chem. Soc. Chem. Commun.* **1970**, No. 20, 1338b–11339. <https://doi.org/10.1039/C2970001338B>.
- (112) Olejniczak, T.; Boratyński, F.; Białońska, A. Fungistatic Activity of Bicyclo[4.3.0]- $\gamma$ -Lactones. *J. Agric. Food Chem.* **2011**, *59* (11), 6071–6081. <https://doi.org/10.1021/jf105019u>.
- (113) Sinz, C. J.; Rychnovsky, S. D. Total Synthesis of the Polyene Macrolide Dermostatin A. *Tetrahedron* **2002**, *58* (32), 6561–6576. [https://doi.org/10.1016/S0040-4020\(02\)00666-X](https://doi.org/10.1016/S0040-4020(02)00666-X).
- (114) Tallmadge, E. H.; Jermaks, J.; Collum, D. B. Structure–Reactivity Relationships in Lithiated Evans Enolates: Influence of Aggregation and Solvation on the Stereochemistry and Mechanism of Aldol Additions. *J. Am. Chem. Soc.* **2016**, *138* (1), 345–355. <https://doi.org/10.1021/jacs.5b10980>.

- (115) Danishefsky, S.; Vaughan, K.; Gadwood, R.; Tsuzuki, K. Total Synthesis of DI-Quadrone. *J. Am. Chem. Soc.* **1981**, *103* (14), 4136–4141. <https://doi.org/10.1021/ja00404a026>.
- (116) G. Williams, D. B.; Cullen, A.; Fourie, A.; Henning, H.; Lawton, M.; Mommsen, W.; Nangu, P.; Parker, J.; Renison, A. Mild Water -Promoted Selective Deacetalisation of Acyclic Acetals. *Green Chem.* **2010**, *12* (11), 1919–1921. <https://doi.org/10.1039/C0GC00280A>.
- (117) Dalpozzo, R.; Nino, A. D.; Maiuolo, L.; Nardi, M.; Procopio, A.; Tagarelli, A. Er(OTf)<sub>3</sub> as a Mild Cleaving Agents for Acetals and Ketals. *Synthesis* **2004**, *2004* (04), 496–498. <https://doi.org/10.1055/s-2004-815941>.
- (118) Chu, X.-J.; Bartkovitz, D.; Danho, W.; Swistok, J.; Cheung, A. W.-H.; Kurylko, G.; Rowan, K.; Yeon, M.; Franco, L.; Qi, L.; Chen, L.; Yagaloff, K. Discovery of 1-Amino-4-Phenylcyclohexane-1-Carboxylic Acid and Its Influence on Agonist Selectivity between Human Melanocortin-4 and -1 Receptors in Linear Pentapeptides. *Bioorg. Med. Chem. Lett.* **2005**, *15* (22), 4910–4914. <https://doi.org/10.1016/j.bmcl.2005.08.012>.
- (119) Lin, C.-T.; Shih, J.-H.; Chen, C.-L.; Yang, D.-Y. Synthesis of Novel Triketone-Based Acidichromic Colorants. *Tetrahedron Lett.* **2005**, *46* (30), 5033–5037. <https://doi.org/10.1016/j.tetlet.2005.05.070>.
- (120) Romanski, S.; Kraus, B.; Guttentag, M.; Schlundt, W.; Rücker, H.; Adler, A.; Neudörfl, J.-M.; Alberto, R.; Amslinger, S.; Schmalz, H.-G. Acyloxybutadiene Tricarbonyl Iron Complexes as Enzyme-Triggered CO-Releasing Molecules (ET-CORMs): A Structure–Activity Relationship Study. *Dalton Trans.* **2012**, *41* (45), 13862–13875. <https://doi.org/10.1039/C2DT30662J>.
- (121) Jacob, J.; Espenson, J. H.; Jensen, J. H.; Gordon, M. S. 1,3-Transposition of Allylic Alcohols Catalyzed by Methyltrioxorhenium. *Organometallics* **1998**, *17* (9), 1835–1840. <https://doi.org/10.1021/om971115n>.
- (122) Akai, S.; Hanada, R.; Fujiwara, N.; Kita, Y.; Egi, M. One-Pot Synthesis of Optically Active Allyl Esters via Lipase–Vanadium Combo Catalysis. *Org. Lett.* **2010**, *12* (21), 4900–4903. <https://doi.org/10.1021/ol102053a>.
- (123) Mori, A.; Yamamoto, H. Resolution of Ketones via Chiral Acetals. Kinetic Approach. *J. Org. Chem.* **1985**, *50* (25), 5444–5446. <https://doi.org/10.1021/jo00225a108>.
- (124) Kitamura, Masato.; Ohkuma, Takeshi.; Inoue, Shinichi.; Sayo, Noboru.; Kumobayashi, Hidenori.; Akutagawa, Susumu.; Ohta, Tetsuo.; Takaya, Hidemasa.;

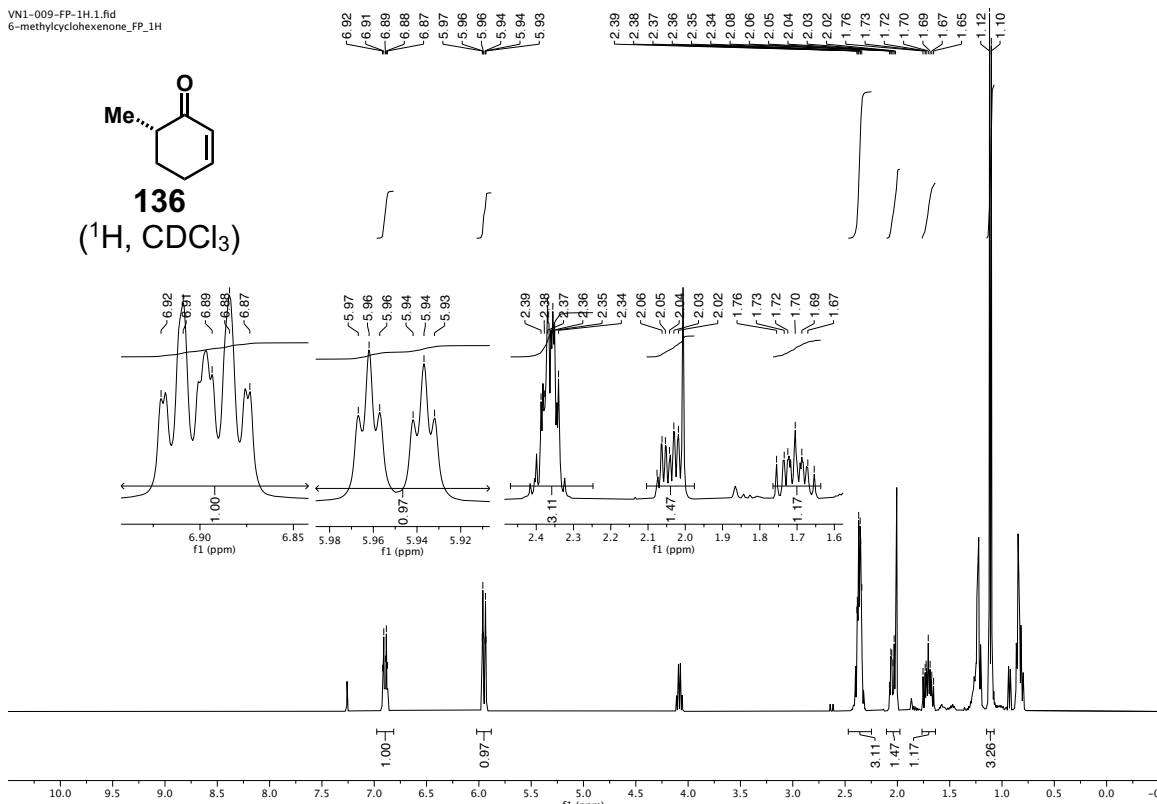
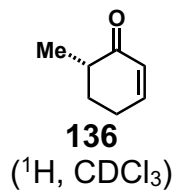
- Noyori, Ryoji. Homogeneous Asymmetric Hydrogenation of Functionalized Ketones. *J. Am. Chem. Soc.* **1988**, *110* (2), 629–631. <https://doi.org/10.1021/ja00210a070>.
- (125) Okabayashi, T.; Iida, A.; Takai, K.; Nawate, Y.; Misaki, T.; Tanabe, Y. Practical and Robust Method for Regio- and Stereoselective Preparation of (E)-Ketene Tert-Butyl TMS Acetals and  $\beta$ -Ketoester-Derived Tert-Butyl (1Z,3E)-1,3-Bis(TMS)Dienol Ethers. *J. Org. Chem.* **2007**, *72* (21), 8142–8145. <https://doi.org/10.1021/jo701456t>.
- (126) Lin, C.-T.; Shih, J.-H.; Chen, C.-L.; Yang, D.-Y. Synthesis of Novel Triketone-Based Acidichromic Colorants. *Tetrahedron Lett.* **2005**, *46* (30), 5033–5037. <https://doi.org/10.1016/j.tetlet.2005.05.070>.
- (127) Salomon, R. G.; Raychaudhuri, S. R. Convenient Preparation of N,N-Dimethylacetamide Dimethyl Acetal. *J. Org. Chem.* **1984**, *49* (19), 3659–3660. <https://doi.org/10.1021/jo00193a045>.
- (128) Su, D.; Duan, H.; Wei, Z.; Cao, J.; Liang, D.; Lin, Y. Condensation of Vilsmeier Salts, Derived from Tetraalkylureas, with Amidoximes: A Novel Approach to Access N,N-Dialkyl-1,2,4-Oxadiazol-5-Amines. *Tetrahedron Lett.* **2013**, *54* (50), 6959–6963. <https://doi.org/10.1016/j.tetlet.2013.10.061>.
- (129) Pauling, H.; Andrews, D. A.; Hindley, N. C. The Rearrangement of  $\alpha$ -Acetylenic Alcohols to  $\alpha$ ,  $\beta$ -Unsaturated Carbonyl Compounds by Silylvanadate Catalysts. *Helv. Chim. Acta* **1976**, *59* (4), 1233–1243. <https://doi.org/10.1002/hlca.19760590426>.
- (130) Johnson, J. W.; Jacobson, A. J.; Brody, J. F.; Rich, S. M. Coordination Intercalation Reactions of the Layered Compounds Vanadyl Phosphate (VOPO<sub>4</sub>) and Vanadyl Arsenate (VOAsO<sub>4</sub>) with Pyridine. *Inorg. Chem.* **1982**, *21* (10), 3820–3825. <https://doi.org/10.1021/ic00140a044>.
- (131) Wang, Z.; Yu, Z.; Kang, D.; Zhang, J.; Tian, Y.; Daelemans, D.; De Clercq, E.; Pannecouque, C.; Zhan, P.; Liu, X. Design, Synthesis and Biological Evaluation of Novel Acetamide-Substituted Doravirine and Its Prodrugs as Potent HIV-1 NNRTIs. *Bioorg. Med. Chem.* **2019**, *27* (3), 447–456. <https://doi.org/10.1016/j.bmc.2018.12.039>.

## 1.7 Selected NMR Spectra

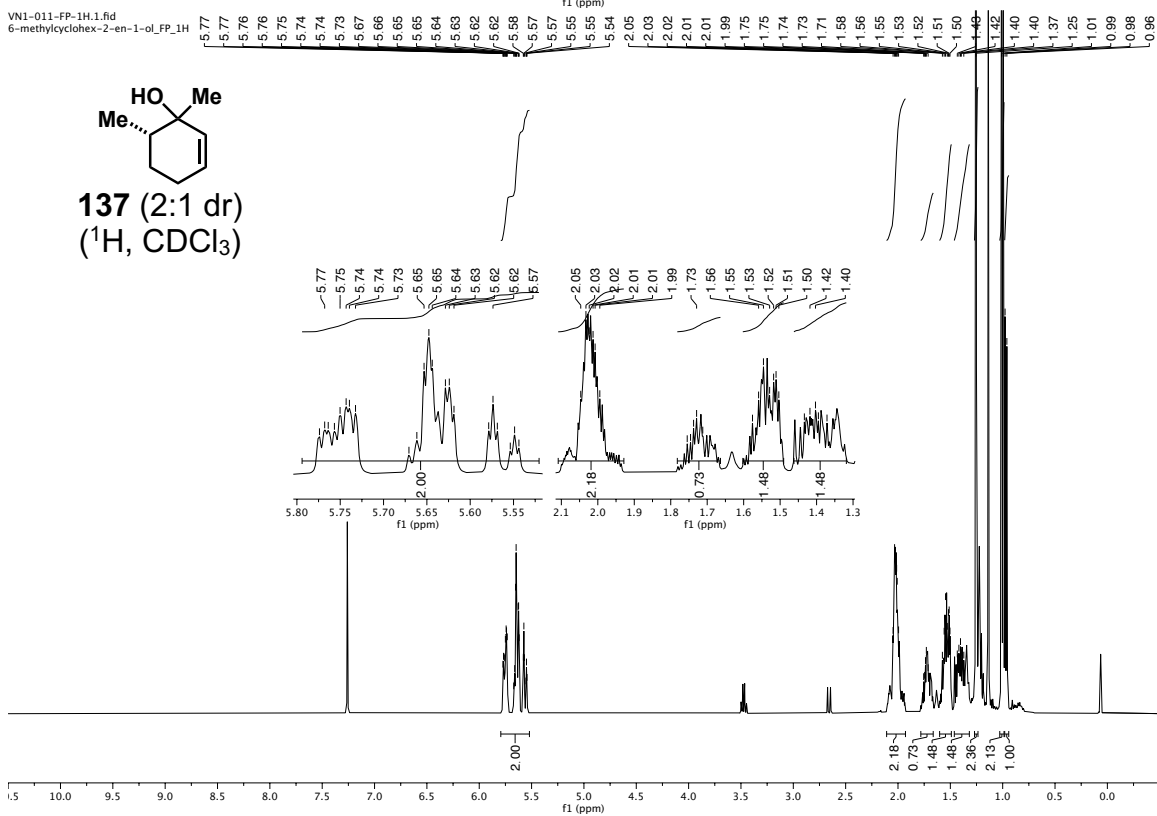
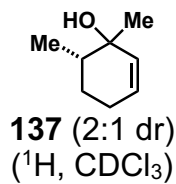
VN2-017-FP-1H.10.fid  
CDCl<sub>3</sub> 400MHz



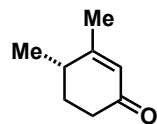
VN1-009-FP-1H.1.fid  
6-methylcyclohexenone\_FP\_1H



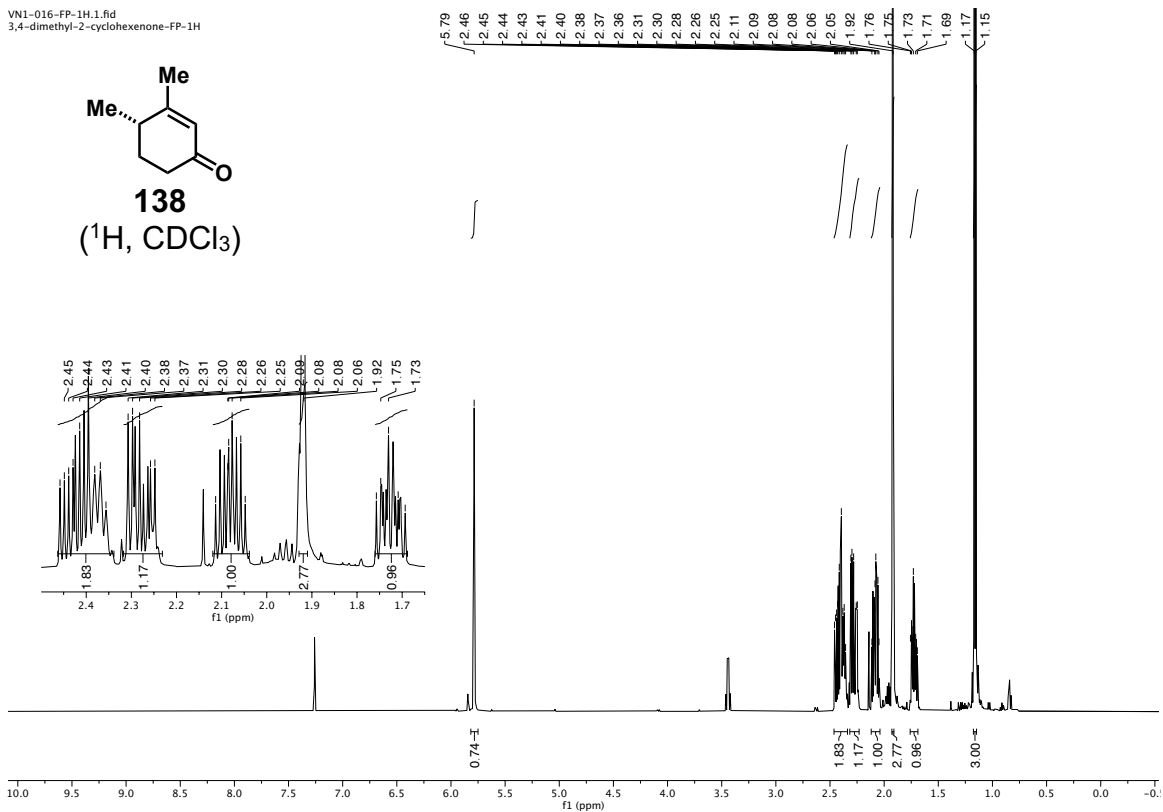
VN1-011-FP-1H.1.fid  
6-methylcyclohex-2-en-1-ol\_FP\_1H



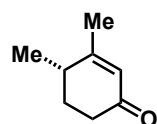
VN1-016-FP-1H.1.fid  
3,4-dimethyl-2-cyclohexenone-FP-1H



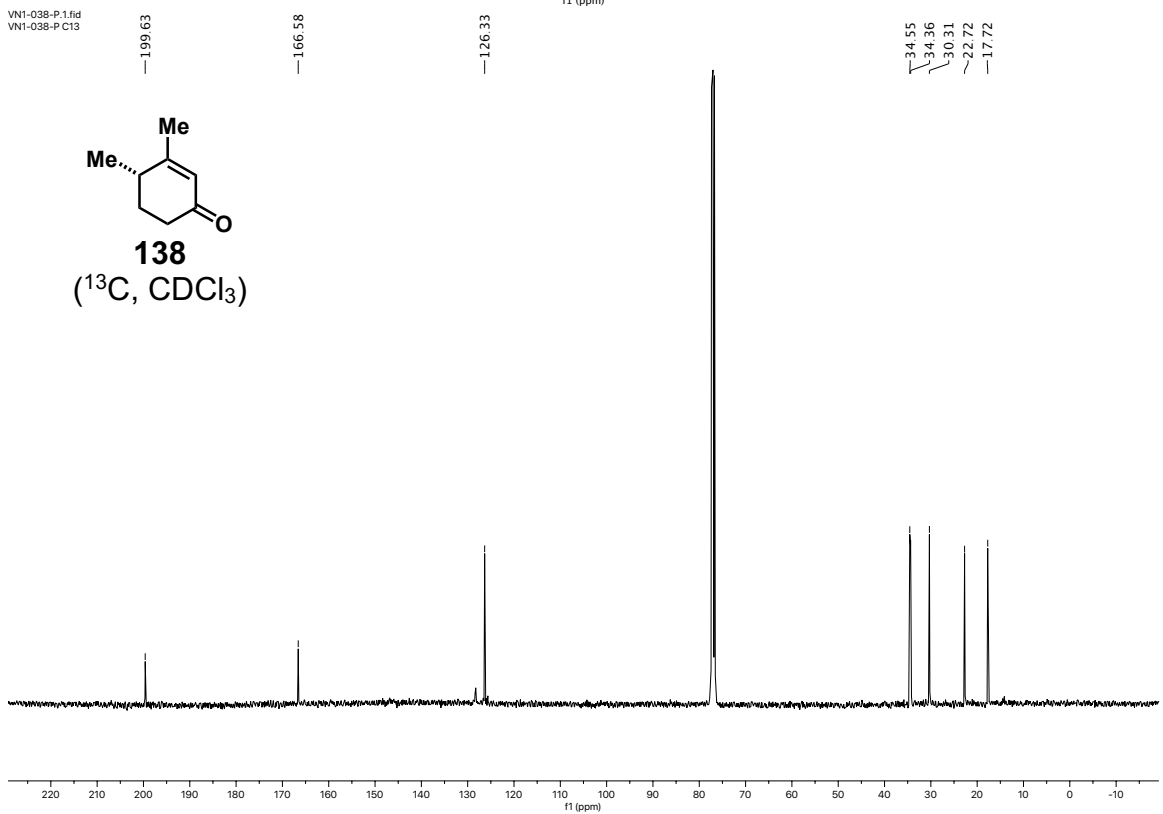
**138**  
(<sup>1</sup>H, CDCl<sub>3</sub>)



VN1-038-P.1.fid  
VN1-038-P.C13

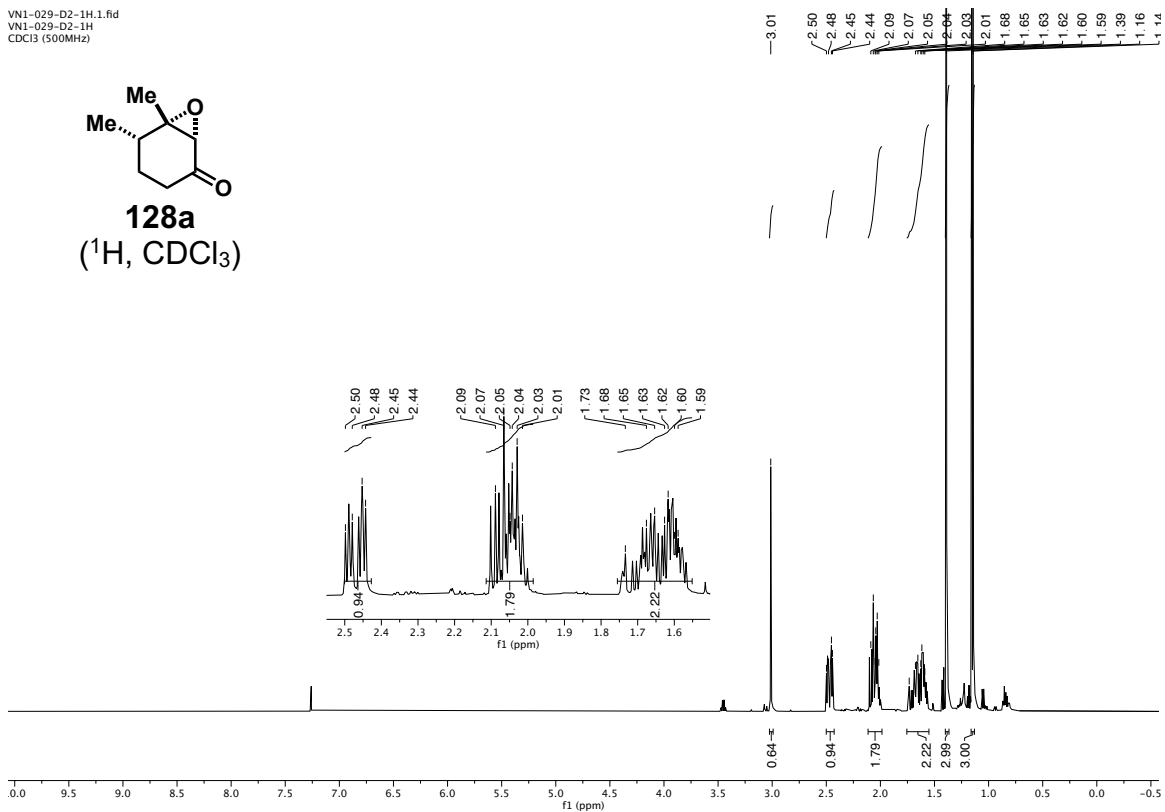
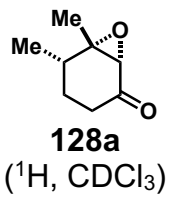


**138**  
(<sup>13</sup>C, CDCl<sub>3</sub>)

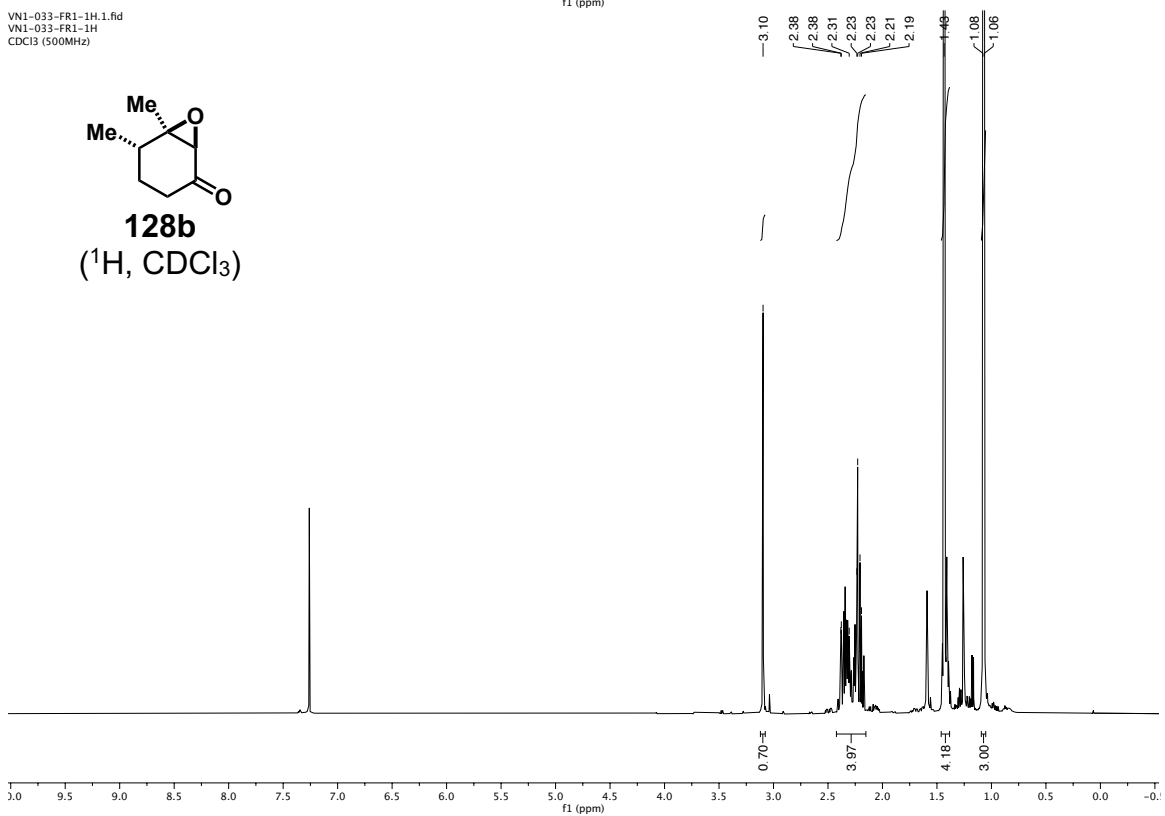
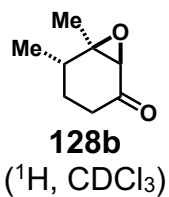




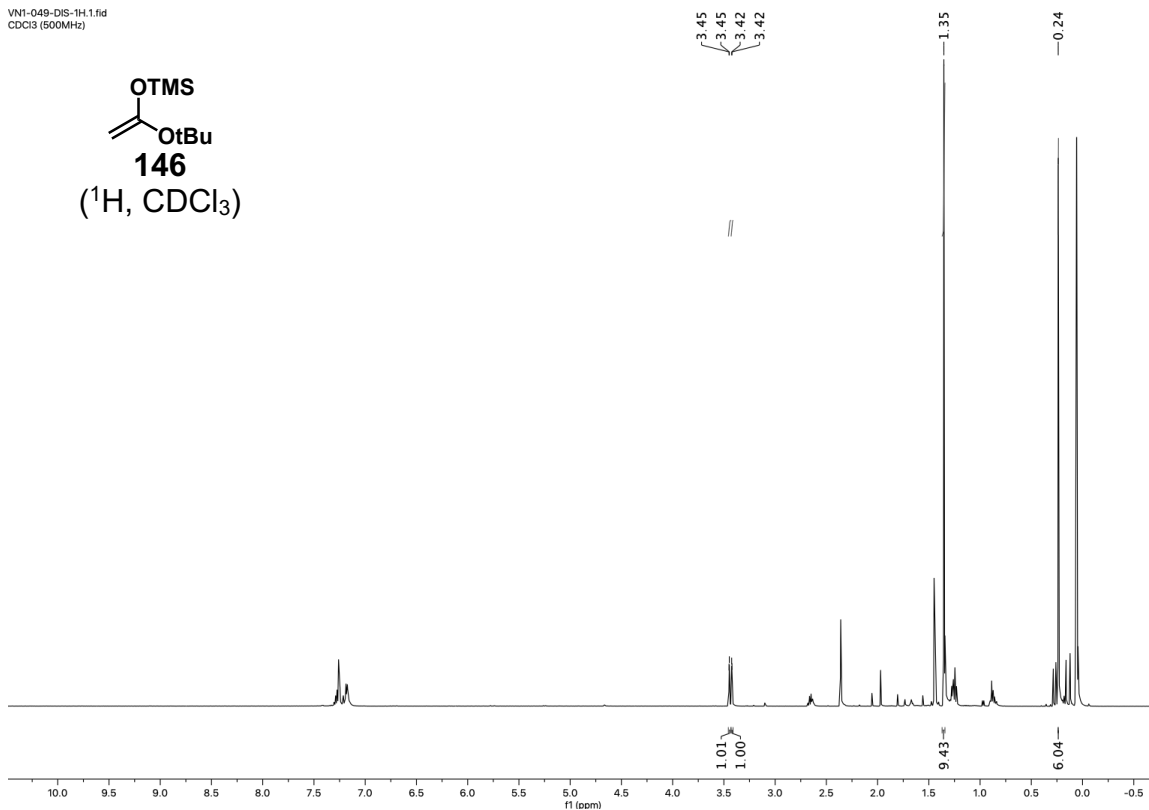
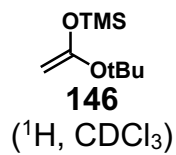
VN1-029-D2-1H.1.fid  
VN1-029-D2-1H  
CDCl<sub>3</sub> (500MHz)



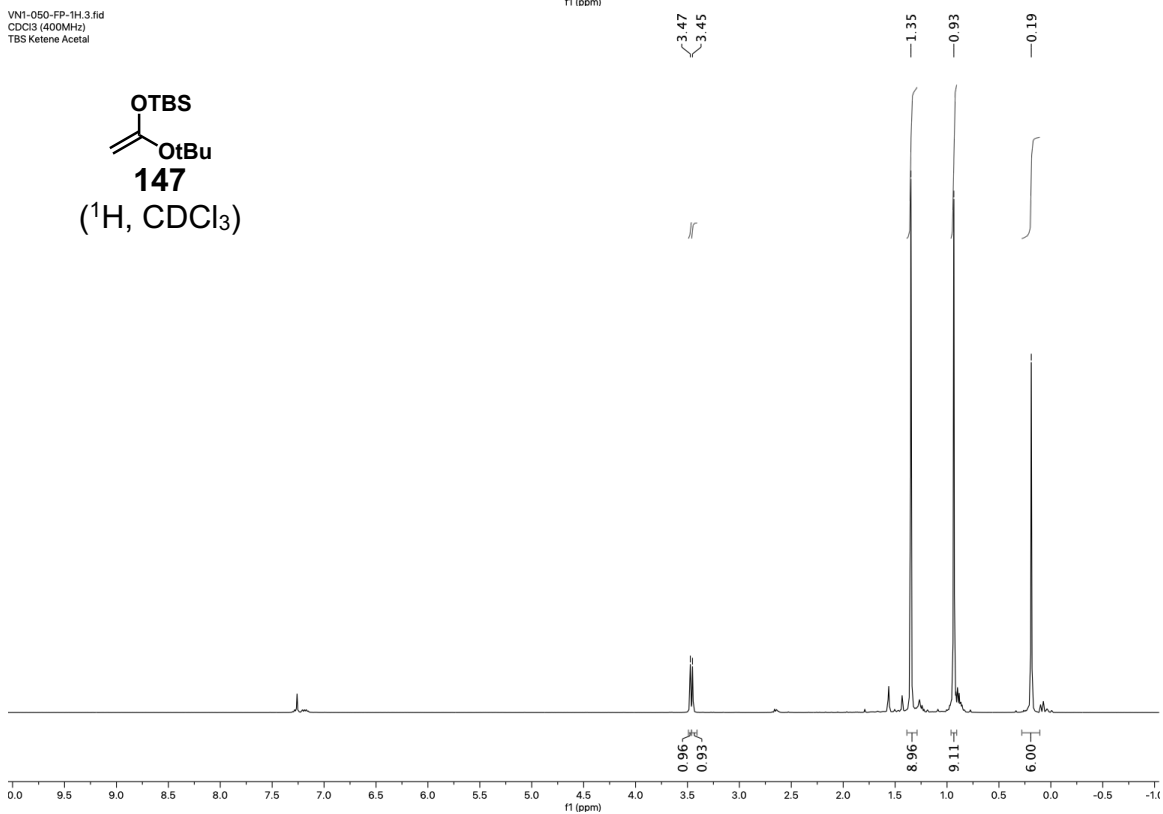
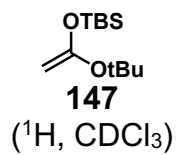
VN1-033-FR1-1H.1.fid  
VN1-033-FR1-1H  
CDCl<sub>3</sub> (500MHz)



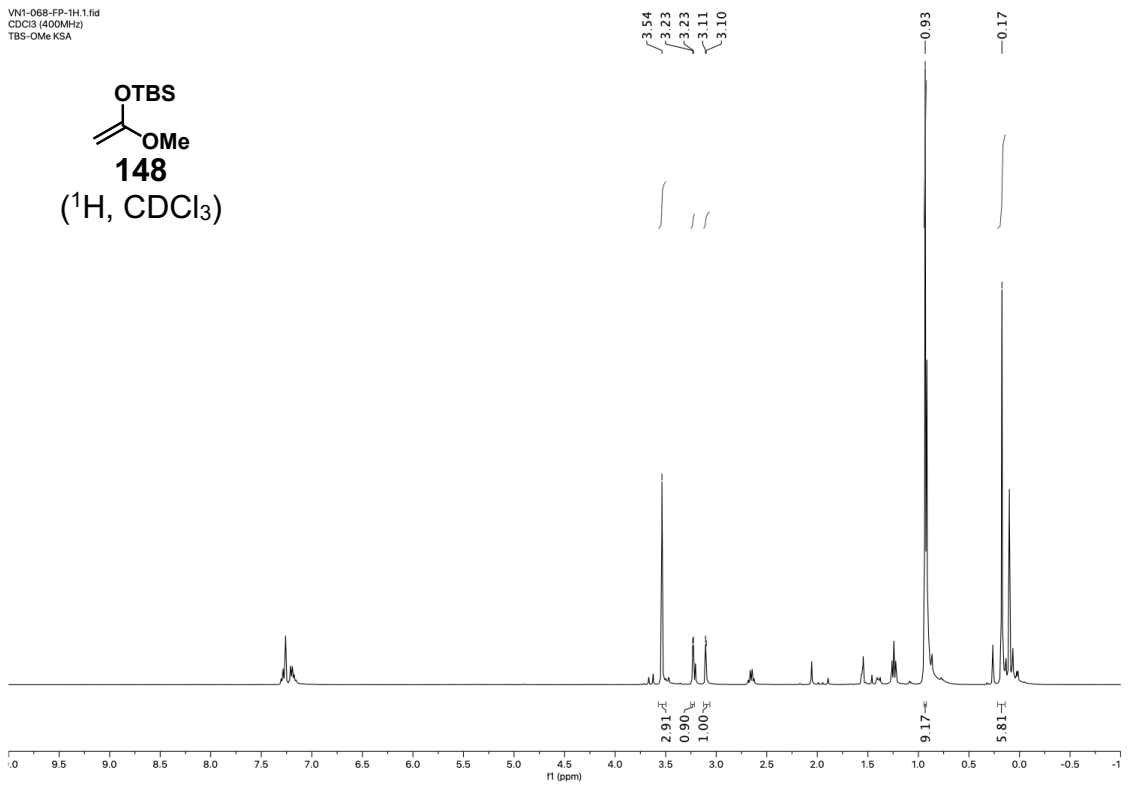
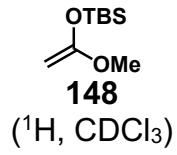
VN1-049-DIS-1H.1.fid  
CDCl3 (500MHz)



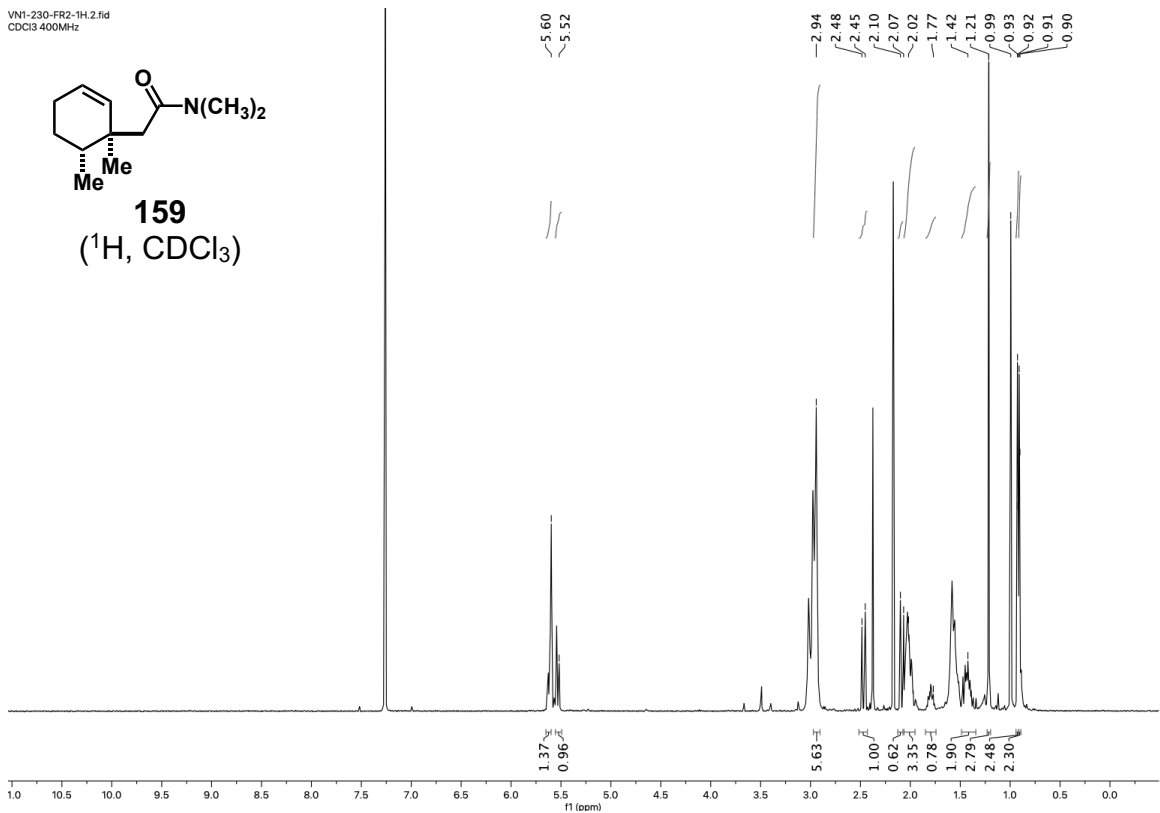
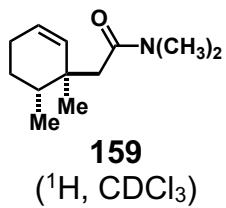
VN1-050-FP-1H.3.fid  
CDCl3 (400MHz)  
TBS Ketene Acetal



VN1-068-FP-1H1.fid  
CDCl3 (400MHz)  
TBS-OMe KSA



VN1-230-FR2-1H2.fid  
CDCl3 400MHz



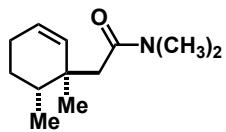
VN1-230-FR1-13C.1.fid  
CDCl<sub>3</sub> 400MHz

—171.86

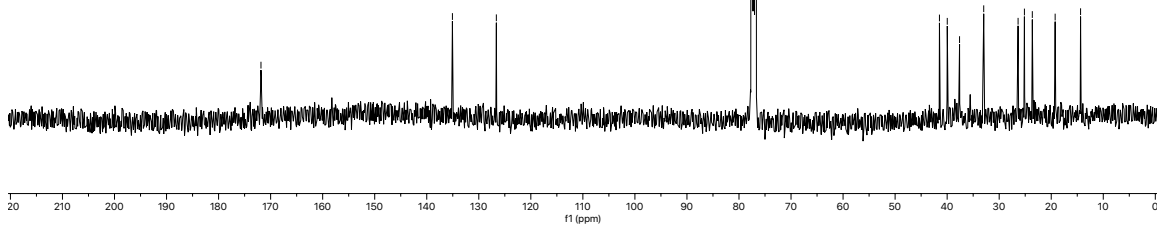
—135.07

—126.63

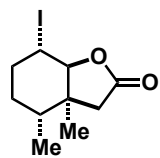
41.48  
39.98  
37.62  
32.97  
26.37  
25.15  
23.63  
19.25  
14.36



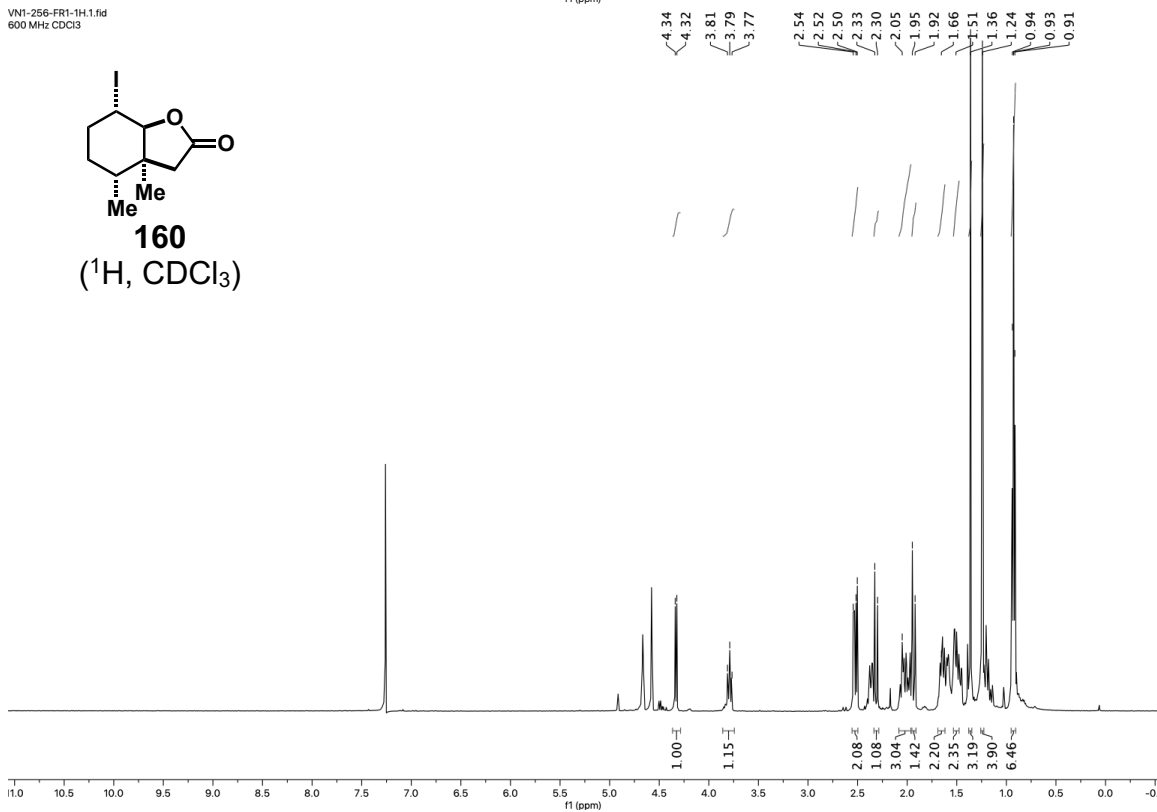
**159**  
(<sup>13</sup>C, CDCl<sub>3</sub>)



VN1-256-FR1-1H.1.fid  
600 MHz CDCl<sub>3</sub>



**160**  
(<sup>1</sup>H, CDCl<sub>3</sub>)

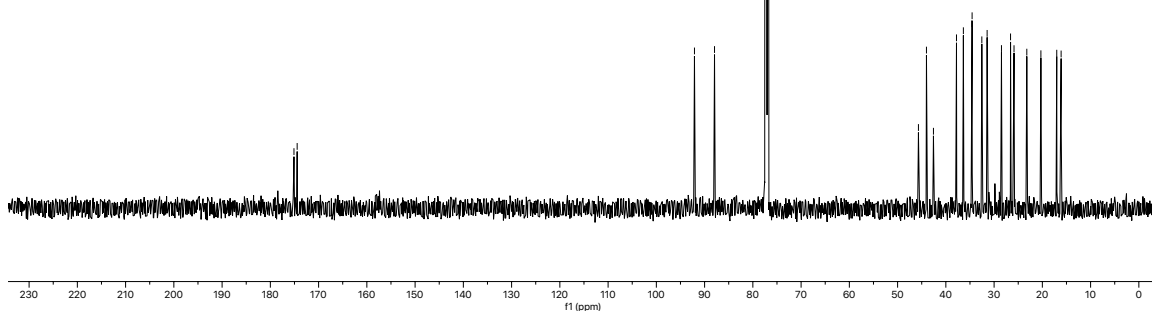
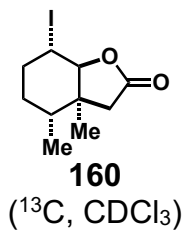


VN1-256-FR1-13C.10.fid  
CDCl<sub>3</sub> 600MHz

175.11  
174.44

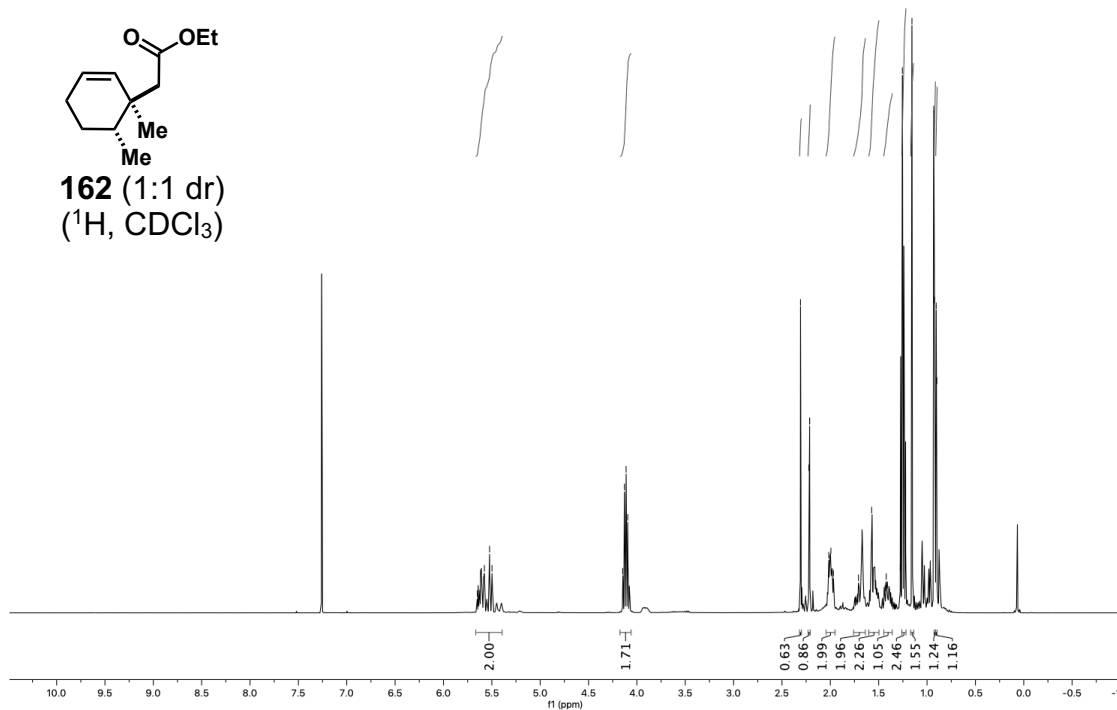
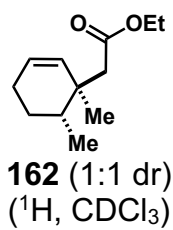
92.10  
87.94

45.68  
44.02  
42.57  
37.79  
36.37  
34.59  
34.56  
32.54  
31.45  
28.47  
26.59  
25.87  
23.22  
20.30  
17.02  
16.11

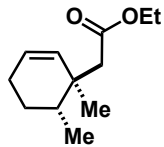


VN1-135-FR1-13C.1.fid  
CDCl<sub>3</sub> (400MHz)  
Johnson-Claisen

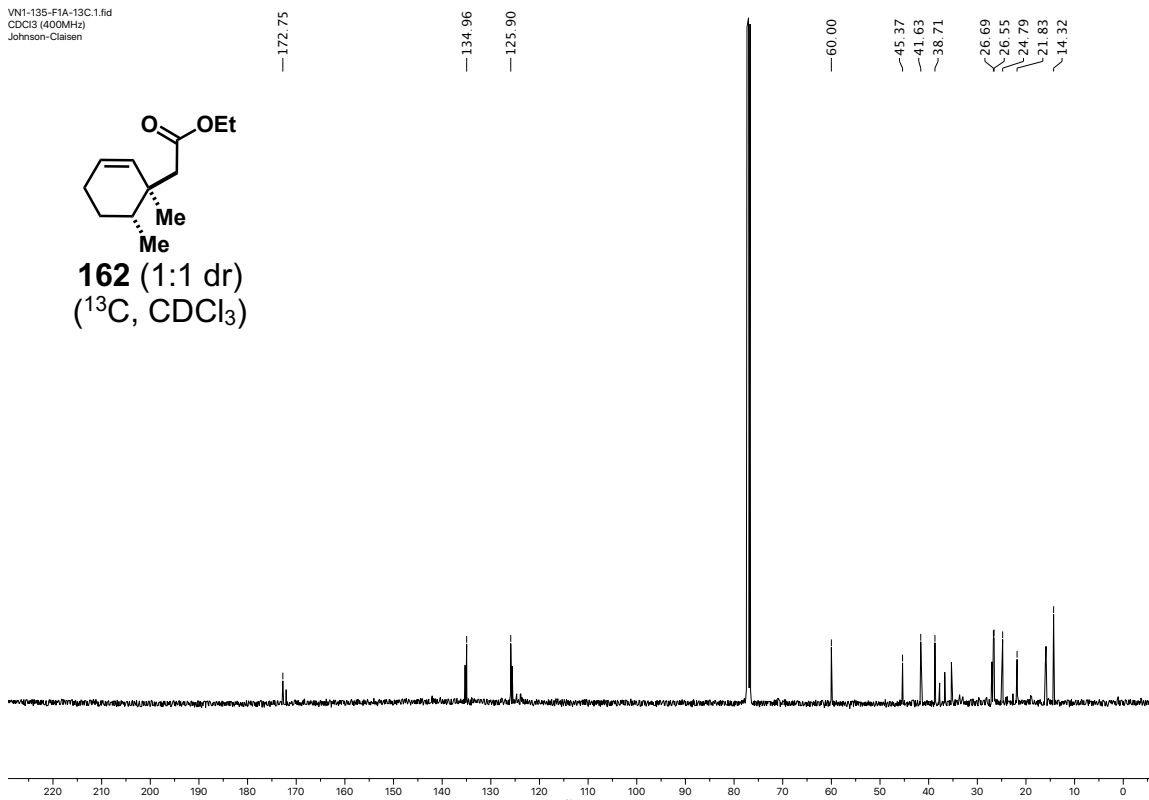
5.65  
5.61  
5.58  
5.52  
5.50  
4.15  
4.13  
4.11  
4.09  
2.31  
2.22  
2.21  
2.21  
2.02  
1.99  
1.97  
1.71  
1.67  
1.57  
1.56  
1.43  
1.43  
1.42  
1.41  
1.28  
1.26  
1.16  
0.93  
0.91  
0.90



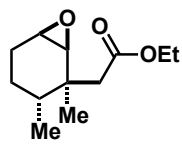
VN1-135-F1A-13C.1.fid  
CDCl<sub>3</sub> (400MHz)  
Johnson-Claisen



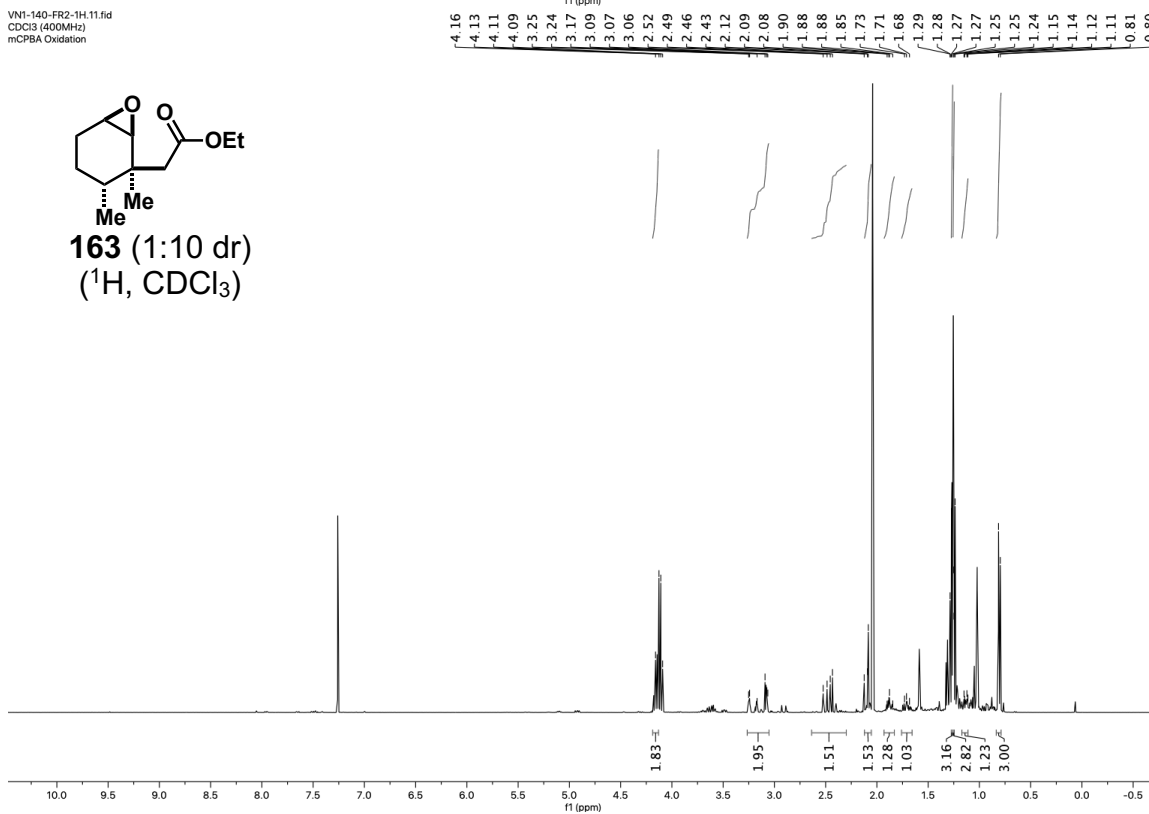
**162** (1:1 dr)  
(<sup>13</sup>C, CDCl<sub>3</sub>)



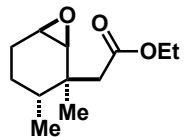
VN1-140-FR2-1H.11.fid  
CDCl<sub>3</sub> (400MHz)  
mCPBA Oxidation



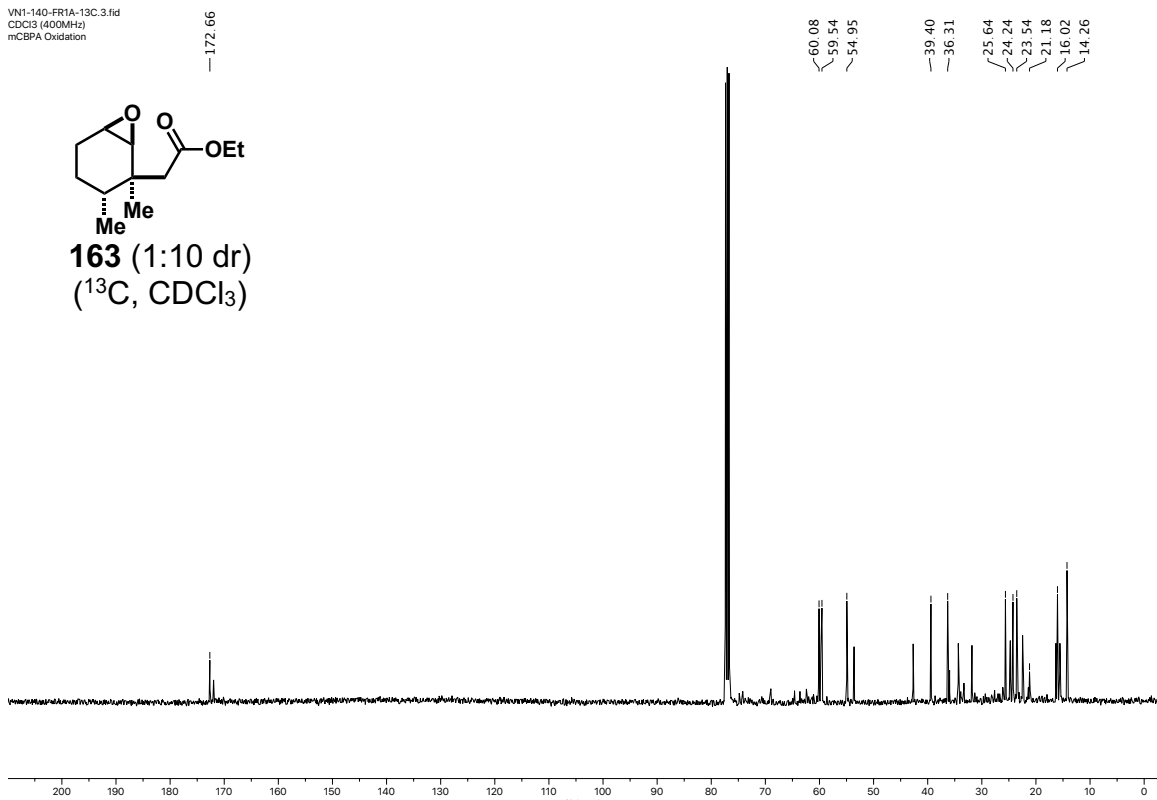
**163** (1:10 dr)  
(<sup>1</sup>H, CDCl<sub>3</sub>)



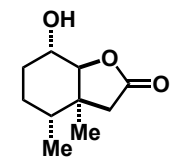
VN1-140-FR1A-13C.3.fid  
CDCl<sub>3</sub> (400MHz)  
mCPBA Oxidation



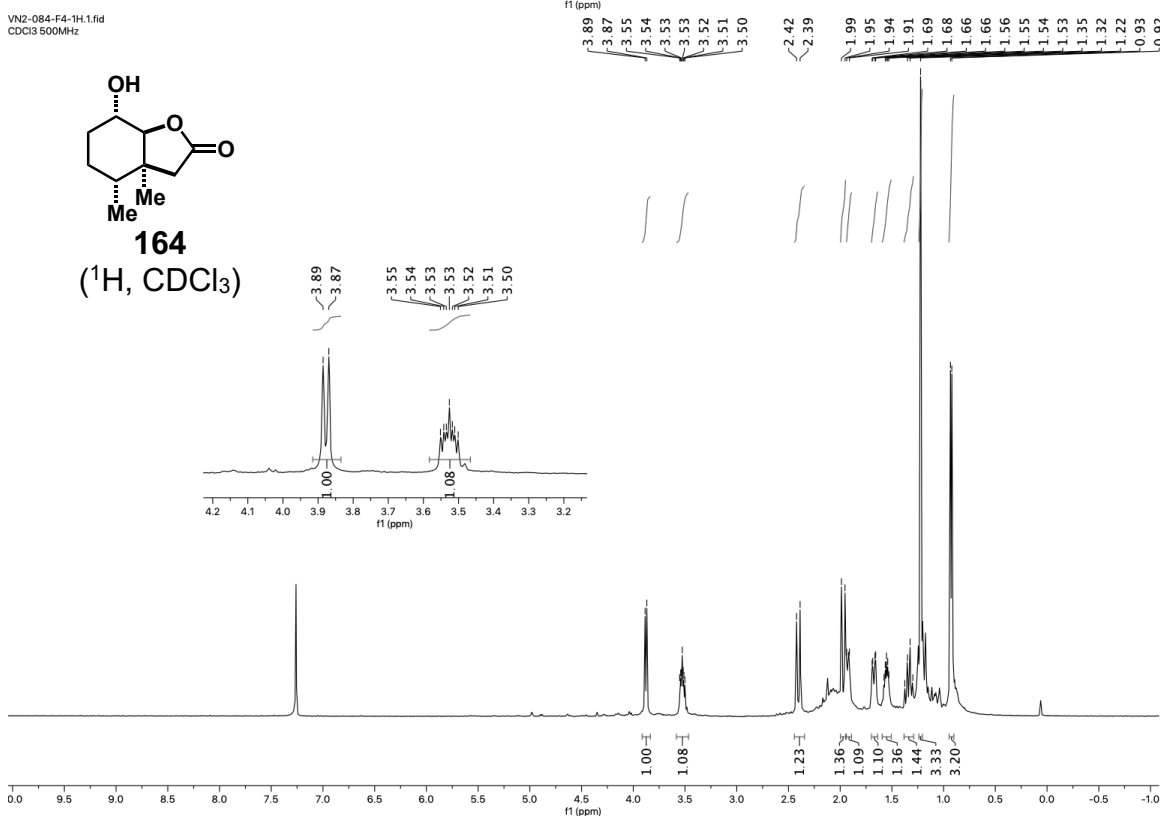
**163** (1:10 dr)  
(<sup>13</sup>C, CDCl<sub>3</sub>)



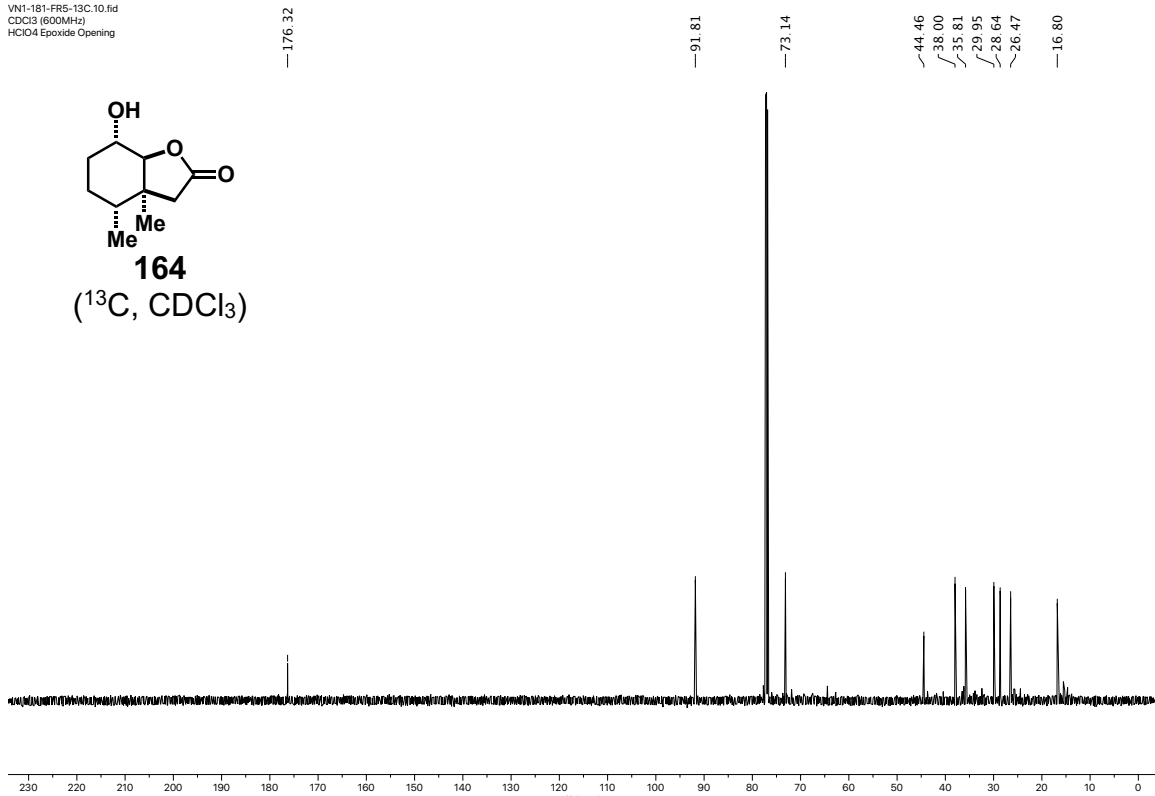
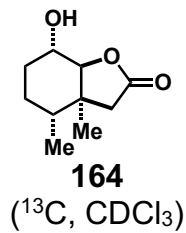
VN2-084-F4-1H.1.fid  
CDCl<sub>3</sub> 500MHz



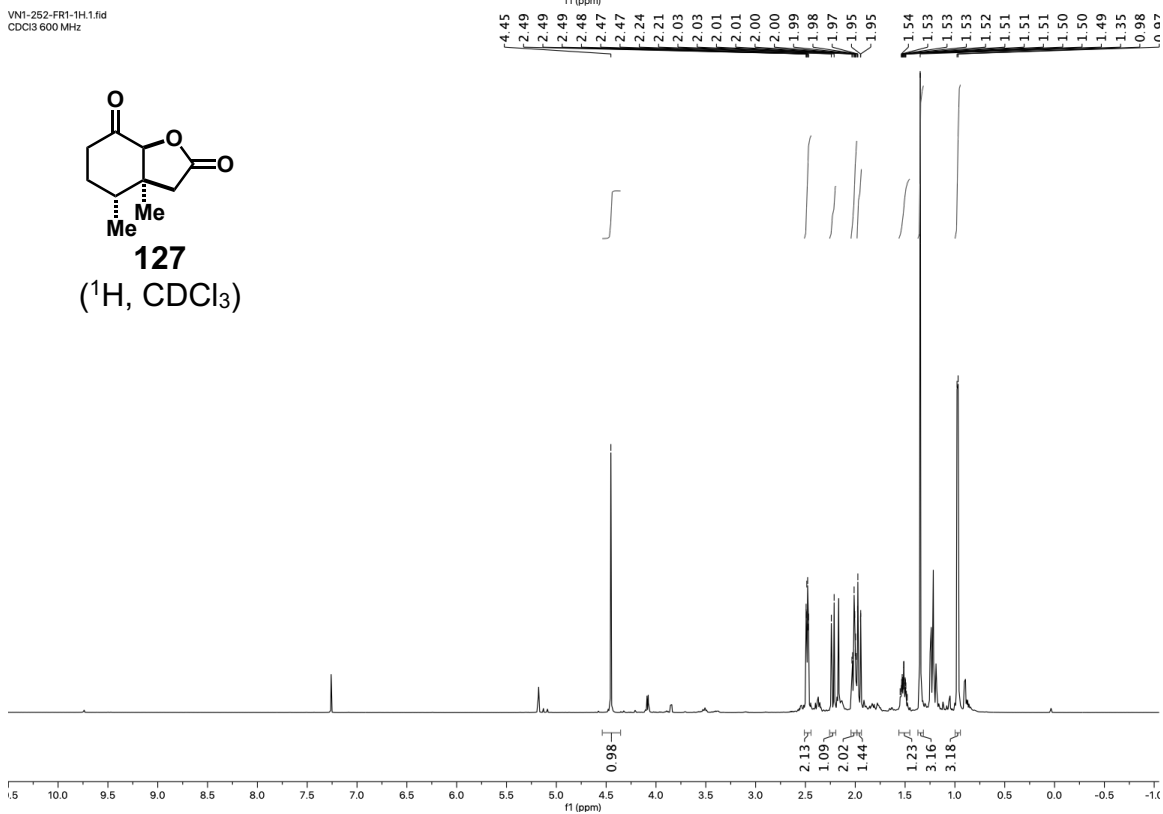
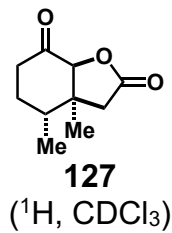
**164**  
(<sup>1</sup>H, CDCl<sub>3</sub>)



VN1-181-FR5-13C.10.fid  
CDCl3 (600MHz)  
HClO4 Epoxide Opening



VN1-252-FR1-1H.1.fid  
CDCl3 600 MHz



VN1\_225-CR-13C.10.fid

—205.17

—174.47

—87.30

—49.90

~39.42

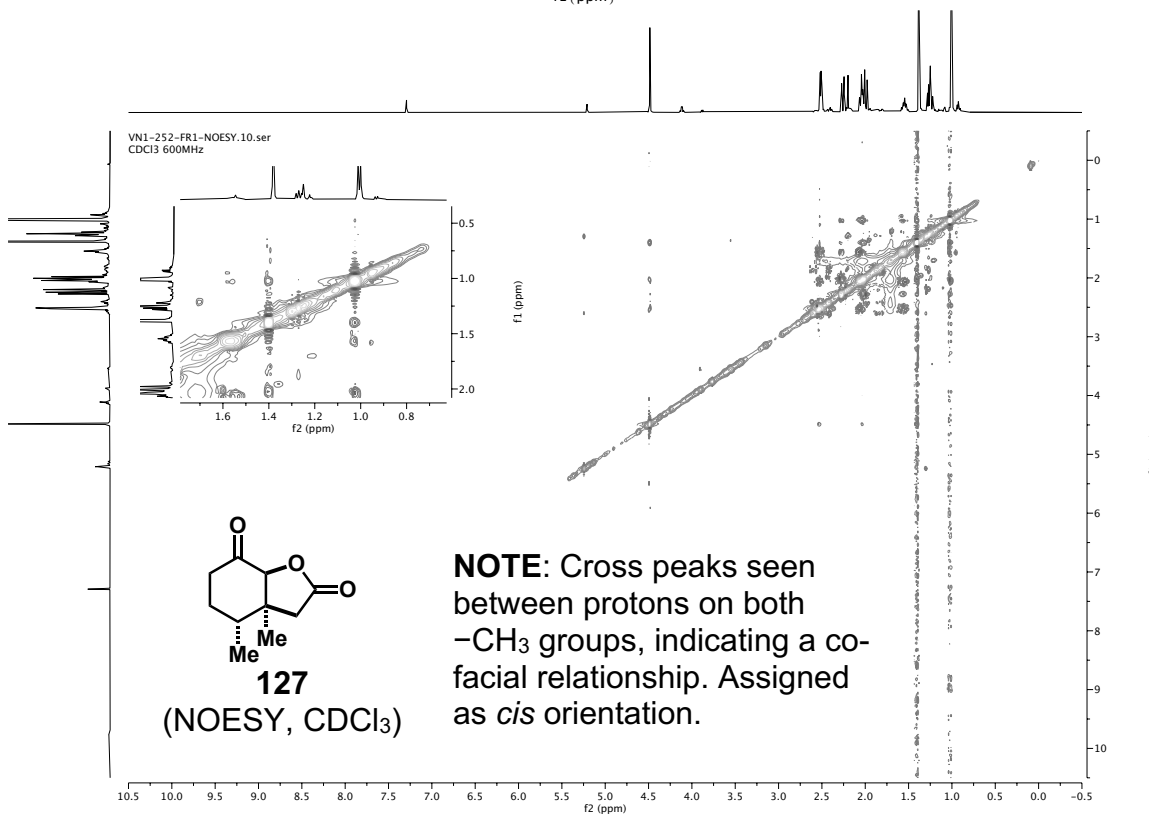
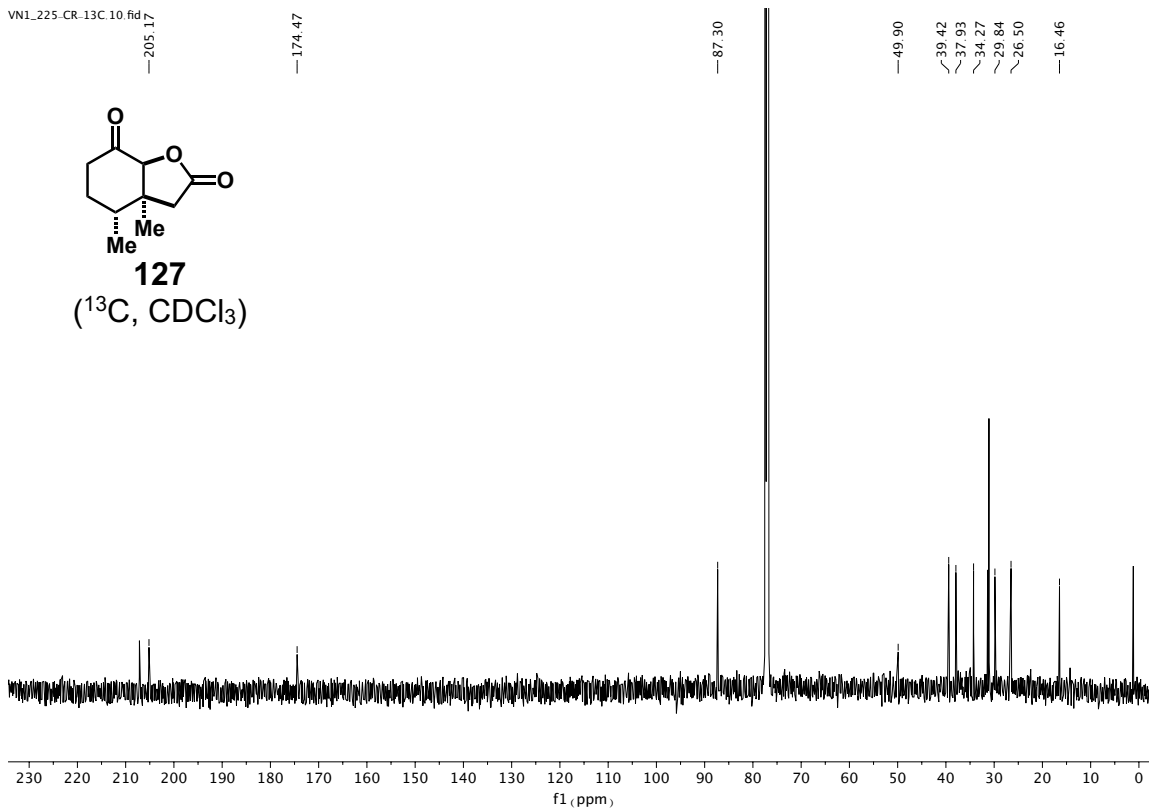
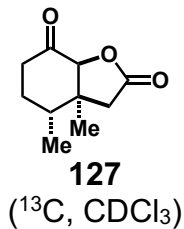
~37.93

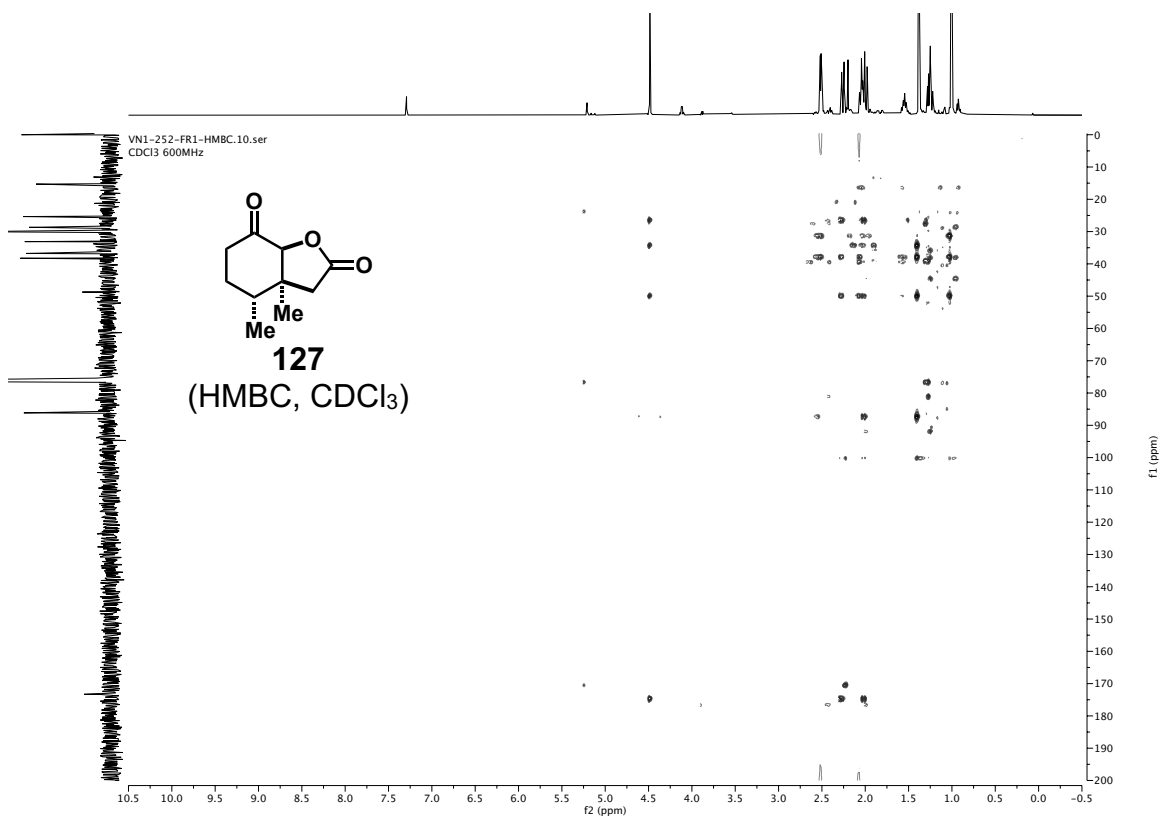
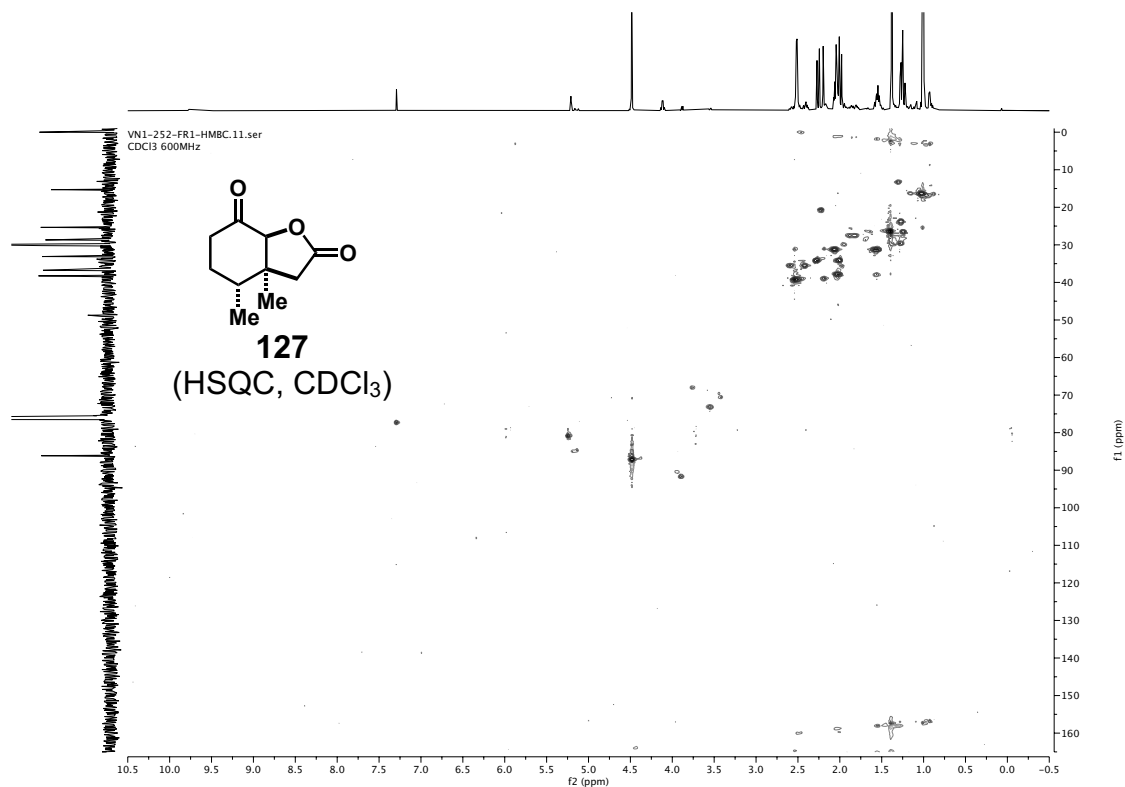
~34.27

~29.84

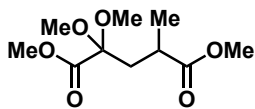
~26.50

—16.46

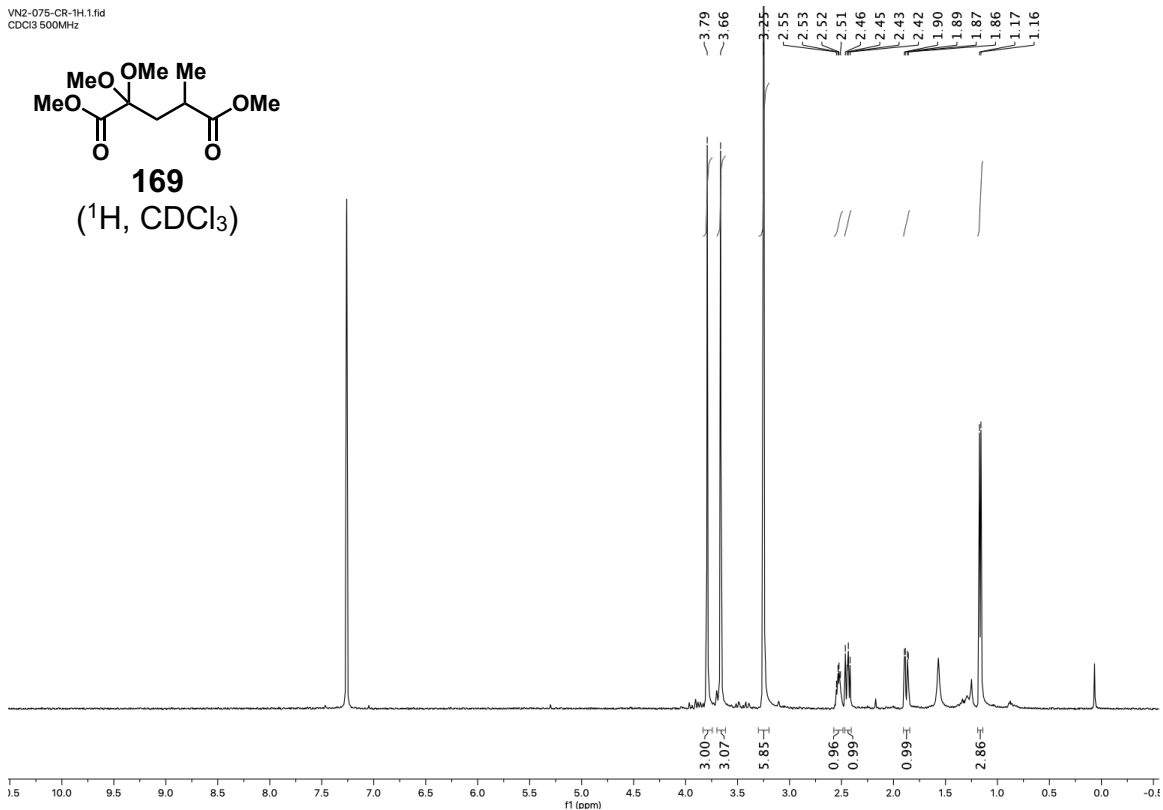




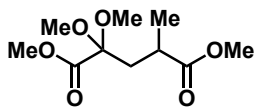
VN2-075-CR-1H.1.fid  
CDCl3 500MHz



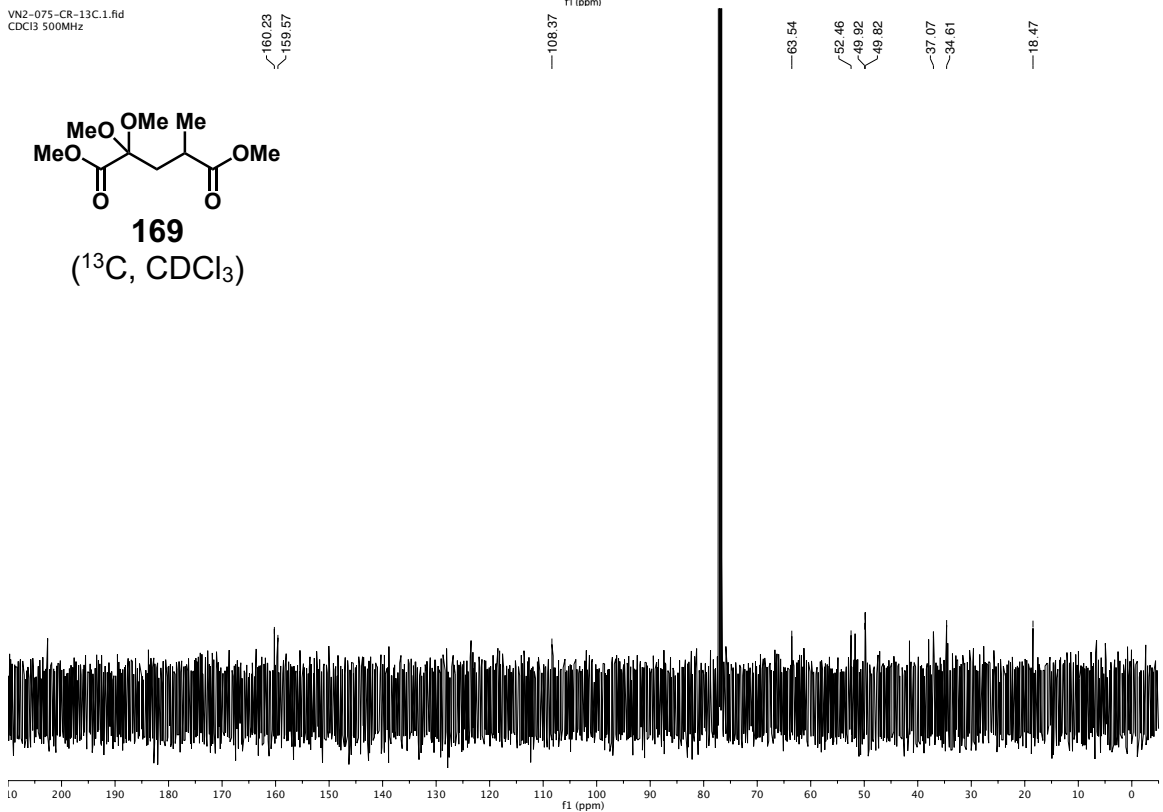
**169**  
(<sup>1</sup>H, CDCl<sub>3</sub>)



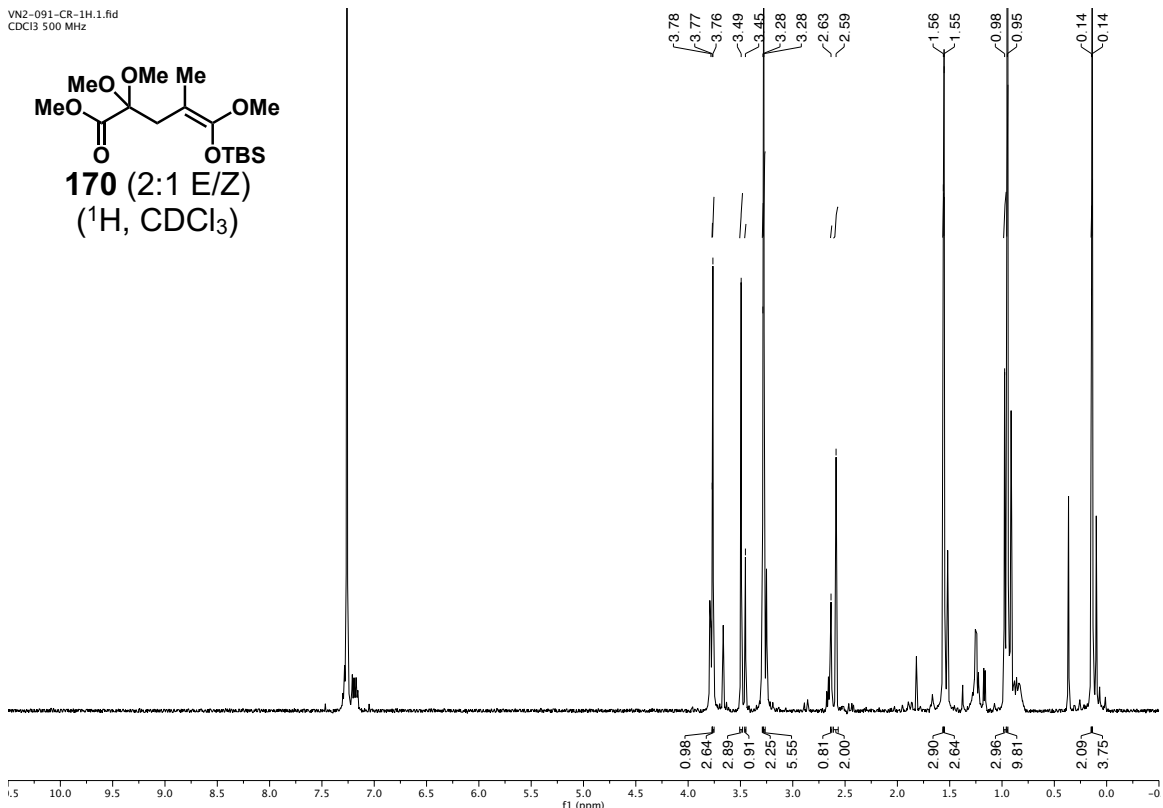
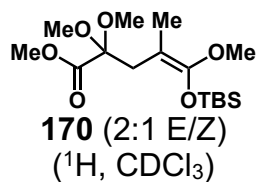
VN2-075-CR-13C.1.fid  
CDCl3 500MHz



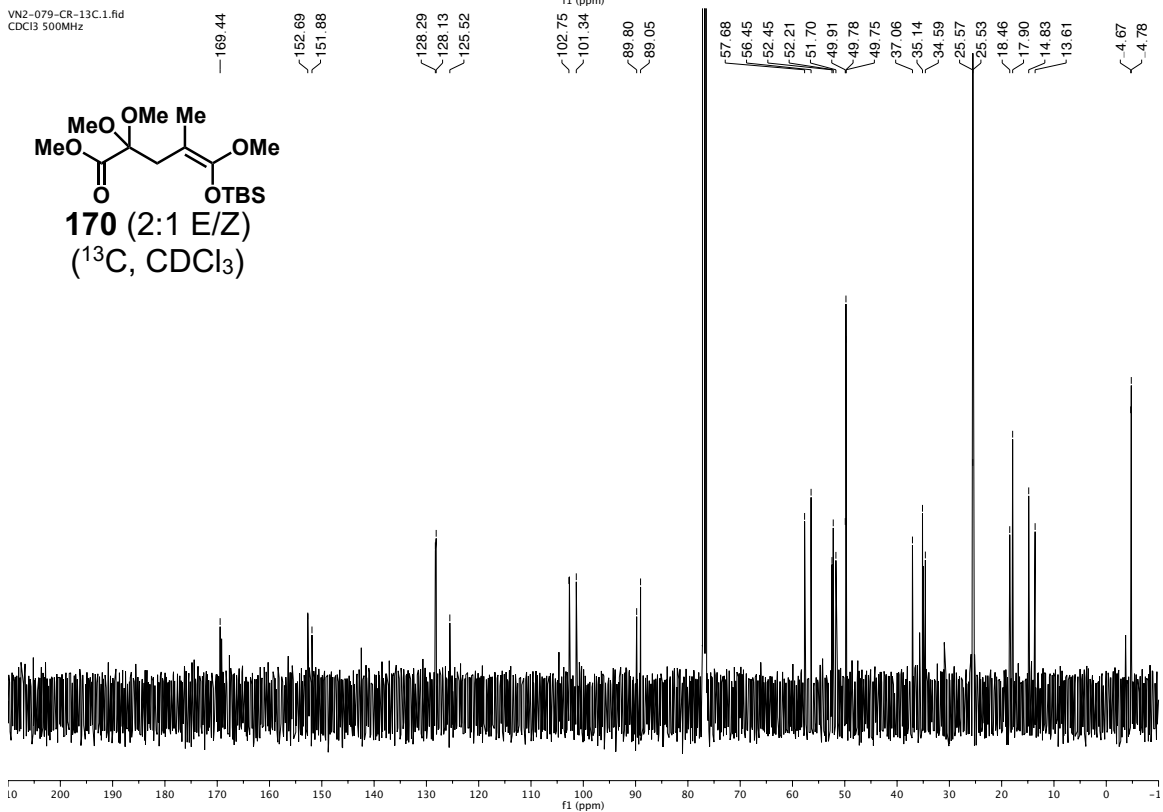
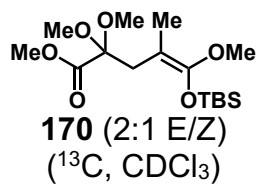
**169**  
(<sup>13</sup>C, CDCl<sub>3</sub>)



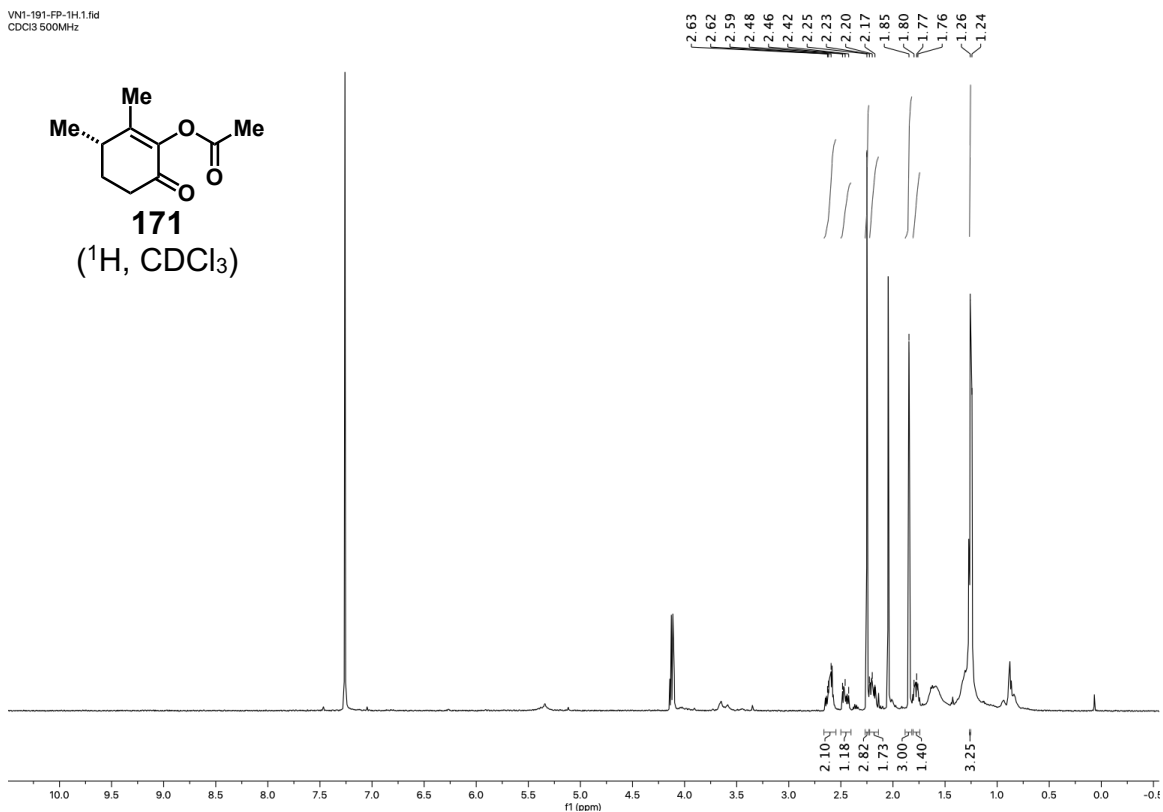
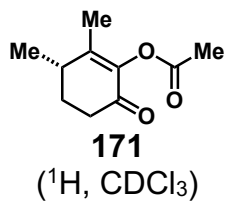
VN2-091-CR-1H.1.fid  
CDCl3 500 MHz



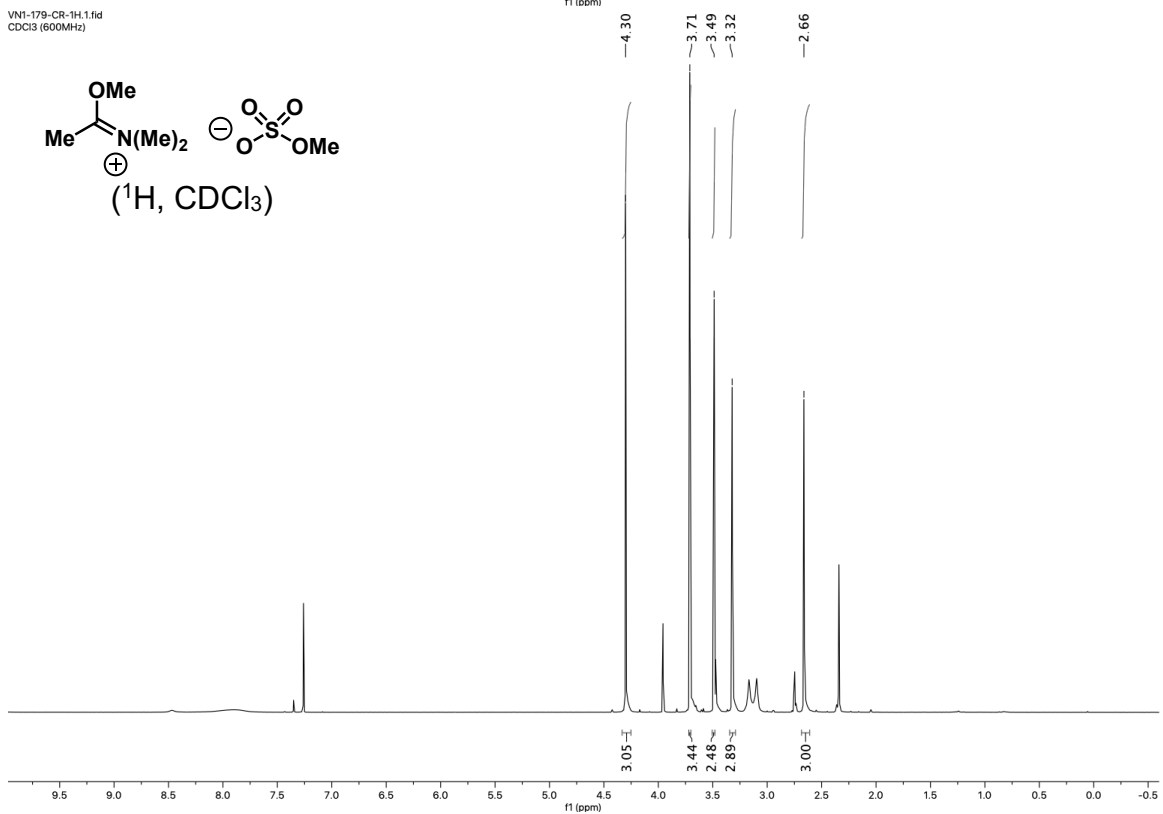
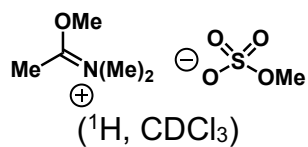
VN2-079-CR-13C.1.fid  
CDCl3 500MHz



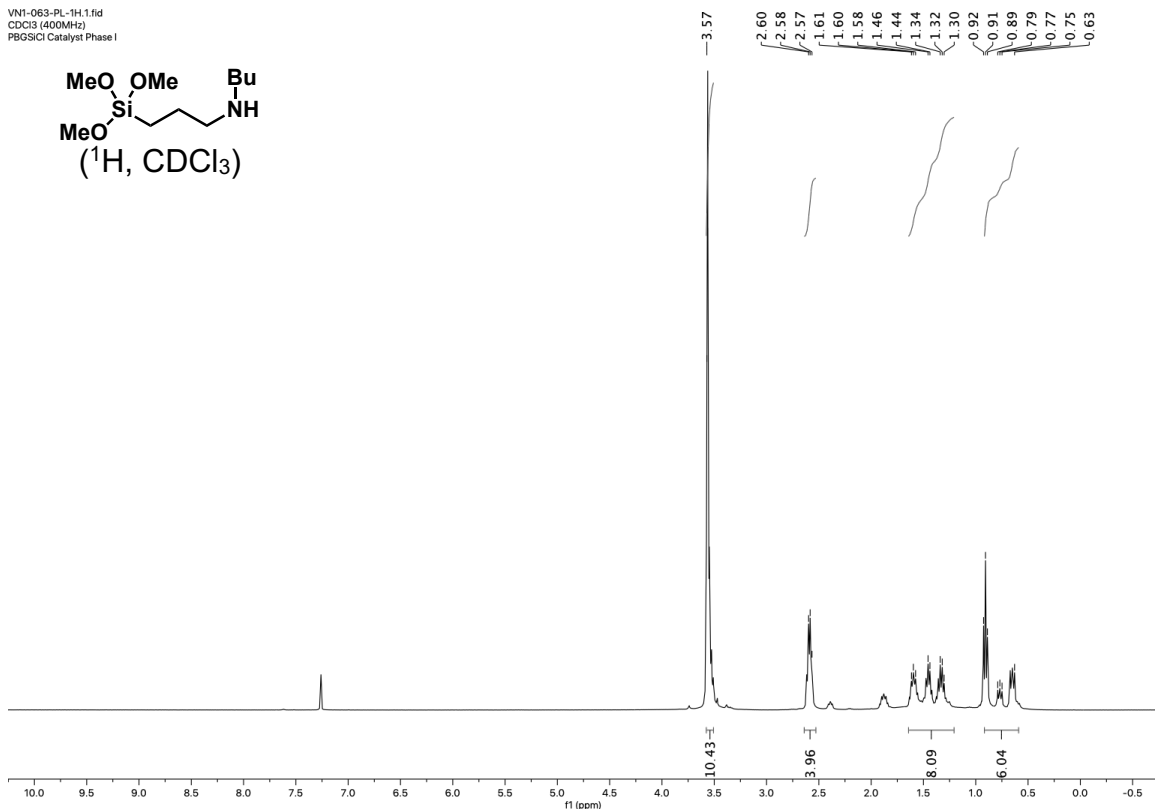
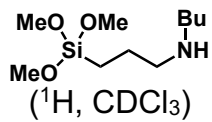
VN1-191-FP-1H.1.fid  
CDCl3 500MHz



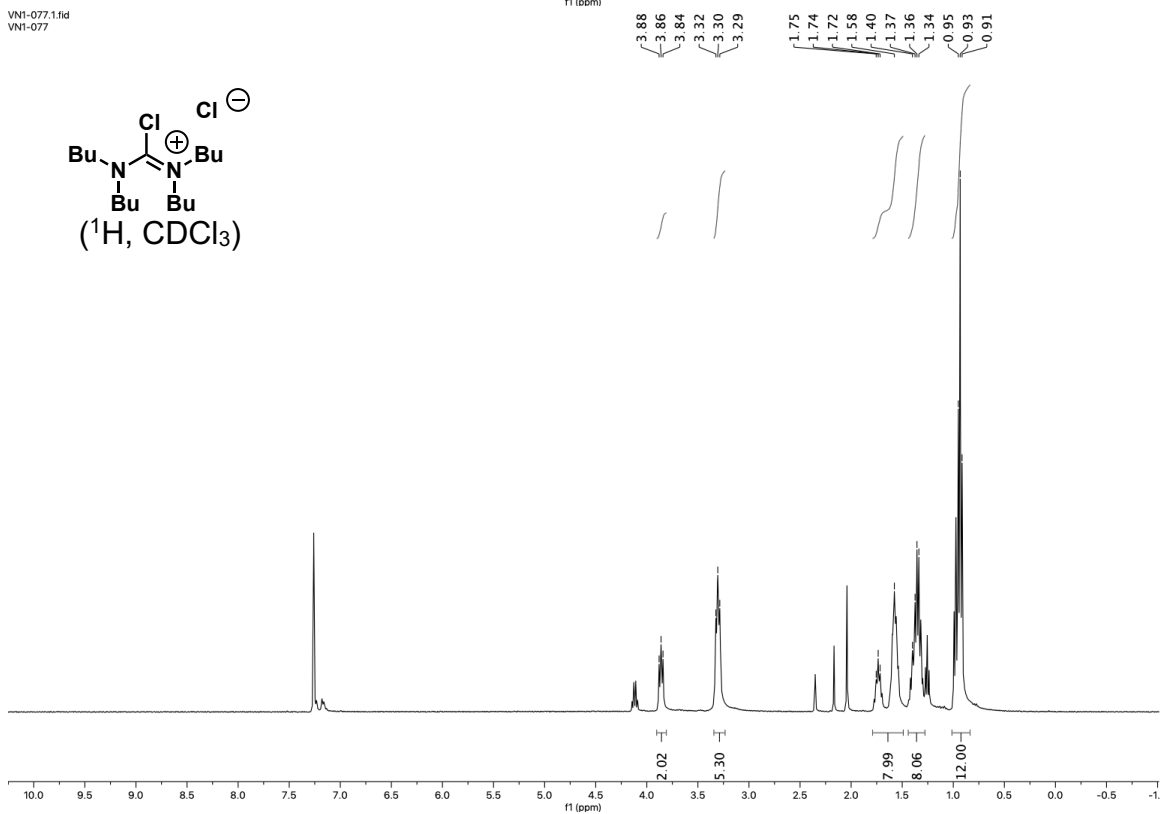
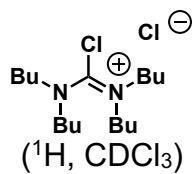
VN1-179-CR-1H.1.fid  
CDCl3 (600MHz)



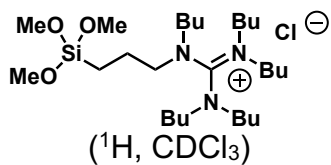
VN1-063-PL-1H.1.fid  
CDCl3 (400MHz)  
PBGSiCl Catalyst Phase I



VN1-077.1.fid  
VN1-077

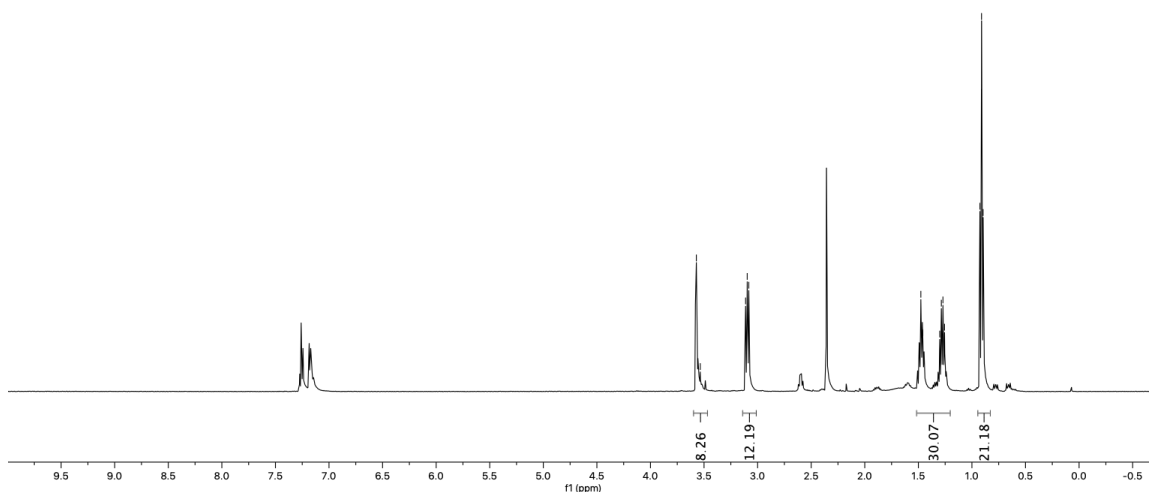


VN1-078-CR-1H.1.fid  
CDCl3 (500MHz)

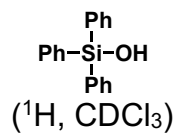


3.57  
3.54  
3.11  
3.10  
3.08

1.49  
1.48  
1.47  
1.46  
1.30  
1.29  
1.27  
1.26  
0.93  
0.91  
0.90

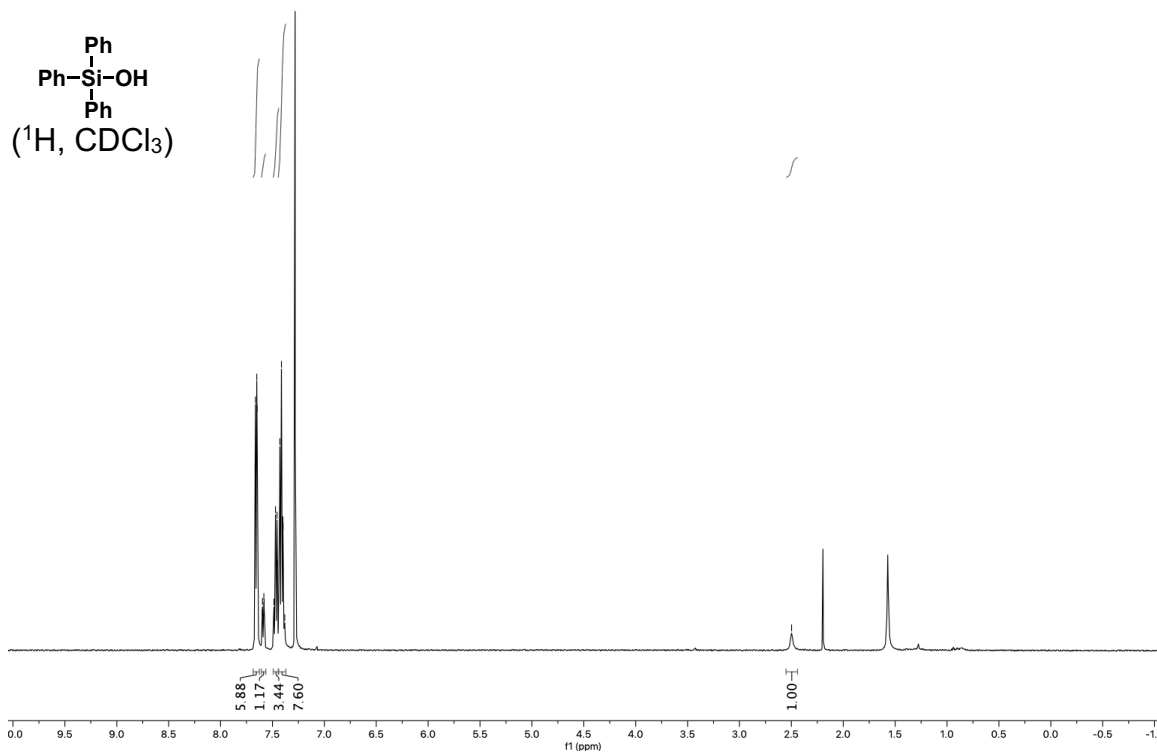


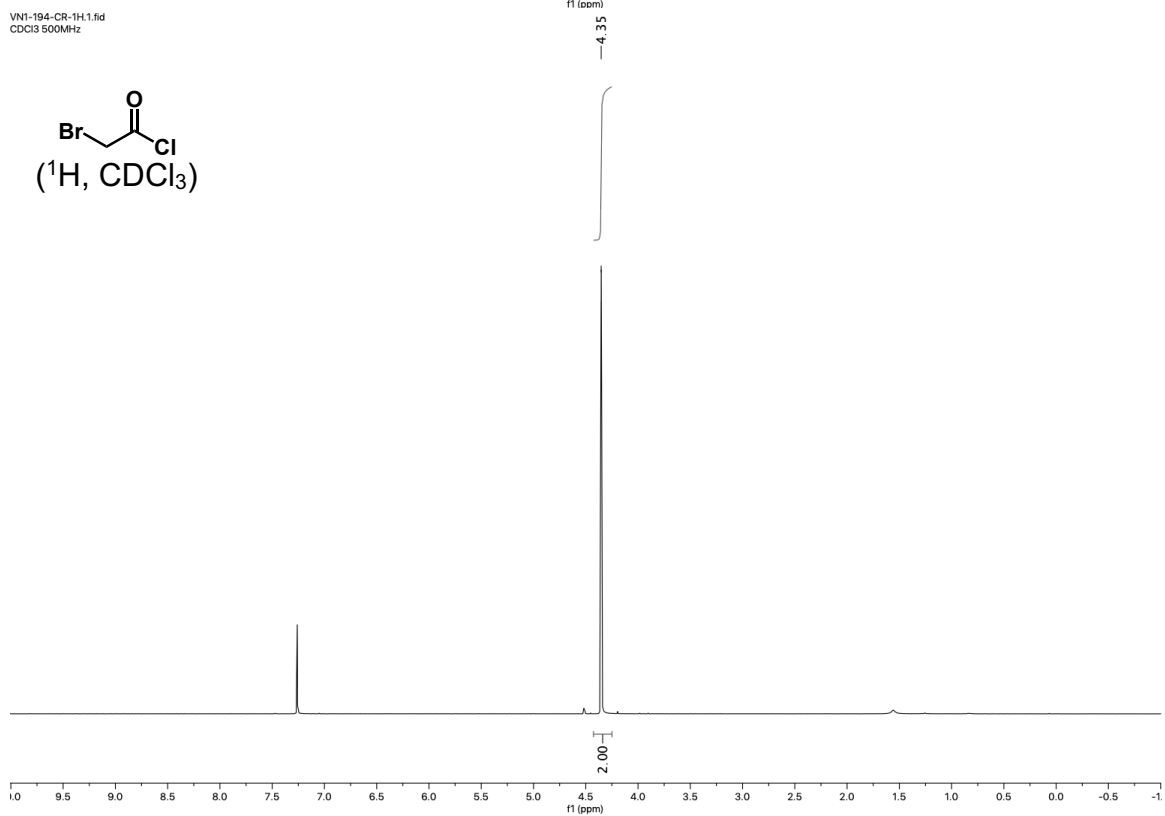
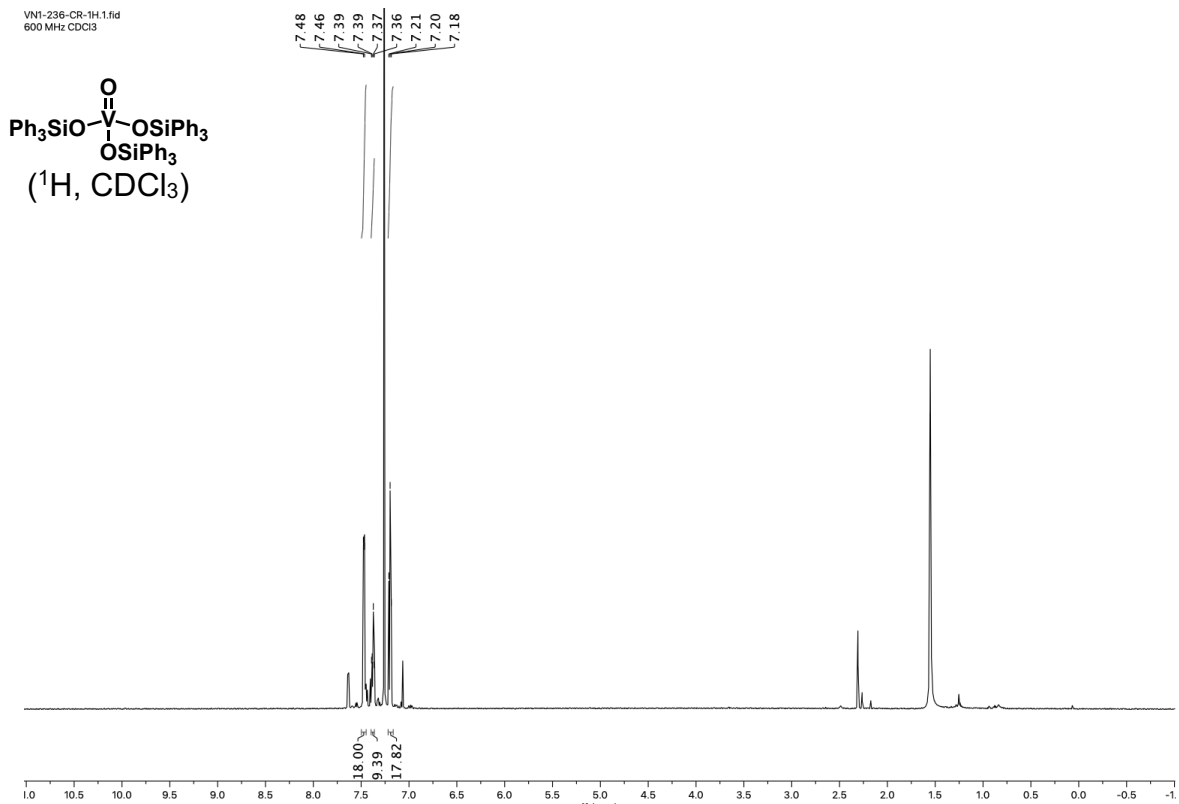
VN1-220-FP-1H.1.fid  
CDCl3 500MHz



7.67  
7.66  
7.65  
7.65  
7.60  
7.60  
7.58  
7.58  
7.49  
7.47  
7.46  
7.45  
7.43  
7.41  
7.40  
7.38

-2.50



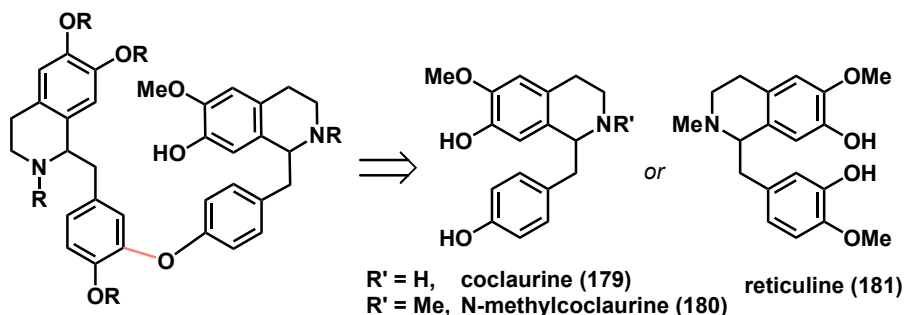


## 2 Chapter Two: Synthetic Efforts Toward Berbamine

### 2.1 Introduction

#### 2.1.1 Classification of Bisbenzylisoquinoline Alkaloids (BisBIAs)

The benzylisoquinoline alkaloids (BIAs) represent a family of over 2500 plant natural products that have been used for centuries as analgesics and wound disinfectants.<sup>1</sup> Some of the active and biosynthetically-related members, have been exploited in modern medicine, for example, morphine for pain, colchicine for gout, and noscapine for cough and cancer.<sup>2</sup> In recent years, the pursuit of bisbenzylisoquinoline alkaloids (bisBIAs), molecules comprising two BIA motifs, is gaining traction. Isolated from the *Berberidaceae*, *Ranunculaceae*, *Lauraceae* and *Menispermaceae* plant families, these compounds can modulate diverse biological functions.<sup>3,4</sup> With varied and rich pharmacology and chemistry, the majority of these alkaloids arise from the condensation of two coclaurine units (**179** or **180**) while some can arise from the condensation of a coclaurine with reticuline (**181**, Scheme 47).<sup>5,6</sup> Based on these distinctions, bisBIAs are often divided into three major classes: bisreticulines, coclaurine-reticulines, and biscoclaurines.<sup>7</sup>



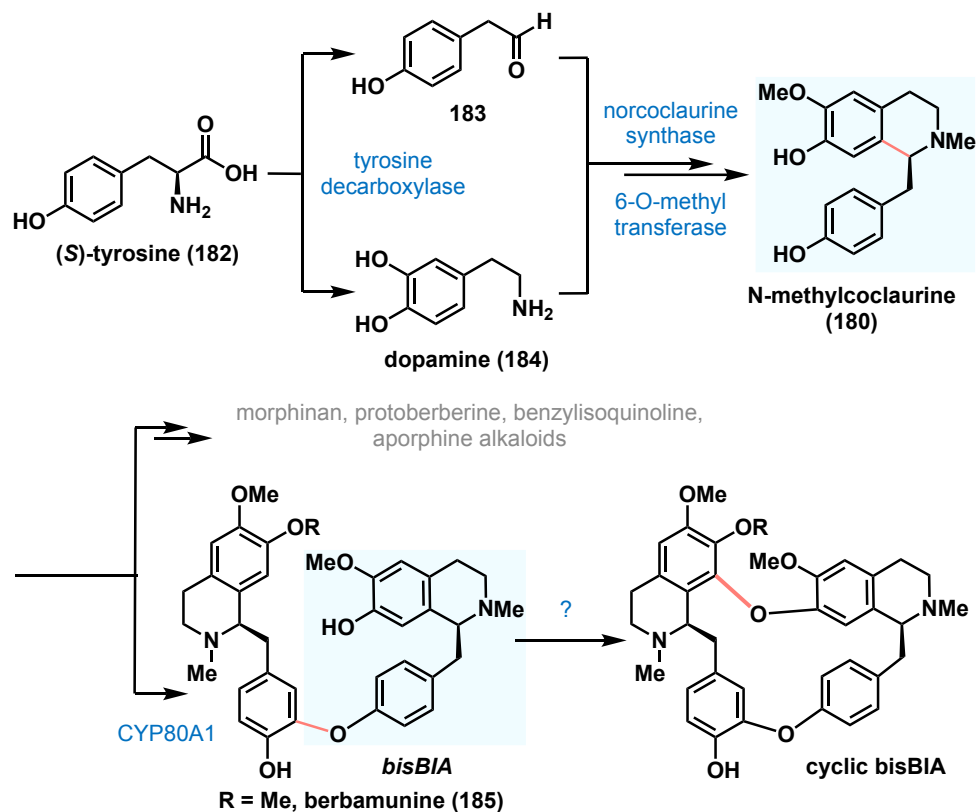
**Scheme 47.** Coclaurine (**179** and **180**) and/or reticuline (**181**) are the biosynthetic building blocks of the majority of bisBIAs

In all instances, the two benzyloquinoline moieties are linked via biphenyl, diphenyl ether, or benzyl phenyl ether bonds.<sup>7</sup> Aromatic rings with hydroxy, methoxy or methylenedioxy substituents and two chiral centers make up the key features of bisBIAs. Therefore, a high degree of variation is observed depending on the number of ether linkages, the sites on the two units at which the linkage originates, the nature of substitution of the nitrogen atoms, and the degree of unsaturation about the heterocycles.

Currently, over five hundred bisBIAs are known and have since been the subject of several review articles detailing their botanical sources as well as spectral and physical data.<sup>1-8</sup> This review highlights the biosynthesis and medicinal implications of bisBIAs. Further attention is given to the prevailing synthesis strategies for preparing these alkaloids.

### 2.1.2 Biosynthesis

BisBIAs are derived from a highly conserved biosynthetic pathway.<sup>8</sup> Catalyzed by tyrosine decarboxylase, the biosynthesis begins with the conversion of amino acid (*S*)-tyrosine (**182**) into 4-hydroxyphenylacetaldehyde (**183**) and dopamine (**184**, Scheme 48).<sup>8,9</sup> A Pictet–Spengler transformation facilitated by the enzyme norcoclaurine synthase combines arylacetaldehyde **183** with dopamine (**184**) to generate (*S*)-norcoclaurine. After two successive enzymatic *O*- and *N*-methylation steps, the core intermediate *N*-methylcoclaurine (**180**) is attained that ultimately gives rise to an array of BIAs.



**Scheme 48.** Current understanding of the bisBIA biosynthetic pathway

For simple bisBIA derivatives, two *N*-methylcoclaurine units are oxidatively dimerized via the P450 enzyme CYP80A1.<sup>8,10</sup> More complex cyclic bisBIAs are produced following a series of downstream biosynthetic modifications that lead to the introduction of additional functionality. Even so, and as noted by Weber and Opatz, the observed structural diversity of bisBIAs is not entirely substantiated by our current understanding of their biosynthesis.<sup>8</sup> For example, the enzyme(s) responsible for the formation of sterically encumbered, electron-rich diaryl ether bonds of cyclic bisBIAs, such as tetrandrine (**186**) and berbamine (**187**) from berbaminine (**185**), has not been identified.

### 2.1.3 Biological Activity

Bisbenzylisoquinoline alkaloids have drawn significant attention due to their potent anti-inflammatory, antiviral, antitumor, analgesic and anti-plasmodial properties.<sup>6,11,12</sup> Formulations containing these alkaloids have been used for centuries as traditional medicines in India, China, sub-Saharan Africa and Southeast Asia.<sup>13</sup> Some active members even have the ability to immobilize skeletal muscle, hence their pronounced use as arrow poisons in South America.<sup>14</sup> Over the past few decades, the quantity of publications concerning the bioactivities of bisBIAs has largely increased. Several extensive studies have examined the antimicrobial and anti-allergenic characteristics of bisBIAs. The antiparasitic influence of twenty unique bisBIAs against *Trypanosoma brucei* and *Leishmania donovani* was explored by Camacho and co-workers.<sup>15</sup> Comparably, these alkaloids exhibited heightened synergistic effects with the antibiotic cefazolin on methicillin-resistant *Staphylococcus aureus* strains.<sup>16</sup>

More recent findings have identified bisBIAs as inhibitors of calcium influx in glial cells and neurons, combatting neuroinflammation and neuroapoptosis.<sup>17</sup> Another example by Medeiros *et al.* reported that the alkaloid curine (**188**) induced vasorelaxation via direct inhibition of L-type voltage-gated calcium current in rat aorta smooth muscle cells, triggering an intracellular decrease in transient calcium stores (Figure 7).<sup>18</sup>

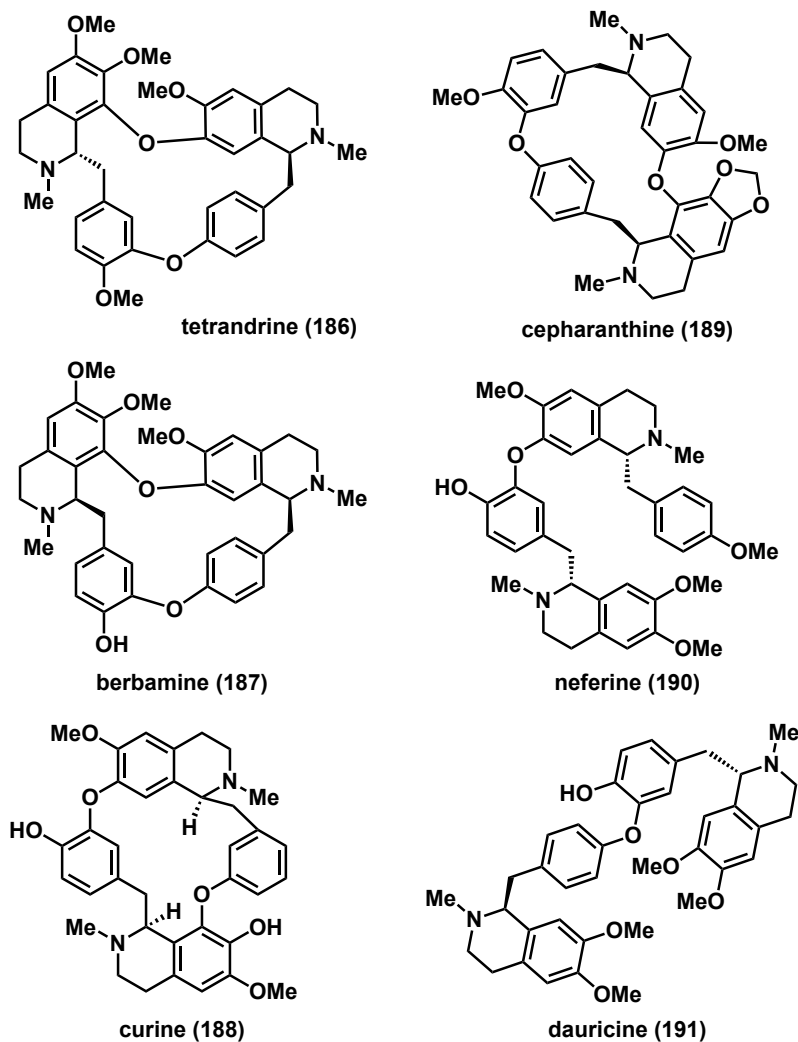


**Figure 7.** Selected bioactive bisBIAs

Of particular interest is the potential of these natural products as latent agents against the novel and highly pathogenic SARS-CoV-2, which is the fundamental cause of coronavirus disease 2019 (COVID-19).<sup>19</sup> Plants of the *Menispermaceae* family are repeatedly used for the treatment of malaria as well as dengue fever and a number of isolated alkaloids exert comparable antiviral consequences.<sup>20,21</sup> He *et al.* identified nine bisBIAs as potent in vitro SARS-CoV-2 entry inhibitors.<sup>22</sup> Tetrandrine (**186**) dramatically

blocked viral S and N protein expression as well as human coronavirus OC43 (HCoV-OC43) replication in MRC-5 human lung cells.<sup>23</sup> Likewise, the approved bisBIA drug cepharanthine (**189**) was shown to inhibit SARS-CoV-2 replication with minimal toxicity at a half maximal effective concentration (EC<sub>50</sub>) of 0.35 μM (Figure 7).<sup>24,25</sup> While the mechanism of action of cepharanthine (**189**) is multifaceted, the antiviral activity not only relies on suppression of nuclear factor-κB (NF-κB) signaling pathways but also induction of plasma membrane rigidity to hamper entry of the pathogen into the cell.<sup>24</sup> These activities highlight a new role for bisBIAs in the prevention and treatment of SARS-CoV-2 infection. Though many bisBIAs have yet to be biologically evaluated, some demonstrate potential as drug candidates and merit special emphasis: tetrandrine (**186**), berbamine (**187**), neferine (**190**), and dauricine (**191**, Figure 7).

#### 2.1.3.1 Tetrandrine

First isolated by Kondo and Tano in 1928, tetrandrine (**186**) is the major bisBIA found in the roots of *Stephania tetrandra* (*Menispermaceae*), a climbing plant used in traditional Chinese and Japanese medicine (Figure 7).<sup>26</sup> Beyond its traditional use for remedying autoimmune disorders, hypertension and cardiovascular diseases, the pharmacological effects of tetrandrine (**186**) have been the focus of various studies since the late-1990s. Its immunologic and vasodilatory properties have been well evaluated, particularly as a latent therapeutic to treat drug-resistant autoimmune diseases and prevent excess fibrosis in patients with severe conjunctival inflammation.<sup>27,28</sup>

The labs of Xu<sup>29</sup> and Huang<sup>30</sup> described the antiproliferative nature of tetrandrine (**186**) on human T and liver cancer cells, respectively, by inhibition of

NF- $\kappa$ B and calcium/calmodulin-dependent protein kinase II, both of which are critical regulators of not only innate immunity, but also cancer-related inflammation. It was even found to upregulate in vitro expression and activation of initiator and effector caspases in glucocorticoid-resistant Jurkat T-cells, contributing to the apoptosis-inducing effect in T cell acute lymphoblastic leukemia (T-ALL).<sup>27,31</sup>

Recently, the alkaloid has been recognized as an antagonist of two-pore channels (TPC), or voltage-dependent calcium channels located on lysosomal membranes, which have been implicated in the pathogenesis of cancer and Ebola virus infection.<sup>32</sup> Sakurai *et al.* determined that in vivo and in vitro Ebola virus entry can be hindered by disrupting TPC channels using submicromolar concentrations of tetrandrine (**186**).<sup>33</sup> The alkaloid also reduced tumor metastasis through inhibition of TPC1 and TPC2 in vivo and in vitro.<sup>34</sup>

An additional pharmacological target of tetrandrine (**186**) is P-glycoprotein (Pgp), a ubiquitous membrane transporter with the ability to efflux drug molecules out of cancer cells, which reduces the efficacy of chemotherapies.<sup>35</sup> Overexpression of Pgp in cancer cells is a crucial factor of multi-drug resistance in a variety of antitumor agents. Among a series of bisBIAs, tetrandrine (**186**) was identified as an effective modulator of Pgp activity.<sup>27,36</sup> Named CBT-1, this alkaloid is being developed by CBA Research Inc. as an adjunctive therapy to chemotherapy in various cancer types with multiple drug resistance, including sarcoma, non-Hodgkin's lymphoma, acute myelogenous leukemia, and multiple myeloma.<sup>37</sup> Prior phase I trials with CBT-1 defined the tolerable dose range and

side effects when administered with doxorubicin.<sup>38</sup> The most recent clinical study is currently investigating the combination of doxorubicin and CBT-1 for the treatment of unresectable, metastatic sarcoma in patients who previously progressed with doxorubicin.<sup>39</sup> A thorough discussion of the synergistic, apoptotic, and autophagic consequences of tetrandrine on multiple cancers, both *in vitro* and *in vivo*, appears in a comprehensive review by Luan *et al.*<sup>36</sup>

From a toxicity perspective, oxidative metabolism involving the 12-O-methoxy group of tetrandrine (**186**) leads to the generation of a highly reactive quinone methide intermediate suspected to be responsible for massive pulmonary edema and hemorrhage in mice models.<sup>40</sup> Likewise, continuous administration of the alkaloid caused a marked pathological change in the liver tissues of dogs.<sup>41</sup>

#### 2.1.3.2 Berbamine

Berbamine (**187**) is a cyclic bisBIA isolated from the traditional Chinese herbal medicine *Berberis amurensis* (Figure 7).<sup>5</sup> There is a well-documented history of its usage in clinical practice for treating inflammation, cancer, and autoimmune diseases.<sup>6</sup> A simple keyword search in scientific databases returns about five hundred publications on berbamine's pharmaceutical assessment spanning from 1969 to present day. Numerous research findings have disclosed its inhibitory effects toward a variety of cancer cell lines, specifically advanced melanoma, ovarian cancer, and chronic myeloid leukemia.<sup>42,43</sup> Its antiproliferative qualities are frequently associated with the inactivation of critical pro-tumorigenic pathways, such as p53, Fas signals, and Ca<sup>2+</sup>/calmodulin-dependent protein kinase II  $\gamma$ .<sup>44</sup>

For example, c-Myc is a transcription factor that regulates cellular metabolism, cell growth, division, and apoptosis.<sup>45</sup> Dysregulated and overexpressed in many cancers including B cell lymphomas and T cell lymphomas, c-Myc is considered an undruggable oncogene.<sup>46</sup> Prof. Wendong Huang's laboratory at City of Hope (COH) National Medical Center, with whom our lab has been actively collaborating with since 2020, first identified CaMKII as a key c-Myc regulator that can be targeted by the bisBIA berbamine (**187**).<sup>47</sup> By inhibiting CaMKII, this natural product destabilizes c-Myc and reduces tumor volume with minimal toxicity in a mouse model, thus establishing berbamine as a CaMKII $\gamma/\delta$  inhibitor and the c-Myc:CaMKII axis as a druggable therapeutic target for aggressive cancers.<sup>44,47-49</sup>

Interestingly, recent studies also uncovered an unforeseen synergy of berbamine (**187**) with an assortment of targeted therapies. Zhao *et al.*<sup>50</sup>, Hu *et al.*<sup>51</sup> and Jia *et al.*<sup>52</sup> demonstrated that berbamine improved the efficacy of sorafenib, gefitinib and paclitaxel, respectively, on advanced hepatocellular carcinoma (HCC), pancreatic cancer and glioma cells through suppression of the STAT3 signaling pathway and reactive oxygen species (ROS)-dependent phospho-Akt protein expression.

#### 2.1.3.3 Neferine and Dauricine

Neferine (**190**) and dauricine (**191**) are the primary bioactive components obtained from the seed embryo of *Nelumbo nucifera* (lotus) and the roots of *Menispermum dauricum* (Asian moonseed), respectively (Figure 7).<sup>6,40</sup> Both compounds display antiviral, antioxidant, antidepressant, antiarrhythmic and anti-cancer actions.<sup>40</sup>

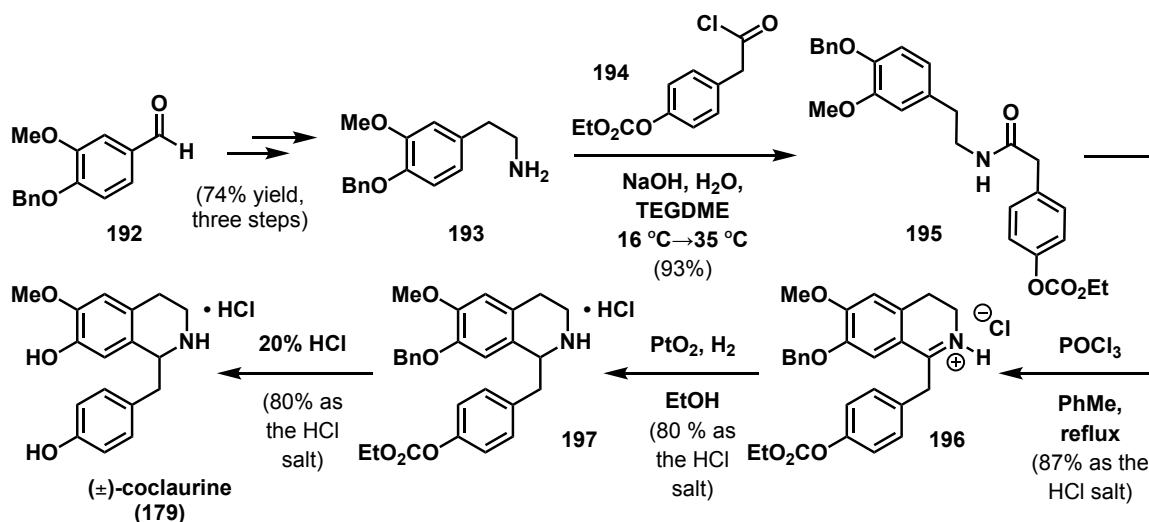
Neferine (**190**) has neuroprotective capabilities and can function as a ROS-mediated autophagy inducer (Figure 7).<sup>53,54</sup> Its anti-diabetic implications were disclosed by Li and co-workers.<sup>55</sup> Their study revealed that compared to untreated diabetic mice, an evident reduction in the blood pressure, body weight, fasting blood sugar glucose, insulin, triglycerides and total cholesterol was seen in type II diabetic mice upon neferine treatment. Additionally, the alkaloid not only bolstered the anti-tumor effects of chemotherapeutic agents, but also reversed multiple drug resistance in both *in vitro* and *in vivo* models of cancer by decreasing epithelial-mesenchymal transition (EMT), a process associated with chemoresistance and tumor invasion.<sup>53,56,57</sup> In a recent investigation, neferine (**190**) reduced the viability of human prostate cancer (PCa) cells and their stem cells in a time- and dose-dependent manner by upregulating cleaved poly-ADP ribose polymerase (PARP), apoptotic caspase-3, and downregulating the expression of anti-apoptotic protein Bcl-2. Intriguingly, neferine (**190**) also elevated the expression of several tumor suppressor genes and downregulated cyclin-dependent kinase 4 (CDK-4) expression, leading to cell cycle arrest at the G<sub>1</sub> phase.<sup>58</sup>

Dauricine (**191**) exerts similar pharmacological attributes with clinical potential. Its cardiovascular, anti-inflammatory, membrane modulating, anti-platelet aggregation and neurological effects are well-documented (Figure 7).<sup>5,6</sup> Outlined by Wang *et al.*, dauricine (**191**) significantly minimizes the *in vitro* secretion level of amyloid beta (A $\beta$ ) and Cu<sup>2+</sup>-induced ROS in human  $\beta$ -amyloid precursor protein (APPs) cells.<sup>59</sup> Hence, it is suggested that the alkaloid could rescue neurons from oxidative stress-induced apoptosis and possibly relieve acute

oxidative damage in Alzheimer's disease (AD) models. The therapeutic capacity of dauricine against lipopolysaccharide (LPS)-induced inflammatory bone loss is more recently demonstrated by Park and co-workers via its action on osteoclasts (OC).<sup>60</sup> Yet, the adverse cytotoxicity of the alkaloid in liver, kidney and lung-derived cell lines is often overlooked.<sup>61</sup>

## 2.1.4 Total Syntheses of bisBIAs

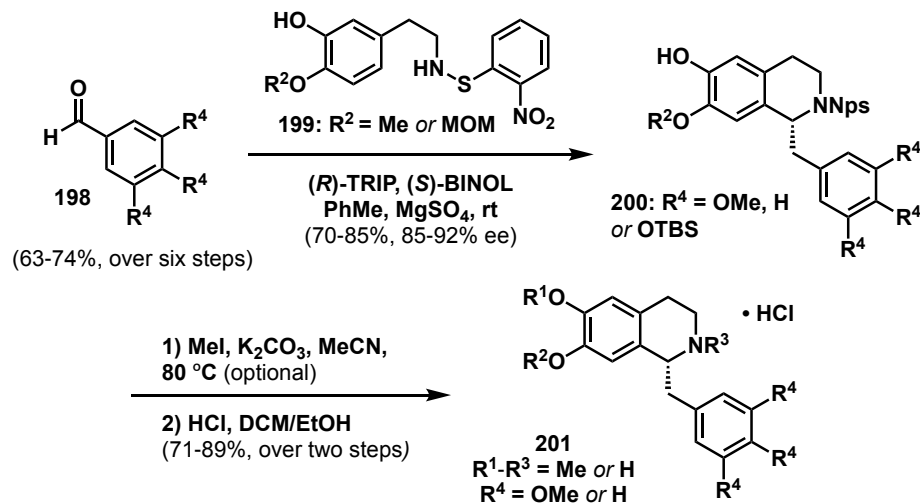
### 2.1.4.1 Synthesis of Coclaurine and its Derivatives



**Scheme 49.** Total synthesis of (±)-coclaurine (**179**)

Besides being structural fragments and precursors, the synthesis of coclaurine (**179**) and its derivatives is imperative in accessing the dimeric bisBIAs. The original strategy of assembling coclaurine (**179**) involved the condensation of 4-benzyloxy-3-methoxyphenylethylamine (**193**) with (4-ethoxycarbonyloxyphenyl)acetyl chloride (**194**), Bischler–Napieralski cyclization of the resultant amide (**195**) to afford the hydrochloride salt of dihydroisoquinoline **196**, PtO<sub>2</sub>-catalyzed reduction of the imine, and phenolic deprotection by acid

hydrolysis (Scheme 49).<sup>62</sup> An Arndt–Eistert reaction between amine (**193**) and 4-methylsulphonyloxydiazoketone has also been employed to synthesize amide **195** en-route to coclaurine (**179**).<sup>63</sup> The above sequence has since been adapted and modified in later syntheses of related tetrahydroisoquinolines. For example, *N*-methylcoclaurine (**180**) was obtained through a LiAlH<sub>4</sub>-mediated reduction of the urethane derivative of dibenzylcoclaurine followed by hydrogenolysis.<sup>64</sup> The Bischler–Napieralski reaction and Noyori reduction is another representative synthesis sequence often applied in the construction of these isoquinoline scaffolds.



**Scheme 50.** Hiemstra's strategy to access ten benzyltetrahydroisoquinolines (**201**)

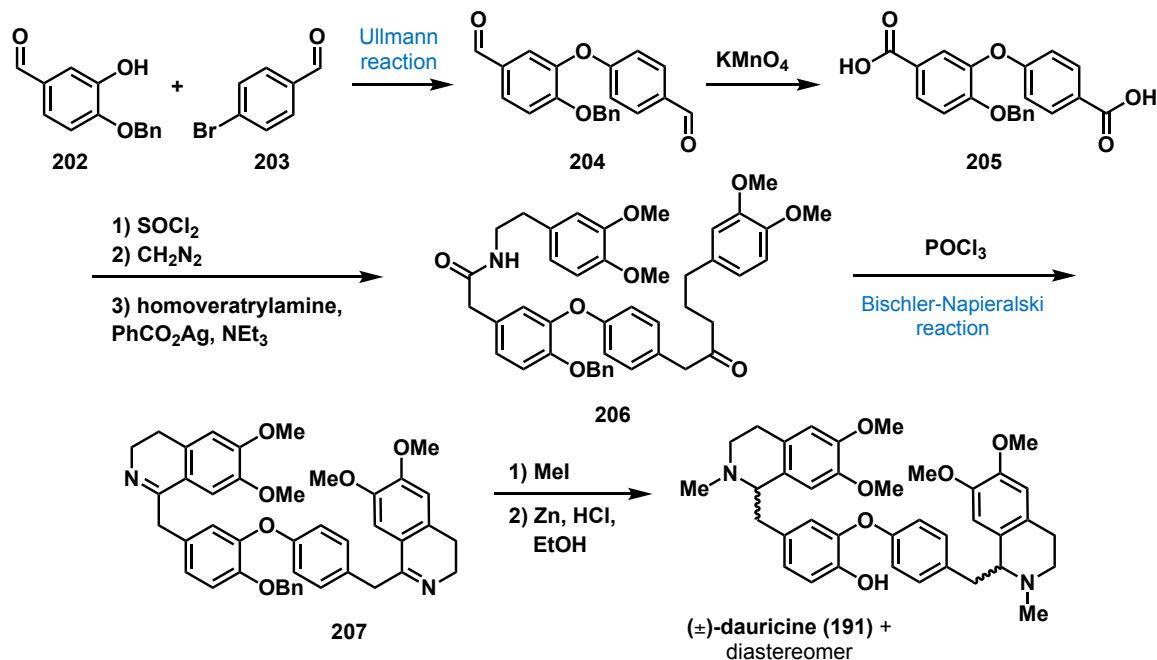
Contemporary synthetic methods have been aimed at utilizing *N*-acyl Pictet–Spengler reactions rather than the conventional Bischler–Napieralski protocols to provide the tetrahydroisoquinolines directly, thus enhancing step-economy. In 2015, Hiemstra and co-workers reported an enantio- and regioselective Pictet–Spengler condensation between aryl acetaldehydes (**198**) and *o*-nitrophenylsulfenyl (Nps)-substituted

arylethylamines (**199**) using (*R*)-TRIP as the chiral catalyst (Scheme 50).<sup>65</sup> This method provided access to several 1-benzyl-1,2,3,4-tetrahydroisoquinolines with up to 92% enantiomeric excess. With this organocatalyzed Pictet–Spengler reaction, the Hiemstra group accomplished the synthesis of ten biologically relevant tetrahydroisoquinoline alkaloids, including (*R*)-coclaurine, (*R*)-reticuline, (*R*)-norprotosinomenine, and other variants. Illustrated in Scheme 50, the steps subsequent to the key (*R*)-TRIP-catalyzed Pictet–Spengler reaction are high yielding and straightforward. *O*-Methylation of the resulting tetrahydroisoquinolines (**200**) using MeI and K<sub>2</sub>CO<sub>3</sub> followed by acid-mediated cleavage of the MOM, TBS, and Nps groups gave the alkaloids (**201**) as their hydrochloride salts in 71–89% overall yield with the ee's being mostly preserved. The *N*-methyl derivatives were fashioned from the unprotected alkaloids via reductive amination with NaCNBH<sub>3</sub> and formaldehyde.

#### 2.1.4.2 Synthesis of Acyclic bisBIAs

There exists two fundamental synthetic approaches to bisBIAs.<sup>8</sup> One is to form diaryl ether bonds for tail-to-tail or head-to-tail connected bisBIAs, to which are subsequently elaborated to isoquinoline fragments (see Scheme 49). The second method is to prefunctionalize both benzyloisoquinoline units and then merge them via diaryl ether bonds. Nearly all syntheses of acyclic and cyclic bisBIAs to-date rely on the classical intra- and intermolecular copper-catalysed Ullmann reaction to generate mono- and (bis)ether linkages, respectively, despite its lack of efficiency: long reaction times, high temperatures, stoichiometric amount of copper salts, and low yields. Variations of the reaction utilizing nickel and palladium have relatively broadened the substrate scope and rendered the reaction

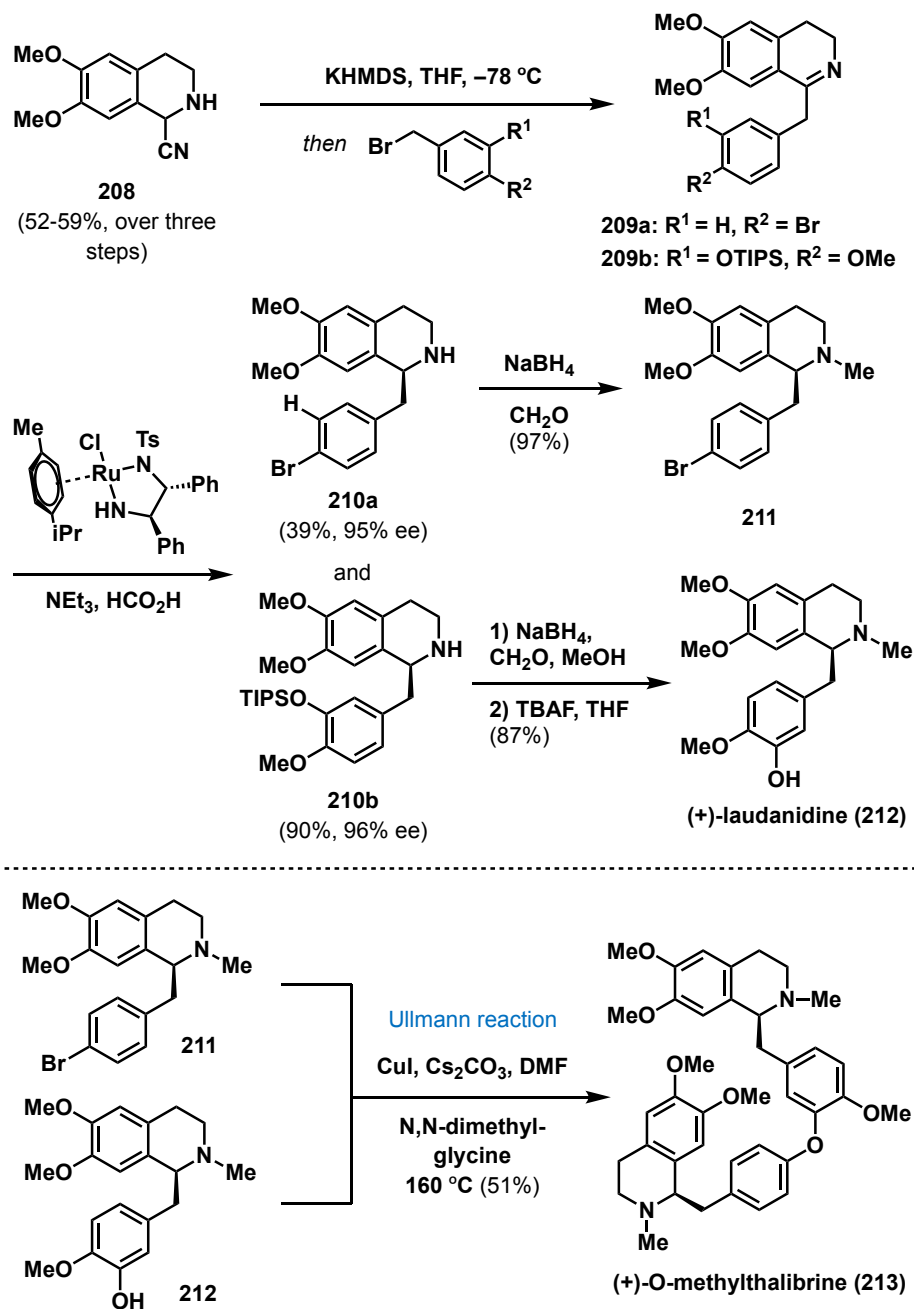
conditions milder. Namely, modern alternatives such as the Chan–Evans–Lam reaction<sup>66</sup> and Buchwald–Hartwig coupling<sup>67</sup> have been explored to assemble the diaryl ether linkages. However, yields remain inconsistent for C–O bond formation, especially in the context of bisBIAs.



**Scheme 51.** Total synthesis of (±)-dauricine (**191**, no yields reported)

One of the early pioneering efforts in the synthesis of the acyclic bisBIA series was in 1955, when a scheme was devised for constructing *O*-methyldauricine via Ullmann coupling between (–)-armepavine and (–)-3-bromo-*O*-methyarmepavine, which was achieved in 24% yield.<sup>68</sup> A similar approach was opted by Kametani and Fukumoto nearly one decade later for the first total synthesis of (±)-dauricine (**191**) and its diastereomer using both the Arndt–Eistert homologation and Bischler–Napieralski reactions (Scheme 51).<sup>69</sup> Other early synthetic iterations of magnolamine, daurinine, magnoline and berbamine

were obtained through reaction sequences analogous to Scheme 49, all of which integrated Ullmann couplings as the key step with yields ranging from 4–20%.<sup>70</sup> A comparable tactic was chosen by Nishimura *et al.* for the synthesis of nelumboferine and three unnatural stereoisomers of neferine (**190**) and *O*-methylneferine.<sup>71</sup> Ullmann coupling of the tetrahydroisoquinoline units with copper(I) bromide and Cs<sub>2</sub>CO<sub>3</sub> in pyridine gave the respective dimers in 34–45% yields.

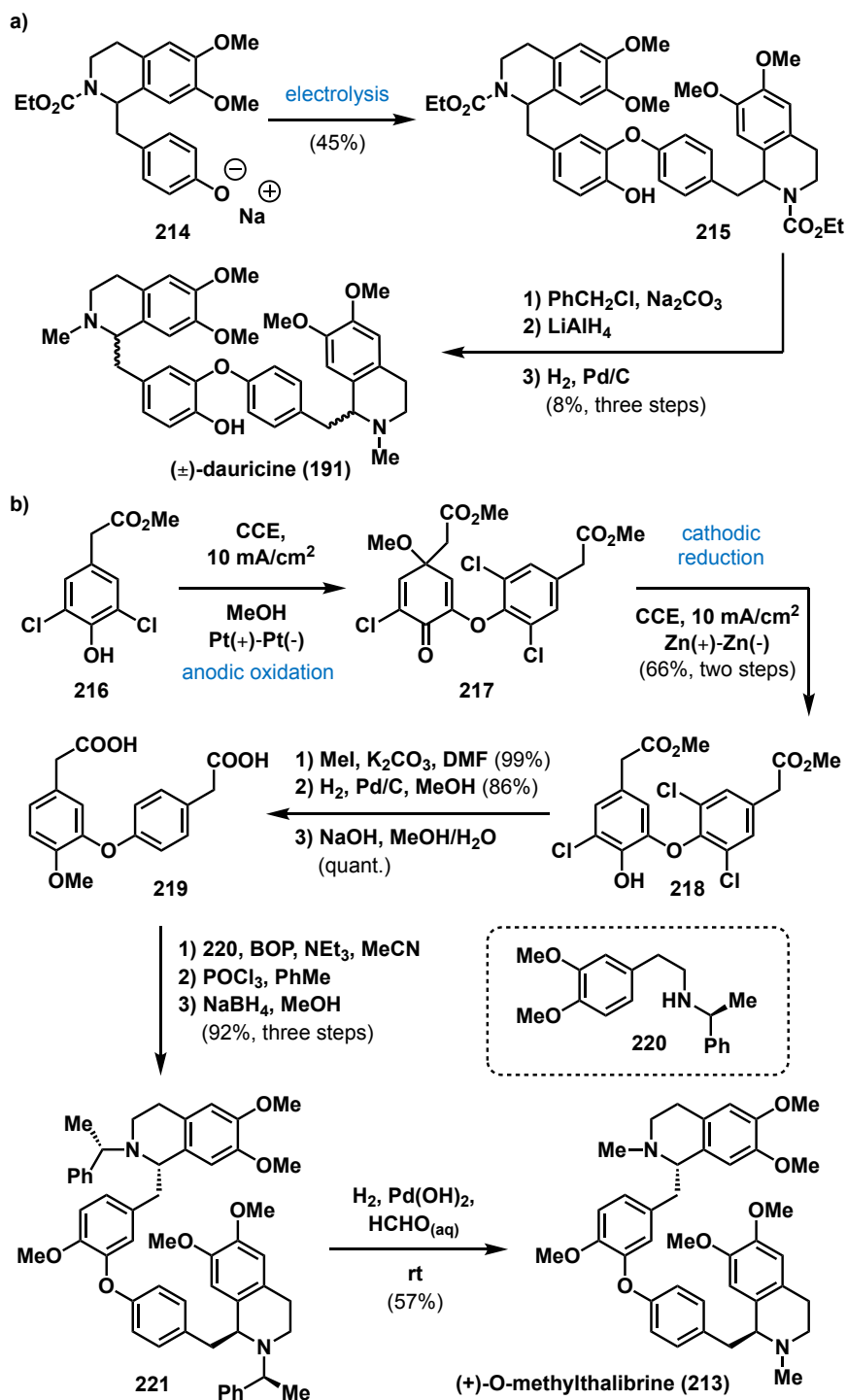


**Scheme 52.** Total synthesis of (+)-*O*-methylthalibrine (**213**).

Modular strategies have been developed for the enantioselective synthesis of bisBIAs. Both benzyloisoquinoline units in the total synthesis of (+)-*O*-methylthalibrine (**213**) arose from 1,2,3,4-tetrahydroisoquinoline-1-carbonitrile

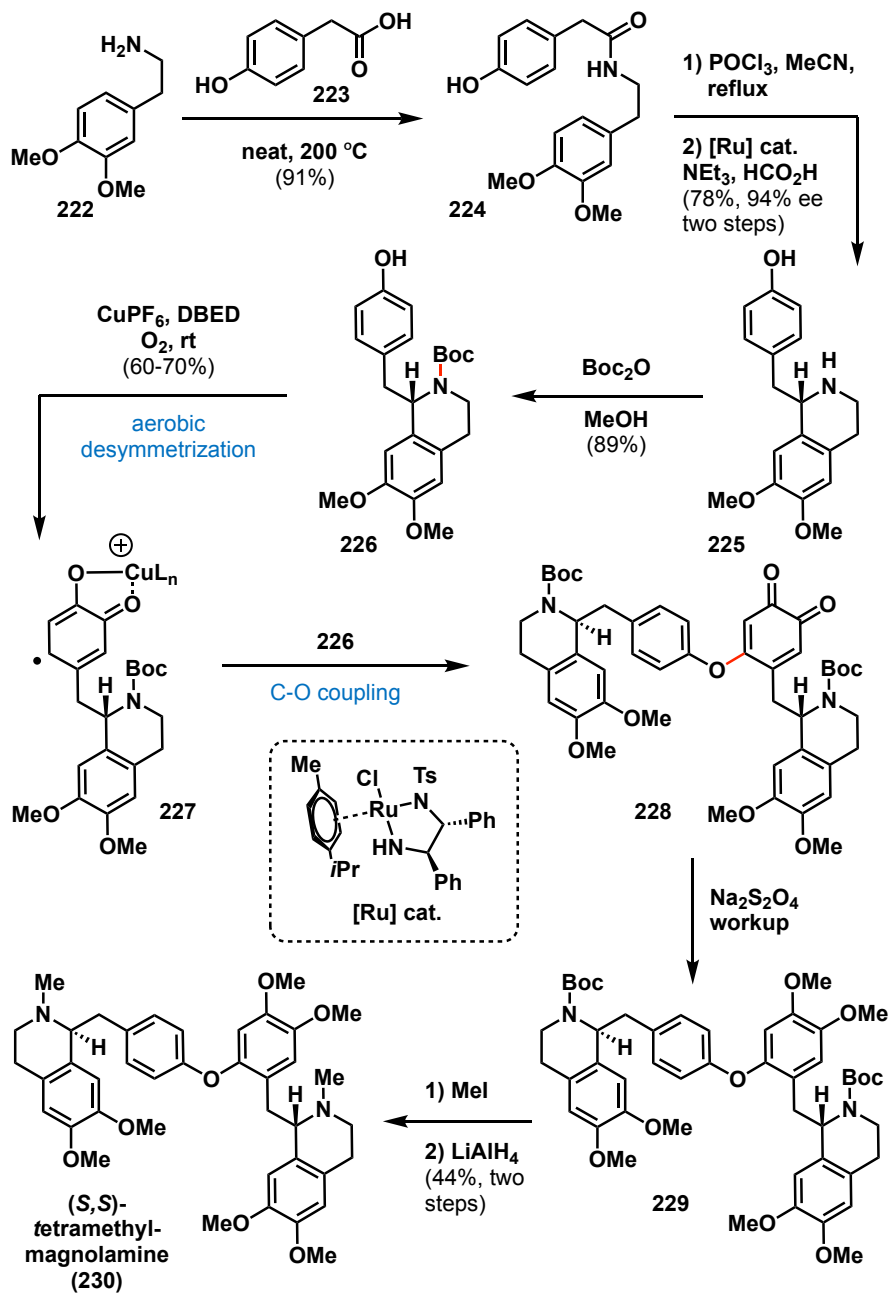
(**208**), which was deprotonated with KHMDS and alkylated to provide 3,4-dihydroisoquinolines **209a** and **209b** (Scheme 52).<sup>72</sup> Noyori transfer hydrogenation, reductive *N*-methylation with NaBH<sub>4</sub> and formaldehyde afforded bromobenzylisoquinoline **211** and (+)-laudanidine (**212**) as the precursors for the final Ullmann coupling, which delivered bisBIA **213** in 51% yield. This protocol was exploited for the asymmetric synthesis of bisbenzylisoquinoline derivative (+)-tetramethylmagnolamine as well as benzylisoquinolines (+)-laudanosine and (+)-armepavine.

Although Ullmann cross-coupling reactions have been extensively applied in aryl ether syntheses, oxidative C–O bond forming reactions have been considered as green and cost-effective surrogates. The first preparation of a naturally occurring bisBIA using an electrolytic oxidation was described in 1971 by Bobbitt and Hallcher.<sup>73</sup> When the sodium salt of (±)-*N*-carbethoxy-*N*-norarmepavine (**214**) was subjected to electrolysis using tetramethylammonium perchlorate as the electrolyte, a graphite anode together with a platinum cathode, a carbon–oxygen (**215**) linked dimer was obtained (Scheme 53a). Subsequent *O*-benzylation, reduction, and catalytic debenylation, furnished a racemic and diastereomeric mixture of dauricine (**191**).



**Scheme 53.** Electrochemical methods to synthesize a) (±)-dauricine (**191**) and b) (+)-*O*-methylthalibrine (**213**)

To install the diaryl ether moieties of bisBIAs at an early stage, Nishiyama and co-workers broadly surveyed electrolytic phenol couplings.<sup>74</sup> Following an extensive screening of electrochemical constraints and reactants, the conditions for the anodic oxidation of phenol **216** and ensuing cathodic reduction of dimer **217** were developed for the preparation of (+)-*O*-methylthalibrine (**213**) and its derivatives (Scheme 53b). *O*-methylation and dehalogenation of dimer **218** yielded diacid **219**. The phenylacetic acid moieties were then coupled to phenylethylamine derivative **220** bearing a chiral auxiliary to achieve two simultaneous asymmetric Bischler–Napieralski reactions. Substitution of the chiral auxiliary groups with methyl groups afforded (+)-*O*-methylthalibrine (**213**) in an overall yield of 29% over ten steps.



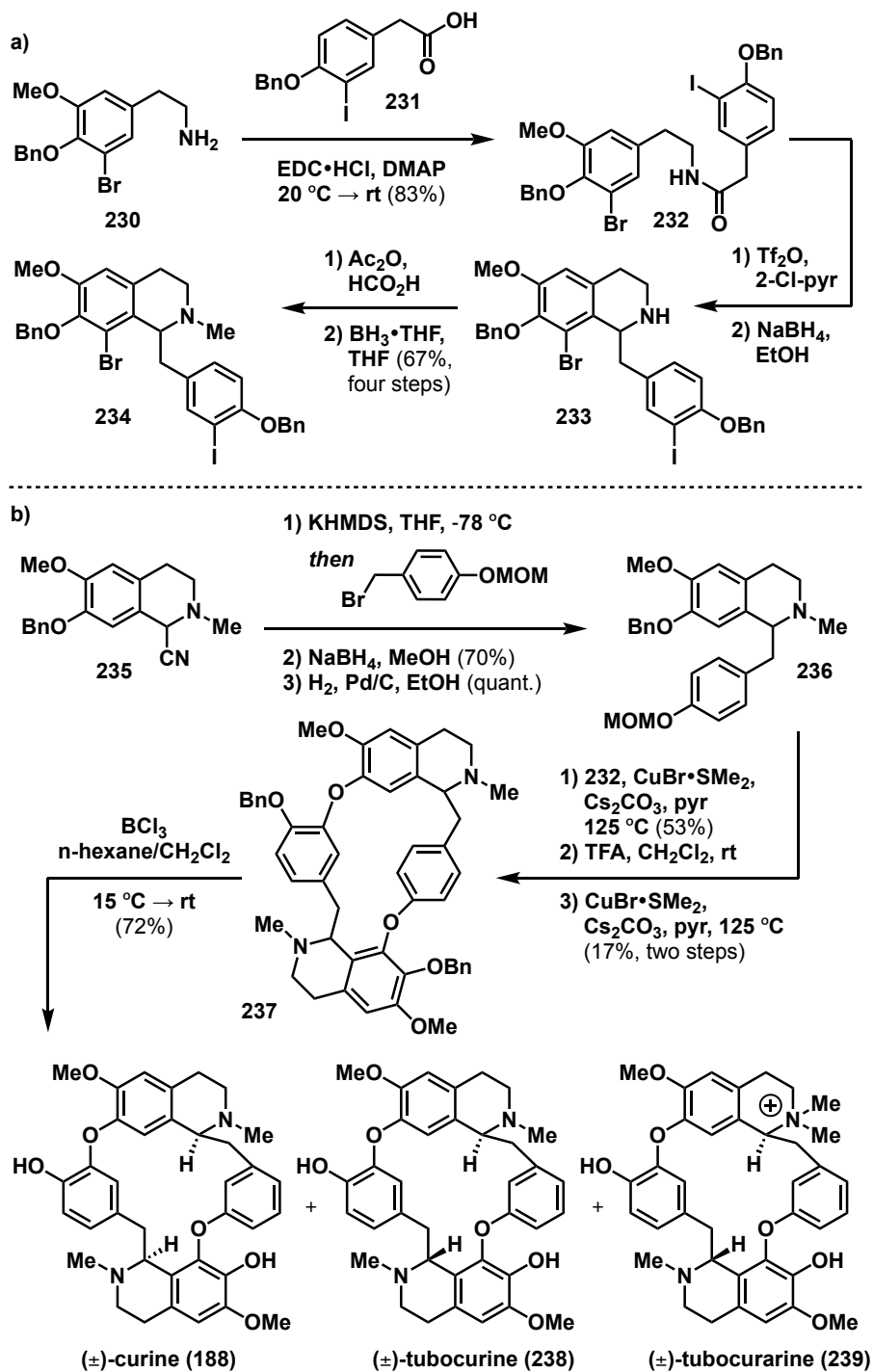
Scheme 54. Huang and Lumb's synthesis of (S,S)-tetramethylmagnolamine (**229**).

DBED = *N,N'*-di-tert-butylethylenediamine

A recent total synthesis of (*S,S*)-tetramethylmagnolamine (**230**) featured a unique instance of catalytic aerobic desymmetrization that took advantage of the alkaloid's inherent pseudosymmetry (Scheme 54).<sup>75</sup> The synthesis commenced with the preparation of Boc-protected tetrahydroisoquinoline **226** via amidation of homoveratrylamine (**222**) and 4-hydroxyphenylacetic acid (**223**). The Bischler–Napieralski cyclization of the accompanying amide (**224**) permitted an asymmetric Noyori hydrogenation to deliver free amine **225** in 70% yield with 94% ee. Upon protection of the amine (**225**) with Boc<sub>2</sub>O, the strategic aerobic oxidative coupling was realized by treatment with O<sub>2</sub> and a catalyst system comprised of CuPF<sub>6</sub> and *N,N'*-di-*tert*-butylethylenediamine (DBED). Reductive workup then gave rise to the corresponding catechol derivative (**229**). Methylation of **229** and reduction of the *N*-Boc groups supplied the dimeric alkaloid (**230**) over seven steps in 21% overall yield. A prior synthesis of **230** by Blank and Opatz required sixteen steps in 14% overall yield and employs a conventional Ullmann coupling to form the key diaryl ether.<sup>72</sup>

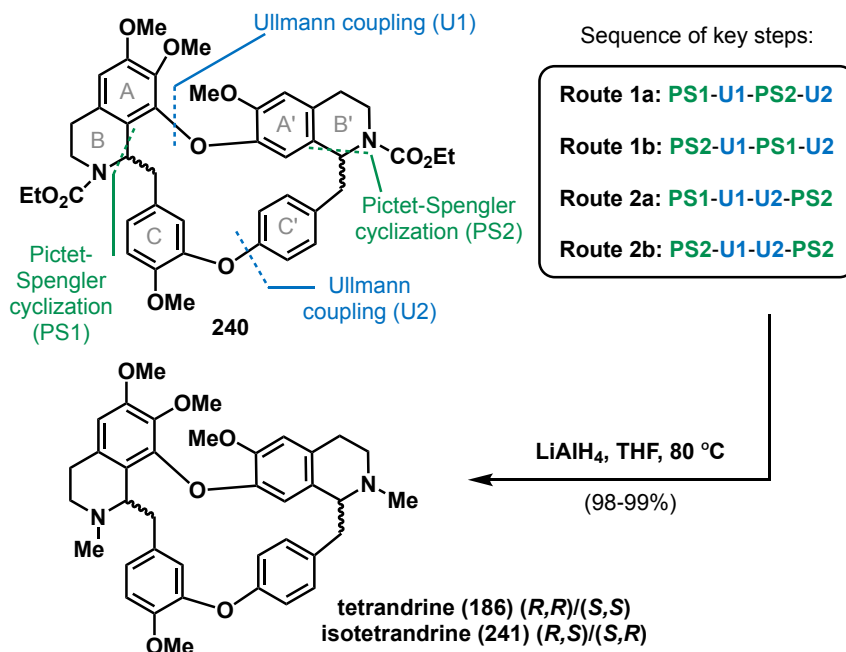
#### 2.1.4.3 Synthesis of Cyclic bisBIAs

Cyclic bisbenzyloisoquinoline alkaloids constitute the more prominent yet challenging class of this natural product family, especially in the context of establishing the appropriate diaryl ether linkages. In 2017, Opatz and co-workers accomplished the racemic synthesis of (±)-curine (**188**) and (±)-tubocurine (**238**) based on two sequential Ullmann-type condensations (Scheme 55).<sup>8,76</sup>



**Scheme 55.** Opatz's synthesis of (±)-curine (**188**) and (±)-tubocurine (**238**) and formal total synthesis of (±)-tubocurarine (**239**)

Preparation of the dihalogenated building block (**234**) began with an amide coupling of phenylethylamine **230** and phenylacetic acid **231** (Scheme 55a). The Bischler–Napieralski reaction of amide **232** mediated by 2-chloropyridine and triflic anhydride generated an imine, which was subsequently reduced to amine **233**. N-methylation of the amine (**233**) provided the dihalide (**234**). Analogous to the protocol shown in Scheme 51, the second MOM-protected benzyloquinoline moiety (**236**) was synthesized from aminonitrile **235** over three steps via an umpolung, alkylation-reduction sequence (Scheme 55b). The rather risky double C–O couplings of precursors **234** and **236** were performed under the reported Ullmann reaction conditions in Scheme 54b. Finally, removal of the benzyl groups delivered (±)-curine (**188**) and (±)-tubocurine (**238**) in a 2:1 diastereomeric ratio. The total synthesis of **238** also embodied the formal synthesis of (±)-tubocurarine (**239**).



**Scheme 56.** Bracher's modular total synthesis of ( $\pm$ )-tetrandrine (**186**) and isotetrandrine (**241**). Conditions for Ullmann couplings: CuBr•SMe<sub>2</sub>, Cs<sub>2</sub>CO<sub>3</sub>, pyridine, 110 °C; Pictet–Spengler reactions: TFA, CH<sub>2</sub>Cl<sub>2</sub>

The aforementioned dual Ullmann reaction was similarly presented in a modular twelve-step synthesis to racemic tetrandrine (**186**) and its diastereomer isotetrandrine (**241**), Scheme 56).<sup>77</sup> Presented in four distinct routes, each strategy incorporated *N*-acyl Pictet–Spengler reactions to access the 1-benzyltetrahydroisoquinoline units and copper-mediated Ullmann-type couplings for C–O bond formation. The first route provided the macrocyclic skeleton (**240**) using two alternating intermolecular Pictet–Spengler cyclizations and an intramolecular diaryl ether coupling. In the second route, an intramolecular *N*-acyl Pictet–Spengler condensation constructed the final alkaloid precursor (**240**). An additional variant for the above routes was also devised, whereby either of the

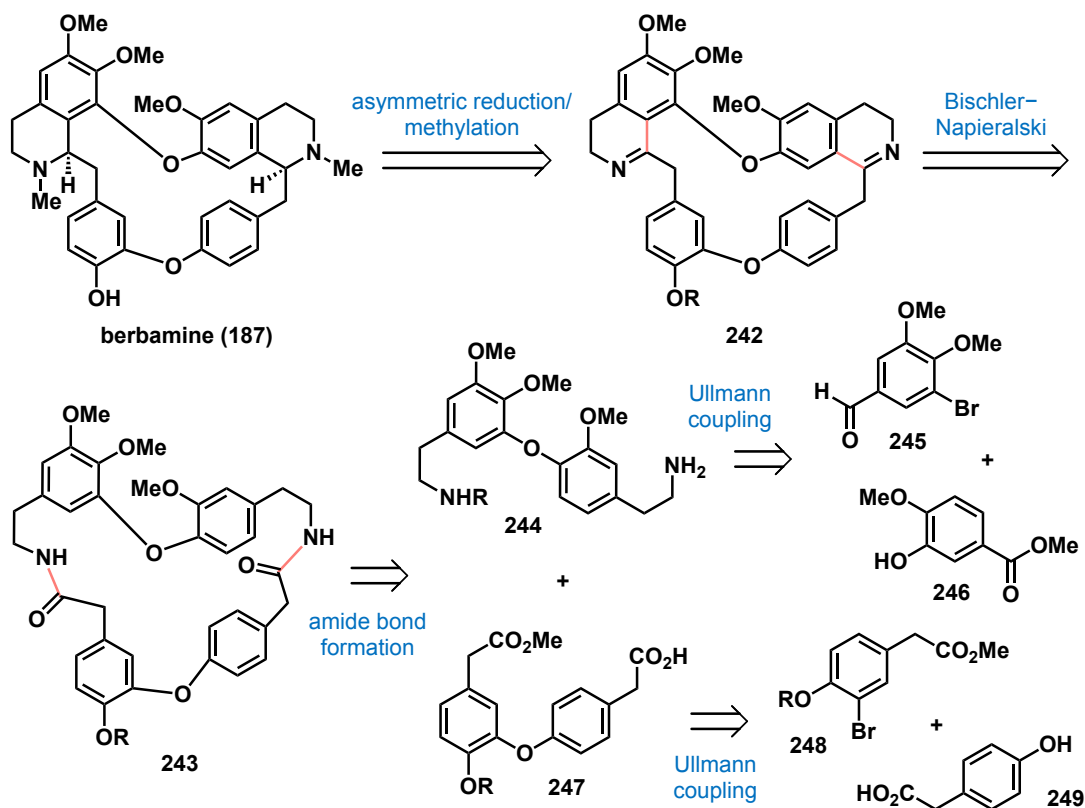
aromatic ring systems (A–C or A'–C') could be assembled at the outset. The final step of all four variants was an LiAlH<sub>4</sub>-reduction of both carbamates in macrocycle **240** to obtain racemic mixtures of (*R,R*)/(*S,S*)-tetrandrine (**186**) and (*S,R*)/(*R,S*)-isotetrandrine (**241**) in 3–19% overall yields. The authors computationally analyzed the observed diastereomeric outcome of the key Pictet–Spengler cyclizations, which revealed that the stereochemistry at the C-1 stereocenter of the macrocycle helps to control the formation of the second chiral center of tetrandrine (**186**).

## 2.2 Berbamine

Reviewed in Section 2.1.3, berbamine (**187**) is the major bioactive component isolated from traditional Chinese herbal medicines such as *Berberis amurensis* (Figure 7). The bioactivities of berbamine consist of anti-hypertensive, antiarrhythmic and anti-inflammatory effects.<sup>40,78</sup> Particularly, numerous findings have divulged its antiproliferative properties toward liver and breast cancers, chronic myeloid leukemia, and melanoma with low toxicity. Observations of berbamine acting synergistically with existing chemotherapeutics have also been documented. Despite its exciting biology, only limited hit-to-lead optimizations of berbamine (**187**) are possible. This is due to not only the lack of functional group handles for derivatizations, but also the absence of a total synthesis for deeper-seated alterations in the core scaffold.<sup>48,79</sup> For example, chemical derivatives of berbamine produced to-date rely on semi-synthesis and traditional organic synthesis protocols to modify the only derivatizable phenolic site.

Hence, current access relies on isolation from natural sources, which are distributed by MilliporeSigma and Santa Cruz Biotechnology and supports numerous biomedical studies.<sup>80-82</sup> Yet, commercial samples acquired by us and our collaborator Dr. Wendong Huang at COH National Medical Center between 2018–2021 revealed compromised authenticities of approximately 0–20% purities by NMR analysis, thus leading to invalid results when used directly. A practical synthesis would provide indisputable access to berbamine and its diverse analogs. Our desire to better understand and elucidate the molecular mechanisms of berbamine (**187**) and expand the diversity of prepared derivatives prompted us to embark on a total synthesis of the bisBIA. Herein, we describe a prospective total synthesis of this compound and the research progress to date.

### 2.3 Retrosynthetic Analysis of Berbamine



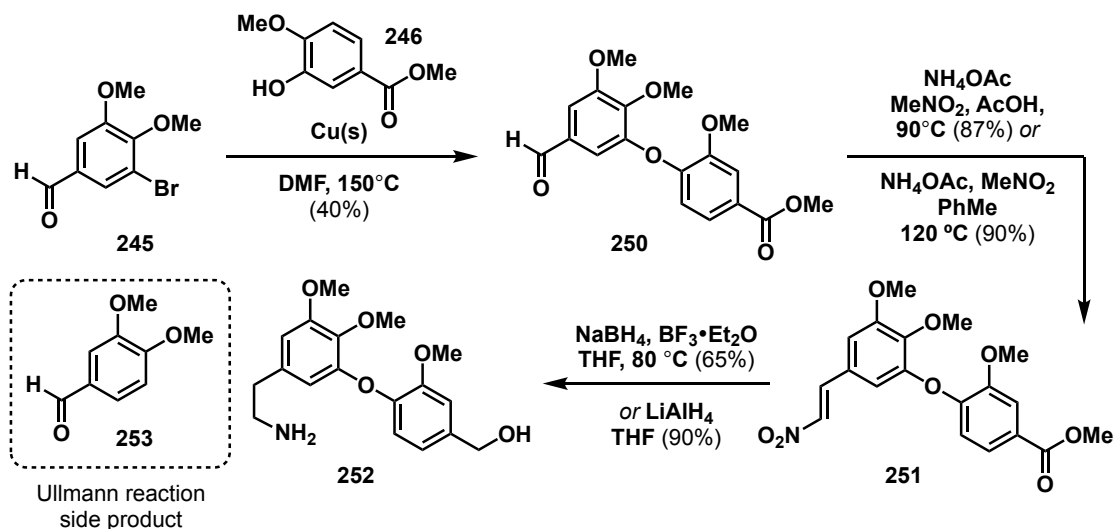
**Scheme 57.** Retrosynthesis of berbamine (**187**)

Retrosynthetically, the tetrahydroisoquinoline core of berbamine (**187**) would arise from cyclic bisdihydroisoquinoline **242** (Scheme 57). In the forward sense, asymmetric hydrogenation followed by *N*-alkylation of the heterochiral (*R,S*)-amine precursor would provide berbamine. Formation of **242** would be realized via a double Bischler–Napieralski cyclization from macro lactam **243**, which would be assembled through coupling of bis(arylethyl)amine **244** and phenylacetic acid **247**. Both of which would be forged via Ullmann coupling between their phenol and aryl halide precursors.

## 2.4 Results and Discussion

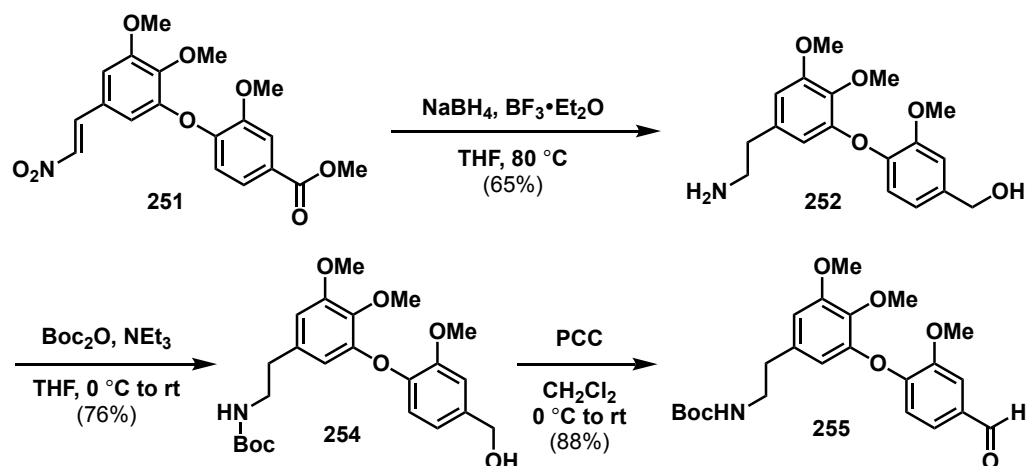
### 2.4.1 Synthesis of Amine Fragment

The northern hemisphere of the molecule, bis(arylethyl)amine **244**, was imagined as coming from commercially available 5-bromovanillin (**245**) and methyl vanillate (**246**, Scheme 57). To forge the preliminary, electron-rich diaryl ether of **250**, the direct coupling between **245** and **246** was examined using different catalysts and solvents (Scheme 58). The first attempt in the presence of 25 mol% of copper(I) or copper(II) oxide catalyst and 1.0 or 2.0 equivalents of  $K_2CO_3$  as the base additive did not effectively promote the C–O cross coupling reaction. Rather,  $^1H$  NMR analysis of the crude material revealed substantial quantities of starting material. Copper(I) thiophene-2-carboxylate (CuTC) and  $Cs_2CO_3$  under the assistance of a bidentate 2,2'-bipyridine (BiPy) ligand in MeCN, PhMe, DMSO, DCE, and dioxane furnished methyl vanillate (**246**) and often veratraldehyde (**253**), resulting from dehalogenation of the original aryl bromide (**245**).<sup>77</sup> Low catalytic amounts of copper(I) iodide and  $Fe(acac)_3$  with 2.0 equivalents of  $K_2CO_3$  likewise did not provide the coupling product **250**. Catalytic copper(I) bromide dimethyl sulfide ( $CuBr \cdot SMe_2$ ), copper(I) iodide (CuI) as well as  $Cu_{(s)}$  were screened with different additives, such as *N*-methoxybenzamide, picolinic acid, and  $K_3PO_4$  were screened, although with no significant outcome. However, 5-bromovanillin (**245**) and methyl vanillate (**246**) were reacted in refluxing DMF with 5.0 equivalents of  $Cu_{(s)}$ , affording the expected dibenzylated diaryl ether **250** in 40% yield.<sup>83</sup> It was noted that a predominant side product was veratraldehyde (**253**), once again due to dehalogenation of **245**.



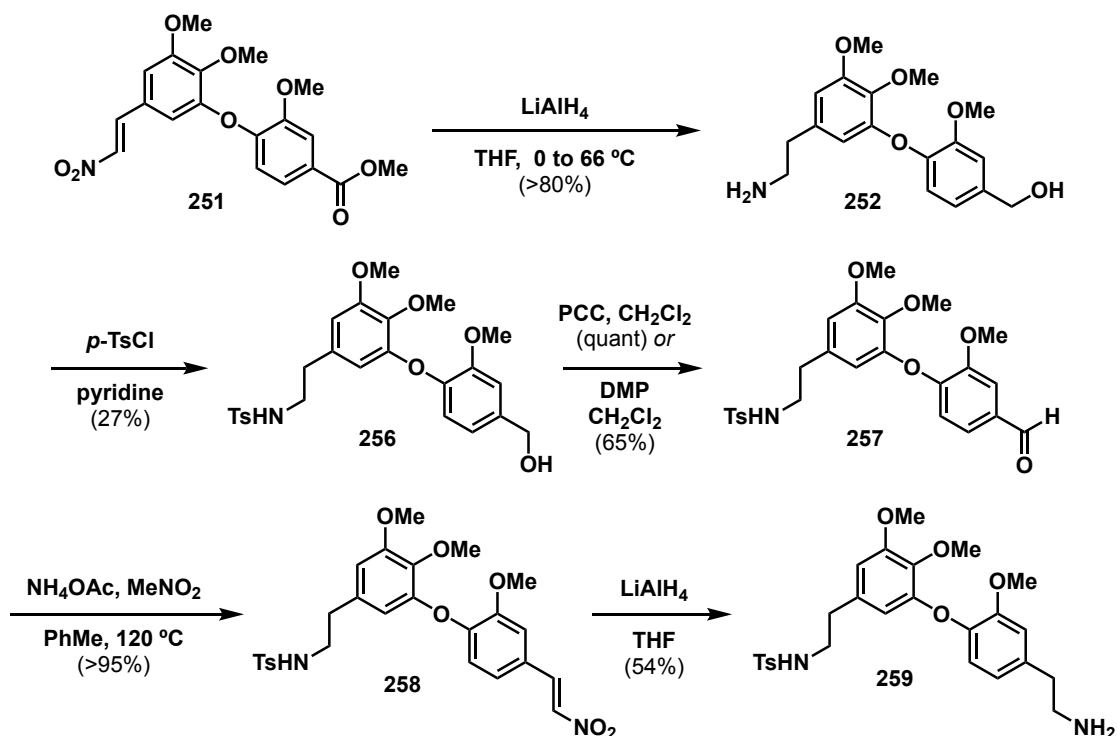
**Scheme 58.** Synthesis of arylethylamine **252**

Diaryl ether **250** possessed an aldehyde that was converted to nitrostyrene **251** in 87% yield via a Henry reaction (Scheme 58).<sup>84</sup> A minor modification of the Henry reaction protocol with PhMe as the solvent instead of AcOH increased the yield of nitrostyrene **251** to 96%. Early attempts to form the ensuing arylethylamine (**252**) were investigated using a Zn(s)-mediated protocol.<sup>85</sup> Based on <sup>1</sup>H NMR analysis of the isolated material, the desired amine (**252**) seemed to have been made in trace amounts, though decomposition of the substrate was observed. A separate reduction protocol using NH<sub>4</sub>HCO<sub>2</sub> and Pd/C suggested only minor formation of the desired amine. However, NaBH<sub>4</sub>-catalyzed reduction of nitrostyrene **251** using BH<sub>3</sub>-THF provided the arylethylamine (**252**) in 23% yield.<sup>86</sup> Later modification by in-situ generated borane in THF from NaBH<sub>4</sub> and BF<sub>3</sub>-Et<sub>2</sub>O furnished amine **252** in 65% yield, which was further amended with LiAlH<sub>4</sub> in THF to increase the yield to 90%.<sup>87,88</sup>



**Scheme 59.** Synthetic route employing *N*-Boc-protected amine (**254**)

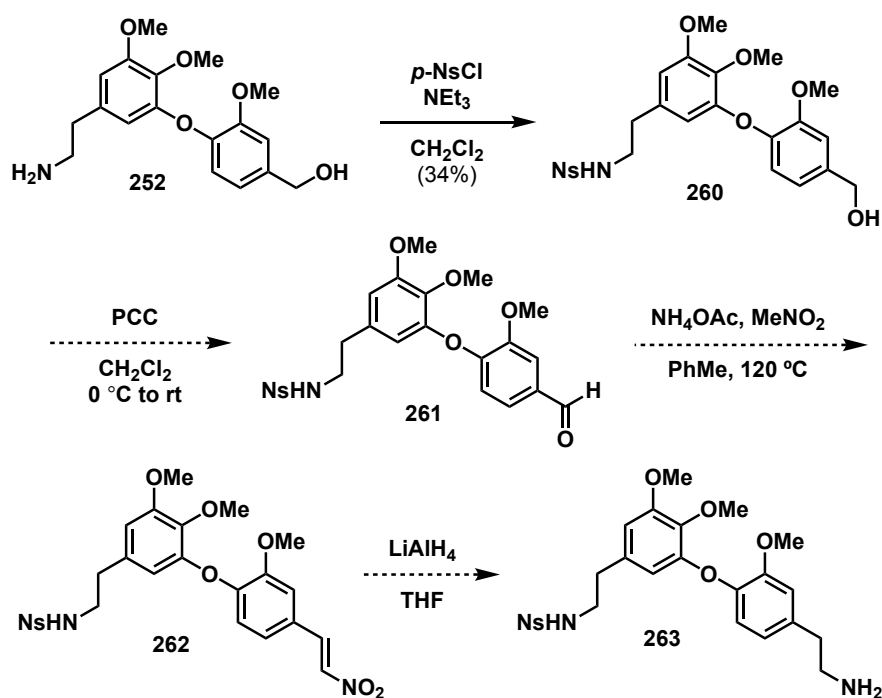
Successive *N*-Boc-protection of the resulting amine (**252**) with  $\text{Boc}_2\text{O}$  and  $\text{NEt}_3$  produced protected amine **254** (76% yield), which was oxidized to the corresponding arylaldehyde **255** in 88% yield (Scheme 59).<sup>89</sup> Reduction and amino alkylation of arylaldehyde **255** was attempted through an analogous Henry reaction–reduction sequence. The Henry reaction of **255** with  $\text{AcOH}$  and  $\text{MeNO}_2$  resulted in the nitrostyrene sans the Boc protecting group, which was cleaved presumably due to the elevated reaction temperature and acidic conditions. Another protocol for the Henry reaction using  $\text{NaOH}_{(s)}$  and  $\text{EtOH}$  was attempted. Yet,  $^1\text{H}$  NMR analyses of the isolated fractions were not indicative of the desired compound. It was hypothesized that the initial nitro aldol reaction was successful, yet the concluding elimination to provide the nitrostyrene did not occur. At this point, an inherent limitation of the *N*-Boc-protected amine (**254**) was realized to be its undesirable conversion to the *N*-methylamine under reducing conditions.



**Scheme 60.** Synthetic route employing *N*-tosyl-protected amine (**256**)

The use of sulfonamide protecting groups, such as *p*-toluenesulfonamide (Ts) and nitrobenzene sulfonamide (Ns), proved to be more accommodating in the present synthetic route. Protection of the amino alcohol (**252**) with *p*-toluene sulfonyl chloride (TsCl) furnished sulfonamide **256** (Scheme 60). Oxidation of the benzylic alcohol (**256**) via PCC or DMP provided *N*-tosyl-protected arylaldehyde **257**, which was followed by an amended Henry reaction–reduction sequence to generate bis(arylethyl)amine **259** in 54% yield. A comparable sequence using *p*-nitrobenzene sulfonyl chloride (NsCl) to generate the *N*-nosyl-protected bis(arylethyl)amine (**263**) was additionally carried out as a suitable alternative to previously discussed *N*-protected amines (Scheme 61).<sup>90</sup> To optimize the yield of **260**, various reaction times, bases, temperatures, and solvents were

investigated.<sup>91-93</sup> Pyridine was replaced as the base and DCE substituted CH<sub>2</sub>Cl<sub>2</sub> as the solvent. Temperatures were also varied from -20 °C, 0 °C, rt to 30-35 °C. Yet, all were unfortunately low yielding, affording largely starting material, *O*-nosylation, or other unidentifiable products. Other conditions will need to be probed to improve the desired reactivity.

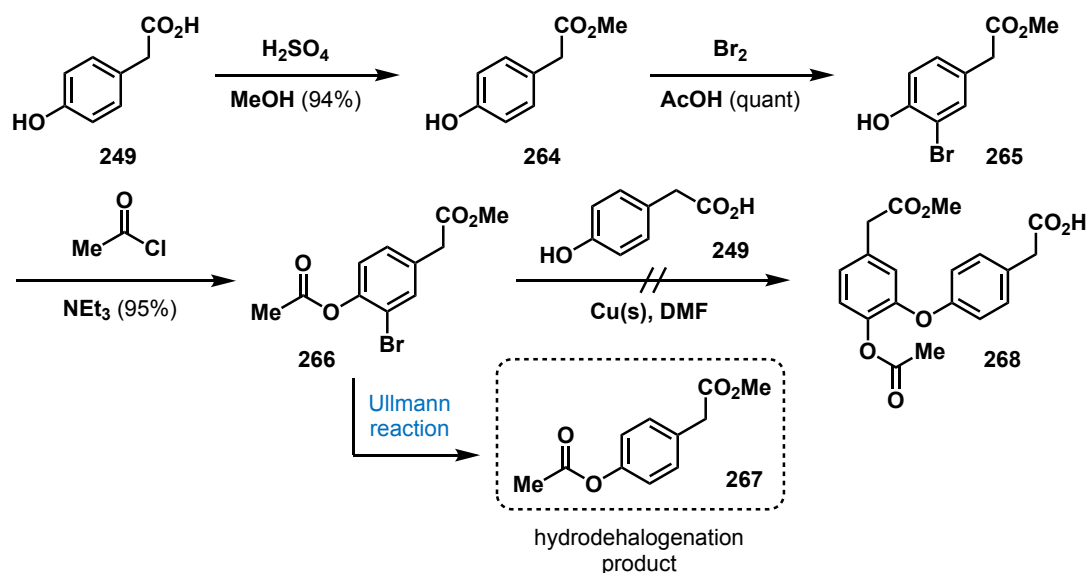


**Scheme 61.** Synthesis of *N*-nosyl-protected bis(arylethyl)amine (**263**)

#### 2.4.2 Synthesis of Phenylacetic Acid **268**

Construction of the southern hemisphere of the molecule, phenylacetic acid **268**, commenced from 4-hydroxyphenylacetic acid (**249**, Scheme 62). Esterification of **249** with H<sub>2</sub>SO<sub>4(aq)</sub> and MeOH generated methyl 4-hydroxyphenylacetate (**264**, 94% yield).<sup>94</sup> An ensuing bromination with Br<sub>2</sub> and AcOH afforded methyl 3-bromo-4-hydroxyphenylacetate (**265**).<sup>95</sup> Treating bromophenylacetate **265** with acetyl chloride

followed by aqueous work-up provided methyl 3-bromo-4-acetoxyphenylacetate (**266**) in 95% yield.<sup>96</sup>

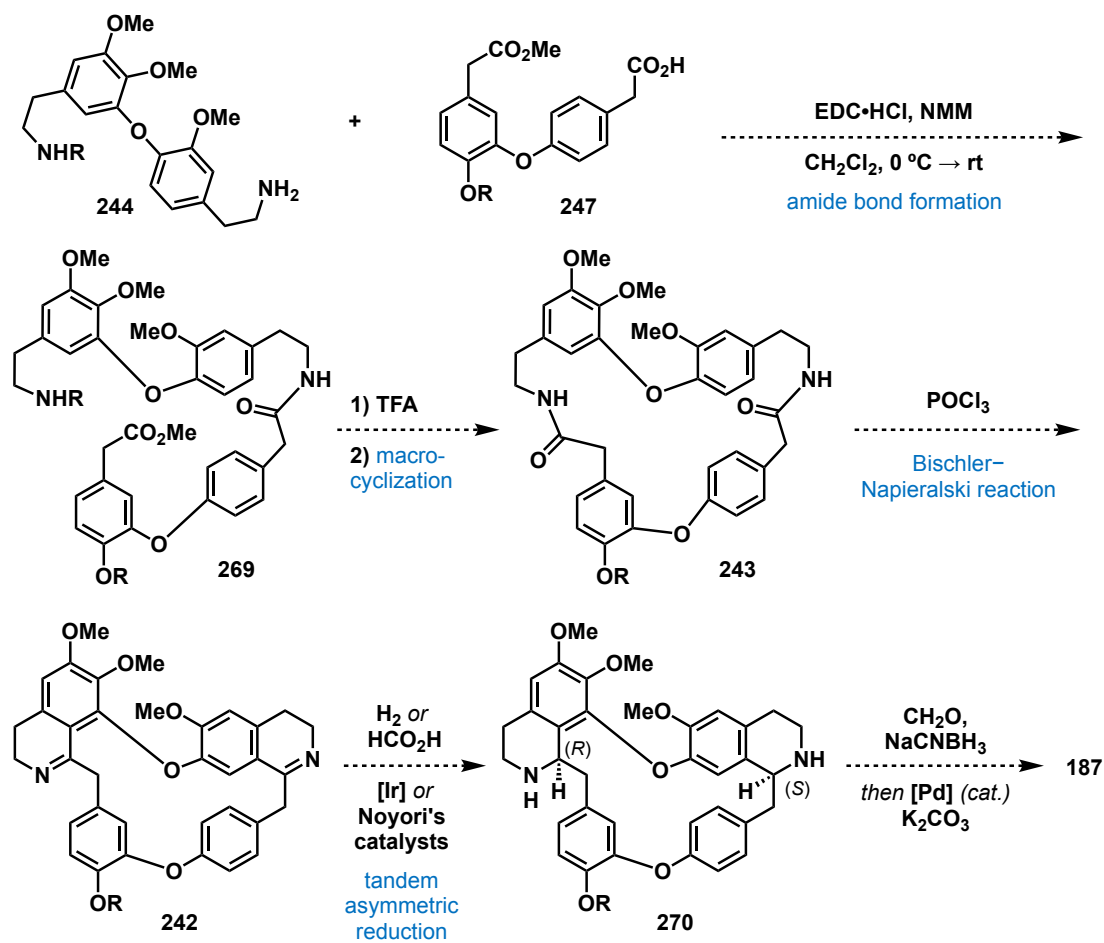


**Scheme 62.** Attempted synthesis of phenylacetic acid (**268**)

Coupling of methyl 3-bromo-4-acetoxyphenylacetate (**266**) and phenylacetic acid (**249**) initially proceeded through the standard Ullmann conditions of Cu<sub>(s)</sub> in refluxing DMF (Scheme 62). Yet, <sup>1</sup>H NMR analysis of the crude reaction mixture indicated primarily starting material. Subjecting acetoxy phenylacetate (**266**) and phenylacetic acid (**249**) to Cu<sub>(s)</sub> and potassium iodide (KI) with K<sub>2</sub>CO<sub>3</sub> in pyridine did not elicit any reactivity. Instead, reversion to aryl bromide **265** was seen, possibly through cleavage of the acyl group. Efforts using other copper sources, such as copper(I) oxide, copper(II) oxide, CuBr•Me<sub>2</sub>S, CuI, and CuTC, along with an assortment of additives and solvent substitutions yielded starting material. Akin to what was observed in Scheme 58, these studies also revealed the existence of methyl 2-(4-acetoxyphenyl)acetate (**267**) as an

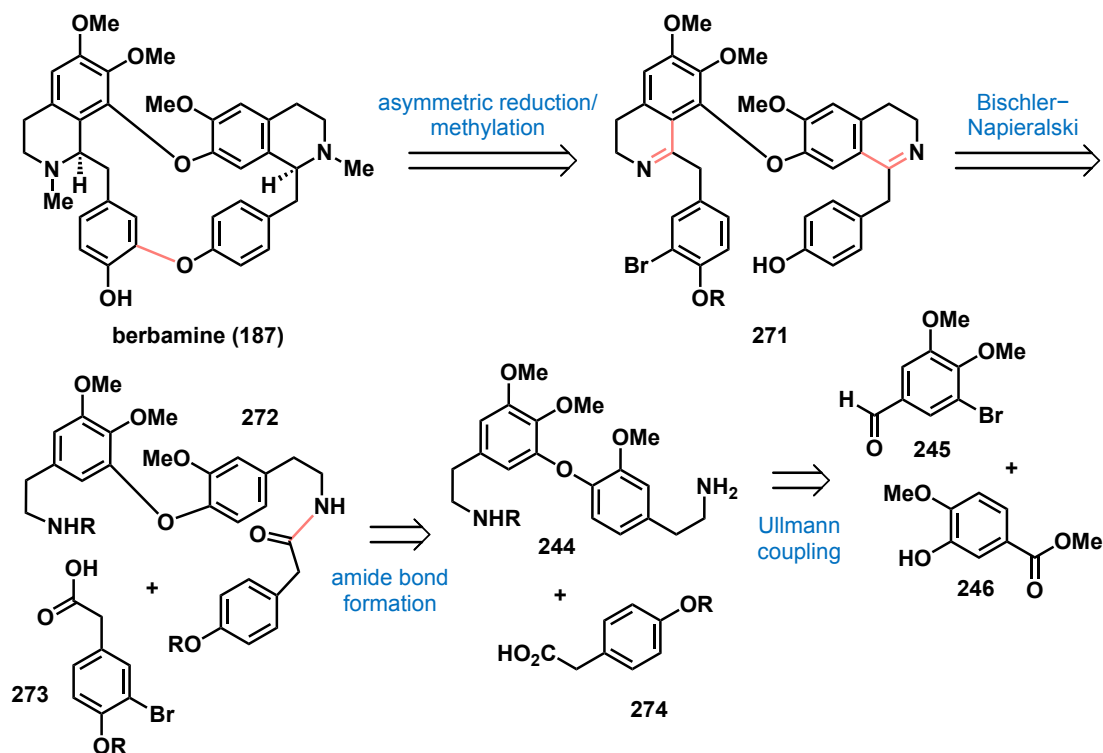
undesired side product, allegedly arising due to hydrodehalogenation of **266**. While hydrodehalogenation side reactions of aryl halides have been previously reported in other copper-catalyzed reactions, the couplings of acetoxy phenylacetate **266** with the methyl and benzyl 4-hydroxyphenylacetate analogs of **249** were attempted to resolve such unsought reactivity.<sup>97-100</sup> Unfortunately, neither yielded any fruitful result as starting material was largely reisolated. Yet, the lack of hydrodehalogenation product **267** in both instances suggested that the carboxylic acid proton to be the most likely hydrogen source in the hydrodehalogenation reaction.

Should generation of **247** be successful, the convergent nature of the synthesis plan would then involve coupling diamine **244** to dicarboxylic acid **247** to generate seco acid ester **269** (Scheme 63). Deprotection and macrocyclization would lead to lactam **243** from which a double Bischler–Napieralski cyclization would generate cyclic bisdihydroisoquinoline **242**.<sup>101</sup> Thus, setting the stage for asymmetric hydrogenation studies to hopefully yield heterochiral (*R,S*)-**270**, the precursor to berbamine (**187**), in a highly efficient manner.<sup>102</sup>



**Scheme 63.** Proposed completion of berbamine (**187**) via macrolactam (**243**) and double Bischler–Napieralski reaction strategy

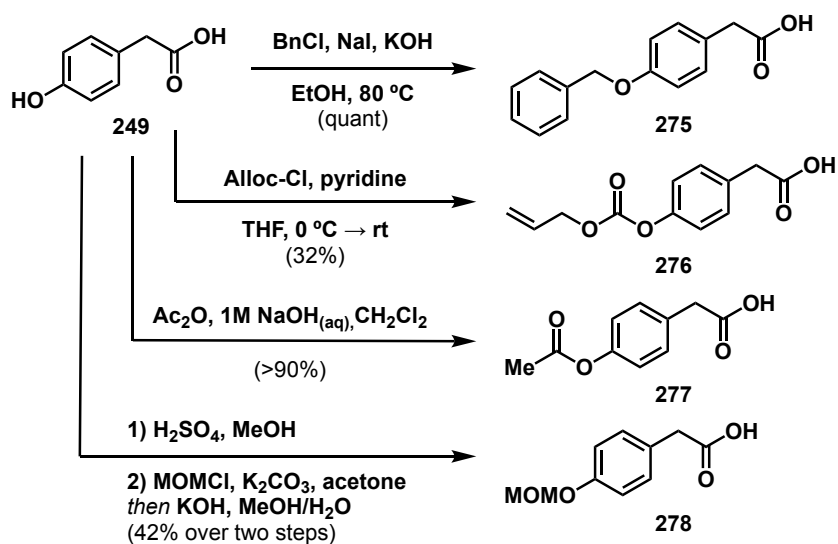
### 2.4.3 Clockwise Approach



**Scheme 64.** Retrosynthesis of **187** incorporating clockwise synthetic strategy

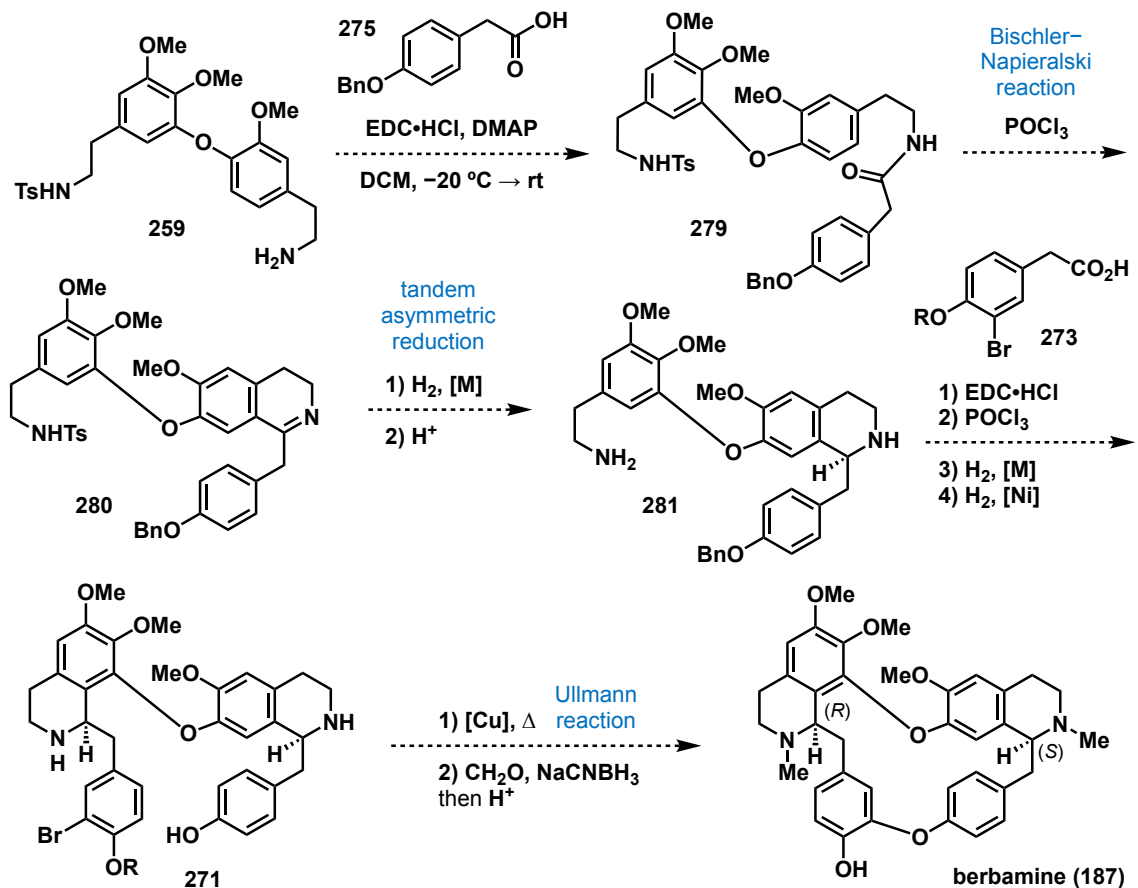
With the prior strategy in mind, another pathway was proposed in which the right-hand, then left-hand tetrahydroisoquinoline cores would be individually assembled starting from an earlier prepared intermediate, bis(arylethyl)amine **244** (Scheme 64). Thus, several variants of phenylacetic acid **274** were pursued as alternative coupling partners for bis(arylethyl)amine **244** as well as a means for any foreseeable protecting group incompatibilities further down the proposed route (Scheme 65). Starting from 4-hydroxyphenylacetic acid (**249**), 2-(4-(benzyloxy)phenyl)acetic acid (**275**) was successfully prepared using a reported protocol that employed KOH, NaI, and benzyl chloride (BnCl), in refluxing EtOH.<sup>103</sup> Installation of the allyloxy carbonyl group (**276**)

and formation of acetyl ester **277** were easily carried out with allyl chloroformate and acetic anhydride in the presence of base in 32% (unoptimized) and 90% yield, respectively.<sup>104,105</sup> The methoxymethyl (MOM) ether **278** was afforded in a two-step sequence involving a H<sub>2</sub>SO<sub>4</sub>-catalyzed Fischer esterification and subsequent saponification.<sup>106</sup>



**Scheme 65.** Synthesis of *O*-protected phenylacetic acid analogs

In a forward sense, we envisaged an amide bond formation and ensuing Bischler–Napieralski cyclization to produce dihydroisoquinoline **280** (Scheme 66). Asymmetric reduction of the resulting imine would produce amine **281**, which can be converted to bisbenzyltetrahydroisoquinoline **271** via an analogous amide bond formation–Bischler–Napieralski–reduction sequence. An intramolecular Ullmann coupling and final *N*-methylation of the two amines would furnish berbamine (**187**).

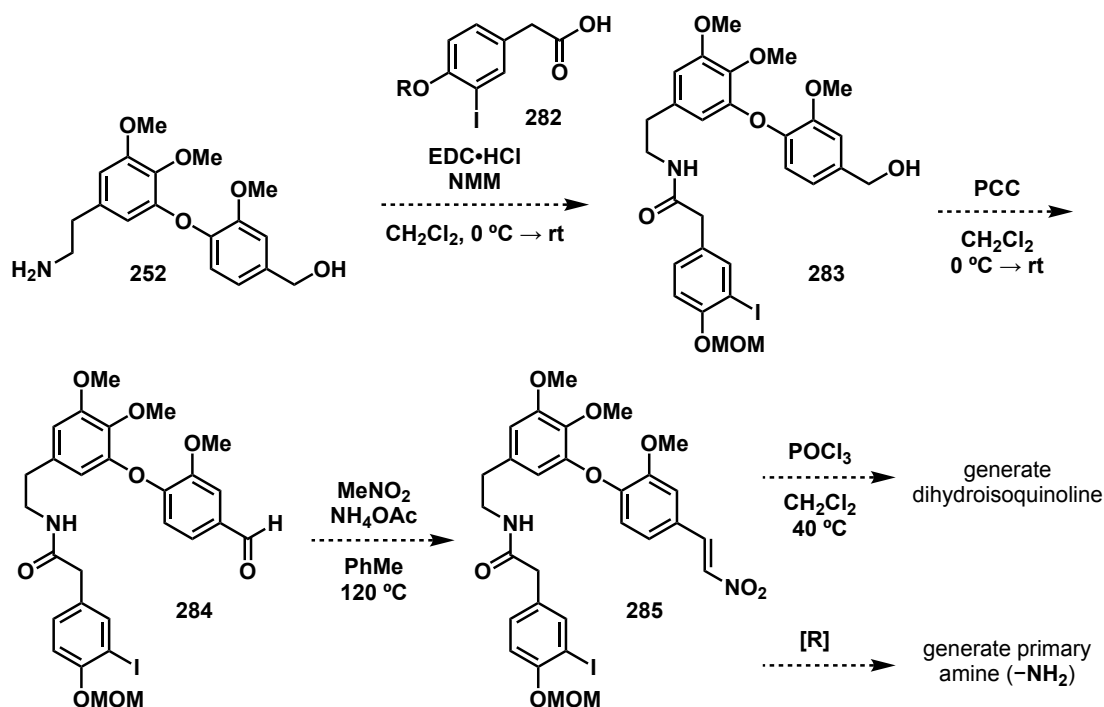


**Scheme 66.** Synthesis of berbamine (**187**) through anticipated clockwise approach

#### 2.4.4 Counterclockwise Approach

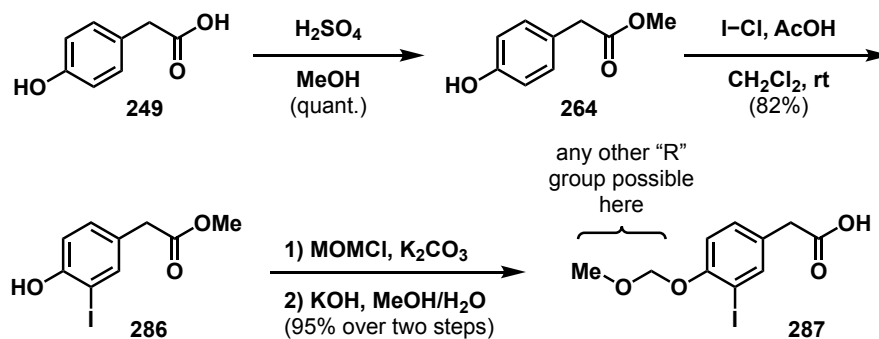
A counterclockwise synthesis was additionally explored to circumvent the protection and deprotection sequence of the bis(arylethyl)amine component, reducing the existing route by two steps. In this regard, a facile amide bond formation between free ethylamine **252** and iodophenylacetic acid **282** would make way for an oxidation enabled by PCC to give arylaldehyde **284** (Scheme 67). Subjecting arylaldehyde **284** to  $\text{MeNO}_2$  and  $\text{NH}_4\text{OAc}$  in  $\text{PhMe}$  would yield nitroalkene **285**, which could be advanced through two distinct pathways. One of which would produce the dihydroisoquinoline via a

Bischler–Napieralski cyclization and the other would involve reduction of the nitroalkene to the free ethylamine that would be taken further down the synthesis to berbamine (**187**) via a comparable route.



**Scheme 67.** Counterclockwise strategy starting from free arylethylamine **252**

For this particular route, construction of an iodinated derivative of phenylacetic acid **249** was undertaken to encourage a more facile late-stage Ullmann reaction (Scheme 68).<sup>76,106</sup> 4-Hydroxyphenylacetic acid (**249**) was subjected to an acid-mediated Fischer esterification leading to 4-hydroxyphenylacetate **264** in nearly quantitative yield. Electrophilic iodination under mildly acidic conditions preferentially gave 4-hydroxy-3-iodophenylacetate (**286**) in 82% yield. Treatment of **286** with MOMCl and K<sub>2</sub>CO<sub>3</sub> followed by hydrolysis of the embedded methyl ester afforded the desired phenolic MOM ether (**287**).

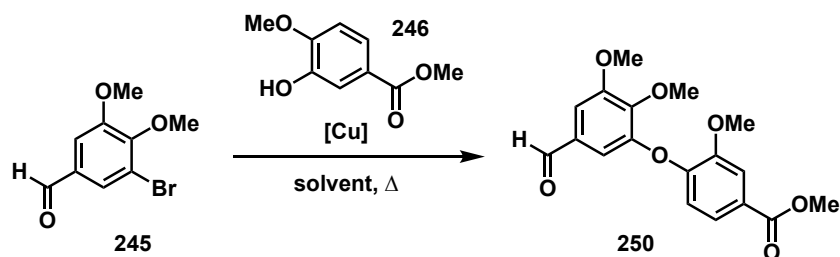


**Scheme 68.** Synthesis of iodophenylacetic acid **287**

#### 2.4.5 Diaryl Ether Studies

Fashioning the diaryl ether linkages in bisBIAs remain a challenge in modern organic synthesis and metal catalysis, with yields ranging from 4–40% using stoichiometric or superstoichiometric copper.<sup>107,108</sup> Concerning the diaryl ether scaffold synthesis, we attempted to optimize the standard Ullmann coupling conditions ( $\text{Cu}_{(s)}$  in refluxing DMF) applied to benzaldehyde **245** and phenol **246** (Table 3). A number of reaction conditions were surveyed. Altering the solvents to DMA and 4-picoline from DMF or incorporating a *N*-methoxybenzamide additive did not improve the yield of the desired diaryl ether (**250**, Entry 2–3). Lowering the initial equivalents of the phenol (**246**, Entry 4–5) also did not lead to improvements. Decreasing the quantity of  $\text{Cu}_{(s)}$  from 5.0 to 4.0 equivalents and prolonging the reaction time to 24 h seemed to have modestly improved the yield to 55% (Entry 7) yet was irreproducible. It was noted that the amounts of weighed  $\text{Cu}_{(s)}$  may have been inconsistent due to irregularities in the glovebox balance.

**Table 3.** Optimization of Ullmann coupling between 5-bromovanillin (**245**) and methyl vanillate (**246**)

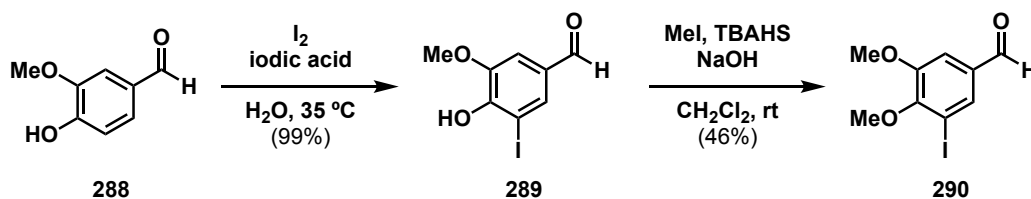


Entry	Ar-X (equiv)	Phenol (equiv)	Cu <sub>(s)</sub> (equiv)	Solvent	Yield (%)
1	1.0	3.0	5.0	DMF	40
2	1.0	3.0	5.0	DMA	30
3	1.0	3.0	5.0	4-picoline	–
4	1.0	2.0	5.0	DMF	37
5	1.0	1.0	5.0	DMF	35
6	3.0	1.0	5.0	DMF	34
7 <sup>a</sup>	1.0	3.0	4.0	DMF	55
8 <sup>a</sup>	1.0	3.0	3.0	DMF	43
9 <sup>a</sup>	1.0	3.0	2.0	DMF	41
10 <sup>a</sup>	1.0	3.0	1.0	DMF	43

<sup>a</sup>24 h reaction time. DMF = dimethylformamide, DMA = dimethylacetamide, 4-picoline = 4-methylpyridine.

An iodinated aryl halide derivative is also being entertained as a substitute for the original 5-bromovanillin (**245**) coupling partner (Scheme 69).<sup>85</sup> Beginning with commercially available vanillin (**288**), treatment with iodine and iodic acid afforded 5-iodovanillin (**289**, 99% yield). **289** was then subjected to a methylation procedure to yield

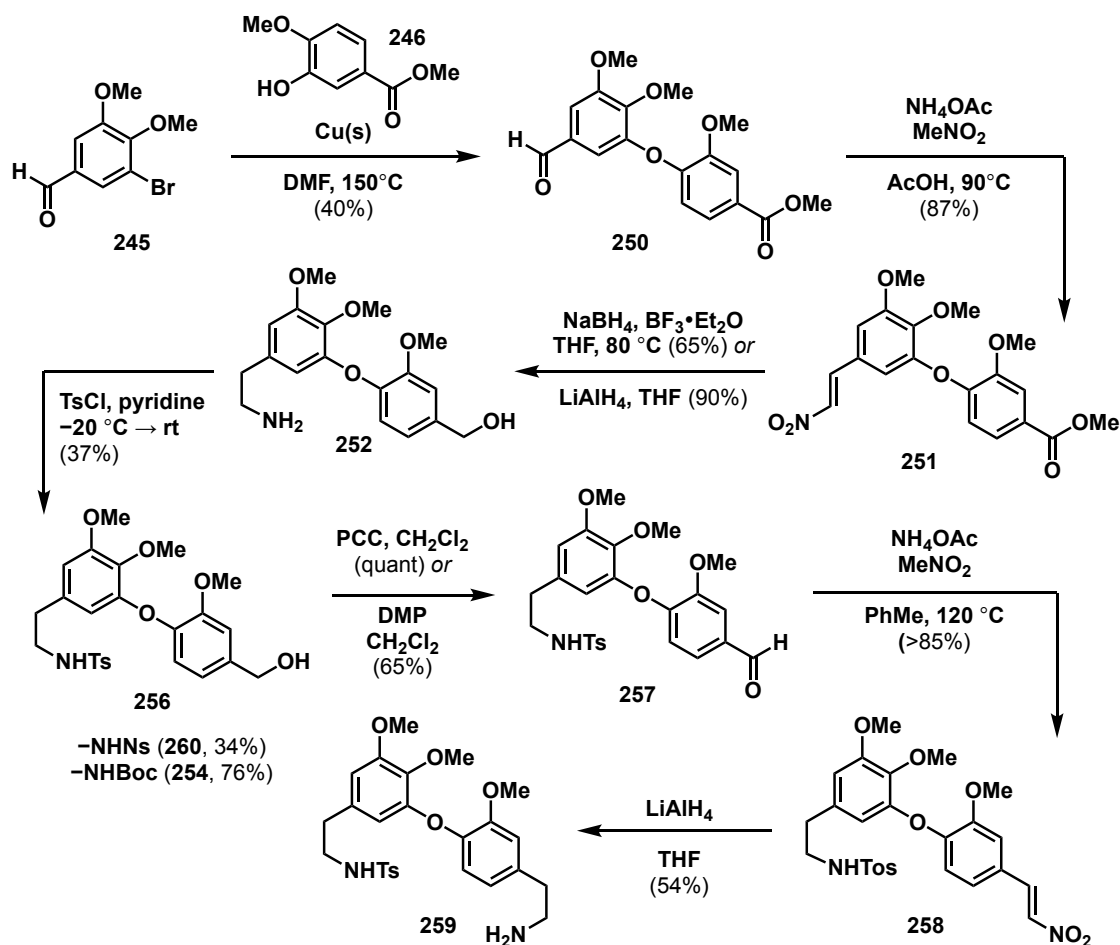
aryl iodide **290** in 46% yield, which was screened accordingly with methyl vanillate (**246**) to see if it may improve the diaryl ether bond formation.



**Scheme 69.** Synthesis of 5-iodovanillin (**290**)

## 2.5 Conclusions

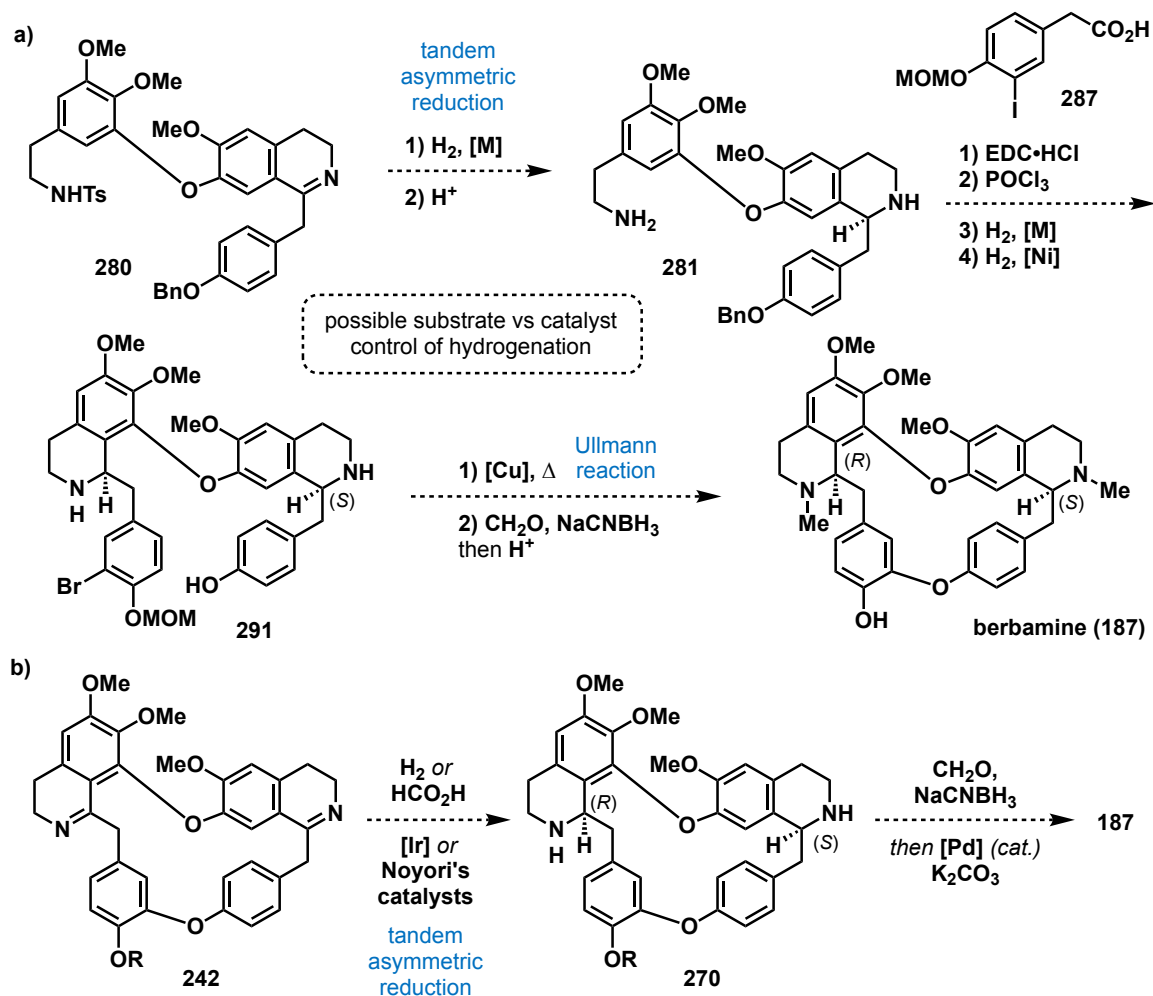
Existing approaches for the total synthesis of bisBIAs underscore limitations in the current state-of-the-art. Not only do the unique structures of bisBIAs serve as inspiration for the development of practical synthetic protocols, but the therapeutic properties of these compounds are also compelling and have spurred numerous efforts in analog synthesis. With continual interest in the function of bisBIAs, advancing synthetic strategies for practical access to enantioenriched bisBIA frameworks is warranted. And so, while the natural product itself has not yet been completed, several strategic developments were made throughout the course of the synthesis of berbamine (**187**). This encompassed the design of three alternative synthetic approaches to not only avoid undesirable side reactivity, but also investigate opportunities for derivatization, substrate-versus catalyst-controlled hydrogenation as well as atropisomerism surrounding the hindered diaryl ether.



**Scheme 70.** Current synthesis toward diethylamine fragment **259**

A scalable, seven-step strategy was thus developed to give *N*-tosyl diethylamine **259** in moderate yields while effectively incorporating the sterically encumbered, electron-rich diaryl ether linkage characteristic of bisBIAs (Scheme 70). This route included an Ullmann coupling between 5-bromovanillin (**245**) and methyl vanillate (**246**) to generate diaryl ether **250**. Further treatment of **250** via a Henry reaction provided nitrostyrene **251**, which was subjected to a LiAlH<sub>4</sub>-mediated reduction leading to the amino alcohol **252**. Following protection of **252** with TsCl, the *N*-tosyl amine **256** underwent an oxidation with either PCC or DMP to provide **257**. Through an additional

Henry-reaction–reduction sequence, the key diethylamine fragment (**259**) was completed, prompting extensive studies farther in the proposed sequences.



**Scheme 71.** Potential remaining synthetic steps to berbamine (**187**)

Therefore, successful completion of berbamine (**187**) will require access to quantities of several key components, notably diethylamine **259** as well as amino alcohol **252**. The remaining steps will focus on generating the requisite tetrahydroisoquinoline (**280** or **242**) core scaffolds (Scheme 71). The atropisomerism of bisBIAs has not been reported and we will also fill this gap by examining how the one stereocenter in

cyclization of precursor **281** influences atropselectivity in diaryl ether formation (Scheme 71a). Particularly, whether it can telescope diastereocontrol via the atropisomeric diaryl ether using an achiral catalyst in the eventual hydrogenation of **281** to **291**. Work in this direction is currently underway in our lab by Berkley Lujan.

## 2.6 Experimental Section

### 2.6.1 General Experimental

Commercial reagents were purchased from MilliporeSigma, Acros Organics, Chem-Impex, TCI, Oakwood, and Alfa Aesar, and used without additional purification. Solvents were purchased from Fisher Scientific, Acros Organics, Alfa Aesar, and Sigma Aldrich. Tetrahydrofuran (THF), diethyl ether (Et<sub>2</sub>O), acetonitrile (MeCN), dichloromethane (CH<sub>2</sub>Cl<sub>2</sub>), toluene (PhMe), 1,4-dioxane, and triethylamine (Et<sub>3</sub>N) were sparged with argon and dried by passing through alumina columns using argon in a Glass Contour (Pure Process Technology) solvent purification system. Benzene (PhH) was distilled over calcium hydride (CaH<sub>2</sub>) under a nitrogen (N<sub>2</sub>) atmosphere, degassed via freeze-pump-thaw (three cycles), and stored over 4 Å molecular sieves in a Strauss flask under N<sub>2</sub>. Dimethylformamide (DMF), dimethyl sulfoxide (DMSO), dichloroethane (DCE), and solutions of MeLi, n-BuLi, and LDA were purchased in Sure/Seal or AcroSeal bottling and dispensed under N<sub>2</sub>. Deuterated solvents were obtained from Cambridge Isotope Laboratories, Inc. or MilliporeSigma.

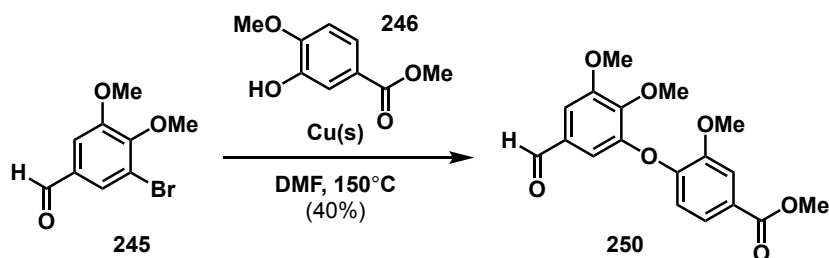
Unless otherwise noted in the experimental procedures, reactions were carried out in flame or oven-dried glassware under a positive pressure of N<sub>2</sub> in anhydrous solvents using standard Schlenk techniques. Reaction progresses were monitored using thin-layer

chromatography (TLC) on EMD Silica Gel 60 F254 or Macherey–Nagel SIL HD (60 Å mean pore size, 0.75 mL/g specific pore volume, 5–17 µm particle size, with fluorescent indicator) silica gel plates. Visualization of the developed plates was performed under UV light (254 nm). Purification and isolation of products were performed via silica gel chromatography (both column and preparative thin-layer chromatography). Organic solutions were concentrated under reduced pressure on IKA® temperature-controlled rotary evaporator equipped with an ethylene glycol/water condenser.

Melting points were measured with the MEL-TEMP melting point apparatus. Proton nuclear magnetic resonance ( $^1\text{H}$  NMR) spectra, carbon nuclear magnetic resonance ( $^{13}\text{C}$  NMR) spectra and fluorine nuclear magnetic resonance ( $^{19}\text{F}$  NMR) spectra were recorded on Bruker Avance NEO 400 (not  $^1\text{H}$  decoupled) or Bruker Avance 600 MHz spectrometers ( $^1\text{H}$  decoupled). Chemical shifts ( $\delta$ ) are reported in ppm relative to the residual solvent signal ( $\delta$  7.26 for  $^1\text{H}$  NMR,  $\delta$  77.16 for  $^{13}\text{C}$  NMR in  $\text{CDCl}_3$ ).<sup>1</sup> Data for  $^1\text{H}$  NMR spectroscopy are reported as follows: chemical shift ( $\delta$  ppm), multiplicity (s = singlet, d = doublet, t = triplet, q = quartet, m = multiplet, br = broad, dd = doublet of doublets, dt = doublet of triplets), coupling constant (Hz), integration. Data for  $^{13}\text{C}$  and  $^{19}\text{F}$  NMR spectroscopy are reported in terms of chemical shift ( $\delta$  ppm). IR spectroscopic data were recorded on a NICOLET 6700 FT-IR spectrophotometer using a diamond attenuated total reflectance (ATR) accessory. Samples are loaded onto the diamond surface either neat or as a solution in organic solvent and the data acquired after the solvent had evaporated. High resolution accurate mass (ESI) spectral data were obtained from the Analytical Chemistry Instrumentation Facility at the University of California,

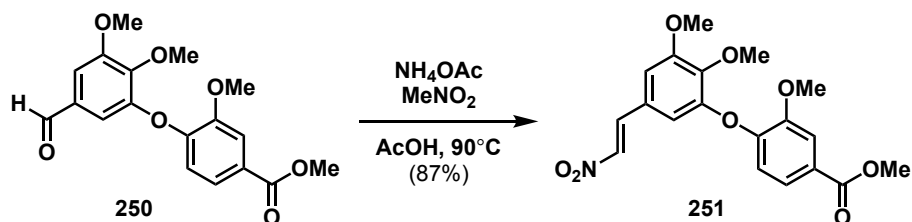
Riverside, on an Agilent 6545 Q-TOF LC/MS instrument (supported by NSF grant CHE-1828782).

## 2.6.2 Experimental Procedures



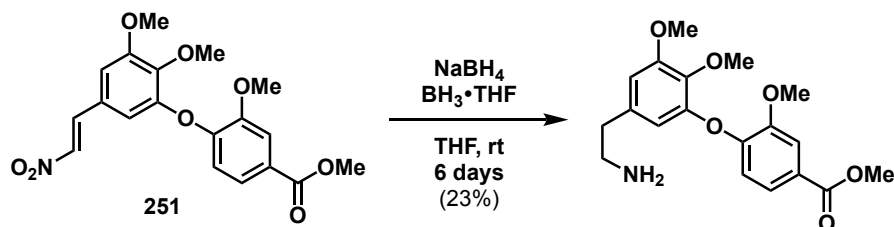
**Methyl-4-(5-formyl-2,3-dimethoxyphenoxy)-3-methoxybenzoate (250)**. A mixture of arylaldehyde **245** (25 mg, 0.10 mmol, 1 equiv), phenol **246** (55 mg, 0.30 mmol, 3 equiv) and copper powder (32 mg, 0.50 mmol, 5 equiv) in dry DMF (0.2 mL) was heated at 150 °C for 16 h. The reaction mixture was cooled to rt, diluted with EtOAc, and filtered over a pad of Celite®, which was further rinsed with EtOAc. Water was added to the filtrate and the aqueous layer was extracted with EtOAc (3 x 2 mL). The combined organic extract was washed with brine (1 x 2 mL), dried over MgSO<sub>4</sub>, filtered, and concentrated in vacuo. The crude product was purified by preparative thin layer chromatography eluting with hexanes/Et<sub>2</sub>O (1:1 v/v) to give compound **250** as a colorless oil (11.3 mg, 40%). R<sub>f</sub>: 0.25 (1:1 hexanes/Et<sub>2</sub>O, UV). <sup>1</sup>H NMR (600 MHz, CDCl<sub>3</sub>) δ 9.77 (s, 1H), 7.68 (s, 1H), 7.61 (d, J = 8.4 Hz, 1H), 7.28 (s, 1H), 7.03 (s, 1H), 6.85 (d, J = 8.3 Hz, 1H), 3.96 (s, 3H), 3.95 (s, 3H), 3.92 (s, 3H), 3.91 (s, 3H). <sup>13</sup>C NMR (400 MHz, CDCl<sub>3</sub>) δ 190.6, 166.6, 154.4, 150.2, 149.7, 145.9, 131.8, 126.4, 123.3, 118.1, 115.7, 113.8, 107.3, 61.3, 56.5, 56.3, 52.4, 29.8. IR (ATR): 3109, 3032, 2955, 2740, 1753, 1738, 1602, 1586, 1541,

1399, 1267, 1119, 1081  $\text{cm}^{-1}$ . HRMS (ESI+)  $m/z$  calculated for  $\text{C}_{18}\text{H}_{19}\text{O}_7$   $[\text{M}+\text{H}]^+$ : 347.1126, found: 347.1125.

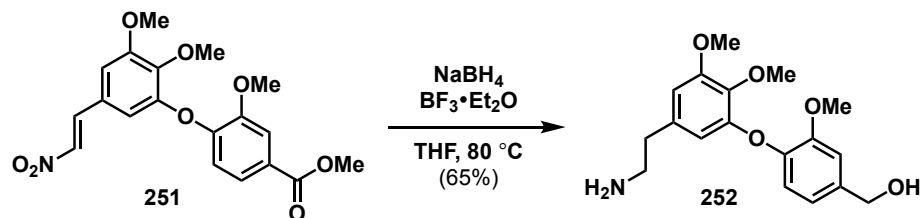


**(E)-Methyl-4-(2,3-dimethoxy-5-(2-nitrovinyl)phenoxy)-3-methoxybenzoate (251).**

Arylaldehyde **250** (11.8 g, 0.03 mmol, 1 equiv) was dissolved in AcOH (50  $\mu\text{L}$ ) and  $\text{NH}_4\text{OAc}$  (9.2 mg, 0.12 mmol, 4 equiv) and anhydrous  $\text{MeNO}_2$  (13  $\mu\text{L}$ , 0.24 mmol, 8 equiv) were added successively under  $\text{N}_2$  atmosphere. The resulting mixture was heated to  $90^\circ\text{C}$  for 19 h. After this time, the reaction mixture was cooled to rt, quenched with  $\text{H}_2\text{O}$  (1 mL) and vacuum filtered. The filtrate was extracted with EtOAc (3 x 2 mL) and the combined organic extract was dried over  $\text{MgSO}_4$ , filtered, and concentrated in vacuo to afford nitrostyrene **251** (11.6 g, 87%) as a dark yellow residue.  $R_f$ : 0.31 (1:1 hexanes/ $\text{Et}_2\text{O}$ , UV).  $^1\text{H}$  NMR (600 MHz,  $\text{CDCl}_3$ )  $\delta$  7.84 (d,  $J = 13.6$  Hz, 1H), 7.69 (s, 1H), 7.62 (d,  $J = 8.4$  Hz, 1H), 7.43 (d,  $J = 13.6$  Hz, 1H), 6.87 (s, 1H), 6.83 (d,  $J = 8.4$  Hz, 1H), 6.74 (s, 1H), 3.94 (s, 3H), 3.93 (s, 3H), 3.92 (s, 3H), 3.91 (s, 3H).  $^{13}\text{C}$  NMR (600 MHz,  $\text{CDCl}_3$ )  $\delta$  166.6, 154.3, 150.0, 149.8, 149.6, 143.8, 138.6, 136.8, 126.3, 125.4, 123.2, 117.9, 113.9, 113.7, 108.5, 61.3, 56.4, 56.2, 52.3. IR (ATR): 3123, 3048, 2979, 1744, 1652, 1628, 1565, 1403, 1192, 822  $\text{cm}^{-1}$ . HRMS (ESI+)  $m/z$  calculated for  $\text{C}_{19}\text{H}_{20}\text{NO}_8$   $[\text{M}+\text{H}]^+$ : 390.1183, found: 390.1172.

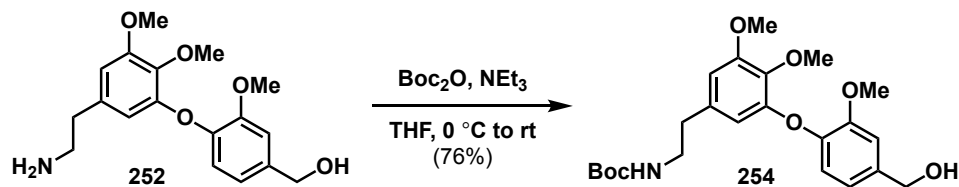


**Methyl-4-(5-(2-aminoethyl)-2,3-dimethoxyphenoxy)-3-methoxybenzoate.** To a solution of  $\text{BH}_3\text{-THF}$  (1.0M, 320  $\mu\text{L}$ , 0.32 mmol, 4 equiv) under  $\text{N}_2$  atmosphere was slowly added a solution of nitrostyrene **251** (30 mg, 0.08 mmol, 1 equiv) in THF (0.2 mL) at 0 °C. The ice-bath was removed and  $\text{NaBH}_4$  (8.0 mg, 0.21 mmol, 2.6 equiv) was added to the resulting mixture, which was then stirred at rt for 6 days. The reaction mixture was quenched with ice-water (5 mL), acidified with 10% HCl (2 mL) and then stirred at 60–65 °C for 2 h. After cooling to rt, the mixture was washed with  $\text{Et}_2\text{O}$  (2 x 5 mL) and the acidic layer was basified with 10%  $\text{NaOH}_{(\text{aq})}$ . Following addition of 10%  $\text{NaOH}_{(\text{aq})}$  (5 mL) and  $\text{NaCl}_{(\text{s})}$  (100 mg), the mixture was extracted with  $\text{Et}_2\text{O}$  (3 x 5 mL), dried over  $\text{Na}_2\text{SO}_4$ , filtered, and concentrated in vacuo to yield the methyl ester (6.7 mg, 23%) as a white solid.  $^1\text{H}$  NMR (500 MHz, MeOD)  $\delta$  7.69 (s, 1H), 7.57 (d,  $J = 8.3$  Hz, 1H), 6.83 – 6.70 (m, 2H), 6.44 (d,  $J = 6.4$  Hz, 1H), 3.91 (s, 3H), 3.89 (s, 6H), 3.88 (s, 3H), 3.03 (t,  $J = 7.5$  Hz, 1H), 2.76 (t,  $J = 7.4$  Hz, 1H).  $^{13}\text{C}$  NMR (600 MHz, MeOD)  $\delta$  166.6, 154.3, 150.0, 149.8, 149.6, 143.8, 138.6, 136.8, 126.3, 125.4, 123.2, 117.9, 113.9, 113.7, 108.5, 61.3, 56.4, 56.2, 52.3. IR (ATR): 3421, 3385, 3041, 2986, 2813, 1739, 1594, 1562, 1401, 1388, 1155  $\text{cm}^{-1}$ . HRMS (ESI+)  $m/z$  calculated for  $\text{C}_{19}\text{H}_{24}\text{NO}_6$   $[\text{M}+\text{H}]^+$ : 362.1598, found: 362.1585.

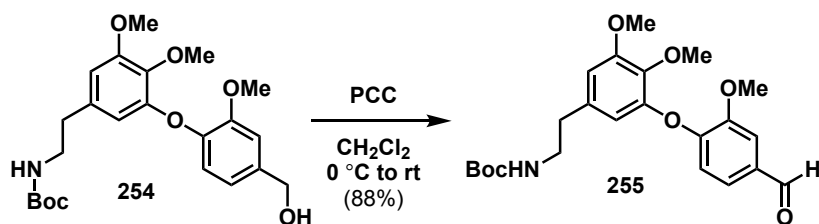


**(4-(5-(2-Aminoethyl)-2,3-dimethoxyphenoxy)-3-methoxyphenyl)methanol (252).**

NaBH<sub>4</sub> (14.4 mg, 0.38 mmol, 4.75 equiv), THF (0.5 mL), and BF<sub>3</sub>·Et<sub>2</sub>O (60 μL, 0.48 mmol, 6 equiv) were added successively under N<sub>2</sub> atmosphere at 0 °C. The ice-bath was removed, and the mixture was stirred at rt for 15 min followed by dropwise addition of a solution of nitrostyrene **251** (30 mg, 0.08 mmol, 1 equiv) in THF (0.5 mL). After stirring at 60–65 °C for 5.5 h, the mixture was cooled to rt, quenched by slow addition of H<sub>2</sub>O (2 mL), acidified with 1 M HCl (2.5 mL), and heated at 80–85 °C for 2 h. After cooling to rt, the mixture was washed with Et<sub>2</sub>O (2 x 5 mL) and basified with 10% NaOH<sub>(aq)</sub> (5 mL). Following addition of NaCl<sub>(s)</sub> (100 mg), the aqueous layer was extracted with Et<sub>2</sub>O (3 x 5 mL), dried over Na<sub>2</sub>SO<sub>4</sub>, filtered, and concentrated in vacuo to yield the benzylic alcohol **252** as a pale-yellow oil (17.3 mg, 65%). <sup>1</sup>H NMR (500 MHz, MeOD) δ 7.12 (d, J = 1.9 Hz, 1H), 6.93 – 6.82 (m, 2H), 6.63 (d, J = 1.9 Hz, 1H), 6.20 (d, J = 1.9 Hz, 1H), 4.59 (s, 2H), 3.87 (s, 3H), 3.81 (s, 3H), 3.79 (s, 3H), 2.81 (t, J = 7.3 Hz, 2H), 2.62 (t, J = 7.3 Hz, 2H). <sup>13</sup>C NMR (500 MHz, MeOD) δ 153.7, 150.9, 150.8, 144.2, 138.2, 137.4, 135.0, 119.6, 119.0, 111.5, 110.1, 107.1, 63.4, 59.8, 55.1, 54.9, 42.2, 37.7. IR (ATR): 3550, 3429, 3023, 2961, 2939, 1602, 1565, 1488, 1203, 1123, 906, 866 cm<sup>-1</sup>. HRMS (ESI+) m/z calculated for C<sub>18</sub>H<sub>23</sub>NO<sub>5</sub> [M+H]<sup>+</sup>: 334.1649, found: 334.1651.

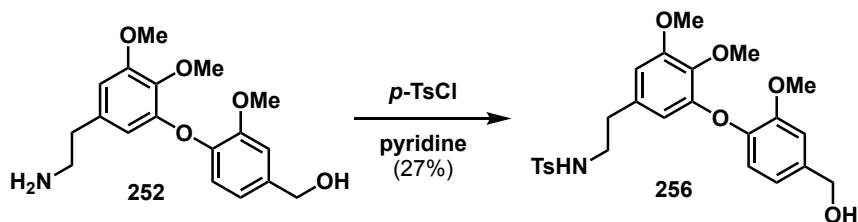


***tert*-Butyl (3-(4-(hydroxymethyl)-2-methoxyphenoxy)-4,5-dimethoxyphenethyl) carbamate (254).** To a solution of amine **252** (35 mg, 0.10 mmol, 1 equiv) in dry THF (0.5 mL) containing NEt<sub>3</sub> (17 μL, 0.12 mmol, 1.1 equiv) was added Boc<sub>2</sub>O (26.2 mg, 0.12 mmol, 1.1 equiv) under N<sub>2</sub> atmosphere at 0 °C. The solution was allowed to gradually warm to rt and was stirred overnight for 16 h. The mixture was diluted with CH<sub>2</sub>Cl<sub>2</sub> (1 mL) and concentrated in vacuo. Purification by column chromatography (eluting with 1:2 acetone/hexanes) yielded Boc-protected amine **254** as a colorless oil (34.7 mg, 76%). <sup>1</sup>H NMR (500 MHz, CDCl<sub>3</sub>) δ 7.02 (s, 1H), 6.83 (s, 2H), 6.48 (s, 1H), 6.24 (s, 1H), 4.65 (s, 2H), 3.86 (s, 6H), 3.84 (s, 4H), 3.26 (q, J = 6.9 Hz, 2H), 2.62 (t, J = 7.2 Hz, 2H), 1.40 (s, 10H). <sup>13</sup>C NMR (101 MHz, CDCl<sub>3</sub>) δ 156.0, 153.8, 150.9, 150.7, 145.2, 138.4, 137.2, 134.7, 119.5, 111.6, 111.5, 107.8, 79.4, 65.2, 61.1, 56.2, 56.1, 41.8, 36.3, 28.5. IR (ATR): 3546, 3468, 3059, 2875, 1774, 1604, 1593, 1478, 1293, 1175, 1163 cm<sup>-1</sup>. HRMS (ESI<sup>+</sup>) m/z calculated for C<sub>23</sub>H<sub>31</sub>NO<sub>7</sub>Na [M+Na]<sup>+</sup>: 456.1998, found: 456.1985.



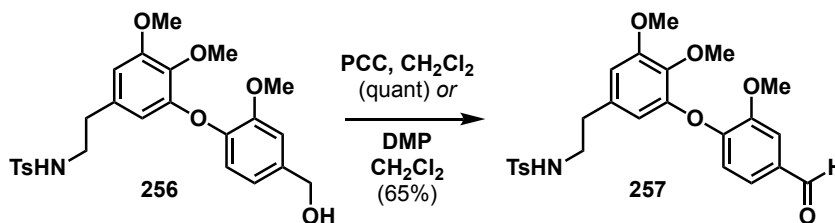
***tert*-Butyl (3-(4-formyl-2-methoxyphenoxy)-4,5-dimethoxyphenethyl)carbamate (255).** Benzyl alcohol **254** (34.7 mg, 0.08 mmol, 1 equiv), CH<sub>2</sub>Cl<sub>2</sub> (1 mL), and PCC (36.6

mg, 0.17 mmol, 2.1 equiv) were added successively under N<sub>2</sub> atmosphere at 0 °C. The mixture was stirred overnight for 20 h at rt. The resulting solution was diluted with CH<sub>2</sub>Cl<sub>2</sub> (3 mL), decanted, and the remaining black resin was washed exhaustively with CH<sub>2</sub>Cl<sub>2</sub>. The combined CH<sub>2</sub>Cl<sub>2</sub> extract was washed with sat. NaHCO<sub>3(aq)</sub> (5 mL) and brine (2 x 5 mL), dried over MgSO<sub>4</sub>, filtered, and concentrated in vacuo to yield aldehyde **255** as a yellow oil (30.7 mg, 88%). <sup>1</sup>H NMR (400 MHz, CDCl<sub>3</sub>) δ 9.86 (d, J = 1.3 Hz, 1H), 7.50 (t, J = 1.4 Hz, 1H), 7.36 – 7.30 (m, 1H), 6.79 (dd, J = 8.2, 0.9 Hz, 1H), 6.61 (d, J = 1.9 Hz, 1H), 6.48 (t, J = 1.4 Hz, 1H), 5.29 (d, J = 1.1 Hz, 1H), 3.97 (s, 3H), 3.87 (s, 3H), 3.77 (s, 3H), 3.32 (t, J = 6.9 Hz, 2H), 2.71 (t, J = 7.1 Hz, 2H), 1.41 (s, 9H). <sup>13</sup>C NMR (101 MHz, CDCl<sub>3</sub>) δ 191.1, 155.9, 154.0, 152.7, 150.3, 148.3, 139.5, 135.3, 131.9, 126.1, 116.3, 114.0, 110.5, 109.6, 79.5, 61.2, 56.3, 56.3, 41.8, 36.2, 28.5. IR (ATR): 3472, 3100, 2994, 2751, 1744, 1745 1595, 1415, 1165, 1056 cm<sup>-1</sup>. HRMS (ESI+) m/z calculated for C<sub>23</sub>H<sub>30</sub>NO<sub>7</sub> [M+H]<sup>+</sup>: 432.2017, found: 432.2006.



***N*-(3-(4-(Hydroxymethyl)-2-methoxyphenoxy)-4,5-dimethoxyphenethyl)-4-methylbenzenesulfonamide (256)**. To a solution of ethylamine **252** (99.4 mg, 0.30 mmol, 1 equiv) in pyridine (0.3 mL) was slowly added *p*-TsCl (74.4 mg, 0.40 mmol, 1.3 equiv) over 10 min under N<sub>2</sub> atmosphere at -20 °C. The cold bath was removed, and the mixture was stirred at rt for 18 h. After 18 h, the mixture was quenched with H<sub>2</sub>O (3 mL) and extracted with CH<sub>2</sub>Cl<sub>2</sub> (3 x 5 mL). The combined organic extract was washed with 2

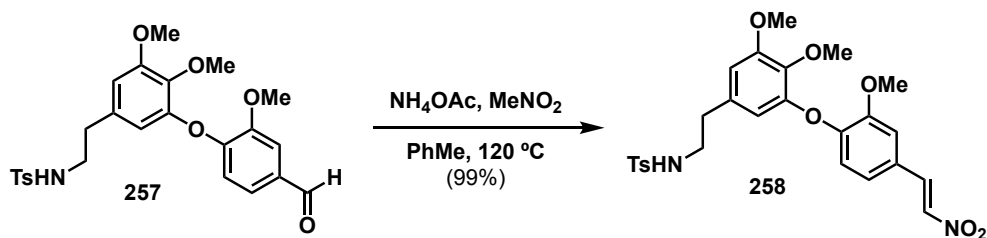
M HCl<sub>(aq)</sub> (3 x 5 mL) and brine (5 mL), then dried over Na<sub>2</sub>SO<sub>4</sub>, filtered, and concentrated in vacuo. Purification by preparative-thin layer chromatography (eluting with 40% acetone/hexanes) yielded Ts-protected amine **256** as a colorless oil (38.2 mg, 27%). <sup>1</sup>H NMR (400 MHz, CDCl<sub>3</sub>) δ 7.62 (d, J = 7.3 Hz, 1H), 7.24 (d, J = 7.6 Hz, 1H), 7.04 (d, J = 1.6 Hz, 1H), 6.84 (t, J = 2.4 Hz, 1H), 6.35 (d, J = 1.9 Hz, 1H), 6.10 (t, J = 1.4 Hz, 1H), 4.66 (s, 1H), 3.86 (d, J = 1.3 Hz, 2H), 3.83 (d, J = 1.7 Hz, 2H), 3.81 (d, J = 1.3 Hz, 3H), 3.09 (qd, J = 6.7, 1.8 Hz, 1H), 2.65 – 2.49 (m, 1H), 2.40 (s, 2H). <sup>13</sup>C NMR (101 MHz, CDCl<sub>3</sub>) δ 153.9, 150.9, 144.8, 143.5, 138.3, 137.5, 136.9, 133.3, 129.8, 127.1, 119.9, 119.5, 111.8, 111.0, 107.4, 65.1, 61.1, 56.2, 56.1, 44.1, 35.7, 21.6. IR (ATR): 3557, 3450, 3092, 2971, 2843, 1606, 1595, 1469, 1401, 1333, 1284, 1002, 917, 798 cm<sup>-1</sup>. HRMS (ESI+) m/z calculated for NaC<sub>25</sub>H<sub>29</sub>NO<sub>7</sub>S [M+Na]<sup>+</sup>: 510.1562, found: 510.1541.



***N*-(3-(4-Formyl-2-methoxyphenoxy)-4,5-dimethoxyphenethyl)-4-**

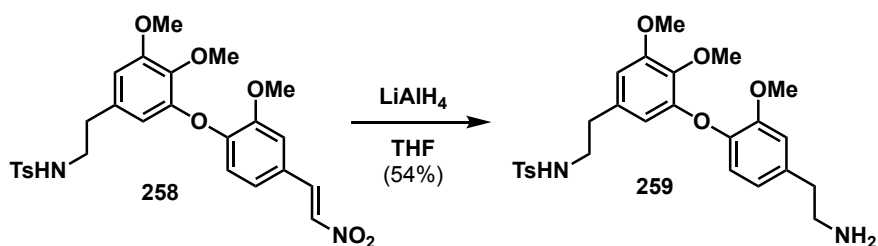
**methylbenzenesulfonamide (257).** To a solution of benzyl alcohol **256** (39.3 mg, 0.08 mmol, 1 equiv) in CH<sub>2</sub>Cl<sub>2</sub> (0.3 mL) under N<sub>2</sub> was added PCC (36.6 mg, 0.17 mmol, 2.1 equiv) at 0 °C. The mixture was stirred overnight at rt. The solution was decanted, and the gummy residue was rinsed exhaustively with CH<sub>2</sub>Cl<sub>2</sub> (5 x 3 mL). The combined organic extracts were washed with sat. NaHCO<sub>3(aq)</sub> (3 mL), brine (2 x 3 mL) then dried over MgSO<sub>4</sub>, filtered, and concentrated in vacuo to yield arylaldehyde **257** as a brown amorphous solid (39.1 mg, quantitative). In an alternative procedure, a solution of

benzylic alcohol **256** (8.0 mg, 0.016 mmol, 1 equiv) in CH<sub>2</sub>Cl<sub>2</sub> (0.1 mL) under N<sub>2</sub> was added a solution of DMP (10.6 mg, 0.025 mmol, 1.5 equiv) in CH<sub>2</sub>Cl<sub>2</sub> (0.1 mL). The mixture was stirred overnight at rt. The solution was quenched with Na<sub>2</sub>S<sub>2</sub>O<sub>3(aq)</sub> (1 mL) and extracted with CH<sub>2</sub>Cl<sub>2</sub> (3 x 1 mL). The combined organic extract was washed with brine (1 mL), dried over Na<sub>2</sub>SO<sub>4</sub>, filtered, and concentrated in vacuo to yield arylaldehyde **257** as a brown oil (5.0 mg, 65%). <sup>1</sup>H NMR (600 MHz, CDCl<sub>3</sub>) δ 9.87 (s, 1H), 7.68 (d, J = 7.6 Hz, 2H), 7.51 (s, 1H), 7.39 – 7.29 (m, 2H), 6.77 (d, J = 8.0 Hz, 1H), 6.52 (s, 1H), 6.35 (s, 1H), 3.96 (d, J = 7.8 Hz, 4H), 3.84 (s, 2H), 3.77 (s, 3H), 3.16 (s, 2H), 2.68 (t, J = 6.5 Hz, 2H), 2.40 (s, 3H). <sup>13</sup>C NMR (101 MHz, CDCl<sub>3</sub>) δ 191.1, 154.2, 152.4, 150.4, 148.5, 143.7, 139.7, 137.0, 133.9, 132.1, 129.9, 127.2, 126.0, 116.4, 113.7, 110.6, 109.6, 61.2, 56.3, 56.3, 44.1, 35.9, 21.7. IR (ATR): 3381, 2927, 2853, 1682, 1579, 1500, 1423, 1264, 1154, 1089 cm<sup>-1</sup>. HRMS (ESI<sup>+</sup>) m/z calculated for C<sub>25</sub>H<sub>28</sub>NO<sub>7</sub>S [M+H]<sup>+</sup>: 486.1581, found: 486.1577.



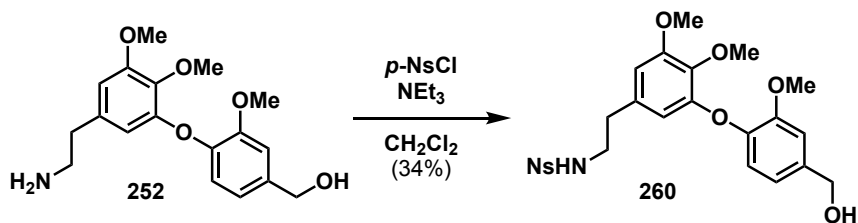
**(E)-N-(3,4-Dimethoxy-5-(2-methoxy-4-(2-nitrovinyl)phenoxy)phenethyl)-4-methylbenzenesulfonamide (258)**. To an oven-dried vessel, **257** (37.8 mg, 0.08 mmol, 1 equiv), NH<sub>4</sub>OAc (37.8 mg, 0.08 mmol, 1 equiv), PhMe (0.8 mL), and MeNO<sub>2</sub> (0.35 mL, 6.4 mmol, 80 equiv) were added successively. The mixture was stirred at 120 °C for 22 h. After 22 h, the mixture was cooled to rt, then quenched with H<sub>2</sub>O (3 mL) and

extracted with EtOAc (3 x 3 mL). The combined organic extracts was washed with brine (2 x 3 mL), then dried over Na<sub>2</sub>SO<sub>4</sub>, filtered, and concentrated in vacuo. Purification by column chromatography (eluting with 1:2 EtOAc/hexanes) yielded nitrostyrene **258** as a yellow oil (66.2 mg, 99%). <sup>1</sup>H NMR (500 MHz, CDCl<sub>3</sub>) δ 7.96 (d, J = 13.6 Hz, 1H), 7.68 (d, J = 1.8 Hz, 2H), 7.54 (d, J = 13.6 Hz, 1H), 7.27 (d, J = 9.7 Hz, 2H), 7.16 – 7.01 (m, 2H), 6.74 (d, J = 8.3 Hz, 1H), 6.50 (d, J = 1.9 Hz, 1H), 6.32 (d, J = 1.9 Hz, 1H), 3.95 (s, 3H), 3.84 (s, 3H), 3.79 (s, 3H), 3.16 (q, J = 6.7 Hz, 2H), 2.67 (t, J = 6.9 Hz, 2H), 2.41 (s, 3H). HRMS (ESI+) m/z calculated for C<sub>26</sub>H<sub>29</sub>N<sub>2</sub>O<sub>8</sub>S [M+H]<sup>+</sup>: 529.1639, found: 529.1617.



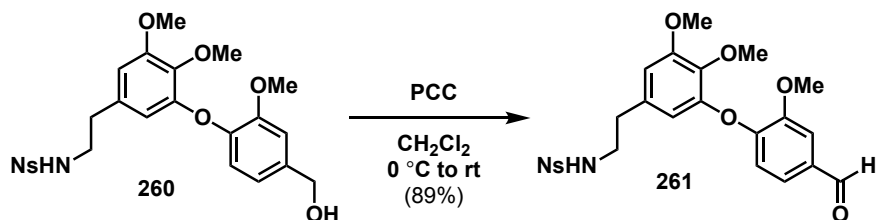
*N*-(3-(4-(2-Aminoethyl)-2-methoxyphenoxy)-4,5-dimethoxyphenethyl)-4-methylbenzenesulfonamide (**259**). To a solution of LiAlH<sub>4</sub> (4.6 mg, 0.12 mmol, 4 equiv) in THF (0.25 mL) under N<sub>2</sub> was slowly added a solution of **258** (16.1 mg, 0.03 mmol, 1 equiv) in THF (0.3 mL) at 0 °C. The reaction mixture was stirred at 66 °C for 3 h, quenched with H<sub>2</sub>O (5 μL), 15% NaOH<sub>(aq)</sub> (5 μL) and H<sub>2</sub>O (15 μL) and allowed to stir at rt for 15 min. The mixture was filtered over a pad of Celite and concentrated in vacuo to afford amine **259** as a pale-yellow oil (8.1 mg, 54%). <sup>1</sup>H NMR (400 MHz, MeOD) δ 7.74 – 7.46 (m, 2H), 7.34 – 7.27 (m, 2H), 7.04 (d, J = 1.7 Hz, 1H), 6.85 (dd, J = 2.8, 1.1

Hz, 2H), 6.53 (d,  $J = 1.9$  Hz, 1H), 6.17 (d,  $J = 1.9$  Hz, 1H), 3.84 (s, 3H), 3.81 (s, 3H), 3.78 (s, 2H), 3.22 (dd,  $J = 8.3, 6.9$  Hz, 2H), 3.06 – 2.91 (m, 4H), 2.55 (t,  $J = 7.0$  Hz, 2H).



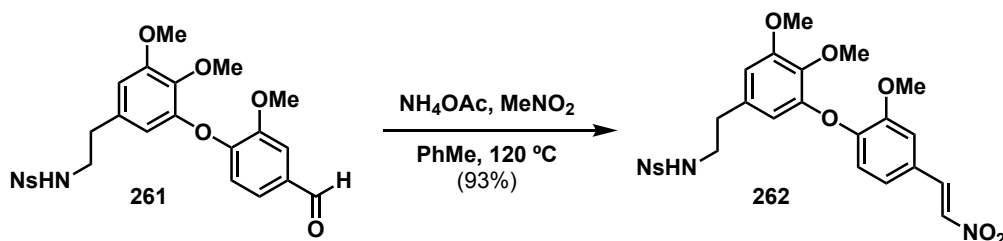
***N*-(3-(4-(Hydroxymethyl)-2-methoxyphenoxy)-4,5-dimethoxyphenethyl)-4-**

**nitrobenzenesulfonamide (260).** To a solution of benzylic alcohol **252** (334.3 mg, 1 mmol, 1 equiv) in CH<sub>2</sub>Cl<sub>2</sub> (2 mL) was added NEt<sub>3</sub> (0.21 mL, 1.5 mmol, 1.5 equiv) and *p*-NsCl (244 mg, 1.10 mmol, 1.1 equiv) under N<sub>2</sub> atmosphere. The mixture was stirred at rt for 20 h. After 20 h, the mixture was diluted with CH<sub>2</sub>Cl<sub>2</sub> (10 mL), then quenched with 1 M HCl<sub>(aq)</sub> (8 mL) and extracted with CH<sub>2</sub>Cl<sub>2</sub> (3 x 8 mL). The combined organic extract was washed with brine (8 mL), then dried over Na<sub>2</sub>SO<sub>4</sub>, filtered, and concentrated in vacuo. Purification by column chromatography (eluting with 50% EtOAc/hexanes) yielded *Ns*-protected amine **260** as a colorless oil (176 mg, 34%). <sup>1</sup>H NMR (400 MHz, CDCl<sub>3</sub>) δ 8.28 (d,  $J = 9.1$  Hz, 1H), 7.92 (d,  $J = 9.0$  Hz, 1H), 7.05 (d,  $J = 1.8$  Hz, 1H), 6.94 – 6.79 (m, 2H), 6.37 (d,  $J = 2.0$  Hz, 1H), 6.07 (d,  $J = 1.9$  Hz, 1H), 4.68 (s, 2H), 3.86 (s, 3H), 3.85 (s, 2H), 3.83 (s, 3H), 3.20 (q,  $J = 6.5$  Hz, 2H), 2.59 (t,  $J = 6.7$  Hz, 2H). <sup>13</sup>C NMR (101 MHz, CDCl<sub>3</sub>) δ 154.0, 151.0, 150.9, 150.0, 145.9, 144.7, 138.5, 137.5, 132.6, 128.2, 124.4, 119.8, 119.5, 111.8, 110.9, 107.4, 65.1, 61.0, 56.2, 56.1, 44.2, 35.7. IR (ATR): 3456, 3113, 2975, 2847, 2744, 1740, 1675, 1578, 1329, 1228, 1164, 1104, 821 cm<sup>-1</sup>. HRMS (ESI<sup>+</sup>)  $m/z$  calculated for NaC<sub>23</sub>H<sub>26</sub>N<sub>2</sub>O<sub>9</sub>S [M+Na]<sup>+</sup>: 541.1257, found: 541.1254.



*N*-(3-(4-Formyl-2-methoxyphenoxy)-4,5-dimethoxyphenethyl)-4-

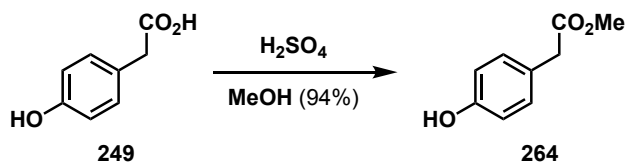
**nitrobenzenesulfonamide (261)**. To a solution of benzylic alcohol **260** (58.1 mg, 0.11 mmol, 1 equiv) in CH<sub>2</sub>Cl<sub>2</sub> (0.5 mL) under N<sub>2</sub> was added PCC (52 mg, 0.24 mmol, 2.1 equiv) at 0 °C. The mixture was stirred overnight at rt. The solution was decanted, and the gummy residue was rinsed exhaustively with CH<sub>2</sub>Cl<sub>2</sub> (5 x 3 mL). The combined organic extract was washed with sat. NaHCO<sub>3(aq)</sub> (3 mL), brine (2 x 3 mL) then dried over MgSO<sub>4</sub>, filtered, and concentrated in vacuo to yield benzaldehyde **261** as a brown amorphous solid (50.9 mg, 89%). <sup>1</sup>H NMR (500 MHz, CDCl<sub>3</sub>) δ 9.88 (s, 1H), 8.33 (d, J = 7.9 Hz, 2H), 7.99 (d, J = 8.1 Hz, 2H), 7.52 (s, 1H), 7.35 (d, J = 8.2 Hz, 1H), 6.77 (d, J = 8.1 Hz, 1H), 6.54 (s, 1H), 6.36 (s, 1H), 3.98 (s, 3H), 3.86 (s, 3H), 3.78 (s, 3H), 3.25 (s, 2H), 2.75 (s, 2H). IR (ATR): 3121, 3040, 2979, 2875, 1783, 1593, 1485, 1441, 1241, 1165, 1110, 889, 869 cm<sup>-1</sup>. HRMS (ESI+) m/z calculated for C<sub>24</sub>H<sub>25</sub>N<sub>2</sub>O<sub>9</sub>S [M+H]<sup>+</sup>: 517.5285, found: 517.5280.



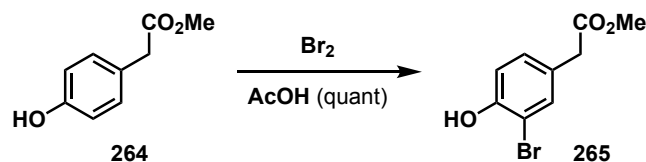
*(E)*-*N*-(3,4-Dimethoxy-5-(2-methoxy-4-(2-nitrovinyl)phenoxy)phenethyl)-4-

**nitrobenzenesulfonamide (262)**. To an oven-dried vessel, **261** (61.3 mg, 0.12 mmol, 1

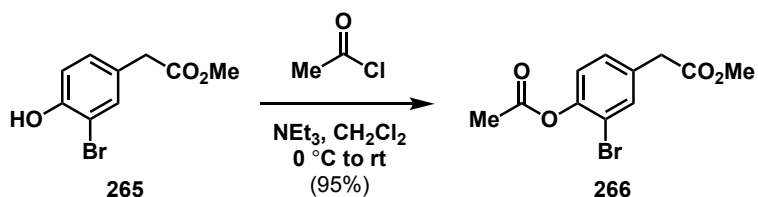
equiv), NH<sub>4</sub>OAc (37.8 mg, 0.13 mmol, 1.1 equiv), PhMe (1.5 mL), and MeNO<sub>2</sub> (0.52 mL, 9.6 mmol, 80 equiv) were added successively. The mixture was stirred at 120 °C for 22 h. After 22 h, the mixture was cooled to rt, then quenched with H<sub>2</sub>O (3 mL) and extracted with EtOAc (3 x 3 mL). The combined organic extract was washed brine (2 x 3 mL), then dried over Na<sub>2</sub>SO<sub>4</sub>, filtered, and concentrated in vacuo. Purification by column chromatography (eluting with 1:2 EtOAc/hexanes) yielded nitrostyrene **262** as a yellow oil (66.9 mg, 93%). <sup>1</sup>H NMR (500 MHz, CDCl<sub>3</sub>) δ 8.33 (d, J = 8.5 Hz, 2H), 8.28 – 7.69 (m, 3H), 7.54 (d, J = 13.6 Hz, 1H), 7.15 – 6.96 (m, 2H), 6.73 (d, J = 8.4 Hz, 1H), 6.51 (d, J = 2.0 Hz, 1H), 6.32 (d, J = 2.0 Hz, 1H), 3.96 (s, 3H), 3.86 (s, 3H), 3.79 (s, 3H), 3.26 (q, J = 6.5 Hz, 2H), 2.73 (t, J = 6.7 Hz, 2H). IR (ATR): 3473, 3104, 3081, 2995, 2863, 1601, 1587, 1423, 1401, 1273, 1245, 1022 cm<sup>-1</sup>. HRMS (ESI+) m/z calculated for NaC<sub>25</sub>H<sub>25</sub>N<sub>3</sub>O<sub>10</sub>S [M+Na]<sup>+</sup>: 582.1158, found: 582.1143.



**Methyl 4-hydroxyphenylacetate (264).** To a solution of phenylacetic acid (**249**, 1.50 g, 9.86 mmol, 1.00 equiv) in MeOH (50 mL) was added H<sub>2</sub>SO<sub>4</sub> (1.4 mL, 25.8 mmol, 2.6 equiv). The mixture was refluxed for 23 h at 70 °C. The resulting solution was quenched with H<sub>2</sub>O (20 mL) and extracted with EtOAc (2 x 25 mL). The combined EtOAc extract was washed with sat. NaHCO<sub>3(aq)</sub> until pH = 7 and brine (2 x 25 mL), dried over Na<sub>2</sub>SO<sub>4</sub>, filtered, and concentrated in vacuo to afford product **264** as a yellow oil (1.54 g, 94%). <sup>1</sup>H NMR (500 MHz, CDCl<sub>3</sub>) δ 7.14 (d, J = 8.5 Hz, 2H), 6.77 (d, J = 8.5 Hz, 2H), 3.69 (s, 3H), 3.56 (s, 2H). All spectroscopic data are consistent with those previously reported.<sup>94</sup>

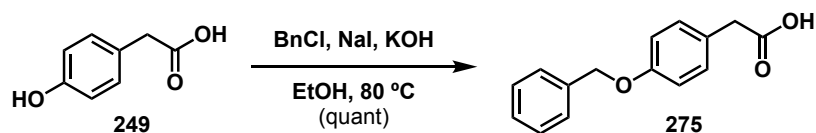


**Methyl 3-bromo-4-hydroxyphenylacetate (265).** To a stirred solution of methyl 4-hydroxyphenylacetate (**264**, 1.54 g, 9.27 mmol, 1 equiv) in AcOH (27 mL) was added Br<sub>2</sub> (0.52 mL) 10.1 mmol, 1.1 equiv) in AcOH (20 mL) over 15 min under N<sub>2</sub> atmosphere. The reaction mixture was stirred for 30 min at rt. The solution was quenched with sat. Na<sub>2</sub>S<sub>2</sub>O<sub>3(aq)</sub> (20 mL) and extracted with CH<sub>2</sub>Cl<sub>2</sub> (3 x 30 mL). The combined organic extracts were washed with sat. NaHCO<sub>3(aq)</sub> (5 mL), dried over Na<sub>2</sub>SO<sub>4</sub>, filtered, and concentrated in vacuo to afford the desired compound **265** as a yellow residue (2.43 g, quantitative). <sup>1</sup>H NMR (600 MHz, CDCl<sub>3</sub>) δ 7.40 (d, J = 2.1 Hz, 1H), 7.13 (dd, J = 8.4, 2.1 Hz, 1H), 6.97 (d, J = 8.3 Hz, 1H), 5.49 (s, 1H), 3.70 (s, 3H), 3.54 (s, 2H). All spectroscopic data are consistent with those previously reported.<sup>95</sup>

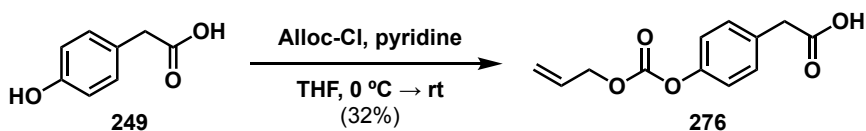


**Methyl 3-bromo-4-acetoxyphenylacetate (265).** Methyl 3-bromo-4-hydroxyphenylacetate (**265**, 1.23 g, 5.02 mmol, 1 equiv), CH<sub>2</sub>Cl<sub>2</sub> (13 mL), and NEt<sub>3</sub> (1.1 mL, 7.53 mmol, 1.5 equiv) were added successively followed by dropwise addition of acetyl chloride (0.45 mL, 6.28 mmol, 1.25 equiv) under N<sub>2</sub> atmosphere at 0 °C. The ice-bath was removed, and the mixture was stirred at rt for 23 h. After 23 h, the mixture was quenched with 5% HCl<sub>(aq)</sub> (5 mL). The biphasic mixture was washed with H<sub>2</sub>O (10 mL)

and sat.  $\text{NaHCO}_{3(\text{aq})}$  (5 mL), then dried over  $\text{Na}_2\text{SO}_4$ , filtered, and concentrated in vacuo to afford the desired product **266** as a brown residue (1.37 g, 95%).  $^1\text{H}$  NMR (400 MHz,  $\text{CDCl}_3$ )  $\delta$  7.55 (d,  $J$  = 2.0 Hz, 1H), 7.24 (d,  $J$  = 2.1 Hz, 1H), 7.08 (d,  $J$  = 8.2 Hz, 1H), 3.71 (s, 3H), 3.59 (s, 2H), 2.35 (s, 3H).  $^{13}\text{C}$  NMR (101 MHz,  $\text{CDCl}_3$ )  $\delta$  171.3, 168.7, 147.5, 134.2, 133.5, 129.6, 123.8, 116.3, 52.4, 40.3, 20.9. IR (ATR): 3105, 3099, 2991, 2981, 1788, 1786, 1441, 1433, 1389, 1121, 1094, 997, 910, 890  $\text{cm}^{-1}$ . HRMS (ESI+)  $m/z$  calculated for  $\text{C}_{11}\text{H}_{12}\text{BrO}_4$   $[\text{M}+\text{H}]^+$ : 286.9913, found: 286.9906.

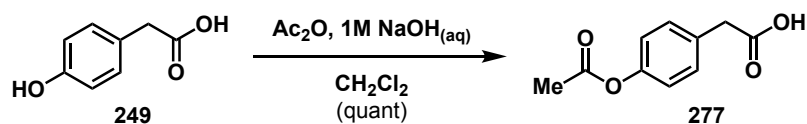


**2-(4-(Benzyloxy)phenyl)acetic acid (275)**. 4-Hydroxyphenylacetic acid (**249**, 300 mg, 1.97 mmol, 1 equiv),  $\text{BnCl}$  (0.24 mL, 2.07 mmol, 1.05 equiv),  $\text{NaI}$  (6.0 mg, 0.04 mmol, 0.02 equiv), and  $\text{KOH}$  (277 mg, 4.93 mmol, 2.5 equiv) were dissolved in  $\text{EtOH}$  (9 mL). The mixture was refluxed at 80  $^\circ\text{C}$  for 23 h. After 23 h, the mixture was cooled to rt, then quenched with 2M  $\text{HCl}_{(\text{aq})}$  (9 mL). The resulting precipitate was filtered, washed with  $\text{H}_2\text{O}$ , and dried under vacuum to afford benzyl acetic acid **275** as a white solid (750.5 mg, quantitative).  $^1\text{H}$  NMR (600 MHz,  $\text{CDCl}_3$ )  $\delta$  7.47 – 7.29 (m, 5H), 7.20 (d,  $J$  = 8.5 Hz, 2H), 7.01 – 6.91 (m, 2H), 5.05 (s, 2H), 3.59 (s, 2H). All spectroscopic data are consistent with those previously reported.<sup>109</sup>



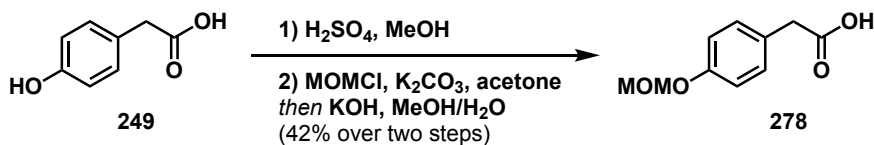
**2-(4-(((Allyloxy)carbonyloxy)phenyl)acetic acid (276)**. To a solution of 4-hydroxyphenylacetic acid (**249**, 250 mg, 1.64 mmol, 1 equiv) in  $\text{THF}$  (5 mL) under  $\text{N}_2$

atmosphere was added pyridine (0.19 mL, 2.3 mmol, 1.4 equiv). The mixture was cooled to 0 °C followed by dropwise addition of allyl chloroformate (0.21 mL, 1.97 mmol, 1.2 equiv). After stirring overnight at rt, the mixture was quenched with H<sub>2</sub>O (10 mL) and extracted with EtOAc (3 x 10 mL). The combined organic extract was washed with 2M HCl<sub>(aq)</sub> (2 x 10 mL) and brine (10 mL), then dried over Na<sub>2</sub>SO<sub>4</sub>, filtered, and concentrated in vacuo. Purification by column chromatography (eluting with 33% EtOAc/hexanes) yielded desired product **276** as a yellow oil (125.8 mg, 32%). <sup>1</sup>H NMR (400 MHz, CDCl<sub>3</sub>) δ 7.15 (d, J = 8.7 Hz, 1H), 6.78 (d, J = 8.6 Hz, 2H), 5.90 (ddt, J = 17.1, 10.4, 5.7 Hz, 1H), 5.34 – 5.12 (m, 3H), 4.59 (dt, J = 5.7, 1.4 Hz, 3H), 3.58 (s, 3H). All spectroscopic data are consistent with those previously reported.<sup>104</sup>

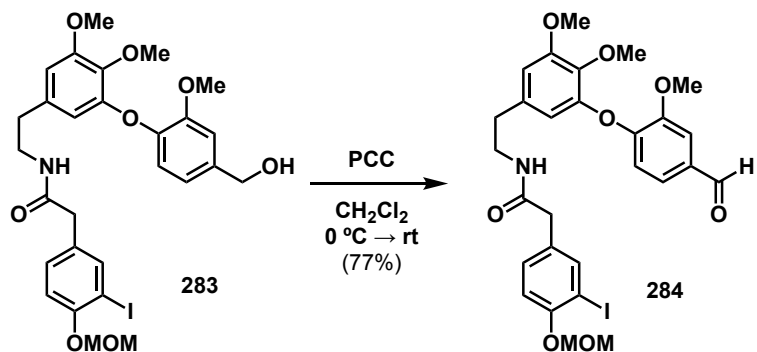


**2-(4-Acetoxyphenyl)acetic acid.** To a solution of 4-hydroxyphenylacetic acid (**249**, 200 mg, 1.31 mmol, 1 equiv) in 1 M NaOH<sub>(aq)</sub> (4 mL) and CH<sub>2</sub>Cl<sub>2</sub> (4 mL) was added Ac<sub>2</sub>O (0.3 mL, 3.15 mmol, 2.4 equiv). The mixture was stirred at rt for 1 h, then acidified with 2M HCl<sub>(aq)</sub> (pH = 2). Following extraction with CH<sub>2</sub>Cl<sub>2</sub> (2 x 10 mL) and EtOAc/MeOH (2 x 10 mL + 1 mL MeOH), the combined organic extract was dried over MgSO<sub>4</sub>, filtered, and concentrated in vacuo. Purification by column chromatography (eluting with 5% MeOH/CH<sub>2</sub>Cl<sub>2</sub>) yielded desired product **277** as a white solid (319.2 mg, quantitative). <sup>1</sup>H NMR (400 MHz, CDCl<sub>3</sub>) δ 7.33 – 7.28 (m, 2H), 7.06 (d, J = 8.7 Hz, 2H), 3.65 (s, 2H), 2.30 (s, 3H). <sup>13</sup>C NMR (101 MHz, CDCl<sub>3</sub>) δ 171.3, 168.7, 147.5, 134.2, 133.5, 129.6,

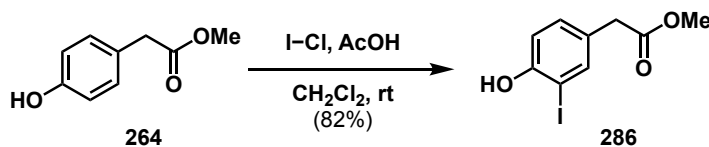
123.8, 116.3, 52.4, 40.3, 20.9. All spectroscopic data are consistent with those previously reported.<sup>110</sup>



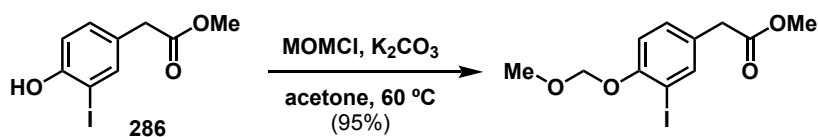
**2-(4-(Methoxymethoxy)phenyl)acetic acid (278)**. A mixture of 4-hydroxyphenylacetic acid (**249**, 300 mg, 1.97 mmol, 1 equiv), concentrated  $\text{H}_2\text{SO}_4$  (5.5  $\mu\text{L}$ , 0.1 mmol, 0.05 equiv) in MeOH (10 mL) was refluxed for 1 h. Following removal of solvent in vacuo, the residue was diluted with  $\text{H}_2\text{O}$  (20 mL), extracted with EtOAc (3 x 15 mL), dried over  $\text{Na}_2\text{SO}_4$ , filtered, and concentrated under reduced pressure. The residue was dissolved in acetone (10 mL) and MOMCl (0.3 mL, 3.94 mmol, 2 equiv) and  $\text{K}_2\text{CO}_3$  (817 mg, 5.91 mmol, 3 equiv) were added. The mixture was heated to 60 °C for 48 h. After filtration of  $\text{K}_2\text{CO}_3$  and removal of the solvent in vacuo, the crude material was passed through a short silica gel column (eluting with 1:15 EtOAc/hexanes). The obtained residue was dissolved in MeOH (11.7 mL) and  $\text{H}_2\text{O}$  (1.3 mL) and KOH (1.11 g, 19.7 mmol, 10 equiv) was added. After stirring at rt for 30 min, the solvent was removed in vacuo and the residue was diluted with  $\text{H}_2\text{O}$  (10 mL), acidified with 4 M  $\text{HCl}_{(\text{aq})}$  (10 mL), and extracted with EtOAc (3 x 10 mL). The combined organic extract was dried over  $\text{Na}_2\text{SO}_4$ , filtered, and concentrated under reduced pressure to provide compound **278** as a yellow oil (159.2 mg, 42%).  $^1\text{H}$  NMR (500 MHz,  $\text{CDCl}_3$ )  $\delta$  7.22 (d,  $J$  = 8.8 Hz, 2H), 7.03 (d,  $J$  = 8.8 Hz, 2H), 5.19 (d,  $J$  = 1.5 Hz, 2H), 3.62 (s, 2H), 3.50 (d,  $J$  = 1.5 Hz, 3H). All spectroscopic data are consistent with those previously reported.<sup>106</sup>



*N*-(3-(4-formyl-2-methoxyphenoxy)-4,5-dimethoxyphenethyl)-2-(3-iodo-4-(methoxymethoxy)phenyl)acetamide (**284**). To a solution of benzyl alcohol **283** (29.7 mg, 0.05 mmol, 1 equiv) in CH<sub>2</sub>Cl<sub>2</sub> (0.2 mL) under N<sub>2</sub> was added PCC (21.1 mg, 0.1 mmol, 2.1 equiv) at 0 °C. The mixture was stirred overnight at rt. The solution was decanted, and the gummy residue was rinsed exhaustively with CH<sub>2</sub>Cl<sub>2</sub> (5 x 1 mL). The combined organic extract was washed with sat. NaHCO<sub>3(aq)</sub> (1 mL), brine (2 x 1 mL) then dried over MgSO<sub>4</sub>, filtered, and concentrated in vacuo to yield benzaldehyde **284** as a brown oil (23.1 mg, 77%). <sup>1</sup>H NMR (400 MHz, CDCl<sub>3</sub>) δ 9.87 (s, 1H), 7.63 (d, *J* = 2.0 Hz, 1H), 7.51 (d, *J* = 1.7 Hz, 1H), 7.35 (dd, *J* = 8.2, 1.8 Hz, 1H), 7.13 – 7.06 (m, 1H), 7.01 (d, *J* = 8.4 Hz, 1H), 6.77 (d, *J* = 8.2 Hz, 1H), 6.57 (d, *J* = 1.9 Hz, 1H), 6.44 (d, *J* = 1.8 Hz, 1H), 5.22 (s, 2H), 3.98 (s, 3H), 3.86 (s, 3H), 3.78 (s, 3H), 3.50 (s, 3H), 3.42 (s, 2H), 2.70 (t, *J* = 7.0 Hz, 2H). <sup>13</sup>C NMR (151 MHz, CDCl<sub>3</sub>) δ 191.0, 170.6, 155.5, 154.0, 152.6, 150.3, 148.2, 140.2, 139.5, 134.9, 131.9, 130.5, 130.1, 126.0, 116.1, 115.1, 113.8, 110.5, 109.5, 95.1, 87.6, 61.2, 56.6, 56.3, 53.6, 42.4, 40.8, 35.6. IR (ATR): 3449, 3118, 3094, 2983, 2895, 2857, 1750, 1609, 1583, 1393, 1281, 1210, 1143, 1012 cm<sup>-1</sup>. HRMS (ESI<sup>+</sup>) *m/z* calculated for C<sub>28</sub>H<sub>30</sub>INO<sub>8</sub>Na [M+Na]<sup>+</sup>: 660.1070, found: 660.1051.

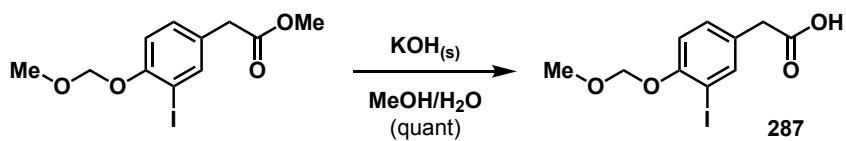


**Methyl 2-(4-hydroxy-3-iodophenyl)acetate (286).** Methyl 4-hydroxyphenylacetate (**264**, 1.04 g, 6.3 mmol, 1 equiv) was dissolved in  $\text{CH}_2\text{Cl}_2$  (19 mL) followed by addition of iodine monochloride (0.4 mL, 6.3 mmol, 1 equiv) and acetic acid (18  $\mu\text{L}$ , 0.3 mmol, 0.05 equiv). The reaction mixture was stirred at rt for 50 h, then quenched with  $\text{H}_2\text{O}$  (10 mL). The mixture was extracted with EtOAc (3 x 10 mL) and the combined organic extract was washed with sat.  $\text{Na}_2\text{S}_2\text{O}_3(\text{aq})$ , then dried over  $\text{Na}_2\text{SO}_4$ . After filtration, the solvent was removed in vacuo to afford aryl iodide **286** as a dark red-yellow oil (1.54 g, 82%).  $^1\text{H}$  NMR (400 MHz,  $\text{CDCl}_3$ )  $\delta$  7.69 – 7.50 (m, 1H), 7.24 – 7.08 (m, 1H), 6.94 (d,  $J = 8.3$  Hz, 1H), 3.70 (s, 3H), 3.52 (s, 2H). All spectroscopic data are consistent with those previously reported.<sup>111</sup>

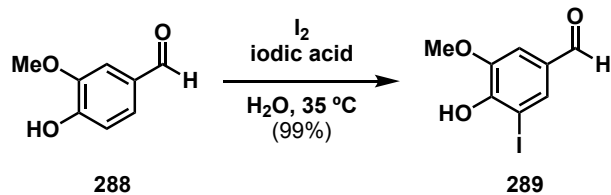


**Methyl 2-(3-iodo-4-(methoxymethoxy)phenyl)acetate.** To a suspension of  $\text{K}_2\text{CO}_3$  (2.61 g, 19 mmol, 3 equiv) in acetone (18 mL) was added a solution of **286** (1.84 g, 6.3 mmol, 1 equiv) in acetone (18 mL) and MOMCl (1 mL, 12.6 mmol, 2 equiv). The mixture was heated to 60  $^\circ\text{C}$  for 19 h, then diluted with  $\text{Et}_2\text{O}$  (20 mL) and  $\text{H}_2\text{O}$  (10 mL). The biphasic solution was extracted with  $\text{Et}_2\text{O}$  (3 x 10 mL) and the combined organic extract was washed with brine (10 mL), dried over  $\text{MgSO}_4$ , filtered, and concentrated in vacuo to yield the desired product as a dark yellow oil (2.02 g, 95%).  $^1\text{H}$  NMR (400

MHz, CDCl<sub>3</sub>) δ 7.70 (d, J = 2.2 Hz, 1H), 7.25 – 7.14 (m, 1H), 7.02 (d, J = 8.4 Hz, 1H), 5.22 (s, 2H), 3.69 (s, 3H), 3.53 (s, 2H), 3.50 (s, 3H). <sup>13</sup>C NMR (151 MHz, CDCl<sub>3</sub>) δ 171.7, 155.3, 140.1, 130.4, 129.3, 114.8, 95.0, 87.2, 56.4, 52.2, 39.7. IR (ATR): 3121, 3040, 2979, 2875, 1783, 1593, 1485, 1441, 1241, 1165, 1110, 889, 869 cm<sup>-1</sup>. HRMS (ESI+) m/z calculated for C<sub>11</sub>H<sub>17</sub>NIO<sub>4</sub> [M+NH<sub>4</sub>]<sup>+</sup>: 354.0188, found: 354.0197.

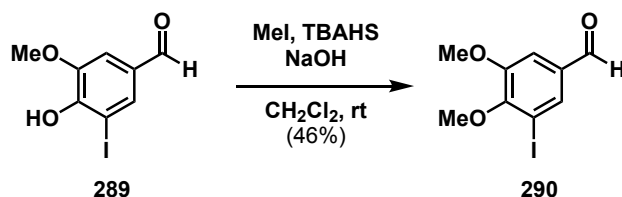


**2-(3-Iodo-4-(methoxymethoxy)phenyl)acetic acid (287).** To a solution of methyl 2-(3-iodo-4-(methoxymethoxy)phenyl)acetate (2.02 g, 6 mmol, 1 equiv) in MeOH (36 mL) and H<sub>2</sub>O (4 mL) was added KOH (3.37 g, 60 mmol, 10 equiv). After stirring at rt for 3 h, the reaction mixture was diluted with H<sub>2</sub>O (10 mL), acidified with 2 M HCl<sub>(aq)</sub> (10 mL), and extracted with EtOAc (3 x 15 mL). The combined organic extract was dried over Na<sub>2</sub>SO<sub>4</sub>, filtered, and concentrated in vacuo to provide compound **287** as a cream colored solid (2.12 g, quantitative). <sup>1</sup>H NMR (400 MHz, CDCl<sub>3</sub>) δ 7.71 (d, J = 2.2 Hz, 1H), 7.29 – 7.14 (m, 2H), 7.03 (d, J = 8.5 Hz, 1H), 5.22 (s, 2H), 3.56 (s, 2H), 3.50 (s, 3H).



**4-Hydroxy-3-iodo-5-methoxybenzaldehyde (289).** To a suspension of vanillin (**288**, 5.0 g, 32.9 mmol, 1 equiv) in EtOH (33 mL) added a solution of iodic acid (1.16 g, 6.6 mmol, 0.2 equiv) in H<sub>2</sub>O (7 mL). The reaction mixture was warmed to 35 °C for 1.5 h. The mixture was filtered over vacuum and the solids were rinsed with sat. Na<sub>2</sub>S<sub>2</sub>O<sub>3(aq)</sub>

(50 mL) and H<sub>2</sub>O (50 mL) to afford the aryl iodide **289** as a cream-colored solid (10.12 g, quantitative). <sup>1</sup>H NMR (500 MHz, CDCl<sub>3</sub>) δ 9.80 (s, 1H), 7.84 (d, *J* = 1.8 Hz, 1H), 7.40 (d, *J* = 1.8 Hz, 1H), 6.68 (d, *J* = 1.5 Hz, 1H), 4.00 (d, *J* = 1.6 Hz, 4H). All spectroscopic data are consistent with those previously reported.<sup>85</sup>



**3-iodo-4,5-dimethoxybenzaldehyde (290)**. To a solution of **289** (1.0 g, 3.6 mmol, 1 equiv) in CH<sub>2</sub>Cl<sub>2</sub> (18 mL) was added an aqueous solution of 0.6M NaOH<sub>(aq)</sub> (18 mL) and phase transfer catalyst tetrabutylammonium hydrogen sulfate (TBAS, 1.22 g, 3.6 mmol, 1 equiv). Once dissolved, MeI (2.7 mL, 43 mmol, 12 equiv) was added and the reaction mixture was allowed to stir at rt for 12 h. After stirring at rt for 12 h, the mixture was extracted with CH<sub>2</sub>Cl<sub>2</sub> (3 x 10 mL). The combined organic extract was washed with brine (10 mL), H<sub>2</sub>O (10 mL), then dried over MgSO<sub>4</sub>, filtered, and concentrated in vacuo to afford the crude material as a yellow solid (2.08 g). Purification by column chromatography (eluting with 20% EtOAc/hexanes) gave aryl halide **290** as a white fluffy solid (481.4 mg, 46%). <sup>1</sup>H NMR (500 MHz, CDCl<sub>3</sub>) δ 9.82 (s, 1H), 7.84 (d, *J* = 1.8 Hz, 1H), 7.40 (d, *J* = 1.8 Hz, 1H), 3.92 (d, *J* = 1.9 Hz, 7H). All spectroscopic data are consistent with those previously reported.<sup>85</sup>

## 2.7 References

- (1) Chougule, M.; Patel, A. R.; Sachdeva, P.; Jackson, T.; Singh, M. Anticancer Activity of Noscapine, an Opioid Alkaloid in Combination with Cisplatin in Human Non-Small Cell Lung Cancer. *Lung Cancer Amst. Neth.* **2011**, *71* (3), 271–282. <https://doi.org/10.1016/j.lungcan.2010.06.002>.
- (2) OpiumPoppy. In *Transgenic Crops VI*; Pua, E.-C., Davey, M. R., Eds.; Biotechnology in Agriculture and Forestry; Springer: Berlin, Heidelberg, 2007; pp 169–187. [https://doi.org/10.1007/978-3-540-71711-9\\_9](https://doi.org/10.1007/978-3-540-71711-9_9).
- (3) Kubitzki, K.; Rohwer, J. G.; Bittrich, V. *Flowering Plants, Dicotyledons : Magnoliid, Hamamelid, and Caryophyllid Families*; Springer-Verlag: Berlin; New York, 1993.
- (4) Liscombe, D. K.; MacLeod, B. P.; Loukanina, N.; Nandi, O. I.; Facchini, P. J. Evidence for the Monophyletic Evolution of Benzylisoquinoline Alkaloid Biosynthesis in Angiosperms. *Phytochemistry* **2005**, *66* (11), 1374–1393. <https://doi.org/10.1016/j.phytochem.2005.04.029>.
- (5) Guha, K. P.; Mukherjee, B.; Mukherjee, R. Bisbenzylisoquinoline Alkaloids--A Review. *J. Nat. Prod.* **1979**, *42* (1), 1–84. <https://doi.org/10.1021/np50001a001>.
- (6) Schiff, P. L. Bisbenzylisoquinoline Alkaloids. *J. Nat. Prod.* **1991**, *54* (3), 645–749. <https://doi.org/10.1021/np50075a001>.
- (7) Guinaudeau, H.; Freyer, A. J.; Shamma, M. Spectral Characteristics of the Bisbenzylisoquinoline Alkaloids. *Nat. Prod. Rep.* **1986**, *3* (0), 477–488. <https://doi.org/10.1039/NP9860300477>.
- (8) Weber, C.; Opatz, T. Chapter One - Bisbenzylisoquinoline Alkaloids. In *The Alkaloids: Chemistry and Biology*; Knölker, H.-J., Ed.; Academic Press, 2019; Vol. 81, pp 1–114. <https://doi.org/10.1016/bs.alkal.2018.07.001>.
- (9) Facchini, P. J.; Huber-Allanach, K. L.; Tari, L. W. Plant Aromatic L-Amino Acid Decarboxylases: Evolution, Biochemistry, Regulation, and Metabolic Engineering Applications. *Phytochemistry* **2000**, *54* (2), 121–138. [https://doi.org/10.1016/S0031-9422\(00\)00050-9](https://doi.org/10.1016/S0031-9422(00)00050-9).
- (10) Aldemir, H.; Richarz, R.; Gulder, T. A. M. The Biocatalytic Repertoire of Natural Biaryl Formation. *Angew. Chem. Int. Ed.* **2014**, *53* (32), 8286–8293. <https://doi.org/10.1002/anie.201401075>.
- (11) Ziegler, J.; Facchini, P. J. Alkaloid Biosynthesis: Metabolism and Trafficking. *Annu. Rev. Plant Biol.* **2008**, *59* (1), 735–769. <https://doi.org/10.1146/annurev.arplant.59.032607.092730>.

- (12) Kutchan, T. M. Alkaloid Biosynthesis—The Basis for Metabolic Engineering of Medicinal Plants. *Plant Cell* **1995**, *7* (7), 1059–1070. <https://doi.org/10.1105/tpc.7.7.1059>.
- (13) Chen, K. K.; Chen, A. L. THE ALKALOIDS OF HAN-FANG-CHI. *J. Biol. Chem.* **1935**, *109* (2), 681–685. [https://doi.org/10.1016/S0021-9258\(18\)75199-5](https://doi.org/10.1016/S0021-9258(18)75199-5).
- (14) Bisset, N. G. Arrow and Dart Poisons. *J. Ethnopharmacol.* **1989**, *25* (1), 1–41. [https://doi.org/10.1016/0378-8741\(89\)90043-3](https://doi.org/10.1016/0378-8741(89)90043-3).
- (15) Camacho, M. del R.; Phillipson, J. D.; Croft, S. L.; Rock, P.; Marshall, S. J.; Schiff, P. L. In Vitro Activity of *Triclisia Patens* and Some Bisbenzylisoquinoline Alkaloids against *Eishmania Donovanii* and *Trypanosoma Brucei Brucei*. *Phytother. Res.* **2002**, *16* (5), 432–436. <https://doi.org/10.1002/ptr.929>.
- (16) Zuo, G.-Y.; Li, Y.; Wang, T.; Han, J.; Wang, G.-C.; Zhang, Y.-L.; Pan, W.-D. Synergistic Antibacterial and Antibiotic Effects of Bisbenzylisoquinoline Alkaloids on Clinical Isolates of Methicillin-Resistant *Staphylococcus Aureus* (MRSA). *Mol. Basel Switz.* **2011**, *16* (12), 9819–9826. <https://doi.org/10.3390/molecules16129819>.
- (17) Meng, X.-L.; Zheng, L.-C.; Liu, J.; Gao, C.-C.; Qiu, M.-C.; Liu, Y.-Y.; Lu, J.; Wang, D.; Chen, C.-L. Inhibitory Effects of Three Bisbenzylisoquinoline Alkaloids on Lipopolysaccharide-Induced Microglial Activation. *RSC Adv.* **2017**, *7* (30), 18347–18357. <https://doi.org/10.1039/C7RA01882G>.
- (18) Medeiros, M. A. A.; Pinho, J. F.; De-Lira, D. P.; Barbosa-Filho, J. M.; Araújo, D. A. M.; Cortes, S. F.; Lemos, V. S.; Cruz, J. S. Curine, a Bisbenzylisoquinoline Alkaloid, Blocks L-Type Ca<sup>2+</sup> Channels and Decreases Intracellular Ca<sup>2+</sup> Transients in A7r5 Cells. *Eur. J. Pharmacol.* **2011**, *669* (1), 100–107. <https://doi.org/10.1016/j.ejphar.2011.07.044>.
- (19) Zhang, Z.-R.; Zhang, Y.-N.; Zhang, H.-Q.; Zhang, Q.-Y.; Li, N.; Li, Q.; Deng, C.-L.; Zhang, B.; Li, X.-D.; Ye, H.-Q. Berbamine Hydrochloride Potently Inhibits SARS-CoV-2 Infection by Blocking S Protein-Mediated Membrane Fusion. *PLoS Negl. Trop. Dis.* **2022**, *16* (4), e0010363. <https://doi.org/10.1371/journal.pntd.0010363>.
- (20) Silva, P. G. da; Fonseca, A. H.; Ribeiro, M. P.; Silva, T. D.; Grael, C. F. F.; Pena, L. J.; Silva, T. M. S.; Oliveira, E. de J. Bisbenzylisoquinoline Alkaloids of *Cissampelos Sympodialis* with Antiviral Activity against Dengue Virus. *Nat. Prod. Res.* **2020**, *0* (0), 1–5. <https://doi.org/10.1080/14786419.2020.1827404>.
- (21) Bero, J.; Frédérick, M.; Quetin-Leclercq, J. Antimalarial Compounds Isolated from Plants Used in Traditional Medicine. *J. Pharm. Pharmacol.* **2009**, *61* (11), 1401–1433. <https://doi.org/10.1211/jpp.61.11.0001>.

- (22) He, C.-L.; Huang, L.-Y.; Wang, K.; Gu, C.-J.; Hu, J.; Zhang, G.-J.; Xu, W.; Xie, Y.-H.; Tang, N.; Huang, A.-L. Identification of Bis-Benzylisoquinoline Alkaloids as SARS-CoV-2 Entry Inhibitors from a Library of Natural Products. *Signal Transduct. Target. Ther.* **2021**, *6* (1), 1–3. <https://doi.org/10.1038/s41392-021-00531-5>.
- (23) Kim, D. E.; Min, J. S.; Jang, M. S.; Lee, J. Y.; Shin, Y. S.; Park, C. M.; Song, J. H.; Kim, H. R.; Kim, S.; Jin, Y.-H.; Kwon, S. Natural Bis-Benzylisoquinoline Alkaloids-Tetrandrine, Fangchinoline, and Cepharanthine, Inhibit Human Coronavirus OC43 Infection of MRC-5 Human Lung Cells. *Biomolecules* **2019**, *9* (11), 696. <https://doi.org/10.3390/biom9110696>.
- (24) Bailly, C. Cepharanthine: An Update of Its Mode of Action, Pharmacological Properties and Medical Applications. *Phytomedicine* **2019**, *62*, 152956. <https://doi.org/10.1016/j.phymed.2019.152956>.
- (25) Wang, Z.; Yang, L. Turning the Tide: Natural Products and Natural-Product-Inspired Chemicals as Potential Counters to SARS-CoV-2 Infection. *Front. Pharmacol.* **2020**, *11*, 1013. <https://doi.org/10.3389/fphar.2020.01013>.
- (26) Bhagya, N.; Chandrashekar, K. R. Tetrandrine – A Molecule of Wide Bioactivity. *Phytochemistry* **2016**, *125*, 5–13. <https://doi.org/10.1016/j.phytochem.2016.02.005>.
- (27) Xu, W.; Chen, S.; Wang, X.; Tanaka, S.; Onda, K.; Sugiyama, K.; Yamada, H.; Hirano, T. Molecular Mechanisms and Therapeutic Implications of Tetrandrine and Cepharanthine in T Cell Acute Lymphoblastic Leukemia and Autoimmune Diseases. *Pharmacol. Ther.* **2021**, *217*, 107659. <https://doi.org/10.1016/j.pharmthera.2020.107659>.
- (28) Kitano, A.; Yamanaka, O.; Ikeda, K.; Ishida-Nishikawa, I.; Okada, Y.; Shirai, K.; Saika, S. Tetrandrine Suppresses Activation of Human Subconjunctival Fibroblasts In Vitro. *Curr. Eye Res.* **2008**, *33* (7), 559–565. <https://doi.org/10.1080/02713680802220817>.
- (29) Xu, W.; Kusano, J.; Chen, S.; Yamamoto, R.; Matsuda, H.; Hara, Y.; Fujii, Y.; Hayashi, S.; Tanaka, S.; Sugiyama, K.; Yamada, H.; Hirano, T. Absolute Configuration of Tetrandrine and Isotetrandrine Influences Their Anti-Proliferation Effects in Human T Cells via Different Regulation of NF- $\kappa$ B. *Z. Für Naturforschung C* **2021**, *76* (1–2), 21–25. <https://doi.org/10.1515/znc-2020-0064>.
- (30) Huang, T.; Xu, S.; Deo, R.; Ma, A.; Li, H.; Ma, K.; Gan, X. Targeting the Ca<sup>2+</sup>/Calmodulin-Dependent Protein Kinase II by Tetrandrine in Human Liver Cancer Cells. *Biochem. Biophys. Res. Commun.* **2019**, *508* (4), 1227–1232. <https://doi.org/10.1016/j.bbrc.2018.12.012>.

- (31) Xu, W.; Wang, X.; Tu, Y.; Masaki, H.; Tanaka, S.; Onda, K.; Sugiyama, K.; Yamada, H.; Hirano, T. Tetrandrine and Cepharanthine Induce Apoptosis through Caspase Cascade Regulation, Cell Cycle Arrest, MAPK Activation and PI3K/Akt/mTOR Signal Modification in Glucocorticoid Resistant Human Leukemia Jurkat T Cells. *Chem. Biol. Interact.* **2019**, *310*, 108726. <https://doi.org/10.1016/j.cbi.2019.108726>.
- (32) Kwan, C.-Y.; Achike, F. I. Tetrandrine and Related Bis-Benzylisoquinoline Alkaloids from Medicinal Herbs: Cardiovascular Effects and Mechanisms of Action. *Acta Pharmacol. Sin.* **2002**, *23* (12), 1057–1068.
- (33) Sakurai, Y.; Kolokoltsov, A. A.; Chen, C.-C.; Tidwell, M. W.; Bauta, W. E.; Klugbauer, N.; Grimm, C.; Wahl-Schott, C.; Biel, M.; Davey, R. A. Two-Pore Channels Control Ebola Virus Host Cell Entry and Are Drug Targets for Disease Treatment. *Science* **2015**, *347* (6225), 995–998. <https://doi.org/10.1126/science.1258758>.
- (34) Nguyen, O. N. P.; Grimm, C.; Schneider, L. S.; Chao, Y.-K.; Atzberger, C.; Bartel, K.; Watermann, A.; Ulrich, M.; Mayr, D.; Wahl-Schott, C.; Biel, M.; Vollmar, A. M. Two-Pore Channel Function Is Crucial for the Migration of Invasive Cancer Cells. *Cancer Res.* **2017**, *77* (6), 1427–1438. <https://doi.org/10.1158/0008-5472.CAN-16-0852>.
- (35) Longley, D. B.; Johnston, P. G. Molecular Mechanisms of Drug Resistance. *J. Pathol.* **2005**, *205* (2), 275–292. <https://doi.org/10.1002/path.1706>.
- (36) Luan, F.; He, X.; Zeng, N. Tetrandrine: A Review of Its Anticancer Potentials, Clinical Settings, Pharmacokinetics and Drug Delivery Systems. *J. Pharm. Pharmacol.* **2020**, *72* (11), 1491–1512. <https://doi.org/10.1111/jphp.13339>.
- (37) Robey, R. W.; Shukla, S.; Finley, E. M.; Oldham, R. K.; Barnett, D.; Ambudkar, S. V.; Fojo, T.; Bates, S. E. Inhibition of P-Glycoprotein (ABCB1)- and Multidrug Resistance-Associated Protein 1 (ABCC1)-Mediated Transport by the Orally Administered Inhibitor, CBT-1®. *Biochem. Pharmacol.* **2008**, *75* (6), 1302–1312. <https://doi.org/10.1016/j.bcp.2007.12.001>.
- (38) Oldham, R. K.; Reid, W. K.; Preisler, H. D.; Barnett, D. A Phase I and Pharmacokinetic Study of CBT-1 as a Multidrug Resistance Modulator in the Treatment of Patients with Advanced Cancer. *Cancer Biother. Radiopharm.* **1998**, *13* (2), 71–80. <https://doi.org/10.1089/cbr.1998.13.71>.
- (39) CBA Research. *A Phase I Trial of CBT-1® in Combination With Doxorubicin in Patients With Locally Advanced or Metastatic, Unresectable Sarcomas Previously to Have Progressed on 150 Mg/M2 or Less of Doxorubicin*; Clinical trial registration

- study/NCT03002805; clinicaltrials.gov, 2019.  
<https://clinicaltrials.gov/ct2/show/study/NCT03002805> (accessed 2021-03-26).
- (40) Tian, Y.; Zheng, J. Chapter Six - Metabolic Activation and Toxicities of Bis-Benzylisoquinoline Alkaloids. In *Advances in Molecular Toxicology*; Fishbein, J. C., Heilman, J. M., Eds.; Elsevier, 2017; Vol. 11, pp 241–272.  
<https://doi.org/10.1016/B978-0-12-812522-9.00006-3>.
- (41) Tainlin, L.; Tingyi, H.; Changqi, Z.; Peipei, Y.; Qiong, Z. Studies of the Chronic Toxicity of Tetrandrine in Dogs: An Inhibitor of Silicosis. *Ecotoxicol. Environ. Saf.* **1982**, 6 (6), 528–534. [https://doi.org/10.1016/0147-6513\(82\)90034-3](https://doi.org/10.1016/0147-6513(82)90034-3).
- (42) Zhang, H.; Jiao, Y.; Shi, C.; Song, X.; Chang, Y.; Ren, Y.; Shi, X. Berbamine Suppresses Cell Proliferation and Promotes Apoptosis in Ovarian Cancer Partially via the Inhibition of Wnt/ $\beta$ -Catenin Signaling. *Acta Biochim. Biophys. Sin.* **2018**, 50 (6), 532–539. <https://doi.org/10.1093/abbs/gmy036>.
- (43) Farooqi, A. A.; Wen, R.; Attar, R.; Taverna, S.; Butt, G.; Xu, B. Regulation of Cell-Signaling Pathways by Berbamine in Different Cancers. *Int. J. Mol. Sci.* **2022**, 23 (5), 2758. <https://doi.org/10.3390/ijms23052758>.
- (44) Gu, Y.; Chen, T.; Meng, Z.; Gan, Y.; Xu, X.; Lou, G.; Li, H.; Gan, X.; Zhou, H.; Tang, J.; Xu, G.; Huang, L.; Zhang, X.; Fang, Y.; Wang, K.; Zheng, S.; Huang, W.; Xu, R. CaMKII  $\gamma$ , a Critical Regulator of CML Stem/Progenitor Cells, Is a Target of the Natural Product Berbamine. *Blood* **2012**, 120 (24), 4829–4839.  
<https://doi.org/10.1182/blood-2012-06-434894>.
- (45) Miller, D. M.; Thomas, S. D.; Islam, A.; Muench, D.; Sedoris, K. C-Myc and Cancer Metabolism. *Clin. Cancer Res.* **2012**, 18 (20), 5546–5553.  
<https://doi.org/10.1158/1078-0432.CCR-12-0977>.
- (46) Toyoshima, M.; Howie, H. L.; Imakura, M.; Walsh, R. M.; Annis, J. E.; Chang, A. N.; Frazier, J.; Chau, B. N.; Loboda, A.; Linsley, P. S.; Cleary, M. A.; Park, J. R.; Grandori, C. Functional Genomics Identifies Therapeutic Targets for MYC-Driven Cancer. *Proc. Natl. Acad. Sci.* **2012**, 109 (24), 9545–9550.  
<https://doi.org/10.1073/pnas.1121119109>.
- (47) Gu, Y.; Zhang, J.; Ma, X.; Kim, B.; Wang, H.; Li, J.; Pan, Y.; Xu, Y.; Ding, L.; Yang, L.; Guo, C.; Wu, X.; Wu, J.; Wu, K.; Gan, X.; Li, G.; Li, L.; Forman, S. J.; Chan, W.-C.; Xu, R.; Huang, W. Stabilization of the C-Myc Protein by CAMKII $\gamma$  Promotes T Cell Lymphoma. *Cancer Cell* **2017**, 32 (1), 115–128.e7.  
<https://doi.org/10.1016/j.ccell.2017.06.001>.
- (48) Liu, X.; Xu, S.; Zhang, J.; Fan, M.; Xie, J.; Zhang, B.; Li, H.; Yu, G.; Liu, Y.; Zhang, Y.; Song, J.; Horne, D.; Chan, W. C.; Chu, X.; Huang, W. Targeting MYC

- and BCL2 by a Natural Compound for “Double-Hit” Lymphoma. *Hematol. Oncol.* **2022**, *40* (3), 356–369. <https://doi.org/10.1002/hon.3010>.
- (49) Meng, Z.; Li, T.; Ma, X.; Wang, X.; Van Ness, C.; Gan, Y.; Zhou, H.; Tang, J.; Lou, G.; Wang, Y.; Wu, J.; Yen, Y.; Xu, R.; Huang, W. Berbamine Inhibits the Growth of Liver Cancer Cells and Cancer-Initiating Cells by Targeting Ca<sup>2+</sup>/Calmodulin-Dependent Protein Kinase II. *Mol. Cancer Ther.* **2013**, *12* (10), 2067–2077. <https://doi.org/10.1158/1535-7163.MCT-13-0314>.
- (50) Zhao, W.; Bai, B.; Hong, Z.; Zhang, X.; Zhou, B. Berbamine (BBM), a Natural STAT3 Inhibitor, Synergistically Enhances the Antigrowth and Proapoptotic Effects of Sorafenib on Hepatocellular Carcinoma Cells. *ACS Omega* **2020**, *5* (38), 24838–24847. <https://doi.org/10.1021/acsomega.0c03527>.
- (51) Hu, B.; Cai, H.; Yang, S.; Tu, J.; Huang, X.; Chen, G. Berbamine Enhances the Efficacy of Gefitinib by Suppressing STAT3 Signaling in Pancreatic Cancer Cells. *OncoTargets Ther.* **2019**, *12*, 11437–11451. <https://doi.org/10.2147/OTT.S223242>.
- (52) Jia, F.; Ruan, S.; Liu, N.; Fu, L. Synergistic Antitumor Effects of Berbamine and Paclitaxel through ROS/Akt Pathway in Glioma Cells. *Evid. Based Complement. Alternat. Med.* **2017**, *2017*, e8152526. <https://doi.org/10.1155/2017/8152526>.
- (53) Prasath, M.; Narasimha, M. B.; Viswanadha, V. P. The Cytoprotective and Anti-Cancer Potential of Bisbenzylisoquinoline Alkaloids from *Nelumbo Nucifera*. *Curr. Top. Med. Chem.* **2019**, *19* (32), 2940–2957.
- (54) Marthandam Asokan, S.; Mariappan, R.; Muthusamy, S.; Velmurugan, B. K. Pharmacological Benefits of Neferine - A Comprehensive Review. *Life Sci.* **2018**, *199*, 60–70. <https://doi.org/10.1016/j.lfs.2018.02.032>.
- (55) Li, G.; Xu, H.; Zhu, S.; Xu, W.; Qin, S.; Liu, S.; Tu, G.; Peng, H.; Qiu, S.; Yu, S.; Zhu, Q.; Fan, B.; Zheng, C.; Li, G.; Liang, S. Effects of Neferine on CCL5 and CCR5 Expression in SCG of Type 2 Diabetic Rats. *Brain Res. Bull.* **2013**, *90*, 79–87. <https://doi.org/10.1016/j.brainresbull.2012.10.002>.
- (56) Deng, G.; Zeng, S.; Ma, J.; Zhang, Y.; Qu, Y.; Han, Y.; Yin, L.; Cai, C.; Guo, C.; Shen, H. The Anti-Tumor Activities of Neferine on Cell Invasion and Oxaliplatin Sensitivity Regulated by EMT via Snail Signaling in Hepatocellular Carcinoma. *Sci. Rep.* **2017**, *7* (1), 41616. <https://doi.org/10.1038/srep41616>.
- (57) Kadioglu, O.; Law, B. Y. K.; Mok, S. W. F.; Xu, S.-W.; Efferth, T.; Wong, V. K. W. Mode of Action Analyses of Neferine, a Bisbenzylisoquinoline Alkaloid of Lotus (*Nelumbo Nucifera*) against Multidrug-Resistant Tumor Cells. *Front. Pharmacol.* **2017**, *8*. <https://doi.org/10.3389/fphar.2017.00238>.

- (58) Erdogan, S.; Turkekul, K. Neferine Inhibits Proliferation and Migration of Human Prostate Cancer Stem Cells through P38 MAPK/JNK Activation. *J. Food Biochem.* **2020**, *44* (7), e13253. <https://doi.org/10.1111/jfbc.13253>.
- (59) Wang, L.; Pu, Z.; Li, M.; Wang, K.; Deng, L.; Chen, W. Antioxidative and Antiapoptosis: Neuroprotective Effects of Dauricine in Alzheimer's Disease Models. *Life Sci.* **2020**, *243*, 117237. <https://doi.org/10.1016/j.lfs.2019.117237>.
- (60) Park, H.-J.; Gholam Zadeh, M.; Suh, J.-H.; Choi, H.-S. Dauricine Protects from LPS-Induced Bone Loss via the ROS/PP2A/NF- $\kappa$ B Axis in Osteoclasts. *Antioxidants* **2020**, *9* (7). <https://doi.org/10.3390/antiox9070588>.
- (61) Jin, H.; Dai, J.; Chen, X.; Liu, J.; Zhong, D.; Gu, Y.; Zheng, J. Pulmonary Toxicity and Metabolic Activation of Dauricine in CD-1 Mice. *J. Pharmacol. Exp. Ther.* **2009**. <https://doi.org/10.1124/jpet.109.162297>.
- (62) Finkelstein, J. The Synthesis of DI-Coclaurine. *J. Am. Chem. Soc.* **1951**, *73* (2), 550–553. <https://doi.org/10.1021/ja01146a012>.
- (63) Kametani, T.; Takano, S.; Masuko, K.; Kuribara, S. Studies on the Syntheses of Heterocyclic Compounds. CIII. *Yakugaku Zasshi* **1965**, *85* (2), 166–168. [https://doi.org/10.1248/yakushi1947.85.2\\_166](https://doi.org/10.1248/yakushi1947.85.2_166).
- (64) Cava, M. P.; Buck, K. T. Some Synthetic Studies in the Isoquinoline Series. *Tetrahedron* **1969**, *25* (14), 2795–2805. [https://doi.org/10.1016/0040-4020\(69\)80023-2](https://doi.org/10.1016/0040-4020(69)80023-2).
- (65) Ruiz-Olalla, A.; Würdemann, M. A.; Wanner, M. J.; Ingemann, S.; van Maarseveen, J. H.; Hiemstra, H. Organocatalytic Enantioselective Pictet–Spengler Approach to Biologically Relevant 1-Benzyl-1,2,3,4-Tetrahydroisoquinoline Alkaloids. *J. Org. Chem.* **2015**, *80* (10), 5125–5132. <https://doi.org/10.1021/acs.joc.5b00509>.
- (66) Chan, D. M. T.; Monaco, K. L.; Wang, R.-P.; Winters, M. P. New N- and O-Arylations with Phenylboronic Acids and Cupric Acetate. *Tetrahedron Lett.* **1998**, *39* (19), 2933–2936. [https://doi.org/10.1016/S0040-4039\(98\)00503-6](https://doi.org/10.1016/S0040-4039(98)00503-6).
- (67) Hartwig, J. F. Transition Metal Catalyzed Synthesis of Arylamines and Aryl Ethers from Aryl Halides and Triflates: Scope and Mechanism. *Angew. Chem. Int. Ed Engl.* **1998**, *37* (15), 2046–2067. [https://doi.org/10.1002/\(SICI\)1521-3773\(19980817\)37:15<2046::AID-ANIE2046>3.0.CO;2-L](https://doi.org/10.1002/(SICI)1521-3773(19980817)37:15<2046::AID-ANIE2046>3.0.CO;2-L).
- (68) Tomita, M.; Ito, K.; Yamaguchi, H. Studies on the Alkaloids of Menispermaceous Plants. CXXX. Synthesis of O-Methylauricine by Ullmann Reaction. *Pharm. Bull.* **1955**, *3* (6), 449–453. <https://doi.org/10.1248/cpb1953.3.449>.

- (69) Kametani, T.; Fukumoto, K. Total Synthesis of (±)-Dauricine. *Tetrahedron Lett.* **1964**, 5 (38), 2771–2775. [https://doi.org/10.1016/S0040-4039\(00\)71728-X](https://doi.org/10.1016/S0040-4039(00)71728-X).
- (70) Shamma, M.; Georgiev, V. St. Chapter 6 Syntheses of Bisbenzylisoqueinoleine Alkaloids. In *The Alkaloids: Chemistry and Physiology*; Elsevier, 1977; Vol. 16, pp 319–392. [https://doi.org/10.1016/S1876-0813\(08\)60073-1](https://doi.org/10.1016/S1876-0813(08)60073-1).
- (71) Nishimura, K.; Horii, S.; Tanahashi, T.; Sugimoto, Y.; Yamada, J. Synthesis and Pharmacological Activity of Alkaloids from Embryo of Lotus, *Nelumbo Nucifera*. *Chem. Pharm. Bull. (Tokyo)* **2013**, 61 (1), 59–68. <https://doi.org/10.1248/cpb.c12-00820>.
- (72) Blank, N.; Opatz, T. Enantioselective Synthesis of Tetrahydroprotoberberines and Bisbenzylisoquinoline Alkaloids from a Deprotonated  $\alpha$ -Aminonitrile. *J. Org. Chem.* **2011**, 76 (23), 9777–9784. <https://doi.org/10.1021/jo201871c>.
- (73) Bobbitt, J. M.; Hallcher, R. C. Electrolytic Oxidation of Armepavine and Its Derivatives. *J. Chem. Soc. Chem. Commun.* **1971**, No. 11, 543–544. <https://doi.org/10.1039/C29710000543>.
- (74) Kawabata, Y.; Naito, Y.; Saitoh, T.; Kawa, K.; Fuchigami, T.; Nishiyama, S. Synthesis of (+)-O-Methylthalibrine by Employing a Stereocontrolled Bischler–Napieralski Reaction and an Electrochemically Generated Diaryl Ether. *Eur. J. Org. Chem.* **2014**, 2014 (1), 99–104. <https://doi.org/10.1002/ejoc.201301128>.
- (75) Huang, Z.; Ji, X.; Lumb, J.-P. Total Synthesis of (S,S)-Tetramethylmagnolamine via Aerobic Desymmetrization. *Org. Lett.* **2019**, 21 (22), 9194–9197. <https://doi.org/10.1021/acs.orglett.9b03559>.
- (76) Otto, N.; Ferenc, D.; Opatz, T. A Modular Access to (±)-Tubocurine and (±)-Curine - Formal Total Synthesis of Tubocurarine. *J. Org. Chem.* **2017**, 82 (2), 1205–1217. <https://doi.org/10.1021/acs.joc.6b02647>.
- (77) Schütz, R.; Meixner, M.; Antes, I.; Bracher, F. A Modular Approach to the Bisbenzylisoquinoline Alkaloids Tetrandrine and Isotetrandrine. *Org. Biomol. Chem.* **2020**, 18 (16), 3047–3068. <https://doi.org/10.1039/D0OB00078G>.
- (78) Wong, C. W.; Seow, W. K.; Zeng, T. S.; Halliday, W. J.; Thong, Y. H. Comparative Immunopharmacology and Toxicology of the Bisbenzylisoquinoline Alkaloids Tetrandrine and Berbamine. *Int. J. Immunopharmacol.* **1991**, 13 (5), 579–585. [https://doi.org/10.1016/0192-0561\(91\)90079-M](https://doi.org/10.1016/0192-0561(91)90079-M).
- (79) Xie, J.; Ma, T.; Gu, Y.; Zhang, X.; Qiu, X.; Zhang, L.; Xu, R.; Yu, Y. Berbamine Derivatives: A Novel Class of Compounds for Anti-Leukemia Activity. *Eur. J. Med. Chem.* **2009**, 44 (8), 3293–3298. <https://doi.org/10.1016/j.ejmech.2009.02.018>.

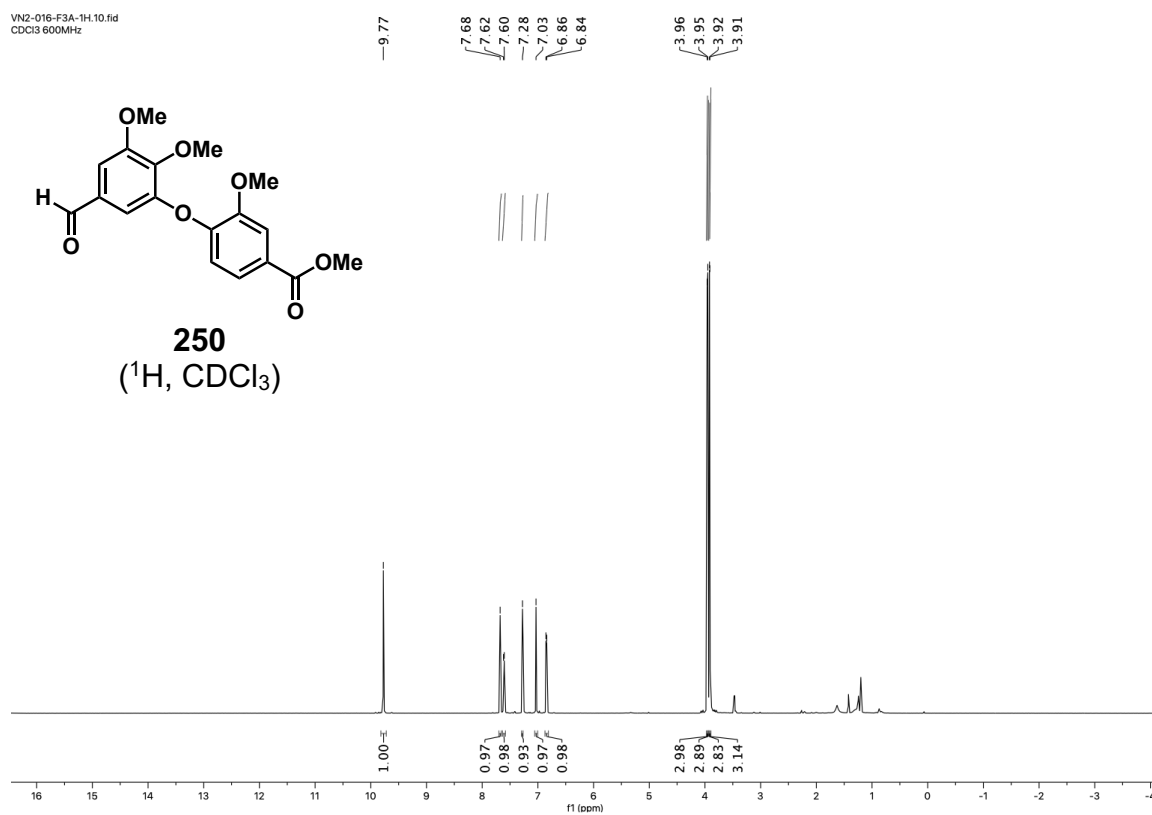
- (80) Jia, X.-J.; Li, X.; Wang, F.; Liu, H.-Q.; Zhang, D.-J. Berbamine Exerts Anti-Inflammatory Effects via Inhibition of NF- $\kappa$ B and MAPK Signaling Pathways. *Cell. Physiol. Biochem.* **2017**, *41* (6), 2307–2318. <https://doi.org/10.1159/000475650>.
- (81) Hudson, A. M.; Lockard, G. M.; Namjoshi, O. A.; Wilson, J. W.; Kindt, K. S.; Blough, B. E.; Coffin, A. B. Berbamine Analogs Exhibit Differential Protective Effects From Aminoglycoside-Induced Hair Cell Death. *Front. Cell. Neurosci.* **2020**, *14*.
- (82) Cloherty, A. P. M.; Rader, A. G.; Patel, K. S.; Pérez-Vargas, J.; Thompson, C. A. H.; Ennis, S.; Niikura, M.; Wildenberg, M. E.; Muncan, V.; Schreurs, R. R. C. E.; Jean, F.; Ribeiro, C. M. S. Berbamine Suppresses Intestinal SARS-CoV-2 Infection via a BNIP3-Dependent Autophagy Blockade. *Emerg. Microbes Infect.* **2023**, *12* (1), 2195020. <https://doi.org/10.1080/22221751.2023.2195020>.
- (83) Vanucci-Bacqué, C.; Camare, C.; Carayon, C.; Bernis, C.; Baltas, M.; Nègre-Salvayre, A.; Bedos-Belval, F. Synthesis and Evaluation of Antioxidant Phenolic Diaryl Hydrazones as Potent Antiangiogenic Agents in Atherosclerosis. *Bioorg. Med. Chem.* **2016**, *24* (16), 3571–3578. <https://doi.org/10.1016/j.bmc.2016.05.067>.
- (84) Ronson, T. O.; Kitsiou, C.; Unsworth, W. P.; Taylor, R. J. K. Synthetic Approaches to Pallimamine and Analogues Using Direct Imine Acylation. *Tetrahedron* **2016**, *72* (40), 6099–6106. <https://doi.org/10.1016/j.tet.2016.05.009>.
- (85) Maresh, J. J.; Ralko, A. A.; Speltz, T. E.; Burke, J. L.; Murphy, C. M.; Gaskell, Z.; Girel, J. K.; Terranova, E.; Richtscheidt, C.; Krzeszowiec, M. Chemoselective Zinc/HCl Reduction of Halogenated  $\beta$ -Nitrostyrenes: Synthesis of Halogenated Dopamine Analogues. *Synlett* **2014**, *25* (20), 2891–2894. <https://doi.org/10.1055/s-0034-1379481>.
- (86) Kabalka, G. W.; Laila, G. M. H.; Varma, R. S. Selected Reductions of Conjugated Nitroalkenes. *Tetrahedron* **1990**, *46* (21), 7443–7457. [https://doi.org/10.1016/S0040-4020\(01\)89059-1](https://doi.org/10.1016/S0040-4020(01)89059-1).
- (87) Winterton, S. E.; Capota, E.; Wang, X.; Chen, H.; Mallipeddi, P. L.; Williams, N. S.; Posner, B. A.; Nijhawan, D.; Ready, J. M. Discovery of Cytochrome P450 4F11 Activated Inhibitors of Stearoyl Coenzyme A Desaturase. *J. Med. Chem.* **2018**, *61* (12), 5199–5221. <https://doi.org/10.1021/acs.jmedchem.8b00052>.
- (88) Muñoz, L.; Rodriguez, A. M.; Rosell, G.; Bosch, M. P.; Guerrero, A. Enzymatic Enantiomeric Resolution of Phenylethylamines Structurally Related to Amphetamine. *Org. Biomol. Chem.* **2011**, *9* (23), 8171–8177. <https://doi.org/10.1039/C1OB06251D>.
- (89) Kurbanov, E. K.; Chiu, T.-L.; Solberg, J.; Francis, S.; Maize, K. M.; Fernandez, J.; Johnson, R. L.; Hawkinson, J. E.; Walters, M. A.; Finzel, B. C.; Amin, E. A.

- Probing the S2' Subsite of the Anthrax Toxin Lethal Factor Using Novel N-Alkylated Hydroxamates. *J. Med. Chem.* **2015**, *58* (21), 8723–8733.  
<https://doi.org/10.1021/acs.jmedchem.5b01446>.
- (90) Lawrence, H. R.; Kazi, A.; Luo, Y.; Kendig, R.; Ge, Y.; Jain, S.; Daniel, K.; Santiago, D.; Guida, W. C.; Sebti, S. M. Synthesis and Biological Evaluation of Naphthoquinone Analogs as a Novel Class of Proteasome Inhibitors. *Bioorg. Med. Chem.* **2010**, *18* (15), 5576–5592. <https://doi.org/10.1016/j.bmc.2010.06.038>.
- (91) Ariyaratna, J. P.; Alom, N.-E.; Roberts, L. P.; Kaur, N.; Wu, F.; Li, W. Lewis Acid-Catalyzed Halonium Generation for Morpholine Synthesis and Claisen Rearrangement. *J. Org. Chem.* **2022**, *87* (5), 2947–2958.  
<https://doi.org/10.1021/acs.joc.1c02804>.
- (92) Ramunno, A.; Cosconati, S.; Sartini, S.; Maglio, V.; Angiuoli, S.; La Pietra, V.; Di Maro, S.; Giustiniano, M.; La Motta, C.; Da Settimo, F.; Marinelli, L.; Novellino, E. Progresses in the Pursuit of Aldose Reductase Inhibitors: The Structure-Based Lead Optimization Step. *Eur. J. Med. Chem.* **2012**, *51*, 216–226.  
<https://doi.org/10.1016/j.ejmech.2012.02.045>.
- (93) Barn, D. R.; Caulfield, W. L.; Cottney, J.; McGurk, K.; Morphy, J. R.; Rankovic, Z.; Roberts, B. Parallel Synthesis and Biological Activity of a New Class of High Affinity and Selective  $\delta$ -Opioid Ligand. *Bioorg. Med. Chem.* **2001**, *9* (10), 2609–2624. [https://doi.org/10.1016/S0968-0896\(01\)00017-7](https://doi.org/10.1016/S0968-0896(01)00017-7).
- (94) Hajji, C.; Roller, S.; Beigi, M.; Liese, A.; Haag, R. Polyglycerol-Supported Chromium-Salen as a High-Loading Dendritic Catalyst for Stereoselective Diels–Alder Reactions. *Adv. Synth. Catal.* **2006**, *348* (12–13), 1760–1771.  
<https://doi.org/10.1002/adsc.200606168>.
- (95) Kita, Y.; Egi, M.; Takada, T.; Tohma, H. Development of Novel Reactions Using Hypervalent Iodine(III) Reagents: Total Synthesis of Sulfur-Containing Pyrroloiminoquinone Marine Product, ( $\pm$ )-Makaluvamine F. *Synthesis* **1999**, *1999* (05), 885–897. <https://doi.org/10.1055/s-1999-3462>.
- (96) Ankner, T.; Fridén-Saxin, M.; Pemberton, N.; Seifert, T.; Grøtli, M.; Luthman, K.; Hilmersson, G. KHMDS Enhanced SmI<sub>2</sub>-Mediated Reformatsky Type  $\alpha$ -Cyanation. *Org. Lett.* **2010**, *12* (10), 2210–2213. <https://doi.org/10.1021/ol100424y>.
- (97) Arai, S.; Hida, M.; Yamagishi, T. The Ullmann Condensation Reaction of Haloanthraquinone Derivatives with Amines in Aprotic Solvents. III. The Formation and Role of Copper(II) Species in the Condensation with 2-Aminoethanol by Copper(I) Catalyst. *Bull. Chem. Soc. Jpn.* **1978**, *51* (1), 277–282.  
<https://doi.org/10.1246/bcsj.51.277>.

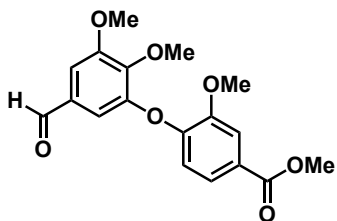
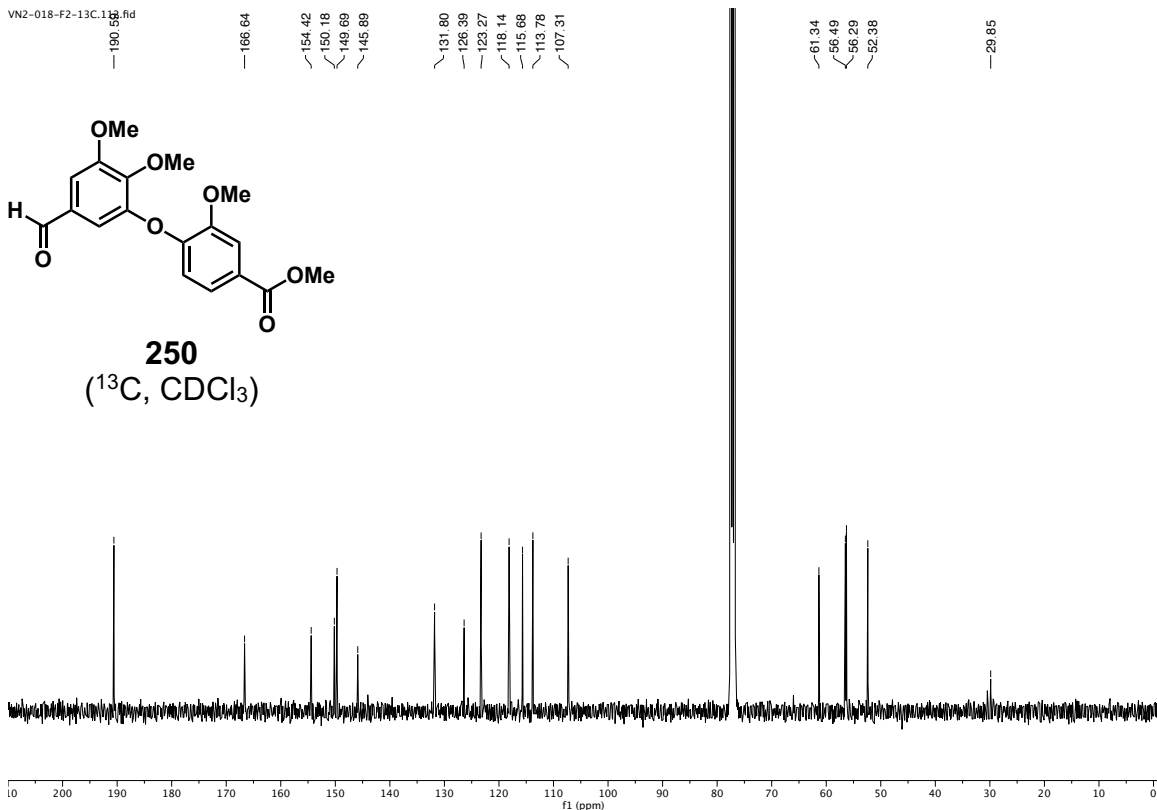
- (98) Cannon, K. A.; Geuther, M. E.; Kelly, C. K.; Lin, S.; MacArthur, A. H. R. Hydrodehalogenation of Aryl Chlorides and Aryl Bromides Using a Microwave-Assisted, Copper-Catalyzed Concurrent Tandem Catalysis Methodology. *Organometallics* **2011**, *30* (15), 4067–4073. <https://doi.org/10.1021/om2003706>.
- (99) Moroz, A. A.; Shvartsberg, M. S. The Ullmann Ether Condensation. *Russ. Chem. Rev.* **1974**, *43* (8), 679. <https://doi.org/10.1070/RC1974v043n08ABEH001845>.
- (100) Fier, P. S.; Hartwig, J. F. Copper-Mediated Difluoromethylation of Aryl and Vinyl Iodides. *J. Am. Chem. Soc.* **2012**, *134* (12), 5524–5527. <https://doi.org/10.1021/ja301013h>.
- (101) Bermejo, A.; Andreu, I.; Suvire, F.; Léonce, S.; Caignard, D. H.; Renard, P.; Pierré, A.; Enriz, R. D.; Cortes, D.; Cabedo, N. Syntheses and Antitumor Targeting G1 Phase of the Cell Cycle of Benzoyldihydroisoquinolines and Related 1-Substituted Isoquinolines. *J. Med. Chem.* **2002**, *45* (23), 5058–5068. <https://doi.org/10.1021/jm020831a>.
- (102) Evanno, L.; Ormala, J.; Pihko, P. M. A Highly Enantioselective Access to Tetrahydroisoquinoline and  $\beta$ -Carboline Alkaloids with Simple Noyori-Type Catalysts in Aqueous Media. *Chem. – Eur. J.* **2009**, *15* (47), 12963–12967. <https://doi.org/10.1002/chem.200902289>.
- (103) Thetiot-Laurent, S. A.-L.; Nadal, B.; Gall, T. L. Synthesis of Bis(Tetronic Acid)s via Double Dieckmann Condensation. *Synthesis* **2010**, 1697–1701. <https://doi.org/10.1055/s-0029-1218738>.
- (104) Dieskau, A. P.; Plietker, B. A Mild Ligand-Free Iron-Catalyzed Liberation of Alcohols from Allylcarbonates. *Org. Lett.* **2011**, *13* (20), 5544–5547. <https://doi.org/10.1021/ol202270g>.
- (105) Trân-Huu-Dâu, M.-E.; Wartchow, R.; Winterfeldt, E.; Wong, Y.-S. New Cyclohexadienone Derivatives: Preparation and Chiral Discrimination in High-Pressure Diels–Alder Cycloadditions. *Chem. – Eur. J.* **2001**, *7* (11), 2349–2369. [https://doi.org/10.1002/1521-3765\(20010601\)7:11<2349::AID-CHEM23490>3.0.CO;2-C](https://doi.org/10.1002/1521-3765(20010601)7:11<2349::AID-CHEM23490>3.0.CO;2-C).
- (106) Takao, K.; Takemura, Y.; Nagai, J.; Kamauchi, H.; Hoshi, K.; Mabashi, R.; Uesawa, Y.; Sugita, Y. Synthesis and Biological Evaluation of 3-Styrylchromone Derivatives as Selective Monoamine Oxidase B Inhibitors. *Bioorg. Med. Chem.* **2021**, *42*, 116255. <https://doi.org/10.1016/j.bmc.2021.116255>.
- (107) Nguyen, V. K.; Kou, K. G. M. The Biology and Total Syntheses of Bisbenzylisoquinoline Alkaloids. *Org. Biomol. Chem.* **2021**, *19* (35), 7535–7543. <https://doi.org/10.1039/D1OB00812A>.

- (108) Kim, A. N.; Ngamnithiporn, A.; Du, E.; Stoltz, B. M. Recent Advances in the Total Synthesis of the Tetrahydroisoquinoline Alkaloids (2002–2020). *Chem. Rev.* **2023**, *123* (15), 9447–9496. <https://doi.org/10.1021/acs.chemrev.3c00054>.
- (109) Kamiyama, A.; Nakajima, M.; Han, L.; Wada, K.; Mizutani, M.; Tabuchi, Y.; Kojima-Yuasa, A.; Matsui-Yuasa, I.; Suzuki, H.; Fukuyama, K.; Watanabe, B.; Hiratake, J. Phosphonate-Based Irreversible Inhibitors of Human  $\gamma$ -Glutamyl Transpeptidase (GGT). GGsTop Is a Non-Toxic and Highly Selective Inhibitor with Critical Electrostatic Interaction with an Active-Site Residue Lys562 for Enhanced Inhibitory Activity. *Bioorg. Med. Chem.* **2016**, *24* (21), 5340–5352. <https://doi.org/10.1016/j.bmc.2016.08.050>.
- (110) McNamara, N.; Rahmani, R.; Sykes, M. L.; Avery, V. M.; Baell, J. Hit-to-Lead Optimization of Novel Benzimidazole Phenylacetamides as Broad Spectrum Trypanosomacides. *RSC Med. Chem.* **2020**, *11* (6), 685–695. <https://doi.org/10.1039/D0MD00058B>.
- (111) Miyakawa, M.; Scanlan, T. S. Synthesis of [125I]-, [2H]-, and [3H]-Labeled 3-Iodothyronamine (T1AM). *Synth. Commun.* **2006**, *36* (7), 891–902. <https://doi.org/10.1080/00397910500466074>.

## 2.8 Selected NMR Spectra

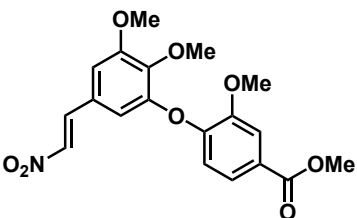
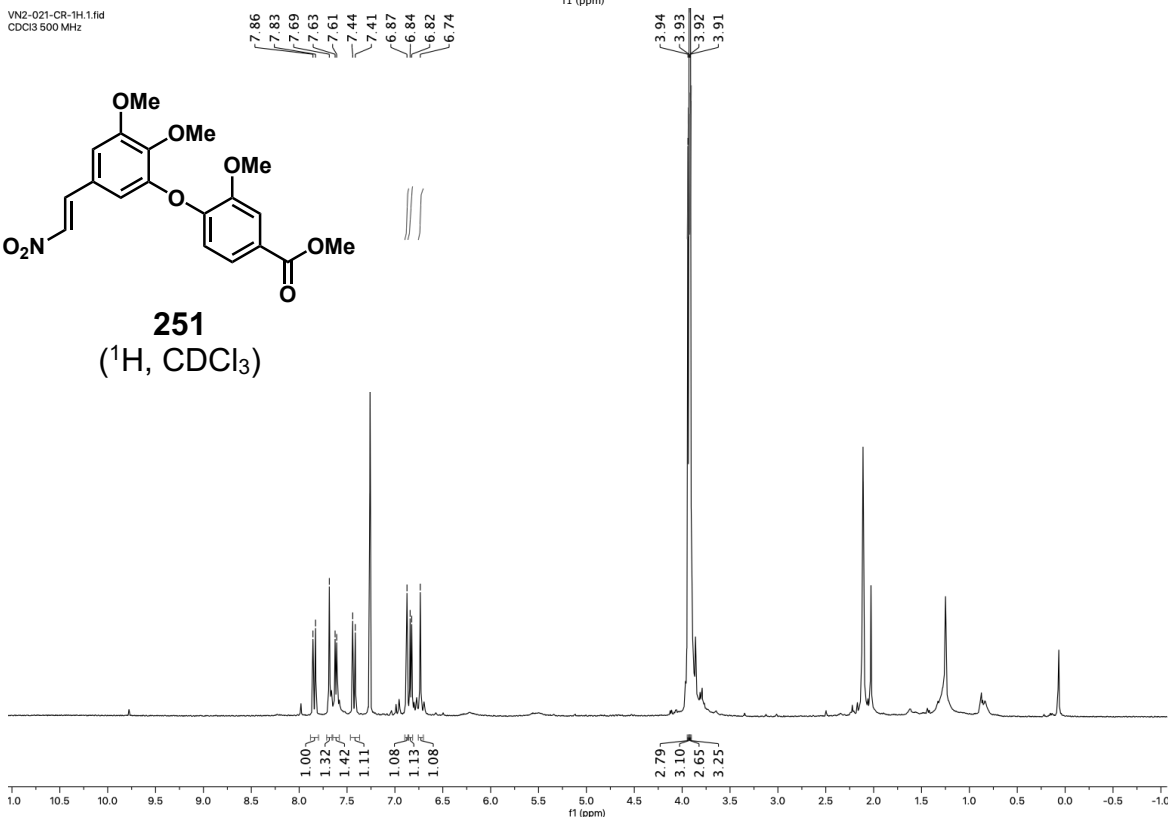


VN2-018-F2-13C.15.fid



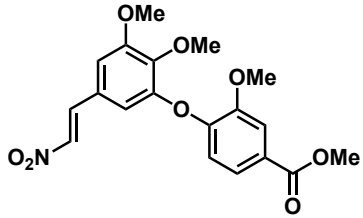
**250**  
(<sup>13</sup>C, CDCl<sub>3</sub>)

VN2-021-CR-1H.1.fid  
CDCl<sub>3</sub> 500 MHz

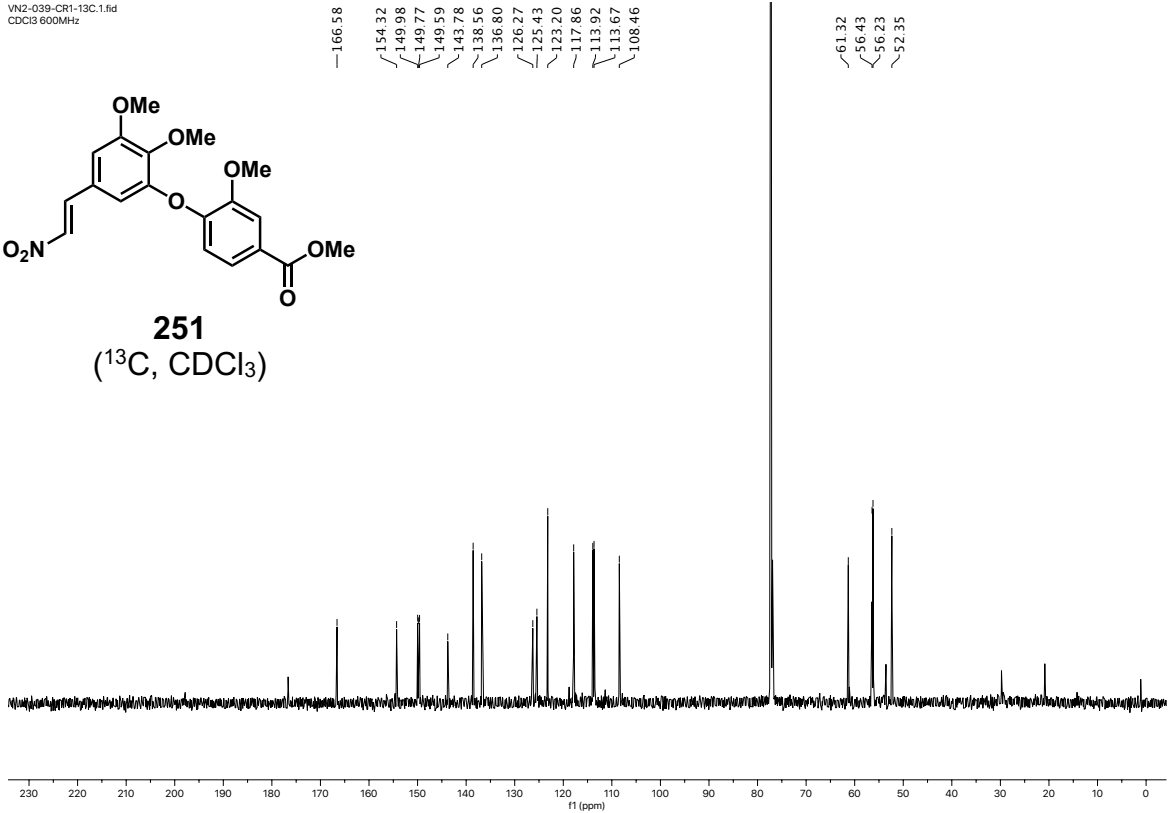


**251**  
(<sup>1</sup>H, CDCl<sub>3</sub>)

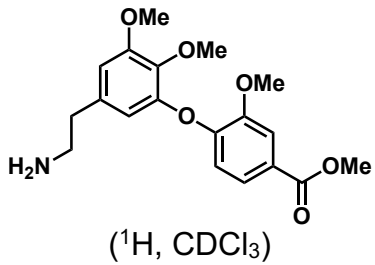
VN2-039-CR1-13C.1.fid  
CDCl3 600MHz



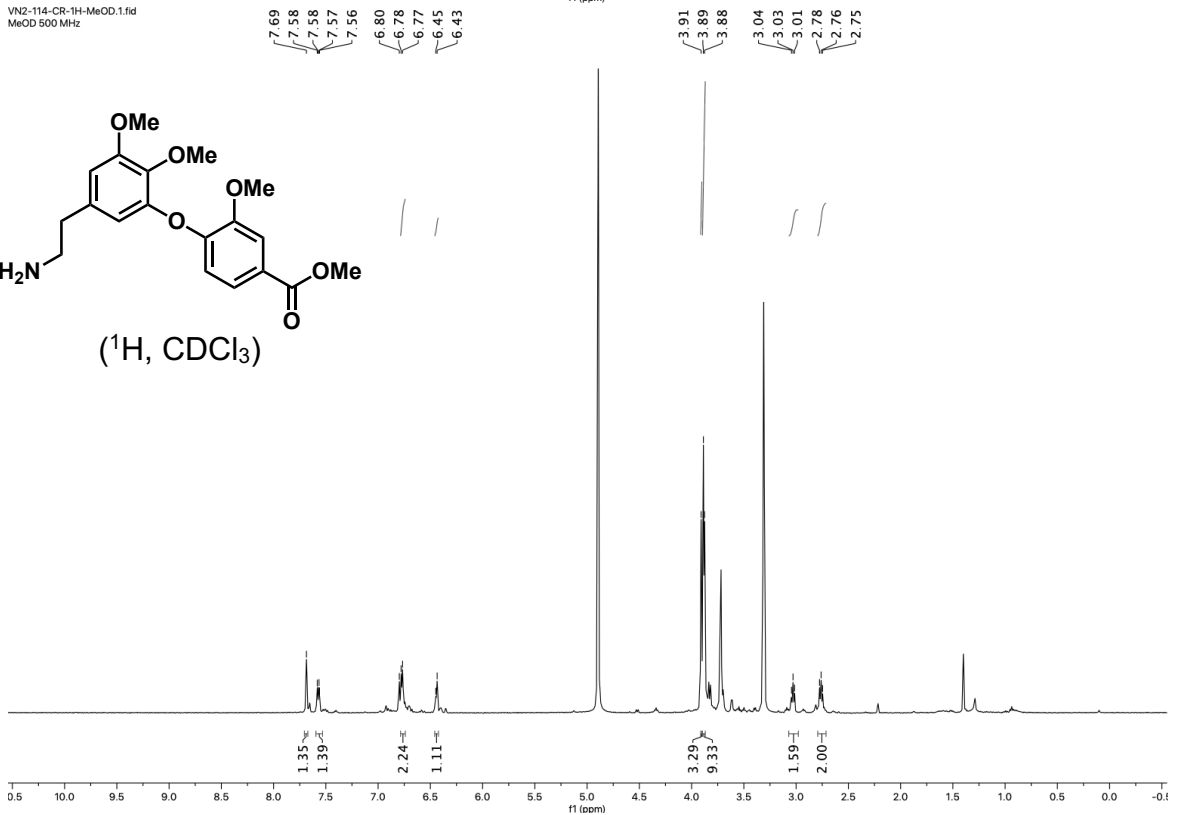
**251**  
(<sup>13</sup>C, CDCl<sub>3</sub>)

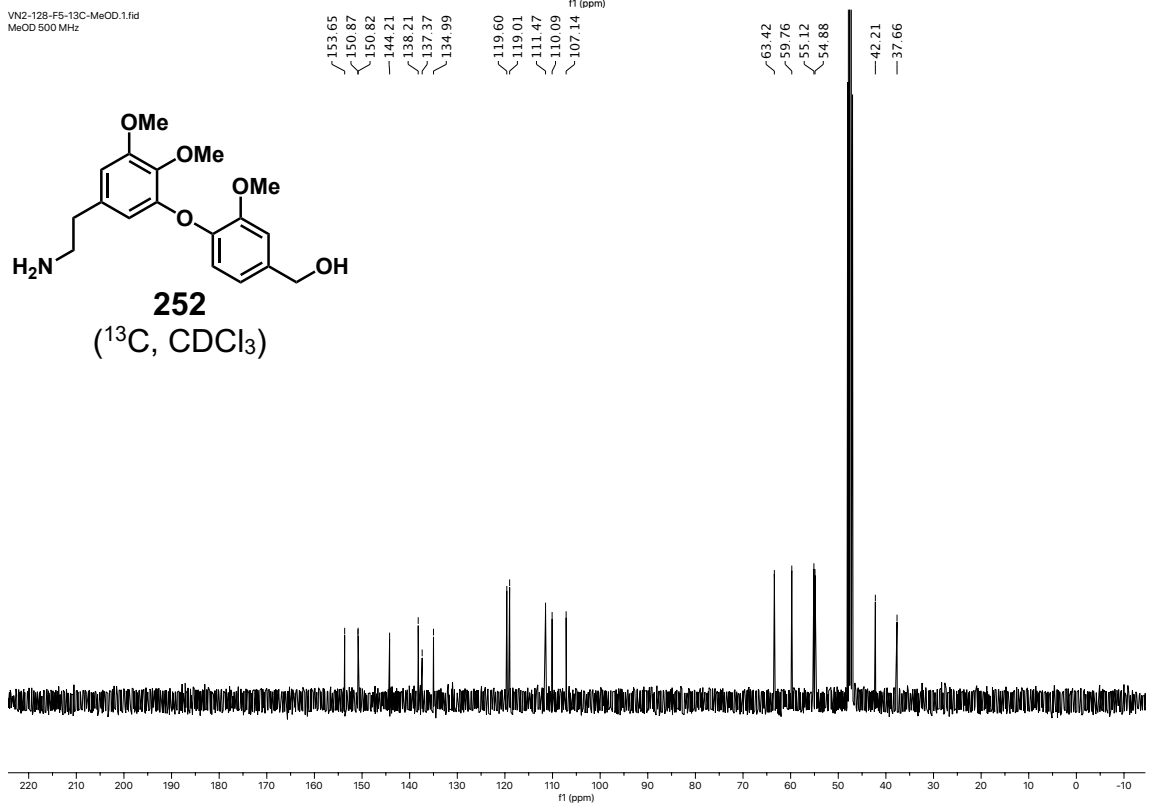
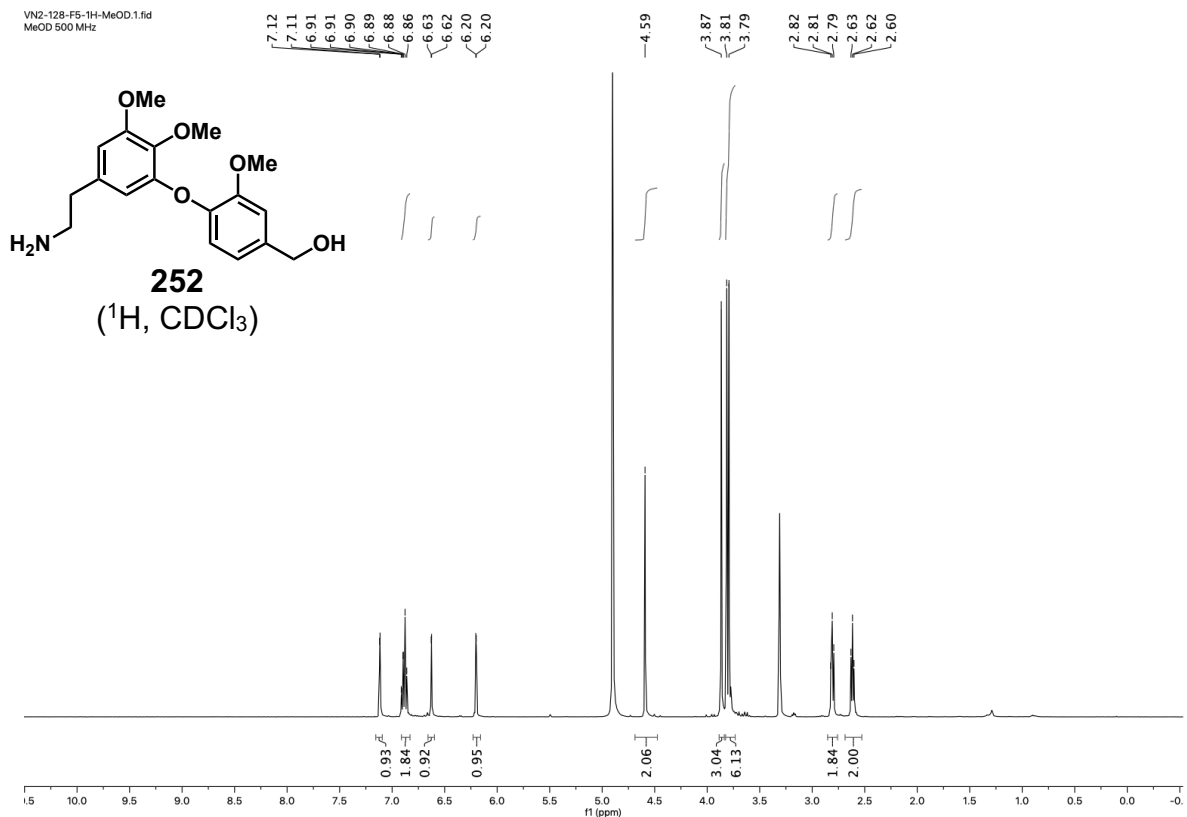


VN2-114-CR-1H-MeOD.1.fid  
MeOD 500 MHz

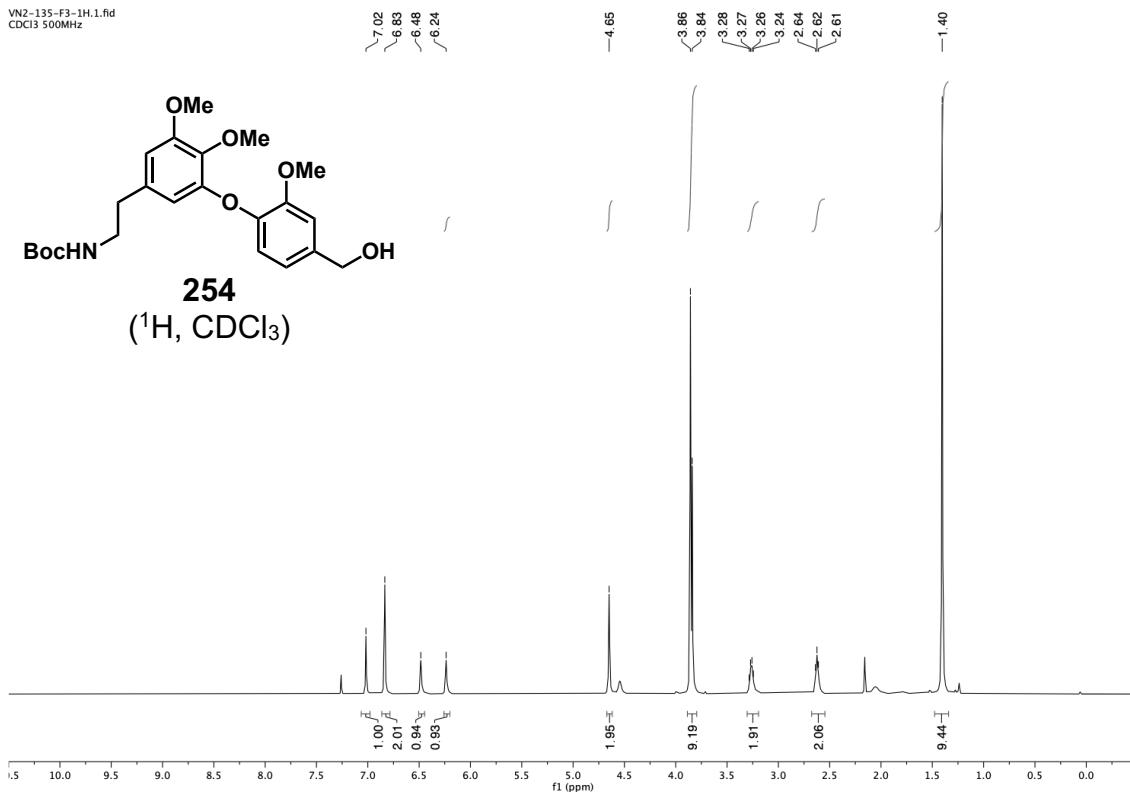


(<sup>1</sup>H, CDCl<sub>3</sub>)





VN2-135-F3-1H.1.fid  
CDCl3 500MHz



VN2-135-F3-13C.2.fid  
400 MHz CDCl<sub>3</sub>

155.95  
153.76  
150.90  
150.67  
145.21  
138.37  
137.23  
134.68

119.50  
111.65  
111.49  
107.76

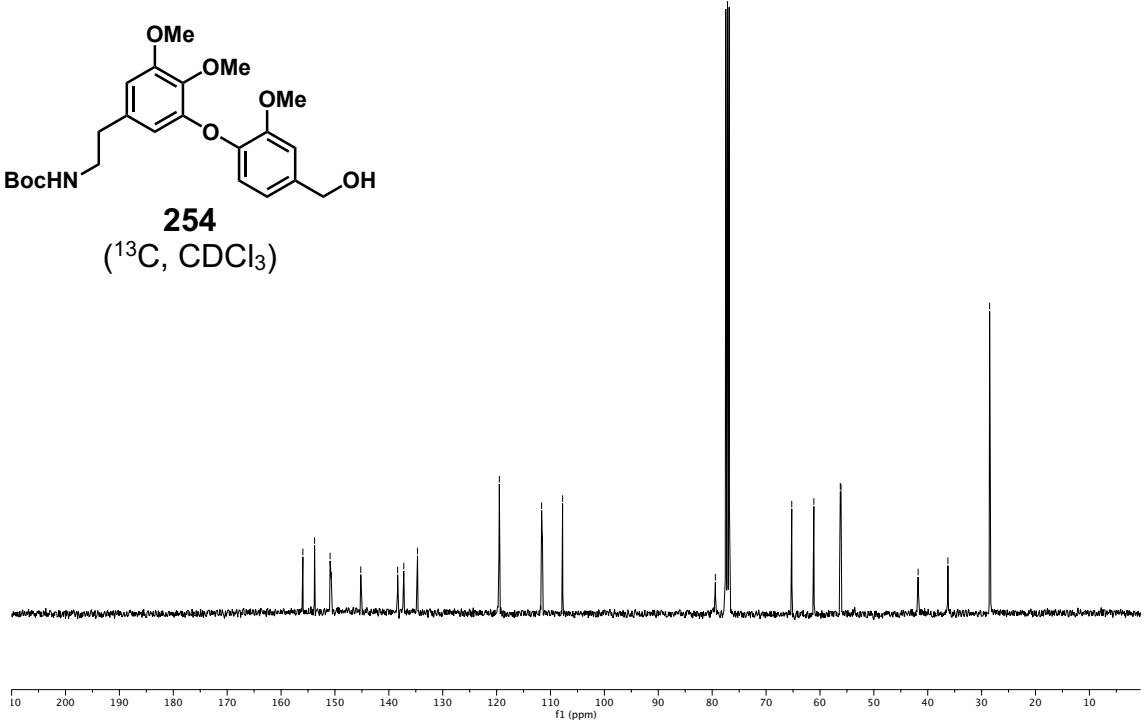
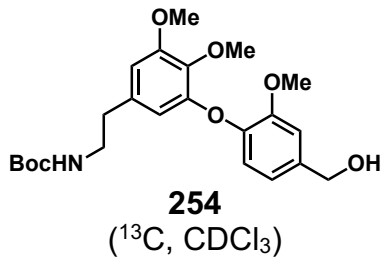
79.41

65.23  
61.13  
56.23  
56.09

41.79

36.26

28.51



VN2-150-CR01H.3.fid  
400 MHz CDCl<sub>3</sub>

7.50  
7.35  
7.32  
6.81  
6.78  
6.61  
6.48

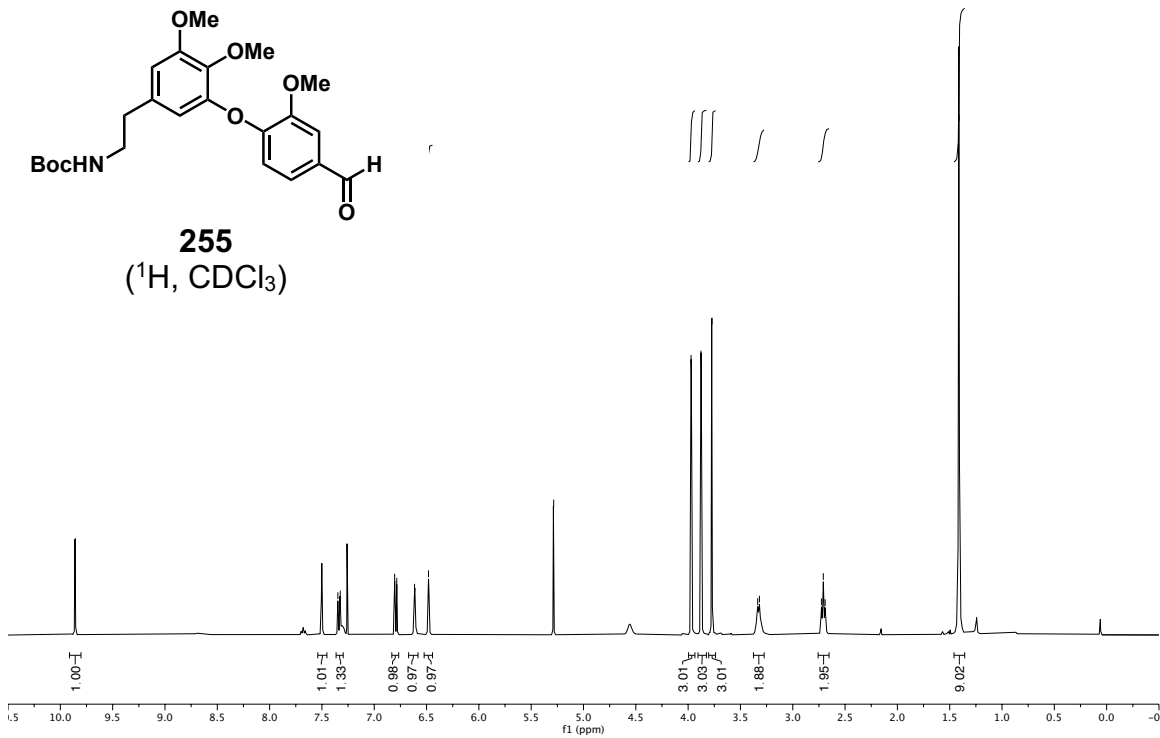
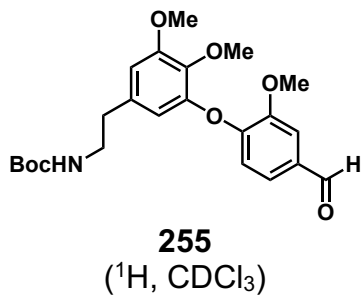
5.28

3.97  
3.88  
3.77

3.34  
3.32

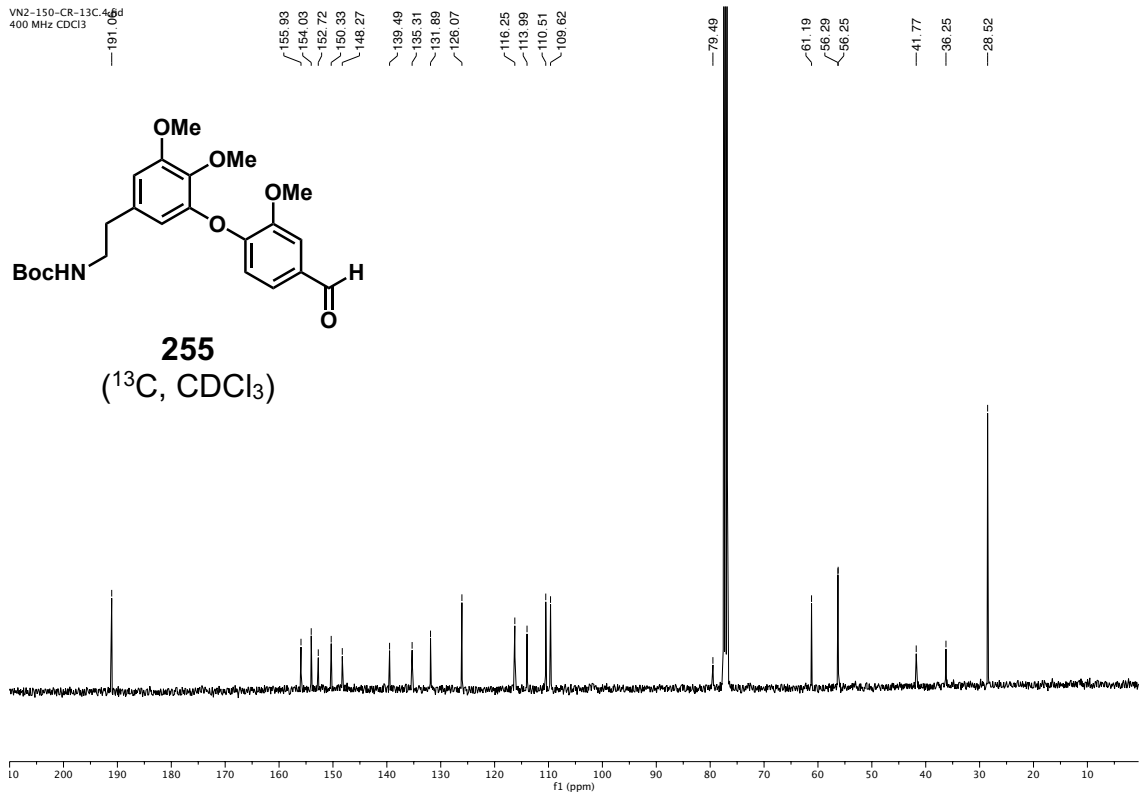
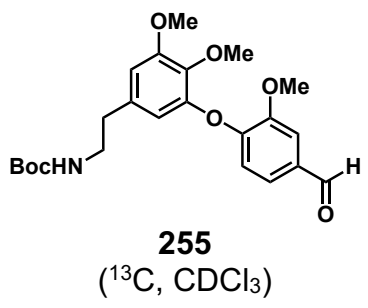
2.73  
2.71  
2.69

1.41



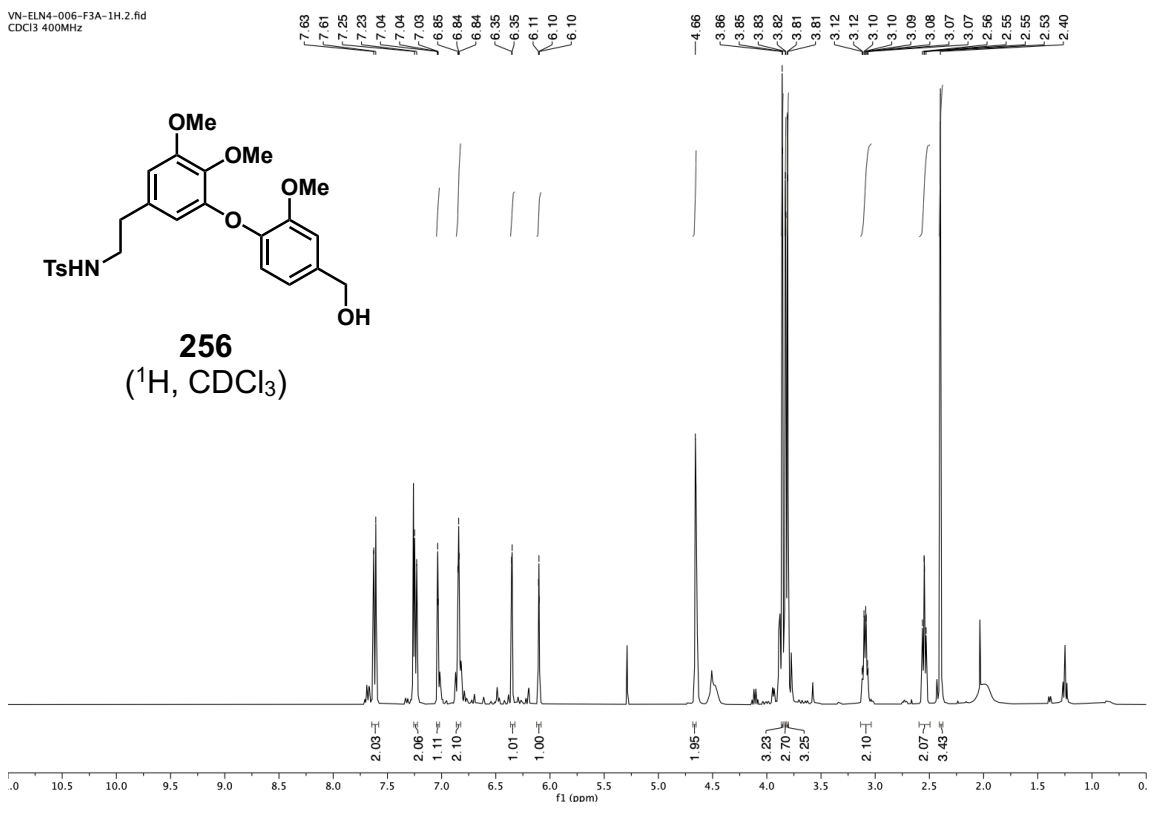
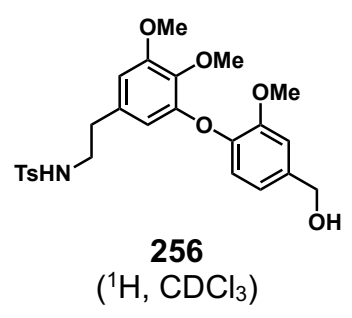
VN2-150-CR-13C-4.fid  
400 MHz CDCl<sub>3</sub>

155.93  
154.03  
152.72  
150.33  
148.27  
139.49  
135.31  
131.89  
126.07  
116.25  
113.99  
110.51  
109.62

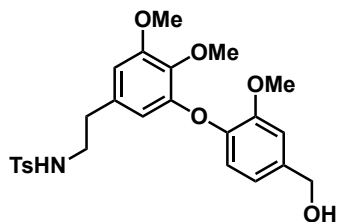


VN-ELN4-006-F3A-1H.2.fid  
CDCl<sub>3</sub> 400MHz

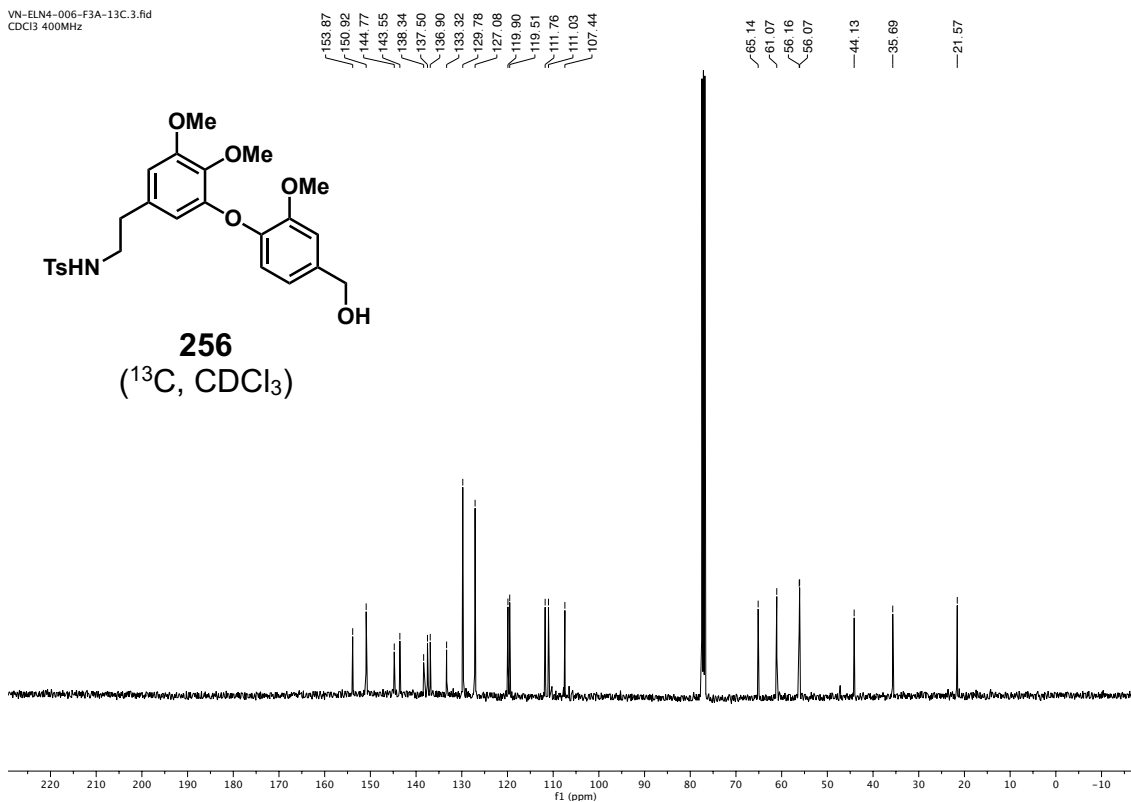
7.63  
7.61  
7.26  
7.23  
7.04  
7.03  
6.85  
6.84  
6.84  
6.35  
6.35  
6.11  
6.10  
6.10  
4.66  
3.86  
3.85  
3.83  
3.82  
3.81  
3.12  
3.12  
3.10  
3.10  
3.09  
3.08  
3.07  
3.07  
2.96  
2.55  
2.55  
2.53  
2.40



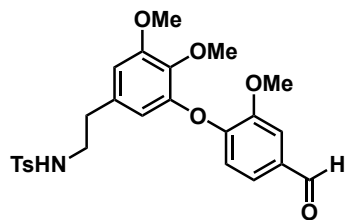
VN-ELN4-006-F3A-13C.3.fid  
CDCl<sub>3</sub> 400MHz



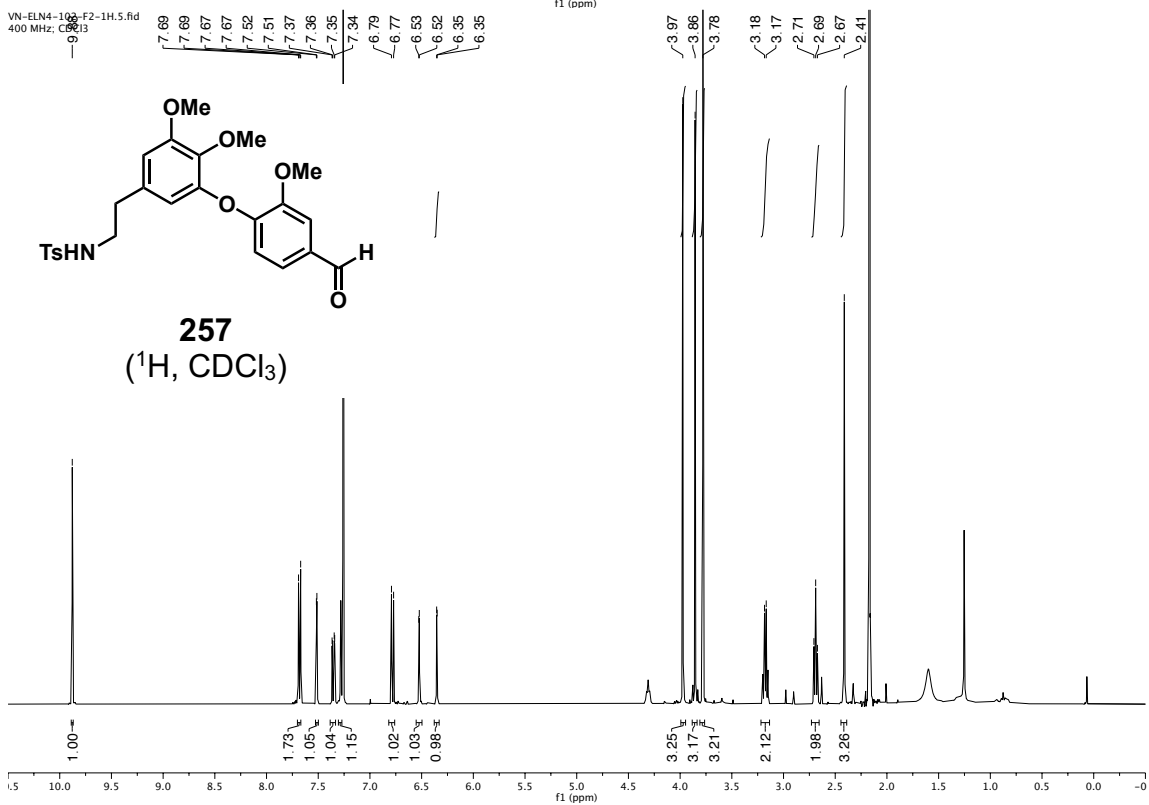
**256**  
(<sup>13</sup>C, CDCl<sub>3</sub>)

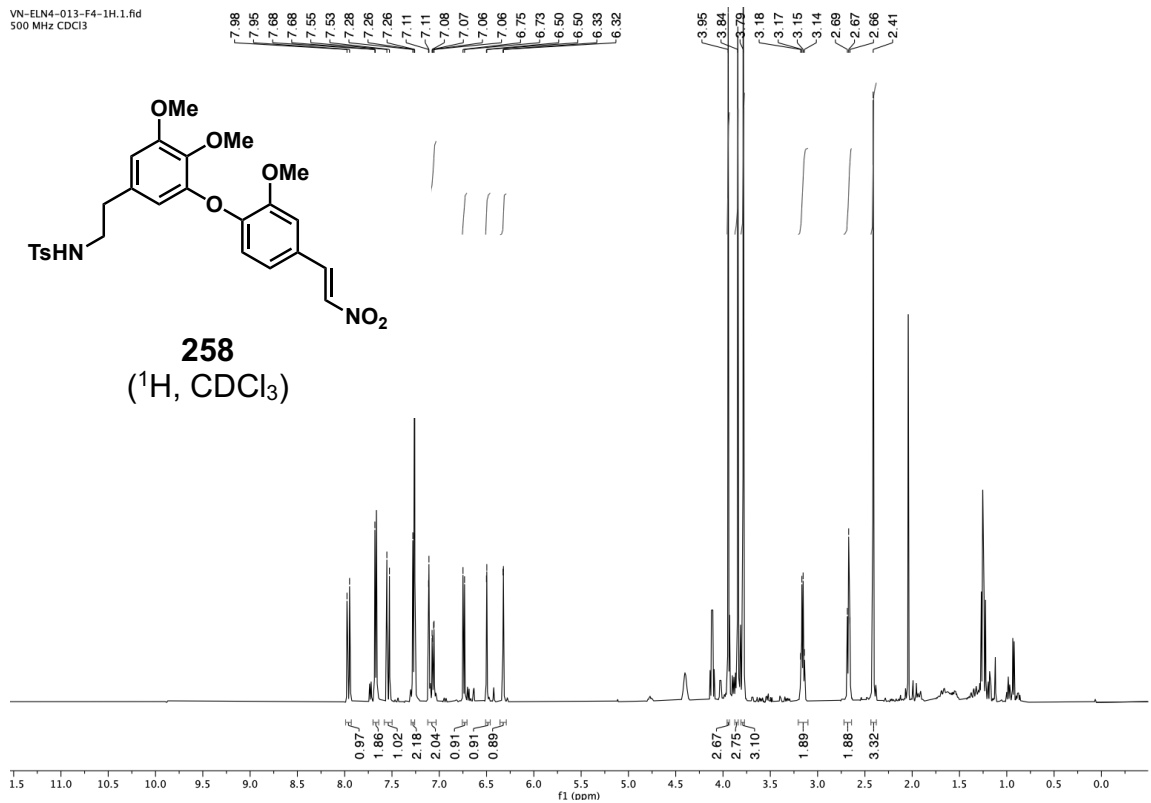
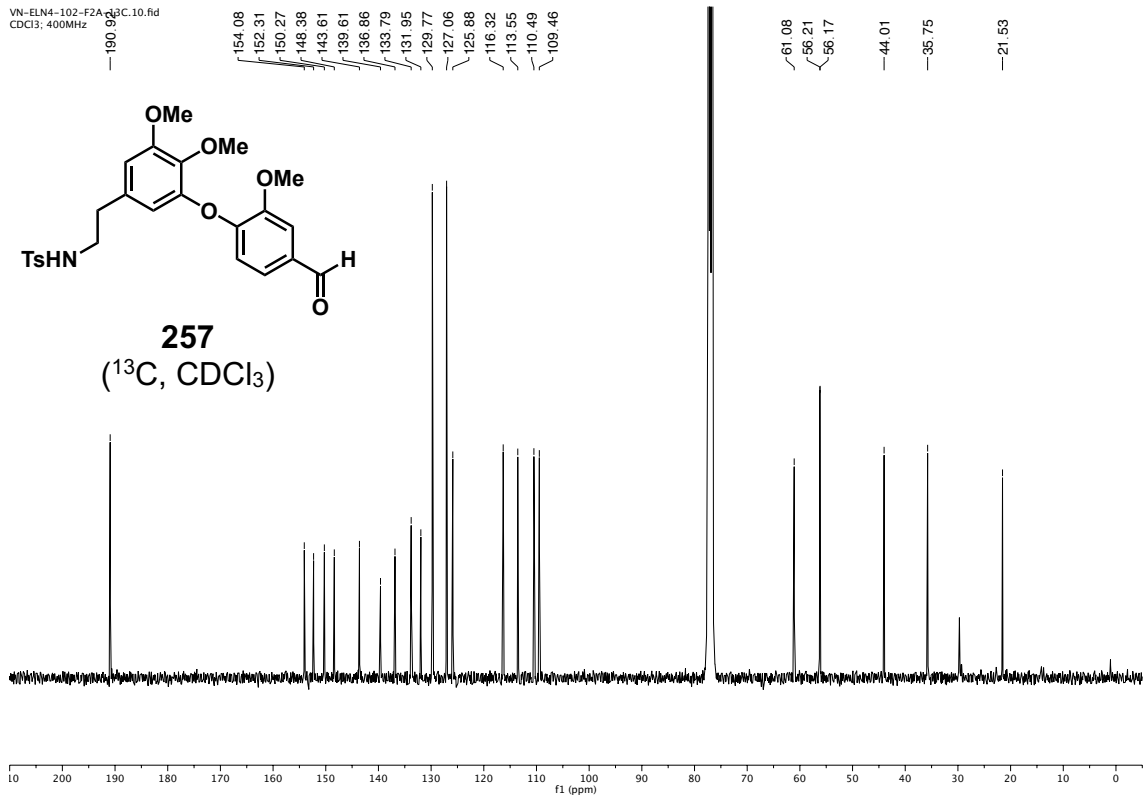


VN-ELN4-102-F2-1H.5.fid  
400 MHz; CDCl<sub>3</sub>

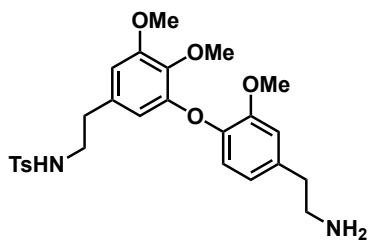


**257**  
(<sup>1</sup>H, CDCl<sub>3</sub>)

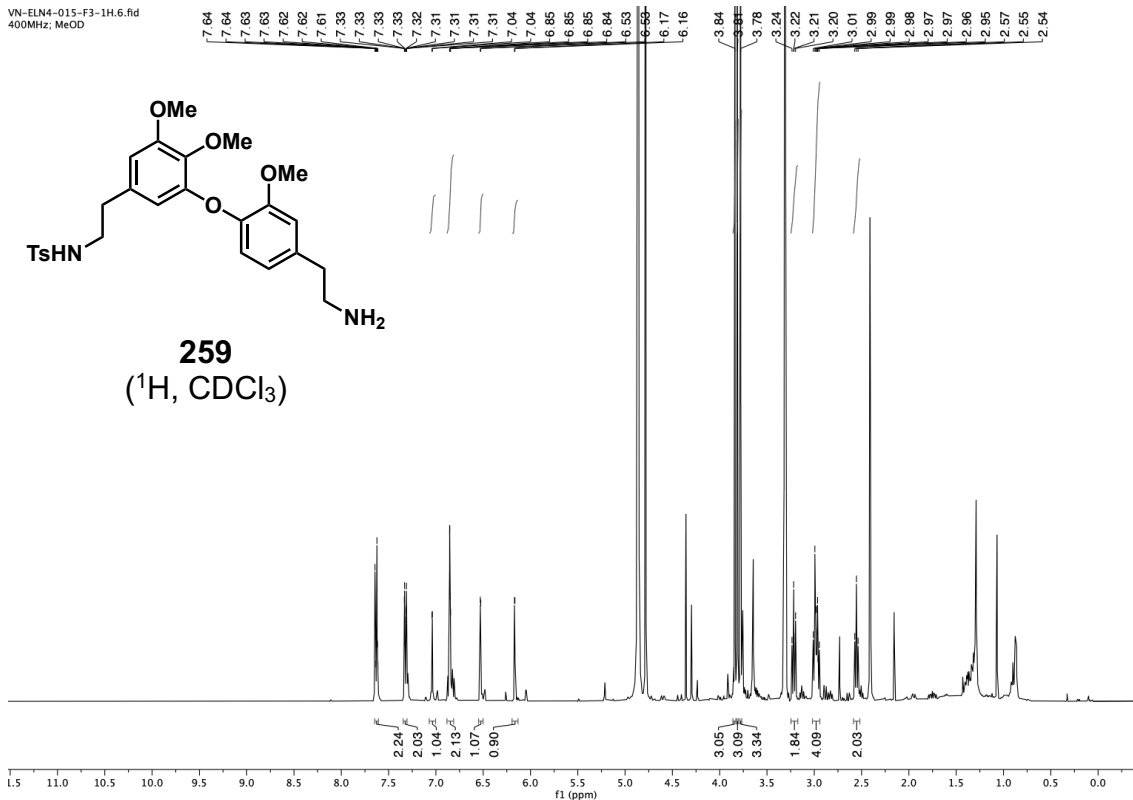




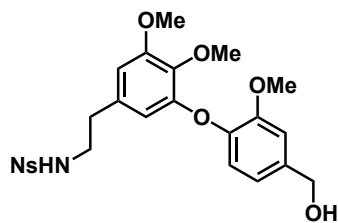
VN-ELN4-015-F3-1H.6.fid  
400MHz; MeOD



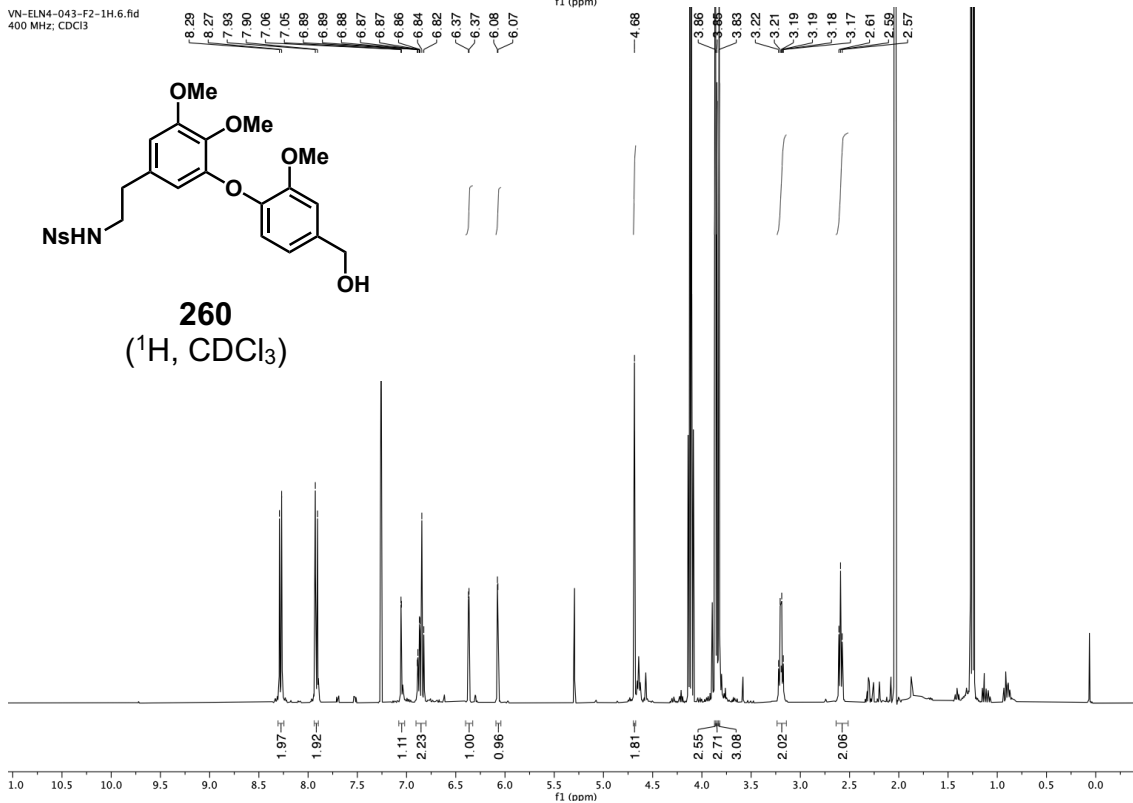
**259**  
(<sup>1</sup>H, CDCl<sub>3</sub>)



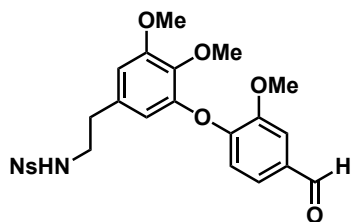
VN-ELN4-043-F2-1H.6.fid  
400 MHz; CDCl<sub>3</sub>



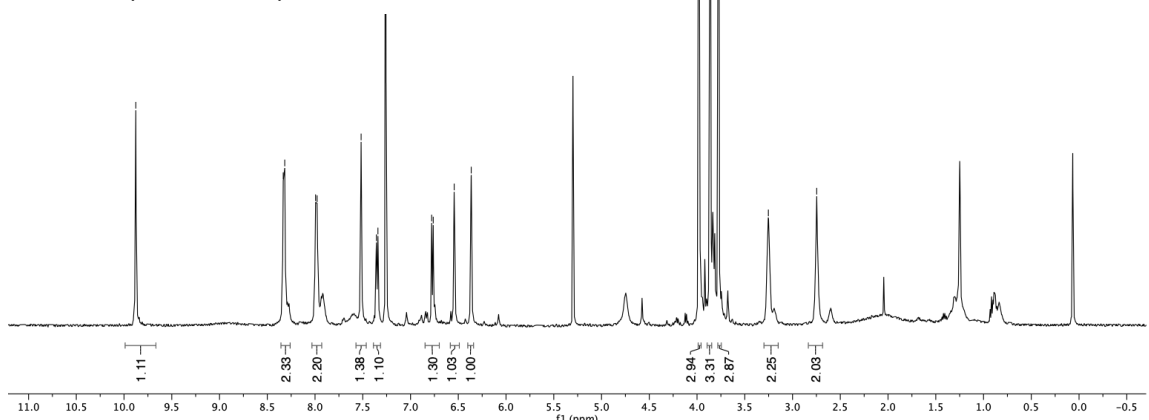
**260**  
(<sup>1</sup>H, CDCl<sub>3</sub>)



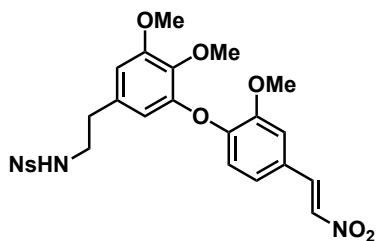
VN-ELN4-045-CR-1H.1.fid  
500 MHz; CDCl<sub>3</sub>



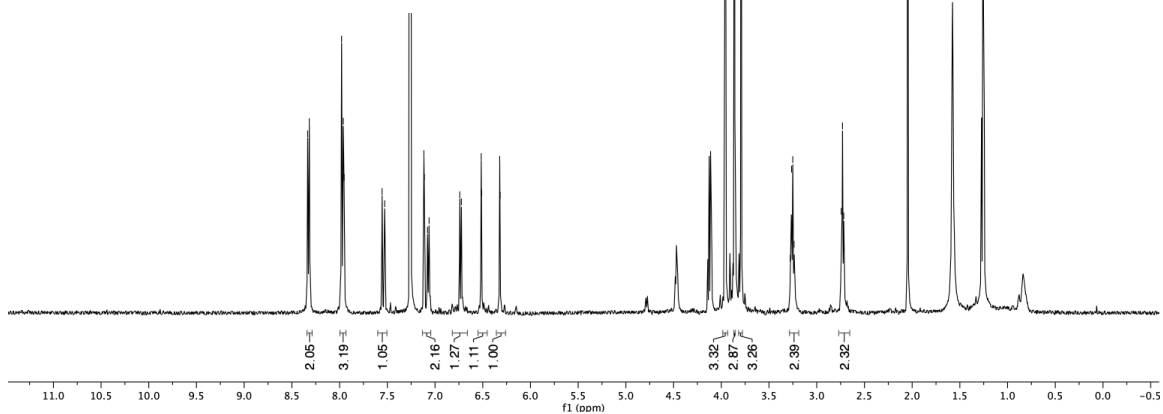
**261**  
(<sup>1</sup>H, CDCl<sub>3</sub>)



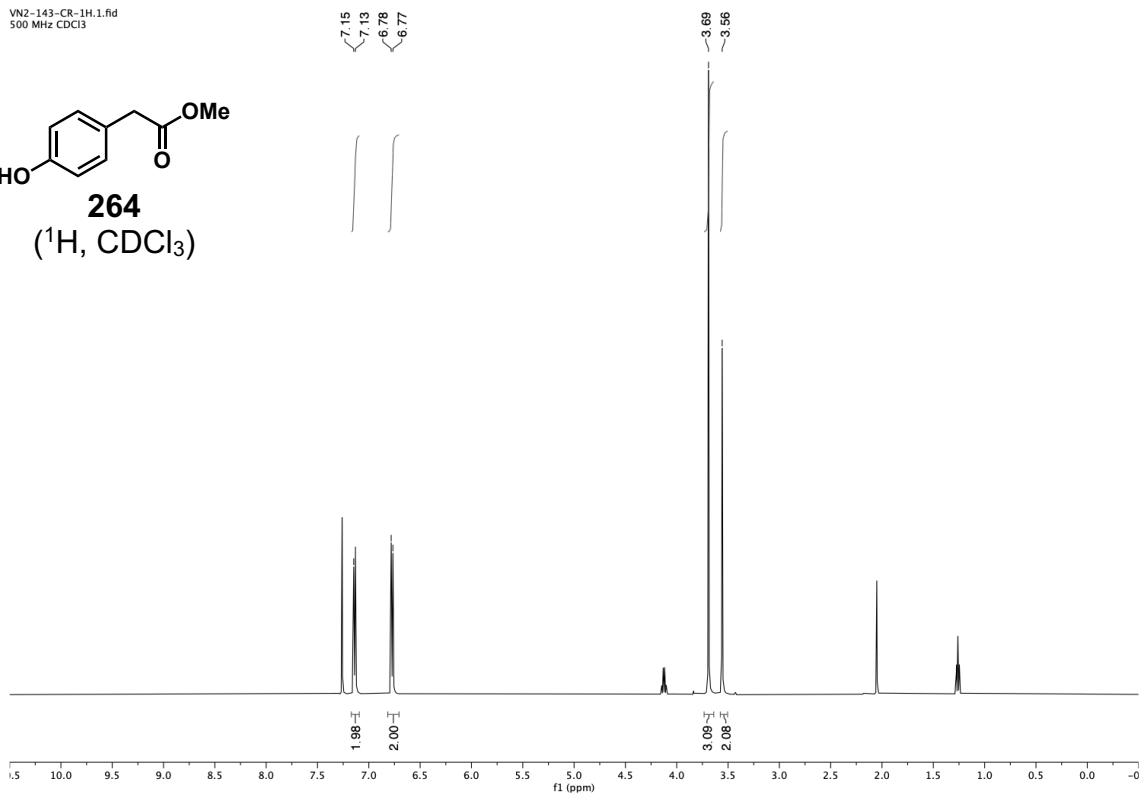
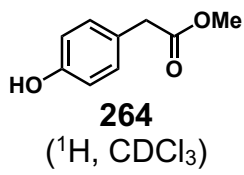
VN-ELN4-049-F1-1H.1.fid  
CDCl<sub>3</sub> 500MHz



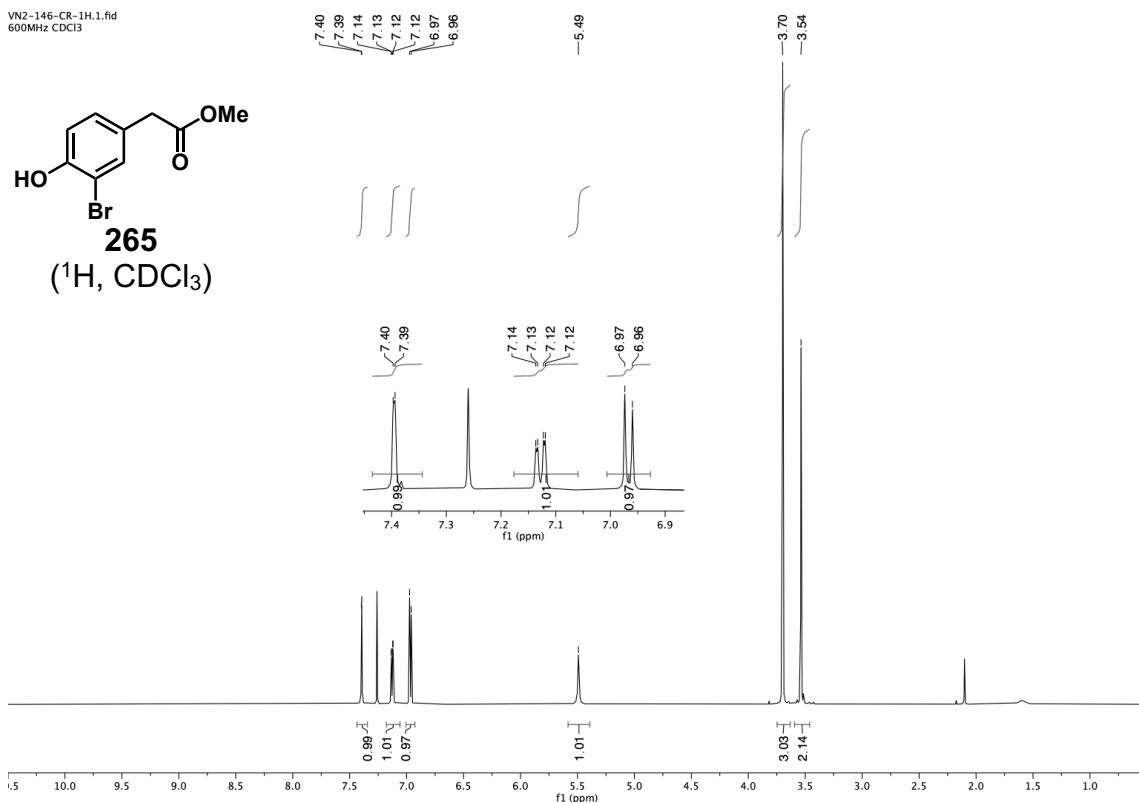
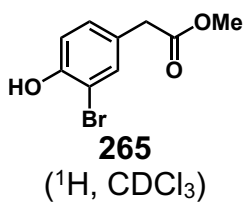
**262**  
(<sup>1</sup>H, CDCl<sub>3</sub>)



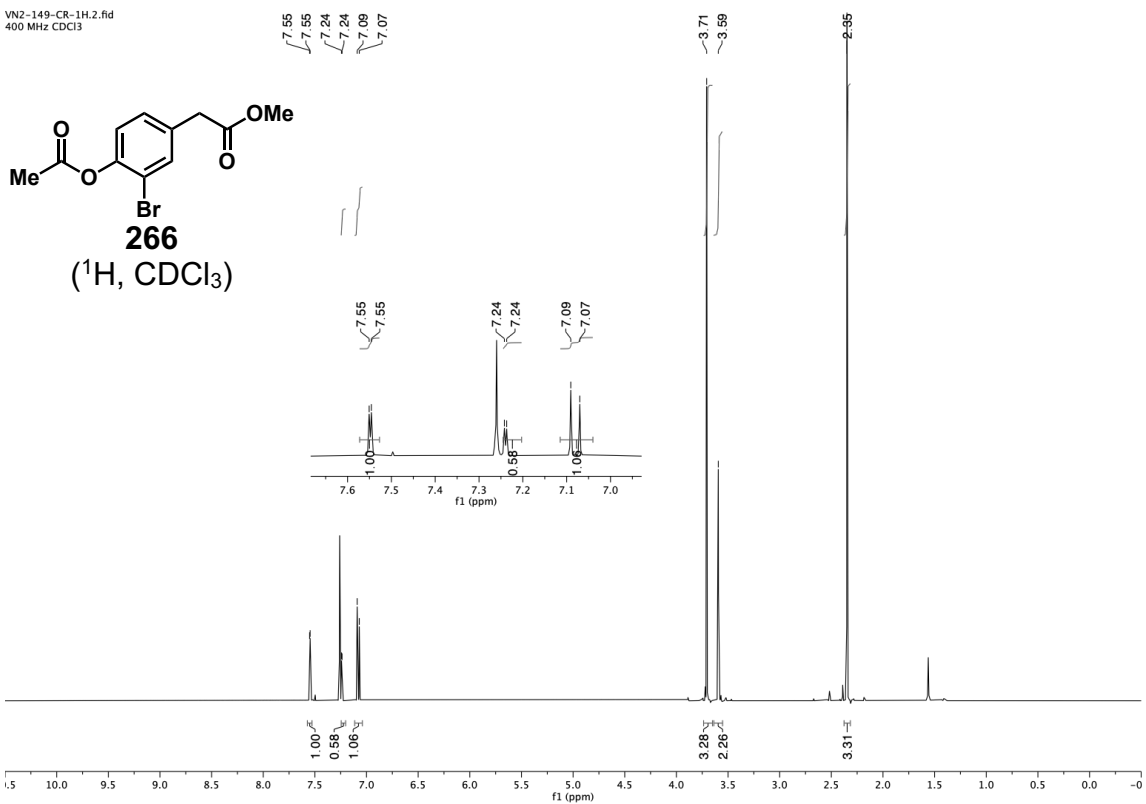
VN2-143-CR-1H.1.fid  
500 MHz CDCl<sub>3</sub>



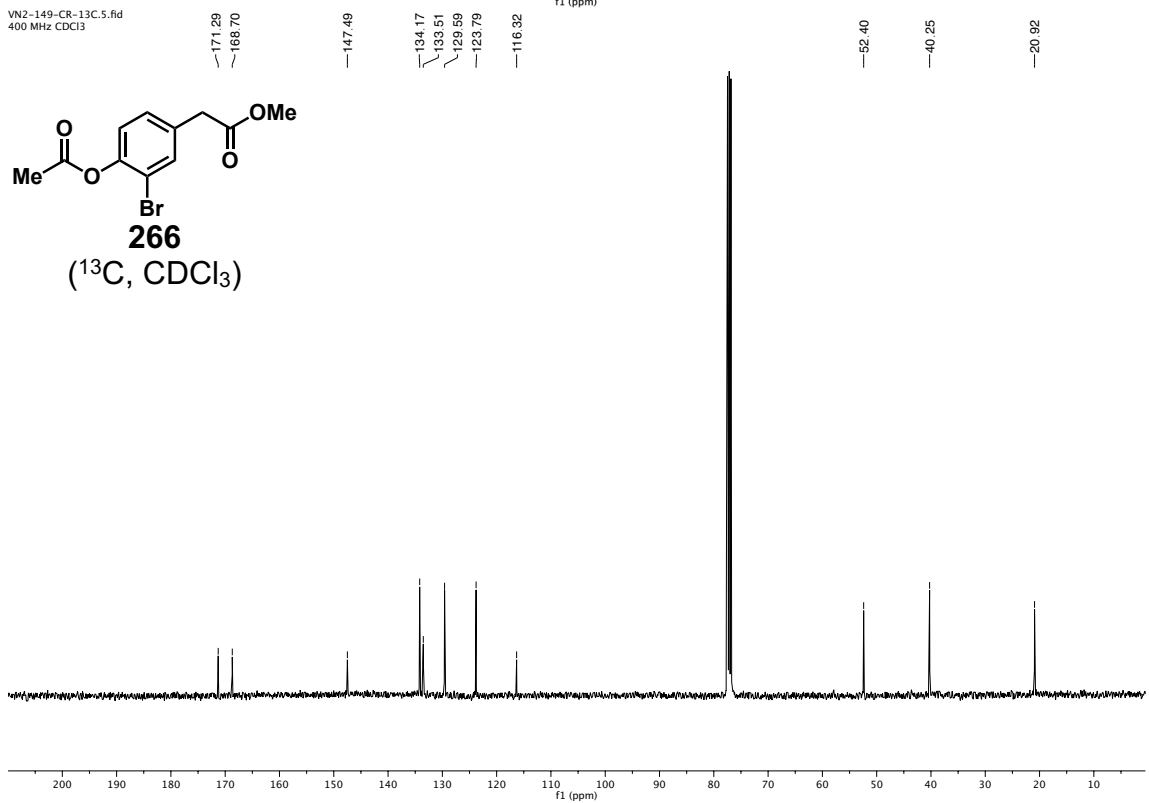
VN2-146-CR-1H.1.fid  
600MHz CDCl<sub>3</sub>



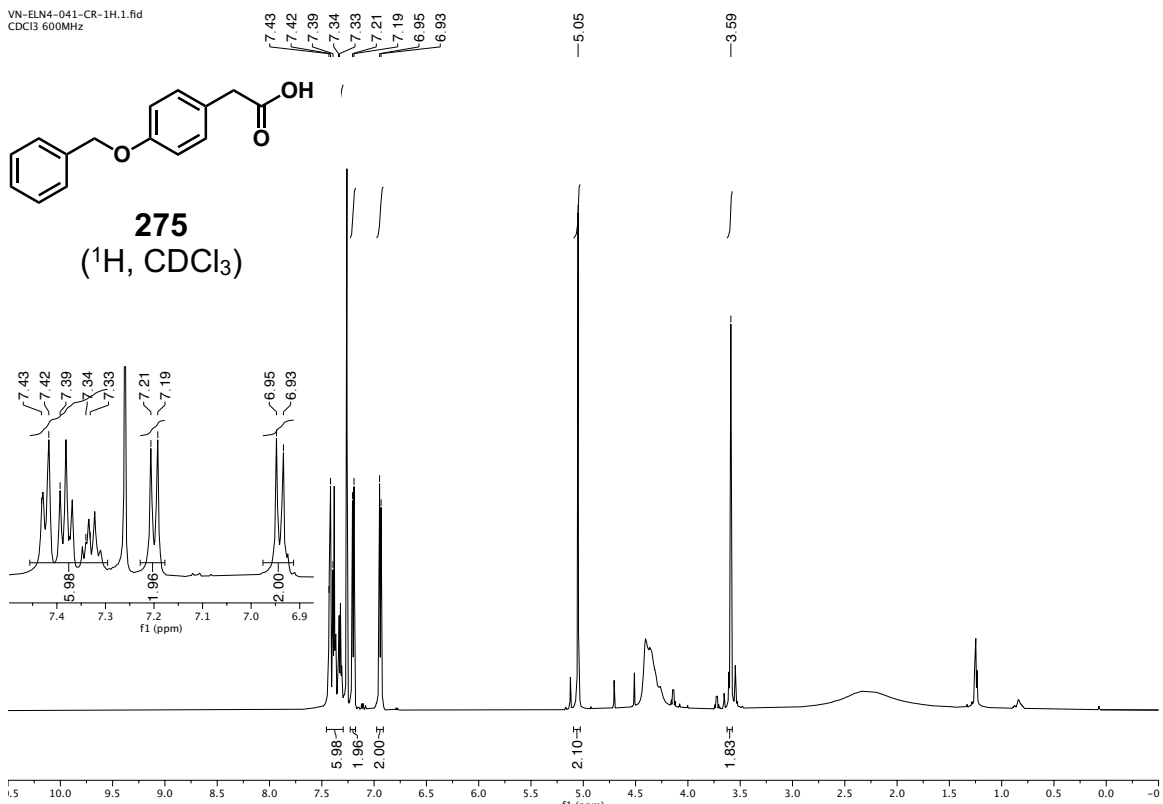
VN2-149-CR-1H.2.fid  
400 MHz CDCl<sub>3</sub>



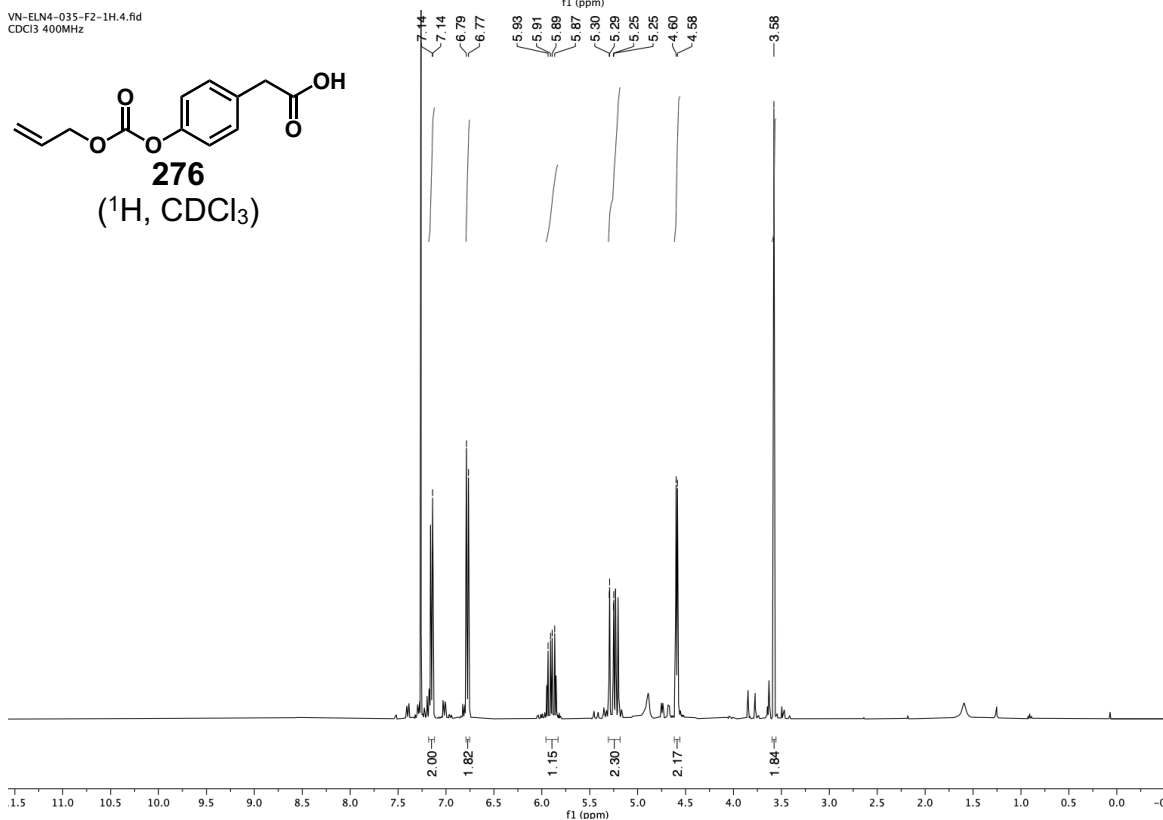
VN2-149-CR-13C.5.fid  
400 MHz CDCl<sub>3</sub>



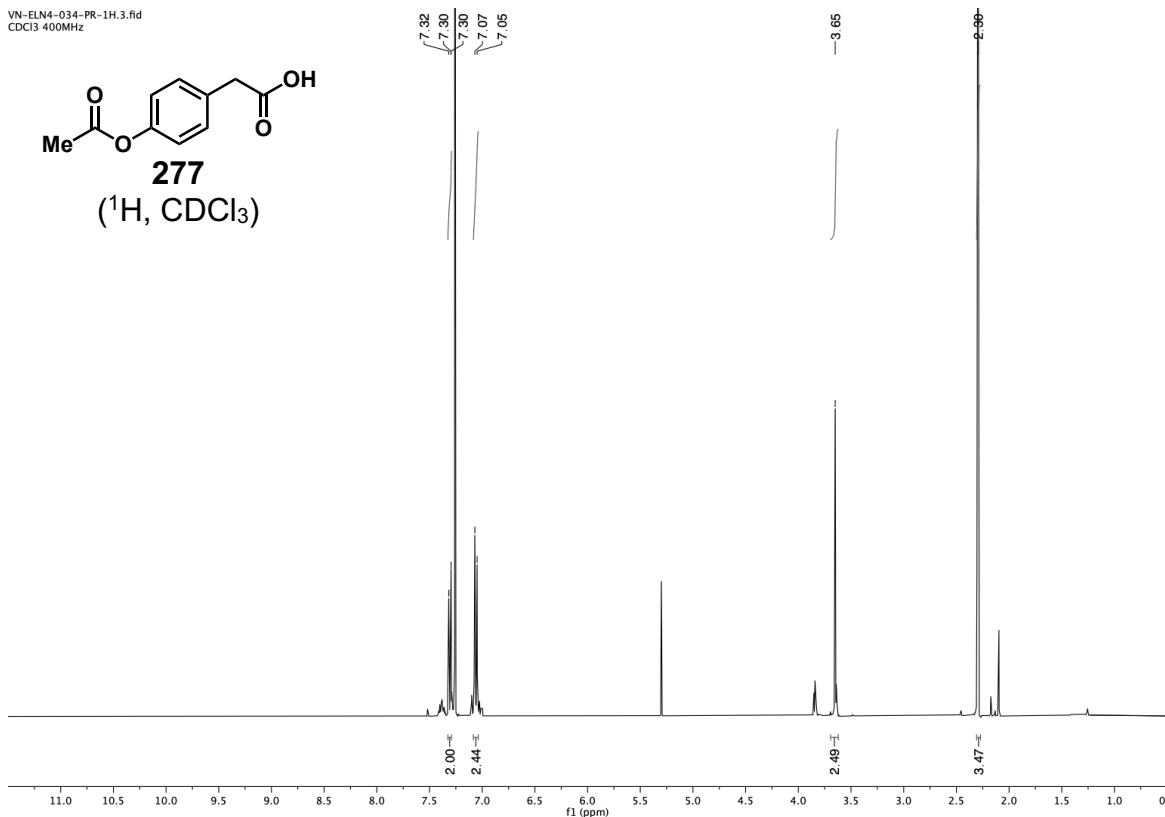
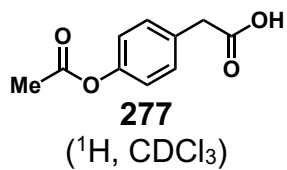
VN-ELN4-041-CR-1H.1.fid  
CDCl3 600MHz



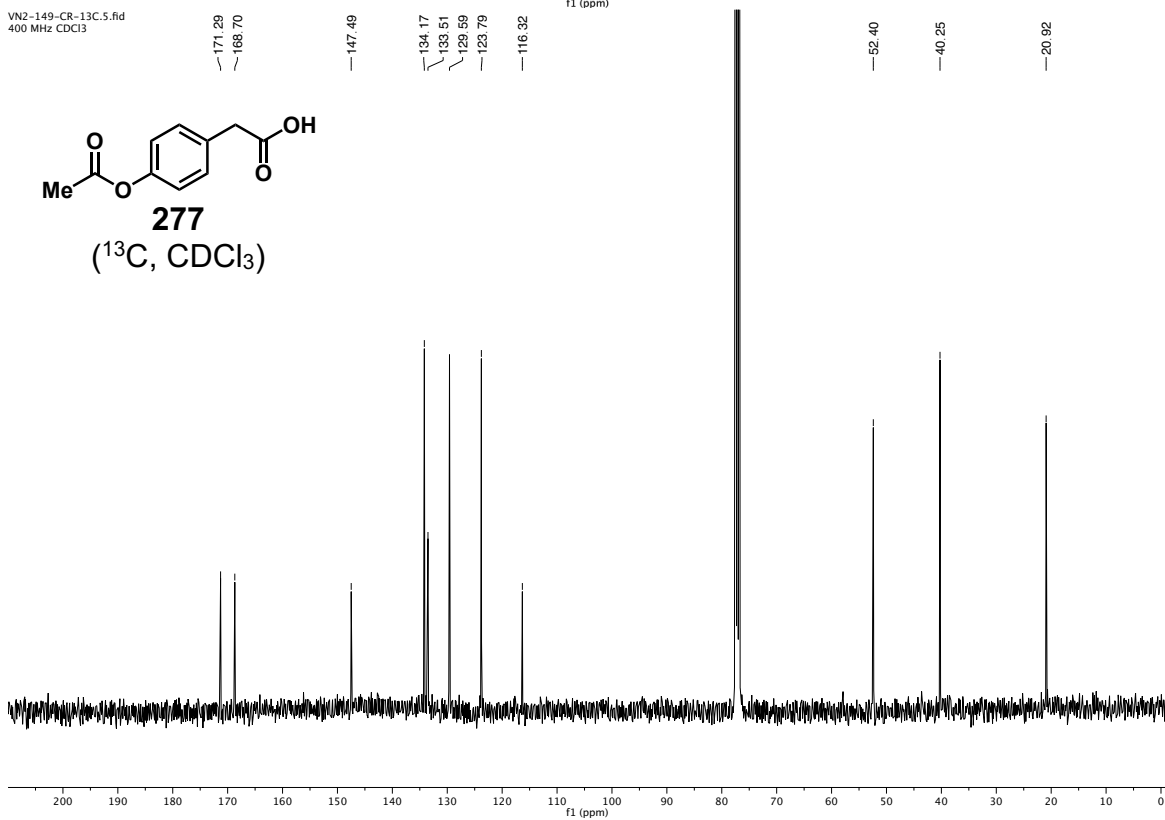
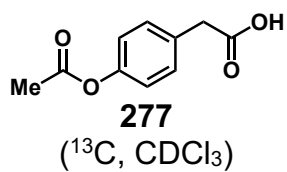
VN-ELN4-035-F2-1H.4.fid  
CDCl3 400MHz



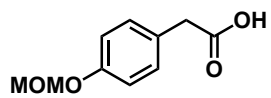
VN-ELN4-034-PR-1H.3.fid  
CDCl3 400MHz



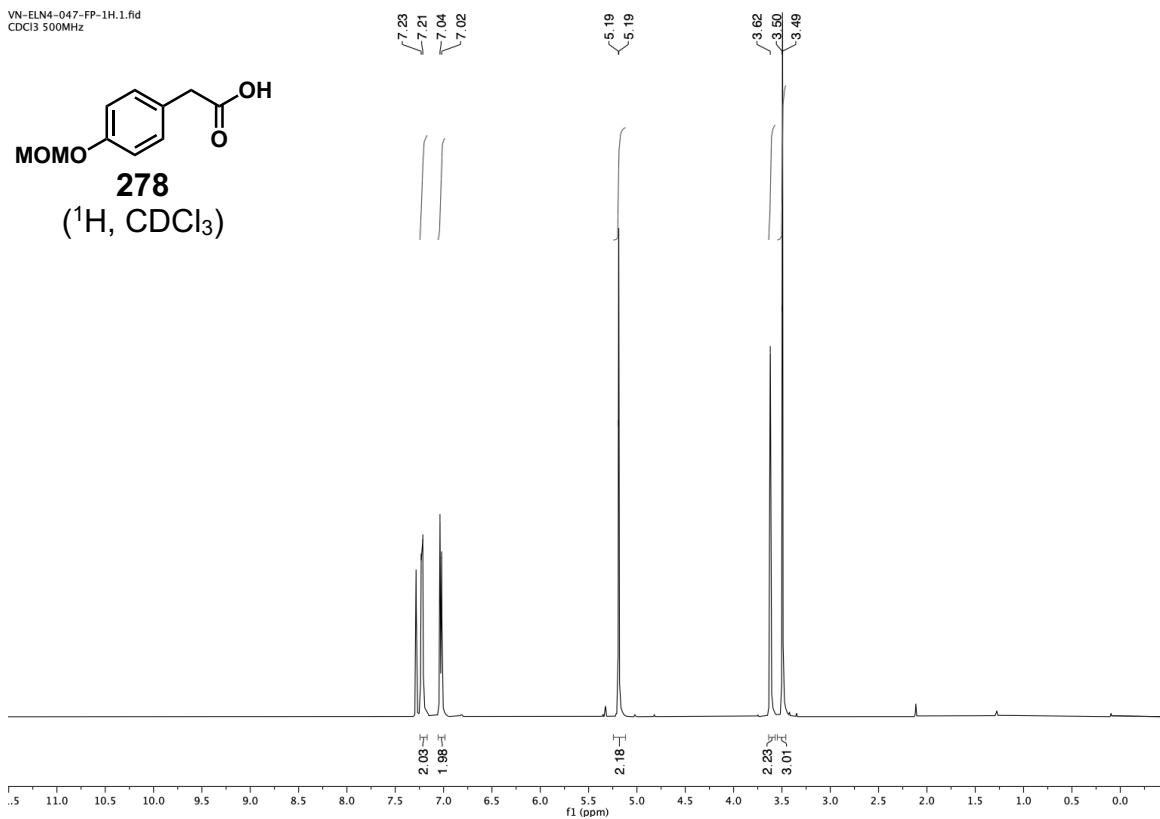
VN2-149-CR-13C.5.fid  
400 MHz CDCl3

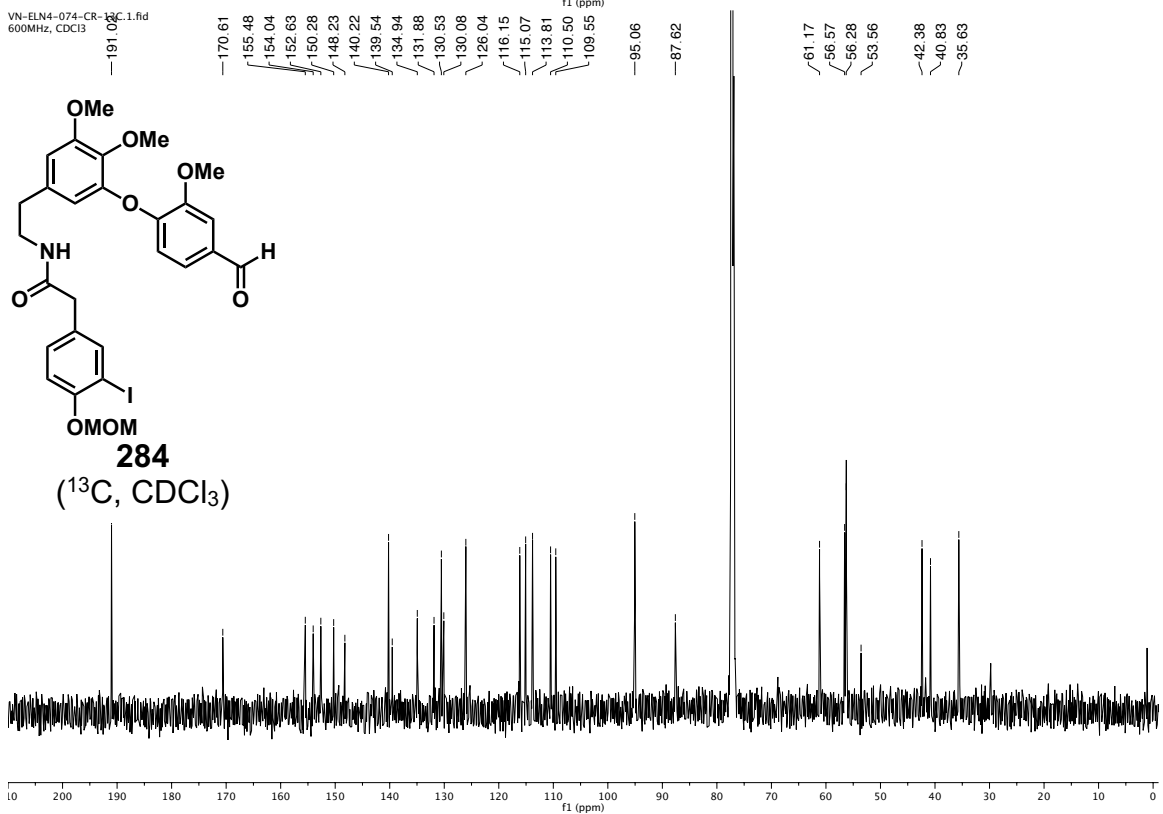
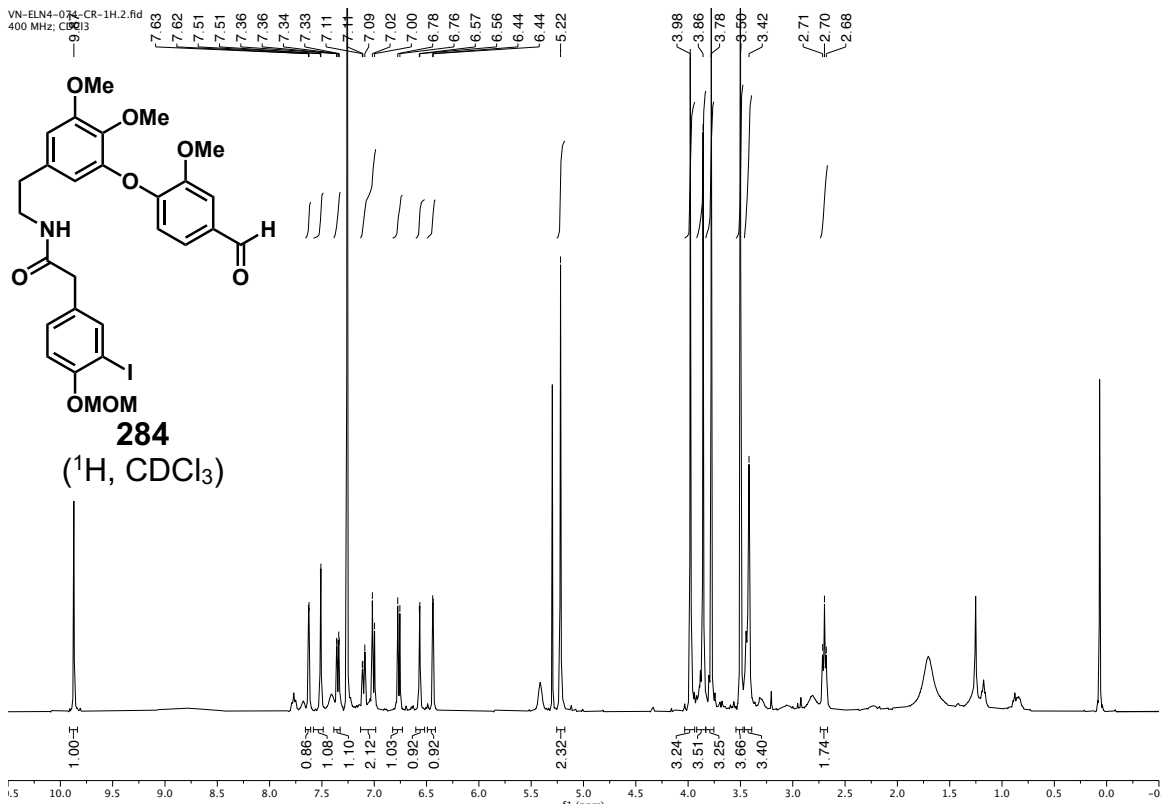


VN-ELN4-047-FP-1H.1.fid  
CDCl<sub>3</sub> 500MHz

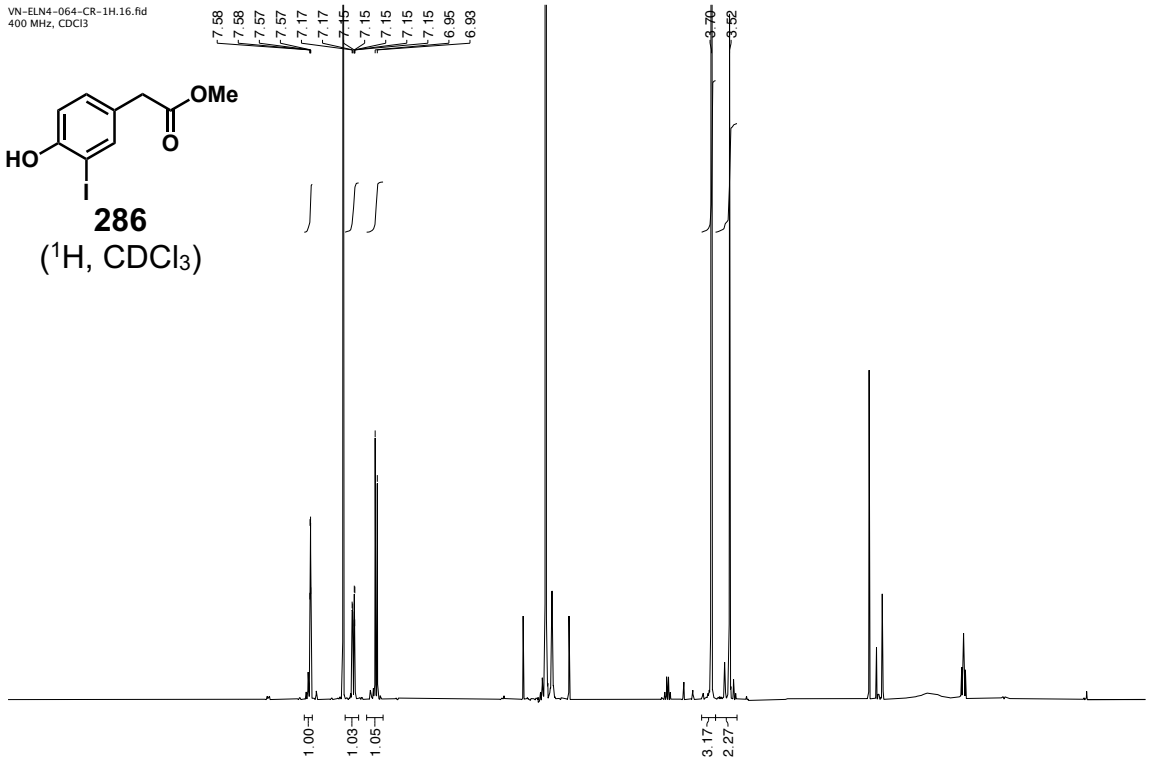


**278**  
(<sup>1</sup>H, CDCl<sub>3</sub>)

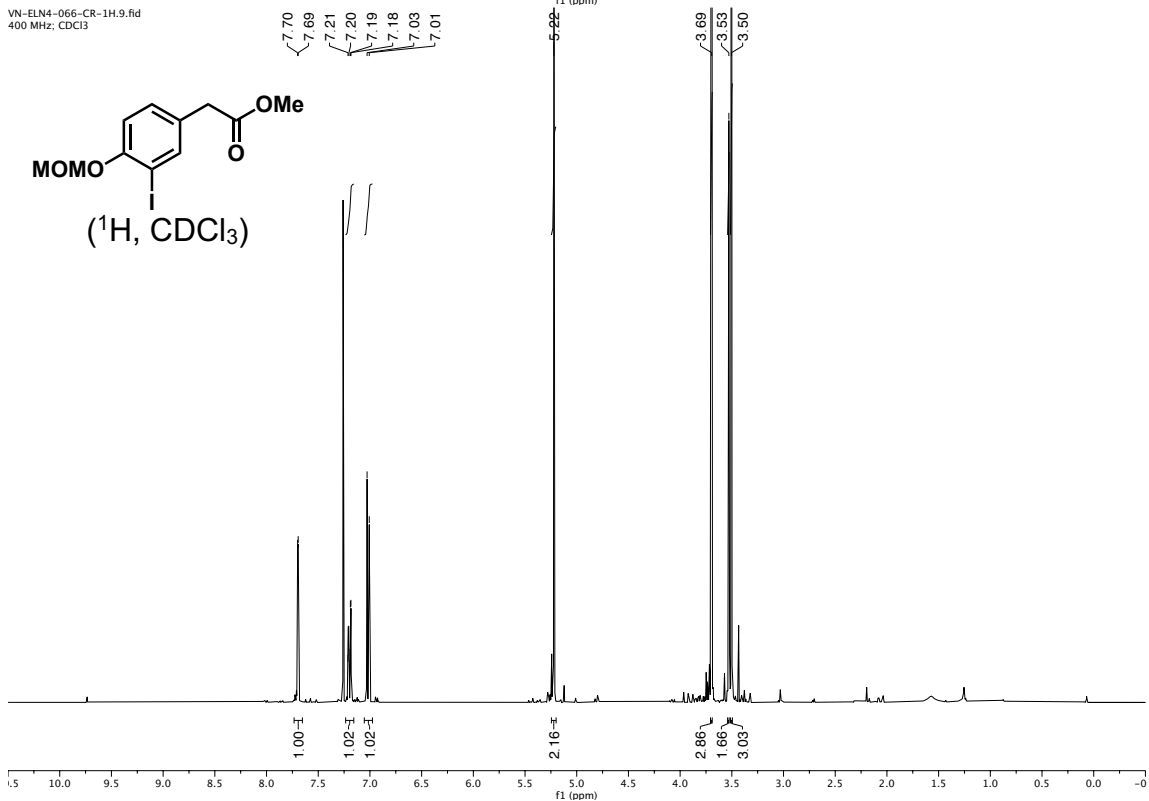




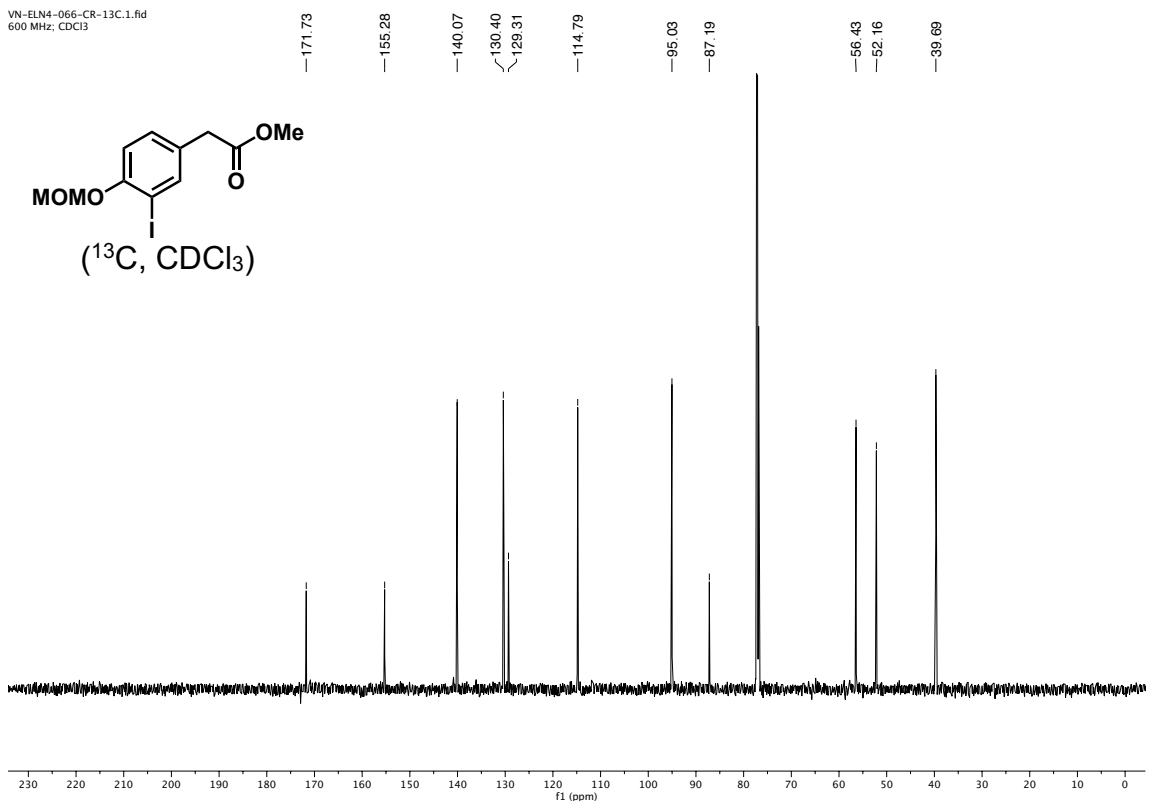
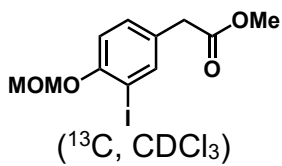
VN-ELN4-064-CR-1H.16.fid  
400 MHz, CDCl<sub>3</sub>



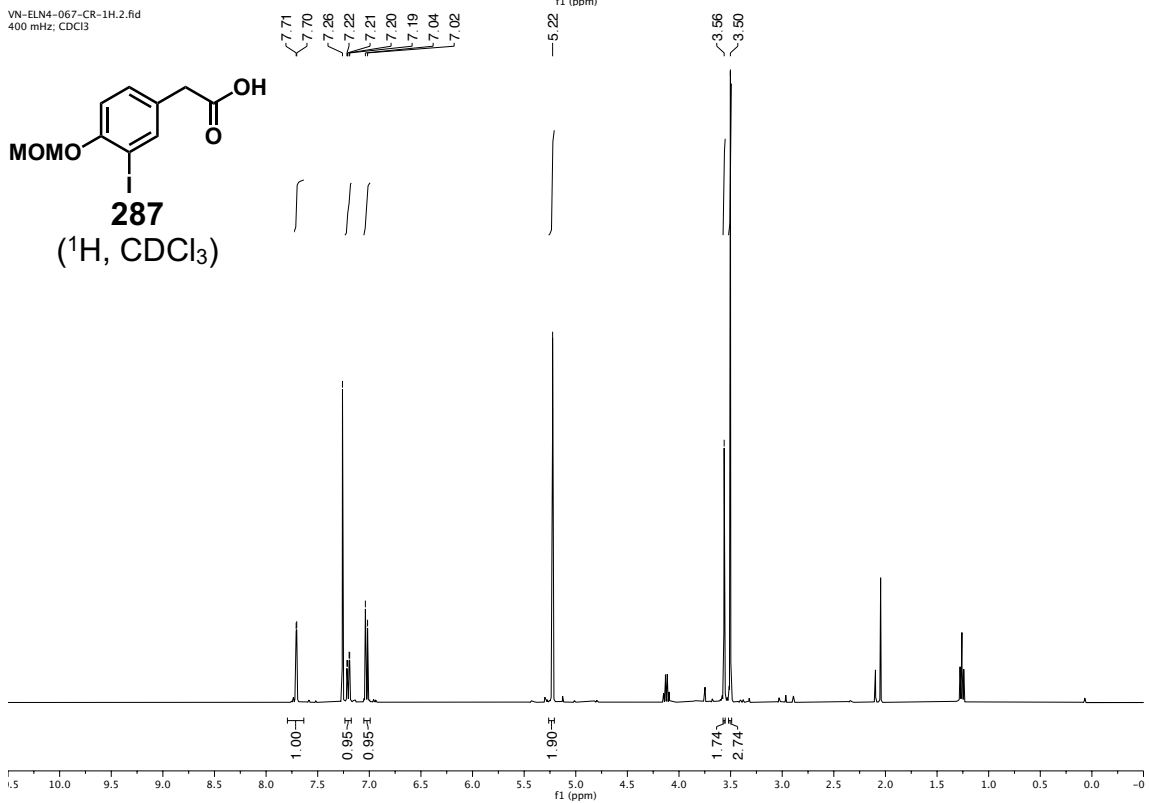
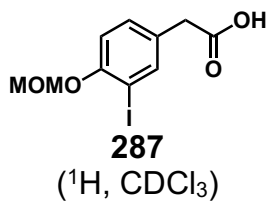
VN-ELN4-066-CR-1H.9.fid  
400 MHz, CDCl<sub>3</sub>



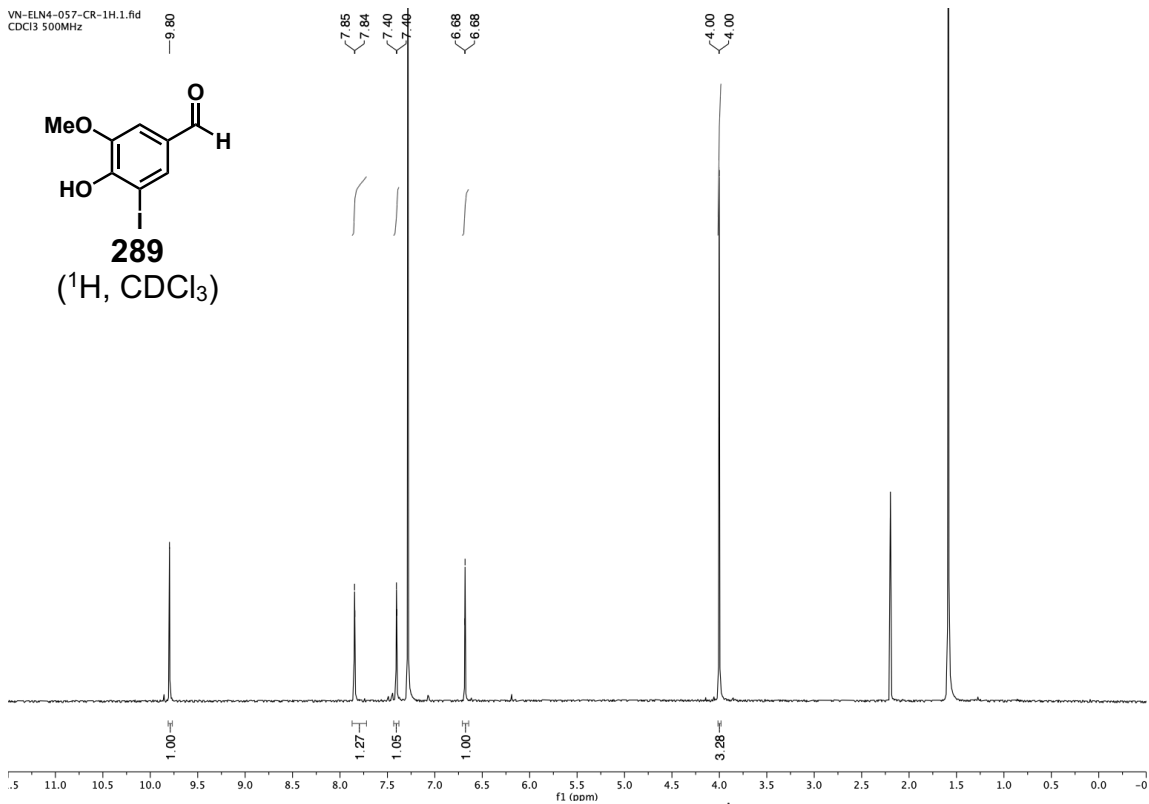
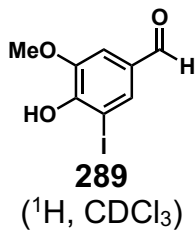
VN-ELN4-066-CR-13C.1.fid  
600 MHz; CDCl<sub>3</sub>



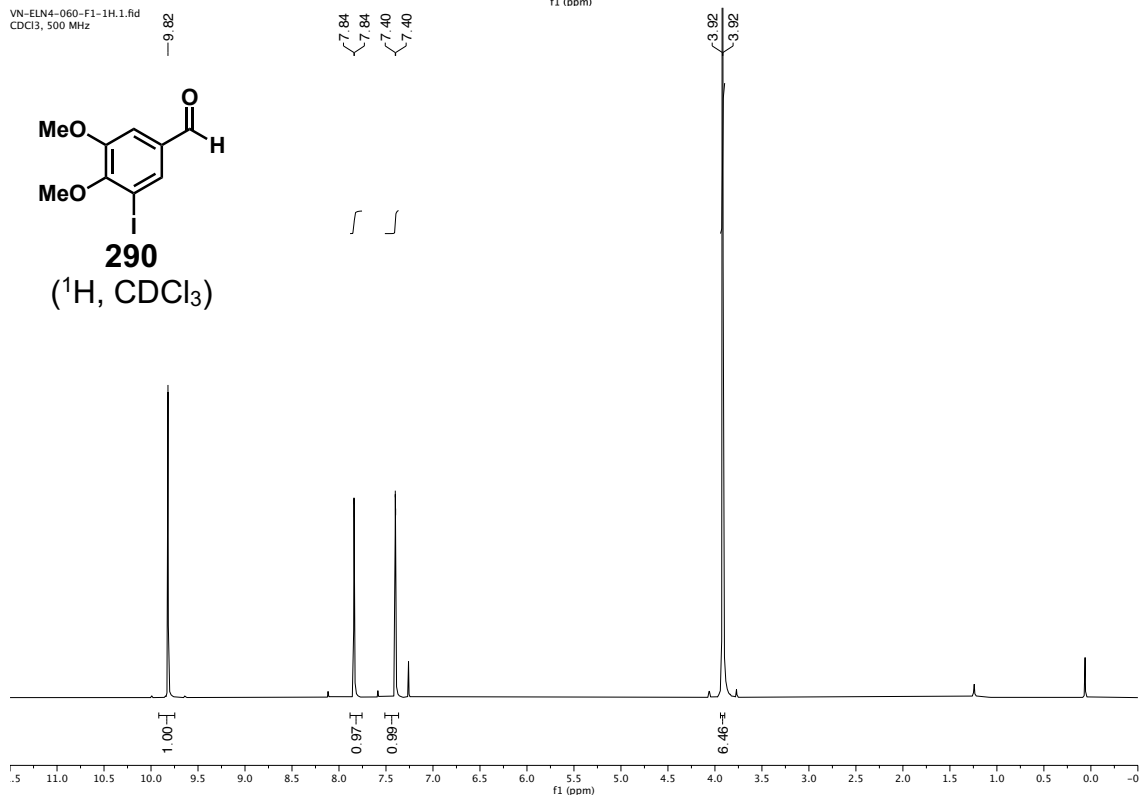
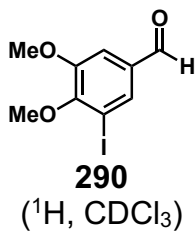
VN-ELN4-067-CR-1H.2.fid  
400 MHz; CDCl<sub>3</sub>



VN-ELN4-057-CR-1H.1.fid  
CDCl<sub>3</sub> 500MHz



VN-ELN4-060-F1-1H.1.fid  
CDCl<sub>3</sub>, 500 MHz

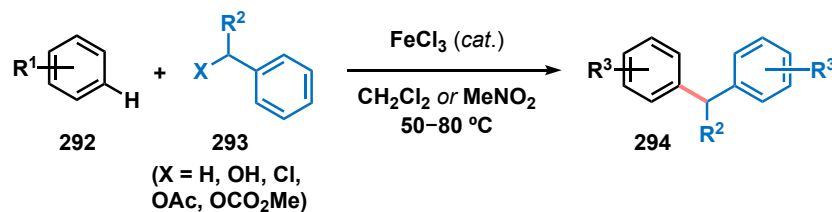


### 3 Chapter Three: Dual Brønsted/Lewis Acid Catalysis for Site-Selective Friedel–Crafts Alkylation of Phenols

#### 3.1 Introduction

##### 3.1.1 Friedel–Crafts Alkylation

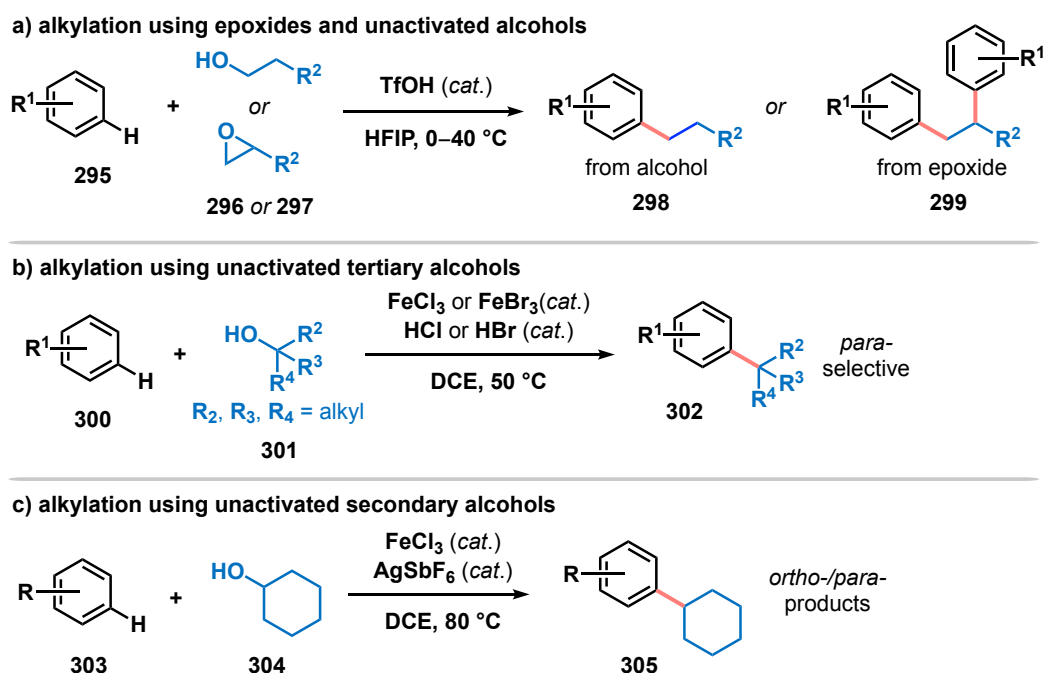
The Friedel–Crafts alkylation provides an intuitive, powerful bond disconnection for C(sp<sup>2</sup>)–C(sp<sup>3</sup>) bond retrosynthesis, and have found importance in the pharmaceutical and fragrance industries.<sup>1–3</sup> The ACS Green Chemistry Institute<sup>®</sup> Pharmaceutical Roundtable has recognized Friedel–Crafts reactions on unactivated substrates and the direct substitution of alcohols as selected synthetic priorities.<sup>4,5</sup> Since then, greener catalytic Friedel–Crafts alkylations using benzylic, propargylic, and allylic alcohols have been advanced to replace some relatively hazardous alkyl halides.<sup>6–10</sup> For example, Iovel *et al.* reported primary and secondary benzylic halides, acetates, and alcohols (**293**) coupling with arenes (**292**) under iron catalysis (Scheme 72).<sup>11</sup>



**Scheme 72.** Iovel's Fe-catalyzed arylation of benzyl alcohols and benzyl carboxylates

Advancing synthetic methodologies that employ non-benzylic, non-propargylic, and non-allylic alcohols in direct aromatic alkylations would complement modern cross-coupling approaches in constructing C(sp<sup>2</sup>)–C(sp<sup>3</sup>) bonds while starting from minimally prefunctionalized reaction precursors. The Moran group demonstrated that the use of trifluoromethanesulfonic acid (TfOH) in hexafluoroisopropanol (HFIP) solvent promotes

a Brønsted acid-assisted Brønsted acid catalysis strategy for arylating a range of alcohols (**296**) and epoxides (**297**, Scheme 73a).<sup>12</sup> Our lab recently reported conditions for setting quaternary carbon centers in para-selective Friedel–Crafts reactions using unactivated tertiary alcohols (**301**) catalyzed by combinations of  $\text{FeX}_3/\text{HX}$  (Scheme 73b),<sup>13</sup> as well as the synthesis of diarylmethane derivatives using methanol as the alkylating agent.<sup>14</sup>



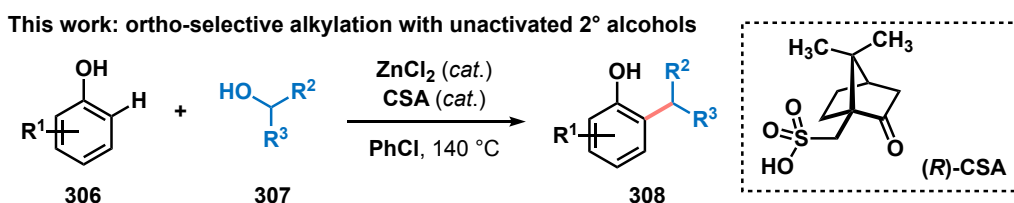
**Scheme 73.** Friedel–Crafts reactions via direct substitution of unactivated alcohols

Aside from a few isolated examples with cycloalkanols,<sup>15–17</sup> the Cook group found that a mixture of  $\text{FeCl}_3/\text{AgSbF}_6$  was effective at arylating unactivated secondary alcohols (**304**), albeit lacking site-selectivity (Scheme 73c).<sup>18</sup> The Newman group also recently reported a Suzuki–Miyaura approach to arylating unactivated tertiary alcohols.<sup>19</sup> Despite these advancements in directly transforming unactivated alcohols, many existing

methods still require excess reagents, costly precious metal additives, or the use of a fluorinated solvent.

### 3.2 Results and Discussion

In the pursuit of more sustainable carbon–carbon bond-forming reactions, we introduce a site-selective Friedel–Crafts alkylation of phenolic derivatives (**306**) with unactivated secondary alcohols (**307**) through dual  $\text{ZnCl}_2$  and camphorsulfonic acid (CSA) catalysis (Scheme 74). Previous research in our lab demonstrated the ability of Lewis acids to enhance the acidity of Brønsted acids.<sup>13</sup> Building on this finding, we hypothesized that this co-catalysis approach could be applied to Friedel–Crafts alkylations using unactivated secondary alcohols. This method offered several advantages over existing approaches, including the use of cost-effective and readily accessible reagents: chlorobenzene instead of HFIP solvent<sup>9,12,20</sup> and Zn/CSA instead of Fe/Ag as catalysts.<sup>18</sup> Note that this work was performed alongside Aaron Pan with the assistance of two undergraduate researchers: Lorraine Rangel and Charlene Fan. My primary contributions involved reaction condition optimization, expansion of the substrate scope, and subsequent analysis of the ortho-selective alkylation.

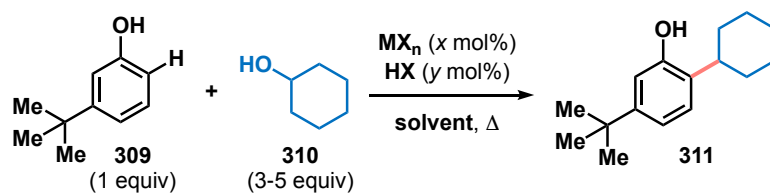


**Scheme 74.** Developed Brønsted/Lewis acid-catalyzed Friedel–Crafts alkylations

### 3.2.1 Optimization Studies

3-*tert*-Butylphenol (**309**) and cyclohexanol (**310**) were selected to test for reactivity since they are readily available and conversion to product could be conveniently quantified by NMR analysis (Table 4). Catalytic amounts of Fe(III) salts (2.5 mol%) were initially examined with stoichiometric quantities of HCl (2 equiv) at 140 °C. The desired alkylation product (**311**) was formed in 50–57% NMR yields (Entries 1–2). Of all the Lewis acid catalysts tested, including Zn(OAc)<sub>2</sub> and Fe(II) salts, ZnCl<sub>2</sub> performed the best, providing the product in 63% yield (Entry 3). Lowering the temperature from 140 °C to 120 °C was detrimental to yield (39%, Entry 4), and increasing the ZnCl<sub>2</sub> loading to 5 mol% enhanced product formation (71%, Entry 5). However, further increasing the amount of Zn-catalyst to 30 mol% did not improve the reaction outcome (Entry 6). CSA was found to be effective at supporting this transformation, albeit providing a lower yield even when cyclohexanol (**310**) was employed as the solvent (39%, Entry 7). Solid CSA was desirable because it addresses the concern of volatile HCl escaping from the reaction vessels at high temperature. Reducing the amount of alkylating agent in the reaction mixture from solvent quantities to 5 equiv improved the yield to 68% (Entry 8). The reactivity was maintained by reducing the amount of CSA from 2 equiv to 0.75 equiv, which resulted in an isolated 74% yield of **311** when using 3 equiv of alcohol **310**. However, reducing the amount of acid to 50 mol% reduced the NMR yield to 52%.

**Table 4.** Survey of conditions for direct Friedel–Crafts alkylation of phenolic **309** with alcohol **310**



Entry	$\text{MX}_n$	$x$	HX	$y$	Solvent	Temp (°C)	% Yield <sup>b</sup>
1	$\text{FeCl}_3$	2.5	HCl	200	PhCl	140	50
2	$\text{FeBr}_3$	2.5	HCl	200	PhCl	140	57
3	$\text{ZnCl}_2$	2.5	HCl	200	PhCl	140	63
4	$\text{ZnCl}_2$	2.5	HCl	200	PhCl	120	39
5	$\text{ZnCl}_2$	5	HCl	200	PhCl	140	71
6	$\text{ZnCl}_2$	30	HCl	200	PhCl	140	61
7	$\text{ZnCl}_2$	5	CSA	200	CyOH	140	39
8	$\text{ZnCl}_2$	5	CSA	200	PhCl	140	68
9	$\text{ZnCl}_2$	5	CSA	75	PhCl	140	(74) <sup>c,d</sup>
10	$\text{ZnCl}_2$	5	CSA	50	PhCl	140	52

<sup>a</sup>Conditions: reactions performed on 0.1 mmol scale, phenol **309** (1 equiv), alcohol **310** (5 equiv), 18 h. <sup>b</sup>Determined by NMR analysis of the crude reaction mixture using 1,3,5-trimethoxybenzene as internal standard. <sup>c</sup>With 3 equiv **310**. <sup>d</sup>Isolated yield.

### 3.2.2 Reaction Scope

Cyclohexanol and cycloheptanol combined with 3-tert-butylphenol (**309**) to forge alkylated **311** and **312** in good yields (69–70%) (Figure 8). The secondary carbocation generated from tetrahydronaphthalen-2-ol (**334**) undergoes 1,2-hydride shift to the corresponding benzylic carbocation under the reaction conditions, which proceeded to diarylmethane derivative **313** in 81% yield. Acyclic secondary alcohols isopropanol, 2-butanol, and 1-adamantyl-1-ethanol were converted to arylated products **314–316** in 54–87% yields. On a larger 1 mmol scale, the reaction proceeded with nearly equimolar alkylating agent (i.e., 1.1 equiv of isopropanol), leading to isopropylated **314** in 70% yield. Strained alcohols such as norborneol and 2-adamantanol were found to be excellent alkylating agents for this catalysis: equimolar quantities of reactants lead to substitution at the ortho-position of 3-tert-butylphenol (**309**) in 82% (**317**) and 76% (**318**) yields, respectively. 3-Isopropylphenol reacted with cyclohexanol in 49% yield and 2-adamantanol in 85% yield to arrive at alkylated arenes **319** and **320**. Likewise, 3-phenylphenol was alkylated with 1-adamantyl-1-ethanol in 38% yield (**321**) and with 2-adamantanol in 64% yield (**322**). In general, reactions with strained secondary alcohols performed better.

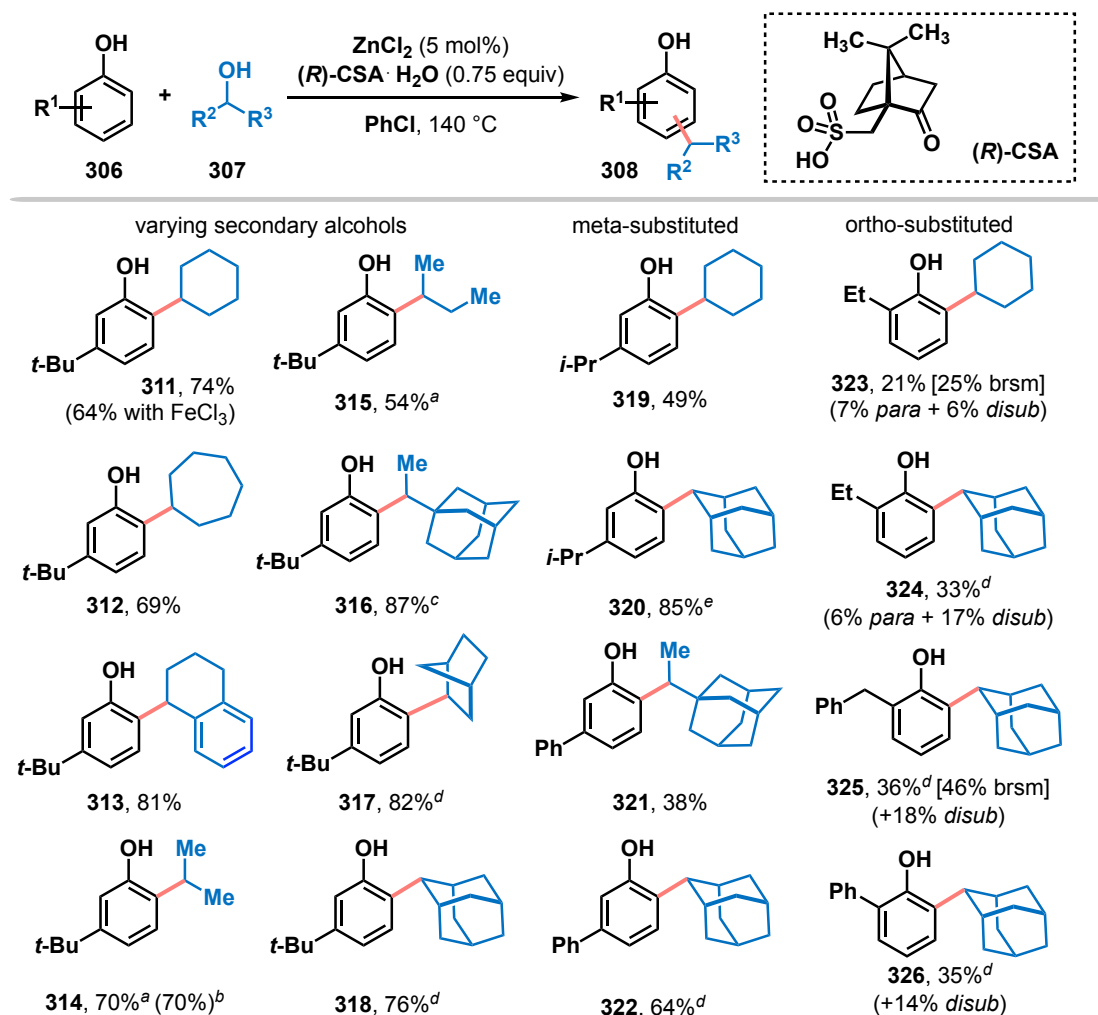


**Figure 8.** Exploring scope of Friedel–Crafts alkylations with unactivated secondary alcohols. Conditions: phenolic **306** (0.2 mmol), alcohol **307** (0.6 mmol), ZnCl<sub>2</sub> (0.01 mmol), (R)-CSA (0.15 mmol), PhCl (0.2 mL, 1 M), 140 °C, 18 h. <sup>a</sup>With 5 equiv alcohol **307**. <sup>b</sup>With phenolic **306** (1 mmol), alcohol **307** (1.1 mmol), ZnCl<sub>2</sub> (0.05 mmol), (R)-CSA (0.75 mmol), PhCl 1 mL, 1 M), 140 °C, 18 h. <sup>c</sup>With 2 equiv alcohol **307**. <sup>d</sup>With 1.1 equiv alcohol **307**. <sup>e</sup>With 1 mol% ZnCl<sub>2</sub>.

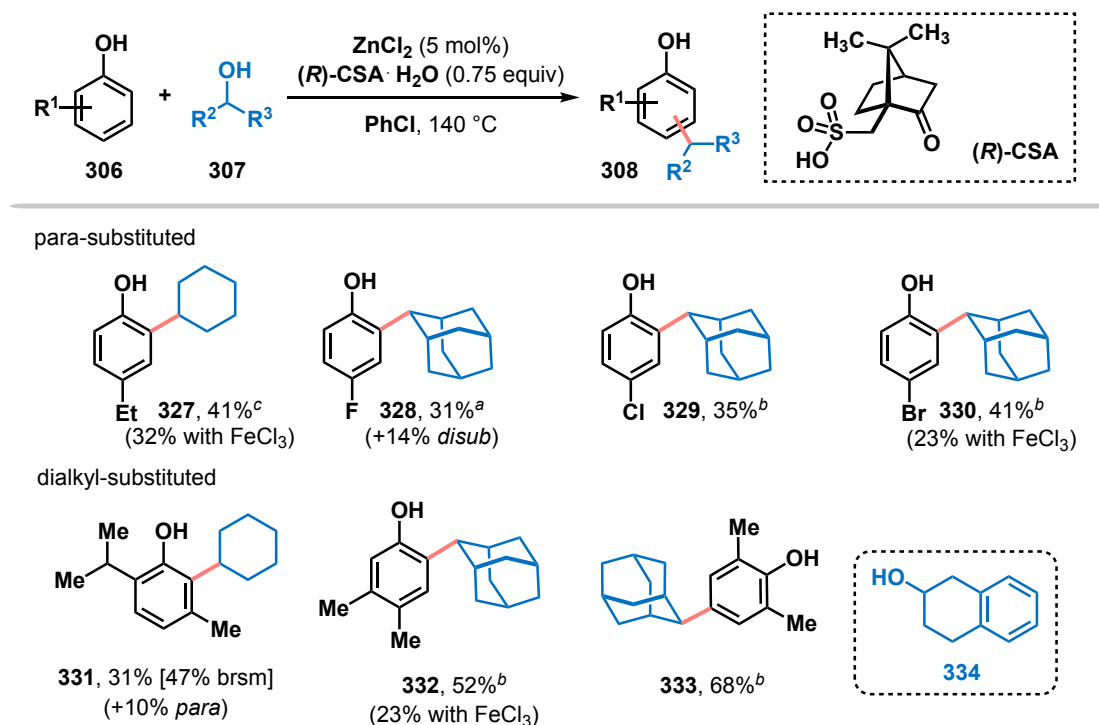


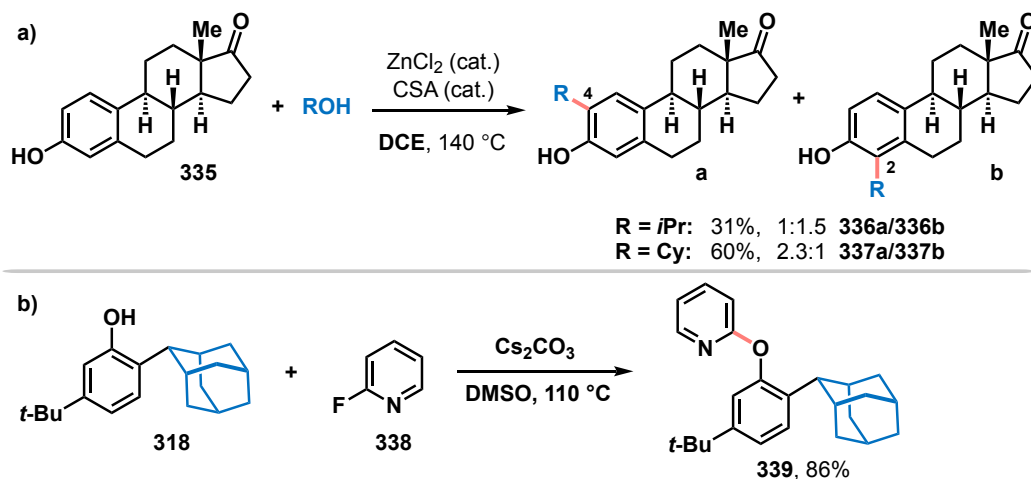
**Figure 9.** Examples of *para*- and dialkyl-substituted phenols. Conditions: phenolic **306** (0.2 mmol), alcohol **307** (0.6 mmol),  $\text{ZnCl}_2$  (0.01 mmol),  $(R)\text{-CSA}$  (0.15 mmol),  $\text{PhCl}$  (0.2 mL, 1 M),  $140^\circ\text{C}$ , 18 h. <sup>a</sup>With 2 equiv alcohol **307**. <sup>b</sup>With 1.1 equiv alcohol **307**. <sup>c</sup>With 1 mol%  $\text{ZnCl}_2$ .

The preference for *ortho*-alkylation extended to *ortho*-substituted phenolic precursors that display a more sterically accessible *para*-site. Cyclohexylation of 2-ethylphenol modestly favored the *ortho*-position, albeit in a low 21% yield of **323**, along with 6% *ortho/para*-dialkylation and 7% *para*-alkylation side products (Figure 8). A similar reactivity pattern was observed between 2-ethylphenol and 2-adamantanol, which gave rise to 33% of phenolic **324**. *ortho/para*-Dialkylated (17%) and *para*-substituted (6%) phenols were formed as minor products. Both 2-benzylphenol and 2-phenylphenol alkylated at their *ortho*-sites with 2-adamantol to afford *ortho/ortho*-dialkylphenols **325**

and **326** in 36% and 35% isolated yields, respectively, along with minor disubstitution side products. In these cases, the *para*-substituted isomers were not isolated nor observed by <sup>1</sup>H NMR analysis of the crude reaction mixtures.

*para*-Substituted, including halogenated phenolic precursors, were mono-alkylated in modest 31–41% yields (**327–330**, Figure 9). Sterically encumbered thymol alkylated with cyclohexanol in 31% yield (47% brsm) predominantly at the most hindered *ortho*-position over the *para*-position (**331**, 10%). In contrast, with two available *ortho*-sites, the flavoring agent 3,4-xylenol underwent alkylation at the less hindered 6-position to furnish 2-adamantyl-4,5-dimethylphenol (**332**) in 52% yield. This selectivity was consistent with all the *meta*-substituted phenolic precursors containing two unsymmetrical *ortho*-sites. With both *ortho*-sites blocked, as in 2,6-xylenol, *para*-alkylation resulted in **333** in 68% yield.

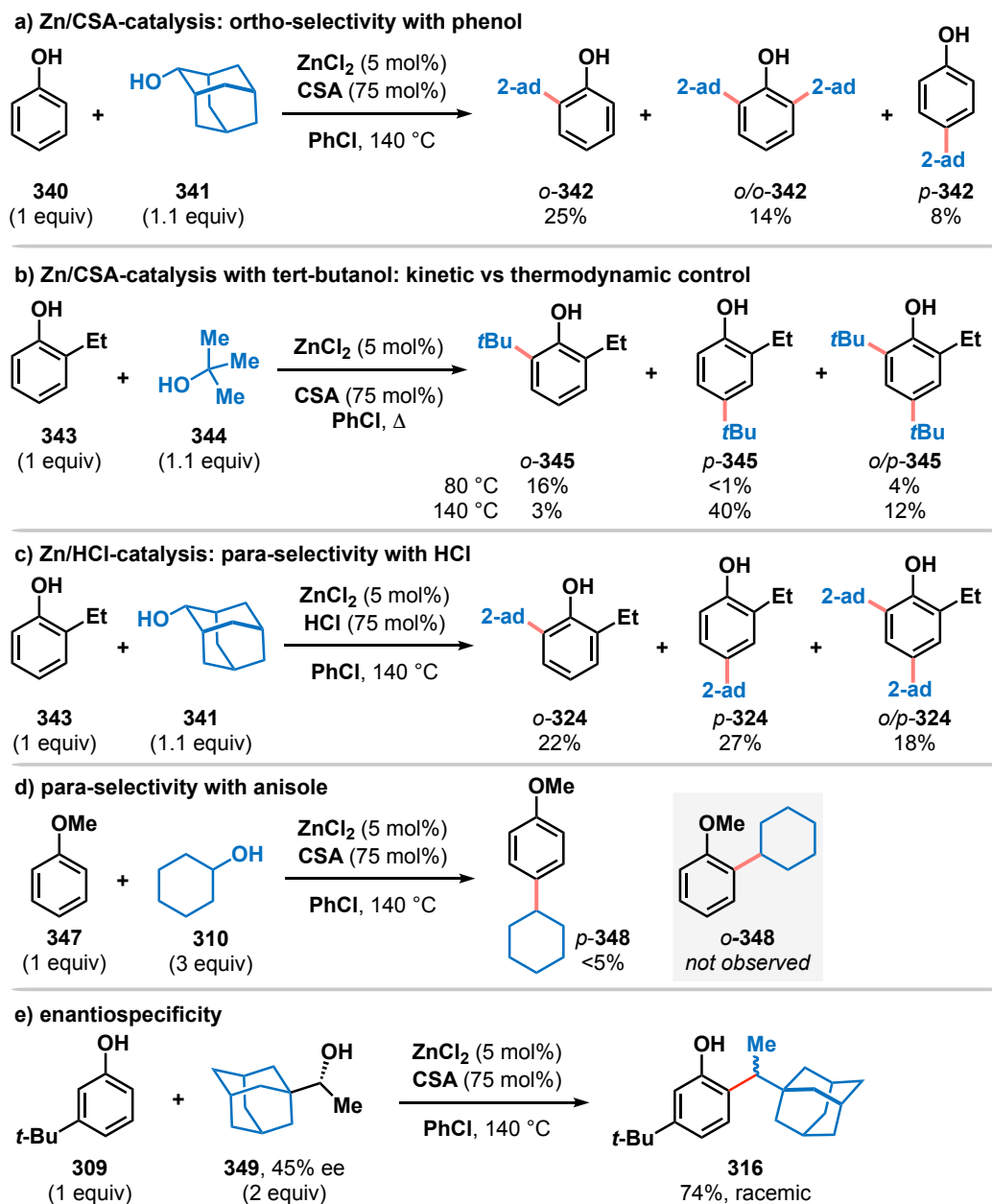
This chemistry was also applied by Pan to the alkylation of more complex molecules like estrone (**335**, Scheme 54a). As examples, its treatment with isopropanol and cyclohexanol furnished a mixture of **336a/336b** in 31% (1:1.5 C4/C2 selectivity) favoring alkylation at the more sterically encumbered *ortho* site and **337a/337b** in 60% yield (2.3:1 C4/C2 selectivity) favoring alkylation at the less hindered *ortho*-site (Scheme 2a). Pan further demonstrated derivatization of the alkylated phenolic compound (**318**) with 2-fluoropyridine (**388**) in a nucleophilic aromatic substitution to access pyridyl aryl ether **339** in 86% yield (Scheme 75b).



**Scheme 75.** Application to late-stage derivatizations

### 3.2.3 Probing the Site-Selectivity

The *ortho*-selective alkylation under Zn/CSA-catalysis conditions was similarly observed between unsubstituted phenol (**340**) and 2-adamantanol (**341**) where a mixture of alkylated products formed, with *o*-alkylation occurring as the major product (25%), followed by *o/o*-dialkylation (14%), and *p*-alkylation (8%) (Scheme 76a). This contrasted from the *para*-selectivity observed in the analogous Fe/HCl-catalyzed Friedel–Crafts alkylation with tertiary alcohols<sup>14</sup> and HFIP-mediated alkylation with tertiary alkyl bromides.<sup>20</sup> In contrast, Pan found that the catalytic Zn/CSA system favored *ortho*-selectivity (*o*-**345**, >16:1 *o/p*) even with the more hindered *tert*-butanol at 80 °C, albeit with lower reactivity compared to the Fe/HCl system (Scheme 76b). At 140 °C, the site-selectivity reversed to favor *p*-**345** (40% yield, 13:1 *p/o*). These experiments suggested a kinetic origin in the observed *ortho*-selectivity. Therefore, the site-selectivity was not simply determined by steric factors, but rather by the catalyst systems. In other words, the Zn/CSA catalyst system inherently favored *ortho*-selectivity.



**Scheme 76.** Mechanistic studies

The site-selectivity largely vanished when CSA was substituted for HCl. The Zn/HCl co-catalyzed reaction between 2-ethylphenol (**343**) and 2-adamantanol (**341**) resulted in a 1:1.2 mixture of *o*-**324**/*p*-**324**, slightly favoring *para*-substitution (Scheme

76c). This highlighted the role of sulfonic acid derivatives in promoting *ortho*-selectivity. We postulated that the Zn and CSA catalysts played roles in templating reactivity and that the phenolic group directed reactivity (through a zinc phenolate species). Upon subjecting anisole (**347**) to the catalysis conditions, only a small amount of the *para*-alkylated product (p-**348**) was observed by NMR analysis (Scheme 76d). This observation emphasized the importance of the free phenolic group in directing both reactivity and selectivity.

### 3.2.4 Mechanism of the Reaction

To probe the substitution mechanism of the reaction, Pan prepared and subjected a non-racemic mixture of 1-adamantyl-1-ethanol (**349**) to Friedel–Crafts alkylation with 3-*tert*-butylphenol (**309**) (Scheme 76e). The loss of enantiomeric excess in forming the chiral racemic product (**316**) strongly suggested involvement of an S<sub>N</sub>1 pathway under the dual ZnCl<sub>2</sub>/CSA catalysis conditions, which was distinct from the S<sub>N</sub>2 pathway promoted by TfOH in HFIP.<sup>13</sup>

We turned to kinetics studies to derive a rate law for this transformation using 3-*tert*-butylphenol (**309**) and 2-adamantanol (**341**) as the model system (Figure 10). Executed by Pan, initial rates of the alkylation reaction were measured by varying the concentrations of ZnCl<sub>2</sub>, CSA, phenolic **309**, alcohol **341**, ZnCl<sub>2</sub>, and CSA. These experiments revealed the rate to be largely independent of the concentration of ZnCl<sub>2</sub>, suggestive of saturation kinetics and sequestration by substrate. In the absence of ZnCl<sub>2</sub>, the initial rate deviated significantly (4.3-fold slower) from the trendline in Figure 9a and was indicative of background reactivity proceeding through a different ZnCl<sub>2</sub>-free

mechanism. The initial rates followed a first-order dependence on the concentration of CSA, half-order dependence on the concentration of phenolic **309**, and first-order dependence on the concentration of 2-adamantanol (**341**), giving the rate law:

$$\text{rate} = k_{\text{obs}}[\text{ZnCl}_2]^0[\text{CSA}]^1[\text{phenolic } \mathbf{309}]^{0.5}[\text{alcohol } \mathbf{341}]^1 \quad (1)$$

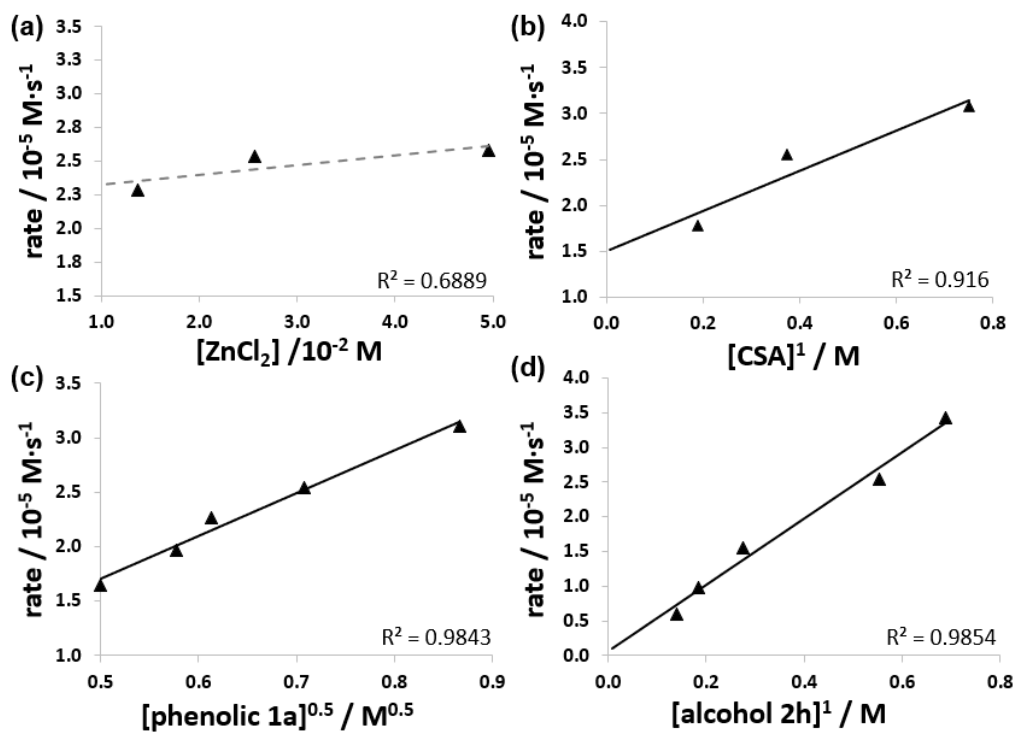
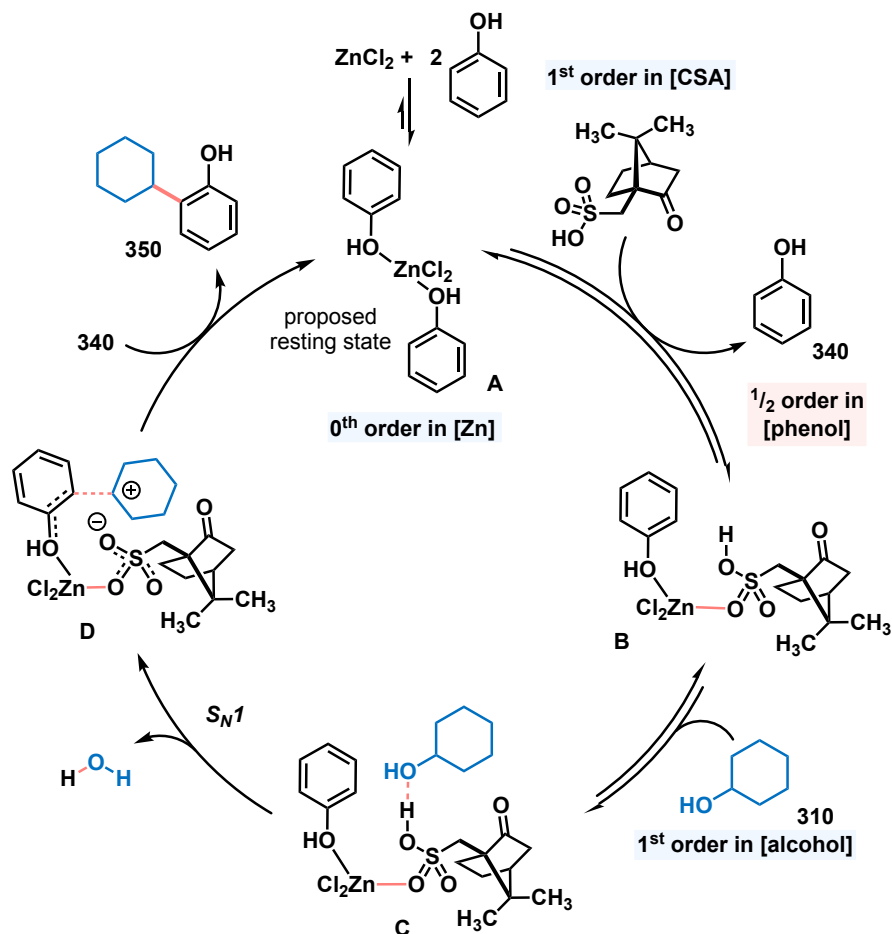


**Figure 10.** Plots of initial rates

(a) [ZnCl<sub>2</sub>] indicating pseudo-zero order dependence, [CSA] = 3.8 × 10<sup>-1</sup> M, [phenol **309**] = 5.0 × 10<sup>-1</sup> M, [alcohol **341**] = 5.5 × 10<sup>-1</sup> M; (b) [CSA] indicating first-order dependence, [ZnCl<sub>2</sub>] = 2.5 × 10<sup>-2</sup> M, [phenol **309**] = 5.0 × 10<sup>-1</sup> M, [alcohol **341**] = 5.5 × 10<sup>-1</sup> M; (c) [phenol **309**] indicating half-order dependence, [ZnCl<sub>2</sub>] = 2.5 × 10<sup>-2</sup> M, [CSA] = 3.8 × 10<sup>-1</sup> M, [alcohol **341**] = 5.5 × 10<sup>-1</sup> M; (d) [alcohol **341**] indicating first-order dependence, [ZnCl<sub>2</sub>] = 2.5 × 10<sup>-2</sup> M, [CSA] = 3.8 × 10<sup>-1</sup> M, [phenol **309**] = 5.0 × 10<sup>-1</sup> M

Based on the experimentally derived rate law, the zinc catalyst was believed to be saturated with phenol ligands in the form of complex **A** (Scheme 77). We therefore proposed it to be the resting state of the catalytic cycle. For the reaction to proceed, one of the phenolate ligands must dissociate from zinc in exchange for CSA to coordinate, leading to complex **B**; hence the half-order dependence on [phenol] and first-order dependence on [CSA]. Complexation of the Brønsted acid to zinc effectively enhances its acidity, enabling it to activate alcohol **310** toward Friedel–Crafts alkylation (see **C**). Ionization, as part of the S<sub>N</sub>1 pathway determined via stereochemical studies (Scheme 3e), leads to loss of water and an ion-pair that can potentially proceed via transition state **D**. The relatively non-polar PhCl solvent favors formation of a tight ion-pair and ortho-selectivity. Release of product in the presence of excess phenolic substrate turns over the zinc catalyst.



**Scheme 77.** Proposed mechanism

### 3.3 Conclusion

In summary, the combination of zinc and CSA catalysts promoted the first direct *ortho*-selective Friedel-Crafts alkylation of phenolic derivatives with unactivated secondary alcohols. The free phenolic group was found to be important for reactivity and site-selectivity, which was rationalized through zinc-mediated templation that biases alkylation at the *ortho*-position over the generally more accessible *para*-position. Mechanistic studies served to elucidate the origin of site-selectivity, favoring an  $\text{S}_{\text{N}}1$  pathway in which zinc and CSA function to scaffold both the phenolic and alcohol

reactants for *ortho*-functionalization. The current catalysis conditions provided a good foundation for developing green and cost-effective conditions for catalytic Friedel–Crafts reactions using readily accessible alcohols as direct alkylating agents. This work also highlighted the efficacy of simple catalysts for achieving C(sp<sup>2</sup>)-C(sp<sup>3</sup>) bond synthesis, departing from conventional transition-metal-catalyzed cross-coupling methods.

### 3.4 Experimental Section

#### 3.4.1 General Experimental

Commercial reagents were purchased from MilliporeSigma, Acros Organics, Chem-Impex, TCI, Oakwood, and Alfa Aesar, and used without additional purification. Solvents were purchased from Fisher Scientific, Acros Organics, Alfa Aesar, and Sigma Aldrich. Tetrahydrofuran (THF), diethyl ether (Et<sub>2</sub>O), acetonitrile (MeCN), dichloromethane (CH<sub>2</sub>Cl<sub>2</sub>), benzene, 1,4-dioxane, and triethylamine (Et<sub>3</sub>N) were sparged with argon and dried by passing through alumina columns using argon in a Glass Contour (Pure Process Technology) solvent purification system. Dimethylformamide (DMF), dimethyl sulfoxide (DMSO), and dichloroethane (DCE) were purchased in Sure/Seal or AcroSeal bottling and dispensed under N<sub>2</sub>. Deuterated solvents were obtained from Cambridge Isotope Laboratories, Inc. or MilliporeSigma.

In general, the catalytic reactions are not air- or moisture-sensitive; however, the iron and zinc salts are hygroscopic and quickly change color when being weighed and added to the reaction vessel. This influences how much metal catalyst is being added because their molecular weights increase on hydration. For consistency and rigor, the iron and zinc salts were weighed and added to vials inside a nitrogen-filled glovebox. All

other reagents, including the solvent, were added outside the glovebox under open air. Reaction progresses were monitored using thin-layer chromatography (TLC) on EMD Silica Gel 60 F254 or Macherey–Nagel SIL HD (60 Å mean pore size, 0.75 mL/g specific pore volume, 5–17 µm particle size, with fluorescent indicator) silica gel plates. Visualization of the developed plates was performed under UV light (254 nm). Purification and isolation of products were performed via silica gel chromatography (both column and preparative thin-layer chromatography). Organic solutions were concentrated under reduced pressure on IKA® temperature-controlled rotary evaporator equipped with an ethylene glycol/water condenser.

Melting points were measured with the MEL-TEMP melting point apparatus.

Proton nuclear magnetic resonance ( $^1\text{H}$  NMR) spectra, carbon nuclear magnetic resonance ( $^{13}\text{C}$  NMR) spectra and fluorine nuclear magnetic resonance ( $^{19}\text{F}$  NMR) spectra were recorded on Bruker Avance NEO 400 (not  $^1\text{H}$  decoupled) or Bruker Avance 600 MHz spectrometers ( $^1\text{H}$  decoupled). Chemical shifts ( $\delta$ ) are reported in ppm relative to the residual solvent signal ( $\delta$  7.26 for  $^1\text{H}$  NMR,  $\delta$  77.16 for  $^{13}\text{C}$  NMR in  $\text{CDCl}_3$ ).<sup>1</sup> Data for  $^1\text{H}$  NMR spectroscopy are reported as follows: chemical shift ( $\delta$  ppm), multiplicity (s = singlet, d = doublet, t = triplet, q = quartet, m = multiplet, br = broad, dd = doublet of doublets, dt = doublet of triplets), coupling constant (Hz), integration. Data for  $^{13}\text{C}$  and  $^{19}\text{F}$  NMR spectroscopy are reported in terms of chemical shift ( $\delta$  ppm). IR spectroscopic data were recorded on a NICOLET 6700 FT-IR spectrophotometer using a diamond attenuated total reflectance (ATR) accessory. Samples are loaded onto the diamond surface either neat or as a solution in organic solvent and the data acquired after the

solvent had evaporated. High resolution accurate mass (ESI) spectral data were obtained from the Analytical Chemistry Instrumentation Facility at the University of California, Riverside, on an Agilent 6545 Q-TOF LC/MS instrument (supported by NSF grant CHE-1828782).

### 3.4.2 Experimental Procedures

General Procedure A: Reductions of Ketones with  $\text{LiAlH}_4$ . To a 50 mL RBF (flame-dried and equipped with a stirring bar) was added  $\text{LiAlH}_4$  (1 equiv) before purging with  $\text{N}_2$  and suspending in dry  $\text{Et}_2\text{O}$  (to produce a 0.2 M suspension). The mixture was cooled to 0 °C before adding dropwise a solution of ketone (1 equiv) in dry  $\text{Et}_2\text{O}$  (1 M). The resulting suspension was allowed to stir at 0 °C for 4 h. The reaction mixture was quenched via the Fieser–Fieser workup conditions: diluted with  $\text{Et}_2\text{O}$  (30 mL), then cooled to 0 °C and dropwise added distilled water ( $\text{dH}_2\text{O}$ ) (2 equiv), 15% (w/v)  $\text{NaOH}_{(\text{aq})}$  (2 equiv), and  $\text{dH}_2\text{O}$  (3 equiv). The mixture was warmed to room temperature and stirred for 15 min, then added anhydrous  $\text{MgSO}_4$  was and stirred for an additional 15 min. The solids were removed by filtration and the filtrate concentrated under reduced pressure to obtain the secondary alcohol product. The alcohols were subsequently used without further purification.

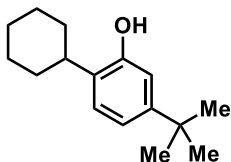
General Procedure B: Alkylations with cyclohexanol. A one-dram vial equipped with a stirring bar was sequentially added  $\text{ZnCl}_2$  or  $\text{FeCl}_3$  (2–10  $\mu\text{mol}$ , 1–5 mol%), arene derivative (0.2 mmol, 1 equiv),  $\text{PhCl}$  (0.2 mL, 1 M), cyclohexanol (62.5  $\mu\text{L}$ , 0.6 mmol, 3 equiv), and (*R*)-camphorsulfonic acid monohydrate (*R*-CSA• $\text{H}_2\text{O}$ ) (37.6 mg, 0.15 mmol, 75 mol%) or (*S*)-camphorsulfonic acid (*S*-CSA) (35 mg, 0.15 mmol, 75 mol%). The

reaction mixture was heated at 140 °C for 18 h, at which time the solution was filtered through a 5" pipette plug of silica gel (approximately one-third filled) and eluted with hexanes/EtOAc (3:1). The solution was concentrated in vacuo and purified via silica gel chromatography to obtain the alkylation product.

General Procedure C: Alkylations with 2-adamantanol. A one-dram vial equipped with a stirring bar was sequentially added ZnCl<sub>2</sub> or FeCl<sub>3</sub> (10 μmol, 5 mol%), arene derivative (0.2 mmol, 1 equiv), PhCl (0.2 mL, 1 M), 2-adamantanol (33.5 mg, 0.22 mmol, 1.1 equiv), (*R*)-camphor sulfonic acid monohydrate (*R*-CSA•H<sub>2</sub>O) (37.6 mg, 0.15 mmol, 75 mol%) or (*S*)-camphor sulfonic acid (*S*-CSA) (35 mg, 0.15 mmol, 75 mol%). The reaction mixture was heated at 140 °C for 18 h, at which time the solution was filtered through a silica gel plug (packed in a 5" glass pipette, approximately one-third filled) and eluted with hexanes/EtOAc (3:1). The solution was concentrated in vacuo and purified via silica gel chromatography to obtain the alkylation product.

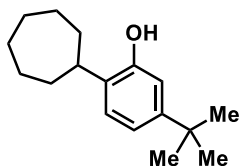
General Procedure D: Alkylations with other secondary alcohols. A one-dram vial equipped with a stirring bar was sequentially added ZnCl<sub>2</sub> (0.01 mmol, 5 mol%), 3-tert-butylphenol (0.2 mmol, 1 equiv), PhCl (0.2 mL, 1 M), secondary alcohol (0.22–1.0 mmol, 1.1–5 equiv), and (*R*)-camphor sulfonic acid monohydrate (*R*-CSA•H<sub>2</sub>O) (37.6 mg, 0.15 mmol, 75 mol%). The reaction mixture was heated at 140 °C for 18 h, at which time the solution was filtered through a silica gel plug (packed in a 5" glass pipette, approximately one-third filled) and eluted with hexanes/EtOAc (9:1) or EtOAc. The solution was concentrated in vacuo and purified via silica gel chromatography to obtain the alkylation product.

### 5-(*tert*-Butyl)-2-cyclohexylphenol (**311**)



Prepared using General Procedure B with 3-*tert*-butylphenol (30.2 mg, 0.2 mmol, 1 equiv), ZnCl<sub>2</sub> (1.5 mg, 0.055 mmol, 0.05 equiv), PhCl (0.2 mL, 1.0 M), cyclohexanol (62.5 μL, 0.6 mmol, 3 equiv), and CSA•H<sub>2</sub>O (37.6 mg, 0.150 mmol, 0.75 equiv). Purification by preparative TLC (eluting with 9:1 hexanes/EtOAc) afforded **311** (34.5 mg, 74%) as a yellow-orange oil. R<sub>f</sub>: 0.33 (19:1 hexanes/EtOAc); <sup>1</sup>H NMR (500 MHz, CDCl<sub>3</sub>) δ 7.12 (d, J = 8.1 Hz, 1H), 6.95 (dd, J = 8.1, 2.0 Hz, 1H), 6.81 (d, J = 2.2 Hz, 1H), 4.74 (s, 1H), 2.77 (qt, J = 6.3, 2.5 Hz, 1H), 1.94–1.83 (m, 5H), 1.82–1.74 (m, 1H), 1.51–1.38 (m, 4H), 1.31 (s, 9H); <sup>13</sup>C NMR (151 MHz, CDCl<sub>3</sub>) δ 152.4, 150.2, 130.5, 126.5, 118.0, 112.7, 37.2, 34.4, 33.3, 31.4, 27.2, 26.4; IR (ATR): 3342, 2925, 2852, 1414, 738 cm<sup>-1</sup>; HRMS (ESI<sup>+</sup>): m/z [M+H]<sup>+</sup> calculated for C<sub>16</sub>H<sub>25</sub>O: 233.1900; found: 233.1902.

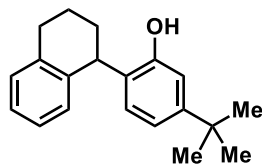
### 5-(*tert*-Butyl)-2-cycloheptylphenol (**312**)



Prepared using General Procedure D with 3-*tert*-butylphenol (30.2 mg, 0.201 mmol, 1 equiv), ZnCl<sub>2</sub> (1.7 mg, 0.012 mmol, 0.05 equiv), PhCl (0.2 mL, 1.0 M), cycloheptanol (69.6 mg, 0.609 mmol, 3 equiv), and CSA•H<sub>2</sub>O (37.8 mg, 0.151 mmol, 0.75 equiv). Purification by preparative TLC (eluting with 19:1 hexanes/EtOAc × 2) afforded **312** (34.0 mg, 69%) as an orange oil. <sup>1</sup>H NMR (500 MHz, CDCl<sub>3</sub>) δ 7.09 (d, J = 8.0 Hz, 1H), 6.91 (dd, J = 8.1, 1.5 Hz, 1H), 6.78 (d, J = 2.0 Hz, 1H), 2.95–2.83 (m, 1H), 1.96–1.87 (m, 2H), 1.85–1.77 (m, 2H), 1.72–1.52 (m, 8H), 1.28 (s, 9H); <sup>13</sup>C NMR (101 MHz, CDCl<sub>3</sub>) δ 151.8, 150.0, 132.4,

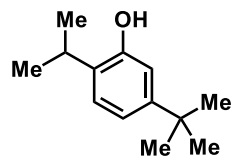
126.8, 118.0, 112.7, 39.3, 35.5, 34.4, 31.5, 28.1, 27.6; IR (ATR): 3380, 2923, 2855, 1617, 1577, 1504, 1460, 1415, 1362, 1292, 1264, 1233, 1203, 1168, 1128, 1089, 931, 863, 814, 738, 705, 651, 576, 554, 485, 458, 451, 440, 404  $\text{cm}^{-1}$ ; HRMS (ESI<sup>+</sup>):  $m/z$  [M+H]<sup>+</sup> calculated for C<sub>17</sub>H<sub>27</sub>O: 247.2056; found: 247.2061.

### 5-(*tert*-Butyl)-2-(1,2,3,4-tetrahydronaphthalen-1-yl)phenol (**313**)



Prepared using General Procedure D with 3-*tert*-butylphenol (30.2 mg, 0.201 mmol, 1 equiv), ZnCl<sub>2</sub> (1.5 mg, 0.011 mmol, 0.05 equiv), PhCl (0.2 mL, 1.0 M), 2-tetralol (**2c**) (53.5  $\mu\text{L}$ , 0.399 mmol, 2 equiv), and CSA•H<sub>2</sub>O (37.5 mg, 0.150 mmol, 0.75 equiv). Purification by preparative TLC (eluting with 19:1 hexanes/EtOAc) afforded **313** (45.4 mg, 81%) as an orange oil.  $R_f$ : 0.27 (19:1 hexanes/EtOAc); <sup>1</sup>H NMR (600 MHz, CDCl<sub>3</sub>)  $\delta$  7.18–7.12 (m, 2H), 7.10–7.04 (m, 1H), 6.98 (d,  $J = 7.8$  Hz, 1H), 6.89–6.84 (m, 2H), 6.81 (d,  $J = 1.8$  Hz, 1H), 4.48 (s, 1H), 4.28 (dd,  $J = 8.8, 5.7$  Hz, 1H), 2.97–2.80 (m, 2H), 2.17–2.08 (m, 1H), 1.99–1.90 (m, 2H), 1.82–1.73 (m, 1H), 1.29 (s, 9H); <sup>13</sup>C NMR (151 MHz, CDCl<sub>3</sub>)  $\delta$  152.9, 151.0, 138.3, 137.9, 130.5, 129.6, 129.5, 129.5, 126.5, 126.3, 117.9, 113.6, 40.9, 34.5, 31.5, 30.9, 29.9, 21.7; IR (ATR): 3312, 2971, 1379, 1087, 1045, 879, 653  $\text{cm}^{-1}$ ; HRMS (ESI<sup>-</sup>):  $m/z$  [M-H]<sup>-</sup> calculated for C<sub>20</sub>H<sub>23</sub>O: 279.1754; found 279.1765.

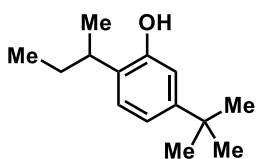
### 5-(*tert*-Butyl)-2-isopropylphenol (**314**)



Prepared using General Procedure D with 3-*tert*-butylphenol (30.1 mg, 0.2 mmol, 1 equiv), ZnCl<sub>2</sub> (1.5 mg, 0.011 mol, 0.05 equiv), PhCl (0.2 mL, 1.0 M), *sec*-butanol (76.5  $\mu\text{L}$ , 1.0 mmol, 5 equiv), and CSA•H<sub>2</sub>O (37.5 mg, 0.15 mmol, 0.75 equiv). Purification by preparative TLC (eluting

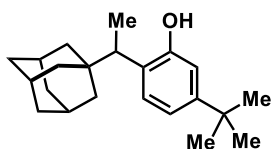
with 19:1 hexanes/EtOAc) afforded **314** (26.7 mg, 70%) as a light-yellow-white solid. M.p. 53–56 °C; R<sub>f</sub>: 0.34 (19:1 hexanes/EtOAc); <sup>1</sup>H NMR (500 MHz, CDCl<sub>3</sub>) δ 7.15 (d, J = 8.0 Hz, 1H), 6.97 (dd, J = 8.0, 2.0 Hz, 1H), 6.81 (d, J = 1.9 Hz, 1H), 4.69 (s, 1H), 3.18 (h, J = 6.9 Hz, 1H), 1.32 (s, 9H), 1.28 (d, J = 6.9 Hz, 6H); <sup>13</sup>C NMR (151 MHz, CDCl<sub>3</sub>) δ 152.4, 150.3, 131.3, 126.0, 118.0, 112.7, 34.4, 31.5, 26.9, 22.8; IR (ATR): 3349, 2960, 2869, 1415, 1156, 1082, 932, 817, 739 cm<sup>-1</sup>; HRMS (ESI<sup>+</sup>): m/z [M+H]<sup>+</sup> calculated for C<sub>13</sub>H<sub>21</sub>O: 193.1587; found: 193.1583.

### 2-(sec-butyl)-5-(tert-butyl)phenol (**315**)



Prepared using General Procedure D with 3-tert-butylphenol (30.1 mg, 0.2 mmol, 1 equiv), ZnCl<sub>2</sub> (1.5 mg, 0.011 mol, 0.05 equiv), PhCl (0.2 mL, 1.0 M), sec-butanol (920 μL, 1 mmol, 5 equiv), and CSA•H<sub>2</sub>O (37.5 mg, 0.15 mmol, 0.75 equiv). Purification by preparative TLC (eluting with 19:1 hexanes/EtOAc) afforded **315** (22.1 mg, 54%) as a colorless oil; <sup>1</sup>H NMR (600 MHz, CDCl<sub>3</sub>) δ 7.07 (d, J = 8.0 Hz, 1H), 6.92 (dt, J = 8.0, 1.5 Hz, 1H), 6.78 (t, J = 1.5 Hz, 1H), 4.57 (s, 1H), 2.89 (sextet, J = 7.0 Hz, 1H), 1.70–1.63 (m, 1H), 1.58 (dq, J = 13.9, 6.9 Hz, 2H), 1.29 (s, 9H), 1.23 (dd, J = 6.9, 1.1 Hz, 3H), 0.88 (td, J = 7.4, 1.1 Hz, 3H); <sup>13</sup>C NMR (151 MHz, CDCl<sub>3</sub>) δ 157.2, 152.7, 150.2, 126.7, 118.0, 112.7, 34.4, 33.9, 31.5, 30.0, 20.5, 12.4; IR (ATR): 3311, 2968, 1417, 1087, 1045, 879, 655 cm<sup>-1</sup>; HRMS (ESI<sup>-</sup>): m/z [M-H]<sup>-</sup> calculated for C<sub>14</sub>H<sub>23</sub>O: 205.1598; found: 205.1601.

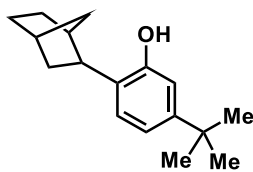
### 2-(1-Adamant-1-yl)ethyl)-5-(tert-butyl)phenol (**316**)



Prepared using General Procedure D with 3-tert-butylphenol (30.0 mg, 0.2 mmol, 1 equiv), ZnCl<sub>2</sub> (1.4 mg, 0.01 mmol, 0.05 equiv),

PhCl (0.2 mL, 1.0 M), 1-(adamant-1-yl)ethanol (**349**) or (R)-1-(adamant-1-yl)ethanol (**(R)-349**) (72.2 mg, 0.40 mmol, 2 equiv), and CSA•H<sub>2</sub>O (37.5 mg, 0.15 mmol, 0.75 equiv). Purification by preparative TLC (eluting with 19:1 hexanes/EtOAc) or flash chromatography (eluting with 0–10% EtOAc in hexanes) afforded **316** (46.5–54.7 mg, 74–87%) as an orange oil. R<sub>f</sub>: 0.37 (19:1 hexanes/EtOAc); <sup>1</sup>H NMR (600 MHz, CDCl<sub>3</sub>) δ 7.02 (d, J = 8.1 Hz, 1H), 6.92–6.87 (m, 1H), 6.78 (d, J = 2.1 Hz, 1H), 4.60 (s, 1H), 2.74 (q, J = 7.3 Hz, 1H), 1.93 (s, 3H), 1.67–1.62 (m, 5H), 1.57 (d, J = 12.6 Hz, 4H), 1.50–1.45 (m, 3H), 1.29 (s, 9H), 1.18 (d, J = 7.2 Hz, 3H); <sup>13</sup>C NMR (151 MHz, CDCl<sub>3</sub>) δ 153.0, 150.0, 129.0, 127.0, 117.3, 112.4, 41.0, 39.7, 37.3, 36.3, 34.4, 31.5, 28.9, 14.4; IR (ATR): 3314, 2971, 1379, 1087, 1045, 879, 657 cm<sup>-1</sup>; HRMS (ESI<sup>-</sup>): m/z [M–H]<sup>-</sup> calculated for C<sub>22</sub>H<sub>31</sub>O: 311.2380; found 311.2395.

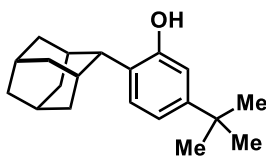
### 2-(norborn-2-yl)-5-(tert-butyl)phenol (**317**)



Prepared using General Procedure D with 3-tert-butylphenol (30 mg, 0.2 mmol, 1 equiv), ZnCl<sub>2</sub> (1.5 mg, 0.055 mmol, 0.05 equiv), PhCl (0.2 mL, 1.0 M), norbornan-2-ol (24.7 mg, 0.22 mmol, 1.1 equiv), and CSA•H<sub>2</sub>O (37.6 mg, 0.15 mmol, 0.75 equiv). Purification by preparative TLC (eluting with 9:1 hexanes/EtOAc) afforded **317** (40.2 mg, 82%) as a yellow-orange oil. <sup>1</sup>H NMR (400 MHz, CDCl<sub>3</sub>) δ 7.14 (d, J = 8.1 Hz, 1H), 6.93 (dd, J = 8.1, 2.0 Hz, 1H), 6.84 (d, J = 2.0 Hz, 1H), 4.73 (s, 1H), 2.82 (dd, J = 9.1, 5.3 Hz, 1H), 2.45–2.24 (m, 2H), 1.81 (ddd, J = 11.7, 8.8, 2.3 Hz, 1H), 1.75–1.51 (m, 4H), 1.47–1.35 (m, 2H), 1.31 (s, 9H), 1.24 (ddd, J = 9.7, 2.3, 1.5 Hz, 1H); <sup>13</sup>C NMR (151 MHz, CDCl<sub>3</sub>) δ 153.1, 150.2, 129.9, 125.7, 117.4, 112.7, 41.1, 40.4, 38.2, 37.0, 36.3, 34.4, 31.5, 30.4, 29.2; IR (ATR): 3341,

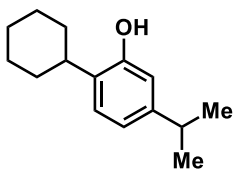
2949, 2867, 1573, 1413, 1295, 1234, 1092, 932, 814  $\text{cm}^{-1}$ ; HRMS (ESI<sup>+</sup>):  $m/z$   $[\text{M}+\text{H}]^+$  calculated for  $\text{C}_{17}\text{H}_{25}\text{O}$ : 245.1900; found: 245.1901.

### 2-(adamantan-2-yl)-5-(tert-butyl)phenol (**318**)



Prepared using General Procedure C with 3-tert-butylphenol (30.1 mg, 0.2 mmol, 1 equiv),  $\text{ZnCl}_2$  (1.5 mg, 0.011 mol, 0.05 equiv),  $\text{PhCl}$  (0.2 mL, 1.0 M), adamantan-2-ol (33.9 mg, 0.2 mmol, 1.1 equiv), and  $\text{CSA}\cdot\text{H}_2\text{O}$  (37.48 mg, 0.15 mmol, 0.75 equiv). Purification by preparative TLC (eluting with 9:1 hexanes/ $\text{EtOAc}$ ) afforded **318** (43 mg, 76%) as a pale-yellow-white solid. M.p. 135–139  $^\circ\text{C}$ ;  $R_f$ : 0.35 (19:1 hexanes/ $\text{EtOAc}$ );  $^1\text{H}$  NMR (500 MHz,  $\text{CDCl}_3$ )  $\delta$  7.37 (d,  $J = 8.1$  Hz, 1H), 6.94 (dd,  $J = 8.1, 2.0$  Hz, 1H), 6.78 (d,  $J = 2.0$  Hz, 1H), 4.67 (s, 1H), 3.15 (s, 1H), 2.38–2.33 (m, 2H), 2.05 (dd,  $J = 12.8, 2.9$  Hz, 2H), 2.02–1.92 (m, 5H), 1.88 (p,  $J = 3.2$  Hz, 1H), 1.82–1.77 (m, 2H), 1.68–1.63 (m, 2H), 1.30 (s, 9H);  $^{13}\text{C}$  NMR (151 MHz,  $\text{CDCl}_3$ )  $\delta$  153.6, 150.2, 128.5, 127.9, 117.3, 113.0, 43.9, 40.1, 38.1, 34.3, 33.0, 31.4, 31.2, 28.3, 27.9; IR (ATR): 3301, 2899, 2849, 1615, 1450, 1411, 1192, 1092, 935, 859, 827, 731, 650  $\text{cm}^{-1}$ ; HRMS (ESI<sup>+</sup>):  $m/z$   $[\text{M}+\text{H}]^+$  calculated for  $\text{C}_{20}\text{H}_{29}\text{O}$ : 285.2213; found 285.2223.

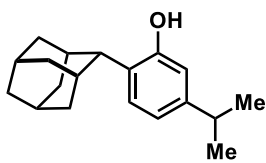
### 2-cyclohexyl-5-isopropylphenol (**319**)



Prepared using General Procedure B with 3-isopropylphenol (27.5  $\mu\text{L}$ , 0.2 mmol, 1 equiv),  $\text{ZnCl}_2$  (1.4 mg, 0.01 mmol, 0.05 equiv),  $\text{PhCl}$  (0.2 mL, 1.0 M), cyclohexanol (62.5  $\mu\text{L}$ , 0.6 mmol, 3 equiv), and  $\text{CSA}\cdot\text{H}_2\text{O}$  (37.4 mg, 0.15 mmol, 0.75 equiv). Purification by preparative TLC (eluting with 9:1 hexanes/ $\text{EtOAc}$ ) afforded **319** (21.5 mg, 49%) as an orange oil.  $R_f$ : 0.27

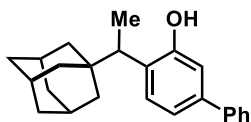
(9:1 hexanes/EtOAc);  $^1\text{H}$  NMR (500 MHz,  $\text{CDCl}_3$ )  $\delta$  7.10 (d,  $J = 7.9$  Hz, 1H), 6.79 (dd,  $J = 7.9, 1.8$  Hz, 1H), 6.64 (t,  $J = 2.0$  Hz, 1H), 4.74 (s, 1H), 2.84 (h,  $J = 6.9$  Hz, 1H), 2.79–2.70 (m, 1H), 1.93–1.81 (m, 4H), 1.81–1.72 (m, 1H), 1.49–1.35 (m, 4H), 1.34–1.24 (m, 1H), 1.23 (d,  $J = 6.9$  Hz, 6H);  $^{13}\text{C}$  NMR (151 MHz,  $\text{CDCl}_3$ )  $\delta$  152.7, 147.8, 130.9, 126.8, 119.1, 113.5, 37.2, 33.7, 33.3, 27.2, 26.5, 24.1; IR (ATR): 3390, 2923, 2850, 1579, 1423, 738  $\text{cm}^{-1}$ ; HRMS (ESI+):  $m/z$   $[\text{M}+\text{H}]^+$  calculated for  $\text{C}_{15}\text{H}_{23}\text{O}$ : 219.1743; found: 219.1744.

### 2-(Adamant-2-yl)-5-isopropylphenol (**320**)



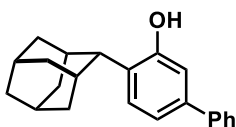
Prepared using General Procedure C with 3-isopropylphenol (27.5  $\mu\text{L}$ , 0.2 mmol, 1 equiv),  $\text{ZnCl}_2$  (1.7 mg, 0.012 mmol, 0.05 equiv),  $\text{PhCl}$  (0.2 mL, 1.0 M), adamantan-2-ol (33.6 mg, 0.22 mmol, 1.1 equiv), and  $\text{CSA}\cdot\text{H}_2\text{O}$  (37.6 mg, 0.15 mmol, 0.75 equiv). Purification by preparative TLC (eluting with 9:1 hexanes/EtOAc) afforded **320** (46.0 mg, 85%) as a yellow-white solid. M.p. 115–118  $^\circ\text{C}$ ;  $R_f$ : 0.41 (9:1 hexanes/EtOAc);  $^1\text{H}$  NMR (500 MHz,  $\text{CDCl}_3$ )  $\delta$  7.34 (d,  $J = 7.9$  Hz, 1H), 6.78 (dd,  $J = 7.8, 1.2$  Hz, 1H), 6.62 (d,  $J = 1.4$  Hz, 1H), 4.59 (s, 1H), 3.13 (s, 1H), 2.83 (dt,  $J = 13.4, 6.3$  Hz, 1H), 2.33 (s, 2H), 2.03 (d,  $J = 12.4$  Hz, 2H), 1.96 (d,  $J = 5.4$  Hz, 5H), 1.78 (s, 2H), 1.64 (d,  $J = 12.7$  Hz, 2H), 1.23 (d,  $J = 6.9$  Hz, 6H);  $^{13}\text{C}$  NMR (151 MHz,  $\text{CDCl}_3$ )  $\delta$  153.9, 147.9, 128.9, 128.1, 118.5, 113.7, 44.0, 40.2, 38.2, 33.6, 33.0, 31.3, 28.3, 27.9, 24.1; IR (ATR): 3411, 2901, 2844, 1619, 1420, 1210, 1094, 1056, 947, 854, 830, 729, 645  $\text{cm}^{-1}$ ; HRMS (ESI–):  $m/z$   $[\text{M}-\text{H}]^-$  calculated for  $\text{C}_{19}\text{H}_{25}\text{O}$ : 269.1911; found 269.1922.

### 2-(1-Adamant-1-yl)ethyl)-5-phenylphenol (**321**)



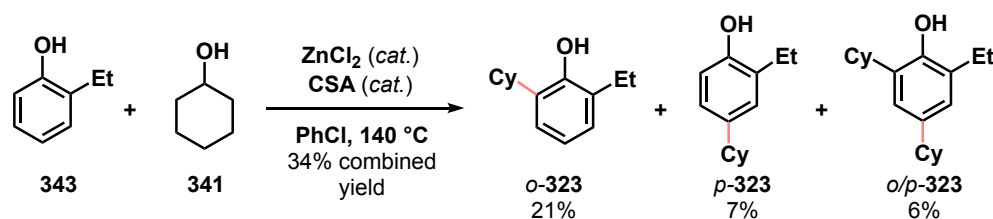
Prepared using General Procedure B with 3-phenylphenol (90% technical grade, 38.1 mg, 0.201 mmol, 1 equiv), ZnCl<sub>2</sub> (1.5 mg, 0.011 mmol, 0.05 equiv), PhCl (0.2 mL, 1.0 M), 1-(adamant-1-yl)ethanol (**2f**) (72.4 mg, 0.401 mmol, 2 equiv), and CSA•H<sub>2</sub>O (37.7 mg, 0.151 mmol, 0.75 equiv). Purification by two cycles of preparatory TLC (eluting with 19:1 hexanes/EtOAc) afforded **321** (25.1 mg, 38%) as an orange-white solid. M.p. 160–162 °C; R<sub>f</sub>: 0.19 (19:1 hexanes/EtOAc); <sup>1</sup>H NMR (500 MHz, CDCl<sub>3</sub>) δ 7.61–7.52 (m, 2H), 7.42 (t, J = 7.5 Hz, 2H), 7.32 (t, J = 7.4 Hz, 1H), 7.20–7.11 (m, 2H), 7.02 (d, J = 1.9 Hz, 1H), 4.73 (s, 1H), 2.84 (q, J = 7.3 Hz, 1H), 1.95 (s, 4H), 1.71–1.48 (m, 11H), 1.22 (d, J = 7.2 Hz, 3H); <sup>13</sup>C NMR (151 MHz, CDCl<sub>3</sub>) δ 153.8, 140.7, 139.7, 129.9, 129.6, 128.8, 127.3, 127.0, 119.1, 113.8, 41.1, 39.8, 37.3, 36.4, 28.9, 14.4; IR (ATR): 3556, 2903, 2885, 2845, 1484, 1447, 1407, 1310, 1220, 1184, 1176, 1115, 1106, 1029, 901, 855, 932, 760, 745, 712, 697, 673, 647, 623, 509 cm<sup>-1</sup>; HRMS (ESI+): m/z [M+H]<sup>+</sup> calculated for C<sub>24</sub>H<sub>28</sub>O: 333.2213; found 333.2200.

### 2-(Adamant-2-yl)-5-phenylphenol (**322**)



Prepared using General Procedure C with 3-phenylphenol (90% technical grade, 37.9 mg, 0.200 mmol, 1 equiv), ZnCl<sub>2</sub> (1.3 mg, 9.5 μmol, 0.05 equiv), PhCl (0.2 mL, 1.0 M), adamantan-2-ol (33.6 mg, 0.221 mmol, 1.1 equiv), and CSA•H<sub>2</sub>O (37.8 mg, 0.151 mmol, 0.75 equiv). Purification by flash chromatography (eluting with 0–20% EtOAc in hexanes) afforded **322** (43.0 mg, 64%) as a light orange-white solid. M.p. 104–107 °C; R<sub>f</sub>: 0.34 (9:1 hexanes/EtOAc); <sup>1</sup>H NMR (500 MHz, CDCl<sub>3</sub>) δ 7.60–7.55 (m, 2H), 7.50 (d, J = 8.0 Hz, 1H), 7.42 (t, J = 7.6

Hz, 2H), 7.32 (t,  $J = 7.3$  Hz, 1H), 7.16 (dd,  $J = 8.8, 1.1$  Hz, 1H), 6.99 (d,  $J = 1.9$  Hz, 1H), 4.77 (s, 1H), 3.22 (s, 1H), 2.39 (s, 2H), 2.07 (d,  $J = 12.8$  Hz, 2H), 2.01–1.98 (m, 4H), 1.90 (s, 1H), 1.80 (s, 2H), 1.68 (d,  $J = 12.5$  Hz, 2H), 1.25 (s, 1H);  $^{13}\text{C}$  NMR (151 MHz,  $\text{CDCl}_3$ )  $\delta$  154.3, 140.7, 139.9, 130.8, 128.8, 128.7, 127.3, 127.0, 119.2, 114.3, 44.1, 40.1, 38.1, 33.0, 31.3, 28.3, 27.9; IR (ATR): 3510, 2897, 2845, 1563, 1485, 1448, 1406, 1172, 1108, 857, 758, 694  $\text{cm}^{-1}$ ; HRMS (ESI $^-$ ):  $m/z$   $[\text{M}-\text{H}]^-$  calculated for  $\text{C}_{22}\text{H}_{23}\text{O}$ : 303.1765; found 303.1765.



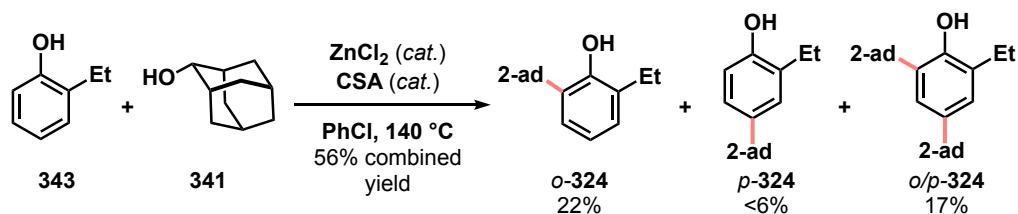
The reaction was performed using General Procedure B with 2-ethylphenol (23.5  $\mu\text{L}$ , 0.20 mmol, 1 equiv),  $\text{ZnCl}_2$  (1.4 mg, 0.01 mmol, 0.05 equiv),  $\text{PhCl}$  (0.2 mL, 1.0 M), cyclohexanol (62.5  $\mu\text{L}$ , 0.6 mmol, 3 equiv), and CSA (35 mg, 0.15 mmol, 0.75 equiv). Purification by preparative TLC (eluting with 19:1 hexanes/ $\text{EtOAc}$ ) afforded an inseparable 3:1 mixture of **323** (8.7 mg, 21%, 25% brsm) and dialkylated *S*-*o/p*-**323** (3.7 mg, 6%, 8% brsm) with compound **323** being the major product. The mono-*para*-substituted *S*-*p*-**323** (7%, 9% brsm) was observed as a minor product.

**2-Cyclohexyl-6-ethylphenol (323):**  $^1\text{H}$  NMR (600 MHz,  $\text{CDCl}_3$ )  $\delta$  7.06 (dd,  $J = 7.7, 1.7$  Hz, 1H), 7.00 (dd,  $J = 7.4, 1.7$  Hz, 1H), 6.87 (t,  $J = 7.7$  Hz, 1H), 4.71 (s, 1H), 2.77 (qd,  $J = 7.2, 3.2$  Hz, 1H), 2.63 (q,  $J = 7.6$  Hz, 2H), 2.07–1.91 (m, 4H), 1.84–1.70 (m, 2H), 1.49–1.35 (m, 4H), 1.26 (t,  $J = 7.6$  Hz, 3H);  $^{13}\text{C}$  NMR (151 MHz,  $\text{CDCl}_3$ )  $\delta$  150.7, 133.1, 129.2, 126.4, 124.5, 120.7, 37.7, 33.4, 27.2, 26.4, 23.3, 14.0. IR (ATR): 3574, 3038,

2963, 1448, 1187, 774  $\text{cm}^{-1}$ ; HRMS (ESI<sup>+</sup>):  $m/z$   $[\text{M}+\text{H}]^+$  calculated for  $\text{C}_{14}\text{H}_{21}\text{O}$ : 205.1587; found: 205.1579.

**2,4-Dicyclohexyl-6-ethylphenol (S-*o/p*-323):**  $^1\text{H}$  NMR (600 MHz,  $\text{CDCl}_3$ )  $\delta$  6.89 (d,  $J = 2.2$  Hz, 1H), 6.84 (d,  $J = 2.2$  Hz, 1H), 4.56 (s, 1H), 2.80 (qd,  $J = 7.2, 3.2$  Hz, 2H), 2.77 (qd,  $J = 7.2, 3.2$  Hz, 1H), 2.63 (q,  $J = 7.6$  Hz, 2H), 2.07–1.91 (m, 4H), 1.84–1.70 (m, 2H), 1.49–1.35 (m, 4H), 1.26 (t,  $J = 7.6$  Hz, 3H);  $^{13}\text{C}$  NMR (151 MHz,  $\text{CDCl}_3$ )  $\delta$  148.7, 140.3, 132.8, 128.8, 124.7, 122.8, 44.3, 37.8, 35.0, 33.4, 27.3, 27.2, 26.5, 26.4, 23.5, 14.1. IR (ATR): 3574, 3038, 2963, 1448, 1187, 774  $\text{cm}^{-1}$ ; HRMS (ESI<sup>+</sup>):  $m/z$   $[\text{M}+\text{H}]^+$  calculated for  $\text{C}_{20}\text{H}_{31}\text{O}$ : 287.2369; found: 287.2359.

**4-Cyclohexyl-2-ethylphenol/4-cyclohexyl-2-ethylphenol (S-*p*-323):** Isolated as an inseparable 2:1 mixture of **343/S-*p*-323** with compound **343** being the major product. The  $^1\text{H}$  NMR data can be extracted from the NMR spectrum of the mixture (600 MHz,  $\text{CDCl}_3$ )  $\delta$  6.98 (d,  $J = 2.2$  Hz, 1H), 6.92 (dd,  $J = 8.1, 2.2$  Hz, 1H), 6.69 (d,  $J = 8.1$  Hz, 1H), 4.53 (s, 1H), 2.63 (q,  $J = 7.6$  Hz, 2H) 2.41 (d,  $J = 10.9$  Hz, 1H), 1.88–1.79 (m, 2H), 1.73 (d,  $J = 13.3$  Hz, 2H), 1.62 (d,  $J = 25.8$  Hz, 2H), 1.49–1.35 (m, 4H), 1.26 (t,  $J = 7.6$  Hz, 3H).



The reaction was performed using General Procedure C with 2-ethylphenol (23.5  $\mu\text{L}$ , 0.20 mmol, 1 equiv),  $\text{ZnCl}_2$  (1.4 mg, 0.01 mmol, 0.05 equiv),  $\text{PhCl}$  (0.2 mL, 1.0 M), 2-adamantanol (33.5 mg, 0.22 mmol, 1.1 equiv), and CSA (35 mg, 0.15 mmol, 0.75 equiv).

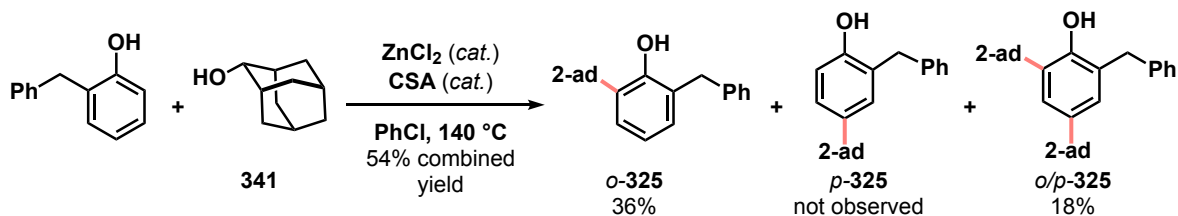
Purification by preparative TLC (eluting with 19:1 hexanes/EtOAc) afforded an inseparable 2:1 mixture of **324** (16.9 mg, 33%) and dialkylated *S-o/p*-**324** (13.2 mg, 17%) with compound **324** being the major product. The mono-para-substituted *S-p*-**324** (<6%) was observed as a minor product.

**2-(Adamantan-2-yl)-6-ethylphenol (324):**  $^1\text{H}$  NMR (500 MHz,  $\text{CDCl}_3$ )  $\delta$  7.32 (d,  $J = 7.8$  Hz, 1H), 7.03 (d,  $J = 7.5$  Hz, 1H), 6.87 (t,  $J = 7.6$  Hz, 1H), 4.70 (s, 1H), 3.17 (s, 1H), 2.62 (q,  $J = 7.6$  Hz, 2H), 2.34 (s, 2H), 2.08–1.93 (m, 7H), 1.92–1.84 (m, 2H), 1.79 (s, 2H), 1.67 (d,  $J = 12.6$  Hz, 2H) 1.25 (t,  $J = 7.5$  Hz, 3H);  $^{13}\text{C}$  NMR (151 MHz,  $\text{CDCl}_3$ )  $\delta$  150.7, 131.1, 129.2, 126.5, 125.8, 120.0, 44.4, 40.3, 38.2, 33.0, 31.4, 28.3, 27.9, 23.2, 14.0. IR (ATR): 3600, 3046, 2901, 1450, 1187, 735  $\text{cm}^{-1}$ ; HRMS (ESI+):  $m/z$   $[\text{M}+\text{H}]^+$  calculated for  $\text{C}_{18}\text{H}_{25}\text{O}$ : 257.1900; found: 257.1892.

**2,4-(Diadamantan-2-yl)-6-ethylphenol (S-o/p-324):**  $^1\text{H}$  NMR (500 MHz,  $\text{CDCl}_3$ )  $\delta$  7.29 (d,  $J = 2.2$  Hz, 1H), 6.98 (d,  $J = 2.2$  Hz, 1H), 4.55 (s, 1H), 3.17 (s, 1H), 2.96 (s, 1H), 2.62 (q,  $J = 7.6$  Hz, 2H), 2.34 (s, 4H), 2.08–1.93 (m, 16H), 1.79 (s, 4H), 1.67 (d,  $J = 12.6$  Hz, 4H) 1.25 (t,  $J = 7.5$  Hz, 3H);  $^{13}\text{C}$  NMR (151 MHz,  $\text{CDCl}_3$ )  $\delta$  149.2, 135.4, 130.5, 128.6, 124.9, 124.2, 46.5, 44.5, 40.3, 39.4, 38.2, 33.2, 33.0, 32.1, 31.5, 31.4, 28.4, 28.3, 28.0, 27.9, 23.7, 14.3. IR (ATR): 3600, 3046, 2901, 1450, 1187, 735  $\text{cm}^{-1}$ ; HRMS (ESI+):  $m/z$   $[\text{M}+\text{H}]^+$  calculated for  $\text{C}_{28}\text{H}_{39}\text{O}$ : 391.2995; found: 391.2985.

**4-(Adamantan-2-yl)-2-ethylphenol (S-p-324):** Isolated as an inseparable 1:1 mixture of an unidentifiable product and *S-p*-**324**. The  $^1\text{H}$  NMR data can be extracted from the NMR spectrum of the mixture (500 MHz,  $\text{CDCl}_3$ )  $\delta$  7.10 (d,  $J = 2.4$  Hz, 1H), 7.05 (dd,  $J = 8.5$ , 2.2 Hz, 1H), 6.73 (d,  $J = 8.2$  Hz, 1H), 4.51 (s, 1H), 2.93 (s, 1H), 2.63 (q,  $J = 7.6$  Hz, 2H),

2.41 (s, 2H), 2.18 – 1.90 (m, 11H), 1.76 (s, 4H), 1.54 (d,  $J = 12.8$  Hz, 4H), 1.24 (t,  $J = 7.6$  Hz, 3H).

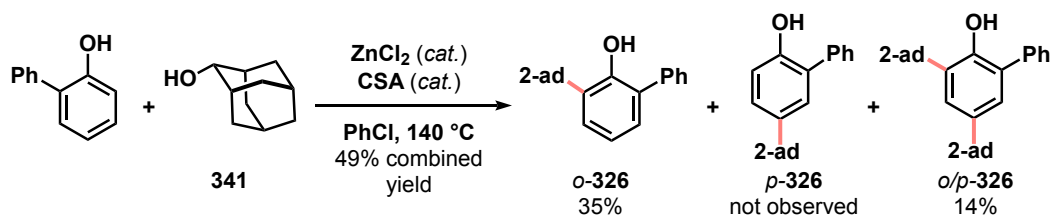


### 2-(Adamantan-2-yl)-6-benzylphenol (*o*-325)

Prepared using General Procedure C with 2-benzylphenol (36.8 mg, 0.20 mmol, 1 equiv), ZnCl<sub>2</sub> (1.4 mg, 0.01 mmol, 0.05 equiv), PhCl (0.2 mL, 1.0 M), 2-adamantanol (33.5 mg, 0.22 mmol, 1.1 equiv), and CSA (35 mg, 0.15 mmol, 0.75 equiv). Purification by preparative TLC (eluting with 19:1 hexanes/Et<sub>2</sub>O) afforded an inseparable 2:1 mixture (54% overall yield, 38.7 mg) of *o*-**325** (22.6 mg, 36%, 46% brsm) and dialkylated *S*-*o/p*-**325** (16.1 mg, 18%, 23% brsm) with compound *o*-**325** being the major product. The *para*-substituted product was not observed by NMR analysis of the crude reaction mixture nor isolated. <sup>1</sup>H NMR of *o*-**325** (400 MHz, CDCl<sub>3</sub>) δ 7.38 (dd,  $J = 7.6, 1.4$  Hz, 1H), 7.33–7.27 (m, 2H), 7.24–7.18 (m, 3H), 7.01 (dd,  $J = 7.4, 1.7$  Hz, 1H), 6.89 (t,  $J = 7.6$  Hz, 1H), 4.65 (s, 1H), 4.00 (s, 2H), 3.14 (s, 1H), 2.30 (q,  $J = 2.9$  Hz, 2H), 2.14–1.92 (m, 7H), 1.88 (dt,  $J = 6.5, 3.2$  Hz, 1H), 1.78 (d,  $J = 3.3$  Hz, 2H), 1.65 (dtt,  $J = 12.7, 2.5, 1.2$  Hz, 2H); <sup>13</sup>C NMR (101 MHz, CDCl<sub>3</sub>) δ 152.4, 139.7, 132.0, 128.9, 128.7, 128.5, 126.7, 126.6, 126.4, 120.1, 44.3, 40.2, 38.1, 37.2, 33.0, 31.4, 28.3, 27.8. IR (ATR): 3544, 2898, 1449, 1187, 730 cm<sup>-1</sup>; HRMS (ESI<sup>+</sup>):  $m/z$  [M+H]<sup>+</sup> calculated for C<sub>23</sub>H<sub>27</sub>O: 319.2056; found: 319.2055.

### 2,4-Diadamantan-2-yl-6-benzylphenol (*S-o/p*-325)

The  $^1\text{H}$  NMR data can be extracted from the NMR spectrum of the mixture (500 MHz,  $\text{CDCl}_3$ )  $\delta$  7.36 (s, 1H), 7.33–7.27 (m, 2H), 7.24–7.18 (m, 3H), 7.04 (s, 1H), 4.67 (s, 1H), 4.00 (s, 2H), 3.14 (s, 2H), 2.30 (q,  $J = 2.9$  Hz, 4H), 2.08–1.92 (m, 14H), 1.90 (dt,  $J = 6.5$ , 3.2 Hz, 2H), 1.78 (d,  $J = 3.3$  Hz, 4H), 1.65 (dtt,  $J = 12.7$ , 2.5, 1.2 Hz, 4H).



### 2-(Adamantan-2-yl)-6-phenylphenol (*o*-326)

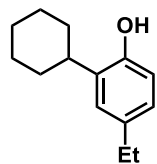
Prepared using General Procedure C with 2-phenylphenol (34 mg, 0.20 mmol, 1 equiv),  $\text{ZnCl}_2$  (1.4 mg, 0.01 mmol, 0.05 equiv),  $\text{PhCl}$  (0.2 mL, 1.0 M), 2-adamantanol (33.5 mg, 0.22 mmol, 1.1 equiv), and CSA (35 mg, 0.15 mmol, 0.75 equiv). Purification by preparative TLC (eluting with 19:1 hexanes/ $\text{Et}_2\text{O}$ ) afforded an inseparable 5:2 mixture (49% overall yield, 33.9 mg) of *o*-326 (21.5 mg, 35%) and dialkylated *S-o/p*-326 (12.4 mg, 14%) with compound *o*-326 being the major product. The para-substituted product was not observed by NMR analysis of the crude reaction mixture.  $^1\text{H}$  NMR of *o*-326 (400 MHz,  $\text{CDCl}_3$ )  $\delta$  7.53–7.43 (m, 5H), 7.40 (t,  $J = 7.0$  Hz, 1H), 7.09 (dd,  $J = 7.5$ , 1.7 Hz, 1H), 6.97 (t,  $J = 7.6$  Hz, 1H), 5.32 (s, 1H), 3.31 (s, 1H), 2.30 (q,  $J = 2.9$  Hz, 2H), 2.14–1.92 (m, 7H), 1.88 (dt,  $J = 6.5$ , 3.2 Hz, 3H), 1.78 (d,  $J = 3.3$  Hz, 1H), 1.65 (dtt,  $J = 12.7$ , 2.5, 1.2 Hz, 1H);  $^{13}\text{C}$  NMR (151 MHz,  $\text{CDCl}_3$ )  $\delta$  150.7, 137.6, 132.4, 129.5, 128.0, 127.9, 127.5, 126.3, 125.8, 119.9, 44.4, 40.2, 38.2, 33.2, 31.3, 28.4, 28.0. IR (ATR): 3547, 2900,

2847, 1467, 1196, 907, 733  $\text{cm}^{-1}$ ; HRMS (ESI+):  $m/z$   $[\text{M}+\text{H}]^+$  calculated for  $\text{C}_{22}\text{H}_{25}\text{O}$ : 305.1900; found: 319.1900.

### 2,4-Diadamantan-2-yl-6-phenylphenol (S-o/p-326)

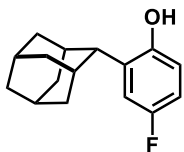
The  $^1\text{H}$  NMR data can be extracted from the NMR spectrum of the mixture (400 MHz,  $\text{CDCl}_3$ )  $\delta$  7.53–7.43 (m, 5H), 7.37 (s, 1H), 7.05 (s, 1H), 5.18 (s, 1H), 3.30 (s, 2H), 2.40 (q,  $J = 2.9$  Hz, 4H), 2.11–2.05 (m, 14H), 2.01–1.88 (dt,  $J = 6.5, 3.2$  Hz, 6H), 1.80 (d,  $J = 5.0$  Hz, 2H), 1.68 (dtd,  $J = 12.8, 2.9, 1.4$  Hz, 2H).

### 2-Cyclohexyl-4-ethylphenol (327)



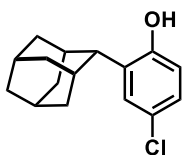
Prepared using General Procedure B with 4-ethylphenol (25.3 mg, 0.2022 mmol, 1 equiv),  $\text{ZnCl}_2$  (0.3 mg, 2.2  $\mu\text{mol}$ , 0.01 equiv),  $\text{PhCl}$  (0.2 mL, 1.0 M), cyclohexanol (62.5  $\mu\text{L}$ , 0.6 mmol, 3 equiv), and  $\text{CSA}\cdot\text{H}_2\text{O}$  (37.6 mg, 0.150 mmol, 0.75 equiv). Purification by preparative TLC (eluting with 19:1 hexanes/ $\text{EtOAc}$ ) afforded **327** (16.9 mg, 41%) as a yellow oil.  $R_f$ : 0.26 (19:1 hexanes/ $\text{EtOAc}$ );  $^1\text{H}$  NMR (500 MHz,  $\text{CDCl}_3$ )  $\delta$  7.03 (d,  $J = 2.2$  Hz, 1H), 6.91 (dd,  $J = 8.1, 2.2$  Hz, 1H), 6.70 (d,  $J = 8.1$  Hz, 1H), 4.75 (s, 1H), 2.81 (tt,  $J = 11.5, 3.0$  Hz, 1H), 2.59 (q,  $J = 7.6$  Hz, 2H), 1.93–1.84 (m, 4H), 1.82–1.76 (m, 1H), 1.52–1.39 (m, 4H), 1.35–1.26 (m, 1H), 1.23 (t,  $J = 7.6$  Hz, 3H);  $^{13}\text{C}$  NMR (151 MHz,  $\text{CDCl}_3$ )  $\delta$  150.7, 136.7, 133.5, 126.5, 125.8, 115.3, 37.5, 33.3, 28.4, 27.2, 26.5, 16.1; IR (ATR): 3341, 2923, 2850, 1504, 1447, 813  $\text{cm}^{-1}$ ; HRMS (ESI+):  $m/z$   $[\text{M}+\text{H}]^+$  calculated for  $\text{C}_{14}\text{H}_{21}\text{O}$ : 205.1587; found: 205.1581.

### 2-(Adamant-2-yl)-4-fluorophenol (**328**)



Prepared using General Procedure C with 3-phenylphenol (22.5 mg, 0.200 mmol, 1 equiv), ZnCl<sub>2</sub> (1.7 mg, 0.012 mmol, 0.05 equiv), PhCl (0.2 mL, 1.0 M), adamantan-2-ol (33.7 mg, 0.221 mmol, 1.1 equiv), and CSA•H<sub>2</sub>O (37.4 mg, 0.150 mmol, 0.75 equiv). Purification by preparatory TLC (eluting with 9:1 hexanes/EtOAc) afforded **328** (15.2 mg, 31%) as a yellow solid. M.p. 90–93 °C; R<sub>f</sub>: 0.32 (9:1 hexanes/EtOAc); <sup>1</sup>H NMR (500 MHz, CDCl<sub>3</sub>) δ 7.15 (dd, J = 10.6, 3.0 Hz, 1H), 6.76 (td, J = 8.2, 3.1 Hz, 1H), 6.66 (dd, J = 8.7, 5.0 Hz, 1H), 4.60 (s, 1H), 3.14 (s, 1H), 2.32 (s, 2H), 2.09 (d, J = 11.6 Hz, 1H), 2.00–1.95 (m, 6H), 1.88 (s, 1H), 1.78 (s, 2H), 1.65 (d, J = 12.8 Hz, 2H); <sup>13</sup>C NMR (151 MHz, CDCl<sub>3</sub>) δ 157.4 (d, J = 236.7 Hz), 149.9, 133.6, 115.9 (d, J = 8.3 Hz), 115.3 (d, J = 23.8 Hz), 112.5 (d, J = 23.2 Hz), 44.3, 40.0, 38.0, 32.8, 31.1, 28.2, 27.7; <sup>19</sup>F NMR (564 MHz, CDCl<sub>3</sub>) δ –124.0; IR (ATR): 3406, 2900, 2847, 1698, 1502, 1427, 1341, 1252, 1178, 1165, 1115, 983, 956, 871, 821, 803, 746, 570, 473 cm<sup>-1</sup>; HRMS (ESI<sup>-</sup>): m/z [M–H]<sup>-</sup> calculated for C<sub>16</sub>H<sub>18</sub>FO: 245.1347; found 245.1359.

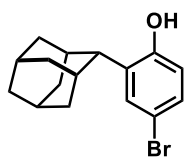
### 2-(Adamant-2-yl)-4-chlorophenol (**329**)



Prepared using General Procedure C with 4-chlorophenol (26.1 mg, 0.203 mmol, 1 equiv), ZnCl<sub>2</sub> (1.4 mg, 0.10 mmol, 0.05 equiv), chlorobenzene (0.2 mL, 1.0 M), adamantan-2-ol (33.6 mg, 0.221 mmol, 1.1 equiv), and CSA•H<sub>2</sub>O (37.8 mg, 0.151 mmol, 0.75 equiv). Purification by flash chromatography (eluting with 0–20% EtOAc in hexanes) afforded **329** (21.4 mg, 41%) as a yellow. R<sub>f</sub>: 0.30 (9:1 hexanes/EtOAc); <sup>1</sup>H NMR (500 MHz, CDCl<sub>3</sub>) δ 7.37 (d, J = 2.5

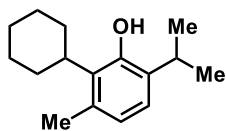
Hz, 1H), 7.04 (dd,  $J = 8.5, 2.5$  Hz, 1H), 6.66 (d,  $J = 8.4$  Hz, 1H), 4.70 (s, 1H), 3.13 (s, 1H), 2.32 (s, 2H), 2.01–1.94 (m, 7H), 1.89 (s, 1H), 1.78 (s, 2H), 1.65 (d,  $J = 12.8$  Hz, 2H);  $^{13}\text{C}$  NMR (151 MHz,  $\text{CDCl}_3$ )  $\delta$  153.3, 134.0, 128.3, 126.1, 124.8, 116.4, 44.1, 40.0, 38.1, 32.9, 30.9, 28.2, 27.8; IR (ATR): 3411, 2898, 2847, 1697, 1491, 1409, 1341, 1212, 1166, 1111, 919, 972, 806, 721, 676, 657, 472  $\text{cm}^{-1}$ ; HRMS (ESI $^-$ ):  $m/z$   $[\text{M}-\text{H}]^-$  calculated for  $\text{C}_{16}\text{H}_{18}\text{ClO}$ : 261.1052; found 261.1063.

### 2-(Adamant-2-yl)-4-bromophenol (**330**)



Prepared using General Procedure C with 4-bromophenol (34.7 mg, 0.200 mmol, 1 equiv),  $\text{ZnCl}_2$  (1.5 mg, 0.11 mmol, 0.05 equiv), chlorobenzene (0.2 mL, 1.0 M), adamantan-2-ol (33.7 mg, 0.221 mmol, 1.1 equiv), and  $\text{CSA}\cdot\text{H}_2\text{O}$  (37.4 mg, 0.150 mmol, 0.75 equiv). Purification by preparatory TLC (eluting with 9:1 hexanes/EtOAc) afforded **330** (18.6 mg, 35%) as an orange-brown oil.  $R_f$ : 0.38 (9:1 hexanes/EtOAc);  $^1\text{H}$  NMR (600 MHz,  $\text{CDCl}_3$ )  $\delta$  7.50 (d,  $J = 2.5$  Hz, 1H), 7.20–7.15 (m, 1H), 6.62 (dd,  $J = 8.6, 1.6$  Hz, 1H), 4.68 (s, 1H), 3.14 (s, 1H), 2.32 (s, 2H), 2.02–1.92 (m, 7H), 1.89 (s, 1H), 1.78 (s, 2H), 1.65 (d,  $J = 12.7$  Hz, 2H);  $^{13}\text{C}$  NMR (151 MHz,  $\text{CDCl}_3$ )  $\delta$  153.2, 134.2, 131.3, 129.4, 117.2, 113.0, 44.2, 40.0, 38.0, 32.8, 31.0, 28.1, 27.7; IR (ATR): 3299, 2900, 1411, 1087, 1045, 879, 627  $\text{cm}^{-1}$ ; HRMS (ESI $^-$ ):  $m/z$   $[\text{M}-\text{H}]^-$  calculated for  $\text{C}_{16}\text{H}_{18}\text{BrO}$ : 305.0547; found 305.0551.

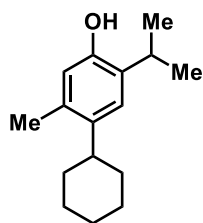
### 2-Cyclohexyl-6-isopropyl-3-methylphenol (**331**)



Prepared using General Procedure B with thymol (30 mg, 0.20 mmol, 1 equiv),  $\text{ZnCl}_2$  (1.4 mg, 0.01 mmol, 0.05 equiv), chlorobenzene (0.2 mL, 1.0 M), cyclohexanol (62.5  $\mu\text{L}$ , 0.6 mmol, 3.0 equiv), and CSA (35 mg, 0.15 mmol,

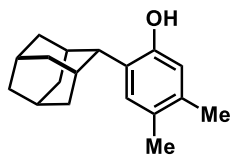
0.75 equiv). Purification by preparative TLC (eluting with 19:1 hexanes/EtOAc) afforded **331** (14.5 mg, 31%, 47% brsm) as a colorless oil. The mono-para-substituted product **S-p-331** was observed as a minor product (10%, 16% brsm).  $^1\text{H}$  NMR (500 MHz,  $\text{CDCl}_3$ )  $\delta$  6.94 (d,  $J = 7.9$  Hz, 1H), 6.73 (d,  $J = 7.7$  Hz, 1H), 4.84 (s, 1H), 3.05 (p,  $J = 6.8$  Hz, 1H), 2.90 (s, 1H), 2.32 (s, 3H), 2.04 (q,  $J = 9.9$  Hz, 2H), 1.86 (d,  $J = 12.5$  Hz, 2H), 1.74 (dd,  $J = 24.5, 12.1$  Hz, 3H), 1.38 (q,  $J = 12.5$  Hz, 3H), 1.26 (d,  $J = 6.8$  Hz, 6H);  $^{13}\text{C}$  NMR (151 MHz,  $\text{CDCl}_3$ )  $\delta$  152.0, 134.7, 132.2, 130.9, 123.1, 120.6, 39.9, 34.4, 30.3, 27.0, 26.5, 22.9, 21.0. IR (ATR): 3620, 2922, 1574, 1486, 767  $\text{cm}^{-1}$ ; HRMS (ESI+):  $m/z$   $[\text{M}+\text{H}]^+$  calculated for  $\text{C}_{16}\text{H}_{25}\text{O}$ : 233.1900; found: 233.1908.

#### 4-(Cyclohexyl)-2-isopropyl-5-methylphenol (**S-p-331**)



Isolated as an inseparable 3:1 mixture of thymol and **S-p-331** with thymol being the major product. The  $^1\text{H}$  NMR data can be extracted from the NMR spectrum of the mixture (600 MHz,  $\text{CDCl}_3$ ) 7.03 (s, 1H), 6.55 (s, 1H), 4.57 (s, 1H), 3.05 (p,  $J = 6.8$  Hz, 1H), 2.90 (s, 1H), 2.62 (m, 1H), 2.25 (s, 3H), 1.85 (m, 1H), 1.78 (m, 2H), 1.66 (dd,  $J = 24.5, 12.1$  Hz, 3H), 1.38 (q,  $J = 12.5$  Hz, 3H), 1.26 (d,  $J = 6.8$  Hz, 6H).

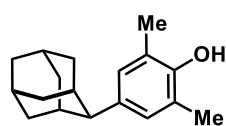
#### 2-(Adamant-2-yl)-4,5-dimethylphenol (**332**)

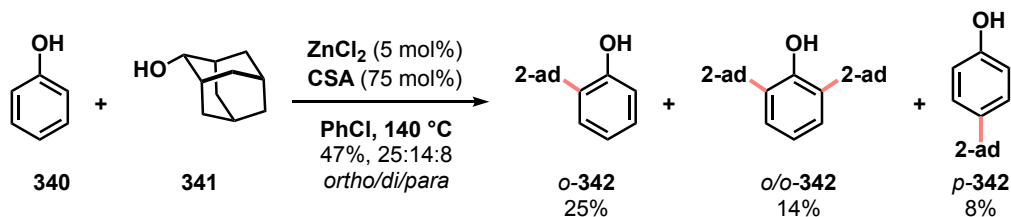


Prepared using General Procedure C with 3,4-xyleneol (24.5 mg, 0.200 mmol, 1 equiv),  $\text{ZnCl}_2$  (1.3 mg, 9.5  $\mu\text{mol}$ , 0.05 equiv), chlorobenzene (0.2 mL, 1.0 M), adamantan-2-ol (33.6 mg, 0.221 mmol, 1.1 equiv), and  $\text{CSA}\cdot\text{H}_2\text{O}$  (37.5 mg, 0.150 mmol, 0.75 equiv). Purification by preparatory TLC (eluting with 9:1 hexanes/EtOAc) afforded **332** (26.9 mg, 52%) as a light brown-white solid. M.p.

105–107 °C;  $R_f$ : 0.38 (19:1 hexanes/EtOAc);  $^1\text{H NMR}$  (500 MHz,  $\text{CDCl}_3$ )  $\delta$  7.17 (s, 1H), 6.55 (s, 1H), 4.42 (s, 1H), 3.13 (s, 1H), 2.34–2.30 (m, 2H), 2.20 (s, 3H), 2.18 (s, 3H), 2.07–2.01 (m, 2H), 1.99–1.94 (m, 5H), 1.88–1.86 (m, 1H), 1.78 (s, 2H), 1.64 (d,  $J = 12.6$  Hz, 2H);  $^{13}\text{C NMR}$  (151 MHz,  $\text{CDCl}_3$ )  $\delta$  151.8, 134.7, 129.5, 128.7, 128.0, 117.0, 43.9, 40.2, 38.2, 33.0, 31.3, 28.3, 27.9, 19.4, 19.3; IR (ATR): 3313, 2898, 2847, 1617, 1449, 1407, 1275, 1198, 1084, 1044, 878, 576, 474  $\text{cm}^{-1}$ ; HRMS (ESI<sup>+</sup>):  $m/z$   $[\text{M}+\text{H}]^+$  calculated for  $\text{C}_{18}\text{H}_{25}\text{O}$ : 257.1900; found 257.1898.

#### 4-(Adamant-2-yl)-2,6-dimethylphenol (**333**)

 Prepared using General Procedure C with 2,6-xylenol (24.6 mg, 0.201 mmol, 1 equiv),  $\text{ZnCl}_2$  (1.3 mg, 9.5  $\mu\text{mol}$ , 0.05 equiv), chlorobenzene (0.2 mL, 1.0 M), adamantan-2-ol (33.6 mg, 0.221 mmol, 1.1 equiv), and  $\text{CSA}\cdot\text{H}_2\text{O}$  (37.7 mg, 0.151 mmol, 0.75 equiv). Purification by flash chromatography (eluting with 0–20% EtOAc in hexanes) afforded **3mh** (34.2 mg, 68%) as a white solid. M.p. 135–139 °C;  $R_f$ : 0.44 (9:1 hexanes/EtOAc);  $^1\text{H NMR}$  (500 MHz,  $\text{CDCl}_3$ )  $\delta$  6.95 (s, 2H), 4.45 (s, 1H), 2.89 (s, 1H), 2.40 (s, 2H), 2.25 (s, 6H), 2.16 (d,  $J = 7.9$  Hz, 1H), 1.98 (d,  $J = 13.0$  Hz, 3H), 1.88 (dd,  $J = 22.6, 12.6$  Hz, 4H), 1.76 (d,  $J = 7.8$  Hz, 3H), 1.52 (s, 1H);  $^{13}\text{C NMR}$  (151 MHz,  $\text{CDCl}_3$ )  $\delta$  149.8, 136.1, 127.1, 122.6, 46.2, 39.3, 38.1, 32.1, 31.2, 28.2, 28.0, 16.3; IR (ATR): 3379, 2897, 2844, 1486, 1447, 1200, 1144, 869, 765, 699, 631  $\text{cm}^{-1}$ ; HRMS (ESI<sup>-</sup>):  $m/z$   $[\text{M}-\text{H}]^-$  calculated for  $\text{C}_{18}\text{H}_{23}\text{O}$ : 255.1754; found 255.1764.



The reaction was performed using General Procedure C with phenol (19.1 mg, 0.203 mmol, 1 equiv), ZnCl<sub>2</sub> (1.4 mg, 0.10 mmol, 0.05 equiv), chlorobenzene (0.2 mL, 1.0 M), adamantan-2-ol (33.7 mg, 0.221 mmol, 1.1 equiv), and CSA•H<sub>2</sub>O (37.7 mg, 0.151 mmol, 0.75 equiv). Purification by preparatory TLC (eluting with 9:1 hexanes/EtOAc) afforded 47% overall yield of three products with **o-242** (12.8 mg, 25%) as an orange oil, **o/o-242** (10.1 mg, 14%) as a yellow-white solid, and **p-242** (4.3 mg, 8%) as a light tan solid.

**2-(Adamant-2-yl)phenol (o-242):** <sup>1</sup>H NMR (500 MHz, CDCl<sub>3</sub>) δ 7.44 (d, J = 7.7 Hz, 1H), 7.11–7.06 (m, 1H), 6.91 (t, J = 7.6 Hz, 1H), 6.75–6.72 (m, 1H), 4.69 (s, 1H), 3.18 (s, 1H), 2.35 (s, 2H), 2.05–1.93 (m, 8H), 1.87 (s, 1H), 1.79 (s, 2H), 1.65 (d, J = 12.6 Hz, 2H). <sup>13</sup>C NMR (151 MHz, CDCl<sub>3</sub>) δ 154.0, 131.7, 128.4, 126.8, 120.5, 115.6, 44.1, 40.1, 38.1, 33.0, 31.2, 28.3, 27.9. The spectral data recorded are consistent with those previously reported.<sup>21</sup>

**2,6-Bis(adamant-2-yl)phenol (o/o-242):** <sup>1</sup>H NMR (500 MHz, CDCl<sub>3</sub>) δ 7.33 (d, J = 7.7 Hz, 2H), 6.90 (t, J = 7.7 Hz, 1H), 4.76 (s, 1H), 3.13 (s, 2H), 2.33–2.29 (m, 4H), 2.05 (d, J = 12.9 Hz, 4H), 2.01–1.95 (m, 10H), 1.90–1.86 (m, 2H), 1.78 (s, 4H), 1.65 (d, J = 12.7 Hz, 4H); <sup>13</sup>C NMR (151 MHz, CDCl<sub>3</sub>) δ 152.3, 131.0, 125.5, 119.5, 44.5, 40.3, 38.1, 33.0, 31.5, 28.3, 27.8; IR (ATR): 3589, 2899, 2847, 1732, 1467, 1451, 1437, 1359, 1340, 1316, 1249, 1217, 1183, 1165, 1116, 1095, 1086, 1061, 1048, 995, 953, 934, 877, 840, 826, 802, 767, 752, 735, 698, 638, 627, 559, 539 cm<sup>-1</sup>; HRMS (ESI<sup>+</sup>): m/z [M+H]<sup>+</sup> calculated for C<sub>26</sub>H<sub>35</sub>O: 363.2682; found 363.2672.

**4-(Adamant-2-yl)phenol (p-242):** <sup>1</sup>H NMR (500 MHz, CDCl<sub>3</sub>) δ 7.21 (d, J = 8.3 Hz, 2H), 6.80 (d, J = 8.3 Hz, 2H), 4.63 (s, 1H), 2.93 (s, 1H), 2.40 (s, 2H), 2.02–1.88 (m, 8H),

1.83 (d,  $J = 12.8$  Hz, 2H), 1.76 (s, 2H). The spectral data recorded are consistent with those previously reported.<sup>21</sup>

### 1-(Cyclohexyl)-4-methoxybenzene (p-348)



Prepared using General Procedure B with anisole (22  $\mu$ L, 0.20 mmol, 1 equiv),  $\text{ZnCl}_2$  (1.4 mg, 0.01 mmol, 0.05 equiv), chlorobenzene (0.2 mL, 1.0 M), cyclohexanol (62.5  $\mu$ L, 0.6 mmol, 3.0 equiv), and CSA (35 mg, 0.15 mmol, 0.75 equiv). Purification by flash chromatography (eluting with 0–20% EtOAc in hexanes) afforded **348** (2.0 mg, 5%) as a colorless oil.  $^1\text{H}$  NMR (500 MHz, Chloroform- $d$ )  $\delta$  7.15 (d,  $J = 8.7$  Hz, 2H), 6.86 (d,  $J = 8.6$  Hz, 2H), 3.81 (s, 3H), 2.47 (t, 1H), 1.86 (dd,  $J = 11.5, 7.6$  Hz, 4H), 1.76 (d,  $J = 13.1$  Hz, 1H), 1.48–1.35 (m, 4H), 0.92–0.83 (m, 2H). The spectral data recorded are consistent with those previously reported.<sup>22</sup>

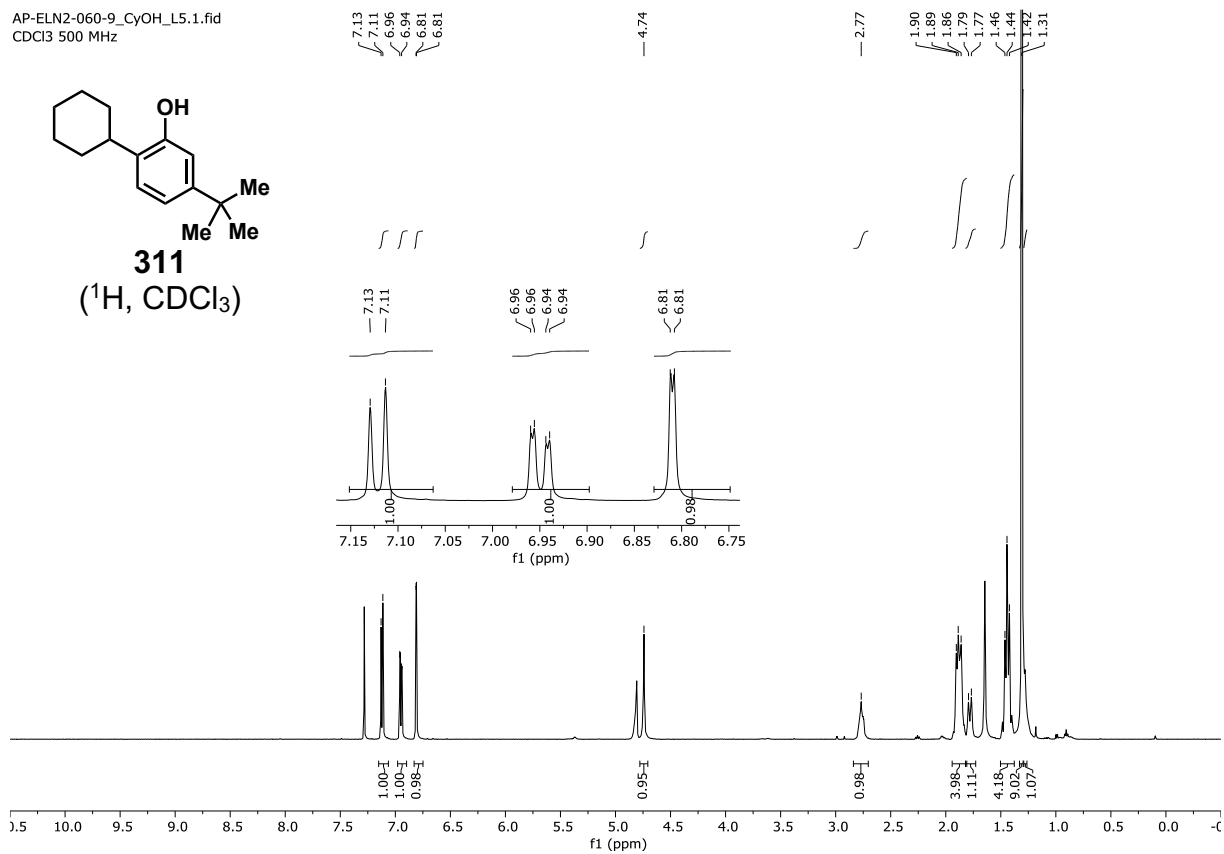
### 3.5 References

- (1) Heravi, M. M.; Zadsirjan, V.; Saedi, P.; Momeni, T. Applications of Friedel–Crafts Reactions in Total Synthesis of Natural Products. *RSC Adv.* **2018**, 8 (70), 40061–40163. <https://doi.org/10.1039/C8RA07325B>.
- (2) Wiley-VCH - Catalytic Asymmetric Friedel-Crafts Alkylations. <https://www.wiley-vch.de/en/areas-interest/natural-sciences/catalytic-asymmetric-friedel-crafts-alkylations-978-3-527-32380-7> (accessed 2023-12-05).
- (3) Surburg, H.; Panten, J. Natural Raw Materials in the Flavor and Fragrance Industry. In *Common Fragrance and Flavor Materials*; John Wiley & Sons, Ltd, 2016; pp 193–264. <https://doi.org/10.1002/9783527693153.ch3>.
- (4) Constable, D. J. C.; Dunn, P. J.; Hayler, J. D.; Humphrey, G. R.; Johnnie L. Leazer, J.; Linderman, R. J.; Lorenz, K.; Manley, J.; Pearlman, B. A.; Wells, A.; Zaks, A.; Zhang, T. Y. Key Green Chemistry Research Areas—a Perspective from Pharmaceutical Manufacturers. *Green Chem.* **2007**, 9 (5), 411–420. <https://doi.org/10.1039/B703488C>.
- (5) Bryan, M. C.; Dunn, P. J.; Entwistle, D.; Gallou, F.; Koenig, S. G.; Hayler, J. D.; Hickey, M. R.; Hughes, S.; Kopach, M. E.; Moine, G.; Richardson, P.; Roschangar, F.; Steven, A.; Weiberth, F. J. Key Green Chemistry Research Areas from a Pharmaceutical Manufacturers’ Perspective Revisited. *Green Chem.* **2018**, 20 (22), 5082–5103. <https://doi.org/10.1039/C8GC01276H>.
- (6) Rueping, M.; Nachtsheim, B. J. A Review of New Developments in the Friedel–Crafts Alkylation – From Green Chemistry to Asymmetric Catalysis. *Beilstein J. Org. Chem.* **2010**, 6 (1), 6. <https://doi.org/10.3762/bjoc.6.6>.
- (7) Chen, L.; Yin, X.-P.; Wang, C.-H.; Zhou, J. Catalytic Functionalization of Tertiary Alcohols to Fully Substituted Carbon Centres. *Org. Biomol. Chem.* **2014**, 12 (32), 6033–6048. <https://doi.org/10.1039/C4OB00718B>.
- (8) Mo, X.; Yakiwchuk, J.; Dansereau, J.; McCubbin, J. A.; Hall, D. G. Unsymmetrical Diarylmethanes by Ferroceniumboronic Acid Catalyzed Direct Friedel–Crafts Reactions with Deactivated Benzylic Alcohols: Enhanced Reactivity Due to Ion-Pairing Effects. *J. Am. Chem. Soc.* **2015**, 137 (30), 9694–9703. <https://doi.org/10.1021/jacs.5b05076>.
- (9) Vuković, V. D.; Richmond, E.; Wolf, E.; Moran, J. Catalytic Friedel–Crafts Reactions of Highly Electronically Deactivated Benzylic Alcohols. *Angew. Chem. Int. Ed.* **2017**, 56 (11), 3085–3089. <https://doi.org/10.1002/anie.201612573>.

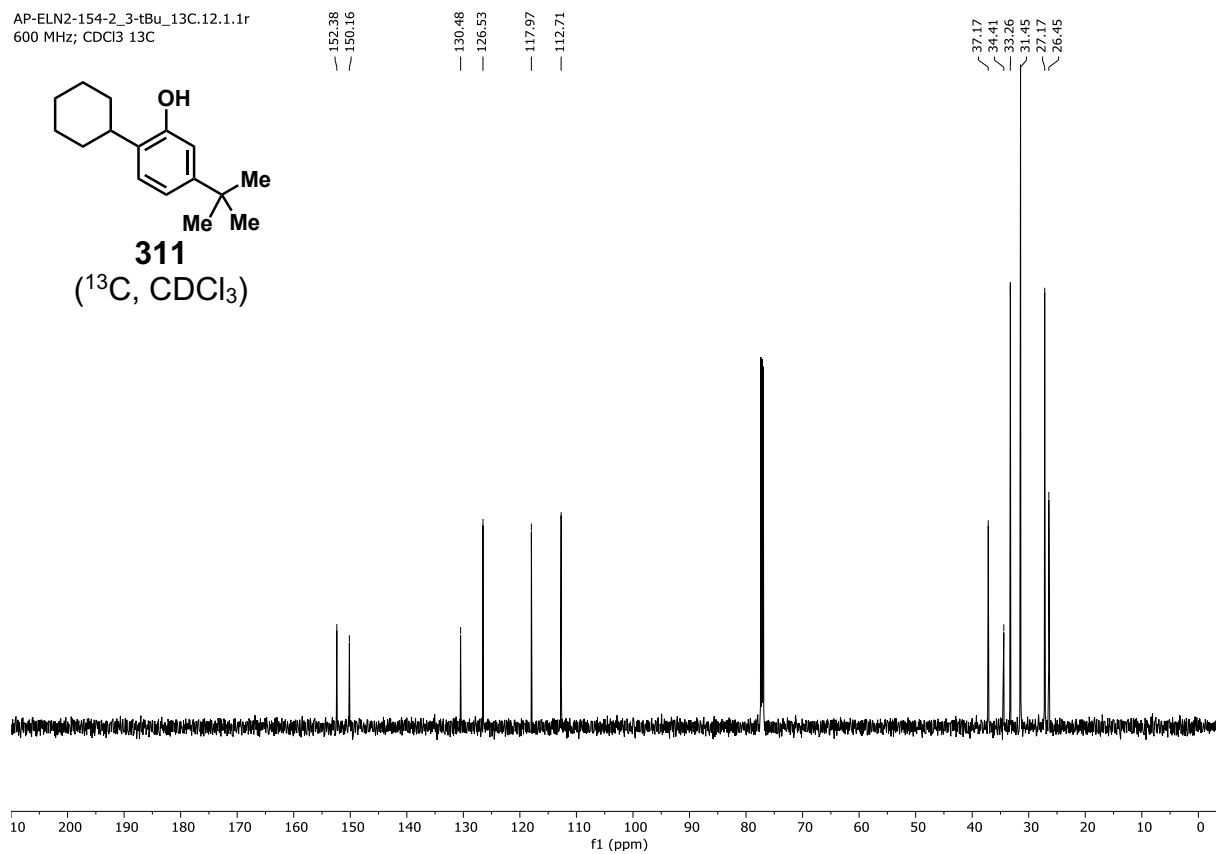
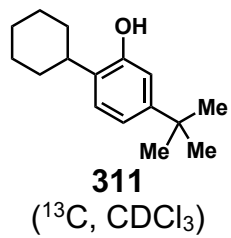
- (10) Oakley, J. V.; Stanley, T. J.; Jesse, K. A.; Melanese, A. K.; Alvarez, A. A.; Prince, A. L.; Cain, S. E.; Wenzel, A. G.; Iafe, R. G. Gold-Catalyzed Friedel–Crafts-Like Reaction of Benzylic Alcohols to Afford 1,1-Diarylalkanes. *Eur. J. Org. Chem.* **2019**, 2019 (42), 7063–7066. <https://doi.org/10.1002/ejoc.201901082>.
- (11) Iovel, I.; Mertins, K.; Kischel, J.; Zapf, A.; Beller, M. An Efficient and General Iron-Catalyzed Arylation of Benzyl Alcohols and Benzyl Carboxylates. *Angew. Chem. Int. Ed.* **2005**, 44 (25), 3913–3917. <https://doi.org/10.1002/anie.200462522>.
- (12) Zhang, S.; Vayer, M.; Noël, F.; Vuković, V. D.; Golushko, A.; Rezajooei, N.; Rowley, C. N.; Leboeuf, D.; Moran, J. Unlocking the Friedel–Crafts Arylation of Primary Aliphatic Alcohols and Epoxides Driven by Hexafluoroisopropanol. *Chem* **2021**, 7 (12), 3425–3441. <https://doi.org/10.1016/j.chempr.2021.10.023>.
- (13) Pan, A.; Chojnacka, M.; Crowley, R.; Göttemann, L.; Haines, B. E.; Kou, K. G. M. Synergistic Brønsted/Lewis Acid Catalyzed Aromatic Alkylation with Unactivated Tertiary Alcohols or Di-Tert-Butylperoxide to Synthesize Quaternary Carbon Centers. *Chem. Sci.* **2022**, 13 (12), 3539–3548. <https://doi.org/10.1039/D1SC06422C>.
- (14) Crowley III, R.; Lujan, B.; Martinez, A.; Manasi, R.; DeBow, J. D.; Kou, K. G. M. A Fenton Approach to Aromatic Radical Cations and Diarylmethane Synthesis. *J. Org. Chem.* **2023**, 88 (21), 15060–15066. <https://doi.org/10.1021/acs.joc.3c01505>.
- (15) Bartlett, J. F.; Garland, C. E. Some Nitrocyclohexylphenols and Their Derivatives I. *J. Am. Chem. Soc.* **1933**, 55 (5), 2064–2068. <https://doi.org/10.1021/ja01332a046>.
- (16) Phukan, P.; Sudalai, A. Regioselective Alkylation of Phenol with Cyclopentanol over Montmorillonite K10: An Efficient Synthesis of 1-(2-Cyclopentylphenoxy)-3-[(1,1-Dimethylethyl)Amino]Propan-2-ol {(S)-Penbutolol}. *J. Chem. Soc. Perkin 1* **1999**, No. 20, 3015–3018. <https://doi.org/10.1039/A902479D>.
- (17) Yi, W.-B.; Cai, C. Rare Earth(III) Perfluorooctanesulfonates Catalyzed Friedel–Crafts Alkylation in Fluorous Biphasic System. *J. Fluor. Chem.* **2005**, 126 (5), 831–833. <https://doi.org/10.1016/j.jfluchem.2005.03.010>.
- (18) Jefferies, L. R.; Cook, S. P. Iron-Catalyzed Arene Alkylation Reactions with Unactivated Secondary Alcohols. *Org. Lett.* **2014**, 16 (7), 2026–2029. <https://doi.org/10.1021/ol500606d>.
- (19) Cook, A.; St. Onge, P.; Newman, S. G. Deoxygenative Suzuki–Miyaura Arylation of Tertiary Alcohols through Silyl Ethers. *Nat. Synth.* **2023**, 2 (7), 663–669. <https://doi.org/10.1038/s44160-023-00275-w>.

- (20) Huang, P.; Jiang, X.; Gao, D.; Wang, C.; Shi, D.-Q.; Zhao, Y. HFIP-Promoted Para-Selective Alkylation of Anilines and Phenols with Tertiary Alkyl Bromides. *Org. Chem. Front.* **2023**, 10 (10), 2476–2481. <https://doi.org/10.1039/D3QO00342F>.
- (21) Arredondo, Y.; Moreno-Mañas, M.; Pleixats, R. Non-Catalyzed C-Alkylation of Phenols With Cyclic Secondary Alkyl Bromides. *Synth. Commun.* **1996**, 26 (21), 3885–3895. <https://doi.org/10.1080/00397919608003808>.
- (22) Rago, A. J.; Vasilopoulos, A.; Dombrowski, A. W.; Wang, Y. Di(2-Picolyl)Amines as Modular and Robust Ligands for Nickel-Catalyzed C(Sp<sup>2</sup>)–C(Sp<sup>3</sup>) Cross-Electrophile Coupling. *Org. Lett.* **2022**, 24 (46), 8487–8492. <https://doi.org/10.1021/acs.orglett.2c03346>.

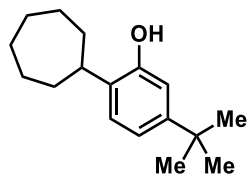
### 3.6 Selected NMR Spectra



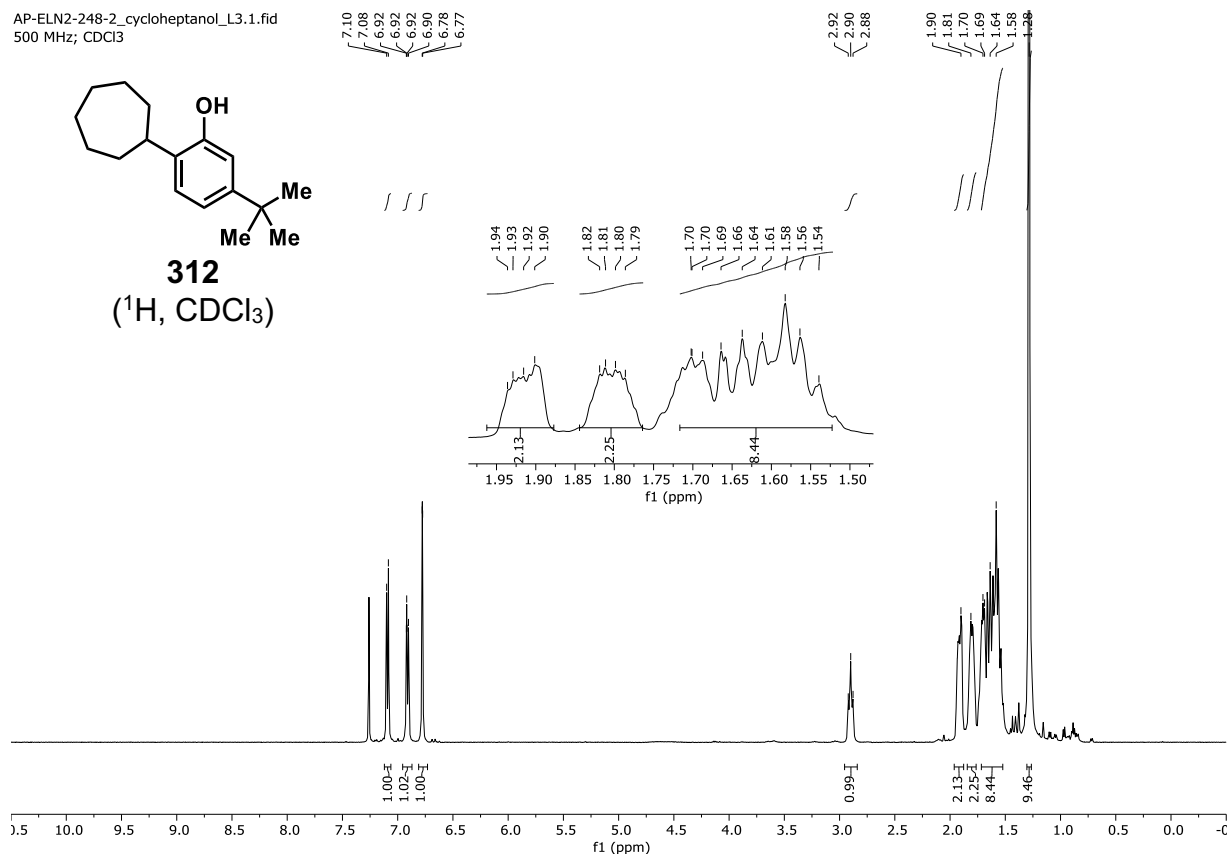
AP-ELN2-154-2\_3-tBu\_13C.12.1.1r  
600 MHz; CDCl<sub>3</sub> 13C



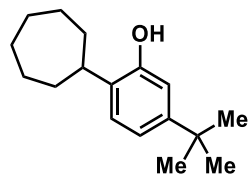
AP-ELN2-248-2\_cycloheptanol\_L3.1.fid  
500 MHz; CDCl<sub>3</sub>



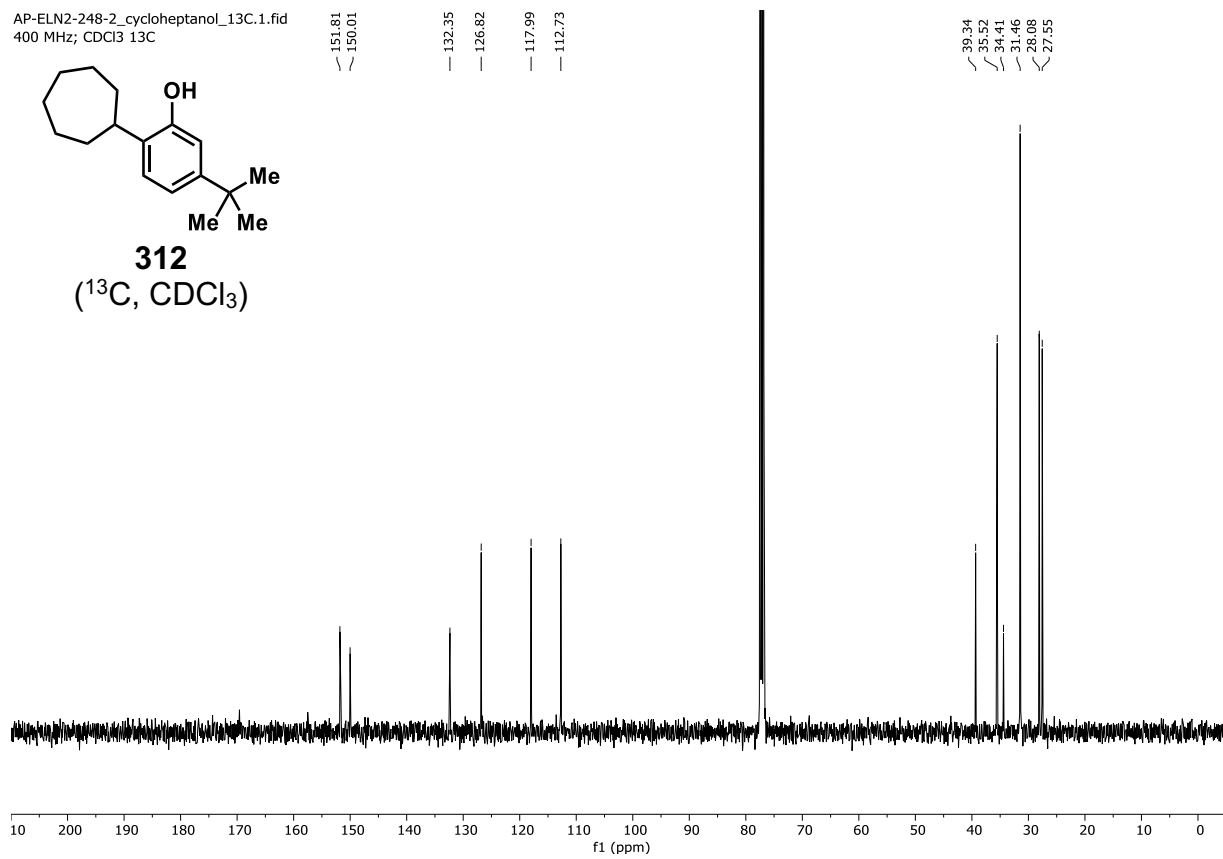
**312**  
(<sup>1</sup>H, CDCl<sub>3</sub>)



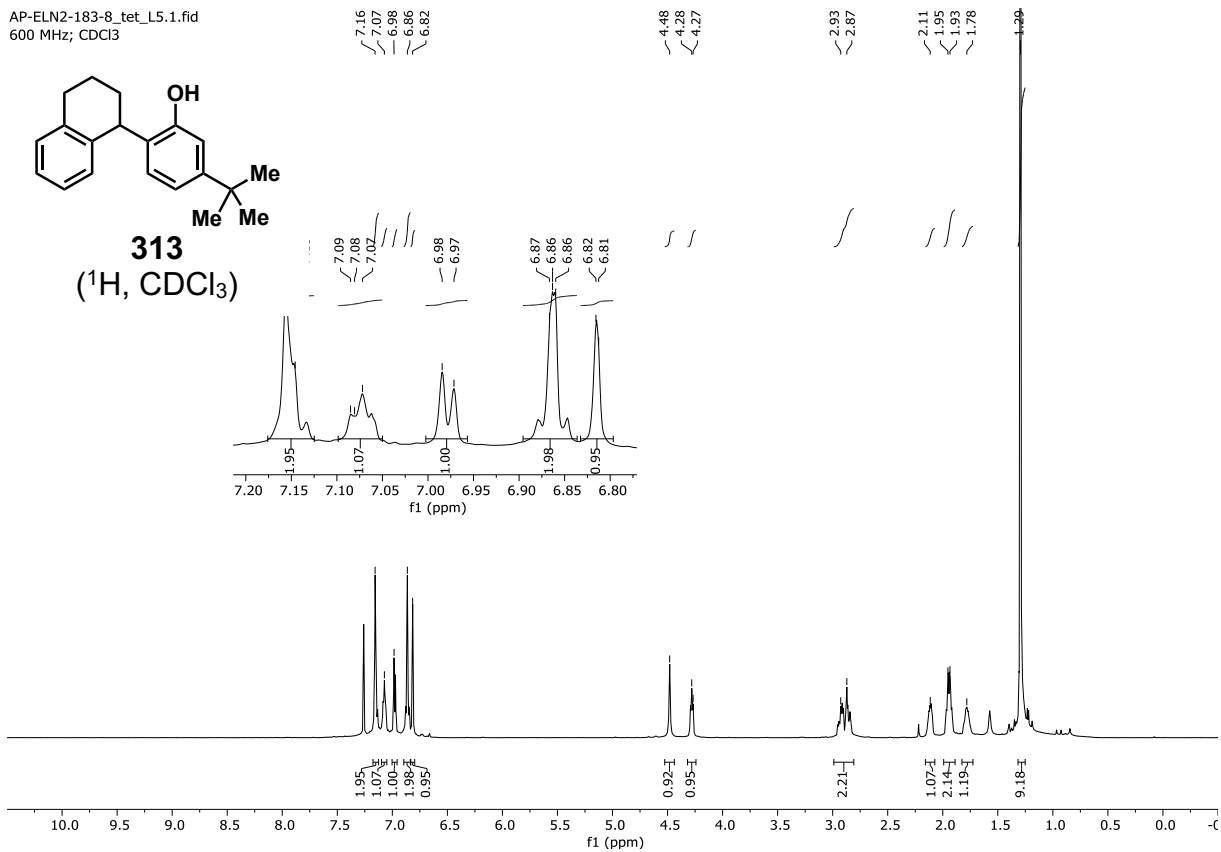
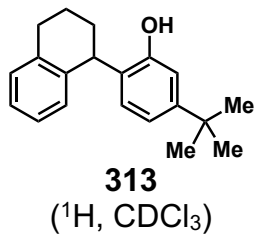
AP-ELN2-248-2\_cycloheptanol\_13C.1.fid  
400 MHz; CDCl<sub>3</sub> 13C



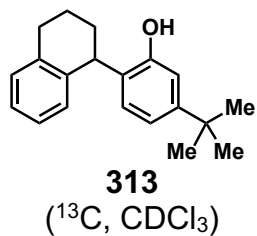
**312**  
(<sup>13</sup>C, CDCl<sub>3</sub>)



AP-ELN2-183-8\_tet\_L5.1.fid  
600 MHz; CDCl<sub>3</sub>

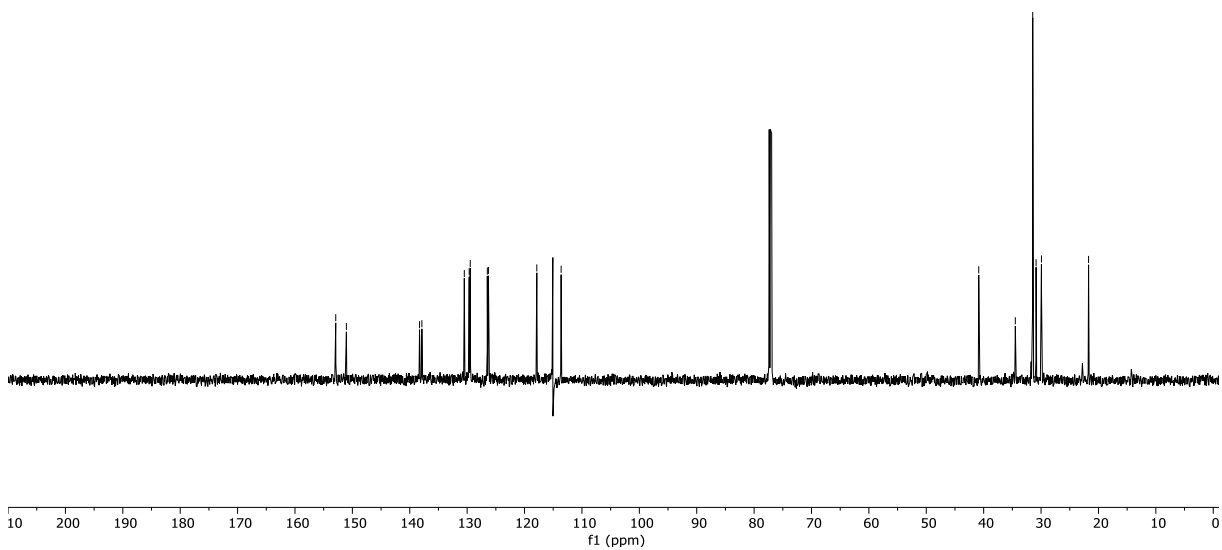


AP-ELN2-183-8\_2-tet\_L5\_13C.1.fid  
600 MHz; CDCl<sub>3</sub> 13X

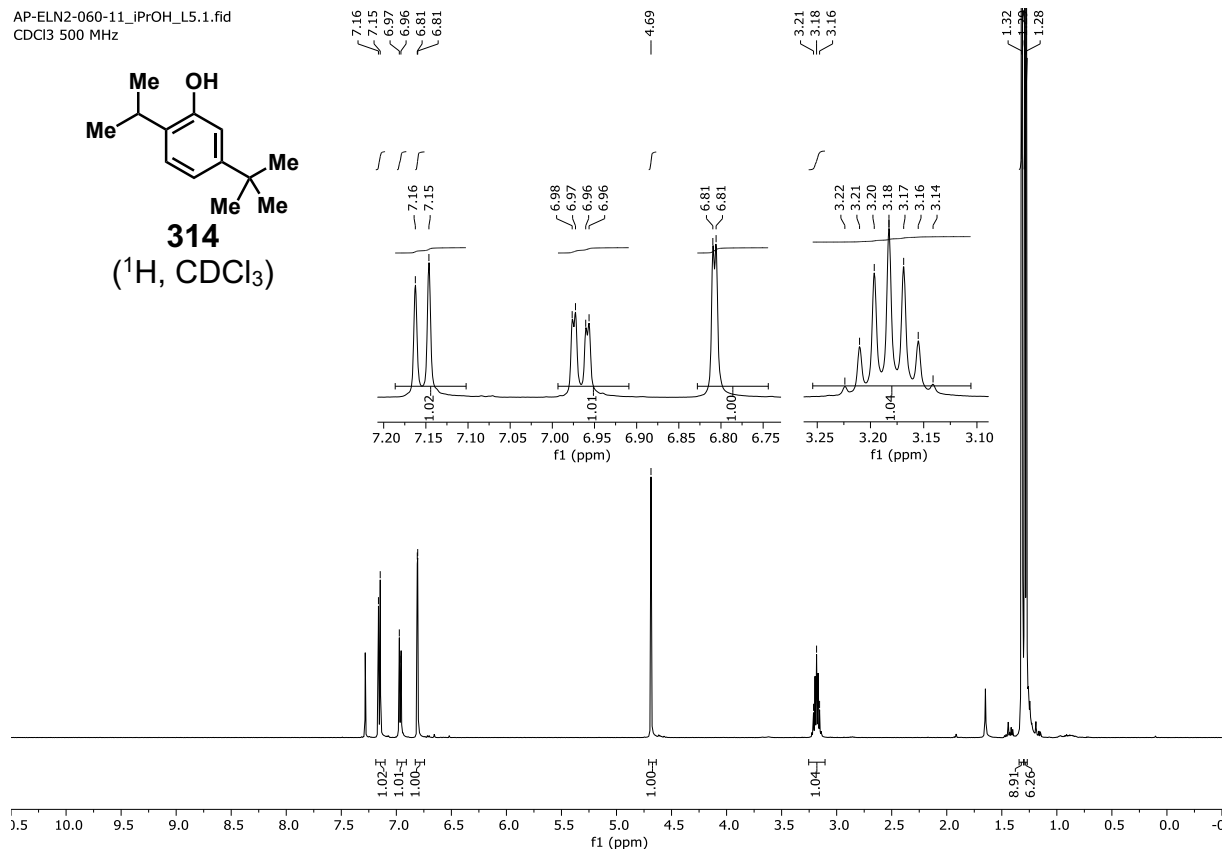
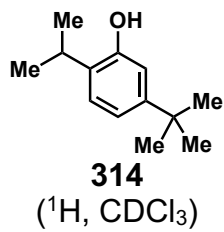


152.90  
151.04  
138.30  
137.89  
130.50  
129.64  
129.52  
129.46  
126.49  
126.29  
117.86  
113.63

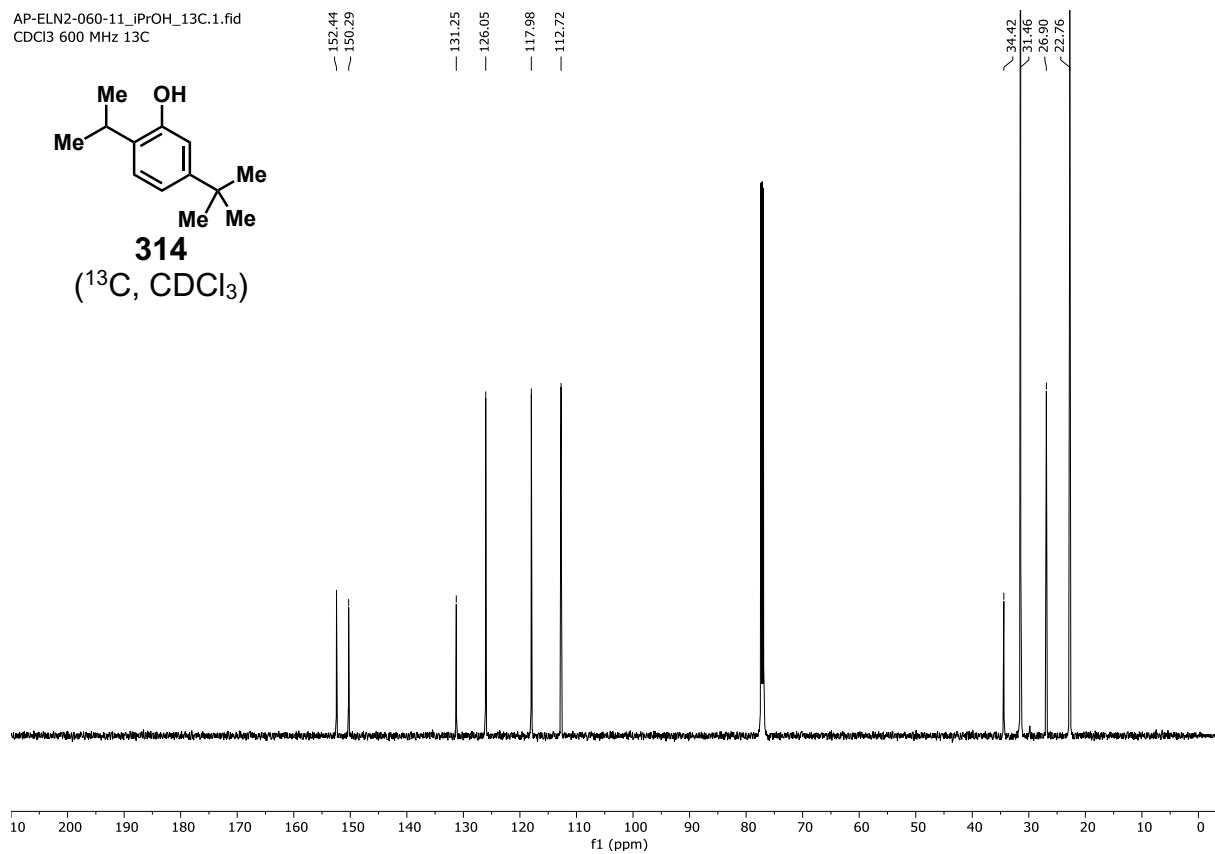
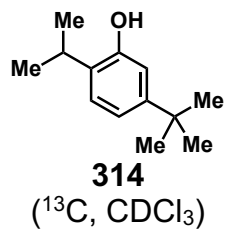
40.86  
34.49  
31.45  
30.87  
29.93  
21.72



AP-ELN2-060-11\_iPrOH\_L5.1.fid  
CDCl3 500 MHz

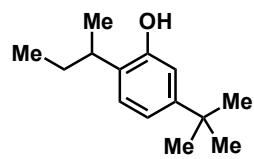


AP-ELN2-060-11\_iPrOH\_13C.1.fid  
CDCl<sub>3</sub> 600 MHz 13C

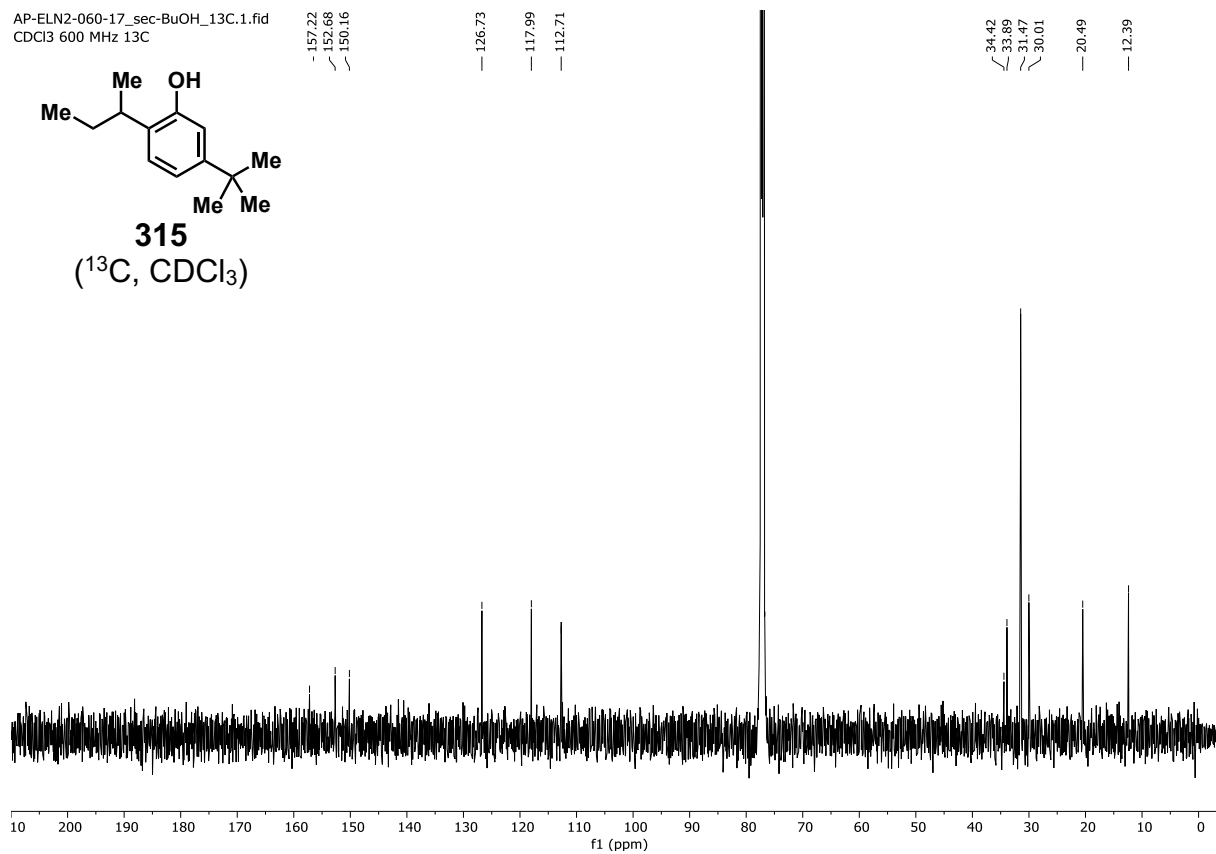




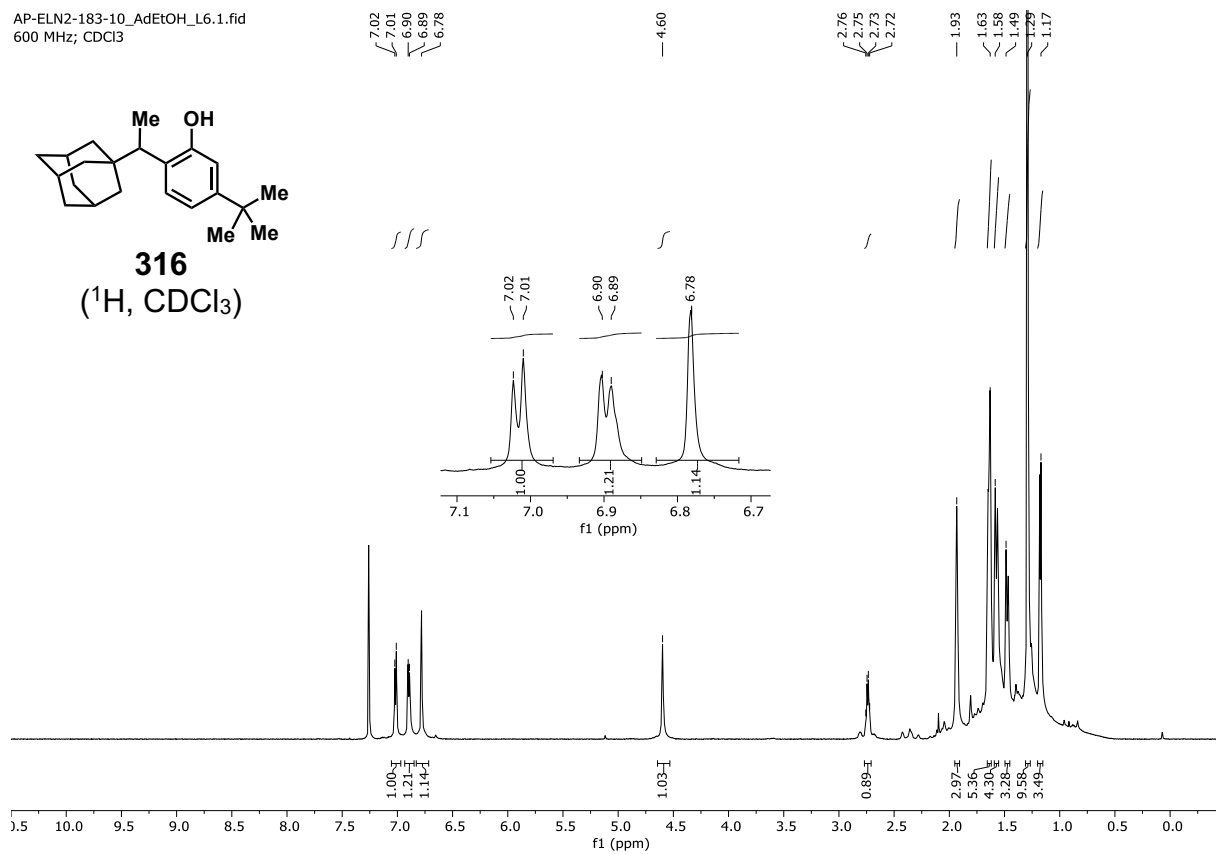
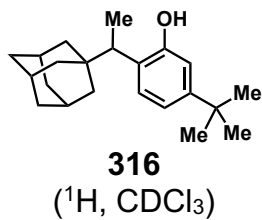
AP-ELN2-060-17\_sec-BuOH\_13C.1.fid  
CDCl3 600 MHz 13C



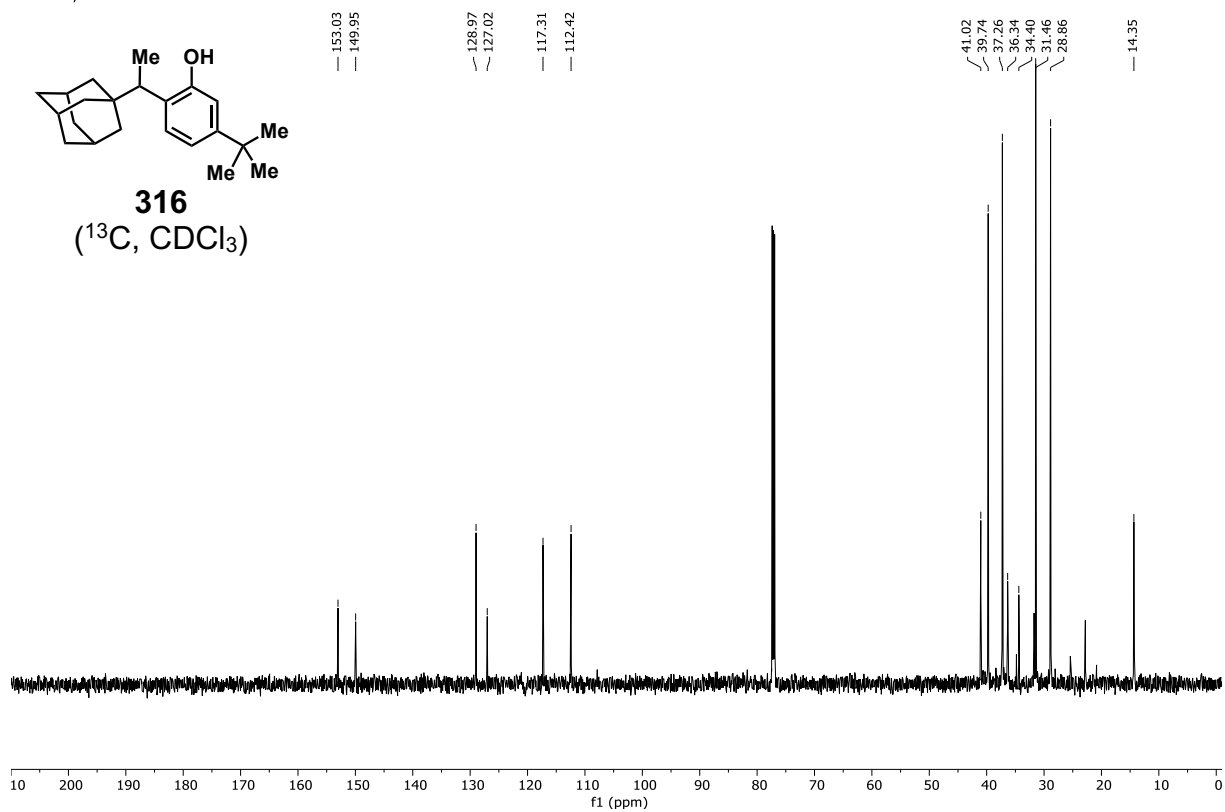
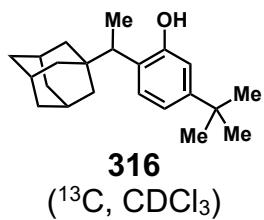
**315**  
(<sup>13</sup>C, CDCl<sub>3</sub>)



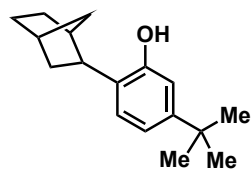
AP-ELN2-183-10\_AdEtOH\_L6.1.fid  
600 MHz; CDCl<sub>3</sub>



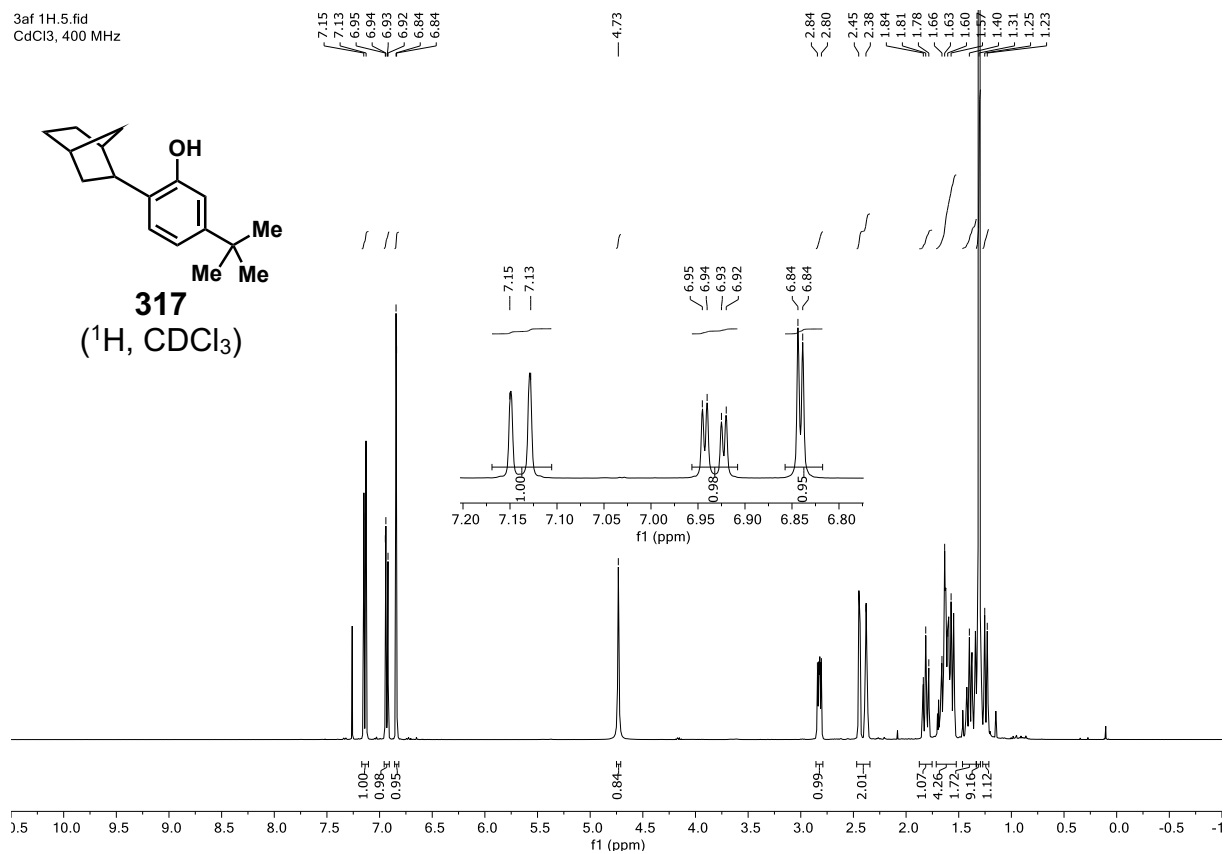
AP-ELN2-183-10\_AdEt\_L6\_13C.1.fid  
600 MHz; CDCl<sub>3</sub> 13X



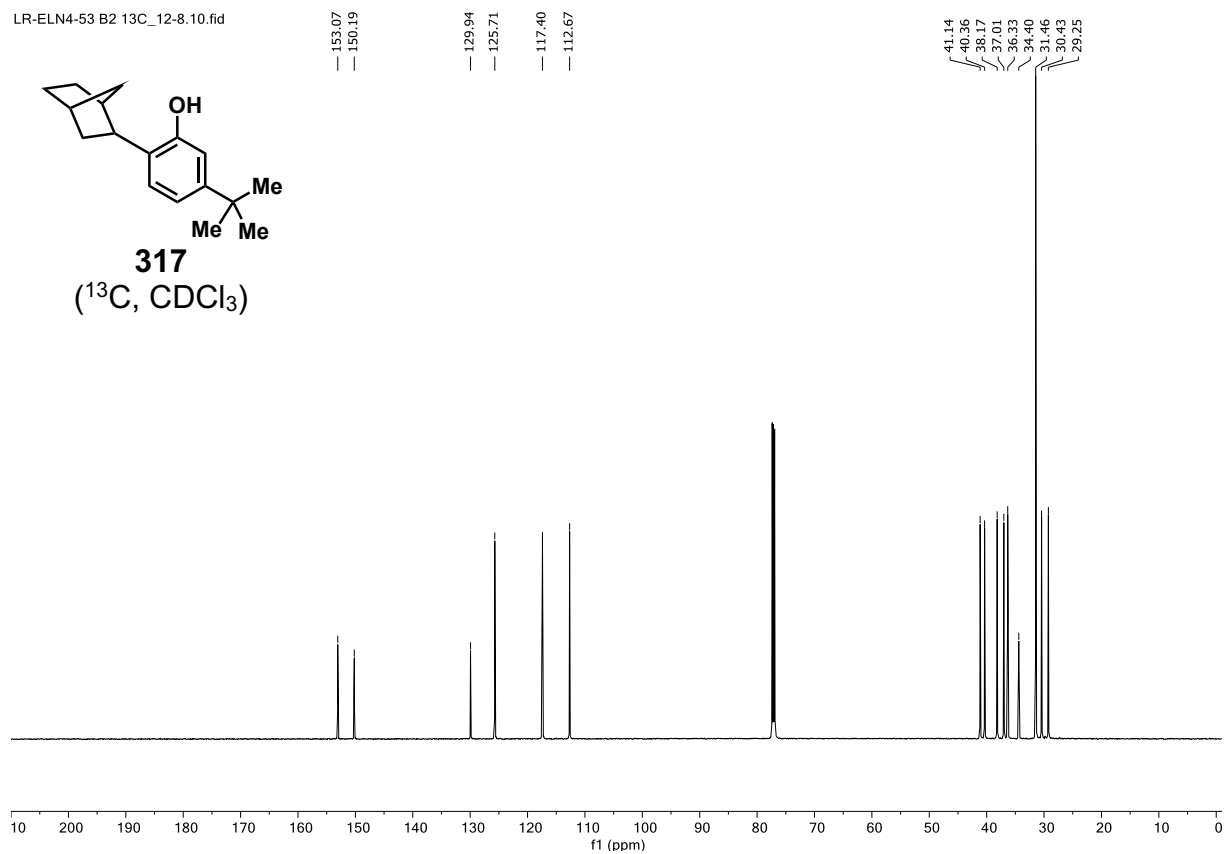
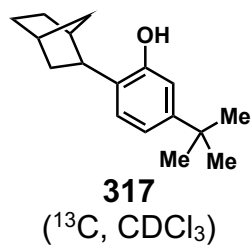
3af 1H.5.fid  
CDCl<sub>3</sub>, 400 MHz



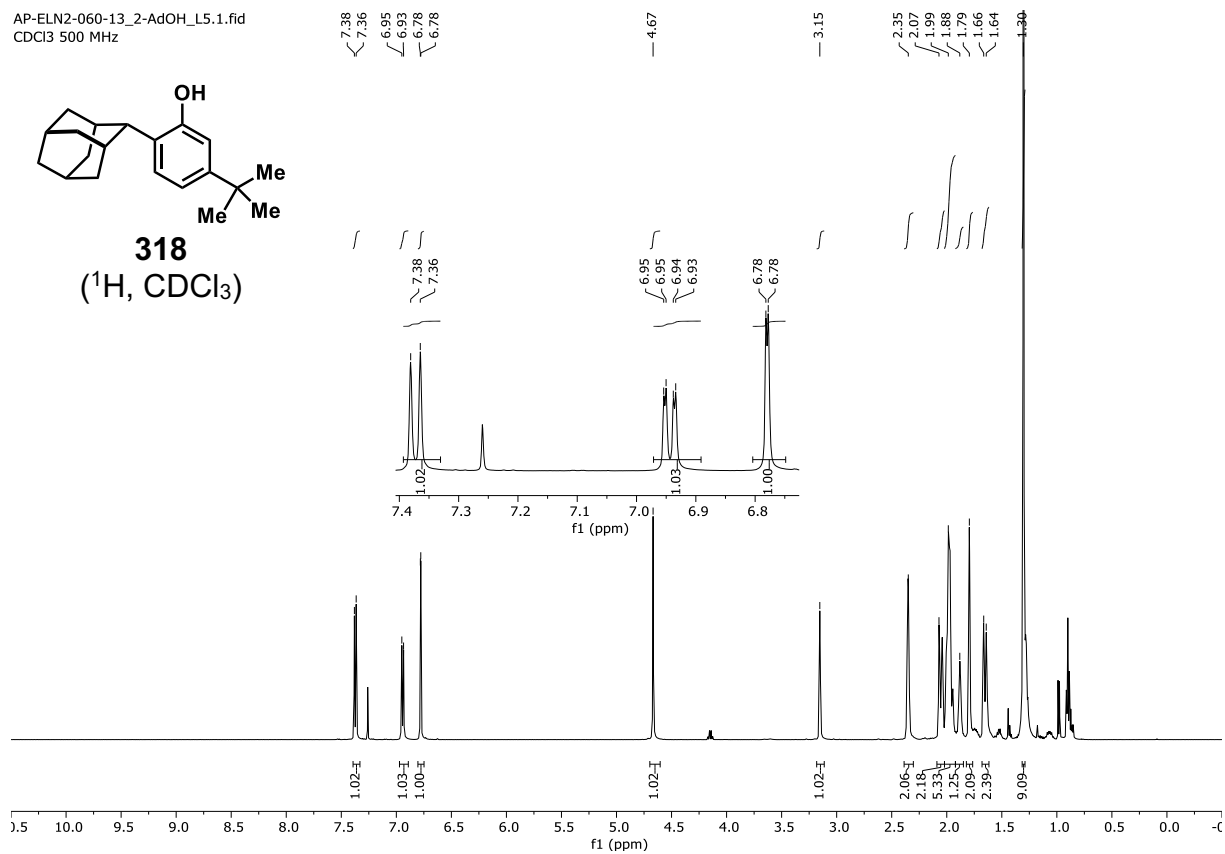
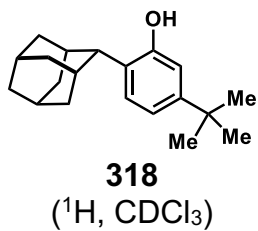
**317**  
(<sup>1</sup>H, CDCl<sub>3</sub>)



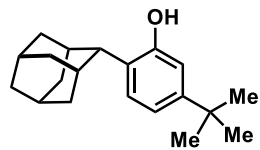
LR-ELN4-53 B2 13C\_12-8.10.fid



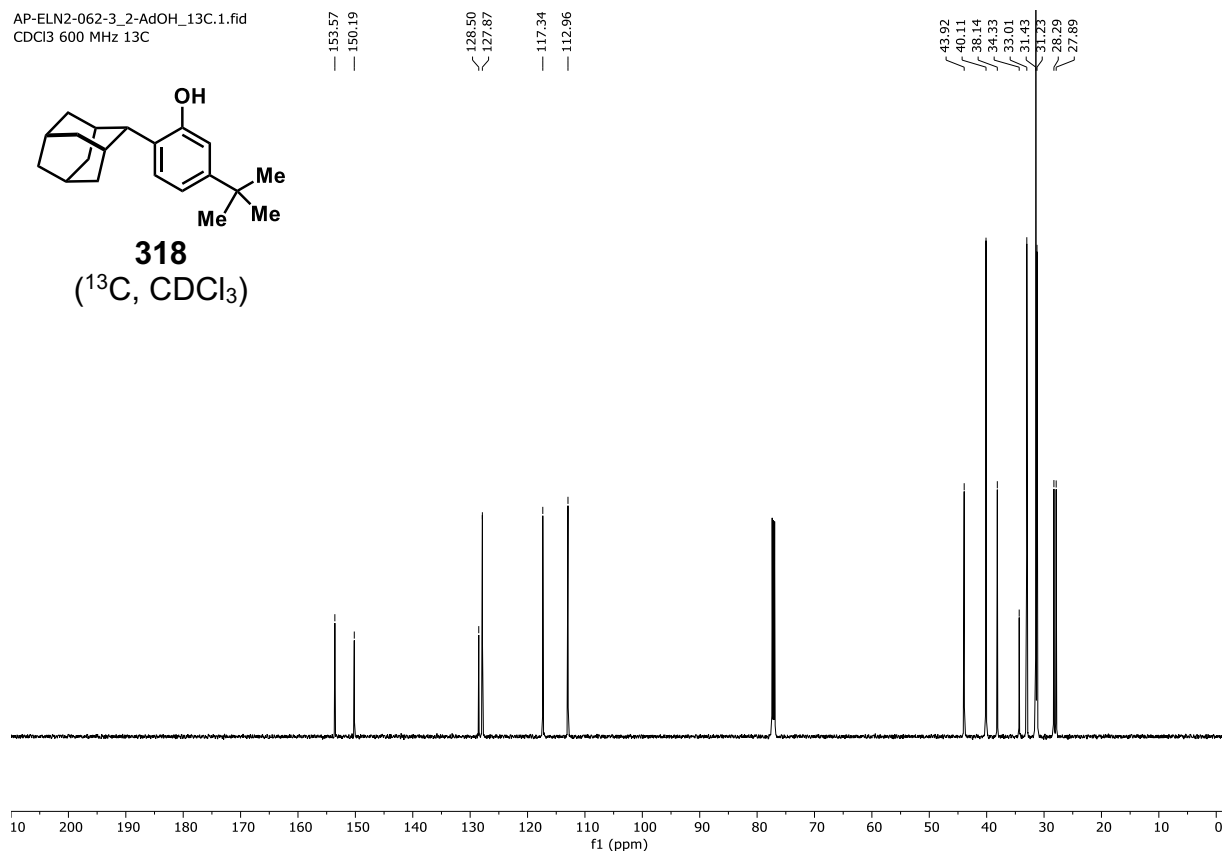
AP-ELN2-060-13\_2-AdOH\_L5.1.fid  
CDCl<sub>3</sub> 500 MHz



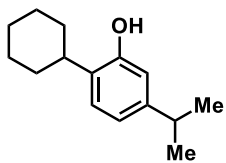
AP-ELN2-062-3\_2-AdOH\_13C.1.fid  
CDCl<sub>3</sub> 600 MHz 13C



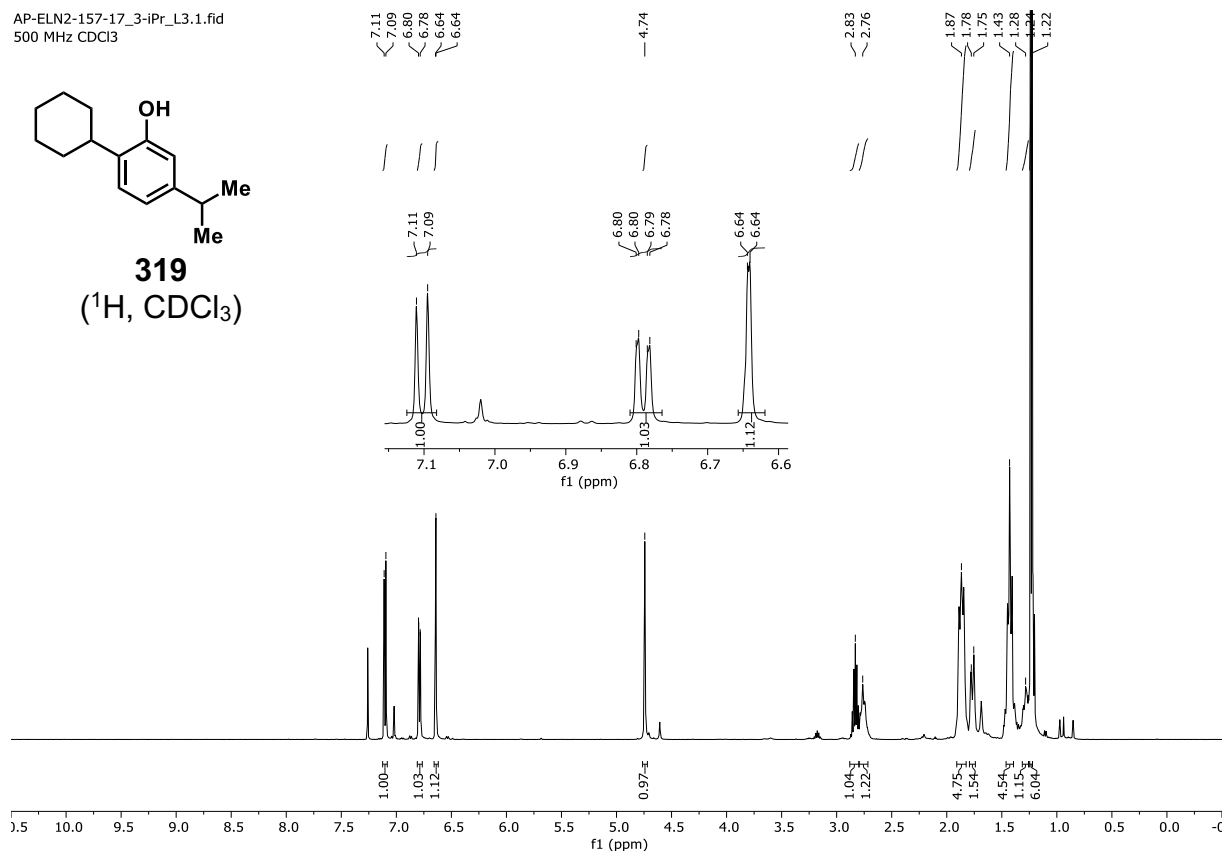
**318**  
(<sup>13</sup>C, CDCl<sub>3</sub>)



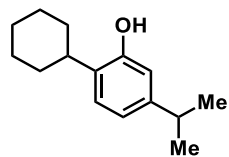
AP-ELN2-157-17\_3-iPr\_L3.1.fid  
500 MHz CDCl<sub>3</sub>



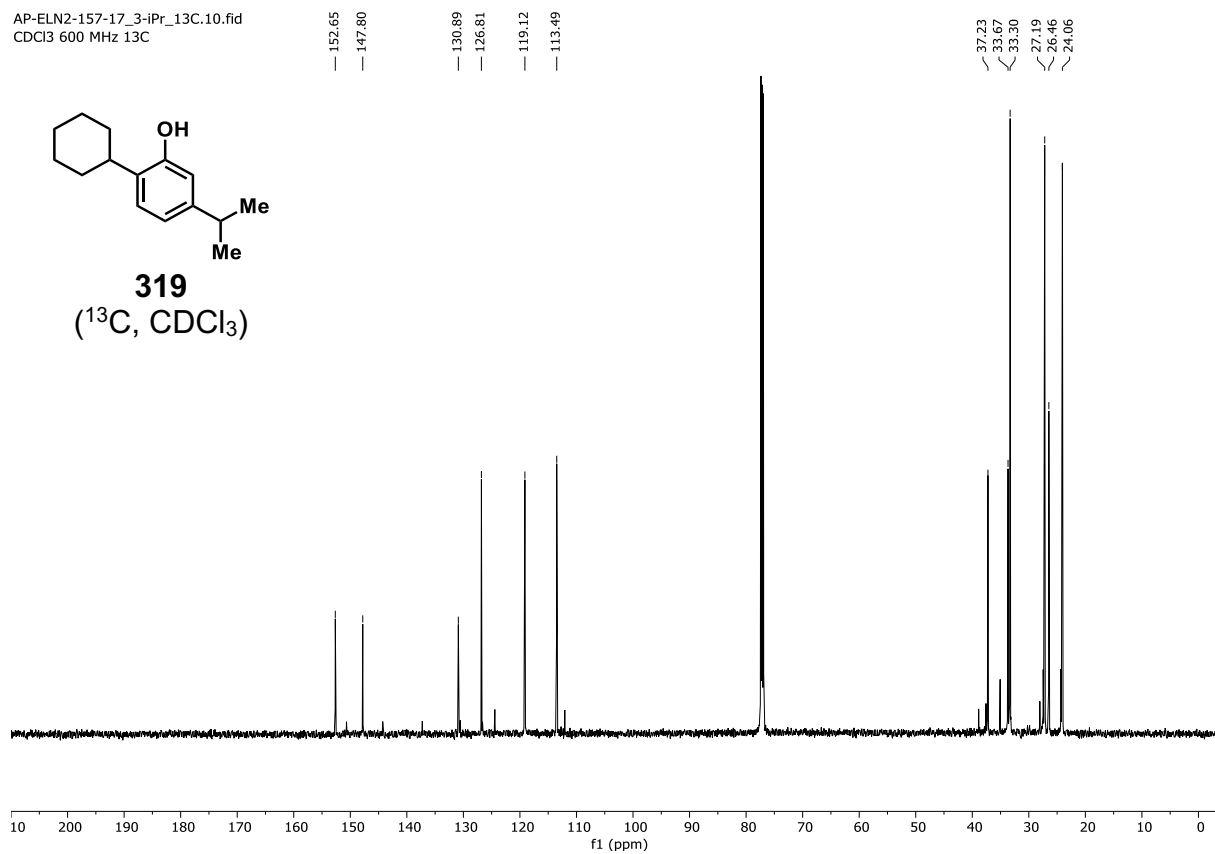
**319**  
(<sup>1</sup>H, CDCl<sub>3</sub>)



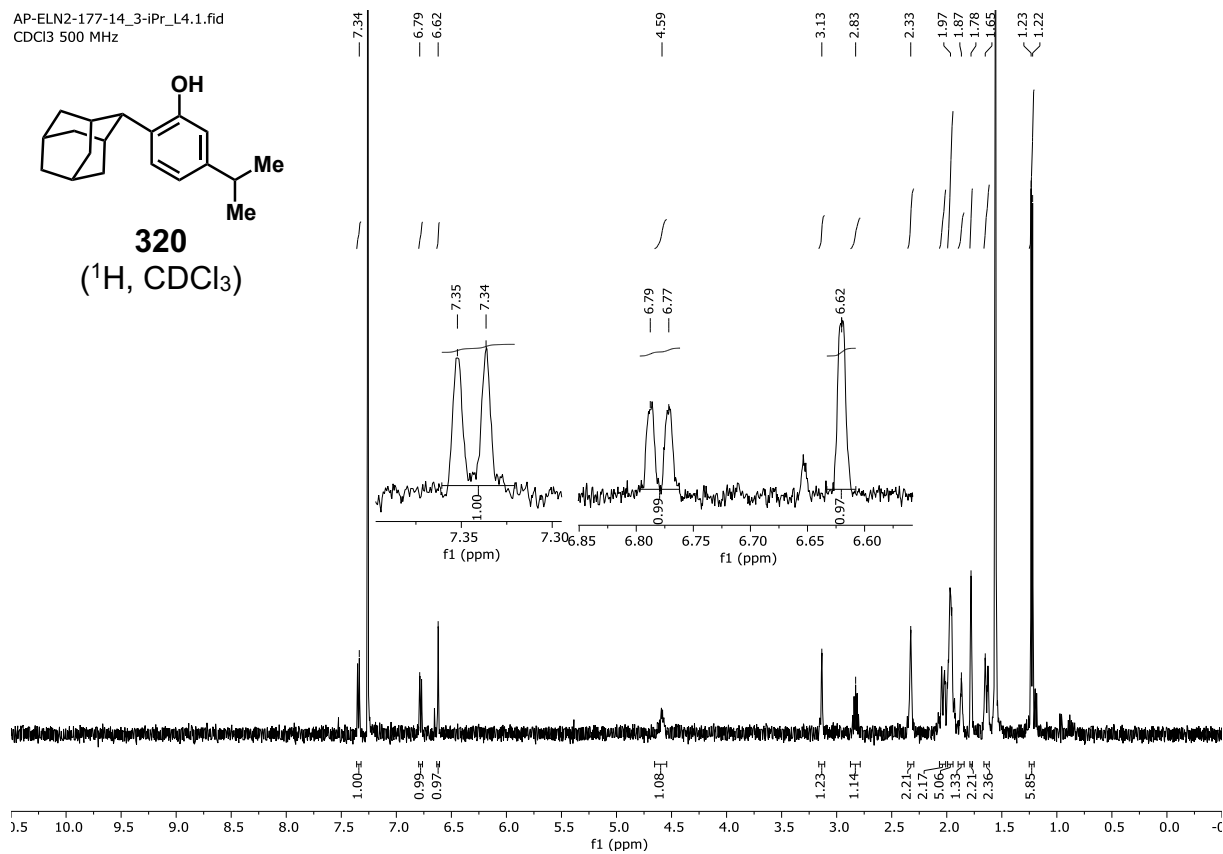
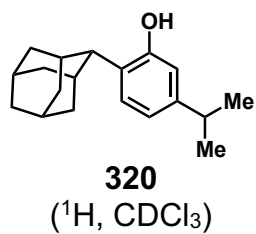
AP-ELN2-157-17\_3-iPr\_13C.10.fid  
CDCl<sub>3</sub> 600 MHz 13C



**319**  
(<sup>13</sup>C, CDCl<sub>3</sub>)



AP-ELN2-177-14\_3-iPr\_L4.1.fid  
CDCl3 500 MHz



AP-ELN2-177-14\_2-(2-Ad)-5-iPr\_13C.1.fid  
CDCl<sub>3</sub> 600 MHz 13C

— 153.85

— 147.86

— 128.86

— 128.14

— 118.52

— 113.73

— 43.99

— 40.15

— 38.16

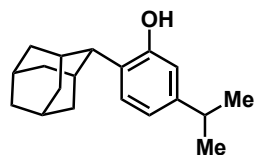
— 33.60

— 31.27

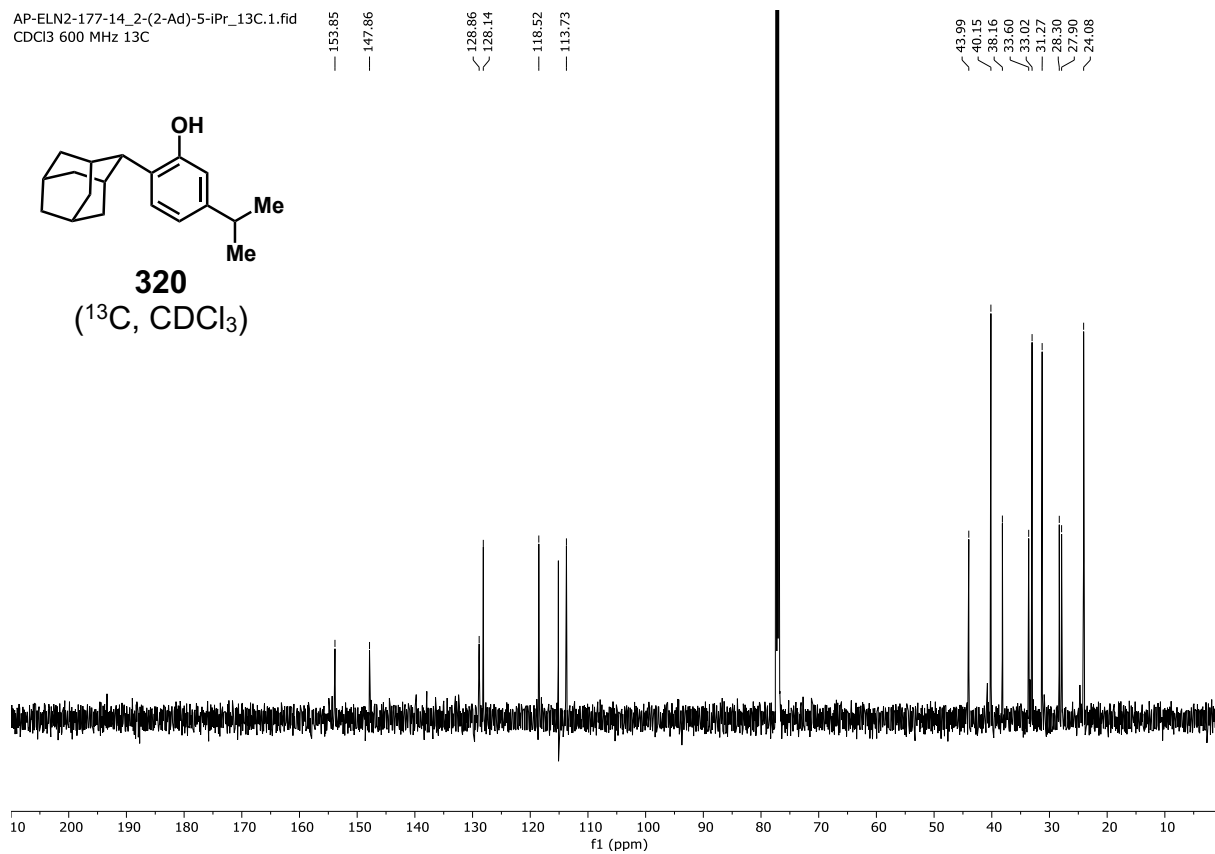
— 28.30

— 27.90

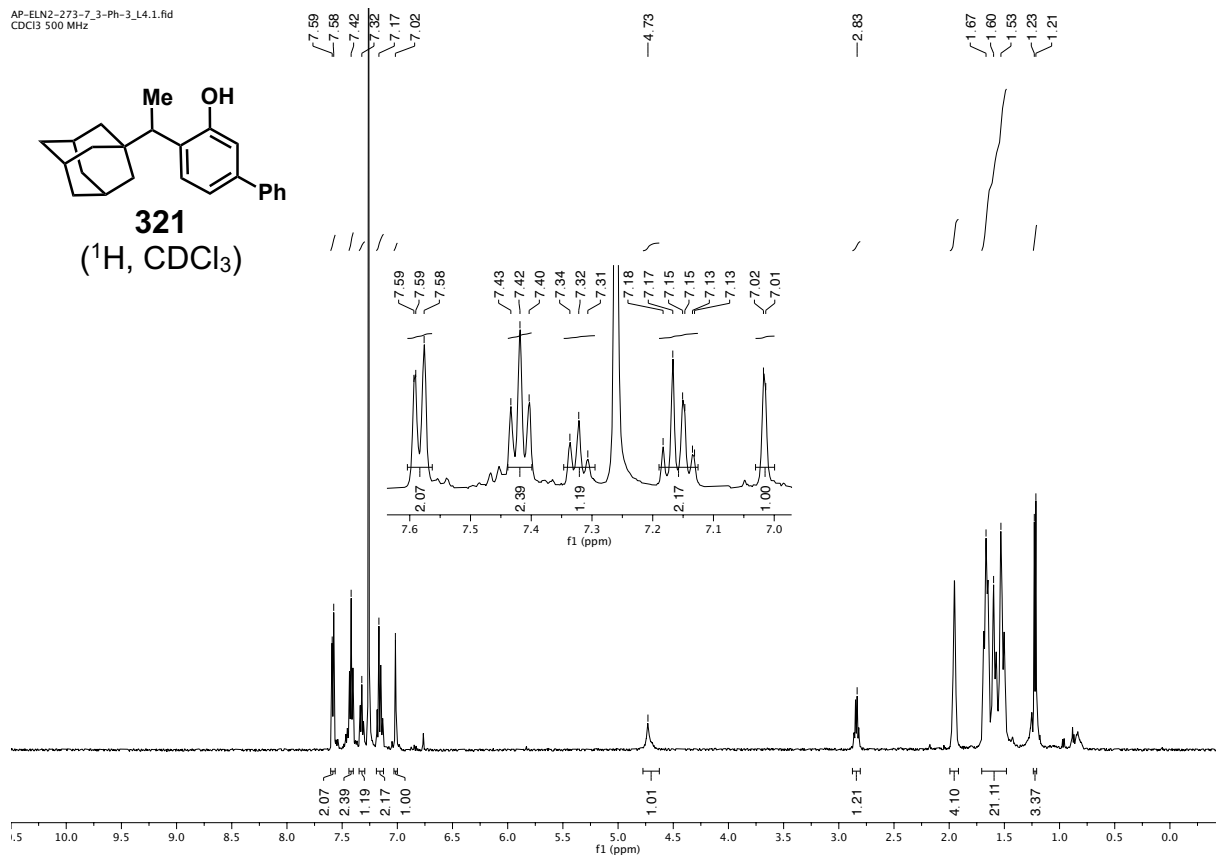
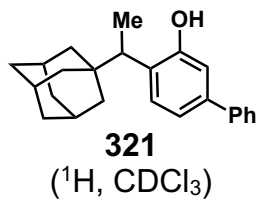
— 24.08



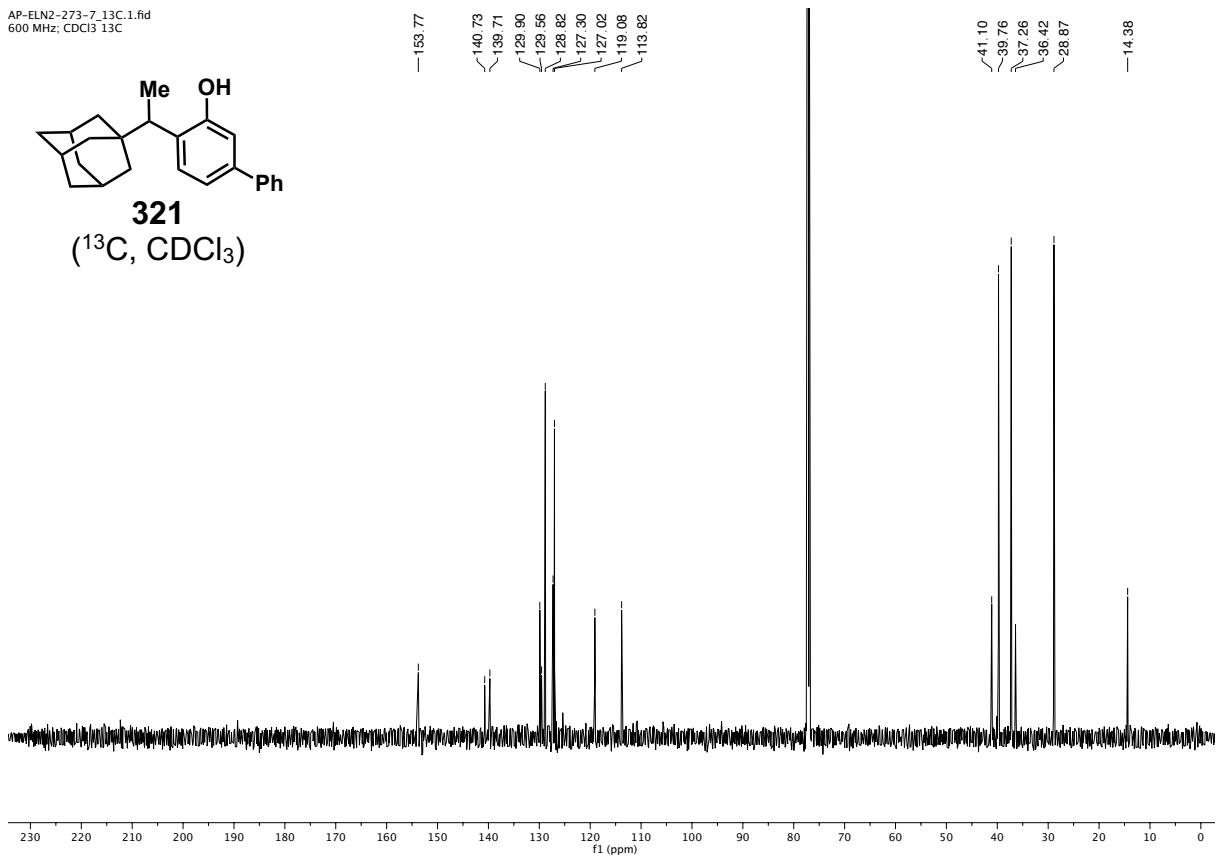
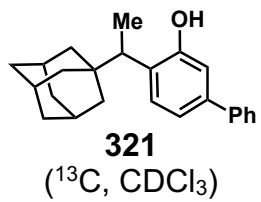
**320**  
(<sup>13</sup>C, CDCl<sub>3</sub>)



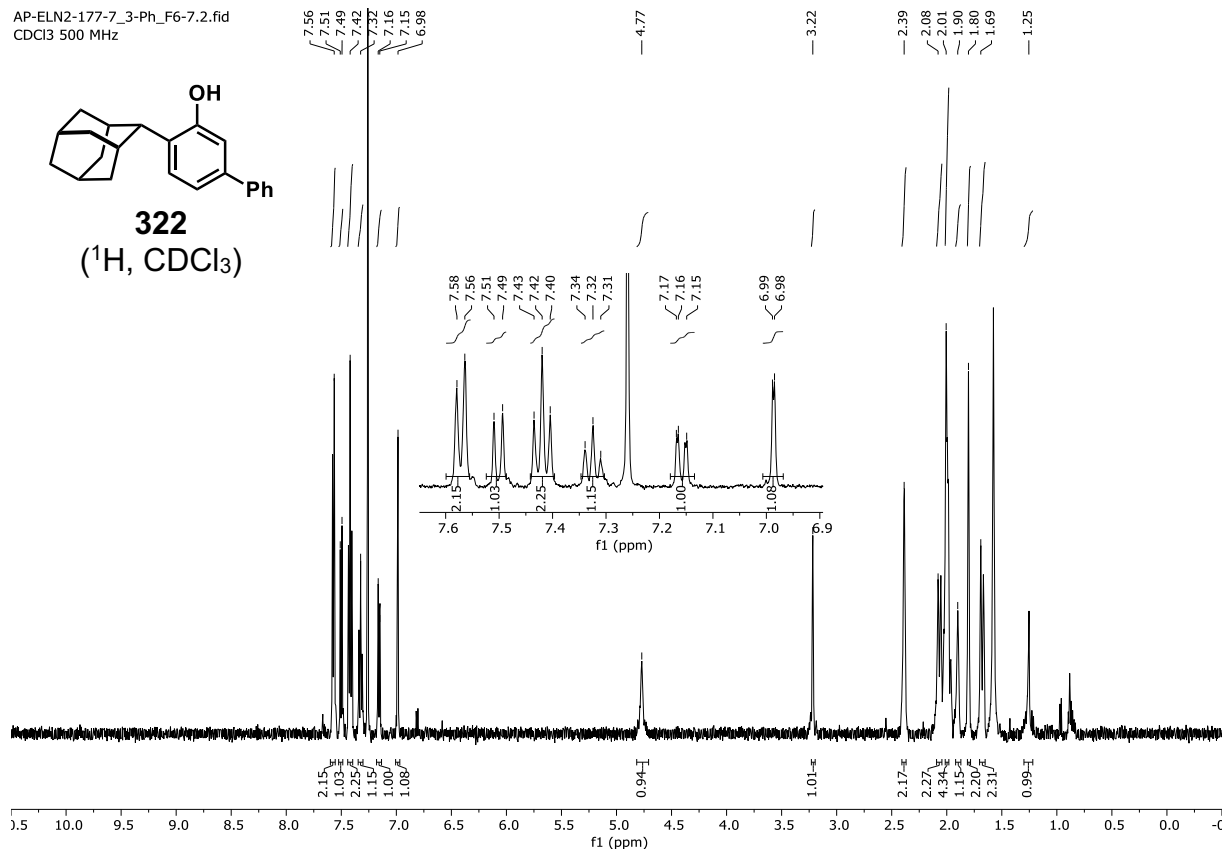
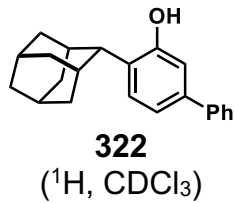
AP-ELN2-273-7\_3-Ph-3\_L4.1.fid  
CDCl3 500 MHz



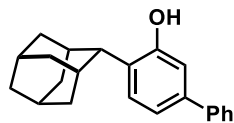
AP-ELN2-273-7\_13C.1.fid  
600 MHz; CDCl<sub>3</sub> 13C



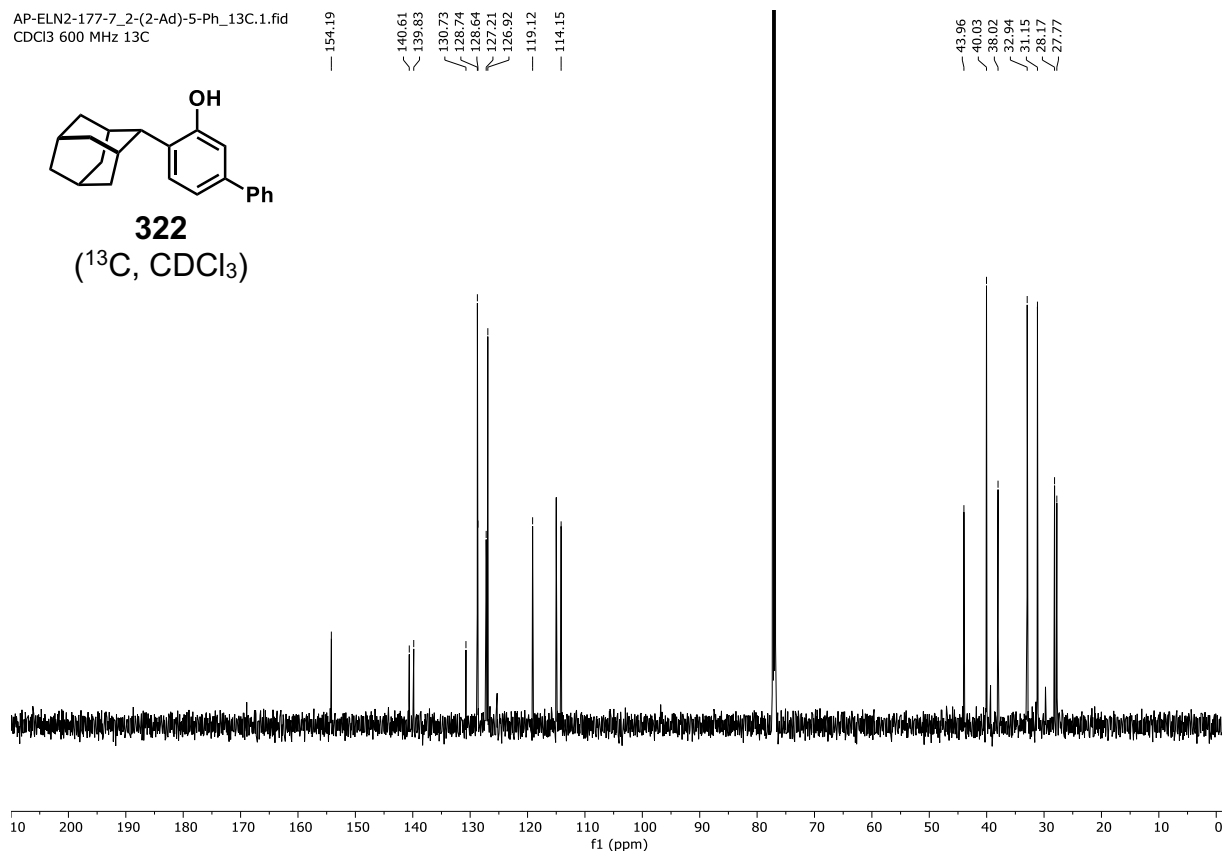
AP-ELN2-177-7\_3-Ph\_F6-7.2.fid  
CDCl3 500 MHz



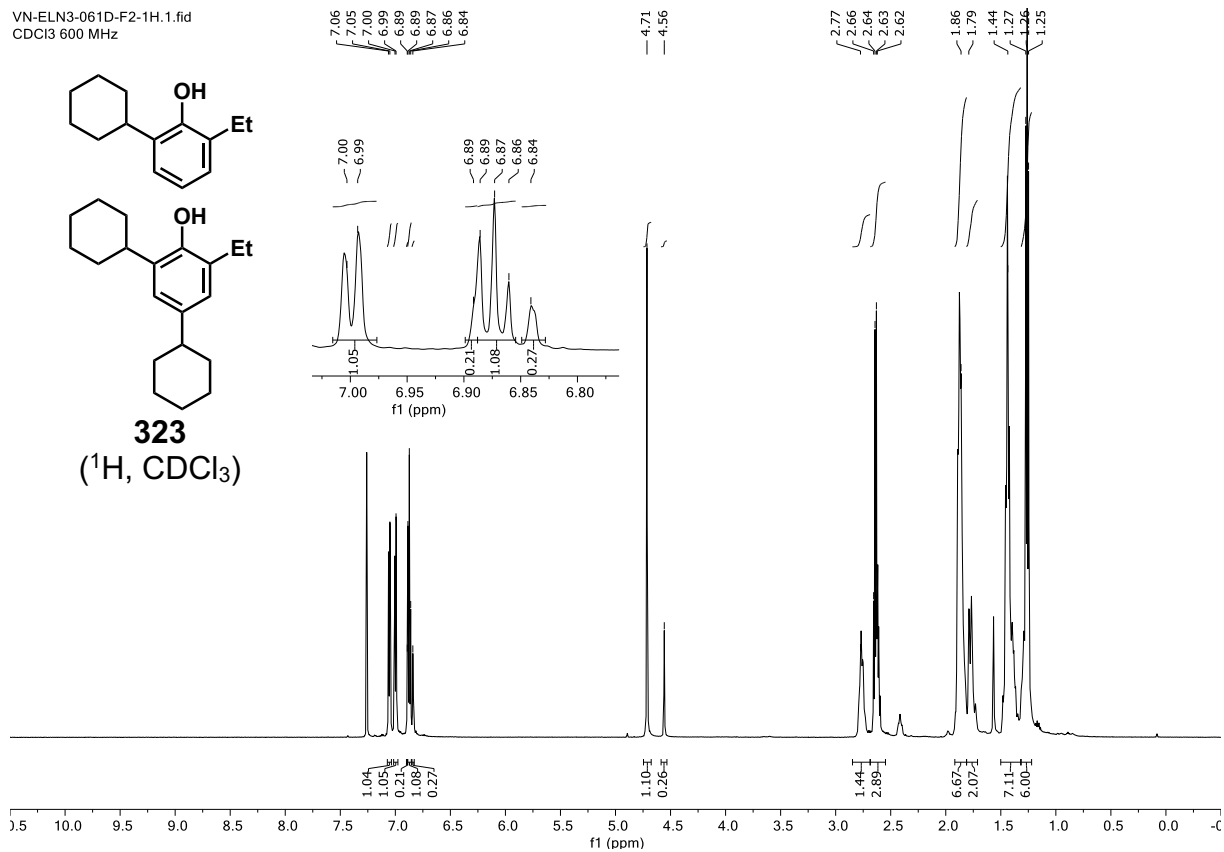
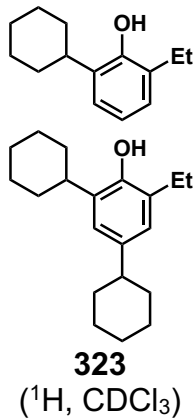
AP-ELN2-177-7\_2-(2-Ad)-5-Ph\_13C.1.fid  
CDCl3 600 MHz 13C



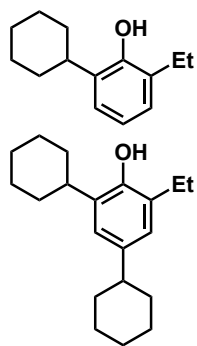
**322**  
(<sup>13</sup>C, CDCl<sub>3</sub>)



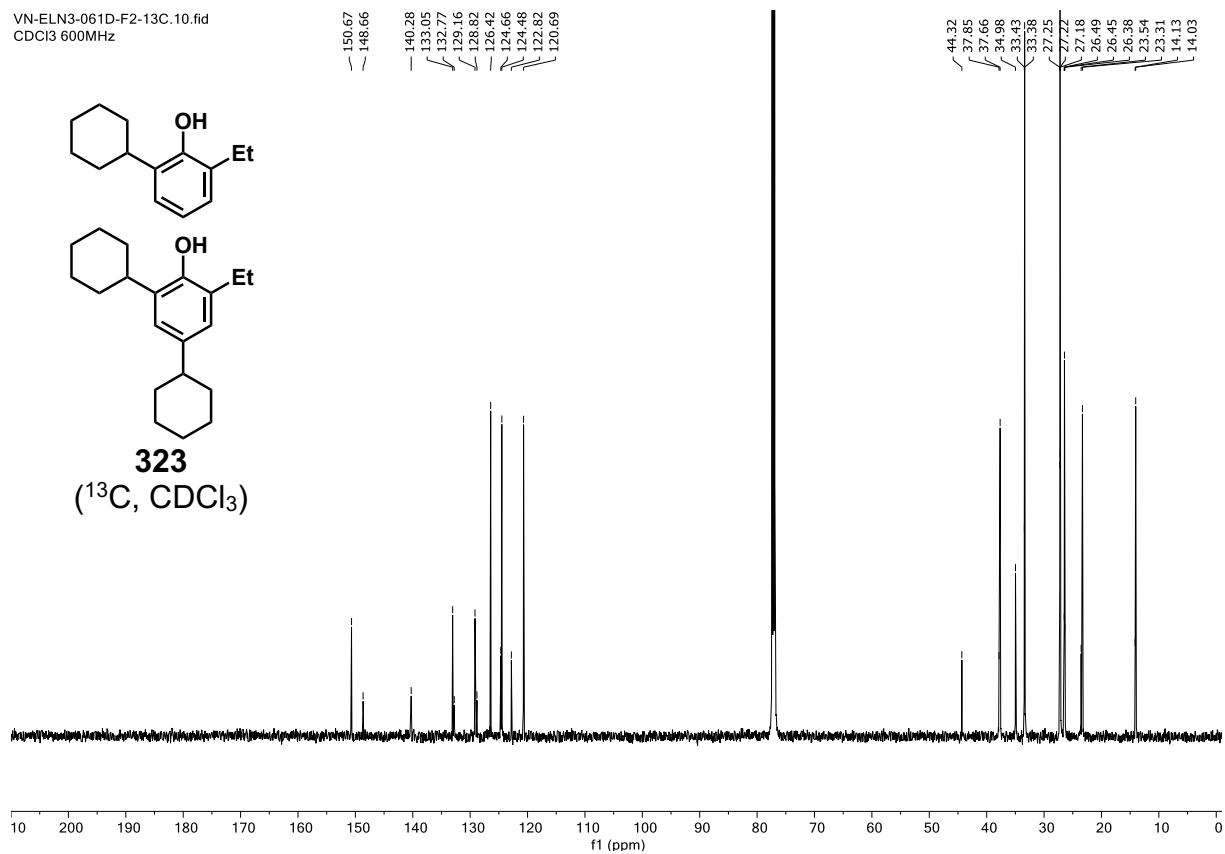
VN-ELN3-061D-F2-1H.1.fid  
CDCl<sub>3</sub> 600 MHz



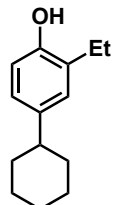
VN-ELN3-061D-F2-13C.10.fid  
CDCl<sub>3</sub> 600MHz



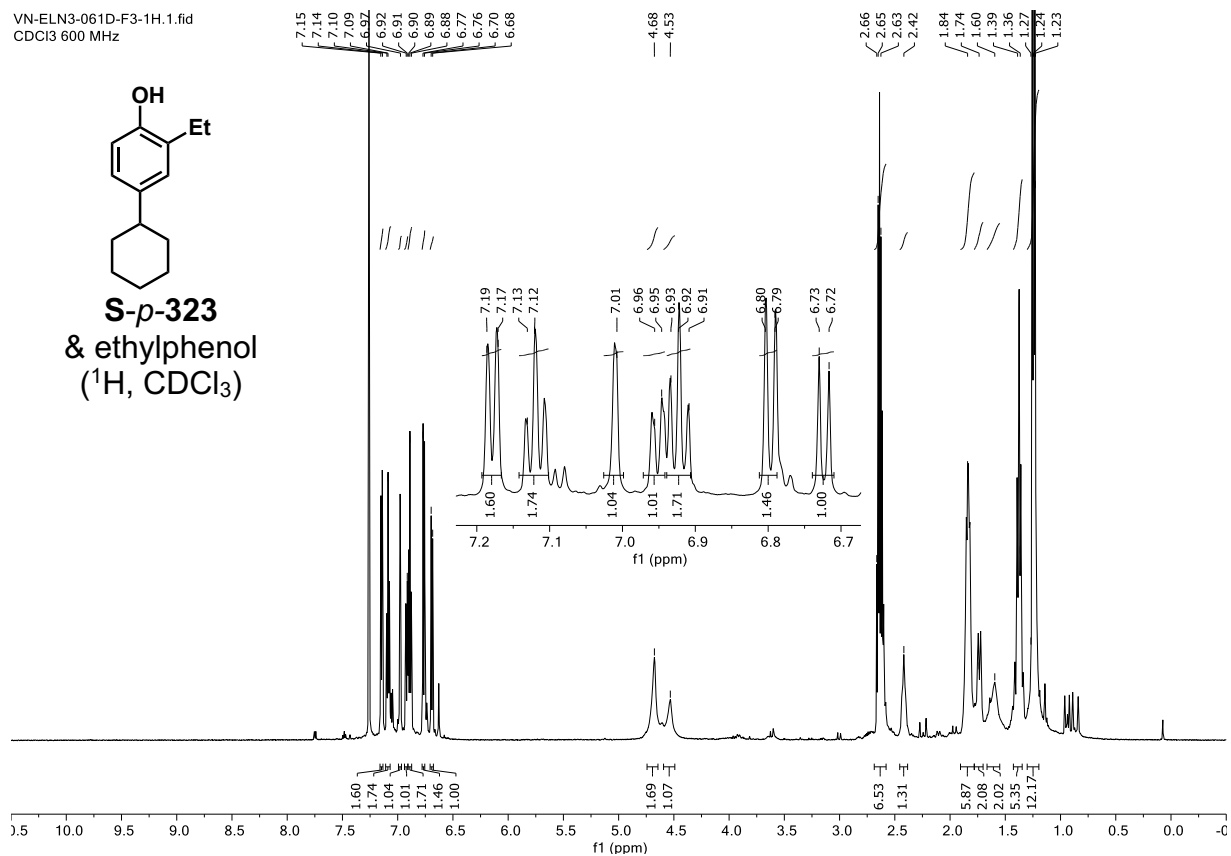
**323**  
(<sup>13</sup>C, CDCl<sub>3</sub>)



VN-ELN3-061D-F3-1H.1.fid  
CDCl3 600 MHz

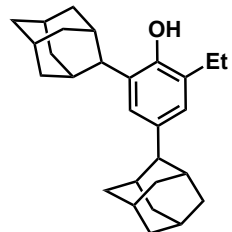
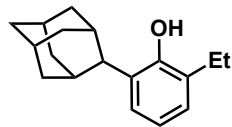


**S-p-323**  
& ethylphenol  
(<sup>1</sup>H, CDCl<sub>3</sub>)

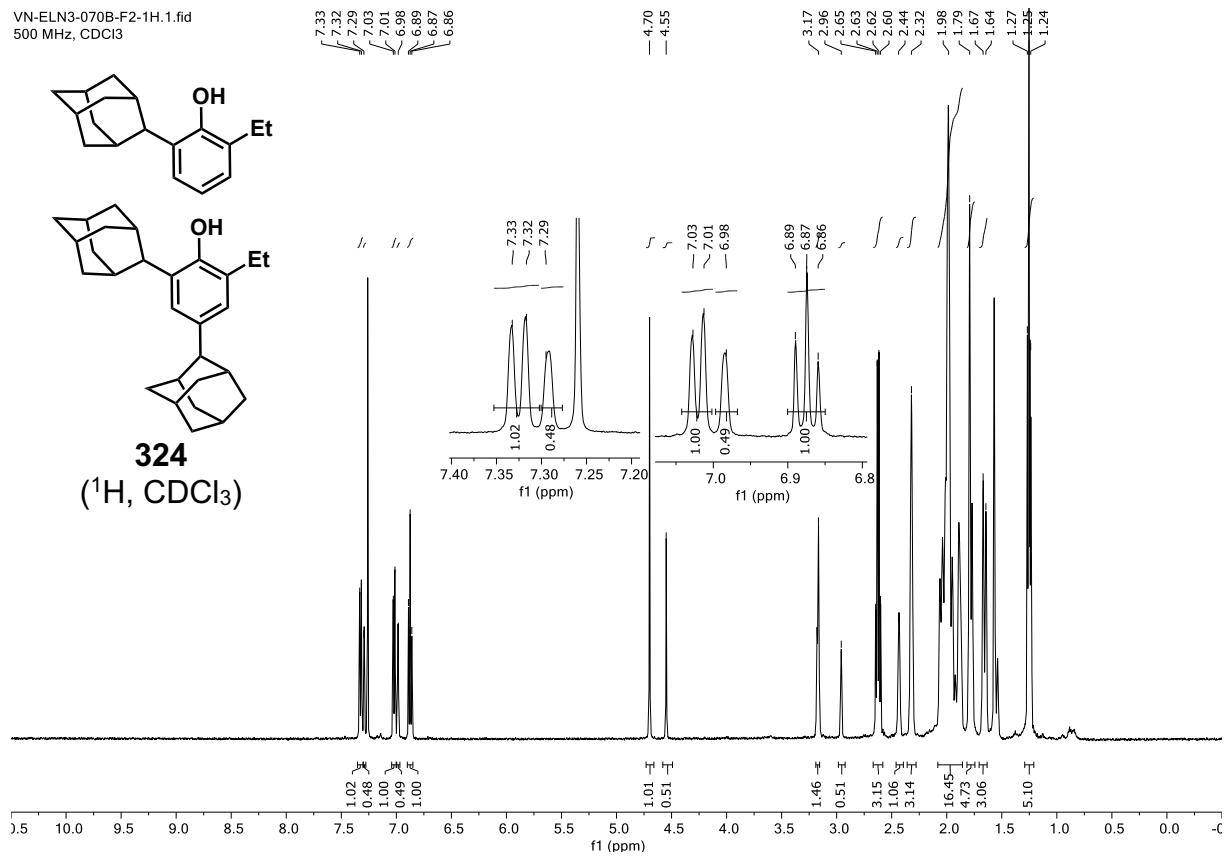




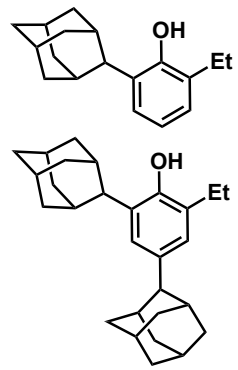
VN-ELN3-070B-F2-1H.1.fid  
500 MHz, CDCl<sub>3</sub>



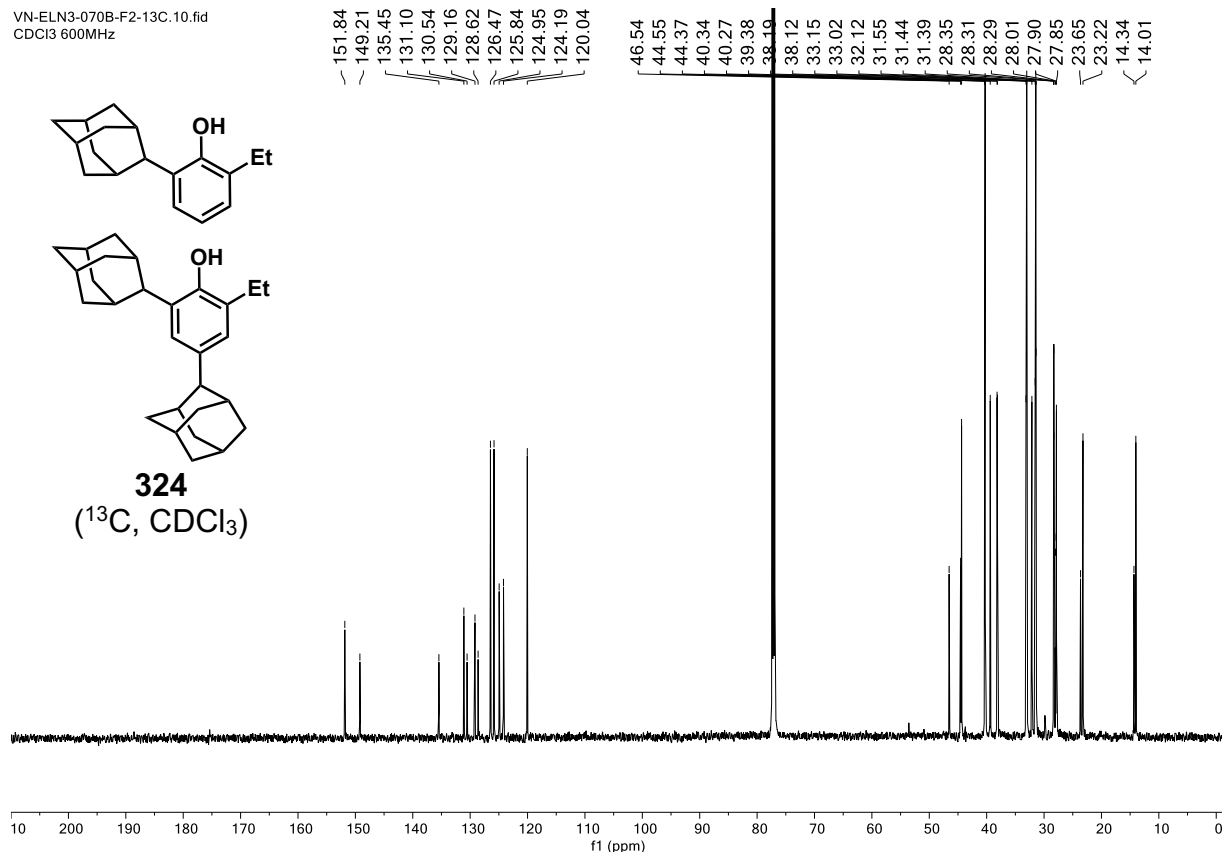
**324**  
(<sup>1</sup>H, CDCl<sub>3</sub>)



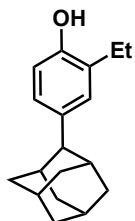
VN-ELN3-070B-F2-13C.10.fid  
CDCl<sub>3</sub> 600MHz



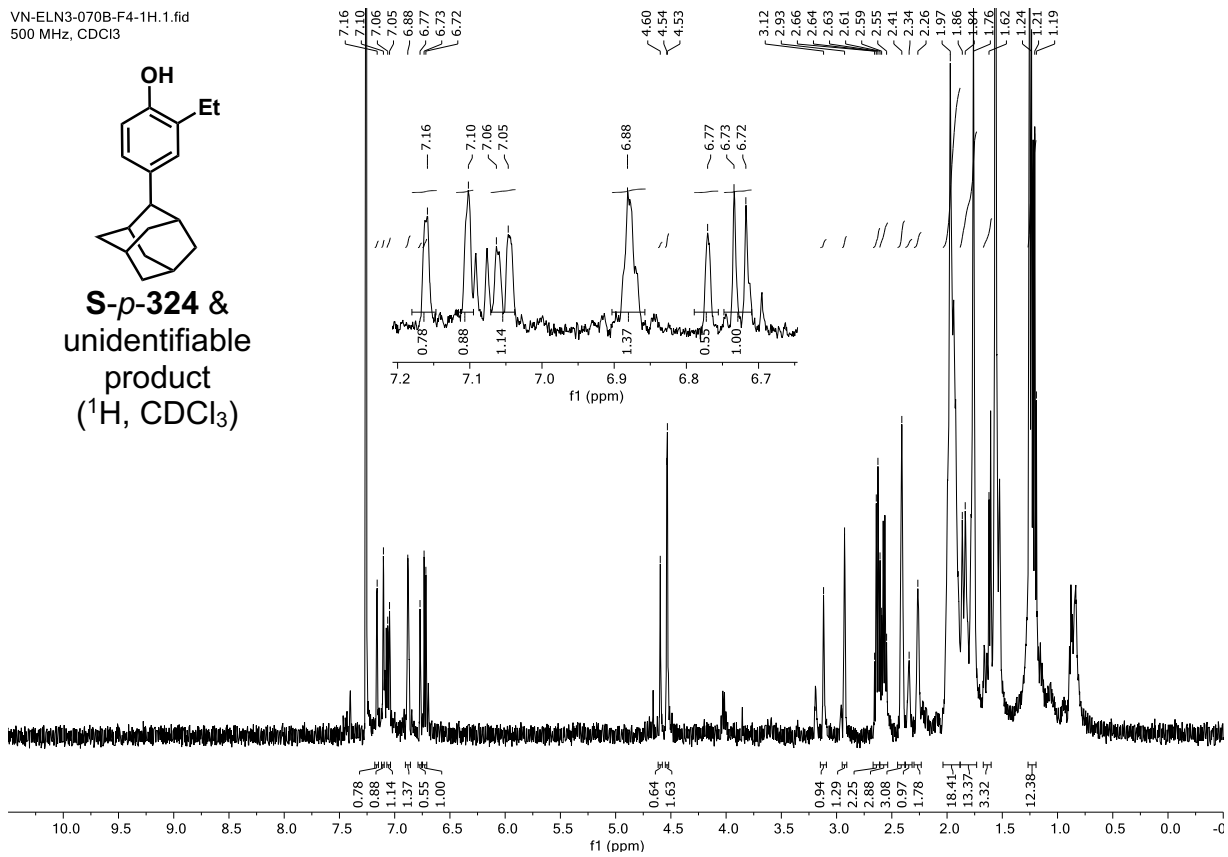
**324**  
(<sup>13</sup>C, CDCl<sub>3</sub>)



VN-ELN3-070B-F4-1H.1.fid  
500 MHz, CDCl<sub>3</sub>

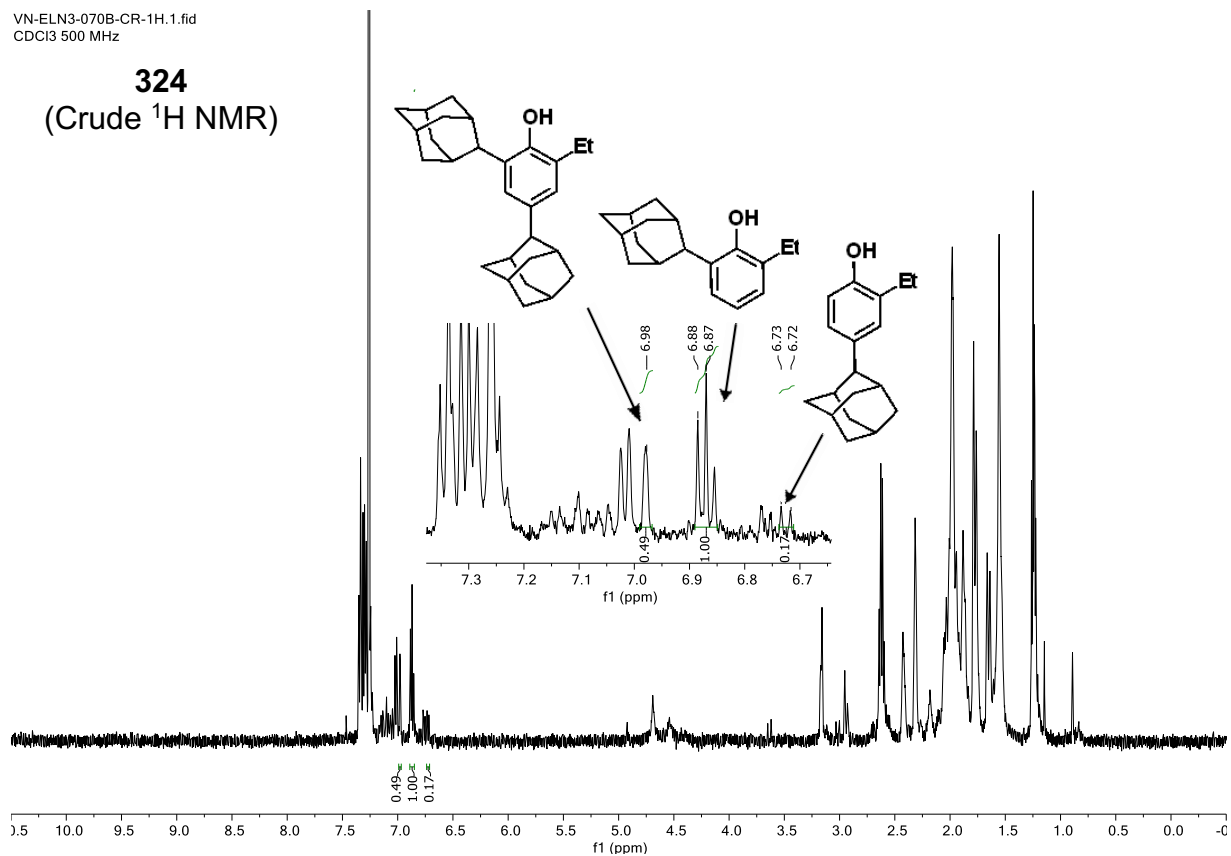


**S-p-324 &  
unidentifiable  
product  
(<sup>1</sup>H, CDCl<sub>3</sub>)**

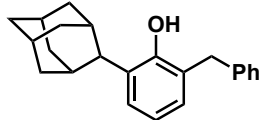


VN-ELN3-070B-CR-1H.1.fid  
CDCl3 500 MHz

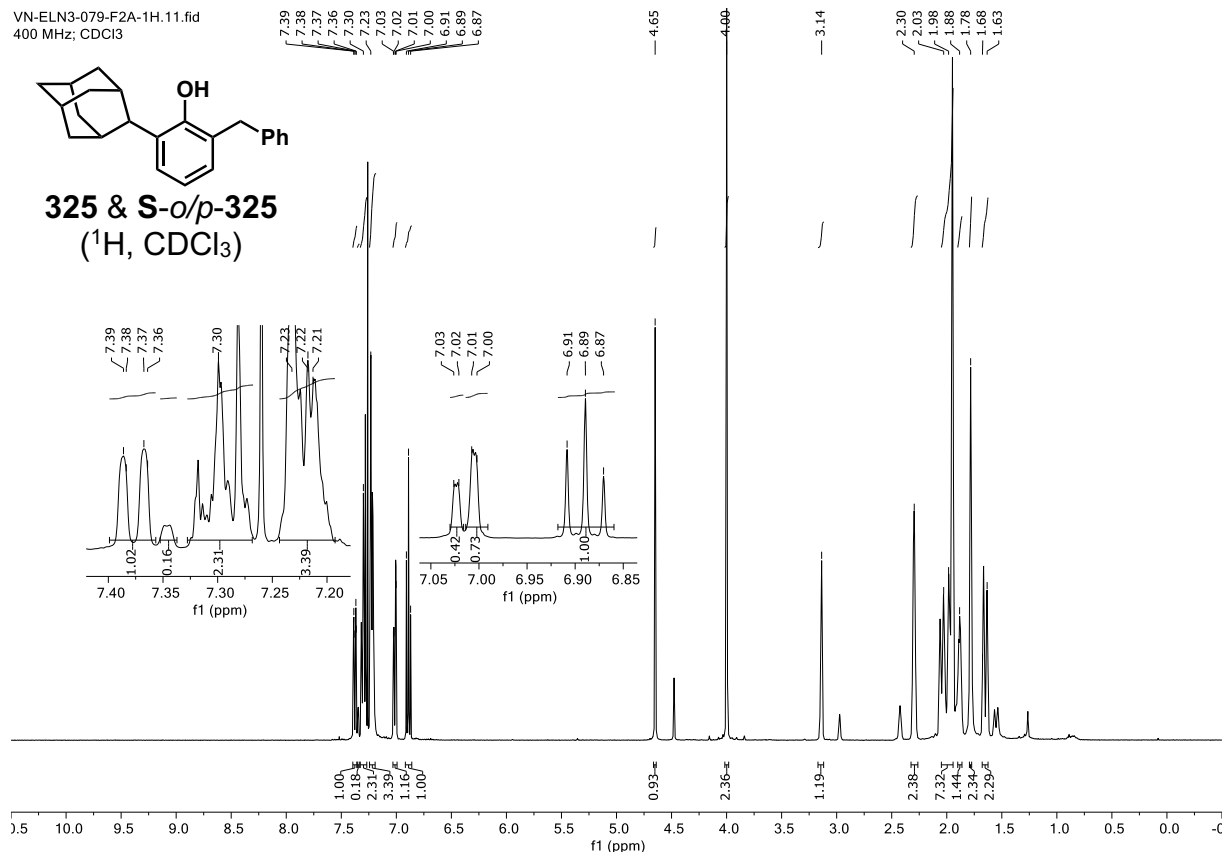
**324**  
(Crude <sup>1</sup>H NMR)



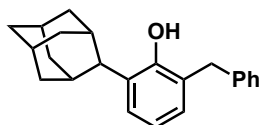
VN-ELN3-079-F2A-1H.11.fid  
400 MHz; CDCl<sub>3</sub>



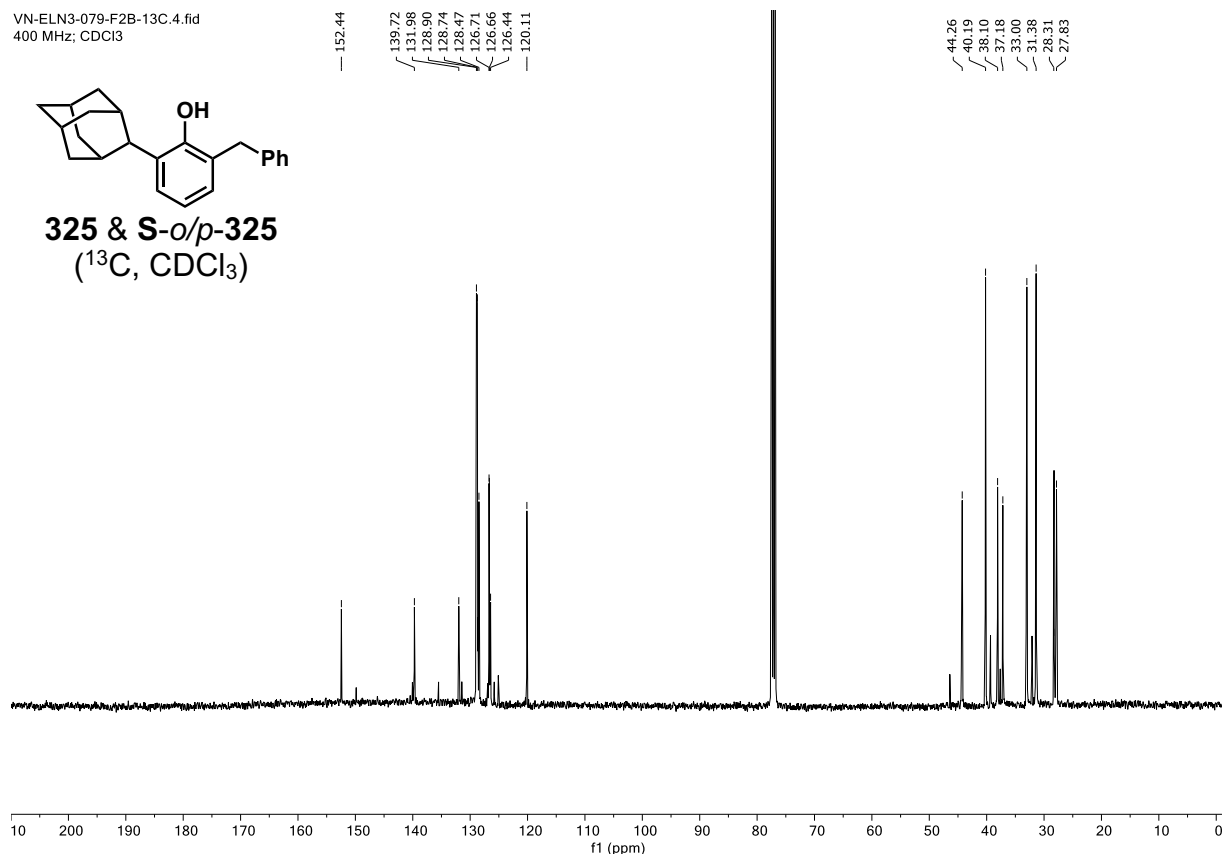
**325 & S-o/p-325**  
(<sup>1</sup>H, CDCl<sub>3</sub>)



VN-ELN3-079-F2B-13C.4.fid  
400 MHz; CDCl<sub>3</sub>

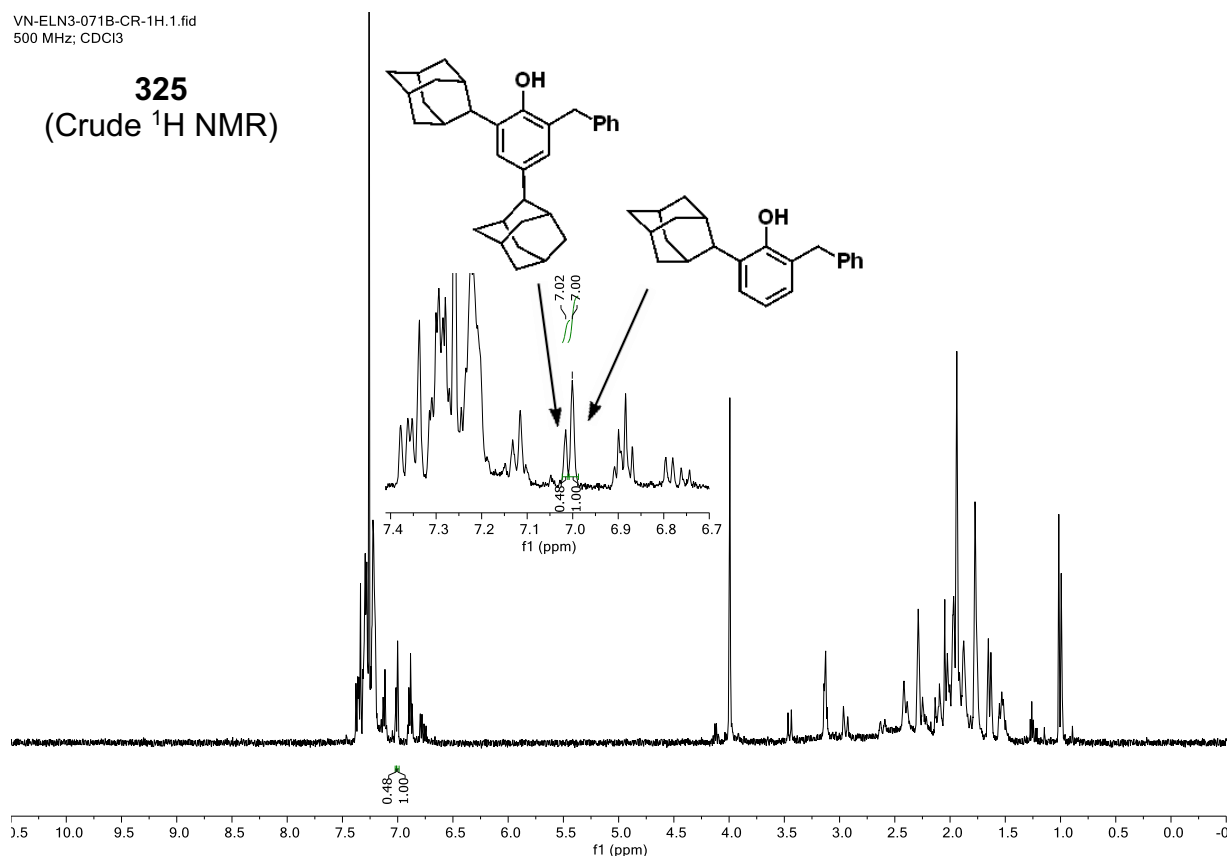


**325 & S-o/p-325**  
(<sup>13</sup>C, CDCl<sub>3</sub>)

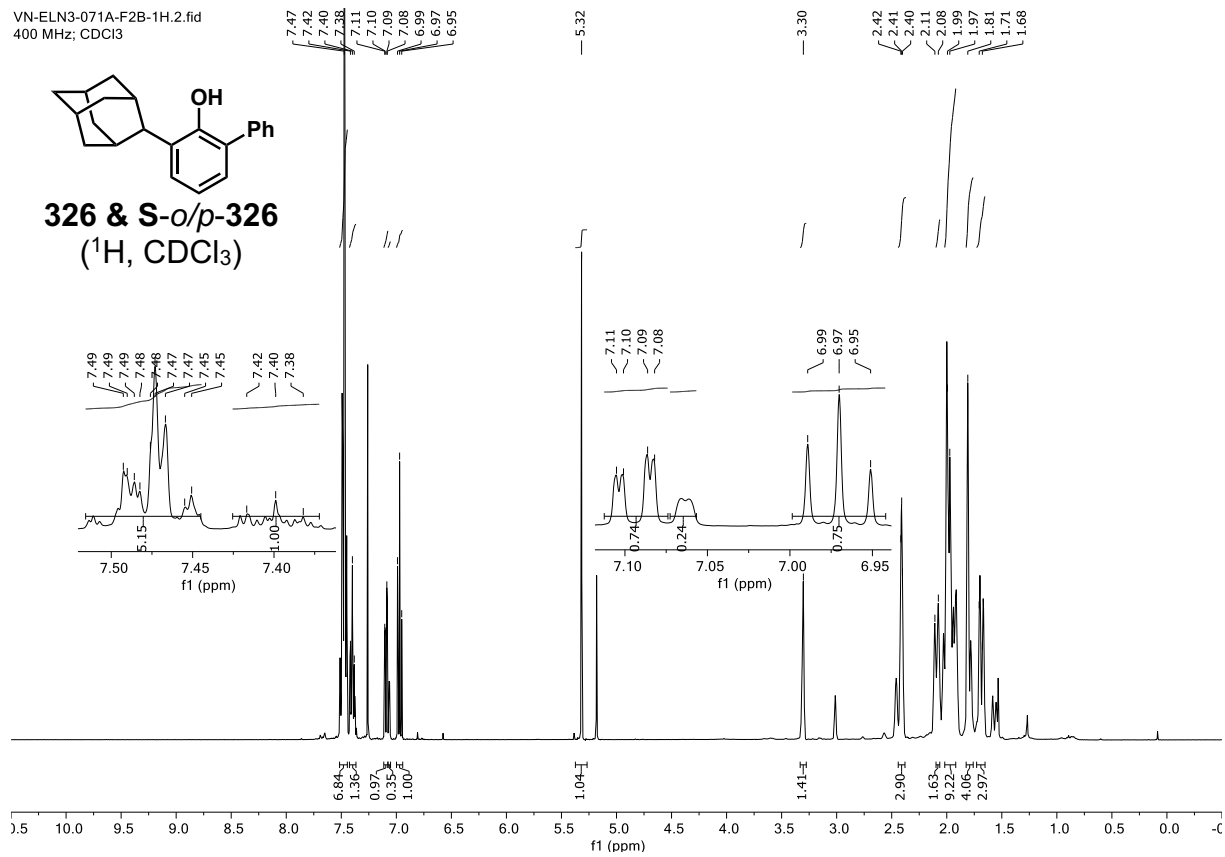
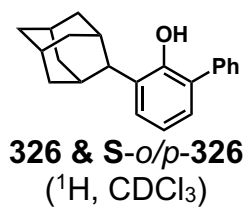


VN-ELN3-071B-CR-1H.1.fid  
500 MHz; CDCl<sub>3</sub>

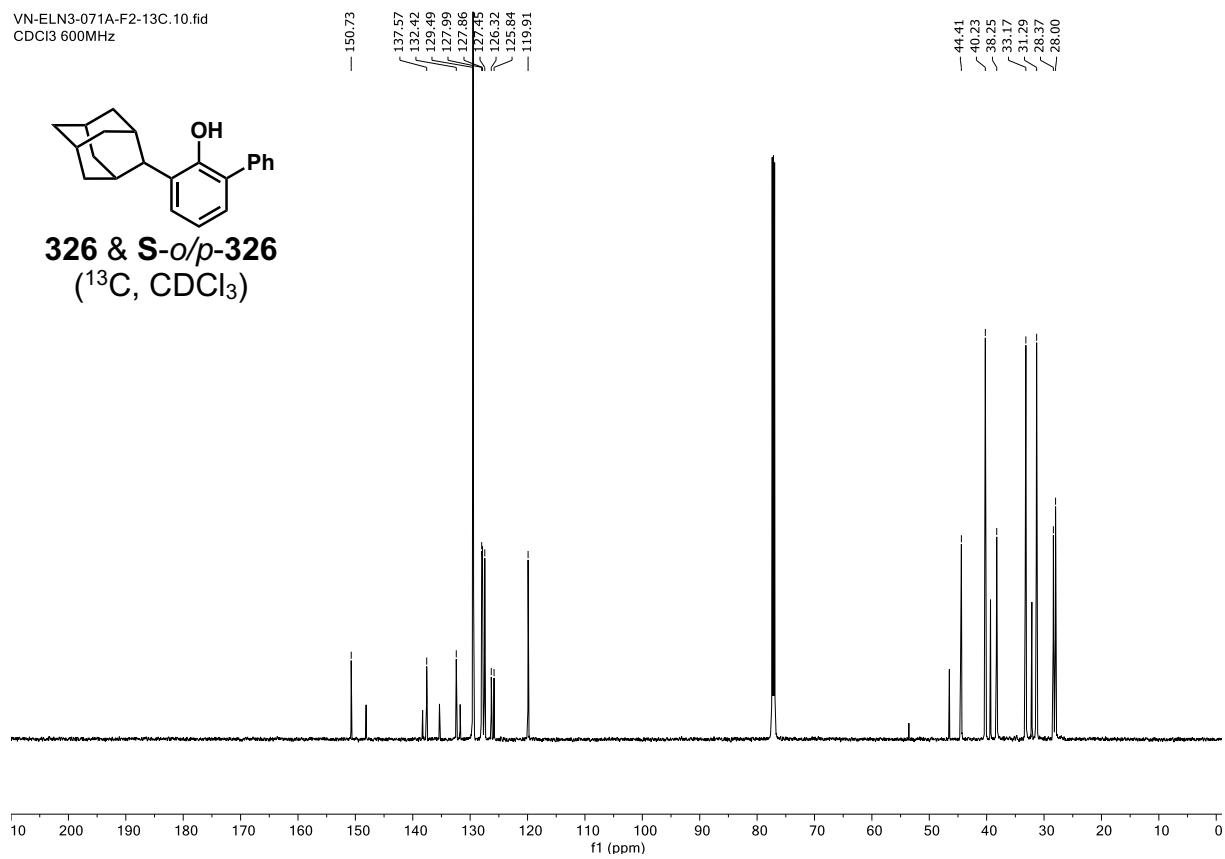
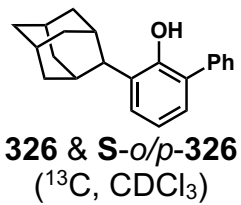
**325**  
(Crude <sup>1</sup>H NMR)



VN-ELN3-071A-F2B-1H.2.fid  
400 MHz; CDCl<sub>3</sub>

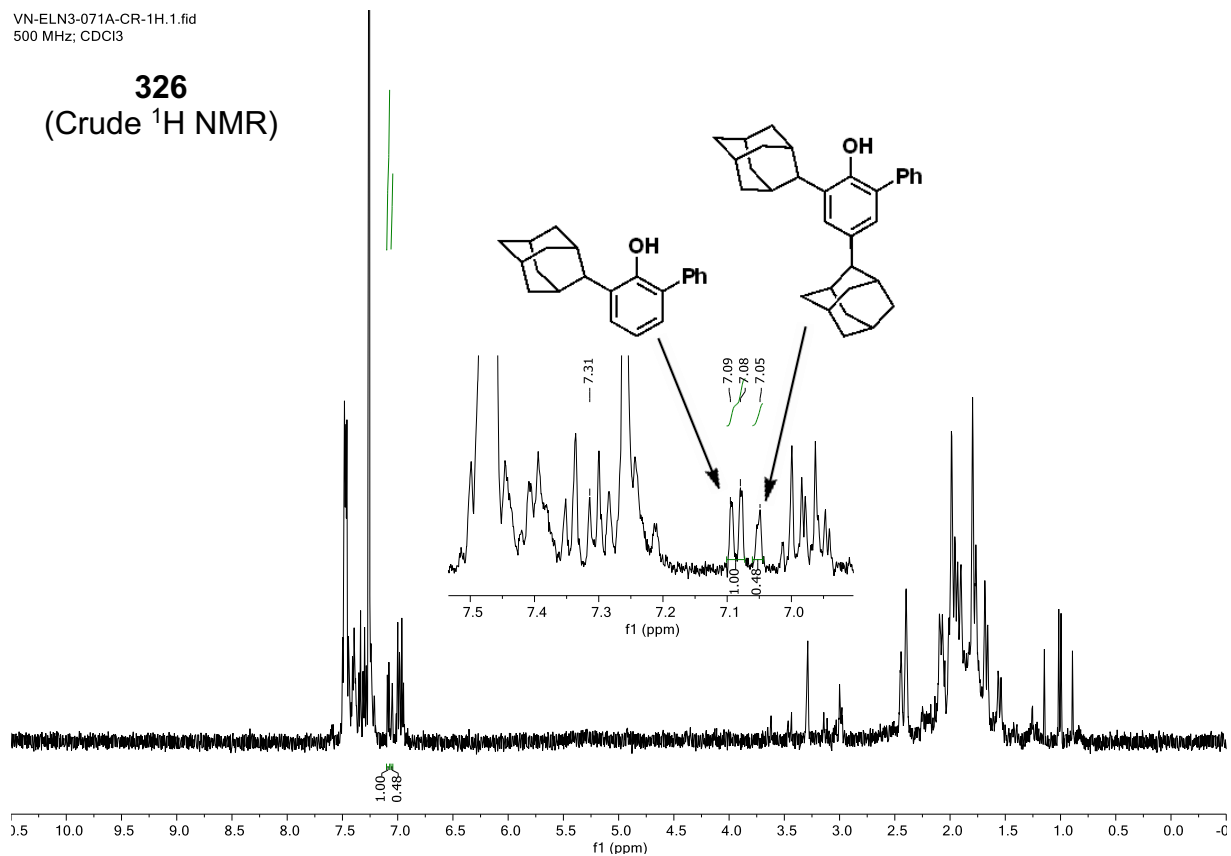


VN-ELN3-071A-F2-13C.10.fid  
CDCl3 600MHz

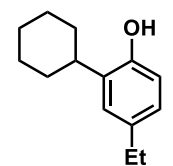


VN-ELN3-071A-CR-1H.1.fid  
500 MHz; CDCl<sub>3</sub>

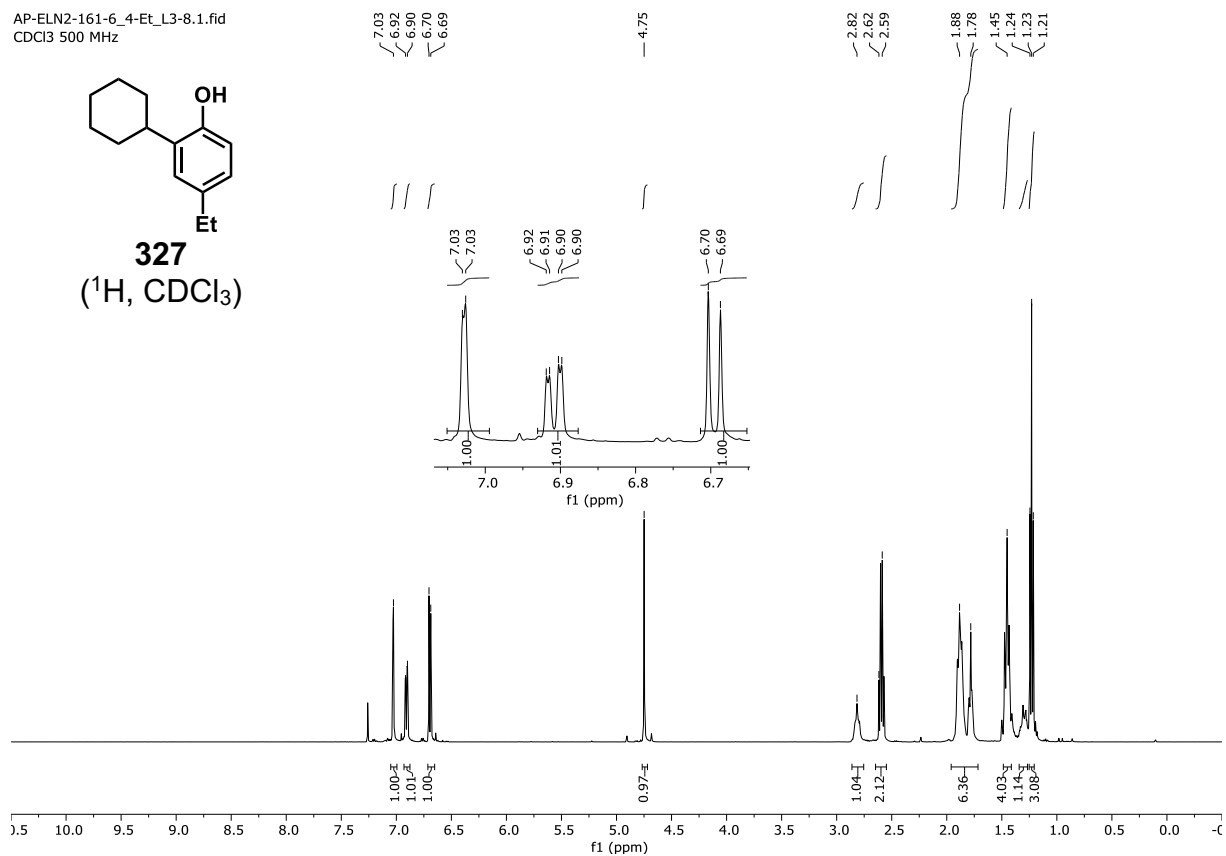
**326**  
(Crude <sup>1</sup>H NMR)



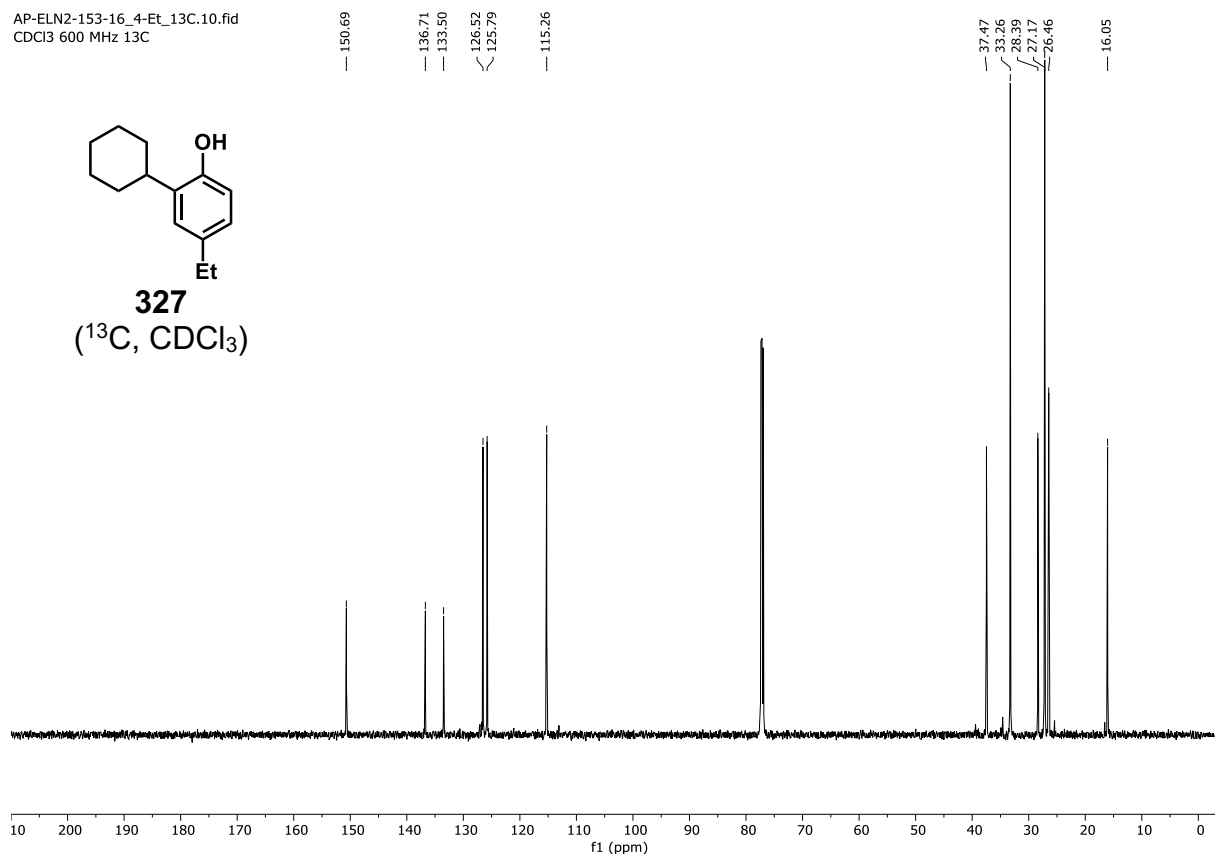
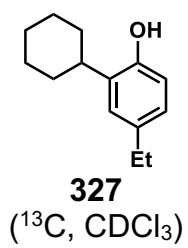
AP-ELN2-161-6\_4-Et\_L3-8.1.fid  
CDCl3 500 MHz



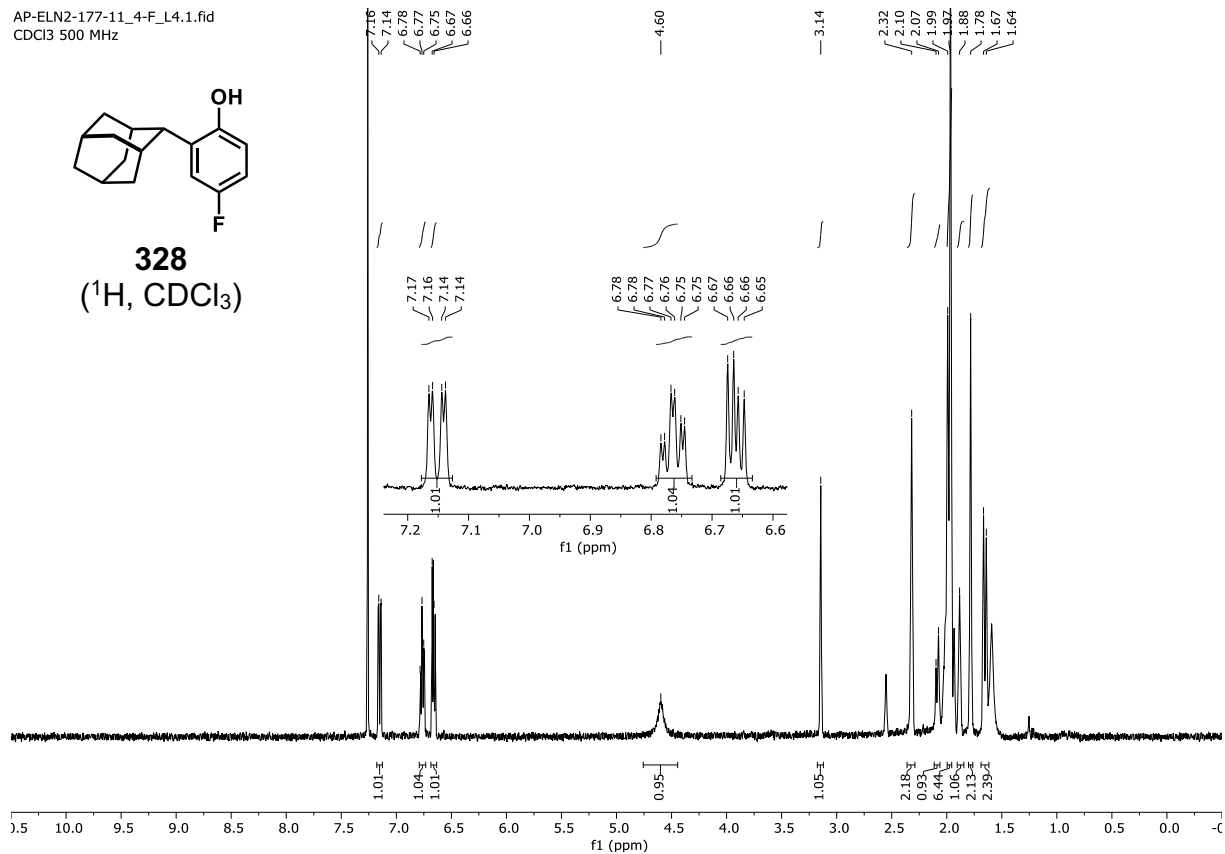
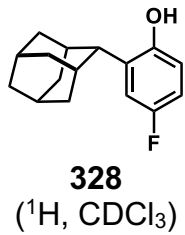
**327**  
(<sup>1</sup>H, CDCl<sub>3</sub>)



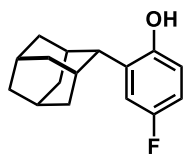
AP-ELN2-153-16\_4-Et\_13C.10.fid  
CDCl<sub>3</sub> 600 MHz 13C



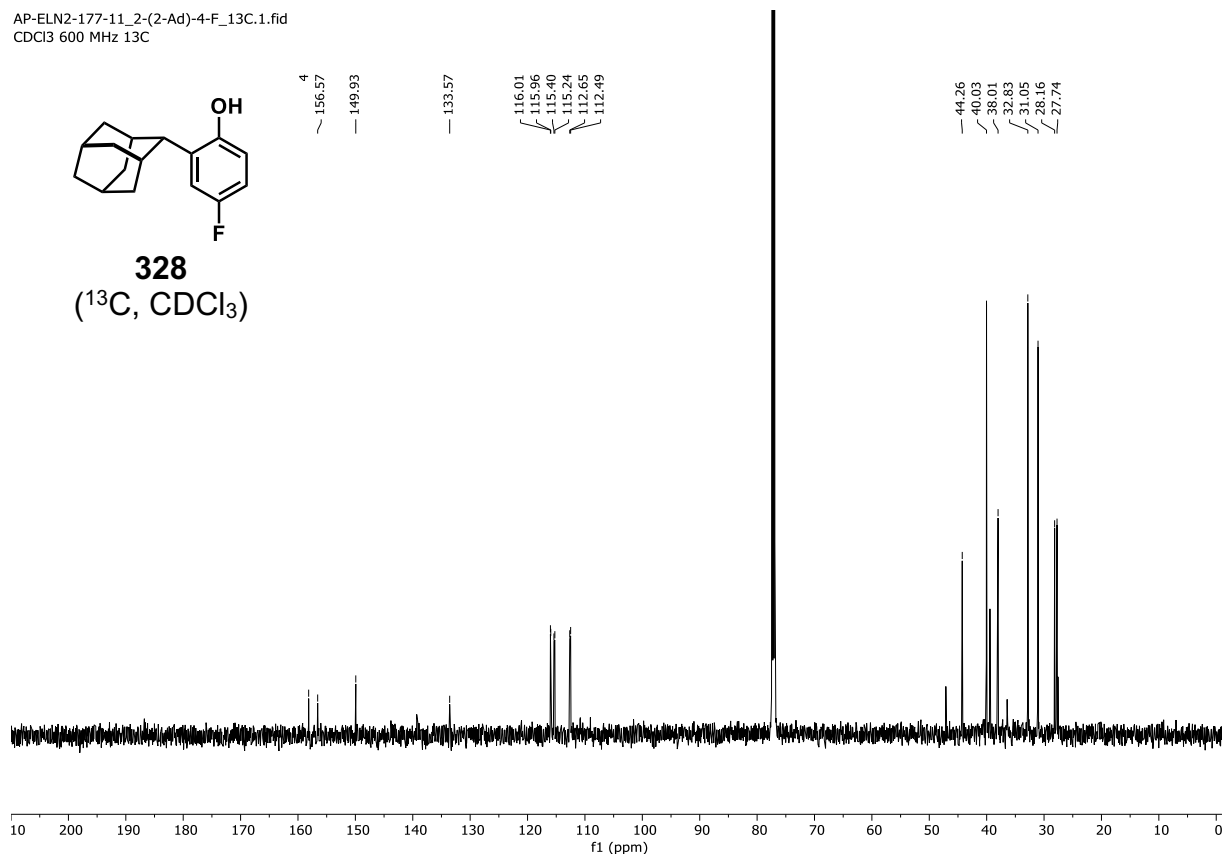
AP-ELN2-177-11\_4-F\_L4.1.fid  
CDCl<sub>3</sub> 500 MHz



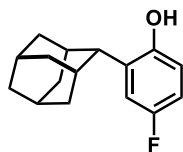
AP-ELN2-177-11\_2-(2-Ad)-4-F\_13C.1.fid  
CDCl3 600 MHz 13C



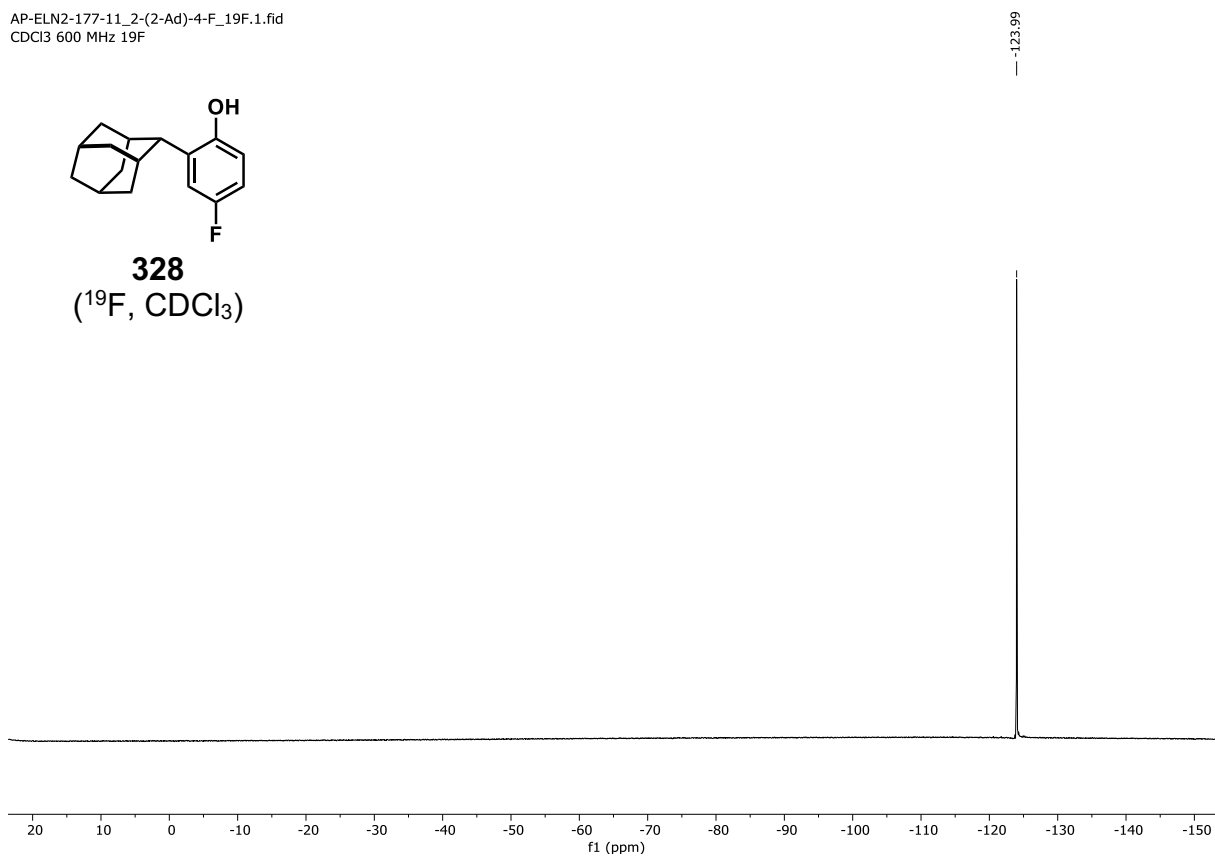
**328**  
(<sup>13</sup>C, CDCl<sub>3</sub>)



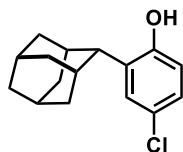
AP-ELN2-177-11\_2-(2-Ad)-4-F\_19F.1.fid  
CDCl<sub>3</sub> 600 MHz 19F



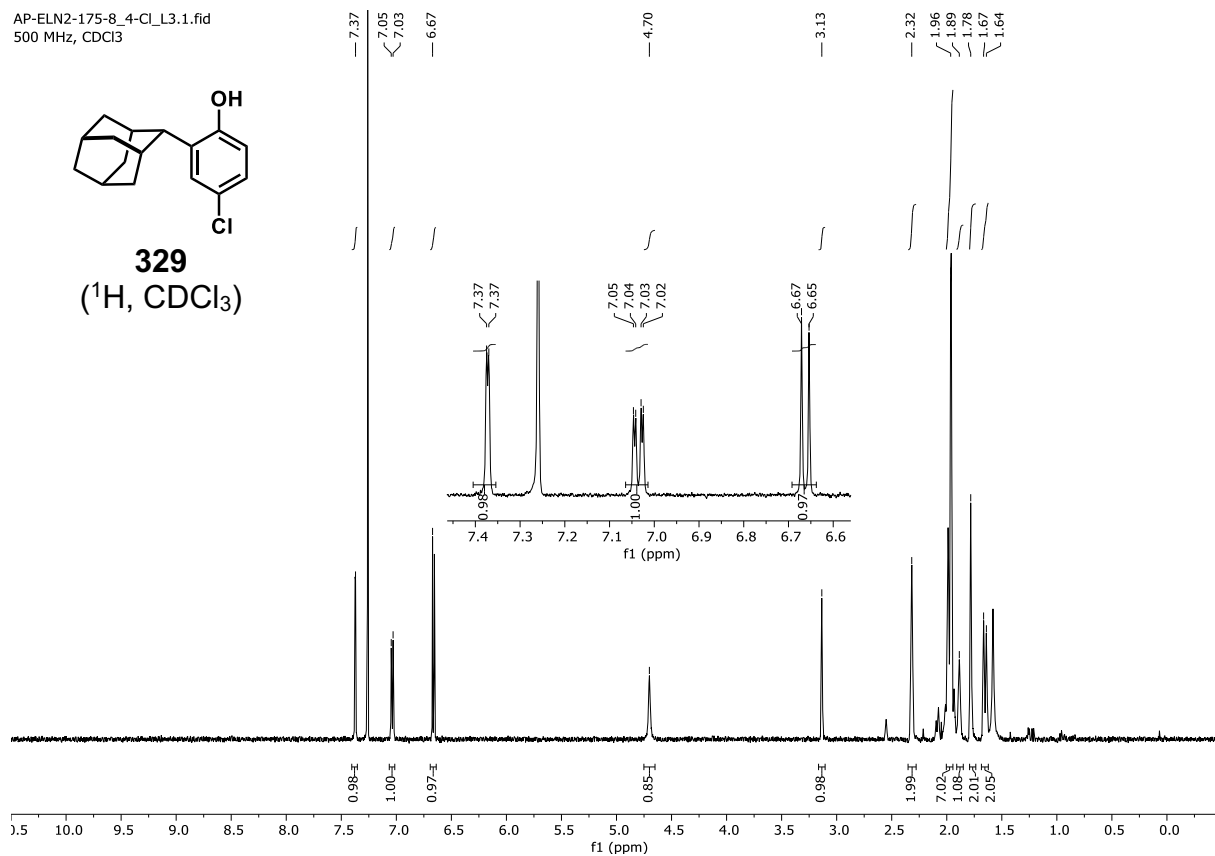
**328**  
(<sup>19</sup>F, CDCl<sub>3</sub>)



AP-ELN2-175-8\_4-Cl\_L3.1.fid  
500 MHz, CDCl<sub>3</sub>



**329**  
(<sup>1</sup>H, CDCl<sub>3</sub>)



AP-ELN2-175-8\_2-(2-Ad)-4-Cl\_13C.2.fid  
CDCl3 600 MHz 13C

— 153.33

— 133.95

— 128.34

— 126.11

— 124.76

— 116.41

— 44.13

— 39.99

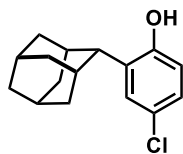
— 38.05

— 32.86

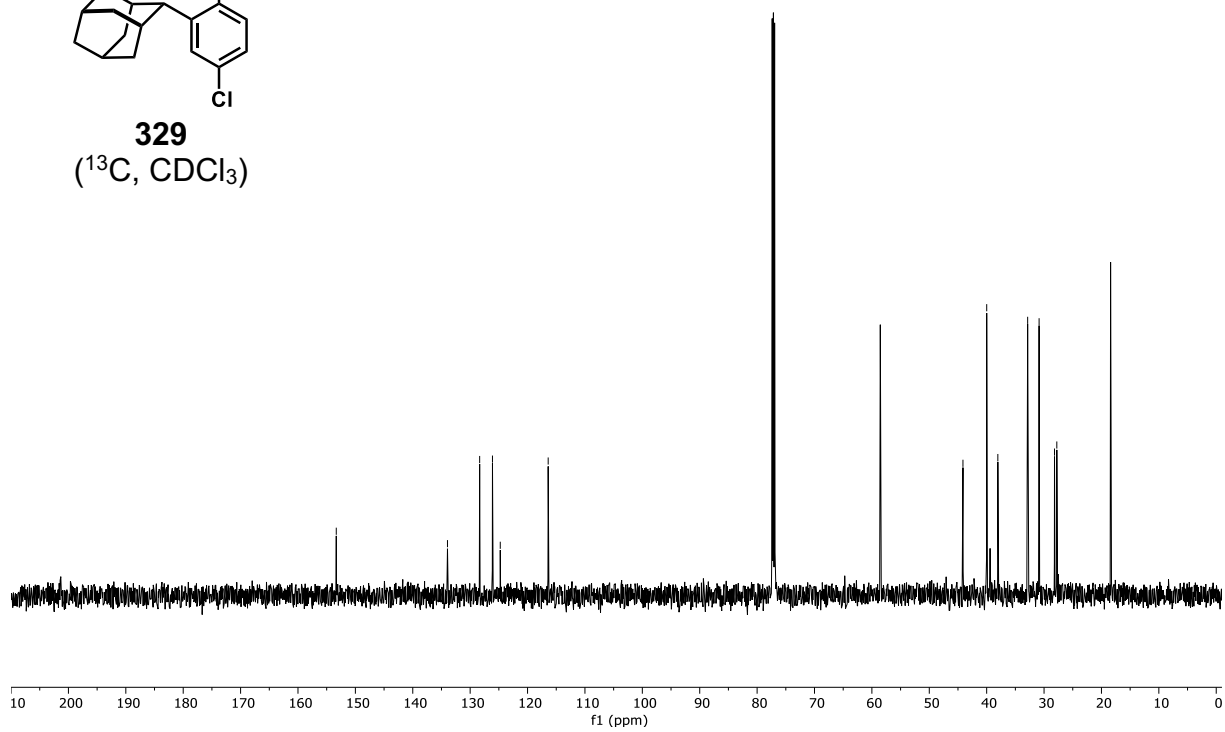
— 30.86

— 28.18

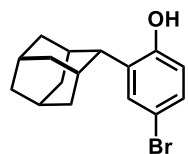
— 27.78



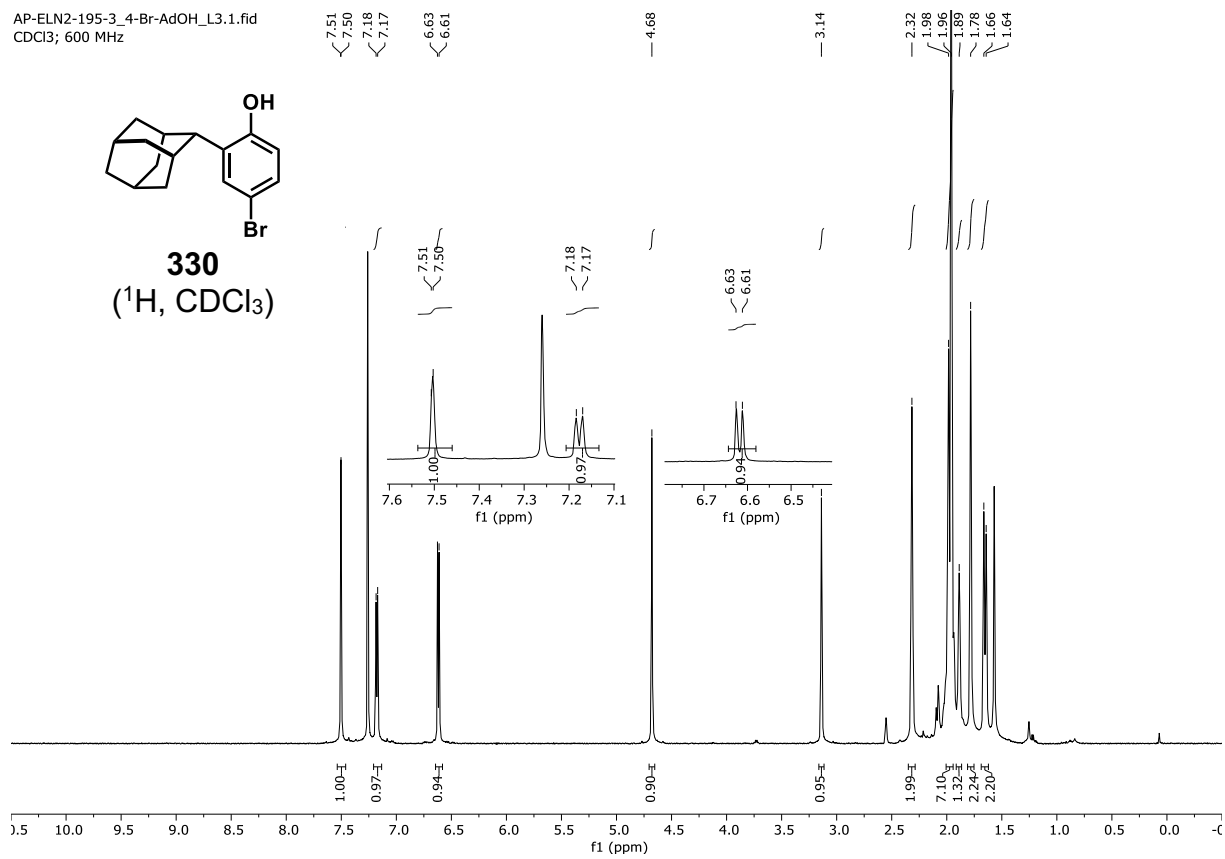
**329**  
(<sup>13</sup>C, CDCl<sub>3</sub>)



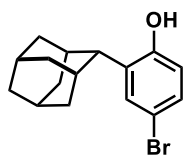
AP-ELN2-195-3\_4-Br-AdOH\_L3.1.fid  
CDCl<sub>3</sub>; 600 MHz



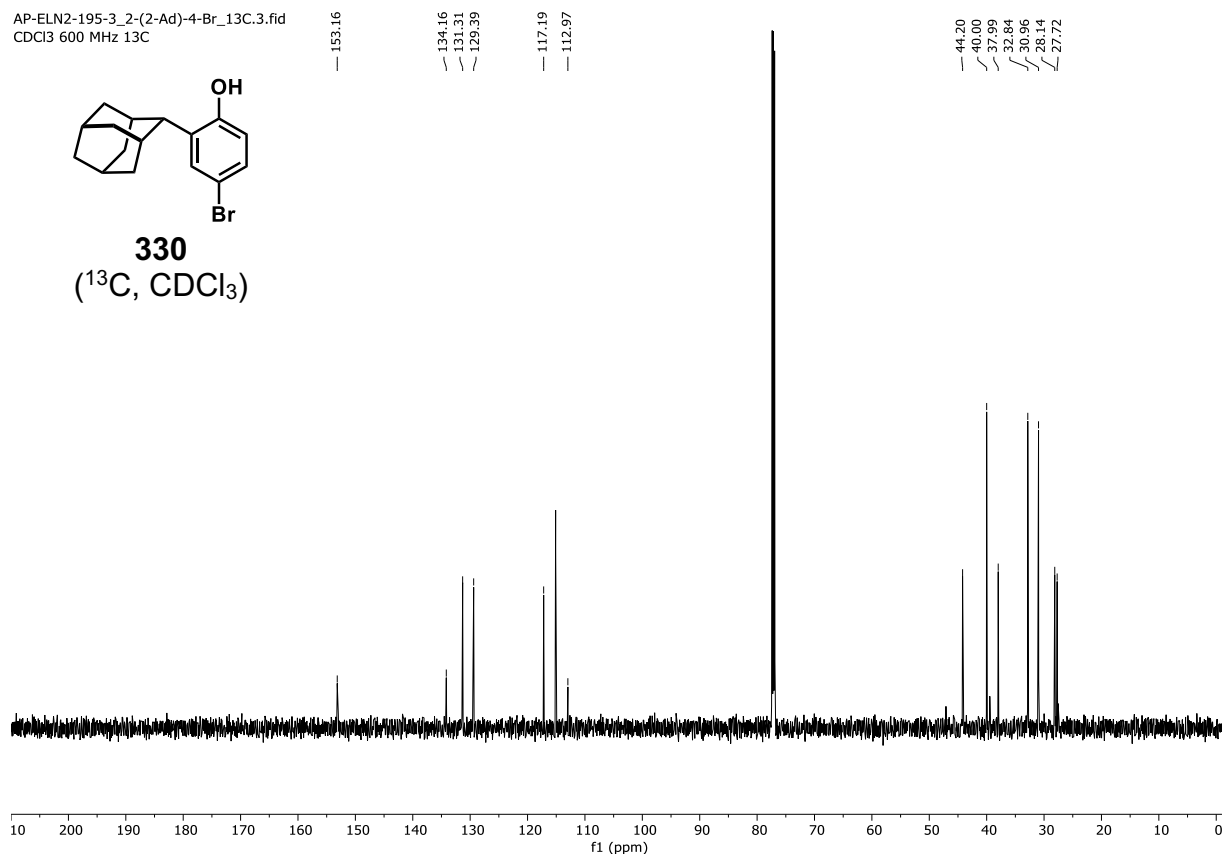
**330**  
(<sup>1</sup>H, CDCl<sub>3</sub>)



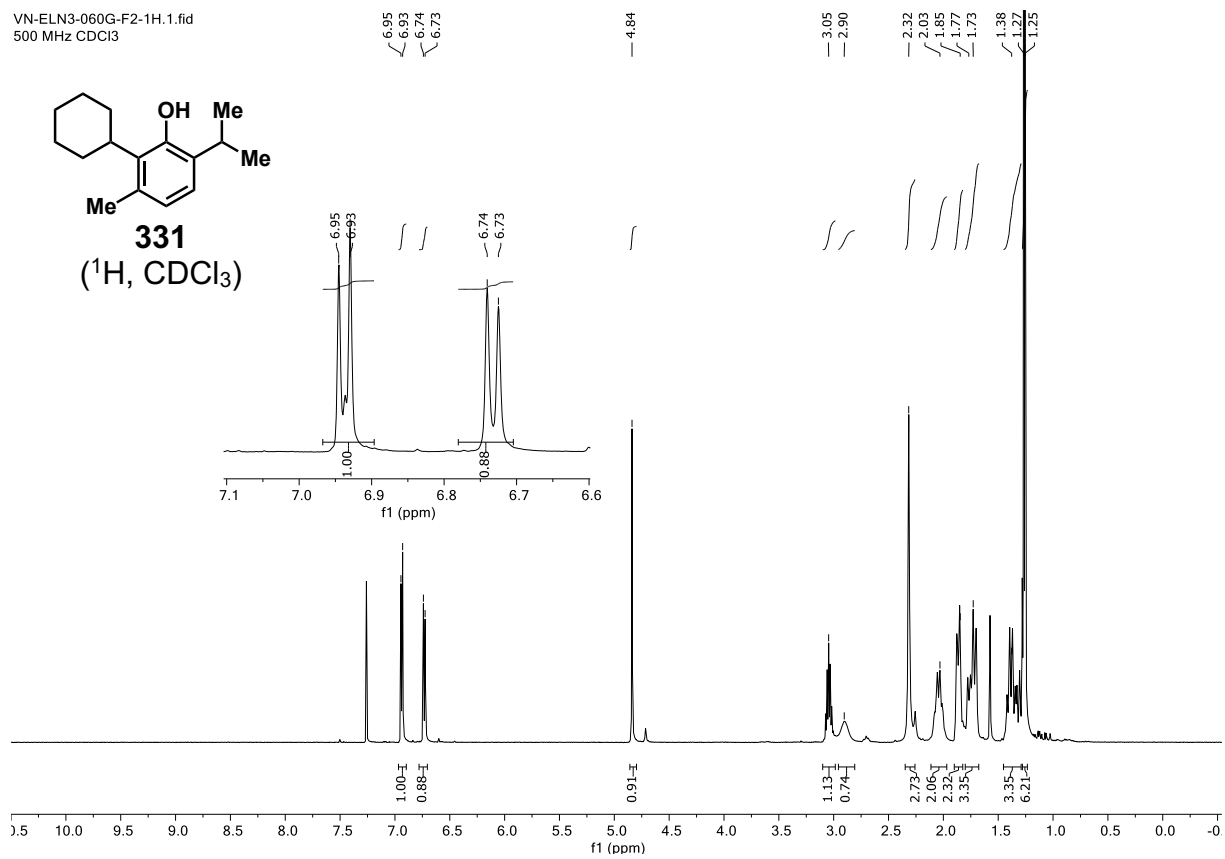
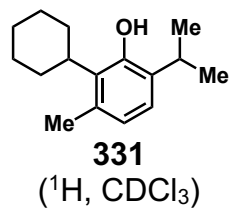
AP-ELN2-195-3\_2-(2-Ad)-4-Br\_13C.3.fid  
CDCl<sub>3</sub> 600 MHz 13C



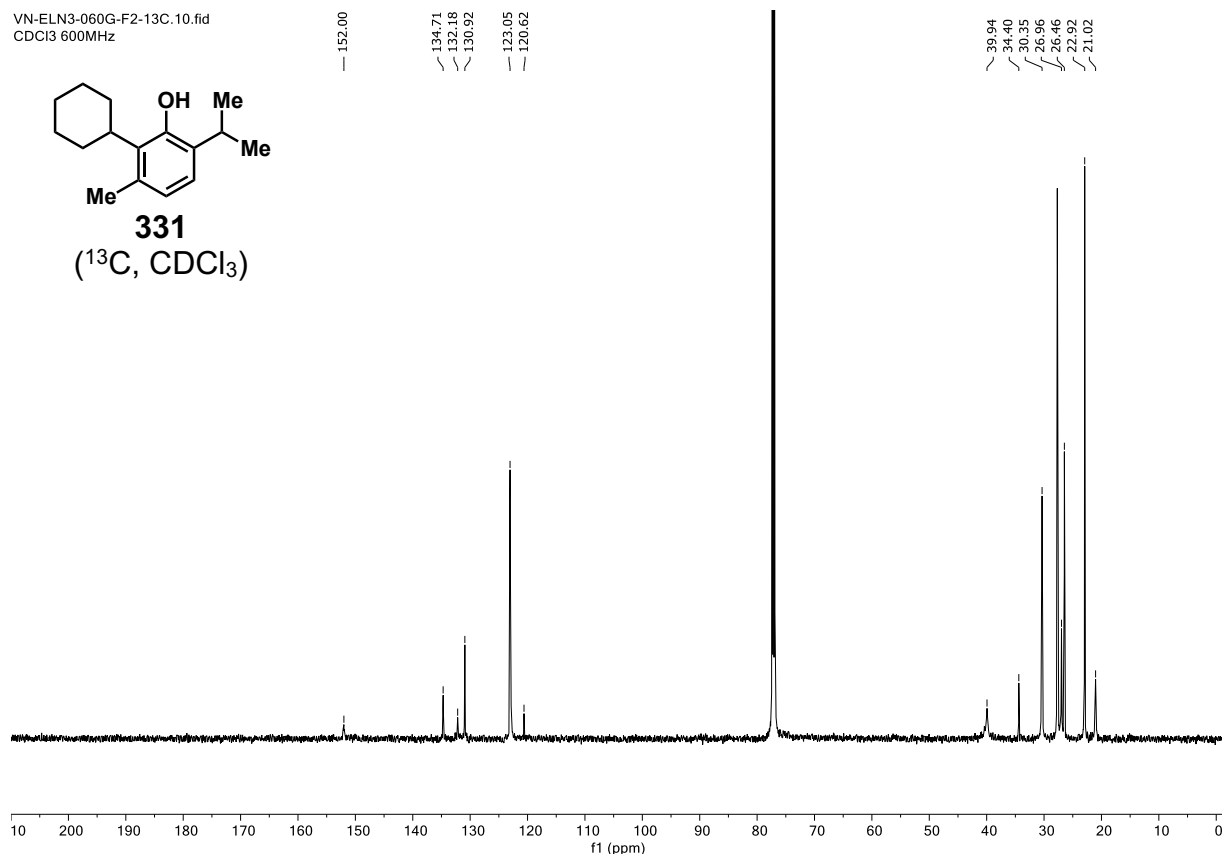
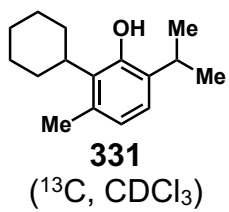
**330**  
(<sup>13</sup>C, CDCl<sub>3</sub>)



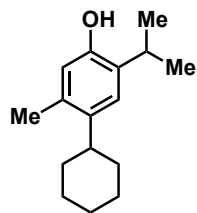
VN-ELN3-060G-F2-1H.1.fid  
500 MHz CDCl<sub>3</sub>



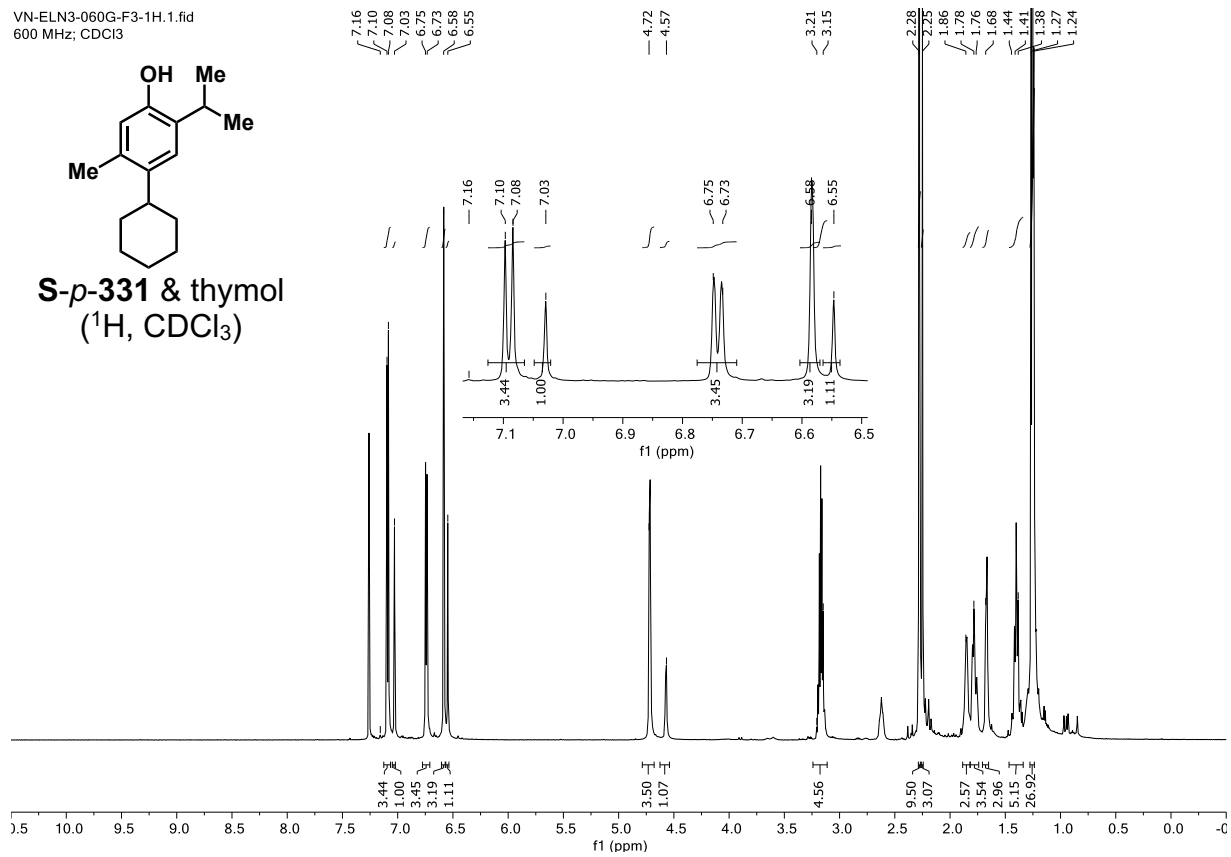
VN-ELN3-060G-F2-13C.10.fid  
CDCl3 600MHz



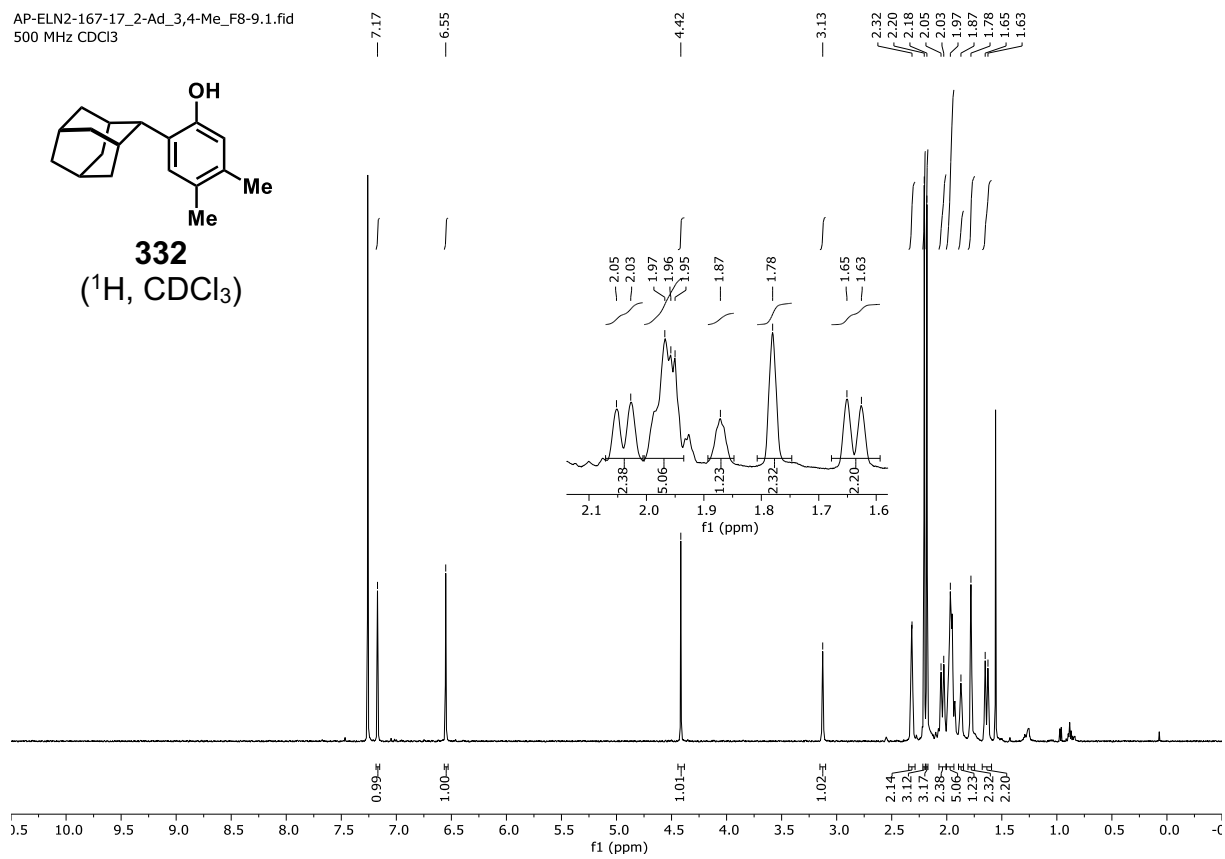
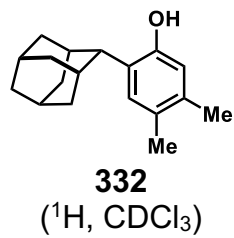
VN-ELN3-060G-F3-1H.1.fid  
600 MHz; CDCl<sub>3</sub>



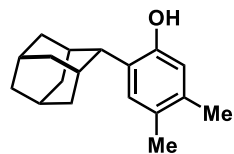
**S-p-331 & thymol**  
(<sup>1</sup>H, CDCl<sub>3</sub>)



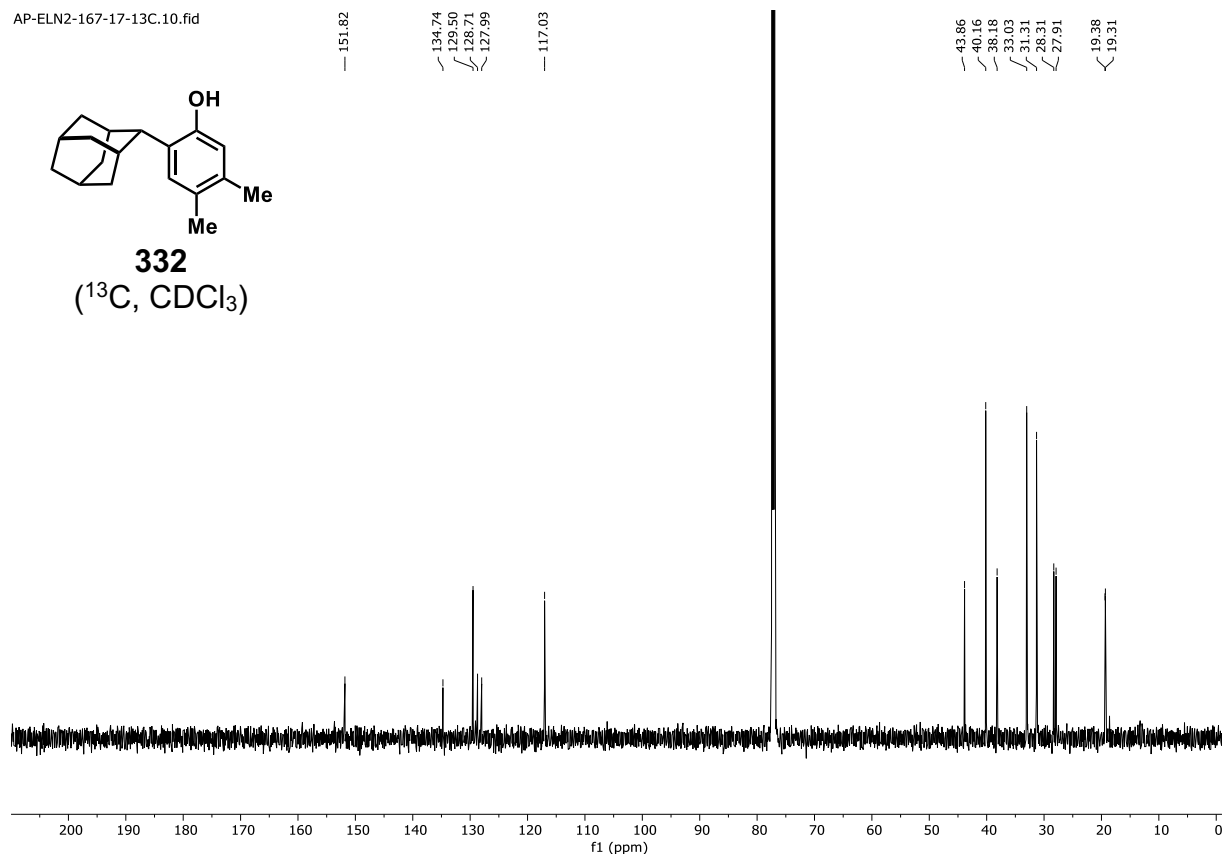
AP-ELN2-167-17\_2-Ad\_3,4-Me\_F8-9.1.fid  
500 MHz CDCl<sub>3</sub>



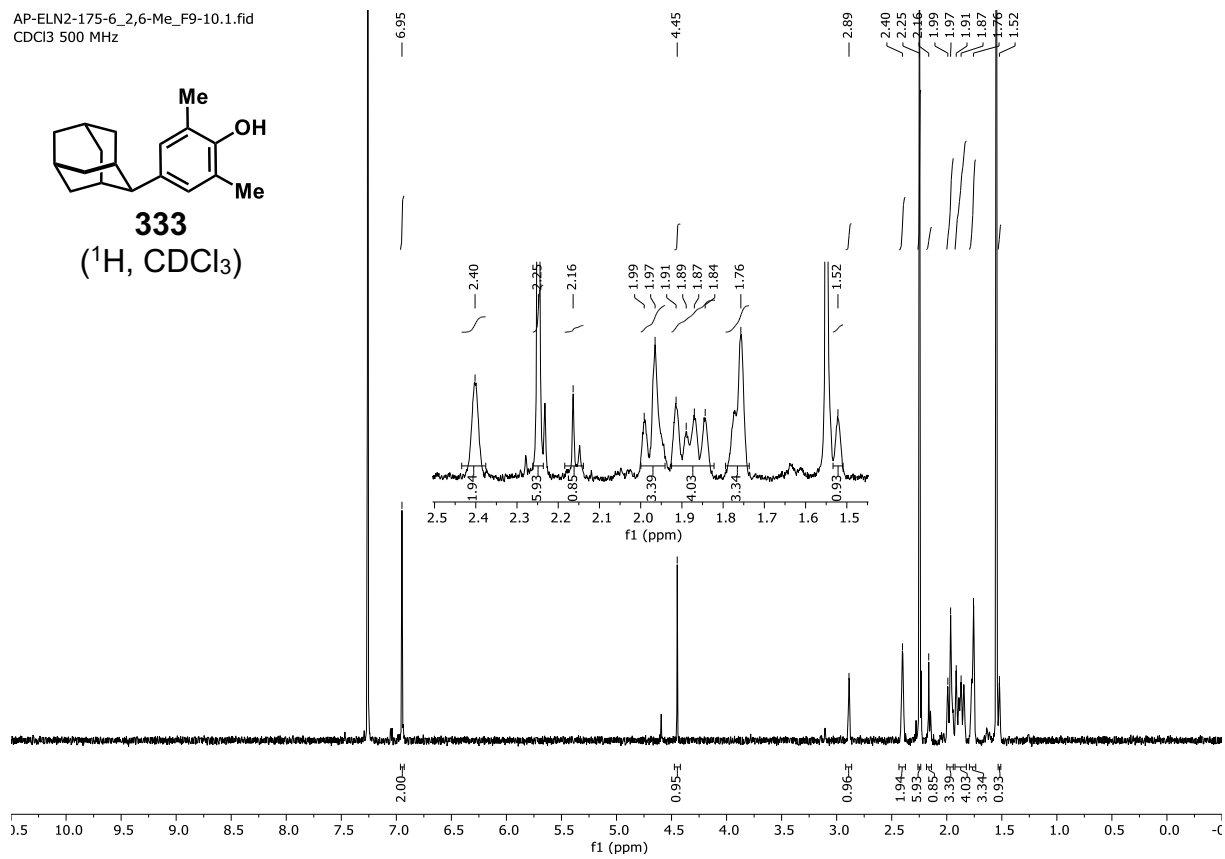
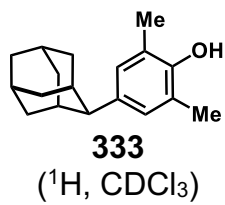
AP-ELN2-167-17-13C.10.fid



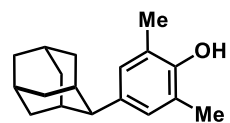
**332**  
(<sup>13</sup>C, CDCl<sub>3</sub>)



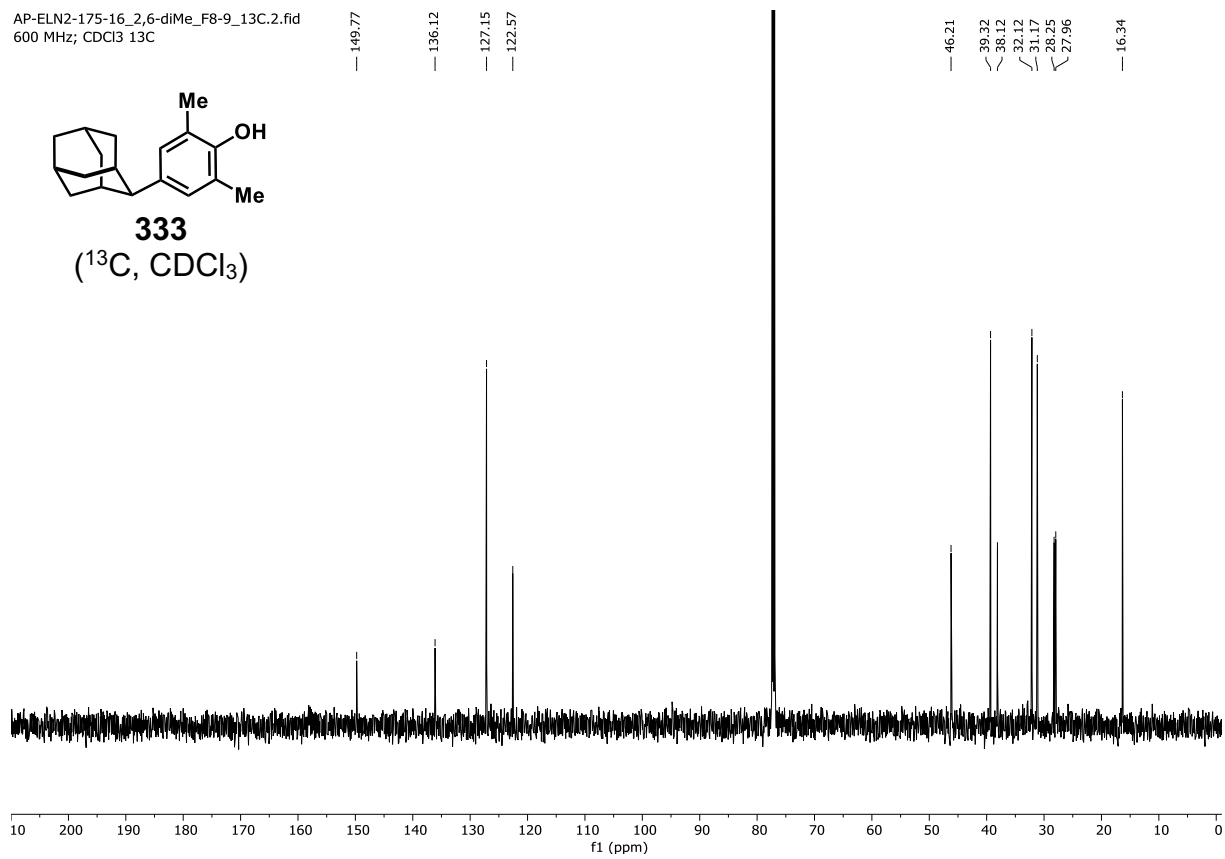
AP-ELN2-175-6\_2,6-Me\_F9-10.1.fid  
CDCl3 500 MHz



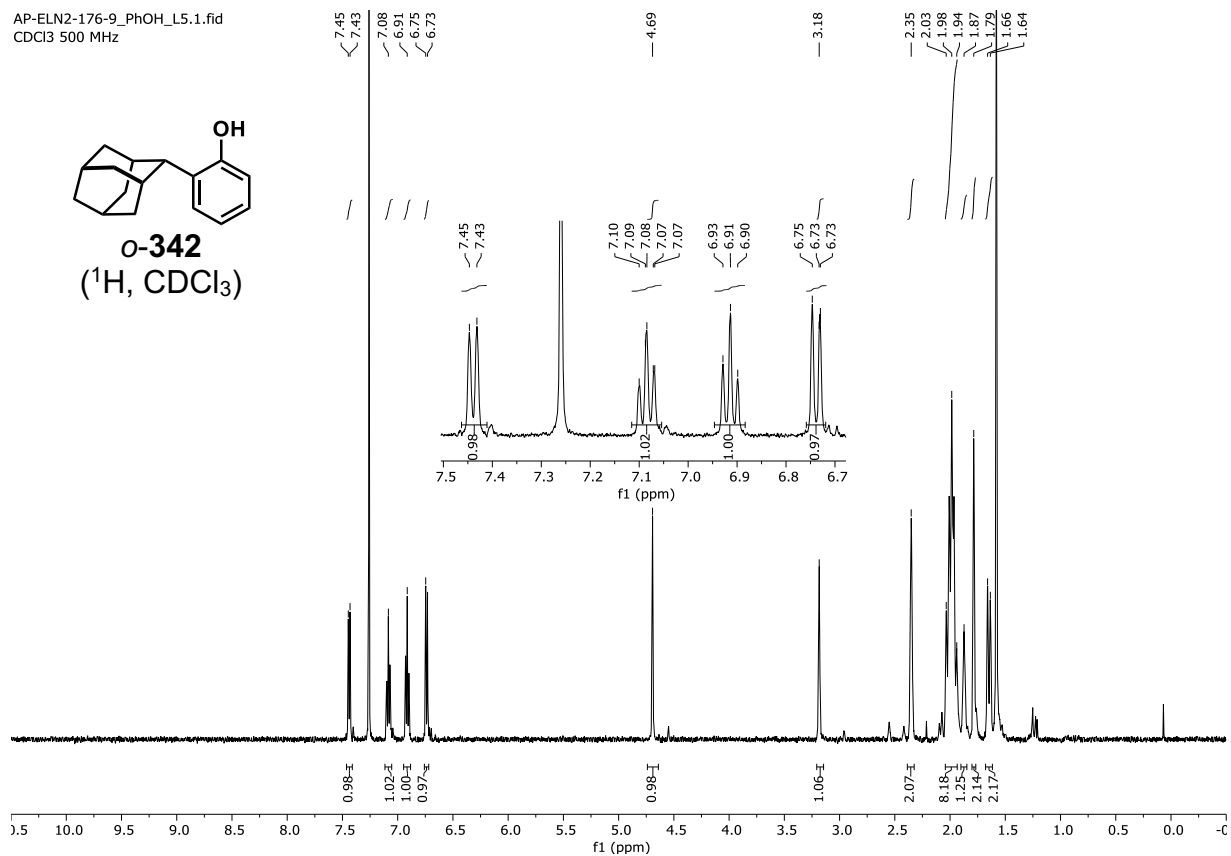
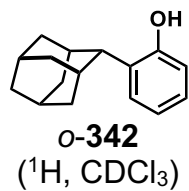
AP-ELN2-175-16\_2,6-diMe\_F8-9\_13C.2.fid  
600 MHz; CDCl<sub>3</sub> 13C



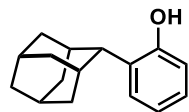
**333**  
(<sup>13</sup>C, CDCl<sub>3</sub>)



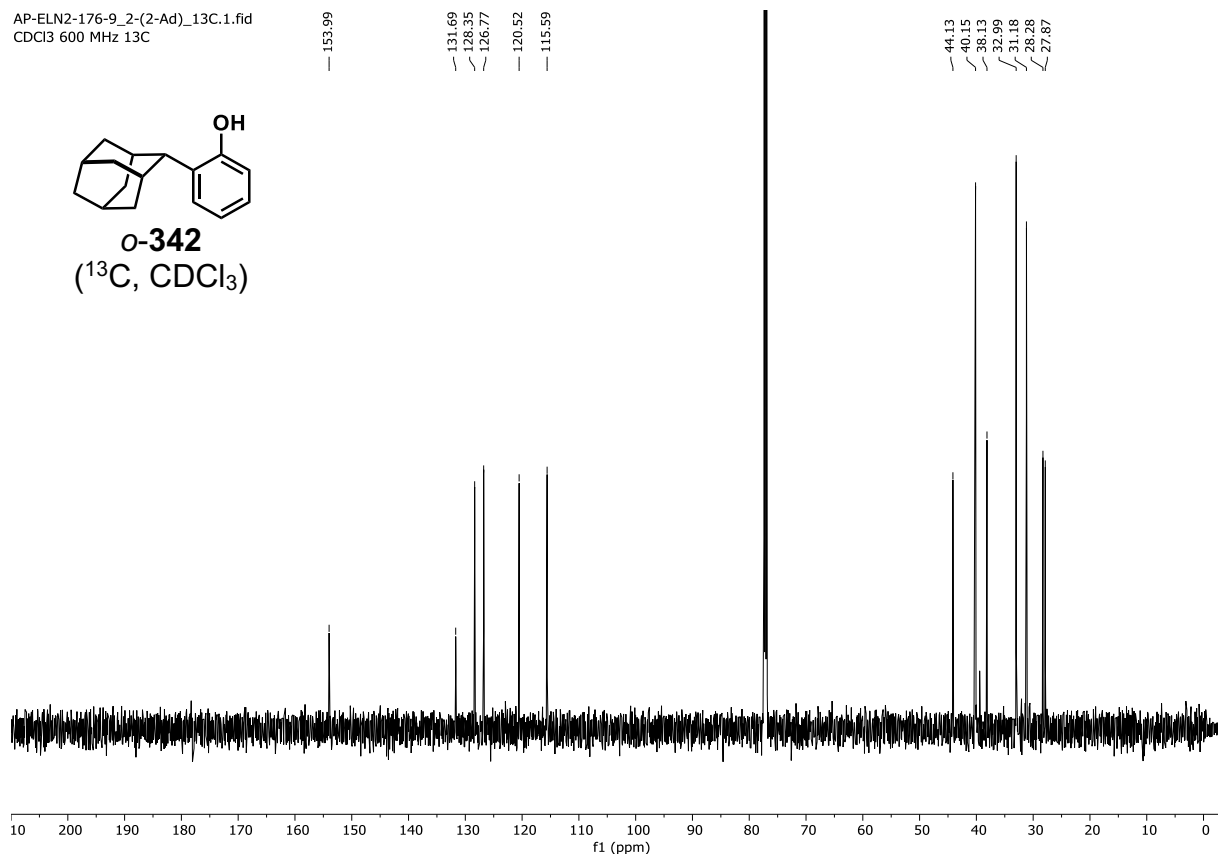
AP-ELN2-176-9\_PHOH\_L5.1.fid  
CDCl3 500 MHz



AP-ELN2-176-9\_2-(2-Ad)\_13C.1.fid  
CDCl3 600 MHz 13C

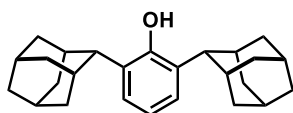


**o-342**  
(<sup>13</sup>C, CDCl<sub>3</sub>)

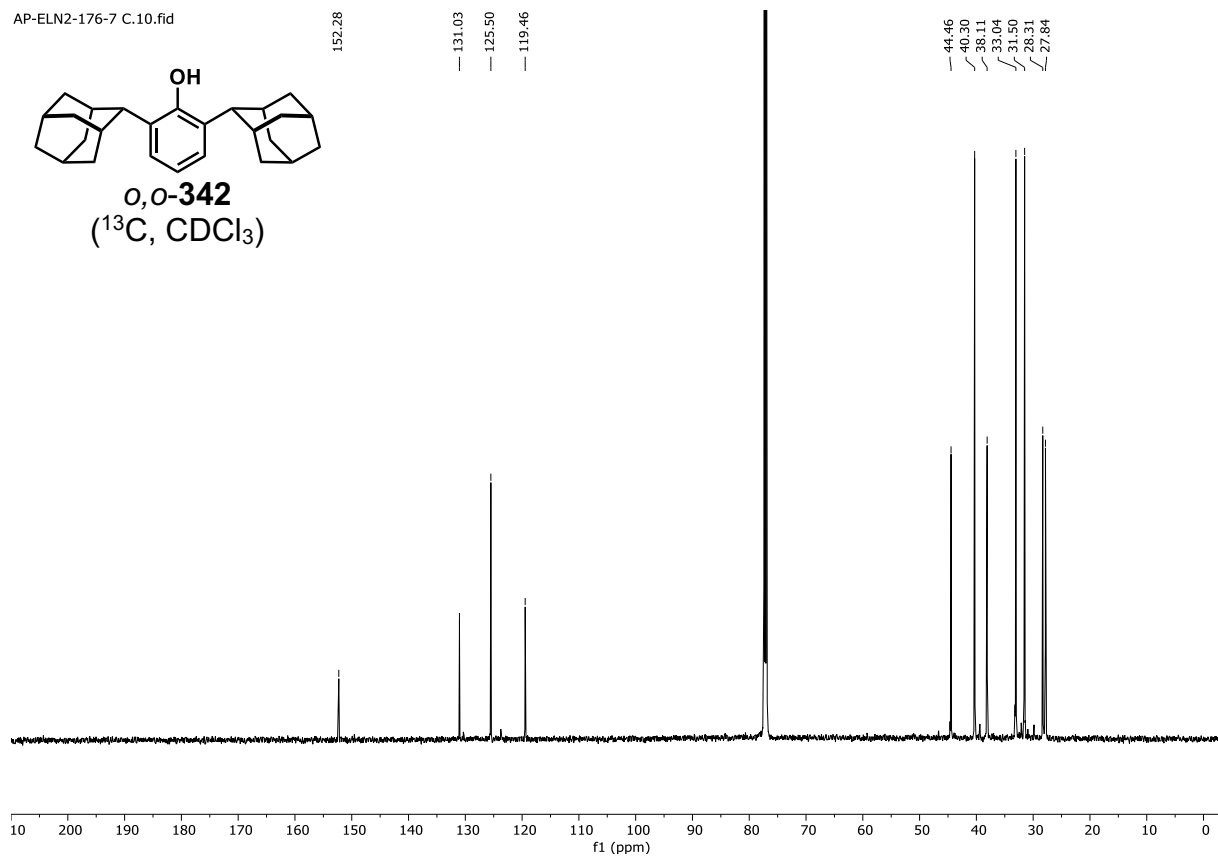




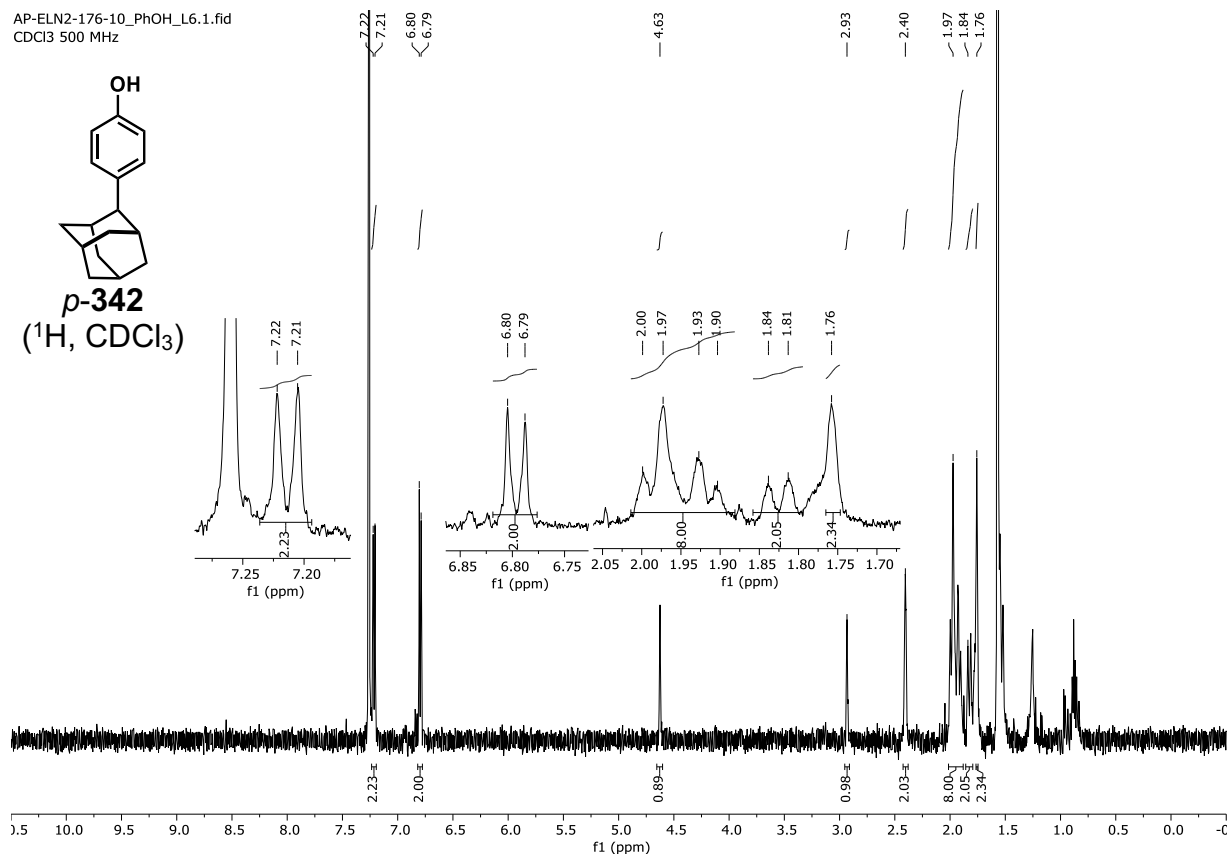
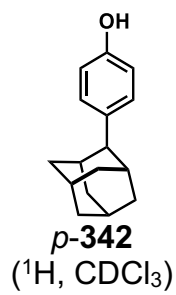
AP-ELN2-176-7 C.10.fid



**o,o-342**  
(<sup>13</sup>C, CDCl<sub>3</sub>)



AP-ELN2-176-10\_PhOH\_L6.1.fid  
CDCl<sub>3</sub> 500 MHz



VN-ELN3-039-F1-1H.1.fid  
500 MHz CDCl<sub>3</sub>

